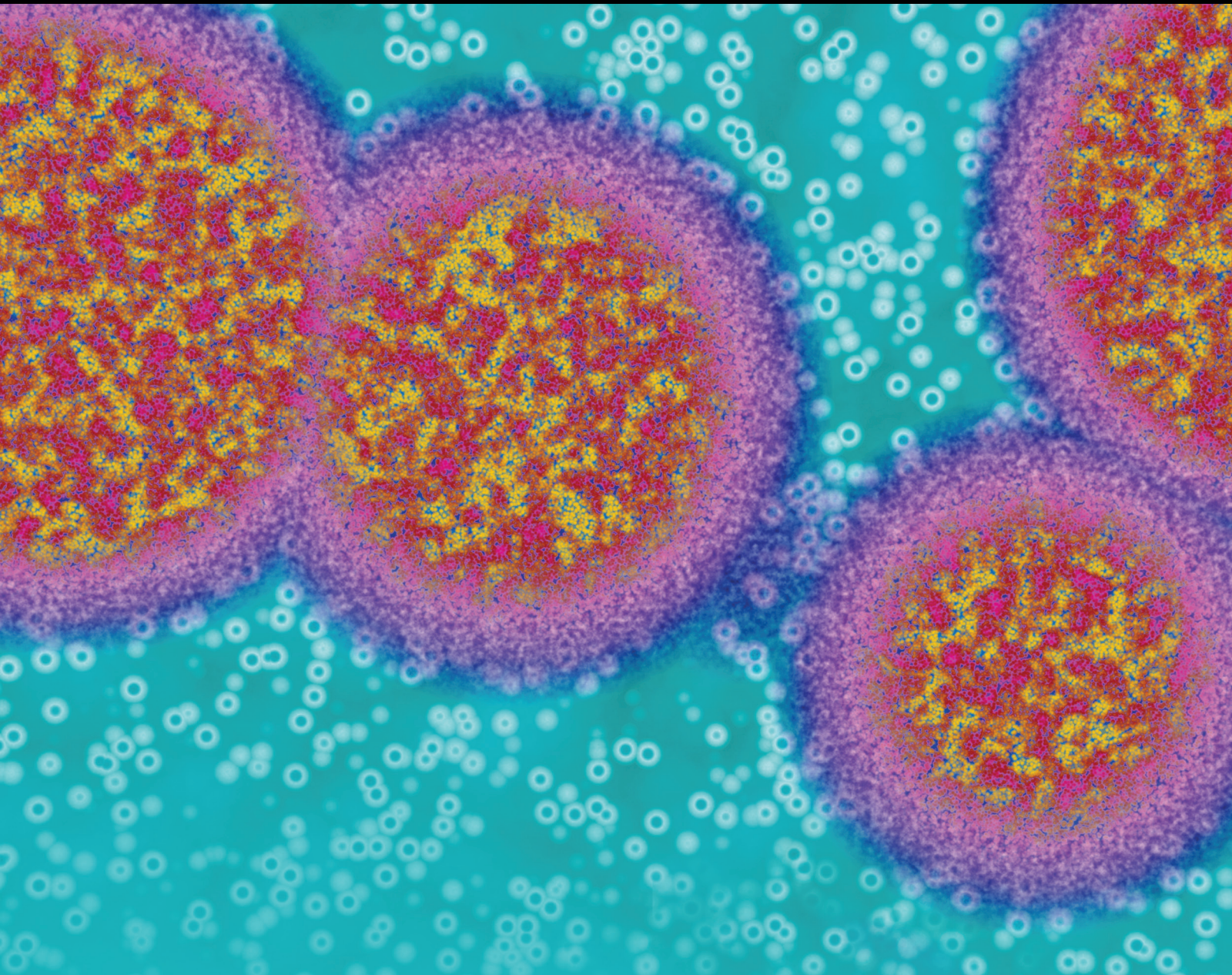


Advances in Hyaluronan Biology: Signaling, Regulation, and Disease Mechanisms

Guest Editors: Paul H. Weigel, Carol de la Motte, Melanie A. Simpson,
and Larry S. Sherman





Advances in Hyaluronan Biology: Signaling, Regulation, and Disease Mechanisms

International Journal of Cell Biology

**Advances in Hyaluronan Biology: Signaling,
Regulation, and Disease Mechanisms**

Guest Editors: Paul H. Weigel, Carol de la Motte,
Melanie A. Simp, and Larry S. Sherman



Copyright © 2015 Hindawi Publishing Corporation. All rights reserved.

This is a special issue published in "International Journal of Cell Biology." All articles are open access articles distributed under the Creative Commons Attribution License, which permits unrestricted use, distribution, and reproduction in any medium, provided the original work is properly cited.

Editorial Board

Paul N. Adler, USA
Emad Alnemri, USA
Avri Ben-Ze'ev, Israel
Jeannette Chloe Bulinski, USA
Michael Bustin, USA
Adrienne D. Cox, USA
Govindan Dayanithi, France
Arun M. Dharmarajan, Australia
William Dunn, USA
Victor Faundez, USA
Roland Foisner, Austria
Hans Hermann Gerdes, Norway
Richard Gomer, USA
Hinrich Gronemeyer, France
Mehran Haidari, USA
Thomas Hays, USA
Wiljan Hendriks, Netherlands
Paul J. Higgins, USA

Michael Hortsch, USA
Pavel Hozak, Czech Republic
Jeremy Hyams, France
Anton M. Jetten, USA
Edward M. Johnson, USA
Daniel P. Kiehart, USA
Sharad Kumar, Australia
Paul Marks, USA
Seamus J. Martin, Ireland
Manuela Martins-Green, USA
Takeshi Noda, Japan
Helga Ógmundsdóttir, Iceland
Shoichiro Ono, USA
Howard Beverley Osborne, France
Markus Paulmichl, Austria
H. Benjamin Peng, Hong Kong
Craig Pikaard, USA
Liza Pon, USA

Maria Roubelakis, Greece
Afshin Samali, Ireland
Michael Peter Sarras, USA
Hirofumi Sawai, Japan
Rony Seger, Israel
Barry D. Shur, USA
Arnoud Sonnenberg, Netherlands
Gary S. Stein, USA
Tung Tien Sun, USA
Ming Tan, USA
Guido Tarone, Italy
Jean-Pierre Tassan, France
Richard Tucker, USA
Andre Van Wijnen, USA
Gerhard Wiche, Austria
Steve Winder, UK
Timothy J. Yen, USA

Contents

Advances in Hyaluronan Biology: Signaling, Regulation, and Disease Mechanisms, Melanie A. Simpson, Carol de la Motte, Larry S. Sherman, and Paul H. Weigel
Volume 2015, Article ID 690572, 2 pages

Correlative Light and Electron Microscopy Reveals the HAS3-Induced Dorsal Plasma Membrane Ruffles, Kirsi Rilla and Arto Koistinen
Volume 2015, Article ID 769163, 8 pages

Regulatory T Cells Resist Cyclosporine-Induced Cell Death via CD44-Mediated Signaling Pathways, Shannon M. Ruppert, Ben A. Falk, S. Alice Long, and Paul L. Bollyky
Volume 2015, Article ID 614297, 10 pages

High Sensitivity Method to Estimate Distribution of Hyaluronan Molecular Sizes in Small Biological Samples Using Gas-Phase Electrophoretic Mobility Molecular Analysis, Lan Do, Christen P. Dahl, Susanne Kerje, Peter Hansell, Stellan Mörner, Ulla Lindqvist, Anna Engström-Laurent, Göran Larsson, and Urban Hellman
Volume 2015, Article ID 938013, 5 pages

Regulated Hyaluronan Synthesis by Vascular Cells, Manuela Viola, Evgenia Karousou, Maria Luisa D'Angelo, Ilaria Caon, Giancarlo De Luca, Alberto Passi, and Davide Vigetti
Volume 2015, Article ID 208303, 8 pages

Extracellular Vesicles from Caveolin-Enriched Microdomains Regulate Hyaluronan-Mediated Sustained Vascular Integrity, Tamara Mirzapoiuzova, Frances E. Lennon, Bolot Mambetsariev, Michael Allen, Jacob Riehm, Valeriy A. Poroyko, and Patrick A. Singleton
Volume 2015, Article ID 481493, 11 pages

The Rise and Fall of Hyaluronan in Respiratory Diseases, Mark E. Lauer, Raed A. Dweik, Stavros Garantziotis, and Mark A. Aronica
Volume 2015, Article ID 712507, 15 pages

Size Matters: Molecular Weight Specificity of Hyaluronan Effects in Cell Biology, Jaime M. Cyphert, Carol S. Trempus, and Stavros Garantziotis
Volume 2015, Article ID 563818, 8 pages

Hyaluronan Synthase 3 Null Mice Exhibit Decreased Intestinal Inflammation and Tissue Damage in the DSS-Induced Colitis Model, Sean P. Kessler, Dana R. Obery, and Carol de la Motte
Volume 2015, Article ID 745237, 13 pages

Carboxymethyl Hyaluronan-Stabilized Nanoparticles for Anticancer Drug Delivery, Jessica L. Woodman, Min Sung Suh, Jianxing Zhang, Yuvabharath Kondaveeti, Diane J. Burgess, Bruce A. White, Glenn D. Prestwich, and Liisa T. Kuhn
Volume 2015, Article ID 249573, 14 pages

Utilization of Glycosaminoglycans/Proteoglycans as Carriers for Targeted Therapy Delivery, Suniti Misra, Vincent C. Hascall, Ilia Atanelishvili, Ricardo Moreno Rodriguez, Roger R. Markwald, and Shibnath Ghatak
Volume 2015, Article ID 537560, 25 pages

Selective Activation of Cancer Stem Cells by Size-Specific Hyaluronan in Head and Neck Cancer,

Marisa Shiina and Lilly Y. W. Bourguignon

Volume 2015, Article ID 989070, 10 pages

Roles of Proteoglycans and Glycosaminoglycans in Wound Healing and Fibrosis, Shibnath Ghatak,

Edward V. Maytin, Judith A. Mack, Vincent C. Hascall, Ilia Atanelishvili, Ricardo Moreno Rodriguez,

Roger R. Markwald, and Suniti Misra

Volume 2015, Article ID 834893, 20 pages

Hyaluronan Synthase: The Mechanism of Initiation at the Reducing End and a Pendulum Model for Polysaccharide Translocation to the Cell Exterior, Paul H. Weigel

Volume 2015, Article ID 367579, 15 pages

Hyperglycemia-Induced Changes in Hyaluronan Contribute to Impaired Skin Wound Healing in Diabetes: Review and Perspective, Sajina Shakya, Yan Wang, Judith A. Mack, and Edward V. Maytin

Volume 2015, Article ID 701738, 11 pages

Hyaluronan Synthesis, Catabolism, and Signaling in Neurodegenerative Diseases, Larry S. Sherman,

Steven Matsumoto, Weiping Su, Taasin Srivastava, and Stephen A. Back

Volume 2015, Article ID 368584, 10 pages

Editorial

Advances in Hyaluronan Biology: Signaling, Regulation, and Disease Mechanisms

Melanie A. Simpson,¹ Carol de la Motte,² Larry S. Sherman,³ and Paul H. Weigel⁴

¹*Department of Biochemistry, University of Nebraska, Lincoln, NE 68588, USA*

²*Department of Pathobiology, Cleveland Clinic Lerner Research Institute, Cleveland, OH 44195, USA*

³*Division of Neuroscience, Oregon National Primate Research Center, Oregon Health & Science University, Beaverton, OR 97006, USA*

⁴*Department of Biochemistry & Molecular Biology, University of Oklahoma Health Sciences Center, Oklahoma City, OK 73104, USA*

Correspondence should be addressed to Paul H. Weigel; paul-weigel@ouhsc.edu

Received 3 June 2015; Accepted 4 June 2015

Copyright © 2015 Melanie A. Simpson et al. This is an open access article distributed under the Creative Commons Attribution License, which permits unrestricted use, distribution, and reproduction in any medium, provided the original work is properly cited.

Hyaluronan is an extracellular glycosaminoglycan polymer consisting of linear disaccharide units containing alternating glucuronate and N-acetylglucosamine. Many cell types make hyaluronan, which unlike most other macromolecules is assembled at the plasma membrane and concurrently translocated through the hyaluronan synthase enzyme. The normal function of large hyaluronan polymers (>1MDa) in tissue cushioning, hydration, and lubrication is well established. The aberrant accumulation and degradation of hyaluronan and the receptor-mediated signaling of smaller hyaluronan fragments have also been extensively implicated in a variety of pathological states including inflammation and cancer. More recently, the discovery that hyaluronan can either be a structural matrix component or appear as smaller processed polymers and oligomers that differentially engage a diverse range of signaling receptors has created an exciting paradigm shift and reenergized hyaluronan research in a broad range of fields. In this special issue, eight review articles focus on summarizing the latest contributions to understanding hyaluronan synthesis and catabolism and the regulation of hyaluronan functions. Seven novel primary research articles also investigate multiple roles of hyaluronan in disease progression and targeting.

The review by P. H. Weigel discusses the mechanism of hyaluronan synthesis and polymer extrusion by the hyaluronan synthase family members as well as topological features of the enzymes, their functional requirement for associated lipids within the plasma membrane, and

a proposed bioenergetic model for the concurrent translocation of hyaluronan to the extracellular space by the enzyme during synthesis. The review by M. Viola et al. addresses the regulation of hyaluronan synthesis by posttranslational modifications of HAS2 and the metabolic conditions that contribute to dysregulated synthesis in atherosclerosis. S. Shakya et al. review the recent data on cellular mechanisms such as autophagic release of hyaluronan-containing vesicles that are triggered in response to glucose overexposure and studies on the impact of altered hyaluronan synthesis in diabetic wound healing. J. M. Cyphert et al. provide an overview of hyaluronan synthesis and degradation, as well as a discussion of the widely differing signaling properties conferred by short processed oligomers versus long newly synthesized polymers of hyaluronan. L. S. Sherman et al. discuss the roles of hyaluronan in nervous system injury and propose a model by which the balance between hyaluronan synthesis and catabolism influences nervous system repair. M. E. Lauer et al. summarizes effects of environmental factors that stimulate hyaluronan production in the lung and review the functional studies that reveal a protective and regenerative role for hyaluronan polymers in lung injury repair. Finally, reviews by S. Misra et al. and S. Ghatak et al. summarize research on the interaction of hyaluronan with proteoglycans in the extracellular space and at the cell surface, in the context of wound healing and fibrosis, and discuss the potential for hyaluronan and proteoglycans to serve as therapeutic targeting agents in diverse disease states.

Novel research articles published in this special issue provide cutting edge methodology advances and insights into the mechanisms by which hyaluronan impacts cancer stem cells, facilitates cancer therapy, promotes inflammation, and controls immune function. The article by M. Shiina and L. Y. W. Bourguignon describes the characterization of microRNA expression induced by hyaluronan of different sizes in cancer stem cells and suggests that specific microRNA induction promotes cancer stem cell self-renewal upon exposure to high molecular mass hyaluronan. J. Woodman et al. provide a novel method for stabilizing cross-linked hyaluronan in nanoparticle construction and test the utility of these constructs for cytotoxic drug delivery in mouse xenografts. S. P. Kessler et al. show that HAS1/HAS3 null mice are less susceptible to chemically induced chronic inflammation than wild-type mice and do not develop colitis, indicating that hyaluronan production in the intestine, primarily by HAS3, is responsible for promoting chronic intestinal inflammation and inducing pathological changes in vasculature and leukocyte infiltration underlying colitis. The article by S. M. Ruppert et al. demonstrates a new role for hyaluronan signaling through CD44 in regulatory T cells undergoing development of resistance to cyclosporine A, independently of canonical IL-2 signaling. Research by T. Mirzapoiazova et al. examines the shedding of hyaluronan in exosomes and microvesicles, revealing that different sizes of hyaluronan are associated with these two very different vesicle types and that these vesicle types have opposite effects in disrupting or preserving vascular integrity. K. Rilla and A. Koistinen discuss the use of superresolution microscopy to visualize the induction of plasma membrane ruffling by HAS3-mediated hyaluronan synthesis. Finally, L. Do et al. describe gas-phase electrophoretic mobility molecular analysis, a novel method that permits highly sensitive size determination of hyaluronan in very small sample sizes.

Collectively, the results and perspectives in this special issue represent the latest description and summary of hyaluronan-mediated control mechanisms in normal and diseased tissues and highlight exciting research advances in a broad range of disease models that exploit novel chemistries and define paradigm-shifting concepts.

*Melanie A. Simpson
Carol de la Motte
Larry S. Sherman
Paul H. Weigel*

Research Article

Correlative Light and Electron Microscopy Reveals the HAS3-Induced Dorsal Plasma Membrane Ruffles

Kirsi Rilla and Arto Koistinen

Institute of Biomedicine and SIB Labs, University of Eastern Finland, 70211 Kuopio, Finland

Correspondence should be addressed to Kirsi Rilla; kirsi.rilla@uef.fi

Received 25 September 2014; Accepted 19 January 2015

Academic Editor: Melanie A. Simpson

Copyright © 2015 K. Rilla and A. Koistinen. This is an open access article distributed under the Creative Commons Attribution License, which permits unrestricted use, distribution, and reproduction in any medium, provided the original work is properly cited.

Hyaluronan is a linear sugar polymer synthesized by three isoforms of hyaluronan synthases (HAS1, 2, and 3) that forms a hydrated scaffold around cells and is an essential component of the extracellular matrix. The morphological changes of cells induced by active hyaluronan synthesis are well recognized but not studied in detail with high resolution before. We have previously found that overexpression of HAS3 induces growth of long plasma membrane protrusions that act as platforms for hyaluronan synthesis. The study of these thin and fragile protrusions is challenging, and they are difficult to preserve by fixation unless they are adherent to the substrate. Thus their structure and regulation are still partly unclear despite careful imaging with different microscopic methods in several cell types. In this study, correlative light and electron microscopy (CLEM) was utilized to correlate the GFP-HAS3 signal and the surface ultrastructure of cells in order to study in detail the morphological changes induced by HAS3 overexpression. Surprisingly, this method revealed that GFP-HAS3 not only localizes to ruffles but in fact induces dorsal ruffle formation. Dorsal ruffles regulate diverse cellular functions, such as motility, regulation of glucose metabolism, spreading, adhesion, and matrix degradation, the same functions driven by active hyaluronan synthesis.

1. Introduction

Hyaluronan is synthesized in the inner face of the plasma membrane by three isoforms of hyaluronan synthases (HAS1, 2, and 3), unique enzymes that simultaneously elongate, bind, and extrude the growing hyaluronan chain directly into extracellular space [1]. Active synthesis of hyaluronan enhances plasma membrane dynamics and formation of several types of actin-based plasma membrane protrusions, like filopodia [2], lamellipodia [3], and membrane ruffles [4].

Ruffles are flat plasma membrane folds that use the actin-based machinery for their dynamic reshaping [5]. Depending on source of studies, their nomenclature is variable, including dorsal ruffles, waves (because they resemble waves on a water surface), linear ruffles [6], or circular dorsal ruffles [7]. Two structurally similar but distinct types of ruffling have been reported, depending on their cellular location. Peripheral ruffling is typically associated with lamellipodia formation and migration [8], while dorsal ruffling is connected to macropinocytosis [9] and internalization of growth factor receptors [10].

Any cell types studied so far like keratinocytes [11], MCF-7 breast cancer cells, MDCK Kidney cells [12], chondrosarcoma cells, [13], fibroblasts, and mesothelial and melanoma cells [14, 15] are induced to grow special plasma membrane protrusions when overexpressing HAS2 or especially HAS3. Moreover, cell types with endogenously high hyaluronan secretion like fibroblasts [16, 17], smooth muscle cells, chondrosarcoma cells [13], neuroblastoma cells [18], and fibroblasts from Shar Pei dogs with high HAS2 expression [19] have high number of plasma membrane protrusions.

The studies of HAS-induced protrusions have been challenging because they are thin and fragile and difficult to preserve by fixation and other processing steps for light and electron microscopy [11–13]. Particularly protrusions arising from apical regions of the plasma membrane that are not adherent to the substratum are easily shrunk and collapsed. Thus their formation and maintenance of structure are still enigmatic and their functions are partly uncharacterized.

The aim of this work was to develop a simple, cost-effective method to correlate fluorescent signal from confocal laser scanning microscopy (CLSM) to fine morphology of the

cells studied with scanning electron microscope (SEM). With this method, we confirmed the GFP-HAS3 localization into the plasma membrane and its protrusions, their bulbous tip complexes, as well as in plasma membrane ruffles. Surprisingly, it was found that in fact ruffle-like plasma membrane folds act as basis of HAS-induced protrusions, which has not been reported previously. Additionally, it was shown in detail for a first time that GFP-HAS3 not only localizes to dorsal ruffles but also induces dorsal ruffle formation. The results obtained in this work will bring us closer to the detailed characterization of hyaluronan-dependent plasma membrane protrusions, their regulation and functions. These structures are putative factors behind hyaluronan-driven effects in diseases like cancer, inflammation, and disorders of glucose metabolism.

2. Methods

2.1. Cell Culture. The human breast adenocarcinoma cell line, MCF-7, was cultured in minimum essential medium alpha (MEM α , EuroClone, Pavia, Italy) supplemented with 5% fetal bovine serum (FBS, HyClone, Thermo Scientific, Epsom, UK), 2 mM glutamine (EuroClone), 50 μ g/mL streptomycin sulfate, and 50 U/mL penicillin (EuroClone). Cells were passaged twice a week at a 1:5 split ratio using 0.05% trypsin (w/v) 0.02% EDTA (w/v) (Biochrom AG, Berlin, Germany).

2.2. Transfections. MCF-7 cells were grown on gridded glass bottom culture dishes (MatTek Corporation, Ashland, MA) before transient transfection with human HAS3 cDNA in-frame with an N-terminal GFP fusion protein [20]. The generation of stable doxycycline-inducible EGFP-HAS3 overexpressing MCF-7 cells was performed as described before [21]. For induction of GFP-HAS3 expression, 0.5 ng/mL of doxycycline (Sigma, St. Louis, MO, USA) was used.

2.3. Imaging, Image Processing, and Analysis. Next day, after transient transfection or induction of stable cells with doxycycline, the fluorescent images were obtained with Zeiss Axio Observer inverted microscope (10 \times NA 1.3 or 63 \times NA 1.4 oil objective) equipped with Zeiss LSM 700 confocal module (Carl Zeiss Microimaging GmbH, Jena, Germany) and an external DIC-capable transmitted-light channel. The cells were fixed with 2% glutaraldehyde either before or immediately after confocal imaging. To control the effect of hyaluronidase digestion on cell morphology, some samples were treated with *streptomyces* hyaluronidase (Seikagaku Kogyo Co., 5 TRU/mL, 30 min at 37°C) prior to fixation. Thereafter, the cells were routinely dehydrated in ascending series of ethanol and hexamethyldisilazane and finally coated with thin layer of gold. After processing, cells were imaged with Zeiss Sigma HD|VP (Zeiss, Oberkochen, Germany) scanning electron microscope at 3 kV. Image processing, like 3-dimensional rendering, analysis of images, and further modification, was performed using ZEN 2012 software (Carl Zeiss Microimaging GmbH), ImageJ 1.32 software (<http://rsb.info.nih.gov/ij/>), and Adobe Photoshop 8.0.

SEM images (8-bit gray-level with pixel resolution of 1024 \times 728) were utilized to quantify the plasma membrane ruffling. From both groups, 20 cells were selected for analysis. Image analysis was carried out using ImageJ. A representative area from apical plasma membrane of the cells was outlined and thresholding was utilized to define ruffles from the background. After thresholding, the images were segmented so that the ruffles were separated with an automatic algorithm. Then the number and areas of discrete ruffles in each cell were calculated. The density of ruffles was presented as the number of ruffles over a cell area of 100 μ m². It should be noticed that the SEM images were recorded using In-Lens detector which is a concentric detector inside the SEM column. The use of the In-Lens detector prevented shadowing effect which is typical to conventional secondary electron imaging.

2.4. Statistical Analysis. Statistical comparison was carried out using IBM SPSS Statistics software (ver. 19; SPSS Inc., Chicago, USA). Mann-Whitney *U* test was used to evaluate the difference in ruffling between the noninduced and induced cells. *P* values less than 0.05 were considered statistically significant.

3. Results

3.1. A simple Correlative Light and Electron Microscopy Method. This study presents a simple and easy process to image live or fixed cells by high resolution CLSM and SEM. The area imaged by CLSM was easily relocalized in SEM by utilizing gridded coverslips (Figure 1). A simultaneous DIC imaging made recognition of the same cells easy via CLSM (Figure 1(a)) and SEM (Figure 1(b)). Some shrinking during fixation and dehydration was detected, but the overall morphology of the cells was well preserved after fixation and processing for SEM. The GFP-HAS3 overexpressing cells were easily detached during processing (arrows in Figure 1), which indicates a decreased adhesion as a result of HAS overexpression, a finding in line with previous results [22].

3.2. Higher Resolution Reveals Tip Expansions of Protrusions and Dorsal Ruffling. More detailed visualization of GFP-HAS3-positive MCF-7 cells was performed with higher magnification. A typical example of single GFP-HAS3-positive MCF-7 cell is shown in Figure 2. The morphology was relatively unchanged after sample processing for SEM (Figure 2) and GFP-HAS3-induced protrusions were preserved. As shown before, many of the HAS-induced protrusions have a dilated tip complex [14, 15], but it has been unclear if this dilation is an artefact resulting from high level of GFP-HAS3 fluorescence and light scattering. SEM confirmed that many of the HAS3-induced protrusions have a dilated tip complex (arrows in Figures 2(d) and 2(e)) and dilated areas are occasionally found also in the body of the protrusions (arrows in Figures 2(g) and 2(h)). The protrusions with dilated tips were similarly formed upon overexpression of HAS3 without GFP-tag (data not shown). Thickness of protrusions expressing high levels of GFP-HAS3 signal is overamplified in confocal microscopy because of light scattering. Protrusions

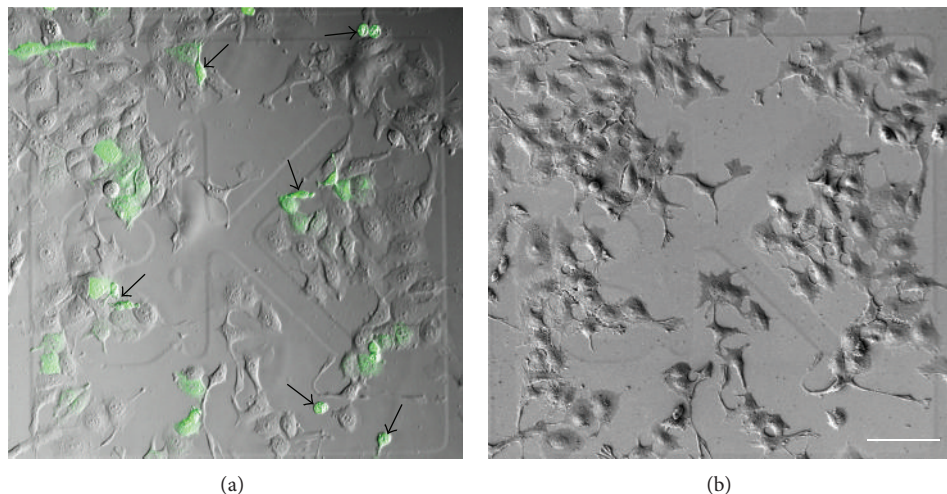


FIGURE 1: Utilization of gridded coverslips for localization of cultured cells for correlative imaging. Low magnification images showing an overview of transiently transfected cells imaged by CLSM and DIC (a) and the corresponding area imaged by SEM (b). Arrows in (a) indicate cells that were detached in the subsequent preparation steps for scanning electron microscopy. Scale bar 100 μm .

also shrink and collapse during fixation and drying for SEM, which increases the differences in thickness observed between CLSM and SEM. As obtained by SEM, the HAS3-induced protrusions are extremely thin, typically between 70 and 130 nm in diameter.

A typical morphology of cells with GFP-HAS3 overexpression was spindle-shaped, with no clear, single lamellipodia or distinguishable “front and rear” (arrows in Figure 3). Another typical feature of GFP-HAS3-positive cells was ruffling of the plasma membrane, appearing mainly on the apical faces of the plasma membrane. Comparison of negative cells (asterisks in Figures 3(a) and 3(b)) and GFP-HAS3-positive cells (arrows in Figures 3(a) and 3(b)) in transiently transfected cultures suggested that overexpression of HAS3 induces dorsal ruffling of the plasma membrane. To control if the ruffles are sensitive to hyaluronidase treatment, samples were treated with *streptomyces* hyaluronidase (5 TRU/mL, 30 min at 37°C) prior to fixation. The results showed that removal of hyaluronan did not completely destroy them (Figures 3(d) and 3(e)). This indicates that their structure is not completely dependent on pericellular hyaluronan.

3.3. Quantification of GFP-HAS3-Induced Plasma Membrane Ruffling. To confirm the findings obtained with transiently transfected cells, the dorsal plasma membrane ruffling was quantified utilizing the stable, inducible MCF-7 cell line expressing GFP-HAS3 [22]. The quantification of these complex structures of variable shape and size would be more time consuming by light microscopy, requiring relatively high magnification and stacks of confocal images. Thus SEM images were utilized for these measurements. The results showed that GFP-HAS3 expression significantly induced both the area and the amount of dorsal plasma membrane ruffling as compared to noninduced cells (Figure 3(c)).

3.4. Ultrastructure of Ruffles. Next high resolution SEM images were utilized to analyze the detailed structure of the

HAS3-induced ruffles. Most of the ruffles appeared on the dorsal surface of the cell (Figures 2(b), 3, and 4) rather than on peripheral areas. GFP-HAS3 signal was detected on the apical plasma membrane of cells and accumulated on the ruffles. Furthermore, SEM revealed that many of the HAS-positive protrusions were embedded in the ruffle, suggesting that ruffles provide a basis for thinner protrusions. There was typically 1–5 or even higher number of protrusions arising from a single ruffle (arrows in Figure 4(b)). This indicates specific modeling of plasma membrane dynamics and the underlying actin network by HAS activity. Most of the ruffles were linear or curved, sheet-like protrusions of variable size, but some circular structures were also found (arrows in Figures 4(a), 4(b), 4(d), and 4(e)), which in line with the suggested dynamic formation of ruffles followed by constriction into circular structures before disappearing [5].

4. Discussion

4.1. CLEM as a Novel Method to Study HAS-Induced Changes in Cell Morphology. In cell biology, multiple imaging methods are usually required to solve a specific scientific problem. However, each imaging technique has its own limitations and separately does not fully answer the specific questions. Since the discovery of HAS3-induced plasma membrane extensions [11, 12, 23], hyaluronan-dependent plasma membrane modifications have been a specific cell biological question waiting for clarification. To solve this question, a straightforward CLEM protocol was developed to combine fluorescent and electron microscopic information of a single cell by using CLSM and SEM. The gridded coverslips were effective in relocating cells quickly and reliably over large areas but also allowed to study the detailed morphology of the plasma membrane. This correlative method is an inexpensive and simple way to image live or fixed cells with confocal microscopy prior to viewing them at the electron microscope

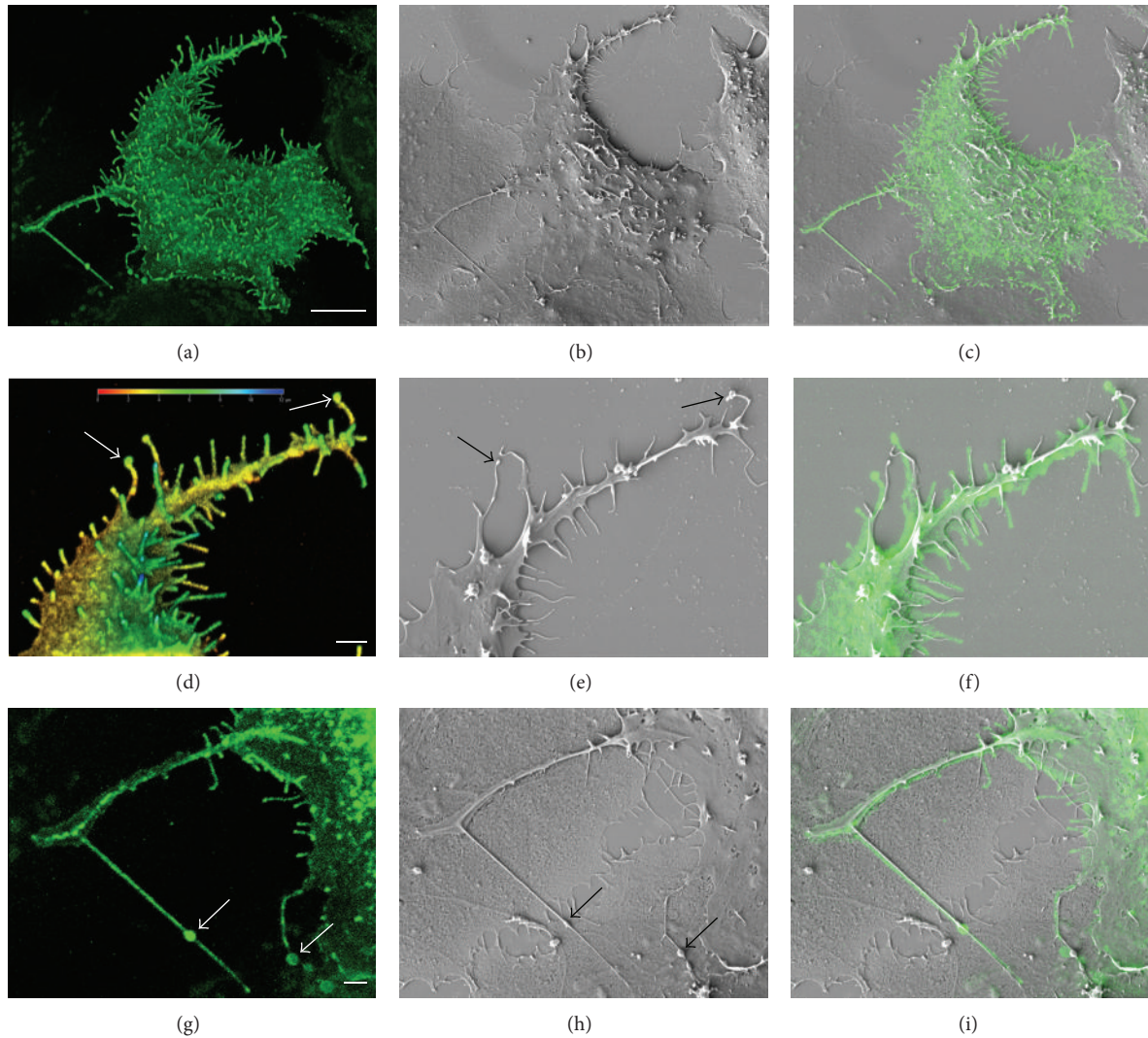


FIGURE 2: GFP-HAS3-induced plasma membrane protrusions imaged by CLEM. A GFP-HAS3 expressing MCF-7 cell imaged by 3D confocal microscopy in (a), (d), and (g) and by SEM in (b), (e), and (h). Merged images are presented in (c), (f), and (i). High magnification images from selected areas of the same cell presented in (a)–(c) are shown in (d)–(i). Arrows in (d), (e), (g), and (h) indicate the GFP-HAS3-positive bulbous expansions in both the body and tips of protrusions. Color depth coding was used to demonstrate the variable length of protrusions in (d). Scale bars 10 μm in (a), 2 μm in (d) and (g).

level. The method can be performed without specific equipment and can be reliably utilized to answer many questions related to detailed localization of proteins and morphology of cultured cells.

4.2. Tip Complexes of Protrusions. We have shown before that many of the HAS-induced protrusions have a dilated tip complex [14, 15], but it has been unclear so far if this dilation is an artefact resulting from accumulation of GFP-HAS3 signal and light scattering. In this work, the existence of GFP-HAS3-positive bulbous expansions was confirmed in both the body and tips of the protrusions. Tip complexes act as putative sites of origin for shedding of hyaluronan-coated extracellular vesicles, which are potential carriers of hyaluronan and other active molecules [14, 15]. Additionally, tip complexes of protrusions are putative enrichment sites for specific proteins

and act as functional areas for glucose uptake [24], which may be crucial for increased needs of glucose for hyaluronan synthesis. Furthermore, growth of protrusions [14, 15] and vesicle shedding [14, 15] are dependent on glucose supply, which makes the future studies of these tip complexes and their role in hyaluronan metabolism especially interesting.

4.3. Hyaluronan and Plasma Membrane Ruffling. Localization of hyaluronan and its receptors into ruffles has been reported in many different cell types, like fibroblasts [25], EGF-induced rat keratinocytes [26], CHO cells [4], and HaCaT cells [20]. Recently, also HAS3 localization into ruffles has been reported [20], but nobody has shown before that activity of hyaluronan synthesis itself induces ruffling of the plasma membrane. In this study, a clear increase was seen in the area and amount of ruffling after induction of HAS3

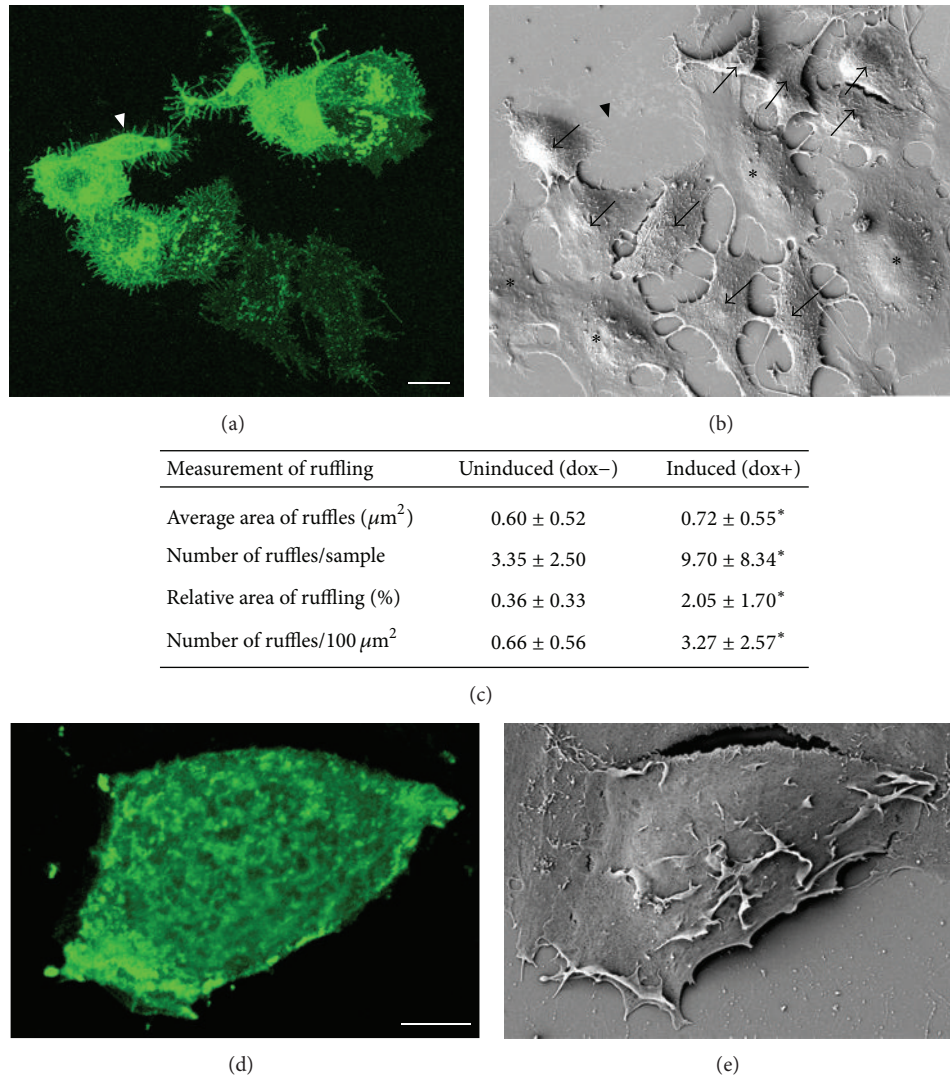


FIGURE 3: GFP-HAS3 expression induces plasma membrane ruffling. Confocal 3D projection of transiently transfected MCF-7 cells imaged by CLSM (a) and the corresponding area by SEM (b). Arrows in (b) indicate GFP-HAS3-positive cells with plasma membrane ruffling, while negative cells (asterisks) have smoother dorsal surface. Arrowheads in (a) and (b) indicate a cell that was lost during SEM processing. Stable, inducible transfections were utilized to quantify the dorsal ruffling of MCF-7 cells, which was significantly increased upon induction of GFP-HAS3. Significant difference ($P < 0.05$) in quantified parameters of ruffling is indicated by an asterisk (*) in table (c). $N = 20$ in both groups. A GFP-HAS3-positive cell treated with hyaluronidase before fixation is shown with CLSM and SEM in (d) and (e), respectively. Scale bars $10 \mu\text{m}$ in (a) and $5 \mu\text{m}$ in (d).

expression. Interestingly, growth factors that induce HAS expression and hyaluronan secretion, like EGF [26] and PDGF [27], induce dorsal membrane ruffling [10, 28]. As shown in this work, plasma membrane ruffling together with thin protrusions is a putative mechanism for HAS to increase the plasma membrane area in order to enhance its own activity. Moreover, small GTPase rac, which is one of the targets of hyaluronan-CD44 signaling [29], is required for membrane ruffling [30]. Furthermore, one of the cofactors of hyaluronan, MMP2 [31], localizes to the tips of ruffles [32], suggesting their role in promoting the degradation of ECM and invasive potential of cells in collaboration with hyaluronan interactions. All of these observations support the

hypothesis that hyaluronan synthesis and plasma membrane ruffling are linked together.

4.4. Putative Mechanisms for Hyaluronan-Associated Plasma Membrane Ruffling. As shown here and before, active hyaluronan synthesis regulates both finger-like protrusions, like filopodia and microvilli, and sheet-like protrusive structures such as lamellipodia and ruffles. As well as finger-like protrusions, ruffles are structures usually erecting vertically from the dorsal cell surface. Pericellular, hydrated hyaluronan coat may provide a pulling force and mechanical support for growth and maintenance of these nonadherent structures. Interestingly, disturbance of the ECM-integrin interactions

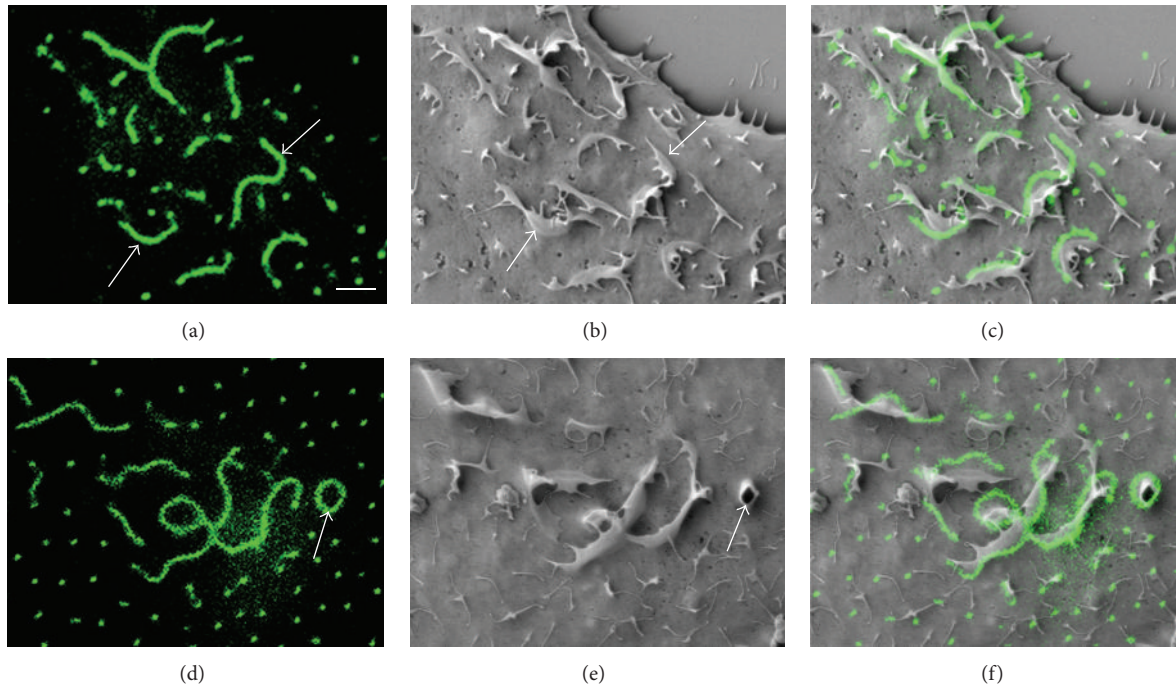


FIGURE 4: Ultrastructure of GFP-HAS3-positive dorsal ruffles. 2D confocal images showing the dorsal GFP-HAS3 signal are shown in (a) and (d) and corresponding SEM images in (b) and (e). Merged images are shown in (c) and (f), respectively. Many of the dorsal ruffles were linear or curved in shape (a) and provided a basis for several thinner protrusions (arrows in (b)). Occasionally, circular ruffles were detected (arrows in (d)-(e)). Scale bar $2 \mu\text{m}$.

induces plasma membrane ruffling [8]. These interactions may be impaired in our model, where excess ventral hyaluronan due to HAS overexpression results in weaker cell attachment to the substratum. Furthermore, dorsal ruffles are suggested to arise as a consequence of inefficient lamellipodia adhesion and impaired migration rate [8], and assembly of ruffles inhibits actin flow to lamellipodia [7]. These findings may explain why highly increased levels of HAS overexpression lead to decreased lamellipodia formation and impaired migration rate [33].

4.5. Hyaluronan-Dependent Protrusions as Potential Sites for Glucose Uptake. Insulin or high glucose induces plasma membrane ruffling with simultaneous recruitment of glucose transporters (GLUT) into the plasma membrane ruffles of muscle cells [34]. Furthermore, GLUT translocation and insulin-stimulated glucose uptake are dependent on cortical actin remodeling and membrane ruffling [35]. These results indicate that hyaluronan, plasma membrane dynamics, and glucose metabolism are linked to each other and suggest that ruffles act as potential sites for cellular glucose uptake. This hypothesis fits well with previous reports on positive correlation between cellular glucose levels and activity of hyaluronan synthesis [14, 15, 36, 37] and suggests that HAS directly or indirectly recruits glucose transporters into the plasma membrane ruffles and protrusion tip complexes to enhance its own activity.

4.6. Future Prospects. We have shown previously that active hyaluronan production induces formation of plasma

membrane extensions [11, 12] and blebbing of extracellular vesicles [14, 15]. The induction of plasma membrane ruffles, the main finding of this work, strengthens the role of active hyaluronan synthesis as a regulator of plasma membrane dynamics, regulating cell behavior in health and disease. Future studies will settle in more detail the dynamics and regulation of HAS-induced ruffles and their relationship with hyaluronan secretion and other cell functions, like secretion of extracellular vesicles and regulation of glucose uptake.

Abbreviations

CLSM: Confocal laser scanning microscopy
 DIC: Differential interference contrast
 ECM: Extracellular matrix
 EGF: Epidermal growth factor
 GFP: Green fluorescent protein
 GLUT: Glucose transporter
 HAS: Hyaluronan synthase
 MMP: Matrix metalloproteinase
 PDGF: Platelet-derived growth factor
 SEM: Scanning electron microscopy.

Conflict of Interests

The authors declare that there is no conflict of interests regarding the publication of this paper.

Acknowledgments

The authors gratefully acknowledge funding from the Regional Council of Northern Savo (HR-SEM Project A32202), the Academy of Finland, Spearhead Funds from the University of Eastern Finland (Cancer Center of Eastern Finland), and Sigrid Juselius foundation. The authors would like to thank Virpi Miettinen and Riikka Kärnä for expert technical assistance.

References

- [1] P. H. Weigel, V. C. Hascall, and M. Tammi, "Hyaluronan syntheses," *The Journal of Biological Chemistry*, vol. 272, no. 22, pp. 13997–14000, 1997.
- [2] D. H. Bernanke and R. R. Markwald, "Effects of hyaluronic acid on cardiac cushion tissue cells in collagen matrix cultures," *Texas Reports on Biology and Medicine*, vol. 39, pp. 271–285, 1979.
- [3] J. Bakkers, C. Kramer, J. Pothof, N. E. M. Quaevdrieg, H. P. Spaink, and M. Hammerschmidt, "Has2 is required upstream of Rac1 to govern dorsal migration of lateral cells during zebrafish gastrulation," *Development*, vol. 131, no. 3, pp. 525–537, 2004.
- [4] P. Bono, E. Cordero, K. Johnson et al., "Layilin, a cell surface hyaluronan receptor, interacts with merlin and radixin," *Experimental Cell Research*, vol. 308, no. 1, pp. 177–187, 2005.
- [5] E. S. Chhabra and H. N. Higgs, "The many faces of actin: matching assembly factors with cellular structures," *Nature Cell Biology*, vol. 9, no. 10, pp. 1110–1121, 2007.
- [6] R. Buccione, J. D. Orth, and M. A. McNiven, "Foot and mouth: podosomes, invadopodia and circular dorsal ruffles," *Nature Reviews Molecular Cell Biology*, vol. 5, no. 8, pp. 647–657, 2004.
- [7] J. L. Hoon, W. K. Wong, and C. G. Koh, "Functions and regulation of circular dorsal ruffles," *Molecular and Cellular Biology*, vol. 32, no. 21, pp. 4246–4257, 2012.
- [8] B. Borm, R. P. Requardt, V. Herzog, and G. Kirfel, "Membrane ruffles in cell migration: indicators of inefficient lamellipodia adhesion and compartments of actin filament reorganization," *Experimental Cell Research*, vol. 302, no. 1, pp. 83–95, 2005.
- [9] R. Warn, D. Brown, P. Dowrick, A. Prescott, and A. Warn, "Cytoskeletal changes associated with cell motility," *Symposia of the Society for Experimental Biology*, vol. 47, pp. 325–338, 1993.
- [10] J. D. Orth, E. W. Krueger, S. G. Weller, and M. A. McNiven, "A novel endocytic mechanism of epidermal growth factor receptor sequestration and internalization," *Cancer Research*, vol. 66, no. 7, pp. 3603–3610, 2006.
- [11] K. Rilla, H. Siiskonen, A. P. Spicer, J. M. T. Hyttinen, M. I. Tammi, and R. H. Tammi, "Plasma membrane residence of hyaluronan synthase is coupled to its enzymatic activity," *The Journal of Biological Chemistry*, vol. 280, no. 36, pp. 31890–31897, 2005.
- [12] A. Kultti, K. Rilla, R. Tiihonen, A. P. Spicer, R. H. Tammi, and M. I. Tammi, "Hyaluronan synthesis induces microvillus-like cell surface protrusions," *The Journal of Biological Chemistry*, vol. 281, no. 23, pp. 15821–15828, 2006.
- [13] K. Rilla, R. Tiihonen, A. Kultti, M. Tammi, and R. Tammi, "Pericellular hyaluronan coat visualized in live cells with a fluorescent probe is scaffolded by plasma membrane protrusions," *Journal of Histochemistry and Cytochemistry*, vol. 56, no. 10, pp. 901–910, 2008.
- [14] K. Rilla, S. Oikari, T. A. Jokela et al., "Hyaluronan synthase 1 (HAS1) requires higher cellular UDP-GlcNAc concentration than HAS2 and HAS3," *The Journal of Biological Chemistry*, vol. 288, no. 8, pp. 5973–5983, 2013.
- [15] K. Rilla, S. Pasonen-Seppänen, A. J. Deen et al., "Hyaluronan production enhances shedding of plasma membrane-derived microvesicles," *Experimental Cell Research*, vol. 319, no. 13, pp. 2006–2018, 2013.
- [16] S. P. Evanko, S. Potter-Perigo, P. Y. Johnson, and T. N. Wight, "Organization of hyaluronan and versican in the extracellular matrix of human fibroblasts treated with the viral mimetic poly I:C," *Journal of Histochemistry and Cytochemistry*, vol. 57, no. 11, pp. 1041–1060, 2009.
- [17] S. Meran, J. Martin, D. D. Luo, R. Steadman, and A. Phillips, "Interleukin-1beta induces hyaluronan and CD44-dependent cell protrusions that facilitate fibroblast-monocyte binding," *The American Journal of Pathology*, vol. 182, no. 6, pp. 2223–2240, 2013.
- [18] A. Pusch, A. Boeckenhoff, T. Glaser et al., "CD44 and hyaluronan promote invasive growth of B35 neuroblastoma cells into the brain," *Biochimica et Biophysica Acta*, vol. 1803, no. 2, pp. 261–274, 2010.
- [19] M. J. Docampo, G. Zanna, D. Fondevila et al., "Increased HAS2-driven hyaluronic acid synthesis in shar-pei dogs with hereditary cutaneous hyaluronosis (mucinosis)," *Veterinary dermatology*, vol. 22, no. 6, pp. 535–545, 2011.
- [20] K. Törrönen, K. Nikunen, R. Kärnä, M. Tammi, R. Tammi, and K. Rilla, "Tissue distribution and subcellular localization of hyaluronan synthase isoenzymes," *Histochemistry and Cell Biology*, vol. 141, no. 1, pp. 17–31, 2014.
- [21] H. Siiskonen, K. Rilla, R. Kärnä et al., "Hyaluronan in cytosol—microinjection-based probing of its existence and suggested functions," *Glycobiology*, vol. 23, no. 2, pp. 222–231, 2013.
- [22] A. J. Deen, K. Rilla, S. Oikari et al., "Rab10-mediated endocytosis of the hyaluronan synthase HAS3 regulates hyaluronan synthesis and cell adhesion to collagen," *The Journal of Biological Chemistry*, vol. 289, no. 12, pp. 8375–8389, 2014.
- [23] A. P. Spicer and J. A. McDonald, "Characterization and molecular evolution of a vertebrate hyaluronan synthase gene family," *Journal of Biological Chemistry*, vol. 273, no. 4, pp. 1923–1932, 1998.
- [24] K. Lange, "Role of microvillar cell surfaces in the regulation of glucose uptake and organization of energy metabolism," *American Journal of Physiology: Cell Physiology*, vol. 282, no. 1, pp. C1–C26, 2002.
- [25] E. A. Turley and J. Torrance, "Localization of hyaluronate and hyaluronate-binding protein on motile and non-motile fibroblasts," *Experimental Cell Research*, vol. 161, no. 1, pp. 17–28, 1985.
- [26] J.-P. Pienimäki, K. Rilla, C. Fülöp et al., "Epidermal growth factor activates hyaluronan synthase 2 in epidermal keratinocytes and increases pericellular and intracellular hyaluronan," *The Journal of Biological Chemistry*, vol. 276, no. 23, pp. 20428–20435, 2001.
- [27] P. Heldin, T. C. Laurent, and C.-H. Heldin, "Effect of growth factors on hyaluronan synthesis in cultured human fibroblasts," *Biochemical Journal*, vol. 258, no. 3, pp. 919–922, 1989.
- [28] K. Mellstrom, C.-H. Heldin, and B. Westermark, "Induction of circular membrane-ruffling on human fibroblasts by platelet-derived growth factor," *Experimental Cell Research*, vol. 177, no. 2, pp. 347–359, 1988.
- [29] L. Y. W. Bourguignon, M. Shiina, and J. J. Li, "Hyaluronan-CD44 interaction promotes oncogenic signaling, microRNA

- functions, chemoresistance, and radiation resistance in cancer stem cells leading to tumor progression,” in *Hyaluronan Signaling and Turnover*, vol. 123 of *Advances in Cancer Research*, pp. 255–275, Elsevier, 2014.
- [30] A. J. Ridley, H. F. Paterson, C. L. Johnston, D. Diekmann, and A. Hall, “The small GTP-binding protein rac regulates growth factor-induced membrane ruffling,” *Cell*, vol. 70, no. 3, pp. 401–410, 1992.
- [31] D. Vigetti, M. Rizzi, M. Viola et al., “The effects of 4-methylumbelliferone on hyaluronan synthesis, MMP2 activity, proliferation, and motility of human aortic smooth muscle cells,” *Glycobiology*, vol. 19, no. 5, pp. 537–546, 2009.
- [32] S. Suetsugu, D. Yamazaki, S. Kurisu, and T. Takenawa, “Differential roles of WAVE1 and WAVE2 in dorsal and peripheral ruffle formation for fibroblast cell migration,” *Developmental Cell*, vol. 5, no. 4, pp. 595–609, 2003.
- [33] J. Brinck and P. Heldin, “Expression of recombinant hyaluronan synthase (HAS) isoforms in CHO cells reduces cell migration and cell surface CD44,” *Experimental Cell Research*, vol. 252, no. 2, pp. 342–351, 1999.
- [34] P. Tong, Z. A. Khayat, C. Huang, N. Patel, A. Ueyama, and A. Klip, “Insulin-induced cortical actin remodeling promotes GLUT4 insertion at muscle cell membrane ruffles,” *The Journal of Clinical Investigation*, vol. 108, no. 3, pp. 371–381, 2001.
- [35] M. Kanzaki and J. E. Pessin, “Insulin-stimulated GLUT4 translocation in adipocytes is dependent upon cortical actin remodeling,” *Journal of Biological Chemistry*, vol. 276, no. 45, pp. 42436–42444, 2001.
- [36] A. Sainio, T. Jokela, M. I. Tammi, and H. Järveläinen, “Hyperglycemic conditions modulate connective tissue reorganization by human vascular smooth muscle cells through stimulation of hyaluronan synthesis,” *Glycobiology*, vol. 20, no. 9, pp. 1117–1126, 2010.
- [37] A. Wang and V. C. Hascall, “Hyaluronan structures synthesized by rat mesangial cells in response to hyperglycemia induce monocyte adhesion,” *The Journal of Biological Chemistry*, vol. 279, no. 11, pp. 10279–10285, 2004.

Research Article

Regulatory T Cells Resist Cyclosporine-Induced Cell Death via CD44-Mediated Signaling Pathways

Shannon M. Ruppert,¹ Ben A. Falk,¹ S. Alice Long,² and Paul L. Bollyky¹

¹Division of Infectious Diseases and Geographic Medicine, Department of Medicine, 300 Pasteur Drive, Stanford University School of Medicine, Stanford, CA 94305-5107, USA

²Benaroya Research Institute, 1201 Ninth Avenue, Seattle, WA 98101, USA

Correspondence should be addressed to Paul L. Bollyky; pbollyky@stanford.edu

Received 27 September 2014; Revised 19 January 2015; Accepted 19 January 2015

Academic Editor: Rony Seger

Copyright © 2015 Shannon M. Ruppert et al. This is an open access article distributed under the Creative Commons Attribution License, which permits unrestricted use, distribution, and reproduction in any medium, provided the original work is properly cited.

Cyclosporine A (CSA) is an immunosuppressive agent that specifically targets T cells and also increases the percentage of pro-tolerogenic CD4⁺Foxp3⁺ regulatory T cells (Treg) through unknown mechanisms. We previously reported that CD44, a receptor for the extracellular matrix glycosaminoglycan hyaluronan (HA), promotes Treg stability in IL-2-low environments. Here, we asked whether CD44 signaling also promotes Treg resistance to CSA. We found that CD44 cross-linking promoted Foxp3 expression and Treg viability in the setting of CSA treatment. This effect was IL-2 independent but could be suppressed using sc-355979, an inhibitor of Stat5-phosphorylation. Moreover, we found that inhibition of HA synthesis impairs Treg homeostasis but that this effect could be overcome with exogenous IL-2 or CD44-cross-linking. Together, these data support a model whereby CD44 cross-linking by HA promotes IL-2-independent Foxp3 expression and Treg survival in the face of CSA.

1. Introduction

In healthy individuals, immunologic tolerance is maintained by populations of regulatory cells, including Foxp3⁺ regulatory T cells (Treg). Treg are a subset of T cells that suppress autoreactive effector T cells (Teff). The absence or depletion of Treg leads to multisystemic autoimmunity in mice and humans [1]. In addition, adoptive transfer of Treg can rescue the healthy phenotype [2, 3].

Treg rely on Interleukin 2 (IL-2) for their suppressive function [4]. IL-2 promotes Foxp3 expression and Treg suppressor functions via signal transducer and activator of transcription 5 (Stat5) signaling [5–10]. However, Foxp3 suppresses autocrine IL-2 production [6], such that Treg rely on other cell types, particularly activated Teff cells, as a source of IL-2. Along with effects on Treg, IL-2 activates Teff lymphocytes as well and promotes their proliferation.

In addition to IL-2, other factors are also known to support Treg maintenance *in vivo* and Treg are present in IL-2^{-/-} as well as CD25^{-/-} mice, though both strains do develop autoimmunity [11]. Furthermore, ambient IL-2 levels in circulation and in peripheral tissues [12–14] are often a

fraction of what Treg require in culture. Finally, while Treg in culture are anergic, *in vivo* their proliferation rate is high [15, 16]. Together, these data suggest that additional factors exist that support Treg maintenance *in vivo*.

Cyclosporine A (CSA) is an immunosuppressive agent that inhibits T cell proliferation by suppressing IL-2 synthesis [17]. CSA inhibits calcineurin-dependent IL-2 production by forming a complex with cyclophilin that inhibits calcineurin phosphatase induced upon T cell activation [18]. In turn, the transcription factor nuclear factor of activated T cells (NFAT) remains in a phosphorylated state and, subsequently, cannot upregulate IL-2 gene expression [19].

The effectiveness of CSA treatment may reflect, in part, changes in the ratio of Treg to Teff cells [20]. Previous clinical and *in vivo* studies have found that treatment with CSA can promote Foxp3 expression in Treg [21, 22]. *In vivo* human data likewise suggests that CSA treatment results in higher levels of circulating Treg than in healthy donors [23]. These data suggest that Treg may have a survival advantage in certain contexts over Teff cells in the face of CSA. However, the mechanisms that underlie the relative sparing of Treg in the setting of CSA treatment are unclear.

One tissue factor known to promote Treg homeostasis in low-IL-2 environments is hyaluronan (HA), an extracellular matrix (ECM) glycosaminoglycan. We and others have demonstrated that high molecular weight HA (HMW-HA) ($>1 \times 10^6$ kDa), characteristic of healing, and uninjured tissues [24] promote the function and persistence of Treg [25–27]. These effects are dependent on HA polymer length and cross-linking of the primary HA receptor, CD44 [28], the expression of which is elevated on Treg [25]. In light of these data, we have proposed that HMW-HA cross-links CD44 and thereby provides Treg with homeostatic signals in injured and healing tissues [26].

We previously reported that CD44 cross-linking allows Treg to resist CSA-mediated cell death [28]. However, the underlying mechanisms remained unclear, as both Foxp3 and CSA are well known to efficiently suppress IL-2 production [6, 18].

Here, we have evaluated the hypothesis that CD44 cross-linking bypasses CSA treatment by recapitulating aspects of IL-2R signaling in the absence of IL-2. We found that CD44 cross-linking promotes Foxp3 expression in an IL-2-independent but Stat5-dependent manner. Moreover, we report that inhibition of HA synthesis impairs Treg homeostasis but that this effect could be overcome with exogenous IL-2 or CD44-cross-linking. Together, these data support a model whereby CD44 cross-linking by HA promotes IL-2-independent and Stat5-dependent Foxp3 expression and Treg survival in the face of CSA.

2. Materials and Methods

2.1. Mice. Foxp3-GFP C57BL/6 mice were the kind gift of Dr. Alexander Rudensky. CD25 deficient C57BL/6 (CD25^{-/-}) mice were purchased from The Jackson Laboratory (Bar Harbor, ME). Foxp3-GFP mice were crossed with CD25^{-/-} mice to generate Foxp3-GFP.CD25^{-/-} mice at our institution. All mice were maintained in specific pathogen-free AAALAC-accredited animal facilities at the BRI and Stanford University and handled in accordance with institutional guidelines.

2.2. Isolation of Leukocyte Populations. Mouse leukocyte populations were isolated from inguinal, axillary, and brachial lymph nodes and spleen cells from 6- to 8-week-old mice. CD4⁺ T cell populations were isolated using a CD4⁺ Isolation Kit (Miltenyi Biotec) as per the manufacturer's instructions. Foxp3/GFP⁺ and Foxp3/GFP⁻ T-cells were then isolated using either a FACS-Vantage Flow Cytometer Cell Sorter or BD FACS Aria. Purity of the resulting cell fractions was reliably $>99.9\%$ Foxp3/GFP⁺.

2.3. Reagents and Cell Lines. Hyaluronan of 1.5×10^6 kDa molecular weight (HMW-HA) was provided by Genzyme. Cyclosporine A (CSA) was obtained from Sigma-Aldrich (St. Louis, MO). Recombinant mouse IL-2R alpha antibody (R&D Systems), IL-2 (Chiron), and neutralizing antibody against CD25 (3C7, BioLegend) were used. HMW-HA conjugated to BSA was used for plate-bound HMW-HA activation studies, as described previously [29].

2.4. Flow Cytometry Analysis. CD44 cross-linking of Treg was performed as follows: 1×10^6 cells/well were cultured in a 96-well round-bottom tissue culture plate. Cells were then treated under different stimulation conditions as follows: media alone, IL-2 (100 IU/mL), and/or plate-bound anti-mouse CD44 Ab (10 μ g/mL, IM7, BD). Alternatively, for analysis following HMW-HA treatment, 1×10^6 cells/well in 96-well round-bottom tissue culture plates were serum starved for 2.5 hours before the assay. The cells were then resuspended in RPMI 1640 (Invitrogen) supplemented with 10% FBS (Hyclone, Logan, UT), 100 μ g/mL Penicillin, 100 U/mL Streptomycin, 50 μ M β me, 2 mM glutamine, and 1 mM sodium pyruvate (Invitrogen) prior to transfer to plates previously coated with 50 μ g/mL BSA-conjugated HMW-HA. On the third day, cells were harvested and washed prior to analysis. Where indicated, the following reagents were incubated at 37°C in a CO₂ incubator with the cells 30 minutes prior to cross-linking CD44: CSA (50 ng/mL or at concentrations indicated) and neutralizing Ab against CD25 (100 μ g/mL; R&D Systems, Cat number AB-223-NA).

Flow cytometry experiments used the following fluorochrome-labeled antibodies: CD3e (145-2C11), CD4 (RM4-5), CD25 (PC61.5), and CD44 (IM7) from BD-Biosciences and eBioscience. Labeled cells resuspended in FACS buffer were analyzed on a LSRII flow cytometer. Analysis was performed using CELLQuest (BD) and FlowJo (TreeStar Inc., Ashland, OR) software. Of note, all FACS plots and MFI values shown were gated on live cells unless otherwise noted.

2.5. Murine Treg Activation Assays. 96-well flat bottom tissue culture plates were precoated with anti-CD3 Ab (0.5 μ g/mL) and anti-CD44 Ab (1 μ g/mL) where relevant. Soluble anti-CD28 Ab was used at 0.5 μ g/mL. Coating with HMW-HA was treated as a second step. Plates were washed with PBS and then either 100 μ L of 100 μ g/mL HMW-HA or 100 μ L of 10% BSA in PBS was added and the plates were incubated at 37°C for 2 hours. Plates were again washed with PBS prior to the addition of 150,000 CD4⁺CD25⁺ Treg in RPMI-10 complete medium. Where noted, CSA (50 ng/mL) or soluble IL-2R α (5 μ g/mL) was added at the inception of the experiment. No exogenous IL-2 was added unless otherwise noted. After three days Treg were stained and analyzed by flow cytometry.

2.6. Statistical Analysis. Graphs were prepared using JMP software (SAS Institute, Cary, NC) and GraphPad Prism (La Jolla, CA). Significance was assessed using paired *t* tests or ANOVA unless otherwise noted.

3. Results

3.1. CSA Increases Treg Percentages in a CD44 Dependent Manner. To evaluate CSA effects on Treg viability and Foxp3 expression, we used tissues isolated from transgenic mice expressing GFP in concert with Foxp3. We purified CD4⁺ T cells from these animals and activated them in culture for 72 hours. Our goal was to test whether CSA increased the fraction of Foxp3⁺ Treg among total CD4⁺ cells *in vitro*, as has been reported *in vivo* [21, 22].

We observed that CSA treatment significantly increased the percentage of Foxp3⁺ Treg among total CD4⁺ T cells. This effect was significant at a range of CSA concentrations but was most pronounced at moderate CSA levels (50 $\mu\text{g}/\text{mL}$) (Figure 1(a)). This effect is due to increased cell death among the GFP/Foxp3⁻, conventional T cell fraction and not the GFP/Foxp3⁺ Treg fraction (data not shown).

No such increase in the GFP/Foxp3 fraction was seen in cells isolated from CD44^{-/-} mice (Figure 1(b)). We also observed that CD44-cross-linking heightened the percentage of Foxp3⁺ Treg, even at high concentrations of CSA (Figure 1(c)). These data indicate that (1) Treg are relatively resistant to CSA, compared to Teff cells, (2) that this resistance is CD44 dependent, and (3) can be magnified by CD44 cross-linking.

3.2. Both CD44 Cross-Linking and IL-2 Promote Foxp3 Expression and Treg Persistence Despite CSA Treatment. The effects of CD44 cross-linking on Foxp3 levels were analogous to what one might expect to see with IL-2 supplementation. We therefore directly compared the effects of CD44 cross-linking and IL-2 supplementation on Treg cultured in the setting of CSA. To this end, we freshly isolated CD4⁺GFP/Foxp3⁺ Treg from GFP/Foxp3 transgenic mice and activated these for three days in the absence or presence of CSA.

We observed that Foxp3 and CD25 expression was abrogated by treatment with CSA but that both CD44 cross-linking and supplementation with 100 IU/mL of IL-2 maintained Foxp3 expression. Indeed, CD44 cross-linking and IL-2 supplementation were roughly equivalent in their ability to promote Treg homeostasis in the setting of CSA (Figures 2(a) and 2(b)). Of note, this beneficial effect of CD44 cross-linking on Foxp3 levels was predicated on the concomitant presence of TCR signals; CD44 cross-linking in the absence of aCD3/28 did not promote resistance to CSA (data not shown).

As with our observation using total CD4⁺ T cells in Figure 1, CD44 cross-linking on purified Treg likewise supported maintenance of Foxp3 expression across a range of CSA concentrations (Figure 2(c)). In addition, we saw comparable effects when we assessed Treg viability upon CSA treatment, as measured by 7-AAD and Annexin V staining. However, CSA treatment of Treg in the absence of CD44 cross-linking led to a significant decrease in viability (Figure 2(d)).

Together, these data indicate that CD44 cross-linking and IL-2 supplementation exert parallel effects on Treg, allowing them to escape cell death caused by treatment with CSA.

3.3. CD44 Cross-linking Promotes Foxp3 Expression in an IL-2-Independent Manner. We previously reported that CD44 cross-linking by HMW-HA promoted Treg maintenance in the absence of exogenous IL-2 [26, 28]. As part of those studies, we observed that CD44 cross-linking allowed Treg to resist CSA-mediated cell death [28]. We had proposed that CD44 cross-linking promoted increased IL-2 production by Treg.

However, this interpretation of the data was problematic for several reasons. First, Foxp3 is known to efficiently

suppress IL-2 production [6]. While we did detect IL-2 in Treg cultures [28], this may be better explained by the propensity of some GFP/Foxp3⁺ Treg to revert to being GFP/Foxp3⁻ Teff cells capable of producing IL-2 [30]. Indeed, upon intracellular staining of these cells for IL-2, we observed that the IL-2 producing cells were uniformly GFP/Foxp3⁻ (data not shown). Second, CSA also suppresses IL-2 production by both Treg and Teff alike in an efficient manner [18]. Consistent with this, the level of IL-2 we detected in these cultures by ELISA, in the 5–20 pg/mL range, would be insufficient to support Treg homeostasis. We therefore sought to better ascertain whether CD44-mediated support of Treg homeostasis was indeed IL-2 independent.

We first neutralized any IL-2 that might be produced in our Treg activation cultures by adding recombinant CD25 (rCD25), the high affinity IL-2 receptor, or antibodies directed at IL-2. However, these reagents did not completely negate the beneficial effect of CD44 cross-linking on Foxp3 expression (Figure 3(a)).

We then obtained CD4⁺GFP/Foxp3⁺ Treg from transgenic GFP/Foxp3 mice lacking CD25, the high affinity IL-2 receptor (GFP/FoxP3.CD25^{-/-} mice). We found that the absence of CD25 had minimal impact on CD44-mediated Foxp3 expression, as the wild type B6 mice and CD25^{-/-} Treg cells had almost equal Foxp3 expression levels (Figure 3(b)).

Because IL-2 effects on Treg homeostasis are dose-dependent, we next tested whether CD44 cross-linking effects were additive with IL-2 supplementation from 0–20 IU/mL (0–4000 pg/mL). We found that the effects of CD44 cross-linking on Foxp3 persistence were most pronounced at low levels of IL-2 and that CD44 cross-linking was functionally equivalent to adding high levels of IL-2 (10–20 IU/mL, equivalent to 2000–4000 pg/mL) to these cultures (Figure 3(c)).

Together, these data support the conclusion that CD44 cross-linking potentiates Foxp3 expression of Treg in an IL-2 and CD25 independent manner.

3.4. Inhibition of HA Synthesis Impairs Treg Homeostasis Which Can Be Overcome with Exogenous IL-2 or CD44-Cross-Linking. We next determined whether the effect of CD44 cross-linking on Foxp3 expression could be induced by its natural ligand HA and whether this source of HA was paracrine or autocrine in origin.

To test this, we incubated CD4⁺/Foxp3⁺ Treg for 72 hours in the presence of HMW-HA, plate-bound CD44 antibody, or IL-2, and examined Foxp3 expression. We observed that cross-linking CD44 receptor through either plate-bound CD44 antibody or HMW-HA promoted Foxp3 expression in CD4⁺ Tregs in a manner similar to IL-2 (Figure 4(a)).

To evaluate whether the HA that promoted Foxp3 expression was paracrine or autocrine in nature, we abrogated endogenously produced HA in CD4⁺ Treg by culturing them in the presence of 4-methylumbelliferone (4-MU), a specific hyaluronan synthase inhibitor [31]. Activated Treg cultured with 4-MU were unable to maintain Foxp3 expression over 72 hours (Figure 4(b)). As expected, IL-2 supplementation could completely rescue Foxp3 expression. Moreover, when these cells were cultured with anti-CD44 antibody, Foxp3

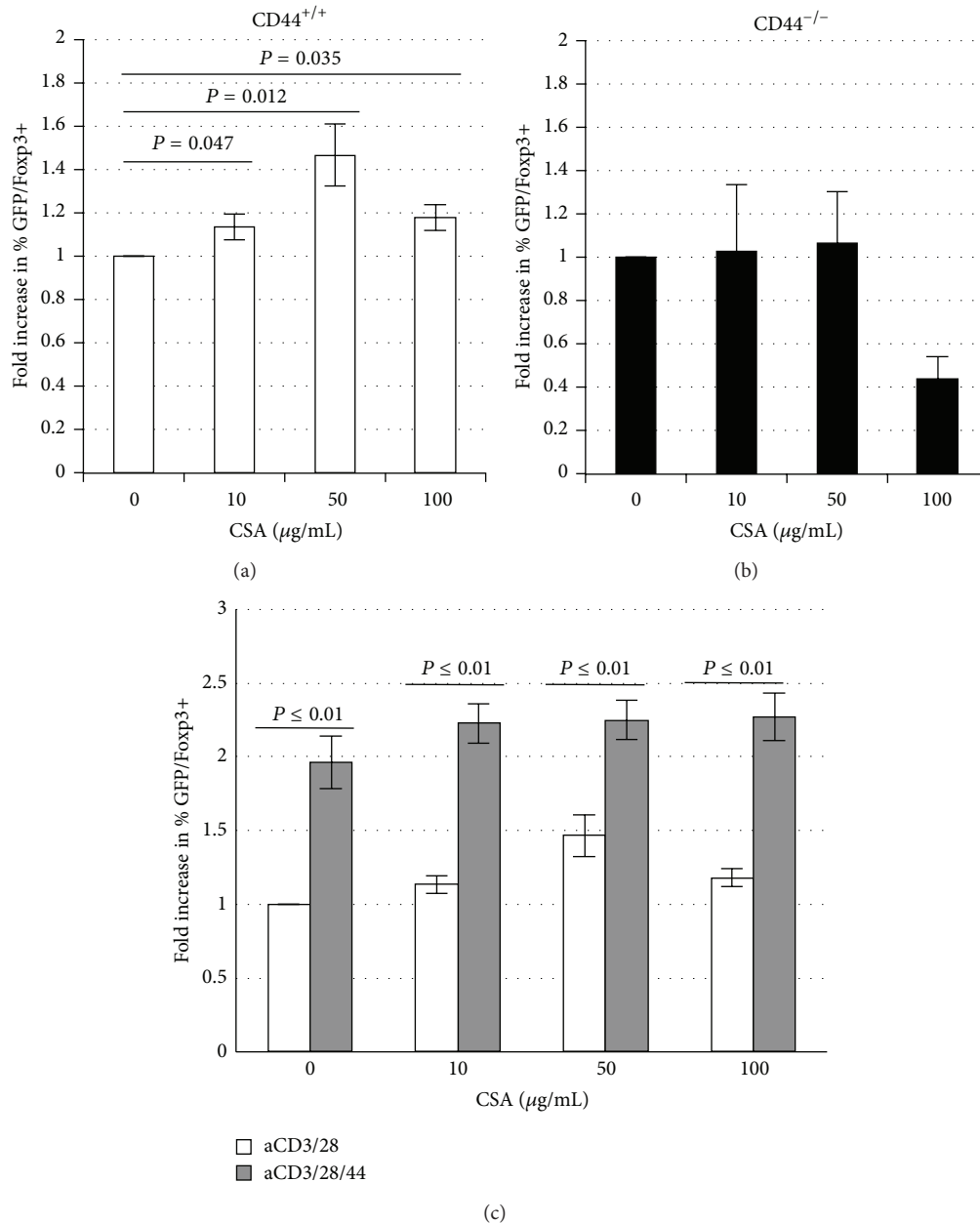


FIGURE 1: CSA increases Treg percentages in a CD44 dependent manner. Fold increase (FI) in the percentage of GFP/Foxp3+ cells of (a) CD44-containing or (b) CD44-deficient, murine CD4+ T cells after 3 days of culture in the settings of anti-CD3 and anti-CD28 with or without CSA in various concentrations. (c) Fold increase (FI) in percentage of GFP/Foxp3+ cells after 3 days of culture in the setting of anti-CD3 and anti-CD28 alone or in conjunction with anti-CD44 Ab. $n = 5$ replicate wells.

expression was maintained at levels similar to controls. These observations were confirmed in multiple experimental replicates (Figure 4(c)). Taken together, these results demonstrate that both endogenous and exogenous HA can potentiate Foxp3 expression and that the loss of HA production can be compensated for by cross-linking of the HA receptor, CD44.

3.5. CD44-Mediated Foxp3 Expression Is Stat5-Dependent. Many of the cytokines known to support Treg homeostasis, including IL-2, signal through Stat5. We therefore evaluated whether the promotion of Foxp3 persistence by CD44 cross-linking is mediated by Stat5 signaling.

We observed that the ability of CD44 cross-linking to promote Foxp3 expression was lost upon treatment with sc-355979, a selective inhibitor of pStat5 (Figure 5(a)). This capacity of sc-355979 to overcome CD44-mediated Foxp3 expression was dose dependent (Figure 5(b)). Finally, whereas CSA treatment alone did not affect Foxp3 expression induced by CD44, combined treatment with CSA and pStat5 inhibition did impair CD44-mediated Foxp3 expression (Figure 5(c)).

Taken together, these results indicate that the CD44-mediated promotion of Foxp3 expression and the ability of

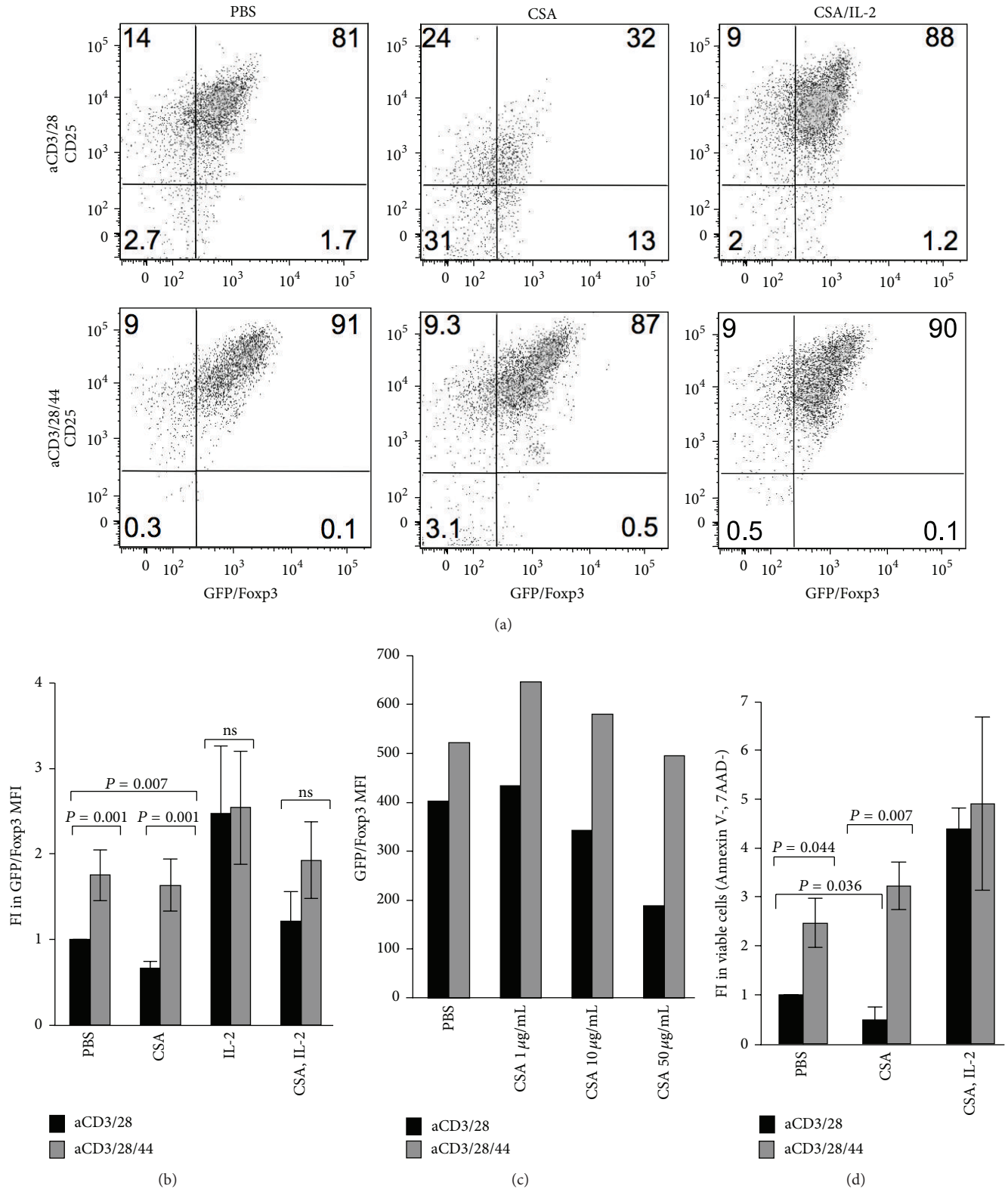


FIGURE 2: CD44 cross-linking and IL-2 both promote Foxp3 expression and Treg persistence despite CSA treatment. (a) Representative flow cytometric analysis of CD25 labeled and GFP/Foxp3+ cells after 3 days in culture in the presence of anti-CD3 and anti-CD28 alone or with the addition of anti-CD44, and with or without CSA (50 ng/mL) alone or together with IL-2 (20 IU/mL). (b) Fold increase (FI) in GFP/Foxp3 MFI after 3 days of culture in the presence of anti-CD3 and anti-CD28 alone or in conjunction with anti-CD44 Ab, with or without CSA (50 ng/mL) alone or together with IL-2 (20 IU/mL). N = 4 independent experiments, among these are included Figure 2(a). (c) Fold Increase in GFP/FoxP3 MFI in the presence of anti-CD3 and anti-CD28 alone, or in conjunction with anti-CD44 and increasing concentrations of CSA. Data are representative of two experiments. (d) Fold increase in the fraction of viable GFP/FoxP3+ cells (Annexin V-, 7AAD-) upon culture with aCD3/28 or aCD3/28/44 with or without CSA (50 ng/mL) alone or together with IL-2 (20 IU/mL). N = 4 experiments among these are included in Figure 2(a) and the other experiments are in Figure 2(b).

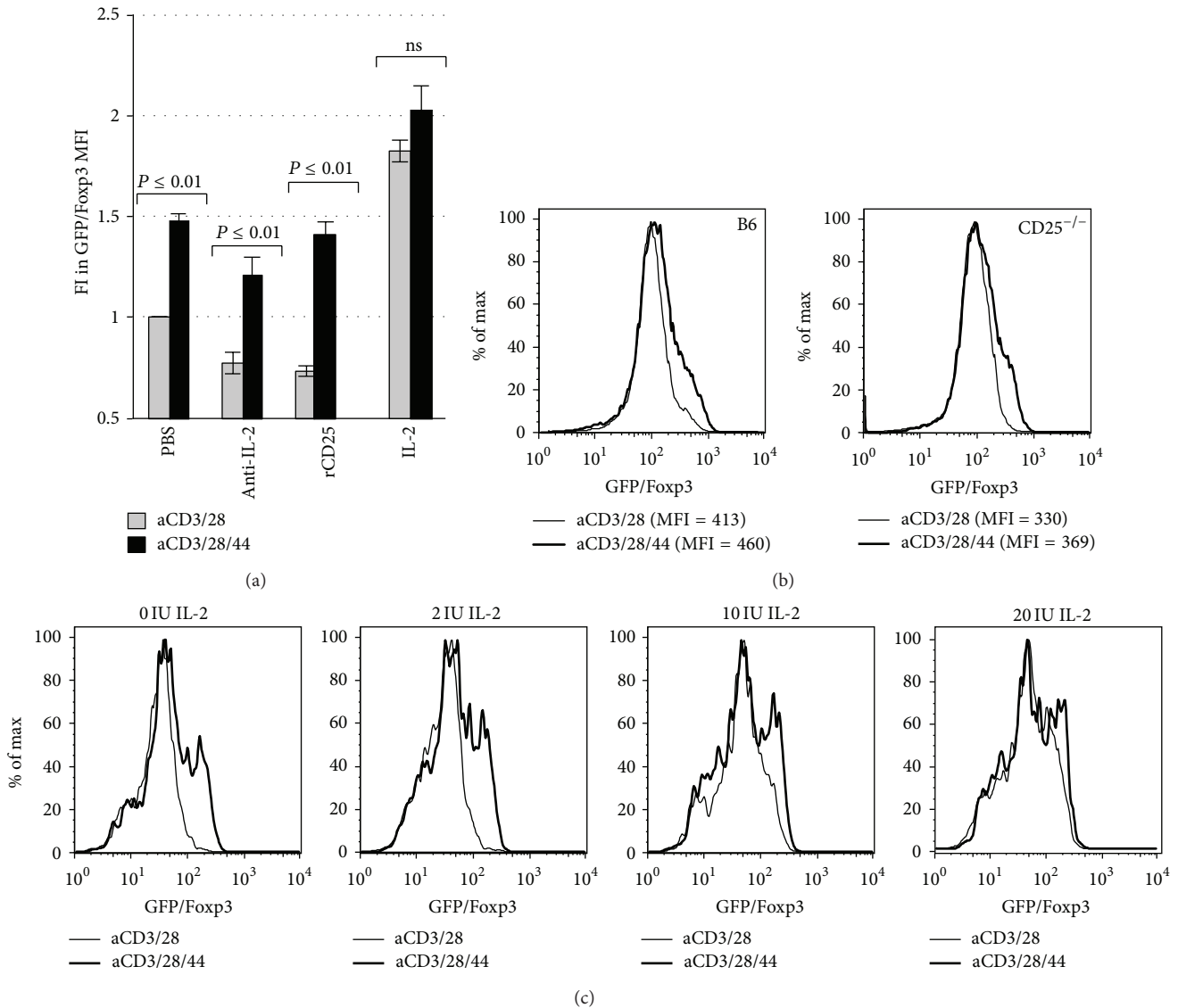


FIGURE 3: CD44 cross-linking promotes Foxp3 expression in an IL-2-independent manner. (a) Fold Increase (FI) in GFP/FoxP3 MFI for Treg activated with anti-CD3 and anti-CD28 Ab alone or in conjunction with plate-bound anti-CD44 Ab with or without anti-IL-2 Ab (Anti-IL-2), recombinant CD25 (rCD25), or IL-2 ($n = 7$). (b) Representative histograms demonstrating GFP/FoxP3 expression by Treg isolated from GFP/FoxP3 knock-in mice on a conventional B6 background mice or on a CD25^{-/-} background (B6 GFP/FoxP3.CD25^{-/-} mice) following 3 days of culture with anti-CD3 and anti-28 alone or in conjunction with plate-bound anti-CD44. (c) Representative histograms illustrating GFP/FoxP3 expression of Treg following 3 days of culture with anti-CD3 and anti-CD28 alone, or in conjunction with plate-bound CD44 Ab, and with or without varying doses of IL-2. Data are representative of two experiments.

CD44 cross-linking to bypass CSA treatment depend on Stat5 activation.

4. Discussion

Cyclosporine (CSA) is a widely used immunosuppressant that selectively targets T cells, thereby preventing antigen-specific immune processes like transplant rejection [32, 33]. There are data that suggest that CSA may selectively spare Treg and it may be that this contributes to CSA efficacy [20–22]. Here, we have identified a novel, CD44-mediated and IL-2 independent mechanism for how Treg may escape CSA suppression.

A role for CD44 in Treg persistence in the face of CSA would be consistent with other lines of evidence supporting a role for CD44 in homeostasis. We previously published that CD44 and HMW-HA promote Treg homeostasis in low IL-2 environments [25–27] and it was recently reported that complexes of CD44 and Galectin-9 promote the stability and function of Treg in a SMAD2/3 signaling dependent manner [34]. CD44 also contributes to Treg function [25, 27, 29] and the capacity to bind HMW-HA is known to characterize the most potent subset of Treg [25]. Of note, CD44 cross-linking did not rescue GFP/Foxp3⁻, conventional T cells from CSA effects in our hands. We speculate that this may reflect the fact that these cells are typically CD44^{lo}. Also of note, it is highly

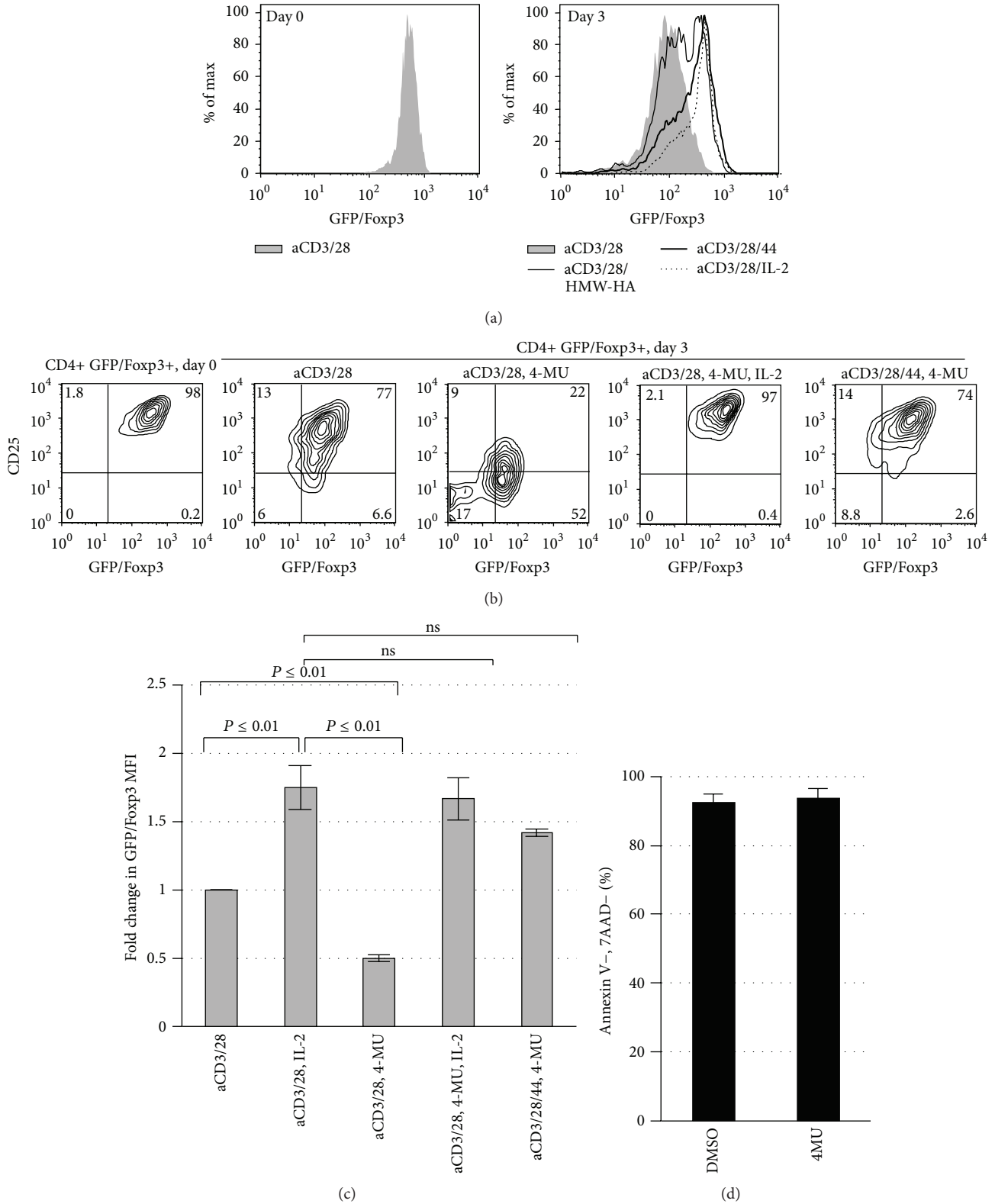


FIGURE 4: Inhibition of HA synthesis impairs Treg homeostasis which can be overcome with exogenous IL-2 or CD44-cross-linking. (a) Representative histograms of GFP/FoxP3 expression of Treg following 3 days of culture in the presence of anti-CD3 and anti-CD28 alone or with IL-2, CD44 cross-linking, or exogenous plate-bound HA. $N = 3$ independent experiments. (b) Representative FACS plots illustrating GFP/Foxp3 and CD25 expression on Day 0 immediately following isolation of CD4+GFP/Foxp3+ Treg from murine splenocytes and following 3 days of culture with anti-CD3 and anti-CD28 Ab alone or in conjunction with plate-bound anti-CD44 Ab, the HA synthesis inhibitor 4-MU, and/or IL-2. (c) Fold change in GFP/Foxp3 MFI for the same conditions as in (b), here for $N = 3$ independent experiments. (d) Viability (the percentage of GFP/Foxp3+ cells negative for 7AAD and Annexin V) for Treg cultured in the setting of either DMSO or 4MU.

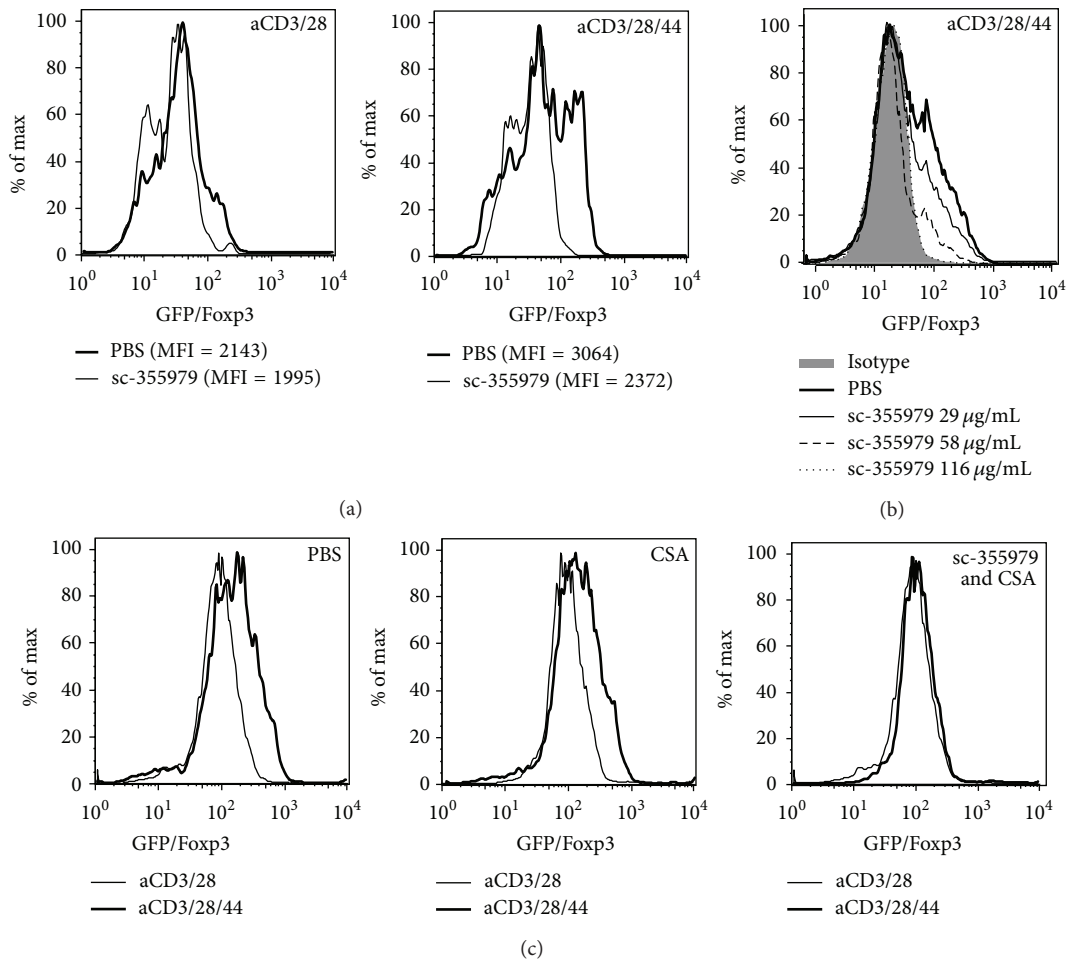


FIGURE 5: *CD44*-mediated *Foxp3* expression is *Stat5*-dependent. (a) Representative histograms for GFP/*Foxp3* expression of CD4+GFP/*Foxp3*+ Treg following culture in the presence of sc-35597, a selective pStat5 inhibitor. (b) Representative histograms for GFP/*Foxp3* following 3 days of culture with aCD3/28/44 together with increasing concentrations of sc-35597. (c) Representative histograms depicting GFP/*Foxp3* persistence following culture with CSA (50 ng/mL) alone or in conjunction with sc-35597. Data for (a–c) are representative of at least 3 experiments.

unlikely that expansion of Treg is responsible for this effect given that it is generally accepted that Treg do not expand *in vitro* in the absence of high dose IL-2 and potent antigenic signals. Induction of Treg from conventional T cells is also highly unlikely given the absence of high dose IL-2, potent antigenic signals, and TGF β [6].

The constitutive expression of CD44 may also promote homeostasis of additional CD44^{hi} T cell subsets. For example, CD44 has been implicated in the homeostasis of memory T cells, which are also CD44^{hi} [35]. In addition to total CD44 levels, the distribution of CD44 on the cell surface, and the make-up of CD44 variant isoforms could also impact T cell homeostasis.

These data may be relevant to understanding seemingly contradictory data indicating that CSA does not uniformly spare Treg (reviewed in [36]). Specifically, there are some reports that CSA inhibits *Foxp3* mRNA expression [37] and induces the reversion of Treg to pro-inflammatory phenotypes [38]. Similarly, *in vivo* studies in which mice underwent MHC-mismatch bone marrow transplantation demonstrated that CSA treatment impaired expansion of Treg and reduced

overall *Foxp3* expression [39]. More recently, it was shown that CSA treatment preferentially inhibits antigen-specific Treg [40]. Miroux and colleagues found that CSA decreased both the activity and proliferation of Treg [41]. Our data suggest that the dose of CSA may impact the ability of Treg to resist CSA. Consistent with this, Kawai and colleagues demonstrated that *in vivo* administration of CSA inhibits the proliferation of Treg at high doses, but not so at low doses [42]. Besides this, our data also support roles for antigenic signals, co-stimulation through CD44, and therefore the local inflammatory milieu as factors that influence Treg susceptibility to suppression by CSA.

Our data support a role for CD44-mediated, IL-2 independent, promotion of Treg resistance to CSA and implicate *Stat5* signaling in this effect [4, 43]. *Stat5* signaling is known to be essential for both the maintenance of *Foxp3* expression and the suppressive function of Treg *in vivo* [44, 45]. This is underscored by the observation that *Stat5* knockout mice exhibit a loss of Treg [46]. Additionally, overexpression of *Stat5* in IL-2 knockout mice can restore *in vivo* Treg numbers [46]. However, avenues for *Stat5* signaling not directly

involving IL-2 are likely to be important for Treg homeostasis. Our current efforts are therefore focused on determining whether CD44 cross-linking directly phosphorylates Stat5 or, alternatively, whether these effects are indirectly mediated.

5. Conclusions

We have identified a role for CD44, a receptor for HA, in promoting Treg resistance to CSA. This effect is IL-2 independent but can be suppressed by inhibition of Stat5 phosphorylation. Moreover, we find that inhibition of HA synthesis impairs Treg homeostasis but that this effect can be overcome with exogenous IL-2 or CD44-cross-linking. Together, these data support a model whereby CD44 cross-linking by HA promotes IL-2-independent Foxp3 expression and Treg survival in the face of CSA.

Abbreviations

ECM:	Extracellular matrix
HA:	Hyaluronan
HMW-HA:	High-molecular-weight hyaluronan
Treg:	Foxp3 ⁺ regulatory T cell.

Conflict of Interests

The authors declare that there are no conflicts of interests regarding the publication of this paper.

Acknowledgments

This work was supported by National Institutes of Health Grants 5 T32 AI07290 (to Shannon M. Ruppert); R01 DK096087-01, R01 HL113294-01A1, and U01 AI101984 (to Paul L. Bollyky).

References

- [1] R. S. Wildin, F. Ramsdell, J. Peake et al., "X-linked neonatal diabetes mellitus, enteropathy and endocrinopathy syndrome is the human equivalent of mouse scurfy," *Nature Genetics*, vol. 27, no. 1, pp. 18–20, 2001.
- [2] E. N. Huter, G. A. Punkosdy, D. D. Glass, L. I. Cheng, J. M. Ward, and E. M. Shevach, "TGF- β -induced Foxp3⁺ regulatory T cells rescue scurfy mice," *European Journal of Immunology*, vol. 38, no. 7, pp. 1814–1821, 2008.
- [3] R. K. Selvaraj and T. L. Geiger, "Mitigation of experimental allergic encephalomyelitis by TGF- β induced Foxp3⁺ regulatory T lymphocytes through the induction of anergy and infectious tolerance," *Journal of Immunology*, vol. 180, no. 5, pp. 2830–2838, 2008.
- [4] T. Y. Wuest, J. Willette-Brown, S. K. Durum, and A. A. Hurwitz, "The influence of IL-2 family cytokines on activation and function of naturally occurring regulatory T cells," *Journal of Leukocyte Biology*, vol. 84, no. 4, pp. 973–980, 2008.
- [5] Q. Chen, Y. C. Kim, A. Laurence, G. A. Punkosdy, and E. M. Shevach, "IL-2 controls the stability of Foxp3 expression in TGF- β -induced Foxp3⁺ T cells in vivo," *The Journal of Immunology*, vol. 186, no. 11, pp. 6329–6337, 2011.
- [6] S. Sakaguchi, R. Setoguchi, H. Yagi, and T. Nomura, "Naturally arising Foxp3-expressing CD25⁺CD4⁺ regulatory T cells in self-tolerance and autoimmune disease," *Current Topics in Microbiology and Immunology*, vol. 305, pp. 51–66, 2006.
- [7] R. Setoguchi, S. Hori, T. Takahashi, and S. Sakaguchi, "Homeostatic maintenance of natural Foxp3⁺ CD25⁺ CD4⁺ regulatory T cells by interleukin (IL)-2 and induction of autoimmune disease by IL-2 neutralization," *The Journal of Experimental Medicine*, vol. 201, no. 5, pp. 723–735, 2005.
- [8] E. Zorn, E. A. Nelson, M. Mohseni et al., "IL-2 regulates FOXP3 expression in human CD4⁺CD25⁺ regulatory T cells through a STAT-dependent mechanism and induces the expansion of these cells in vivo," *Blood*, vol. 108, no. 5, pp. 1571–1579, 2006.
- [9] M. de la Rosa, S. Rutz, H. Dorninger, and A. Scheffold, "Interleukin-2 is essential for CD4⁺CD25⁺ regulatory T cell function," *European Journal of Immunology*, vol. 34, no. 9, pp. 2480–2488, 2004.
- [10] W. Liao, J.-X. Lin, L. Wang, P. Li, and W. J. Leonard, "Modulation of cytokine receptors by IL-2 broadly regulates differentiation into helper T cell lineages," *Nature Immunology*, vol. 12, no. 6, pp. 551–559, 2011.
- [11] T. R. Malek, A. Yu, L. Zhu, T. Matsutani, D. Adeegbe, and A. L. Bayer, "IL-2 family of cytokines in T regulatory cell development and homeostasis," *Journal of Clinical Immunology*, vol. 28, no. 6, pp. 635–639, 2008.
- [12] L. M. Anderson, T. C. Dumsha, N. J. McDonald, and J. K. Spitznagel Jr., "Evaluating IL-2 levels in human pulp tissue," *Journal of Endodontics*, vol. 28, no. 9, pp. 651–655, 2002.
- [13] O. Lesur, A. Kokis, C. Hermans, T. Fülöp, A. Bernard, and D. Lane, "Interleukin-2 involvement in early acute respiratory distress syndrome: relationship with polymorphonuclear neutrophil apoptosis and patient survival," *Critical Care Medicine*, vol. 28, no. 12, pp. 3814–3822, 2000.
- [14] T. M. Phillips, "Measurement of total and bioactive interleukin-2 in tissue samples by immunoaffinity-receptor affinity chromatography," *Biomedical Chromatography*, vol. 11, no. 4, pp. 200–204, 1997.
- [15] A. N. Akbar, M. Vukmanovic-Stejic, L. S. Taams, and D. C. Macallan, "The dynamic co-evolution of memory and regulatory CD4⁺ T cells in the periphery," *Nature Reviews Immunology*, vol. 7, no. 3, pp. 231–237, 2007.
- [16] M. Vukmanovic-Stejic, Y. Zhang, A. N. Akbar, and D. C. Macallan, "Measurement of proliferation and disappearance of regulatory T cells in human studies using deuterium-labeled glucose," *Methods in Molecular Biology*, vol. 707, pp. 243–261, 2011.
- [17] H. G. Kang, D. Zhang, N. Degauque, C. Mariat, S. Alexopoulos, and X. X. Zheng, "Effects of cyclosporine on transplant tolerance: the role of IL-2," *American Journal of Transplantation*, vol. 7, no. 8, pp. 1907–1916, 2007.
- [18] J. Liu, J. D. Farmer Jr., W. S. Lane, J. Friedman, I. Weissman, and S. L. Schreiber, "Calcineurin is a common target of cyclophilin-cyclosporin A and FKBP-FK506 complexes," *Cell*, vol. 66, no. 4, pp. 807–815, 1991.
- [19] C.-W. Chow, M. Rincón, and R. J. Davis, "Requirement for transcription factor NFAT in interleukin-2 expression," *Molecular and Cellular Biology*, vol. 19, no. 3, pp. 2300–2307, 1999.
- [20] W. Gao, Y. Lu, B. El Essawy, M. Oukka, V. K. Kuchroo, and T. B. Strom, "Contrasting effects of cyclosporine and rapamycin in de novo generation of alloantigen-specific regulatory T cells," *The American Journal of Transplantation*, vol. 7, no. 7, pp. 1722–1732, 2007.
- [21] E. F. Knol, I. M. Haeck, A. A. van Kraats et al., "Modulation of lymphocyte function *In Vivo* via inhibition of calcineurin or

- purine synthesis in patients with atopic dermatitis," *Journal of Investigative Dermatology*, vol. 132, no. 10, pp. 2476–2479, 2012.
- [22] Z. Y. Li, Q. Wu, Z. Yan et al., "Prevention of acute GVHD in mice by treatment with *Tripterygium hypoglaucum* Hutch combined with cyclosporin A," *Hematology*, vol. 18, no. 6, pp. 352–359, 2013.
- [23] F. Meloni, M. Morosini, N. Solari et al., "Peripheral CD4⁺CD25⁺ Treg cell expansion in lung transplant recipients is not affected by calcineurin inhibitors," *International Immunopharmacology*, vol. 6, no. 13-14, pp. 2002–2010, 2006.
- [24] R. Stern, A. A. Asari, and K. N. Sugahara, "Hyaluronan fragments: an information-rich system," *European Journal of Cell Biology*, vol. 85, no. 8, pp. 699–715, 2006.
- [25] M. Firan, S. Dhillon, P. Estess, and M. H. Siegelman, "Suppressor activity and potency among regulatory T cells is discriminated by functionally active CD44," *Blood*, vol. 107, no. 2, pp. 619–627, 2006.
- [26] P. L. Bollyky, B. A. Falk, R. P. Wu, J. H. Buckner, T. N. Wight, and G. T. Nepom, "Intact extracellular matrix and the maintenance of immune tolerance: high molecular weight hyaluronan promotes persistence of induced CD4⁺CD25⁺ regulatory T cells," *Journal of Leukocyte Biology*, vol. 86, no. 3, pp. 567–572, 2009.
- [27] P. L. Bollyky, J. D. Lord, S. A. Masewicz et al., "Cutting edge: high molecular weight hyaluronan promotes the suppressive effects of CD4⁺CD25⁺ regulatory T cells," *Journal of Immunology*, vol. 179, no. 2, pp. 744–747, 2007.
- [28] P. L. Bollyky, B. A. Falk, S. A. Long et al., "CD44 costimulation promotes FoxP3⁺ regulatory T cell persistence and function via production of IL-2, IL-10, and TGF- β ," *Journal of Immunology*, vol. 183, no. 4, pp. 2232–2241, 2009.
- [29] T. Liu, L. Soong, G. Liu, R. König, and A. K. Chopra, "CD44 expression positively correlates with Foxp3 expression and suppressive function of CD4⁺ T_{reg} cells," *Biology Direct*, vol. 4, article 40, 2009.
- [30] C. Koenecke, N. Czeloth, A. Bubke et al., "Alloantigen-specific de novo-induced Foxp3⁺ Treg revert in vivo and do not protect from experimental GVHD," *European Journal of Immunology*, vol. 39, no. 11, pp. 3091–3096, 2009.
- [31] I. Kakizaki, K. Kojima, K. Takagaki et al., "A novel mechanism for the inhibition of hyaluronan biosynthesis by 4-methylumbelliferone," *The Journal of Biological Chemistry*, vol. 279, no. 32, pp. 33281–33289, 2004.
- [32] A. Glazier, P. J. Tutschka, E. R. Farmer, and G. W. Santos, "Graft-versus-host disease in cyclosporin A-treated rats after syngeneic and autologous bone marrow reconstitution," *The Journal of Experimental Medicine*, vol. 158, no. 1, pp. 1–8, 1983.
- [33] E. K. Gao, D. Lo, R. Cheney, O. Kanagawa, and J. Sprent, "Abnormal differentiation of thymocytes in mice treated with cyclosporin A," *Nature*, vol. 336, no. 6195, pp. 176–179, 1988.
- [34] C. Wu, T. Thalhamer, R. F. Franca et al., "Galactin-9-CD44 interaction enhances stability and function of adaptive regulatory T cells," *Immunity*, vol. 41, no. 2, pp. 270–282, 2014.
- [35] B. J. G. Baaten, C.-R. Li, M. F. Deiro, M. M. Lin, P. J. Linton, and L. M. Bradley, "CD44 regulates survival and memory development in Th1 cells," *Immunity*, vol. 32, no. 1, pp. 104–115, 2010.
- [36] S. A. de Serres, M. H. Sayegh, and N. Najafian, "Immunosuppressive drugs and tregs: a critical evaluation!," *Clinical Journal of the American Society of Nephrology*, vol. 4, no. 10, pp. 1661–1669, 2009.
- [37] C. C. Baan, B. J. Van Der Mast, M. Klepper et al., "Differential effect of calcineurin inhibitors, anti-CD25 antibodies and rapamycin on the induction of FOXP3 in human T cells," *Transplantation*, vol. 80, no. 1, pp. 110–117, 2005.
- [38] C. Miroux, O. Moralès, A. Carpentier et al., "Inhibitory effects of cyclosporine on human regulatory T cells in vitro," *Transplantation Proceedings*, vol. 41, no. 8, pp. 3371–3374, 2009.
- [39] R. Zeiser, V. H. Nguyen, A. Beilhack et al., "Inhibition of CD4⁺CD25⁺ regulatory T-cell function by calcineurin-dependent interleukin-2 production," *Blood*, vol. 108, no. 1, pp. 390–399, 2006.
- [40] T. Wu, L. Zhang, K. Xu et al., "Immunosuppressive drugs on inducing Ag-specific CD4⁺CD25⁺Foxp3⁺ Treg cells during immune response *in vivo*," *Transplant Immunology*, vol. 27, no. 1, pp. 30–38, 2012.
- [41] C. Miroux, O. Morales, K. Ghazal et al., "In vitro effects of cyclosporine a and tacrolimus on regulatory T-cell proliferation and function," *Transplantation*, vol. 94, no. 2, pp. 123–131, 2012.
- [42] M. Kawai, H. Kitade, C. Mathieu, M. Waer, and J. Pirenne, "Inhibitory and stimulatory effects of cyclosporine A on the development of regulatory T cells in vivo," *Transplantation*, vol. 79, no. 9, pp. 1073–1077, 2005.
- [43] J. D. Goldstein, R. S. Balderas, and G. Marodon, "Continuous activation of the CD122/STAT-5 signaling pathway during selection of antigen-specific regulatory T cells in the murine thymus," *PLoS ONE*, vol. 6, no. 4, Article ID e19038, 2011.
- [44] A. M. Thornton, "Signal transduction in CD4⁺CD25⁺ regulatory T cells: CD25 and IL-2," *Frontiers in Bioscience*, vol. 11, no. 1, pp. 921–927, 2006.
- [45] T. R. Malek, "The biology of interleukin-2," *Annual Review of Immunology*, vol. 26, no. 1, pp. 453–479, 2008.
- [46] A. Antov, L. Yang, M. Vig, D. Baltimore, and L. van Parijs, "Essential role for STAT5 signaling in CD25⁺CD4⁺ regulatory T cell homeostasis and the maintenance of self-tolerance," *The Journal of Immunology*, vol. 171, no. 7, pp. 3435–3441, 2003.

Research Article

High Sensitivity Method to Estimate Distribution of Hyaluronan Molecular Sizes in Small Biological Samples Using Gas-Phase Electrophoretic Mobility Molecular Analysis

Lan Do,^{1,2} Christen P. Dahl,³ Susanne Kerje,⁴ Peter Hansell,⁵ Stellan Mörner,¹ Ulla Lindqvist,⁶ Anna Engström-Laurent,⁷ Göran Larsson,² and Urban Hellman¹

¹Cardiology, Heart Centre and Department of Public Health and Clinical Medicine, Division of Medicine, Umeå University, 901 85 Umeå, Sweden

²Department of Medical Biochemistry and Biophysics-Unit of Research Education and Development Östersund, Umeå University, 831 31 Umeå, Sweden

³Department of Cardiology, Oslo University Hospital, Faculty of Medicine and K.G. Jebsen Cardiac Research Center and Center for Heart Failure Research, University of Oslo, 0327 Oslo, Norway

⁴Department of Medical Biochemistry and Microbiology, Science for Life Laboratory, Uppsala University, 751 23 Uppsala, Sweden

⁵Division of Integrative Physiology, Department of Medical Cell Biology, Uppsala University, 751 23 Uppsala, Sweden

⁶Department of Medical Sciences, Uppsala University, 751 85 Uppsala, Sweden

⁷Division of Medicine, Department of Public Health and Clinical Medicine, Umeå University, 901 85 Umeå, Sweden

Correspondence should be addressed to Urban Hellman; urban.hellman@umu.se

Received 25 September 2014; Revised 24 December 2014; Accepted 7 January 2015

Academic Editor: Carol de la Motte

Copyright © 2015 Lan Do et al. This is an open access article distributed under the Creative Commons Attribution License, which permits unrestricted use, distribution, and reproduction in any medium, provided the original work is properly cited.

Hyaluronan is a negatively charged polydisperse polysaccharide where both its size and tissue concentration play an important role in many physiological and pathological processes. The various functions of hyaluronan depend on its molecular size. Up to now, it has been difficult to study the role of hyaluronan in diseases with pathological changes in the extracellular matrix where availability is low or tissue samples are small. Difficulty to obtain large enough biopsies from human diseased tissue or tissue from animal models has also restricted the study of hyaluronan. In this paper, we demonstrate that gas-phase electrophoretic molecular mobility analyzer (GEMMA) can be used to estimate the distribution of hyaluronan molecular sizes in biological samples with a limited amount of hyaluronan. The low detection level of the GEMMA method allows for estimation of hyaluronan molecular sizes from different parts of small organs. Hence, the GEMMA method opens opportunity to attain a profile over the distribution of hyaluronan molecular sizes and estimate changes caused by disease or experimental conditions that has not been possible to obtain before.

1. Introduction

Hyaluronan (HA) is a negatively charged polysaccharide consisting of an unbranched repetitive dimer of *N*-acetyl-D-glucosamine and D-glucuronic acid [1]. It is unsulfated, in contrast to other glycosaminoglycans, and only rarely exist covalently bound to proteins. It is a polydisperse molecule, usually with an average molecular weight between 200 and 2000 kDa but it can occur up to 10^7 Da as a single molecule [2].

In vertebrates, so far, three HA synthases are described, HA synthases 1, 2, and 3 (HAS 1–3) [3, 4] and approximately one-third of total amount of HA is turned over every day. Degradation takes place enzymatically by hyaluronidases (HYAL) or by oxidation. In humans, there are 6 genes for HYAL where 4 can give rise to functional enzymes [5].

HA is present in various forms in the tissues of the body: as a freely circulating molecule bound to hyaluronan-binding proteins, loosely associated with tissue or anchored to the cell membrane via receptors. A complex of HA bound to

proteins has different properties and functions depending on its molecular weight, concentration, and the protein [6–8]. HA can also bind to cell membrane receptors, for example, CD44, which through intracellular signaling regulates cell proliferation, migration, and inflammation [9].

The various functions of HA depend on its molecular weight [10–16]. High molecular weight (HMW) HA, so-called native HA, has in some cases been shown to have opposite effect compared to fragmented HA [17, 18]. If the balance between synthesis and degradation of HA is disrupted, an accumulation of fragmented low molecular weight (LMW) HA can be formed. This is often harmful to tissues, which then cause a pathological condition.

To understand the role of HA in pathological conditions as well as in developmental processes, it is important to analyze its molecular size distribution with a reliable method suitable also for small amounts of tissues and fluids.

Gas-phase electrophoretic molecular mobility analyzer (GEMMA) (TSI Corp., MN) was originally established for globular proteins and relatively weak protein complexes [19, 20] and we have previously shown *in vitro* that the method can also be used for estimation of HA molecular size determination [21]. The method utilizes a differential mobility analyzer to determine the electrophoretic mobility (EMD) of a single charged molecule in air, which is proportional to the retention time and hence the electrophoretic diameter and the molecular size, of the particle. The advantage of GEMMA is the low detection level where reliable GEMMA analyses can be achieved with HA concentrations of 50 ng/mL or less, in small sample volumes of no more than 20 μ L [21]. The low sample concentration also ensures that the analysis is done at concentrations far below the critical concentration at which HA domain overlap occurs [22].

Due to the physical properties of HA and the shape dependence of the GEMMA method, a higher resolution is achieved in the LMW range than in the HMW range of HA [21]. The GEMMA easily separates LMW HA up to ca 100 kDa, whereas the resolution for HMW is poorer. However, in studies of biological or pathological samples this is not usually a disadvantage. The method still separates HMW from LMW HA where the resolution is high, and it is this LMW regime of HA size that shows strong cell signaling effects.

The low detection level of the GEMMA method opens new opportunities to study HA molecular size distributions from tissues in diseases that have not been possible to study before. In this paper, we demonstrate that the GEMMA method can be used for estimation of HA molecular weight distributions in biological samples with a limited amount of HA, such as from small biopsies with only few mg of available tissue.

2. Material

Adult white Leghorn chicken controls from a commercial population were bred and maintained at the Animal Facilities at the National Veterinary Institute in Uppsala, Sweden. A sagittal sample was collected from the middle part of the comb. These samples were frozen in -80°C . Approval from

TABLE 1: Average weight of a series of tissue biopsies used for HA isolation and subsequent GEMMA analysis. The purified chicken comb sample contained so much HA so it needed to be diluted before analysis in the GEMMA.

	Wet weight (mg)	Dry weight (mg)	Sample dilution
Heart ($n = 24$)	52	12	1x
Kidney ($n = 15$)	54	9	1x
Chicken comb ($n = 10$)	19	2,5	100x

the Ethical Committee for animal experiments in Uppsala was obtained for all experiments involving the chickens (C307/11).

A heart from a wild moose was a kind gift from a local moose hunter. The heart was kept in -20°C and myocardial septum tissue samples were taken for analysis.

Human myocardial septum tissue was obtained from Oslo, Norway, from a cardiac donor who was rejected for surgical reasons. The myocardium was kept on ice for 1–4 hours before tissue sampling with subsequent freezing in -80°C . Approval for the study was obtained from the Regional Ethical Committee (Regional Etisk Komité) in Norway.

Kidney tissue was excised from adult Sprague-Dawley rats and samples from the inner medulla (papilla) were frozen in -80°C . Approval from the Ethical Committee for animal experiments in Uppsala was obtained for all experiments involving the rats (C169/11).

Except the wild moose, all animals in this project were handled by trained personnel and reared according to the guidelines from the Swedish Board of Agriculture.

3. Methods

3.1. Isolation and Purification of HA. To isolate HA from tissue samples a slightly modified protocol from Tolg et al. [23] was used. Depending on sample, between 5 and 60 mg of wet tissue was dried using a vacuum rotary evaporator (Table 1). When the tissues were completely dried, they were homogenized by grinding.

A brief summary of the protocol follows.

To digest proteins in the homogenized tissues proteinase K (Sigma-Aldrich) was used in a deferoxamine mesylate containing buffer to prevent HA degradation. HA was extracted in chloroform by liquid-liquid extraction and precipitated by ethanol (EtOH) 99%.

To digest nucleic acids, the HA containing pellets were dissolved in a buffer containing benzonase (Sigma-Aldrich) followed by digestion of chondroitin by chondroitinase ABC (Sigma-Aldrich). To avoid digestion of HA the chondroitin digestions were allowed to carry on for exactly 10 min at 37°C [24]. Chloroform extraction and precipitation by ethanol were repeated.

The crude HA-samples were purified on an anion exchange minispin column (Thermo Scientific). To remove the salt, the eluted HA fractions were dialyzed thoroughly against 20 mM of ammonium acetate at pH 8.0. The final

aliquots were ready for GEMMA analysis and were subsequently diluted according to Table 1. Since the GEMMA method is not specific for HA, the purification of chicken comb was checked for impurities by GEMMA analysis before and after hyaluronidase treatment.

3.2. Molecular Weight Estimation with GEMMA Analysis. All HA molecular weight analyses were performed using GEMMA. Depending on the tissue origin, sample size, and initial concentration the HA samples were diluted between 1 and 100 times prior to GEMMA analysis. The final volume for all GEMMA measurements was adjusted to ca 20 μ L before the start of the measurements, and each GEMMA run used between 125 and 300 nL of sample. All GEMMA measurements were performed as described in Malm et al. [21] with the only exception that the differential mobility analyzer (DMA) was adjusted to scan for electrophoretic mobility of molecules with an apparent diameter between 1.72 and 54.2 nm instead of 2.55 and 25.5 nm.

4. Results

To show the potential of GEMMA analysis in HA research we show examples of HA size distribution in four different tissues and species, heart tissue from human and wild moose, chicken comb, and rat kidney.

Weight needed for analysis was about 50 mg wet weight for heart and kidney and ca 20 mg for chicken comb samples. Purified HA extract of the heart and kidney were not necessary to dilute whereas the chicken comb HA required a 100-fold dilution prior to analysis to prevent overload of the instrument (Table 1). Differences in HA molecular size distribution were observed between all samples. The raw data from GEMMA analysis are reported as the electrophoretic mobility diameter (EMD) of the different samples. The EMD was converted to molecular weight by analyzing HA standards from Hyalose L.L.C. (Figure 1) [21]. HA from moose heart and chicken comb both showed uniform peaks around EMD 7.2 nm, which is consistent with HMW HA of ca 5000 kDa. In contrast, HA from rat kidney both showed the HMW peak seen in the moose and chicken samples, and in addition a broad peak with a center around EMD 5.2 nm, corresponding to a low molecular weight of ca 30 kDa [21]. Human heart also showed presence of LMW HA in the same range as in rat kidney but the HMW HA content was of apparent greater size than the other three examples shown.

5. Discussion

In this paper, some examples are given that demonstrate the ability of GEMMA to separate LMW from HMW HA in small biological samples. This opens up for the possibility to study the involvement of LMW HA in pathological conditions which have not been possible before due to lack of material.

The strength of the GEMMA compared to other methods for HA molecular size determination is the low detection level. SEC with multiangle light scattering (MALS), sedimentation techniques, flow field-flow fractionation, or gel electrophoresis usually has a detection limit of >0.01 mg/mL

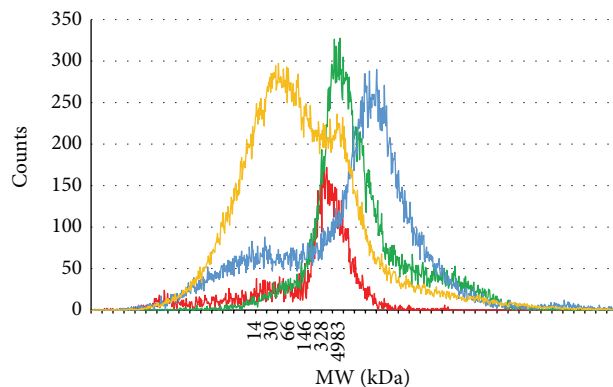


FIGURE 1: GEMMA data profile. Molecular size distribution of HA extracted from four different tissues and species, rat kidney (orange), chicken comb (green), human heart (blue), and moose heart (red), one of each. The electrophoretic molecule diameter analyzed in the GEMMA was converted to molecular weight by analyzing HA standards from Hyalose L.L.C. ranging from 30 kDa to 2400 kDa samples [21]. HA from moose heart and chicken comb both showed uniform HMW HA peaks around ca 5000 kDa. HA from rat kidney showed the HMW peak and an additional broad peak with a center around 30 kDa. Human heart also showed presence of LMW HA in the same range as in rat kidney but the HMW HA content was of apparent greater size than the other three examples shown.

[25–28]. Since the GEMMA method is at least 200 times more sensitive, it is possible to analyze very small amounts of tissues, for example, comparing left and right wall in a rat heart. GEMMA can therefore be used to estimate the molecular size distribution of HA in samples with very low concentrations, something that is crucial when extracting HA from small tissue samples. However, if a more exact molecular weight determination is needed and enough material is available, then, for example, gel electrophoresis is better suited [29, 30].

As expected, moose cardiac tissue and adult chicken comb showed HMW HA content around 5000 kDa. In contrast, besides the native HMW HA seen in the inner medulla of rat kidney, a large fraction of LMW HA around 30 kDa was also found. Both overexpression of hyaluronidase 2 or hyaluronidase 1 deficiency could potentially lead to accumulation of fragmented LMW HA as seen for this sample. However, in the kidney the amount of HA changes rapidly according to body hydration, and an extensive turnover of HA in a dehydrated kidney is to be expected [31]. Thus, since the tissue analyzed within this study was from a dehydrated rat, the large fraction of fragmented HA is anticipated.

Analysis of HA standards and ladders from Hyalose L.L.C. showed that also the biggest molecular weight (6 MDa) did not have an EMD over 9 nm (data not shown). The GEMMA spectrum of the human heart sample showed a peak center at EMD ca 9 nm, indicating abnormally large HA. This could possibly be cross-linked HA molecules or HA cross-linked with proteins. The latter case would indicate a protection of the crosslinking protein from degradation during the extraction process by HA shielding it.

We have seen this very high molecular weight HA in samples from very young chicken combs (data not shown). Thus, it is likely that this very high molecular weight HA is extracted only from certain types of tissues, for example, human heart and young chicken comb tissues which excludes the extraction process as source of the crosslinking. The very high molecular weight HA in the young chicken comb is degraded by hyaluronidases but possible trace amount of some other molecules forcing crosslinking could hide in the baseline noise. This highlights the need to develop a reliable HA specific affinity extraction which would be useful for all variants of HA molecular size determination methods.

6. Conclusion

Up to now, it has been very difficult to study diseases with pathological changes in the extracellular matrix where availability is low or tissue samples are small in size. Difficulty to obtain large enough biopsies for HA analysis from tissues of human disease or animal disease models has in many cases restricted the study of HA in such diseases. The low detection level of the GEMMA method now allows for studies of diseases where HA is involved. In addition, the method allows for estimation of the distribution of HA molecular sizes from different parts of small organs, for example, rat kidney (Figure 1). Hence, the GEMMA gives an opportunity to attain a profile over the distribution of HA molecular weight and estimate changes caused by disease or experimental conditions that has not been possible to obtain before.

Conflict of Interests

The authors declare that there is no conflict of interests regarding the publication of this paper.

References

- [1] B. Weissmann and K. Meyer, "The structure of hyalobiuronic acid and of hyaluronic acid from umbilical cord," *Journal of the American Chemical Society*, vol. 76, no. 7, pp. 1753–1757, 1954.
- [2] B. P. Toole, "Hyaluronan: from extracellular glue to pericellular cue," *Nature Reviews Cancer*, vol. 4, no. 7, pp. 528–539, 2004.
- [3] P. H. Weigel and P. L. DeAngelis, "Hyaluronan synthases: a decade-plus of novel glycosyltransferases," *The Journal of Biological Chemistry*, vol. 282, no. 51, pp. 36777–36781, 2007.
- [4] N. Itano, T. Sawai, M. Yoshida et al., "Three isoforms of mammalian hyaluronan synthases have distinct enzymatic properties," *The Journal of Biological Chemistry*, vol. 274, no. 35, pp. 25085–25092, 1999.
- [5] R. Stern, "Hyaluronan catabolism: a new metabolic pathway," *European Journal of Cell Biology*, vol. 83, no. 7, pp. 317–325, 2004.
- [6] C. B. Knudson and W. Knudson, "Hyaluronan-binding proteins in development, tissue homeostasis, and disease," *The FASEB Journal*, vol. 7, no. 13, pp. 1233–1241, 1993.
- [7] E. A. Turley, P. W. Noble, and L. Y. W. Bourguignon, "Signaling properties of hyaluronan receptors," *The Journal of Biological Chemistry*, vol. 277, no. 7, pp. 4589–4592, 2002.
- [8] A. J. Day and G. D. Prestwich, "Hyaluronan-binding proteins: tying up the giant," *The Journal of Biological Chemistry*, vol. 277, no. 7, pp. 4585–4588, 2002.
- [9] W. Knudson, G. Chow, and C. B. Knudson, "CD44-mediated uptake and degradation of hyaluronan," *Matrix Biology*, vol. 21, no. 1, pp. 15–23, 2002.
- [10] R. Stern, A. A. Asari, and K. N. Sugahara, "Hyaluronan fragments: an information-rich system," *European Journal of Cell Biology*, vol. 85, no. 8, pp. 699–715, 2006.
- [11] M. S. Pandey, B. A. Baggenstoss, J. Washburn, E. N. Harris, and P. H. Weigel, "The hyaluronan receptor for endocytosis (HARE) activates NF- κ B-mediated gene expression in response to 40–400-kDa, but not smaller or larger, hyaluronans," *The Journal of Biological Chemistry*, vol. 288, no. 20, pp. 14068–14079, 2013.
- [12] X. Tian, J. Azpurua, C. Hine et al., "High-molecular-mass hyaluronan mediates the cancer resistance of the naked mole rat," *Nature*, vol. 499, no. 7458, pp. 346–349, 2013.
- [13] R. Stern, "Devising a pathway for hyaluronan catabolism: are we there yet?" *Glycobiology*, vol. 13, no. 12, pp. 105R–115R, 2003.
- [14] M. R. Horton, C. M. McKee, C. Bao et al., "Hyaluronan fragments synergize with interferon- γ to induce the C-X-C chemokines mig and interferon-inducible protein-10 in mouse macrophages," *The Journal of Biological Chemistry*, vol. 273, no. 52, pp. 35088–35094, 1998.
- [15] M. R. Horton, M. A. Olman, and P. W. Noble, "Hyaluronan fragments induce plasminogen activator inhibitor-1 and inhibit urokinase activity in mouse alveolar macrophages. A potential mechanism for impaired fibrinolytic activity in acute lung injury," *Chest*, vol. 116, supplement 1, p. 17S, 1999.
- [16] P. W. Noble, C. M. McKee, M. Cowman, and H. S. Shin, "Hyaluronan fragments activate an NF- κ B/I- κ B α autoregulatory loop in murine macrophages," *Journal of Experimental Medicine*, vol. 183, no. 5, pp. 2373–2378, 1996.
- [17] P. Rooney, M. Wang, P. Kumar, and S. Kumar, "Angiogenic oligosaccharides of hyaluronan enhance the production of collagens by endothelial cells," *Journal of Cell Science*, vol. 105, part 1, pp. 213–218, 1993.
- [18] R. Deed, P. Rooney, P. Kumar et al., "Early-response gene signalling is induced by angiogenic oligosaccharides of hyaluronan in endothelial cells. Inhibition by non-angiogenic, high-molecular-weight hyaluronan," *International Journal of Cancer*, vol. 71, no. 2, pp. 251–256, 1997.
- [19] S. L. Kaufman, J. W. Skogen, F. D. Dorman, F. Zarrin, and K. C. Lewis, "Macromolecule analysis based on electrophoretic mobility in air: globular proteins," *Analytical Chemistry*, vol. 68, no. 11, pp. 1895–1904, 1996.
- [20] G. Bacher, W. W. Szymanski, S. L. Kaufman, P. Zllner, D. Blaas, and G. Allmaier, "Charge-reduced nano electrospray ionization combined with differential mobility analysis of peptides, proteins, glycoproteins, noncovalent protein complexes and viruses," *Journal of Mass Spectrometry*, vol. 36, no. 9, pp. 1038–1052, 2001.
- [21] L. Malm, U. Hellman, and G. Larsson, "Size determination of hyaluronan using gas-phase electrophoretic mobility molecular analyzer," *Glycobiology*, vol. 22, no. 1, pp. 7–11, 2012.
- [22] P. Gribbon, B. C. Heng, and T. E. Hardingham, "The molecular basis of the solution properties of hyaluronan investigated by confocal fluorescence recovery after photobleaching," *Biophysical Journal*, vol. 77, no. 4, pp. 2210–2216, 1999.
- [23] C. Tolg, S. R. Hamilton, E. Zalinska et al., "A RHAMM mimetic peptide blocks hyaluronan signaling and reduces inflammation and fibrogenesis in excisional skin wounds," *The American Journal of Pathology*, vol. 181, no. 4, pp. 1250–1270, 2012.
- [24] F. Grøndahl, H. Tveit, L. K. Akslen-Hoel, and K. Prydz, "Easy HPLC-based separation and quantitation of chondroitin

- sulphate and hyaluronan disaccharides after chondroitinase ABC treatment,” *Carbohydrate Research*, vol. 346, no. 1, pp. 50–57, 2011.
- [25] S. Hokputsa, K. Jumel, C. Alexander, and S. E. Harding, “A comparison of molecular mass determination of hyaluronic acid using SEC/MALLS and sedimentation equilibrium,” *European Biophysics Journal*, vol. 32, no. 5, pp. 450–456, 2003.
- [26] M. K. Cowman and R. Mendichi, “Methods for determination of hyaluronan molecular weight,” in *Chemistry and Biology of Hyaluronan*, H. G. Garg and C. A. Hales, Eds., pp. 41–69, Elsevier, Amsterdam, The Netherlands, 2004.
- [27] M. H. Moon, “Flow field-flow fractionation and multiangle light scattering for ultrahigh molecular weight sodium hyaluronate characterization,” *Journal of Separation Science*, vol. 33, no. 22, pp. 3519–3529, 2010.
- [28] P. S. Harmon, E. P. Maziarz, and X. M. Liu, “Detailed characterization of hyaluronan using aqueous size exclusion chromatography with triple detection and multiangle light scattering detection,” *Journal of Biomedical Materials Research Part B, Applied Biomaterials*, vol. 100, no. 7, pp. 1955–1960, 2012.
- [29] M. K. Cowmana, C. C. Chen, M. Pandya et al., “Improved agarose gel electrophoresis method and molecular mass calculation for high molecular mass hyaluronan,” *Analytical Biochemistry*, vol. 417, no. 1, pp. 50–56, 2011.
- [30] S. Bhilocha, A. Ripal, M. Pandya et al., “Agarose and polyacrylamide gel electrophoresis methods for molecular mass analysis of 5- to 500-kDa hyaluronan,” *Analytical Biochemistry*, vol. 417, no. 1, pp. 41–49, 2011.
- [31] P. Hansell, V. Goransson, C. Odling, B. Gerdin, and R. Hallgren, “Hyaluronan content in the kidney in different states of body hydration,” *Kidney International*, vol. 58, no. 5, pp. 2061–2068, 2000.

Review Article

Regulated Hyaluronan Synthesis by Vascular Cells

Manuela Viola, Evgenia Karousou, Maria Luisa D'Angelo, Ilaria Caon, Giancarlo De Luca, Alberto Passi, and Davide Vigetti

Department of Surgical and Morphological Sciences, University of Insubria, 21100 Varese, Italy

Correspondence should be addressed to Davide Vigetti; davide.vigetti@uninsubria.it

Received 23 October 2014; Accepted 27 January 2015

Academic Editor: Paul H. Weigel

Copyright © 2015 Manuela Viola et al. This is an open access article distributed under the Creative Commons Attribution License, which permits unrestricted use, distribution, and reproduction in any medium, provided the original work is properly cited.

Cellular microenvironment plays a critical role in several pathologies including atherosclerosis. Hyaluronan (HA) content often reflects the progression of this disease in promoting vessel thickening and cell migration. HA synthesis is regulated by several factors, including the phosphorylation of HA synthase 2 (HAS2) and other covalent modifications including ubiquitination and O-GlcNAcylation. Substrate availability is important in HA synthesis control. Specific drugs reducing the UDP precursors are able to reduce HA synthesis whereas the hexosamine biosynthetic pathway (HBP) increases the concentration of HA precursor UDP-N-acetylglucosamine (UDP-GlcNAc) leading to an increase of HA synthesis. The flux through the HBP in the regulation of HA biosynthesis in human aortic vascular smooth muscle cells (VSMCs) was reported as a critical aspect. In fact, inhibiting O-GlcNAcylation reduced HA production whereas increased O-GlcNAcylation augmented HA secretion. Additionally, O-GlcNAcylation regulates HAS2 gene expression resulting in accumulation of its mRNA after induction of O-GlcNAcylation with glucosamine treatments. The oxidized LDLs, the most common molecules related to atherosclerosis outcome and progression, are also able to induce a strong HA synthesis when they are in contact with vascular cells. In this review, we present recent described mechanisms involved in HA synthesis regulation and their role in atherosclerosis outcome and development.

1. Introduction

Cardiovascular diseases, which include heart attacks, strokes, and peripheral vascular disease, are the first cause of death in Asia, Europe, and United States [1]. Atherosclerosis is the underlying cause of such vascular disorders, and even though its pathogenesis has been actively investigated in the last decades, several aspects are still elusive. Among the factors involved in plaque formation and progression as well as in vessel thickening (i.e., neointima formation after vascular surgery such as angioplasty or stent placement), extracellular matrix (ECM) plays a pivotal role [2]. ECM composition modifies the behavior of different cell types, including the vascular cells. In fact, the cell microenvironment is involved in most diseases by altering several cell functions. Furthermore, several factors influence the ECM architecture promoting endothelial dysfunction [3, 4].

Arteries consist of three layers, known also as tunica, named intima, media, and adventitia, whose architecture differs in cell population and ECM composition. The intima

layer, which is in contact with the bloodstream, is mainly composed of endothelial cells (ECs) attached to the basement membrane. The media are composed of smooth muscle cells (SMCs) producing elastin and small amounts of ECM. The adventitia, the outermost layer, is made by a sheath of fibroblasts with a dense ECM.

Atherosclerotic lesions consist of asymmetric intima thickenings due to a chronic inflammatory response of the arterial wall, initiated by injury caused by hyperglycemia, modified low-density lipoprotein (LDL), or hypertension [5]. The earliest changes that lead to formation of atherosclerotic lesions are due to EC dysfunction [3] and include lowered production of nitric oxide or augmented lipoprotein permeability, immune cell adhesion (by increased ICAM and VCAM), and thrombotic potential [6]. The recruitment of monocytes, which differentiate into macrophages in the intima, is the signal for the secretion of proinflammatory chemokines, including IL-1 β and TNF α . Moreover, activated macrophages produce reactive oxygen species that cause LDL oxidation. In fact, when LDL particles become

trapped in the vessel wall, they undergo progressive oxidation, and they can be internalized by macrophages through scavenger receptors, which are not regulated and lead to the formation of foam cells [7].

The next stage is fatty streak formation, which initially consists of lipid-laden monocytes and macrophages that are engaged with oxidized LDL (oxLDL) forming foam cells together with T lymphocytes. Subsequently, SMC migration from media to fatty streak increases the number of cells in this area [6]. Thus, in the center of atheromatous plaque, foam cells and extracellular lipid droplets form a core region that is surrounded by a cap of SMCs and a collagen-rich matrix [6, 8].

These events drive to a structural reorganization of ECM and as consequence have a crucial role in altered cellular behavior. In the media portion of vascular wall, the ECM in healthy conditions consists largely of type I and type III fibrillar collagens and elastin, whereas in atherosclerotic lesions it consists mainly of proteoglycans (PGs), such as versican and HA, intermixed with loosely scattered collagen fibrils [9]. PGs represent a special class of glycoproteins that are heavily glycosylated by one or more covalently attached glycosaminoglycan (GAG) chains. These GAG chains are long, linear carbohydrate polymers that are negatively charged under physiological conditions, due to the occurrence of O-sulfation, N-sulfation, and glucuronic/ iduronic acid groups. On the other hand, HA, made of the glucuronic acid (GlcUA) and N-acetylglucosamine (GlcNAc) disaccharide repeats, is the unique GAG and is not covalently linked to core proteins and not sulfated or epimerized. HA synthesis is catalyzed by three HA synthases (HAS) located on the plasma membrane [10–12]. HA synthesis, therefore, differs completely from that of the other GAGs, which is a typical process localized in the Golgi. HA synthesis is finely regulated by cytokines, growth factors, and prostaglandins, as well as by the precursor availability (i.e., UDP-GlcNAc and UDP-GlcUA), which modulates HAS gene expression [13, 14]. While collagen inhibits cell growth, PGs and HA stimulate SMC proliferation and migration contributing to vessel wall thickening [15–17]. How ECM can modulate cell growth and motility is only partially known. However, PGs can form highly hydrated ECMs that facilitate migration and diffusion of mitogenic molecules, growth factors, and inflammatory mediators. Moreover, ECM remodeling can release active fragments, known as matrikines, of other signaling compounds bound to PGs and GAGs that easily can reach cell surface receptors [18]. Additionally, HA can interact with several cell surface receptors, including CD44, RHAMM, and TLR2/4 that are largely distributed on different cell types, which can trigger internal cell signaling and modulate differentiation, proliferation, migration, and development [19, 20].

In addition to this complex picture, low molecular mass HA can be produced during inflammation due to oxidative stresses, enzymatic degradation by hyaluronidases, and/or aberrations during the HA synthetic process [17]. Interestingly, it was shown that HA synthesis can be induced in ECs by the action of IL-15 in an inflammation model [21]. Although high molecular mass HA exerts antiproliferative,

anti-inflammatory, and protective properties on cells, low molecular mass HA has the surprising ability to activate Toll-like receptor (TLR) 2/4 signaling leading to enhancement cell replication, MMP secretion, and invasive properties [11, 20, 22]. In inflammatory responses, the important role of HA receptors in transition of monocytes to macrophages has been reported [11, 23–26].

This review will describe the known strategies that vascular cells adopt to regulate HA synthesis, which could identify future targets for pharmacological treatments in vascular pathologies.

2. HA Regulation in ECs

ECs are the most inner lining in blood vessels that control transport of nutrients and other substances from the bloodstream into the tissues. Moreover, the endothelium regulates vascular SMC tone, blood clotting, and angiogenesis. ECs also have a critical role in the inflammation mediating the adhesion and the extravasation of immune cells. Typical endothelial proteins like ICAM-1, P-selectin, and VCAM-1 are key molecules in adhesiveness of circulating cells.

Glycocalyx, a complex network of membrane-bound PGs, glycoproteins, and HA that lumenally covers the endothelium, is the real interface between cells and bloodstream. Many cellular properties depend on the glycocalyx composition and integrity [27]. HA in the glycocalyx has a protective role against platelet adhesion and immune cell-EC interactions and therefore fulfills an antithrombotic and anti-inflammatory role [28–30]. As a proof of concept Nagy et al. [31] demonstrated damage of the glycocalyx after treatment with 4-methylumbelliferone (a well-known HA synthesis inhibitor [32]), EC dysfunction, increased macrophage driven plaque inflammation, and increased atherosclerosis.

The basal membrane produced by ECs in healthy vessels is mainly composed by collagen IV and laminin. In the early stage of the progression of atherosclerosis, which means before the monocytes are recruited, the inflammatory condition changes the basal membrane into a transitional matrix, which contains fibronectin and fibrinogen [33]. Such a switch alters EC response to flow and shear stress and induces NF- κ B activating integrins. As a consequence, the new integrin binding to the inflammatory ECM changes gene expression and enhances endothelial permeability [34].

HA synthesis has been found to be inducible in EC cultures, and its synthesis is triggered by proinflammatory mediators such as IL-1 β , IL15, TNF- α , and lipopolysaccharide [35]. The increased secretion of HA during inflammation is due to the overexpression of the isoenzyme HAS2 [21, 36]. The cellular pathway that leads to HAS2 expression involves a NF- κ B pathway. Increased HA, together with an augment of the typical adhesion molecules, is responsible for the increased binding of immune cells to ECs and is critical for regulating tissue inflammation. Interestingly, CD44 is also overexpressed in ECs treated with proinflammatory mediators, suggesting a particular model of EC/immune cell interaction. In this model, newly synthesized HA would be kept above the endothelium by CD44, and leukocytes

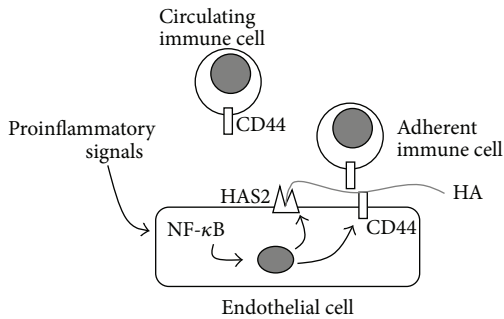


FIGURE 1: Schematic representation of the regulation of HA synthesis in ECs and the effects on immune cell-EC adhesion. Through their receptors, proinflammatory signals (i.e., cytokines) trigger NF- κ B pathway that regulates both HAS2 and CD44 (and other adhesive molecules such as ICAM-1, E-selectin, VCAM-1, and MHC class I genes) [38]. HAS2 synthesizes high molecular weight HA that interacts with CD44 present on both ECs and immune cells (i.e., leukocytes) in the “sandwich model,” which drives immune cells to adhere to ECs contributing to inflammation. Gray circle represents the nucleus.

would be bound to HA through their own CD44 [37]. Thus, this model highlights the importance of HA synthesis and confirms the critical role of HAS2 in triggering HA synthesis after proinflammatory signal treatments. Figure 1 summarizes the concepts expressed in this paragraph. Together with the alteration of the basal membrane, HA deposition seems therefore to be the earliest signal of the onset of a vascular disease.

3. HA Synthesis Regulation in Vascular Smooth Muscle Cells

Vessel wall ECM is mainly synthesized by SMCs in the media. Different from EC, vascular SMC (VSMC) cultures produce large amounts of HA that can be easily found in the conditioned medium as well as in the VSMC pericellular space. High expression of HAS2 and HAS3 is necessary for HA synthesis in VSMCs as well as the presence of the enzymes for production of substrates via the UDP-glucose dehydrogenase and hexosamine biosynthetic pathway (HBP) [36, 39–41]. From a metabolic point of view, the entering of nutrients in anabolic pathways is a very finely tuned process as all the cellular energetic requirements should be satisfied before biosynthesis of HA is allowed [19]. As the synthesis of HA sugar nucleotide precursors is a high energetic demanding process, we found that adenosine monophosphate activated protein kinase (AMPK) deeply affects HA synthesis [38].

AMPK has a pivotal role in regulating energy homeostasis in eukaryotic cells. In response to a decrease in cellular ATP levels, AMPK reduces the rate of anabolic pathways (ATP-utilizing) and increases the rate of catabolic pathways (ATP-producing) [42]. Through the capacity to detect the ATP:AMP ratio, AMPK acts as a metabolic master switch and phosphorylates key target proteins that control flux through metabolic pathways in order to maintain energy homeostasis. HAS2 is a substrate of AMPK, which

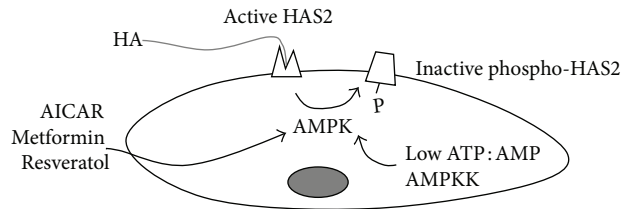


FIGURE 2: Schematic representation of the regulation of HA synthesis by AMPK in SMCs. Through the action of compounds such as AICAR, metformin, and resveratrol or by sensing ATP:AMP ratio or by the action of AMPK upstream kinases (AMPKK), AMPK phosphorylates HAS2 threonine 110 residue inhibiting HAS2 activity and reducing the HA production.

phosphorylates threonine 110 to inhibit HAS2 enzymatic activity [38]. Interestingly, AMPK does not alter the synthesis of other GAGs secreted by VSMCs, highlighting the specificity of AMPK action on HA synthesis. This aspect could explain the vasoprotective effect of AMPK activation, obtained also by the antidiabetic drug metformin, to reduce neointima formation in animal models for atherosclerosis [43] (Figure 2).

Glucose is a major cell substrate, and its utilization is finely regulated allosterically as well as hormonally. HBP represents an alternative glucose pathway in the cells which leads to the formation of the crucial sugar nucleotide UDP-GlcNAc [44]. Besides being a substrate for HA and other glycoconjugate biosyntheses, UDP-GlcNAc is the substrate of O-GlcNAc transferase (OGT), the critical enzyme for protein O-GlcNAcylation [45], which is the reversible modification of nuclear or cytosolic proteins by attachment of a single β -GlcNAc moiety by O-linkage to specific serine/threonine residues. O-GlcNAcylation increased typically in hyperglycemic conditions, due to the entering of the excess of glucose in the HBP, and is involved in several diabetic complications [46–48]. As angiopathies are one of the main complications of diabetes and HA is altered in human diabetic patients [49] as well as in animal models of this pathology [50], it is not surprising that HA synthesis is induced by HAS2 O-GlcNAcylation (Figure 3) [39].

O-GlcNAcylation of HAS2 occurs on serine 221 in the cytoplasmic loop, which stabilizes the enzyme in plasma and cytosolic membranes. This allows the enzyme to have a half-life of more than 5 hours before proteasomal degradation (although in other cell types HAS2 is ubiquitinated [51]). In contrast, HAS2 without this modification only has a half-life of 17 minutes [39].

O-GlcNAcylation is also able to modulate gene expression, and in VSMCs this glycosylation leads to an increment of HAS2 mRNA [52]. The molecular mechanism of such regulation is complex and does not involve the typical O-GlcNAcylated transcription factors that are known to regulate HA synthesis like YY1 and SPI1, which are able to interact with the HAS2 promoter [13]. By using ChIP analyses from mice with high O-GlcNAcylation levels, we found a significant signal in correspondence with the natural antisense transcript for HAS2 (HAS2-AS1), which is a particular long noncoding RNA transcribed using the opposite strand of

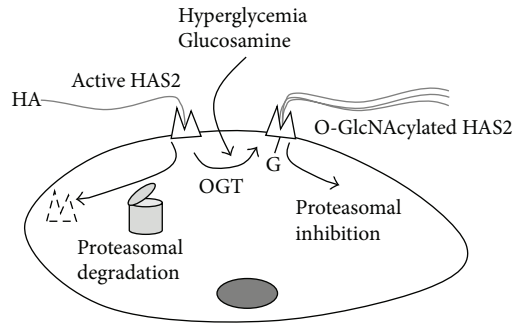


FIGURE 3: Schematic representation of the regulation of HA synthesis by OGT in SMCs. In normal conditions HAS2 in plasma membrane is active but can be rapidly degraded in a 26 S proteasome dependent manner. In hyperglycemic condition or after glucosamine treatments, OGT catalyzes the O-GlcNAcylation of HAS2 serine 221 residue, which greatly stabilizes HAS2 favoring HA production.

HAS2 locus on chromosome 8 [53]. HAS2 and HAS2-AS1 RNA molecules share about 200 base pairs and can form a RNA:RNA duplex. In previous papers antisense transcripts have been described to stabilize their sense mRNA [54, 55], but this mechanism did not work with VSMCs. In contrast, we found that HAS2-AS1 transcription is initiated by O-GlcNAcylation of RelA (a component of NF- κ B complex) [56], and HAS2-AS1 was necessary to change chromatin structure around the HAS2 promoter to allow more efficient binding of RNA polymerase 2, thereby enhancing HAS2 gene expression (Figure 4) [52]. In vivo analyses confirmed the crucial role of HAS2-AS1 in the regulation of HAS2 in humans and in animal models for vascular pathologies [52]. Although investigations are still in progress, our hypothesis is that HAS2-AS1 could alter the epigenetic signature of the HAS2 promoter by switching it into a more active chromatin. The more recent theories about the long noncoding RNA functions highlight their role in recruiting enzymes able to modify histones and DNA in particular loci of the genome [57–60].

4. LDL and HA Metabolism

Despite the great challenge to discover specific markers for the onset of atherosclerosis, at the moment the unique factors routinely evaluated in the clinical practice are the quantification of circulating LDL-cholesterol and the ratio LDL/HDL. The presence within the intima of cholesterol-rich macromolecules induces the formation of foam cells, originating from both macrophages and SMCs [6, 61] encircled by altered ECM. As recently reported, upon activation with the endotoxin LPS, macrophages undergo activation to the M1 phenotype [62] with a concomitant rapid increase in Has1 mRNA and inhibition of hyaluronidases 1 and 2, the major HA degrading enzymes. Nevertheless, HA deposition could only be detected after inhibiting lysosomal and endosomal activities with chloroquine, indicating a rapid turnover and degradation of HA from the ECM [63]. These results are in line with the increasing evidence of the pivotal role of

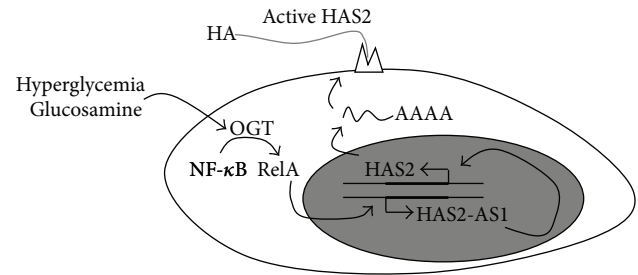


FIGURE 4: Schematic representation of the regulation of HAS2 expression by OGT in SMCs. In normal conditions, basal HAS2 and HAS2-AS1 expression are allowed. After the induction of O-GlcNAcylation (due to hyperglycemia or after glucosamine treatments), the NF- κ B subunit RelA can be modified with O-GlcNAc by OGT. In the cell nucleus, glycosylated RelA can activate HAS2-AS1 transcription, which, in turn, changes chromatin structure around the HAS2 promoter (probably altering chromatin signature) favoring HAS2 expression leading to HA accumulation.

SMCs as ECM modulators. When SMCs resident in the tunica intima and media [64] get in contact with chemically modified LDL, they produce the inflammatory ECM of the plaques. Given the numerous oxidative events associated with the development of an inflammatory atherosclerotic plaque, LDLs, which are accumulated early in the intima primarily from enhanced retention by the GAGs, are converted into oxLDL or into aggregate LDL (aggLDL). Oxidation is the most representative modification, and several enzymatic and nonenzymatic oxidant candidates have been described to be involved [65]. Oxidation may affect both lipid and protein moieties of the particles, and as a result, a series of biologically active species including peroxides, aldehydes, and oxysterols may be produced [66, 67]. The two different modifications of LDL exert different roles in VSMCs. Only oxLDL induced the neosynthesis and deposition of HA, while aggLDL engulfed the cells with lipids without affecting the ECM.

Several scavenger receptors have been reported to be able to internalize oxLDL (e.g., SR-PSOX, SR-AI, CD36, LOX-1, and LRP1). However, even though some of them are present on the SMC membrane, only LOX-1 was upregulated after oxLDL exposure [68, 69]. The oxLDL entrance via LOX-1 has various effects inside the cells: upregulation of LOX-1, increasing the load of lipids and ROS in ER leading to ER stress, and overexpression of HAS2 and HAS3 with concomitant deposition of HA in the ECM (Figure 5), all of which occur during atherosclerosis progression. The increase in HA in the SMC ECM promotes macrophage adhesion and activation as well as their higher migration ability.

LOX-1 is a well-known receptor expressed by vascular ECs, where LOX-1 mediates oxLDL-induced EC apoptosis via an elevation of intracellular NADPH oxidase, which in turn activates the ER stress pathway [70]. However, remarkably, there is no information given for HA metabolism.

The ER stress rescue (also named UPR, unfolded protein response) mechanism is induced in both SMCs and ECs after oxLDL loading, including the expression of several proteins, including CHOP and GRP78, that can modify the activity of transcription factors in the cell nucleus [71]. This intriguing

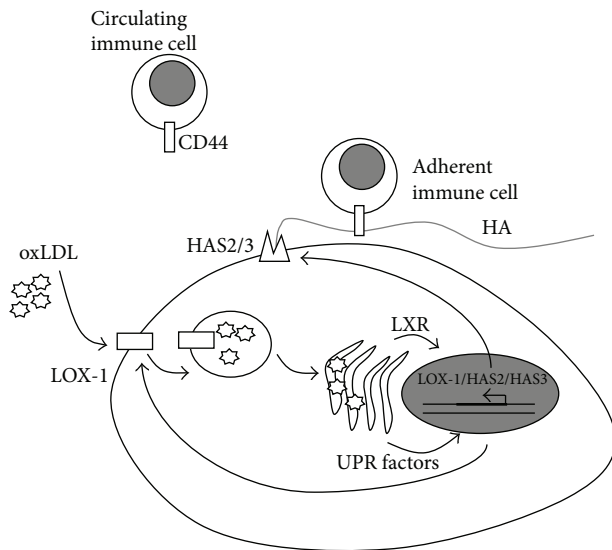


FIGURE 5: Schematic representation of HA metabolism in SMCs loaded with oxidized LDL (oxLDL). Nontoxic concentrations of oxLDL are driven inside the SMCs by the upregulation of the scavenger receptor LOX-1. Accumulation of oxLDL leads to ER stress with overexpression of the UPR factors CHOP and GRP78 as well as activation of the LXR sterol sensor system. One or both systems induce the overexpression in the nucleus of several genes: LOX-1, HAS2, and HAS3. The HASs are active on the plasma membrane where they synthesize HA that interacts with CD44 present on immune cells, driving their adhesion, which contributes to the inflammatory status of the atherosclerotic lesion.

mechanism has been taken into consideration in the investigation of several ECM molecules, including HA [72, 73]. Given the role of LDL in cholesterol metabolism, a key factor in this context is the LXR/RXR sterol sensor system [74]. Liver X receptors (LXR) of the nuclear receptor superfamily are factors that regulate the transcription of several genes involved in cholesterol metabolism. It is noteworthy that the use of cholesterol depleted ox-LDL fails to stimulate HAS2 overexpression and HA synthesis. Interestingly HAS3 was upregulated by these macromolecules; moreover, cholesterol and oxysterols control the expression of HAS3 while only oxysterols can regulate HAS2 transcript levels [69]. It seems therefore evident that a different control of the two enzymes HAS2 and HAS3, regulated by oxysterols/LXR/RXR and/or UPR factors, can reflect their different role in cell behavior.

5. Conclusions

Vessel wall ECM components have a great impact on cell behaviour and, therefore, on vascular pathologies. The critical effect of HA was demonstrated in different ways, and a better knowledge of the mechanisms that control HAS expression could identify future targets for pharmacological treatments of circulatory diseases.

Abbreviations

ECM: Extracellular matrix
HA: Hyaluronan

PGs: Proteoglycans
GAGs: Glycosaminoglycans
MMP: Matrix metalloproteinase
ECs: Endothelial cells
SMCs: Smooth muscle cells
UDP-GlcNAc: Uridine diphosphate-N-acetylglucosamine
HAS: Hyaluronan synthase
AMPK: Adenosine monophosphate activated protein kinase
HBP: Hexosamine biosynthetic pathway
oxLDL: Oxidized low-density lipoproteins.

Conflict of Interests

The authors declare that there is no conflict of interests regarding the publication of this paper.

Acknowledgments

This work was supported by FAR, PRIN, and EU grant IRSES INFLAMA to Alberto Passi. The authors acknowledge the Ph.D. School in Biological and Medical Sciences for Maria Luisa D'Angelo and Ilaria Caon fellowships.

References

- [1] V. L. Roger, A. S. Go, D. M. Lloyd-Jones et al., "Heart disease and stroke statistics—2012 update: a report from the American Heart Association," *Circulation*, vol. 125, no. 1, pp. e2–e220, 2012.
- [2] P. M. Vanhoutte, "Endothelial dysfunction—the first step toward coronary arteriosclerosis," *Circulation Journal*, vol. 73, no. 4, pp. 595–601, 2009.
- [3] M. J. Merrilees, B. W. Beaumont, K. R. Braun et al., "Neointima formed by arterial smooth muscle cells expressing versican variant V3 is resistant to lipid and macrophage accumulation," *Arteriosclerosis, Thrombosis, and Vascular Biology*, vol. 31, no. 6, pp. 1309–1316, 2011.
- [4] B. Messner and D. Bernhard, "Smoking and cardiovascular disease: mechanisms of endothelial dysfunction and early atherogenesis," *Arteriosclerosis, Thrombosis, and Vascular Biology*, vol. 34, no. 3, pp. 509–515, 2014.
- [5] L. Badimon and G. Vilahur, "LDL-cholesterol versus HDL-cholesterol in the atherosclerotic plaque: inflammatory resolution versus thrombotic chaos," *Annals of the New York Academy of Sciences*, vol. 1254, no. 1, pp. 18–32, 2012.
- [6] J. X. Rong, M. Shapiro, E. Trogan, and E. A. Fisher, "Transdifferentiation of mouse aortic smooth muscle cells to a macrophage-like state after cholesterol loading," *Proceedings of the National Academy of Sciences of the United States of America*, vol. 100, no. 23, pp. 13531–13536, 2003.
- [7] J. G. Dickhout, Š. Lhoták, B. A. Hilditch et al., "Induction of the unfolded protein response after monocyte to macrophage differentiation augments cell survival in early atherosclerotic lesions," *The FASEB Journal*, vol. 25, no. 2, pp. 576–589, 2011.
- [8] D. Vigetti, P. Moretto, M. Viola et al., "Matrix metalloproteinase 2 and tissue inhibitors of metalloproteinases regulate human aortic smooth muscle cell migration during in vitro aging," *The FASEB Journal*, vol. 20, no. 8, pp. 1118–1130, 2006.

- [9] R. Ross, "Atherosclerosis—an inflammatory disease," *The New England Journal of Medicine*, vol. 340, no. 2, pp. 115–126, 1999.
- [10] D. Jiang, J. Liang, and P. W. Noble, "Hyaluronan in tissue injury and repair," *Annual Review of Cell and Developmental Biology*, vol. 23, pp. 435–461, 2007.
- [11] D. Jiang, J. Liang, and P. W. Noble, "Hyaluronan as an immune regulator in human diseases," *Physiological Reviews*, vol. 91, no. 1, pp. 221–264, 2011.
- [12] E. G. Karousou, M. Viola, A. Genasetti et al., "Application of polyacrylamide gel electrophoresis of fluorophore-labeled saccharides for analysis of hyaluronan and chondroitin sulfate in human and animal tissues and cell cultures," *Biomedical Chromatography*, vol. 19, no. 10, pp. 761–765, 2005.
- [13] R. H. Tammi, A. G. Passi, K. Rilla et al., "Transcriptional and post-translational regulation of hyaluronan synthesis," *FEBS Journal*, vol. 278, no. 9, pp. 1419–1428, 2011.
- [14] D. Vigetti, M. Viola, E. Karousou, G. de Luca, and A. Passi, "Metabolic control of hyaluronan synthases," *Matrix Biology*, vol. 35, pp. 8–13, 2014.
- [15] S. P. Evanko, J. C. Angello, and T. N. Wight, "Formation of hyaluronan- and versican-rich pericellular matrix is required for proliferation and migration of vascular smooth muscle cells," *Arteriosclerosis, Thrombosis, and Vascular Biology*, vol. 19, no. 4, pp. 1004–1013, 1999.
- [16] D. Vigetti, M. Viola, E. Karousou et al., "Hyaluronan-CD44-ERK1/2 regulate human aortic smooth muscle cell motility during aging," *The Journal of Biological Chemistry*, vol. 283, no. 7, pp. 4448–4458, 2008.
- [17] D. Kothapalli, L. Zhao, E. A. Hawthorne et al., "Hyaluronan and CD44 antagonize mitogen-dependent cyclin D1 expression in mesenchymal cells," *The Journal of Cell Biology*, vol. 176, no. 4, pp. 535–544, 2007.
- [18] J. C. Monboisse, J. B. Oudart, L. Ramont, S. Brassart-Pasco, and F. X. Maquart, "Matrikines from basement membrane collagens: a new anti-cancer strategy," *Biochimica et Biophysica Acta*, vol. 1840, no. 8, pp. 2589–2598, 2014.
- [19] D. Vigetti, E. Karousou, M. Viola, S. Deleonibus, G. de Luca, and A. Passi, "Hyaluronan: biosynthesis and signaling," *Biochimica et Biophysica Acta (BBA)—General Subjects*, vol. 1840, no. 8, pp. 2452–2459, 2014.
- [20] M. Nardini, M. Ori, D. Vigetti, R. Gornati, I. Nardi, and R. Perris, "Regulated gene expression of hyaluronan synthases during *Xenopus laevis* development," *Gene Expression Patterns*, vol. 4, no. 3, pp. 303–308, 2004.
- [21] P. Estess, A. Nandi, M. Mohamadzadeh, and M. H. Siegelman, "Interleukin 15 induces endothelial hyaluronan expression *in vitro* and promotes activated T cell extravasation through a CD44-dependent pathway *in vivo*," *The Journal of Experimental Medicine*, vol. 190, no. 1, pp. 9–19, 1999.
- [22] D. Vigetti and A. Passi, "Hyaluronan synthases posttranslational regulation in cancer," in *Advances in Cancer Research*, vol. 123, pp. 95–119, Elsevier, 2014.
- [23] M. Afanasyeva, D. Georgakopoulos, D. F. Belardi et al., "Quantitative analysis of myocardial inflammation by flow cytometry in murine autoimmune myocarditis: correlation with cardiac function," *The American Journal of Pathology*, vol. 164, no. 3, pp. 807–815, 2004.
- [24] K. L. Brown, A. Maiti, and P. Johnson, "Role of sulfation in CD44-mediated hyaluronan binding induced by inflammatory mediators in human CD14⁺ peripheral blood monocytes," *Journal of Immunology*, vol. 167, no. 9, pp. 5367–5374, 2001.
- [25] S. Shahrara, C. C. Park, V. Temkin, J. W. Jarvis, M. V. Volin, and R. M. Pope, "RANTES modulates TLR4-induced cytokine secretion in human peripheral blood monocytes," *Journal of Immunology*, vol. 177, no. 8, pp. 5077–5087, 2006.
- [26] C. Termeer, F. Benedix, J. Sleeman et al., "Oligosaccharides of hyaluronan activate dendritic cells via Toll-like receptor 4," *Journal of Experimental Medicine*, vol. 195, no. 1, pp. 99–111, 2002.
- [27] S. Reitsma, D. W. Slaaf, H. Vink, M. A. M. J. van Zandvoort, and M. G. A. Oude Egbrink, "The endothelial glycocalyx: composition, functions, and visualization," *Pflugers Archiv European Journal of Physiology*, vol. 454, no. 3, pp. 345–359, 2007.
- [28] B. M. van den Berg, H. Vink, and J. A. E. Spaan, "The endothelial glycocalyx protects against myocardial edema," *Circulation Research*, vol. 92, no. 6, pp. 592–594, 2003.
- [29] A. A. Constantinescu, H. Vink, and J. A. E. Spaan, "Endothelial cell glycocalyx modulates immobilization of leukocytes at the endothelial surface," *Arteriosclerosis, Thrombosis, and Vascular Biology*, vol. 23, no. 9, pp. 1541–1547, 2003.
- [30] H. Vink, A. A. Constantinescu, and J. A. E. Spaan, "Oxidized lipoproteins degrade the endothelial surface layer: implications for platelet-endothelial cell adhesion," *Circulation*, vol. 101, no. 13, pp. 1500–1502, 2000.
- [31] N. Nagy, T. Freudenberger, A. Melchior-Becker et al., "Inhibition of hyaluronan synthesis accelerates murine atherosclerosis: novel insights into the role of hyaluronan synthesis," *Circulation*, vol. 122, no. 22, pp. 2313–2322, 2010.
- [32] T. Nakamura, K. Takagaki, S. Shibata, K. Tanaka, T. Higuchi, and M. Endo, "Hyaluronic-acid-deficient extracellular matrix induced by addition of 4-methylumbelliferone to the medium of cultured human skin fibroblasts," *Biochemical and Biophysical Research Communications*, vol. 208, no. 2, pp. 470–475, 1995.
- [33] A. W. Orr, J. M. Sanders, M. Bevard, E. Coleman, I. J. Sarembock, and M. A. Schwartz, "The subendothelial extracellular matrix modulates NF- κ B activation by flow: a potential role in atherosclerosis," *Journal of Cell Biology*, vol. 169, no. 1, pp. 191–202, 2005.
- [34] A. W. Orr, R. Stockton, M. B. Simmers et al., "Matrix-specific p21-activated kinase activation regulates vascular permeability in atherogenesis," *Journal of Cell Biology*, vol. 176, no. 5, pp. 719–727, 2007.
- [35] A. Genasetti, D. Vigetti, M. Viola et al., "Hyaluronan and human endothelial cell behavior," *Connective Tissue Research*, vol. 49, no. 3–4, pp. 120–123, 2008.
- [36] D. Vigetti, A. Genasetti, E. Karousou et al., "Proinflammatory cytokines induce hyaluronan synthesis and monocyte adhesion in human endothelial cells through hyaluronan synthase 2 (HAS2) and the nuclear factor- κ B (NF- κ B) pathway," *The Journal of Biological Chemistry*, vol. 285, no. 32, pp. 24639–24645, 2010.
- [37] B. Ruffell and P. Johnson, "The regulation and function of hyaluronan binding by CD44 in the immune system," 2009.
- [38] D. Vigetti, M. Clerici, S. Deleonibus et al., "Hyaluronan synthesis is inhibited by adenosine monophosphate-activated protein kinase through the regulation of HAS2 activity in human aortic smooth muscle cells," *Journal of Biological Chemistry*, vol. 286, no. 10, pp. 7917–7924, 2011.
- [39] D. Vigetti, S. Deleonibus, P. Moretto et al., "Role of UDP-N-acetylglucosamine (GlcNAc) and O-GlcNacylation of hyaluronan synthase 2 in the control of chondroitin sulfate and hyaluronan synthesis," *The Journal of Biological Chemistry*, vol. 287, no. 42, pp. 35544–35555, 2012.

- [40] D. Vigetti, M. Ori, M. Viola et al., "Molecular cloning and characterization of UDP-glucose dehydrogenase from the amphibian *Xenopus laevis* and its involvement in hyaluronan synthesis," *Journal of Biological Chemistry*, vol. 281, no. 12, pp. 8254–8263, 2006.
- [41] D. Vigetti, M. Rizzi, M. Viola et al., "The effects of 4-methylumbelliferone on hyaluronan synthesis, MMP2 activity, proliferation, and motility of human aortic smooth muscle cells," *Glycobiology*, vol. 19, no. 5, pp. 537–546, 2009.
- [42] H. D. Grahame, "AMPK: a target for drugs and natural products with effects on both diabetes and cancer," *Diabetes*, vol. 62, no. 7, pp. 2164–2172, 2013.
- [43] I. Pernicova and M. Korbonits, "Metformin—mode of action and clinical implications for diabetes and cancer," *Nature Reviews Endocrinology*, vol. 10, no. 3, pp. 143–156, 2014.
- [44] C. Butkinaree, K. Park, and G. W. Hart, "O-linked β -N-acetylglucosamine (O-GlcNAc): extensive crosstalk with phosphorylation to regulate signaling and transcription in response to nutrients and stress," *Biochimica et Biophysica Acta (BBA)—General Subjects*, vol. 1800, no. 2, pp. 96–106, 2010.
- [45] G. W. Hart, M. P. Housley, and C. Slawson, "Cycling of O-linked β -N-acetylglucosamine on nucleocytoplasmic proteins," *Nature*, vol. 446, no. 7139, pp. 1017–1022, 2007.
- [46] M. G. Buse, "Hexosamines, insulin resistance, and the complications of diabetes: current status," *American Journal of Physiology—Endocrinology and Metabolism*, vol. 290, no. 1, pp. E1–E8, 2006.
- [47] B. Laczy, B. G. Hill, K. Wang et al., "Protein O-GlcNAcylation: a new signaling paradigm for the cardiovascular system," *The American Journal of Physiology—Heart and Circulatory Physiology*, vol. 296, no. 1, pp. H13–H28, 2009.
- [48] J. Nigro, N. Osman, A. M. Dart, and P. J. Little, "Insulin resistance and atherosclerosis," *Endocrine Reviews*, vol. 27, no. 3, pp. 242–259, 2006.
- [49] L. Heickendorff, T. Ledet, and L. M. Rasmussen, "Glycosaminoglycans in the human aorta in diabetes mellitus: a study of tunica media from areas with and without atherosclerotic plaque," *Diabetologia*, vol. 37, no. 3, pp. 286–292, 1994.
- [50] T. O. McDonald, R. G. Gerrity, C. Jen et al., "Diabetes and arterial extracellular matrix changes in a porcine model of atherosclerosis," *Journal of Histochemistry and Cytochemistry*, vol. 55, no. 11, pp. 1149–1157, 2007.
- [51] E. Karousou, M. Kamiry, S. S. Skandalis et al., "The activity of hyaluronan synthase 2 is regulated by dimerization and ubiquitination," *The Journal of Biological Chemistry*, vol. 285, no. 31, pp. 23647–23654, 2010.
- [52] D. Vigetti, S. Deleonibus, P. Moretto et al., "Natural antisense transcript for hyaluronan synthase 2 (HAS2-AS1) induces transcription of HAS2 via protein O-GlcNAcylation," *The Journal of Biological Chemistry*, vol. 289, no. 42, pp. 28816–28826, 2014.
- [53] H. Chao and A. P. Spicer, "Natural antisense mRNAs to hyaluronan synthase 2 inhibit hyaluronan biosynthesis and cell proliferation," *The Journal of Biological Chemistry*, vol. 280, no. 30, pp. 27513–27522, 2005.
- [54] D. R. Michael, A. O. Phillips, A. Krupa et al., "The human hyaluronan synthase 2 (HAS2) gene and its natural antisense RNA exhibit coordinated expression in the renal proximal tubular epithelial cell," *The Journal of Biological Chemistry*, vol. 286, no. 22, pp. 19523–19532, 2011.
- [55] M. A. Faghihi, F. Modarresi, A. M. Khalil et al., "Expression of a noncoding RNA is elevated in Alzheimer's disease and drives rapid feed-forward regulation of beta-secretase," *Nature Medicine*, vol. 14, no. 7, pp. 723–730, 2008.
- [56] D. F. Allison, J. J. Wamsley, M. Kumar et al., "Modification of RelA by O-linked N-acetylglucosamine links glucose metabolism to NF- κ B acetylation and transcription," *Proceedings of the National Academy of Sciences of the United States of America*, vol. 109, no. 42, pp. 16888–16893, 2012.
- [57] D. Vigetti, M. Viola, E. Karousou et al., "Epigenetics in extracellular matrix remodeling and hyaluronan metabolism," *FEBS Journal*, vol. 281, no. 22, pp. 4980–4992, 2014.
- [58] T. R. Mercer and J. S. Mattick, "Structure and function of long noncoding RNAs in epigenetic regulation," *Nature Structural and Molecular Biology*, vol. 20, no. 3, pp. 300–307, 2013.
- [59] M. Magistri, M. A. Faghihi, G. St Laurent, and C. Wahlestedt, "Regulation of chromatin structure by long noncoding RNAs: focus on natural antisense transcripts," *Trends in Genetics*, vol. 28, no. 8, pp. 389–396, 2012.
- [60] J. T. Lee, "Epigenetic regulation by long noncoding RNAs," *Science*, vol. 338, no. 6113, pp. 1435–1439, 2012.
- [61] A. C. Doran, N. Meller, and C. A. McNamara, "Role of smooth muscle cells in the initiation and early progression of atherosclerosis," *Arteriosclerosis, Thrombosis, and Vascular Biology*, vol. 28, no. 5, pp. 812–819, 2008.
- [62] A. Sica and A. Mantovani, "Macrophage plasticity and polarization: in vivo veritas," *The Journal of Clinical Investigation*, vol. 122, no. 3, pp. 787–795, 2012.
- [63] M. Y. Chang, Y. Tanino, V. Vidova et al., "Reprint of: a rapid increase in macrophage-derived versican and hyaluronan in infectious lung disease," *Matrix Biology*, vol. 35, pp. 162–173, 2014.
- [64] P. Libby, P. M. Ridker, and G. K. Hansson, "Progress and challenges in translating the biology of atherosclerosis," *Nature*, vol. 473, no. 7347, pp. 317–325, 2011.
- [65] R. Stocker and J. F. Kearney Jr., "Role of oxidative modifications in atherosclerosis," *Physiological Reviews*, vol. 84, no. 4, pp. 1381–1478, 2004.
- [66] T. Hevonoja, M. O. Pentikäinen, M. T. Hyvönen, P. T. Kovanen, and M. Ala-Korpela, "Structure of low density lipoprotein (LDL) particles: basis for understanding molecular changes in modified LDL," *Biochimica et Biophysica Acta*, vol. 1488, no. 3, pp. 189–210, 2000.
- [67] H. Yoshida and R. Kisugi, "Mechanisms of LDL oxidation," *Clinica Chimica Acta*, vol. 411, no. 23–24, pp. 1875–1882, 2010.
- [68] S. Mitra, T. Goyal, and J. L. Mehta, "Oxidized LDL, LOX-1 and atherosclerosis," *Cardiovascular Drugs and Therapy*, vol. 25, no. 5, pp. 419–429, 2011.
- [69] M. Viola, B. Bartolini, D. Vigetti et al., "Oxidized low density lipoprotein (LDL) affects hyaluronan synthesis in human aortic smooth muscle cells," *The Journal of Biological Chemistry*, vol. 288, no. 41, pp. 29595–29603, 2013.
- [70] D. Hong, Y.-P. Bai, H.-C. Gao et al., "Ox-LDL induces endothelial cell apoptosis via the LOX-1-dependent endoplasmic reticulum stress pathway," *Atherosclerosis*, vol. 235, no. 2, pp. 310–317, 2014.
- [71] I. Tabas and D. Ron, "Integrating the mechanisms of apoptosis induced by endoplasmic reticulum stress," *Nature Cell Biology*, vol. 13, no. 3, pp. 184–190, 2011.
- [72] D. Vigetti, A. Genasetti, E. Karousou et al., "Modulation of hyaluronan synthase activity in cellular membrane fractions," *The Journal of Biological Chemistry*, vol. 284, no. 44, pp. 30684–30694, 2009.

- [73] D. Vigetti, E. Karousou, M. Viola, and A. Passi, "Analysis of hyaluronan synthase activity," in *Glycosaminoglycans*, vol. 1229 of *Methods in Molecular Biology*, pp. 201–208, Springer, New York, NY, USA, 2015.
- [74] A. C. Calkin and P. Tontonoz, "Transcriptional integration of metabolism by the nuclear sterol-activated receptors LXR and FXR," *Nature Reviews Molecular Cell Biology*, vol. 13, no. 4, pp. 213–224, 2012.

Research Article

Extracellular Vesicles from Caveolin-Enriched Microdomains Regulate Hyaluronan-Mediated Sustained Vascular Integrity

Tamara Mirzapoiazova,¹ Frances E. Lennon,² Bolot Mambetsariev,¹ Michael Allen,¹ Jacob Riehm,¹ Valeriy A. Poroyko,³ and Patrick A. Singleton^{1,4}

¹Department of Medicine, Section of Pulmonary and Critical Care, Pritzker School of Medicine, The University of Chicago, Chicago, IL, USA

²Department of Medicine, Section of Hematology/Oncology, Pritzker School of Medicine, The University of Chicago, Chicago, IL, USA

³Department of Surgery, Pritzker School of Medicine, The University of Chicago, Chicago, IL, USA

⁴Department of Anesthesia and Critical Care, Pritzker School of Medicine, The University of Chicago, Chicago, IL, USA

Correspondence should be addressed to Patrick A. Singleton; psinglet@medicine.bsd.uchicago.edu

Received 5 September 2014; Accepted 8 December 2014

Academic Editor: Hans Hermann Gerdes

Copyright © 2015 Tamara Mirzapoiazova et al. This is an open access article distributed under the Creative Commons Attribution License, which permits unrestricted use, distribution, and reproduction in any medium, provided the original work is properly cited.

Defects in vascular integrity are an initiating factor in several disease processes. We have previously reported that high molecular weight hyaluronan (HMW-HA), a major glycosaminoglycan in the body, promotes rapid signal transduction in human pulmonary microvascular endothelial cells (HPMVEC) leading to barrier enhancement. In contrast, low molecular weight hyaluronan (LMW-HA), produced in disease states by hyaluronidases and reactive oxygen species (ROS), induces HPMVEC barrier disruption. However, the mechanism(s) of sustained barrier regulation by HA are poorly defined. Our results indicate that long-term (6–24 hours) exposure of HMW-HA induced release of a novel type of extracellular vesicle from HPMVEC called enlargeosomes (characterized by AHNAK expression) while LMW-HA long-term exposure promoted release of exosomes (characterized by CD9, CD63, and CD81 expression). These effects were blocked by inhibiting caveolin-enriched microdomain (CEM) formation. Further, inhibiting enlargeosome release by annexin II siRNA attenuated the sustained barrier enhancing effects of HMW-HA. Finally, exposure of isolated enlargeosomes to HPMVEC monolayers generated barrier enhancement while exosomes led to barrier disruption. Taken together, these results suggest that differential release of extracellular vesicles from CEM modulate the sustained HPMVEC barrier regulation by HMW-HA and LMW-HA. HMW-HA-induced specialized enlargeosomes can be a potential therapeutic strategy for diseases involving impaired vascular integrity.

1. Introduction

Vascular integrity (i.e., the maintenance of blood vessel continuity) is required for normal cardiovascular homeostasis [1, 2]. Several mechanisms regulate basal vascular integrity including the endothelial glycocalyx and endothelial cell-cell junctions which are controlled by tight junctions, adherens junctions, and caveolin-enriched microdomains (CEM), a subset of lipid rafts containing the scaffolding protein caveolin-1 [1, 3–7]. Certain pathologies, including atherosclerosis, sepsis, ischemia/reperfusion, acute lung injury, diabetes, and cancer metastasis, induce degradation of the glycocalyx and disruption of EC-EC junctions causing

leakage of fluids and proteins into the underlying tissue [1, 2, 4, 8, 9]. Therefore, understanding the mechanism(s) of EC barrier regulation can have important clinical utility.

The major nonsulfated glycosaminoglycan in most tissues, hyaluronan (HA), plays a fundamental role in the maintenance of vascular integrity [4, 8, 10–17]. We have previously demonstrated that HA and its major cell surface receptor, CD44, regulate pulmonary vascular integrity and that HMW-HA could potentially be utilized as a therapeutic intervention for defects in vascular integrity [5, 18, 19]. Specifically, HMW-HA (~1 million Da) binds to the transmembrane receptor, CD44s (standard form), in CEM which initiates a rapid signal transduction cascade. CD44s transactivates the barrier

enhancing SIP1 receptor within CEM which results in the serine/threonine kinase, Akt-mediated activation of the Rac1 guanine nucleotide exchange factor, Tiam1, and Rac1-GTP formation leading to cortical actin formation and strengthening of EC-EC contacts. Further, HMW-HA recruits several other actin regulatory proteins to CEM including protein S100-A10, filamin-A, and filamin-B which enhance cortical actin formation and vascular integrity. In contrast to HMW-HA, LMW-HA (~2,500 Da) binds to and activates the HA receptor, CD44v10 (variant 10) in CEM. CD44v10 then transactivates the barrier disruptive SIP3 receptor. These events promote RhoA guanine nucleotide exchange factor (RhoGEF) activation and RhoA-GTP formation which stimulates the serine/threonine kinase, rho kinase (ROCK). This leads to actin stress fiber formation and EC barrier disruption. However, the long-term sustained pulmonary EC barrier regulatory mechanism(s) by HA is poorly defined.

Extracellular vesicles (EVs) come in several types including microvesicles, exosome-like vesicles, exosomes, and membrane particles [20, 26–29]. Each type has specific protein markers and is formed from either budding of the plasma membrane or release of intracellular multivesicular endosomes [20]. EVs range in size from 20 to 1,000 nm and are released by a variety of cells including EC [20]. EVs are believed to be a means of cell-cell communication and can transport proteins, mRNA, and miRNA to target cells [20, 30]. Enlargeosomes are specialized vesicles enriched in AHNAK and annexin II that have been observed intracellularly, fusing to the plasma membrane and shedding from the plasma membrane [21–23]. However, the role(s) of EV in HA-mediated sustained vascular integrity are unknown.

In the current study, we investigated the mechanism of HA-mediated long-term EC barrier regulation. We have identified that ~6 hours after HA addition, human EC differentially release EVs that contain caveolin-1 and are regulated by CEM. Utilizing several novel techniques including atomic force microscopy and nanosight nanoparticle tracking analysis (NTA), we have characterized these EVs as exosomes (for LMW-HA) and enlargeosomes (for HMW-HA). Importantly, isolated LMW-HA-induced exosomes promote EC barrier disruption while isolated HMW-HA-induced enlargeosomes induce EC barrier enhancement. Inhibiting HMW-HA-induced enlargeosome release reduces the sustained barrier enhancing properties of HMW-HA. These EVs differentially express HA, HA binding proteins, and microRNA which can potentially contribute to their differential EC barrier regulatory effects. Our findings demonstrate an important mechanism of HA-induced sustained vascular integrity through differential release of EV from human EC. Further, utilization of isolated HMW-HA-induced specialized enlargeosomes and/or their bioactive components can be a potential therapeutic strategy for diseases involving impaired vascular integrity.

2. Materials and Methods

2.1. Antibodies and Reagent. Antibodies utilized in this study include anti-CD9 (Santa Cruz Biotechnology Inc.,

Dallas, TX), anti-CD63 (Abcam, Cambridge, MA), anti-CD81 (GeneTex Inc., Irvine, CA), anti-AHNAK 1 (Thermo Scientific, Waltham, MA), anti-HABP2 (Abnova, Walnut, CA), anti-CD44 (IM7 clone) (BD Biosciences), anti-CD44v10 (Novus Biologicals), and anti-actin (Sigma). Hyaluronic acid (sodium salt from *Streptococcus zooepidemicus*), LPS, ATP, and ionomycin were purchased from Sigma. Reagents for SDS-PAGE electrophoresis were purchased from Bio-Rad (Richmond, CA) and Immobilon-P transfer membrane was purchased from Millipore (Millipore Corp., Bedford, MA).

2.2. Human Pulmonary Microvascular Endothelial Cell (HPMVEC) Culture. Primary human pulmonary microvascular cells were purchased from Lonza and maintained in EBM-2 growth media supplemented with EGM-2-MV Bulletkit and 10% fetal bovine serum. Cells were maintained at 37°C in a humidified atmosphere of 5% CO₂-95% air and used for experimentation at passages 3–6.

2.3. Preparation of LMW-HA. LMW-HA was prepared similar to that as we have previously described [9, 31]. Briefly 500 mg of hyaluronan sodium salt from *Streptococcus zooepidemicus* was digested with 20,000 units of bovine testicular hyaluronidase (Type VI-S, lyophilized powder, 3,000–15,000 units/mg (Sigma, H3631) in digestion buffer (0.1 M sodium acetate, pH 5.4, 0.15 M NaCl) for 24 h), and the reaction stopped with 10% trichloroacetic acid. The resulting solution was centrifuged in an Ultrafree-MC Millipore 5 kDa MW cutoff filter and the flow-through was dialyzed against distilled water for 24 h at 4°C in 500 Da cutoff Spectra-Por tubing (Pierce-Warriner, Chester, UK). LMW-HA was quantitated using an ELISA-like competitive binding assay with a known amount of fixed HA and biotinylated HA binding peptide (HABP) as the indicator (Echelon Inc). LMW-HA solutions were filtrated through 0.22 µm filters and kept in sterile tubes. In some cases, both low and high MW HA were subject to boiling, proteinase K (50 µg/mL) digestion, hyaluronidase SD digestion (*Streptococcus dysgalactiae*, NorthStar Bioproducts Associates of Cape Cod Inc., East Falmouth, MA (100741-1A), 100 mU/mL utilized), or addition of boiled (inactivated) hyaluronidase SD to test for possible protein/lipid contaminants. To test for endotoxin contamination of HA, a lipopolysaccharides (LPS) bioAssay ELISA kit (USBiological Life Sciences) was utilized. LMW-HA with HA standards (Sigma and Enzo Life Sciences) were run on 4–20% Tris/Borate/EDTA (TBE) gels and stained with Stains-All (Sigma) or Alcian blue to confirm LMW-HA purity and size.

2.4. Inhibition of Protein Expression in Human EC Utilizing siRNA. Human lung microvascular EC were transfected with siRNA against human annexin II mRNA (Santa Cruz Biotechnology, Santa Cruz, CA) using siPORT Amine as the transfection reagent (Ambion, TX) according to the protocol provided by Ambion. Cells (~40% confluent) were serum-starved for 1 hour followed by incubation with 250 nM of target siRNA (or scramble siRNA or no siRNA) for 6 hours in serum-free media. The serum-containing media were

then added (10% serum final concentration) for 42 h before biochemical experiments and/or functional assays were conducted. Effective silencing of target protein expression was determined with immunoblot analysis of siRNA-transfected EC lysates using specific antibodies.

2.5. Extracellular Vesicle (EV) Isolation. EVs were isolated from cell-free media from treated EC for 0, 1, 2, 3, 6, 12, or 24 hours. The conditioned media were centrifuged at $300 \times g$ for 15 min, $2,000 \times g$ for 30 min, and $12,000 \times g$ for 45 min to remove whole cells and debris. The resultant supernatant was passed through a 0.22 mm filter sterilized Steritop (Millipore, Billerica, MA, USA) and then centrifuged at $100,000 \times g$ for 75 min (Thermo Fisher Scientific Ins., Asheville, NC, USA, Sorvall, SureSpin 630/36, fixed angle rotor). The pellet was resuspended in PBS, pH = 7.4, washed, and recentrifuged ($100,000 \times g$, 75 min). The pellet was then resuspended in PBS and overlaid on a discontinuous OptiPrep gradient (40, 20, 10, and 5% OptiPrep solution in 0.25 M sucrose, 10 mM Tris, pH 7.5) and centrifuged at $100,000 \times g$ for 16 h. The EVs float at a density of 1.10–1.12 g/mL OptiPrep. Fractions were collected from the top of the gradient, diluted with 10 mM Tris buffer, and centrifuged at $100,000 \times g$ for 3 h; the subsequent pellets were resuspended in PBS, pH = 7.4, and subjected to EV characterization [32, 33].

2.6. Immunoblotting. Extracellular vesicles from treated or untreated HPMVEC were incubated with IP buffer (50 mM HEPES (pH 7.5), 150 mM NaCl, 20 mM $MgCl_2$, 1% Nonidet P-40 (NP-40), 0.4 mM Na_3VO_4 , 40 mM NaF, 50 μM okadaic acid, 0.2 mM phenylmethylsulfonyl fluoride, and 1:250 dilution of Calbiochem protease inhibitor mixture 3). The samples were then run on SDS-PAGE in 4–15% polyacrylamide gels, transferred onto Immobilon membranes, and developed with specific primary and secondary antibodies. Visualization of immunoreactive bands was achieved using enhanced chemiluminescence (Amersham Biosciences). In some instances, computer-assisted densitometry was utilized to quantitate immunoreactive bands.

2.7. Isolation of Exosomal RNA and RNA Analysis. Exosomal pellets were dissolved in lysis buffer from RNAs isolation kit mirVana (Ambion/Life Technologies, Carlsbad, CA) and processed for small RNA isolation using column based methods according to the manufacturer's instruction. For detection and analysis of the extracted exosomal small RNAs, we used an Agilent 2100 Bioanalyzer with a small RNA chip kit (Agilent Technologies).

2.8. Transendothelial Electrical Resistance (TER). For EC barrier function, human pulmonary microvascular endothelial cells were grown to confluence in polycarbonate wells containing evaporated gold microelectrodes (surface area, $10\text{--}3\text{ cm}^2$) in series with a large gold counter electrode (1 cm^2) connected to a phase-sensitive lock-in amplifier as described previously. Measurements of transendothelial electrical resistance (TER) were performed using an electrical cell-substrate impedance sensing system (ECIS) (Applied BioPhysics Inc.).

Briefly, current was applied across the electrodes by a 4,000-Hz AC voltage source with amplitude of 1 V in series with a $1\text{ M}\Omega$ resistance to approximate a constant current source ($1\ \mu A$). As cells adhere and spread out on the microelectrode, TER increases (maximal at confluence), whereas cell retraction, rounding, or loss of adhesion is reflected by a decrease in TER. These measurements provide a highly sensitive biophysical assay that indicates the state of cell shape and focal adhesion. Values from each microelectrode were pooled at discrete time points and plotted versus time as the mean \pm SE of the mean [34–37].

2.9. Atomic Force Microscopy (AFM). AFM was utilized similar to that as we have previously described [34]. Briefly, AFM offers a novel way to analyze the morphology and size of EV [38]. Isolate EVs were diluted in PBS, pH = 7.4, and plated on mica. AFM (tapping mode) was then utilized on a DI multimode AFM (Digital Instruments, Santa Barbara, CA) using a V-shaped oxide-sharpened silicon nitride cantilever with an optical scanning speed of ~ 1.0 Hz to obtain surface topology maps.

2.10. Nanosight Nanoparticle Tracking Analysis (NTA). EVs as described above were subjected to NTA analysis as previously described [39]. NTA utilizes the properties of both light scattering and Brownian motion in order to predict particle size distributions of dilute samples in liquid suspension. A 635 nm laser beam was passed through a prism-edged glass flat under the ultrathin sample chamber. The angle of incidence of the laser and the refractive index of the glass are designed to illuminate the sample chamber, and the light is refracted by particles in the sample solution. The scattered beam light from a sample of EV diluted in PBS, pH = 7.4, was visualized using a 20x magnification microscope objective fitted to a conventional optical microscope. A high-sensitivity complementary metal oxide semiconductor camera recorded 30 frames per second video of the scattered light. A triplicate of 60 s video files was recorded for each sample, advancing the sample solution to a new $100\ \mu m \times 80\ \mu m \times 10\ \mu m$ field of view for each recording. The Nanosight software (v3.0) was then used to identify and track individual particles on a frame-by-frame basis. The mean squared two-dimensional displacement of each tracked particle was recorded and, coupled with the temperature, viscosity of the suspension media, and the Stokes-Einstein equation, was used to estimate a sphere equivalent hydrodynamic radius. The software tracked multiple EVs, with parameters set by the user, to provide a particle size distribution and concentration of the sample.

2.11. Statistical Analysis. Results are expressed as mean \pm standard deviation of three independent experiments. For data analysis, experimental samples were compared to controls by unpaired Student's *t*-test. For multiple-group comparisons, a one-way variance analysis (ANOVA) and post hoc multiple comparisons tests were used. Differences between groups were considered statistically significant when *P* value was less than 0.05. All statistical analyses were performed

using the GraphPad Prism program (GraphPad Software Inc., USA).

3. Results

In order to identify potential mechanism(s) of hyaluronan-(HA-) mediated sustained human endothelial cell (EC) barrier function, we first determined the kinetics of HA-induced extracellular vesicle (EV) release. Human pulmonary microvascular EC (HPMVEC) were grown to confluence and placed in serum-free media, and no HA (control), 100 nm HMW-HA, or 100 nm LMW-HA were added for 0, 1, 2, 3, 6, 12, or 24 hours. Treated media were then collected and analyzed using nanosight nanoparticle tracking analysis (NTA) to determine EV concentrations (see Section 2). The results of Figure 1(a) indicate that HPMVEC secrete basal levels of EV. However, there is a dramatic increase in EV release from HPMVEC with either LMW-HA or HMW-HA addition starting at ~6 hours.

Since caveolin-1 has been implicated in EV release [40] and we have previously demonstrated that caveolin-enriched microdomains (CEM) are crucial for EC barrier function [5–7, 41, 42], we next examined whether CEM regulate HA-induced EV secretion in HPMVEC. Figure 1(b) indicates that inhibiting CEM formation with methyl-beta-cyclodextrin ($M\beta CD$) inhibits both LMW-HA and HMW-HA-induced EV from HPMVEC (24-hour treatment) indicating the important role of this specialized plasma membrane microdomain in HA-induced EV secretion.

We next characterized HA-induced EV using biomarker analysis and atomic force microscopy (AFM). The results of Figure 2(a) indicate that LMW-HA induces EV with biomarkers consistent with exosomes (CD9, CD63, and CD81). In contrast, HMW-HA induces EV with biomarkers consistent with a novel vesicle called an enlargeosome. Enlargeosomes are specialized vesicles enriched in AHNAK and annexin II that have been observed intracellularly, fusing to the plasma membrane and shedding from the plasma membrane [21–23]. Intrigued with these results, we further analyzed the HA-induced EV with AFM. Figure 2(b) indicates control EV and exosomes are round in shape and have a relatively smooth surface. In contrast, enlargeosomes are relatively round in shape but have a rough uneven surface topology. Control EV and exosomes have a diameter of ~50 nm which is consistent with the accepted exosome size range of 30–100 nm [20]. HMW-HA-induced enlargeosomes appear slightly larger in comparison to exosomes.

To further investigate HMW-HA-induced enlargeosome dynamics in HPMVEC, confluent monolayers were treated with HMW-HA for 6 hours. ATP and ionomycin were used as controls due to their previously reported ability to stimulate enlargeosome exocytosis [21–24]. The samples were then fixed and subjected to immunocytochemical analysis using AHNAK antibodies (green). Plasma membranes were labeled with Alexa Fluor 594 wheat germ agglutinin (red) and nuclei were stained with Hoechst 33342 (blue). The results of Figure 3 indicate that control HPMVEC exhibit diffuse cytoplasmic AHNAK staining. When stimulated with HMW-HA,

intracellular AHNAK redistributes to a “vesicular” pattern which is similar to treatment with ATP and ionomycin.

Considering the results of Figures 2 and 3, we further investigated these HA-induced EVs to determine the presence or absence of potential bioactive agents. Interestingly, Alcian blue stained TBE gels revealed that purified enlargeosomes contain HA of ~1 million Da (see arrow) consistent with HMW-HA which we have previously demonstrated to be barrier enhancing [4, 5, 7, 8]. In contrast, control, LMW-HA, or LPS-induced EV contained negligible HA (Figure 4(a)). Considering that the HA receptor, CD44, has previously been reported to be expressed on exosomes [43, 44], we next analyzed HA binding protein expressed in our purified HA-induced EV. Figure 4(b) indicates that HMW-HA-induced enlargeosomes express the EC barrier enhancing CD44 isoform, CD44s (standard form) [4, 7]. In contrast, LMW-HA-induced exosomes express the EC barrier disrupting HA binding proteins, CD44 isoform CD44v10, and the extracellular serine protease, HABP2 [7, 25]. Basally secreted EVs (control) have low expression of these molecules. In addition, EVs are believed to serve as carriers of RNAs [27, 28]. Figure 4(c) indicates that, compared to control EV, LMW-HA-induced EVs have less total RNA and microRNA while HMW-HA-induced enlargeosomes have ~2-fold higher levels of total RNA and microRNA.

Since we observed differential expression of bioactive agents in EV in Figure 4 that could impact vascular integrity, we next determined the role(s) of isolated HA-induced EV in human EC barrier function. HPMVEC were plated on transendothelial electrical resistance (TER) electrodes, grown to confluence, and switched to serum-free media and either isolated LMW-HA-induced exosomes or isolated HMW-HA-induced enlargeosomes were then added. Figure 5(a) indicates that addition of isolated LMW-HA-induced exosomes to human EC monolayers promotes barrier disruption in a dose-dependent manner. In contrast, Figure 5(b) indicates that addition of isolated HMW-HA-induced enlargeosomes to human EC monolayers induces barrier enhancement in a dose-dependent manner.

To determine whether HMW-HA-induced enlargeosomes affect sustained human EC barrier function, we silenced the expression of annexin II which has previously been reported to be crucial for enlargeosome exocytosis [23]. Figure 6(a) indicates that we can successfully inhibit annexin II expression with siRNA in human EC. Silencing of annexin II significantly reduces HMW-HA-, but not LMW-HA-, mediated EV secretion from human EC (Figure 6(b)). Importantly, silencing of annexin II did not affect the sustained human EC barrier disruptive effects of LMW-HA (Figure 6(c)) but almost completely inhibited the sustained HMW-HA barrier enhancing effects (Figure 6(d)).

4. Discussion

Since defects in vascular integrity are an initiating factor in several disease processes, understanding the mechanism(s) of endothelial barrier function can have important clinical implications. We have previously determined that the glycosaminoglycan, hyaluronan (HA), initiates rapid endothelial

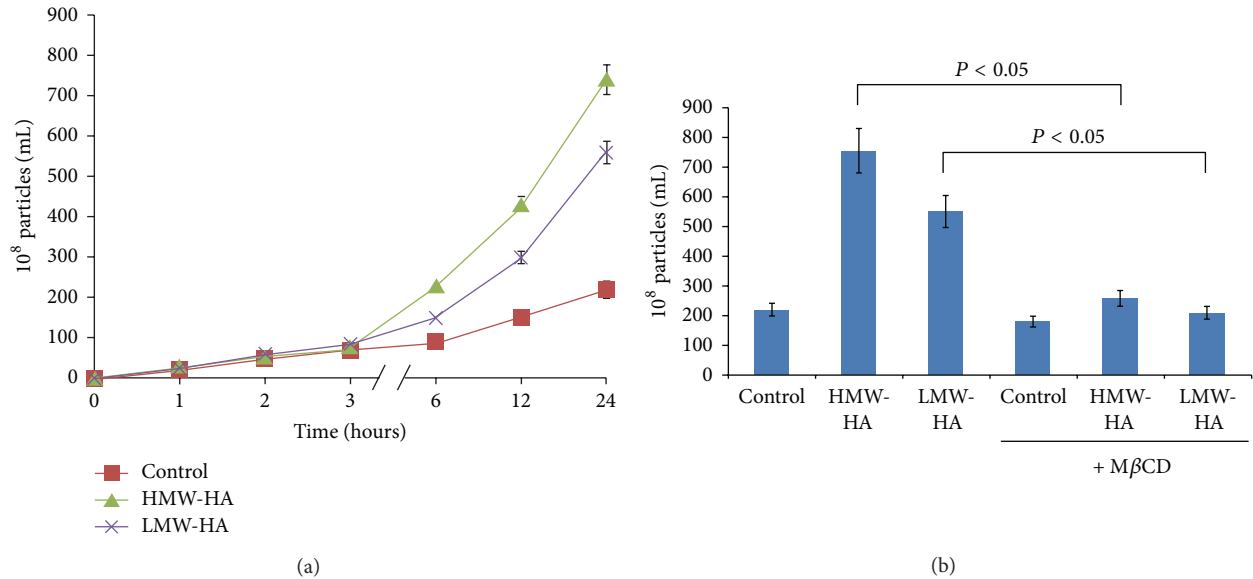


FIGURE 1: Determination of extracellular vesicle (EV) release kinetics and caveolin-enriched microdomain (CEM) dependence in human endothelial cells (EC). Panel (a): graphical representations of the kinetics of HA-induced EV release from human pulmonary microvascular endothelial cells (HPMVEC). Human EC monolayers were placed in serum-free media and the resulting media containing EV were collected at 0, 1, 2, 3, 6, 12, and 24 hours. The concentrations of EV were determined utilizing nanosight nanoparticle tracking analysis (NTA). HPMVEC exhibit basal secretion of EV (control). However, addition of 100 nM HMW-HA or 100 nM LMW-HA dramatically increased the production of EV starting at ~6 hours posttreatment. $N = 3$ per group and error bars = standard deviation. Panel (b): graphical representation of the role of CEM in HA-mediated EV production from human EC. HPMVEC monolayers were either untreated or treated with 5 mM methyl- β -cyclodextrin (M β CD, a CEM disrupting agent) with or without addition of 100 nM LMW-HA or 100 nM HMW-HA (24 hours). EVs were analyzed as described in Panel (a). Inhibiting CEM formation significantly inhibited both LMW-HA and HMW-HA-mediated EV secretion with $n = 3$ per group and error bars = standard deviation.

signal transduction events leading to changes in barrier function. In this study, we investigated the potential long-term mechanism(s) of HA-mediated endothelial cell (EC) barrier regulation. We have identified that ~6 hours after HA addition, human EC differentially release extracellular vesicles (EVs) that contain caveolin-1 and are regulated by caveolin-enriched microdomains (CEM). Utilizing several novel techniques including atomic force microscopy and nanosight nanoparticle tracking analysis (NTA), we have characterized these EVs as a novel type of EV called enlargeosomes (for HMW-HA) and exosomes (for LMW-HA, produced in disease states from HMW-HA by hyaluronidases and ROS). Importantly, isolated LMW-HA-induced exosomes promote EC barrier disruption while isolated HMW-HA-induced enlargeosomes induce EC barrier enhancement. Inhibiting HMW-HA-induced enlargeosome release reduces the sustained barrier enhancing properties of HMW-HA. These findings demonstrate an important mechanism of HA-induced sustained vascular integrity through differential release of EV from human EC.

We have previously reported that CEM are important plasma membrane microdomains involved in rapid protein recruitment and signal transduction leading to endothelial barrier regulation [4–8, 41, 45]. The results of the current study expand the role of CEM to include regulation of HA-induced EV release from human EC. Specifically, our data

indicate that inhibiting CEM attenuates both LMW-HA-induced exosome release and HMW-HA-induced enlargeosome release. Further, these EVs contain caveolin-1, a crucial component of CEM [46, 47]. Interestingly, although basally secreted control EVs also contain caveolin-1, CEM do not appear to be involved in their secretion. The fact that these control EVs do not contain markers for exosomes or enlargeosomes indicates that they belong to a different class of EV, possibly exosome-like vesicles or apoptotic bodies [28]. Further analysis is needed to determine the identity of these EVs.

HMW-HA treatment of human pulmonary microvascular EC (HPAEC) causes recruitment of the Ca^{2+} -dependent phospholipid and actin-binding protein, annexin II, and the scaffolding protein, AHNAK, to CEM [5]. These proteins are biomarkers of enlargeosomes which are specialized vesicles that occur intracellularly, fusing to the plasma membrane and shedding from the plasma membrane [21–23]. They are implicated in membrane repair which is consistent with their role in sustained HMW-HA-mediated EC barrier enhancement. It is interesting to note the difference in surface topology of control EV and exosomes compared to enlargeosomes. Control EV and exosomes are round in shape and have a relatively smooth surface. In contrast, enlargeosomes are relatively round in shape but have a rough uneven surface topology potentially indicating greater surface protein expression.

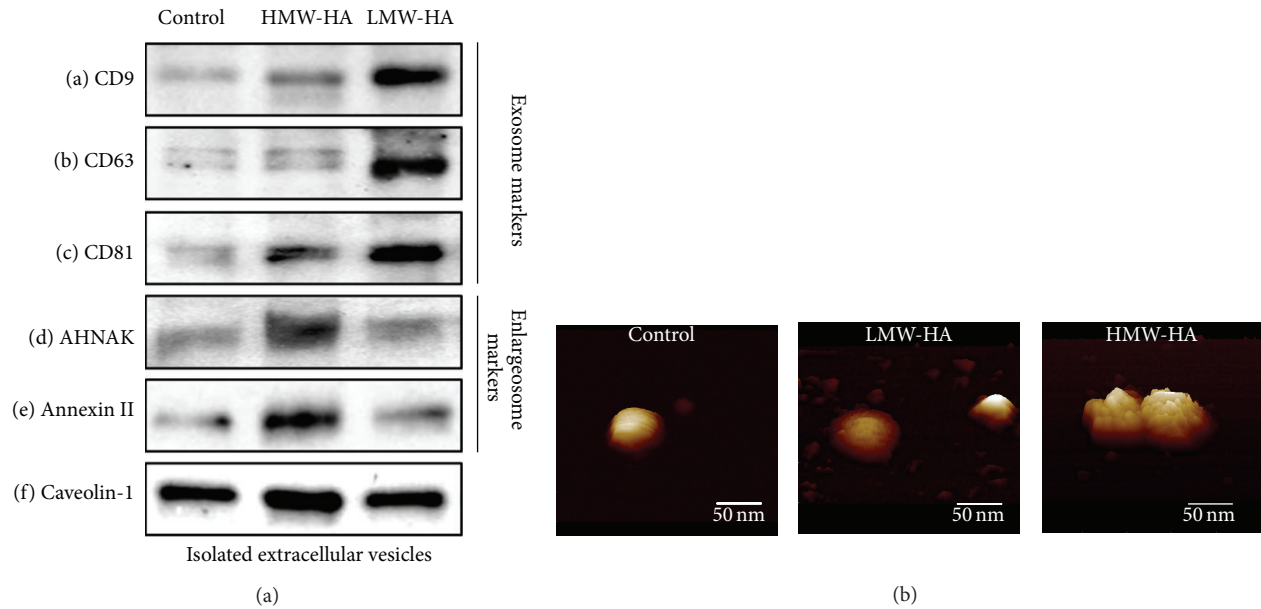


FIGURE 2: Identification of LMW-HA and HMW-HA-induced EV from human EC. Panel (a): biomarker analysis of HA-induced EV. HPMVEC were grown to confluence and switched to serum-free media and either no HA (control), 100 nM HMW-HA, or 100 nM LMW-HA for 24 hours. EVs were then isolated, run on SDS-PAGE, and immunoblotted with anti-CD9 (a), anti-CD63 (b), anti-CD81 (c), anti-AHNAK (d), antiannexin II (e), or anti-caveolin-1 (f) antibodies. LMW-HA-induced EV expressed exosome markers while HMW-HA-induced EV expressed enlargeosome markers. EV also expressed caveolin-1, a crucial component of caveolin-enriched microdomains (CEM). Panel (b): topographical images of HA-induced EV using atomic force microscopy (AFM). Isolated HA-induced EVs as described in Panel (a) were plated on mica and subjected to AFM analysis (see Section 2). The vesicles were never dried and are shown as imaged under buffer. Control EV and exosomes were round in shape and had a relatively smooth surface. In contrast, enlargeosomes were relatively round in shape but had a rough uneven surface topology. Control EV and exosomes had a diameter of ~50 nm which is consistent with the accepted exosome size range of 30–100 nm [20]. HMW-HA-induced enlargeosomes appeared slightly larger in comparison to exosomes.

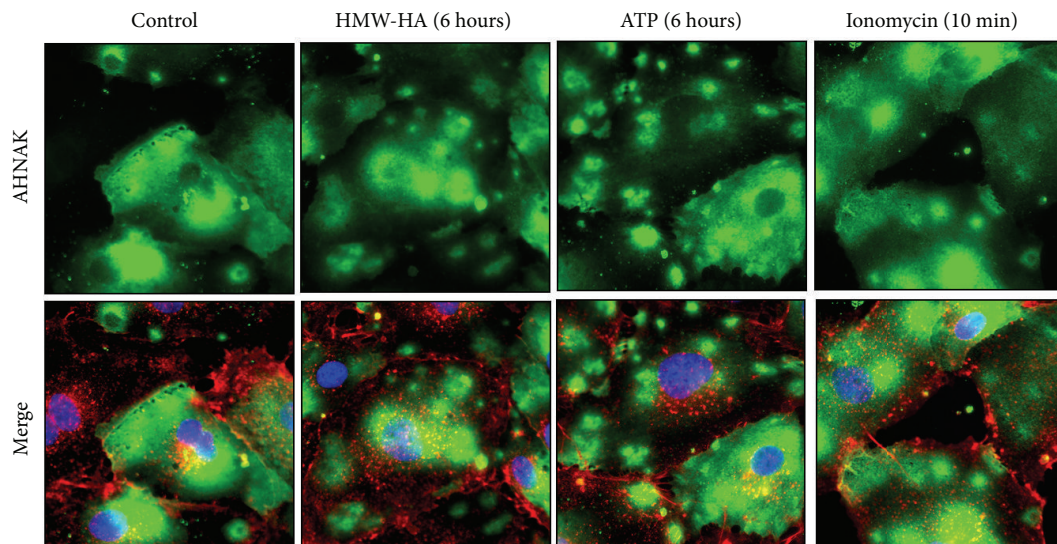


FIGURE 3: Analysis of HMW-HA-induced AHNK redistribution in human EC. HPMVEC were grown to confluence on glass coverslips and treated with 100 nM HMW-HA for 6 hours. 50 μ M ATP (six hours) and 3 μ M ionomycin (10 minutes) were used as controls due to their previously reported ability to stimulate enlargeosome exocytosis [21–24]. The samples were then fixed in 4% paraformaldehyde and subjected to immunocytochemical analysis using AHNK antibodies (green). Plasma membranes were labeled with Alexa Fluor 594 wheat germ agglutinin (red) and nuclei were stained with Hoechst 33342 (blue). Control HPMVEC exhibited diffuse cytoplasmic AHNK staining. When stimulated with HMW-HA, intracellular AHNK redistributed to a “vesicular” pattern which is similar to treatment with ATP and ionomycin.

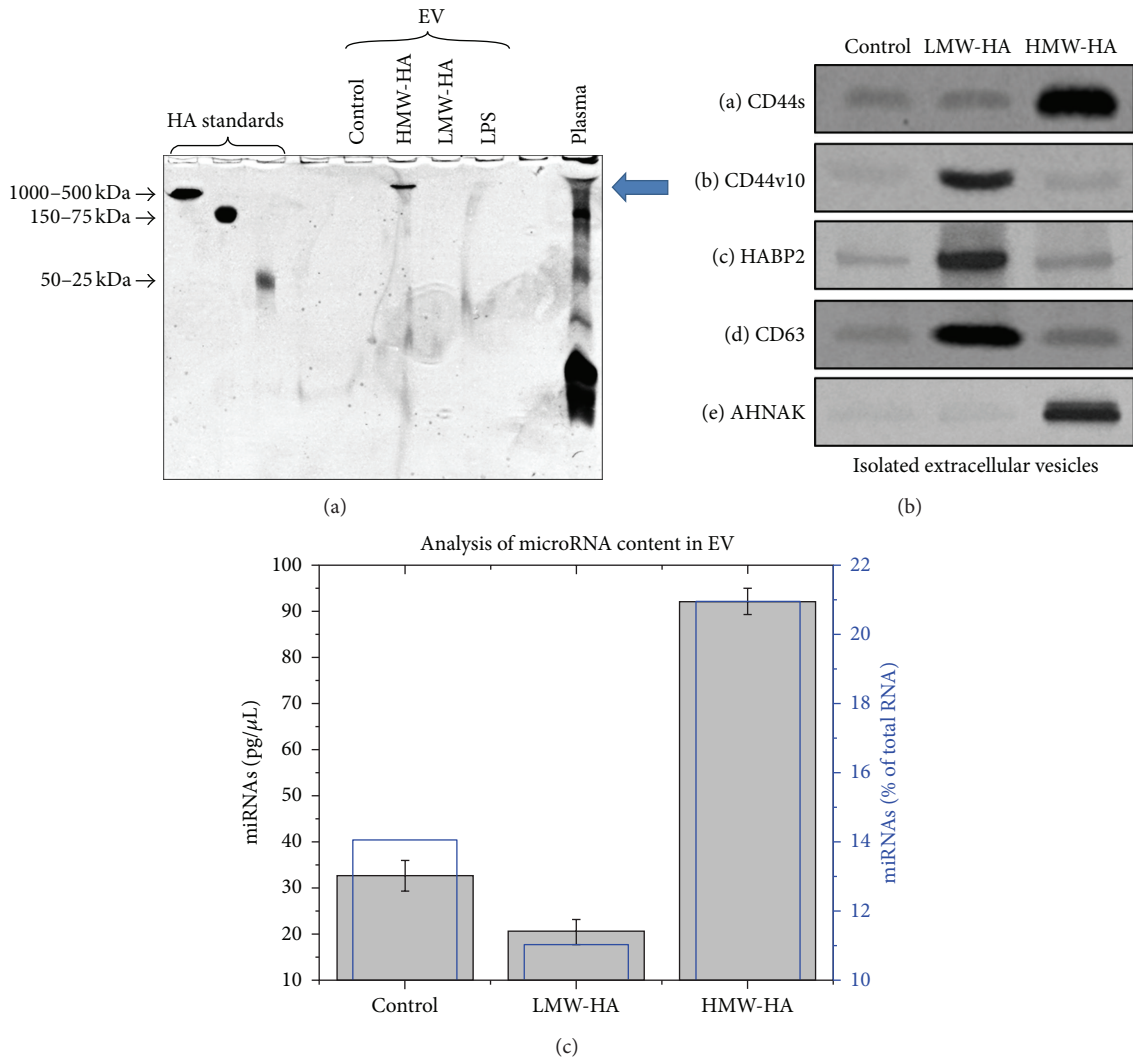


FIGURE 4: Characterization of potential bioactive components in HA-induced EV. Panel (a): HPMVEC were grown to confluence and switched to serum-free media and either no HA (control), 100 nM HMW-HA, 100 nM LMW-HA, or 500 ng/mL LPS for 24 hours. EVs were then isolated, run on 4–20% TBE gels, and stained with Alcian blue. Purified enlargeosomes contained HA of ~1 million Da (see arrow) consistent with HMW-HA which we have previously demonstrated to be barrier enhancing [4, 5, 7, 8]. In contrast, control, LMW-HA, or LPS-induced EV contained negligible HA. Human plasma was used as a control. Panel (b): HPMVEC were grown to confluence and switched to serum-free media and either no HA (control), 100 nM HMW-HA, or 100 nM LMW-HA for 24 hours. EVs were then isolated, run on SDS-PAGE, and immunoblotted with anti-CD44 (IM-7) (a), anti-CD44v10 (b), anti-HABP2 (c), anti-CD63 (d), or anti-AHNAK (e) antibodies. HMW-HA-induced enlargeosomes expressed the EC barrier enhancing CD44 isoform, CD44s (standard form) [4, 7]. In contrast, LMW-HA-induced exosomes expressed the EC barrier disrupting HA binding proteins, CD44 isoform CD44v10, and the extracellular serine protease, HABP2 [7, 25]. Basally secreted EV (control) had low expression of these molecules. Panel (c): isolated EVs as described in Panel (b) were subjected to RNA isolation and analysis (see Section 2). Compared to control EV, LMW-HA-induced EV had less total RNA and microRNA while HMW-HA-induced enlargeosomes had ~2-fold higher levels of total RNA and microRNA.

Control EV and exosomes have a diameter of ~50 nm which is consistent with the accepted exosome size range of 30–100 nm [20, 28]. HMW-HA-induced enlargeosomes have increased size in comparison to exosomes but do not reach the range of larger EV including microsomes [28]. Further, it has been reported that, in astrocyte stellation, there is a Rac1-dependent remodeling of the cytoskeleton with concomitant exocytosis of enlargeosomes [48]. Considering our previous published data that HMW-HA induces Rac1 activation in EC

[7], it is possible that Rac1 might also play a role in HMW-HA mediated enlargeosome exocytosis to enhance EC barrier function. In another cellular function, neurite outgrowth, enlargeosomes, and another distinct type of exocytotic vesicle are required for the enlargement of the cell surface [49, 50]. Therefore, we cannot rule out the cooperation of distinct EVs during EC barrier regulation.

Another important result of the current study is that EVs differentially express HA and HA binding proteins which

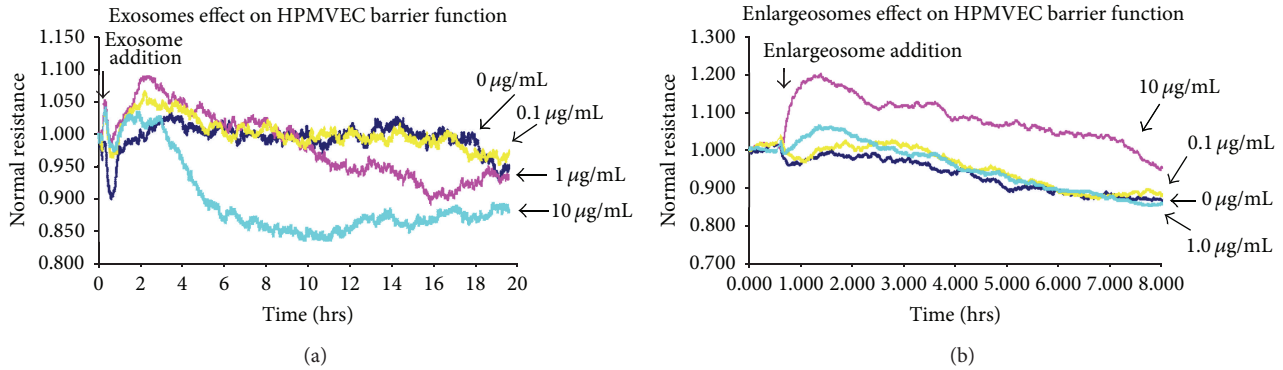


FIGURE 5: The effects of isolated LMW-HA and HMW-HA-induced EV on human EC barrier function. Panel (a): HPMVEC were plated on transendothelial electrical resistance (TER) electrodes, grown to confluence, and switched to serum-free media and 0, 0.1, 1, or 10 $\mu\text{g/mL}$ isolated LMW-HA-induced exosomes were then added. Addition of isolated LMW-HA-induced exosomes to human EC monolayers promoted barrier disruption in a dose-dependent manner. Panel (b): HPMVEC were plated on transendothelial electrical resistance (TER) electrodes, grown to confluence, and switched to serum-free media and 0, 0.1, 1, or 10 $\mu\text{g/mL}$ isolated HMW-HA-induced enlargeosomes were then added. Addition of isolated HMW-HA-induced enlargeosomes to human EC monolayers induces barrier enhancement in a dose-dependent manner.

can potentially contribute to their differential EC barrier regulatory effects. Control EV and EV from barrier disruptive agents (LMW-HA and LPS) did not appear to have significant amounts of HA. In contrast, the novel HMW-HA-induced enlargeosomes, in which little compositional information is known, contain HA of ~ 1 million Da which can potentially contribute to the paracellular propagation of the sustained HMW-HA endothelial barrier enhancing response [5]. Our data indicate that there is differential expression of CD44 isoforms in EV induced by LMW-HA versus HMW-HA. Alternative splicing of the CD44 transcript can give rise to a number of CD44 variants, which express an extra insert in their extracellular membrane proximal domain [51]. HMW-HA-induced enlargeosomes mainly express the barrier enhancing, CD44s (standard form, which lacks extra exon insertions), while LMW-HA-induced exosomes express CD44v10 (variant 10) which contains an extra exon insert and is involved in EC barrier disruption [4]. The precise role of differential CD44 isoform expression in EV function is currently being investigated in our laboratory. In addition, LMW-HA-induced exosomes express the extracellular serine protease, hyaluronan binding protein 2 (HABP2) which we have previously demonstrated to promote endothelial barrier disruption through activation of protease-activated receptor- (PAR receptor-) mediated signal transduction [25]. We are currently examining the expression of HABP2 and another class of HA binding proteins, hyaluronidases, in HA-induced endothelial EV function [25, 52].

MicroRNAs are small noncoding RNA molecules (~ 22 nucleotides) that function in RNA silencing and post-transcriptional regulation of gene expression [53–55]. Our data indicate that HA-induced EVs contain RNA with a significant fraction of microRNAs. Specifically, compared to control EV, LMW-HA-induced EVs have less total RNA and microRNA while HMW-HA-induced enlargeosomes have ~ 2 -fold higher levels of total RNA and a higher percentage of microRNAs. Considering the pleiotropic effects of

these molecules, it is plausible to speculate that differential expression of microRNAs in LMW-HA-induced exosomes and HMW-HA-induced enlargeosomes can contribute to differential endothelial barrier function. Indeed, it has been reported that EC treated with hypoxia, TNF- α , high glucose, and mannose produce exosomes with altered protein and RNA content [56]. Further, curcumin treatment of EC produces exosomes that promote EC barrier function [57] while cancer-secreted exosomes containing miR-105 inhibit EC barrier function and promote metastasis [58].

In conclusion, our findings demonstrate an important mechanism of HA-induced sustained vascular integrity through CEM-regulated differential release of EV from human EC. Specifically, LMW-HA treatment of HPMVEC induces release of endothelial barrier disruptive exosomes while HMW-HA promotes secretion of a novel type of EV, enlargeosomes, which promote sustained endothelial barrier enhancement. Further, these EVs contain differential expression of HA, HA binding proteins, and miRNAs which can contribute to their barrier regulatory properties. Utilization of isolated HMW-HA-induced specialized enlargeosomes and/or their bioactive components can be a potential therapeutic strategy for diseases involving impaired vascular integrity.

Conflict of Interests

The authors declare that there is no conflict of interests regarding the publication of this paper.

Acknowledgments

The authors would like to thank the Department of Biomedical Engineering at the Illinois Institute of Technology for their assistance in Nanosight Nanoparticle Tracking Analysis (NTA). This research was supported by the American

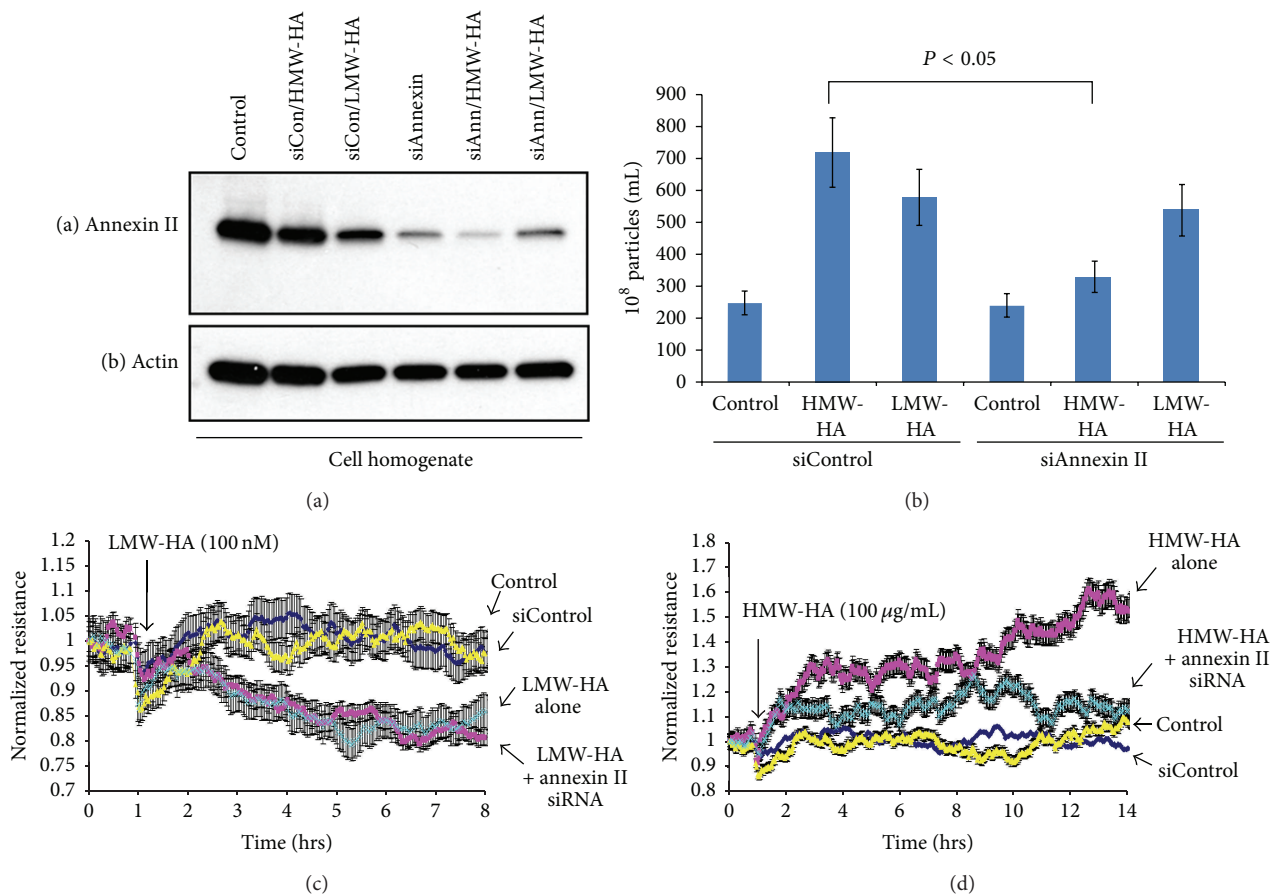


FIGURE 6: Inhibiting enlargesome release attenuates HMW-HA-mediated sustained human EC barrier enhancement. Panel (a): inhibition of annexin II expression using siRNA in HPMVEC. Human EC were plated at ~50% confluence and treated with either no siRNA (control), siControl, or siAnnexin II with or without 100 nM LMW-HA or 100 nM HMW-HA for 48 hours. EC lysates were then obtained, run on SDS-PAGE, and immunoblotted with anti-annexin II (a) or anti-actin (b) antibodies. Panel (b): graphical representation of the role of annexin II inhibition in HA-mediated EV production from human EC. HPMVEC were treated as described in Panel (a) and EVs were analyzed utilizing nanosight nanoparticle tracking analysis (NTA). Silencing of annexin II, which has previously been reported to be crucial for enlargesome exocytosis [23], significantly reduces HMW-HA-, but not LMW-HA-, mediated EV secretion from human EC with $n = 3$ per group and error bars = standard deviation. Panel (c): HPMVEC previously treated with either no siRNA (control), siControl, or annexin II siRNA were plated on transendothelial electrical resistance (TER) electrodes, grown to confluence, and switched to serum-free media and 100 nM LMW-HA was then added. Silencing of annexin II did not affect the sustained human EC barrier disruptive effects of LMW-HA with $n = 3$ per group and error bars = standard deviation. Panel (d): HPMVEC previously treated with either no siRNA (control), siControl, or annexin II siRNA were plated on transendothelial electrical resistance (TER) electrodes, grown to confluence, and switched to serum-free media and 100 nM HMW-HA was then added. In contrast to LMW-HA, silencing annexin II almost completely inhibited the sustained barrier enhancing effects of HMW-HA with $n = 3$ per group and error bars = standard deviation.

Heart Association National Scientist Development Grant no. 0730277N (to Patrick A. Singleton), NIH NHLBI Award R01-HL 095723 (to Patrick A. Singleton), and NIH R01NS067247 (to Michael Allen).

References

- [1] M. Murakami and M. Simons, "Regulation of vascular integrity," *Journal of Molecular Medicine*, vol. 87, no. 6, pp. 571–582, 2009.
- [2] E. Dejana, E. Tournier-Lasserre, and B. M. Weinstein, "The control of vascular integrity by endothelial cell junctions: molecular basis and pathological implications," *Developmental Cell*, vol. 16, no. 2, pp. 209–221, 2009.
- [3] T. F. Luscher and M. Barton, "Biology of the endothelium," *Clinical Cardiology*, vol. 20, no. 12, pp. II-3–II-10, 1997.
- [4] F. E. Lennon and P. A. Singleton, "Hyaluronan regulation of vascular integrity," *American Journal of Cardiovascular Disease*, vol. 1, pp. 200–213, 2011.
- [5] P. A. Singleton, T. Mirzapoiazova, Y. Guo et al., "High-molecular-weight hyaluronan is a novel inhibitor of pulmonary vascular leakiness," *The American Journal of Physiology—Lung Cellular and Molecular Physiology*, vol. 299, no. 5, pp. L639–L651, 2010.
- [6] P. A. Singleton, S. Chatchavalvanich, P. Fu et al., "Akt-mediated transactivation of the slp1 receptor in caveolin-enriched microdomains regulates endothelial barrier enhancement by oxidized phospholipids," *Circulation Research*, vol. 104, no. 8, pp. 978–986, 2009.

- [7] P. A. Singleton, S. M. Dudek, S.-F. Ma, and J. G. N. Garcia, "Transactivation of sphingosine 1-phosphate receptors is essential for vascular barrier regulation: novel role for hyaluronan and CD44 receptor family," *The Journal of Biological Chemistry*, vol. 281, no. 45, pp. 34381–34393, 2006.
- [8] F. E. Lennon and P. A. Singleton, "Role of hyaluronan and hyaluronan-binding proteins in lung pathobiology," *The American Journal of Physiology—Lung Cellular and Molecular Physiology*, vol. 301, no. 2, pp. L137–L147, 2011.
- [9] F. E. Lennon, T. Mirzapozova, N. Mambetsariev, B. Mambetsariev, R. Salgia, and P. A. Singleton, "Transactivation of the receptor-tyrosine kinase ephrin receptor A2 is required for the low molecular weight hyaluronan-mediated angiogenesis that is implicated in tumor progression," *The Journal of Biological Chemistry*, vol. 289, no. 35, pp. 24043–24058, 2014.
- [10] K. S. Girish and K. Kemparaju, "The magic glue hyaluronan and its eraser hyaluronidase: a biological overview," *Life Sciences*, vol. 80, no. 21, pp. 1921–1943, 2007.
- [11] D. Jiang, J. Liang, and P. W. Noble, "Hyaluronan in tissue injury and repair," *Annual Review of Cell and Developmental Biology*, vol. 23, pp. 435–461, 2007.
- [12] R. C. Savani, G. Cao, P. M. Pooler, A. Zaman, Z. Zhou, and H. M. DeLisser, "Differential involvement of the hyaluronan (HA) receptors CD44 and receptor for HA-mediated motility in endothelial cell function and angiogenesis," *The Journal of Biological Chemistry*, vol. 276, no. 39, pp. 36770–36778, 2001.
- [13] R. Stern, "Hyaluronan metabolism: a major paradox in cancer biology," *Pathologie Biologie*, vol. 53, no. 7, pp. 372–382, 2005.
- [14] M. I. Tammi, A. J. Day, and E. A. Turley, "Hyaluronan and homeostasis: a balancing act," *The Journal of Biological Chemistry*, vol. 277, no. 7, pp. 4581–4584, 2002.
- [15] B. P. Toole, "Hyaluronan: from extracellular glue to pericellular cue," *Nature Reviews Cancer*, vol. 4, no. 7, pp. 528–539, 2004.
- [16] A. Wang, C. de La Motte, M. Lauer, and V. Hascall, "Hyaluronan matrices in pathobiological processes," *FEBS Journal*, vol. 278, no. 9, pp. 1412–1418, 2011.
- [17] P. H. Weigel and P. L. DeAngelis, "Hyaluronan synthases: a decade-plus of novel glycosyltransferases," *The Journal of Biological Chemistry*, vol. 282, no. 51, pp. 36777–36781, 2007.
- [18] P. A. Singleton, S. M. Dudek, S.-F. Ma, and J. G. N. Garcia, "Transactivation of sphingosine 1-phosphate receptors is essential for vascular barrier regulation. Novel role for hyaluronan and CD44 receptor family," *The Journal of Biological Chemistry*, vol. 281, no. 45, pp. 34381–34393, 2006.
- [19] P. A. Singleton, R. Salgia, L. Moreno-Vinasco et al., "CD44 regulates hepatocyte growth factor-mediated vascular integrity: role of c-Met, Tiam1/Rac1, dynamin 2, and cortactin," *The Journal of Biological Chemistry*, vol. 282, no. 42, pp. 30643–30657, 2007.
- [20] B. György, T. G. Szabó, M. Pásztói et al., "Membrane vesicles, current state-of-the-art: emerging role of extracellular vesicles," *Cellular and Molecular Life Sciences*, vol. 68, no. 16, pp. 2667–2688, 2011.
- [21] E. Cocucci, G. Racchetti, P. Podini, and J. Meldolesi, "Enlargeosome traffic: exocytosis triggered by various signals is followed by endocytosis, membrane shedding or both," *Traffic*, vol. 8, no. 6, pp. 742–757, 2007.
- [22] E. Cocucci, G. Racchetti, P. Podini, M. Rupnik, and J. Meldolesi, "Enlargeosome, an exocytic vesicle resistant to nonionic detergents, undergoes endocytosis via a nonacidic route," *Molecular Biology of the Cell*, vol. 15, no. 12, pp. 5356–5368, 2004.
- [23] A. Lorusso, C. Covino, G. Priori, A. Bachi, J. Meldolesi, and E. Chierregatti, "Annexin2 coating the surface of enlargeosomes is needed for their regulated exocytosis," *The EMBO Journal*, vol. 25, no. 23, pp. 5443–5456, 2006.
- [24] I. Prada, E. Cocucci, G. Racchetti, and J. Meldolesi, "The Ca²⁺-dependent exocytosis of enlargeosomes is greatly reinforced by genistein via a non-tyrosine kinase-dependent mechanism," *FEBS Letters*, vol. 581, no. 25, pp. 4932–4936, 2007.
- [25] N. Mambetsariev, T. Mirzapozova, B. Mambetsariev et al., "Hyaluronic Acid binding protein 2 is a novel regulator of vascular integrity," *Arteriosclerosis, Thrombosis, and Vascular Biology*, vol. 30, no. 3, pp. 483–490, 2010.
- [26] V. Muralidharan-Chari, J. W. Clancy, A. Sedgwick, and C. D'Souza-Schorey, "Microvesicles: mediators of extracellular communication during cancer progression," *Journal of Cell Science*, vol. 123, no. 10, pp. 1603–1611, 2010.
- [27] S. Mathivanan, H. Ji, and R. J. Simpson, "Exosomes: extracellular organelles important in intercellular communication," *Journal of Proteomics*, vol. 73, no. 10, pp. 1907–1920, 2010.
- [28] G. Raposo and W. Stoorvogel, "Extracellular vesicles: exosomes, microvesicles, and friends," *The Journal of Cell Biology*, vol. 200, no. 4, pp. 373–383, 2013.
- [29] C. D'Souza-Schorey and J. W. Clancy, "Tumor-derived microvesicles: shedding light on novel microenvironment modulators and prospective cancer biomarkers," *Genes & Development*, vol. 26, no. 12, pp. 1287–1299, 2012.
- [30] C. Lässer, V. Seyed Alikhani, K. Ekström et al., "Human saliva, plasma and breast milk exosomes contain RNA: uptake by macrophages," *Journal of Translational Medicine*, vol. 9, article 9, 2011.
- [31] P. A. Singleton, "Hyaluronan regulation of endothelial barrier function in cancer," in *Hyaluronan Signaling and Turnover*, vol. 123 of *Advances in Cancer Research*, pp. 191–209, 2014.
- [32] H. Kalra, C. G. Adda, M. Liem et al., "Comparative proteomics evaluation of plasma exosome isolation techniques and assessment of the stability of exosomes in normal human blood plasma," *Proteomics*, vol. 13, no. 22, pp. 3354–3364, 2013.
- [33] S. Mathivanan, J. W. E. Lim, B. J. Tauro, H. Ji, R. L. Moritz, and R. J. Simpson, "Proteomics analysis of A33 immunoaffinity-purified exosomes released from the human colon tumor cell line LIM1215 reveals a tissue-specific protein signature," *Molecular & Cellular Proteomics*, vol. 9, no. 2, pp. 197–208, 2010.
- [34] S. M. Dudek, E. T. Chiang, S. M. Camp et al., "Abl tyrosine kinase phosphorylates nonmuscle myosin light chain kinase to regulate endothelial barrier function," *Molecular Biology of the Cell*, vol. 21, no. 22, pp. 4042–4056, 2010.
- [35] Y. Ephstein, P. A. Singleton, W. Chen et al., "Critical role of SIP1 and integrin β 4 in HGF/c-Met-mediated increases in vascular integrity," *The Journal of Biological Chemistry*, vol. 288, no. 4, pp. 2191–2200, 2013.
- [36] J. H. Finigan, S. M. Dudek, P. A. Singleton et al., "Activated protein C mediates novel lung endothelial barrier enhancement: role of sphingosine 1-phosphate receptor transactivation," *The Journal of Biological Chemistry*, vol. 280, no. 17, pp. 17286–17293, 2005.
- [37] Y. Guo, P. A. Singleton, A. Rowshan et al., "Quantitative proteomics analysis of human endothelial cell membrane rafts: evidence of MARCKS and MRP regulation in the sphingosine 1-phosphate-induced barrier enhancement," *Molecular & Cellular Proteomics*, vol. 6, no. 4, pp. 689–696, 2007.
- [38] S. Sharma, H. I. Rasool, V. Palanisamy et al., "Structural-mechanical characterization of nanoparticle exosomes in

- human saliva, using correlative AFM, FESEM, and force spectroscopy,” *ACS Nano*, vol. 4, no. 4, pp. 1921–1926, 2010.
- [39] P. Hole, K. Sillence, C. Hannell et al., “Interlaboratory comparison of size measurements on nanoparticles using nanoparticle tracking analysis (NTA),” *Journal of Nanoparticle Research*, vol. 15, article 2101, 2013.
- [40] M. Logozzi, A. de Milito, L. Lugini et al., “High levels of exosomes expressing CD63 and caveolin-1 in plasma of melanoma patients,” *PLoS ONE*, vol. 4, no. 4, Article ID e5219, 2009.
- [41] P. A. Singleton, R. Salgia, L. Moreno-Vinasco et al., “CD44 regulates hepatocyte growth factor-mediated vascular integrity. Role of c-Met, Tiam1/Rac1, dynamin 2, and cortactin,” *The Journal of Biological Chemistry*, vol. 282, no. 42, pp. 30643–30657, 2007.
- [42] P. A. Singleton, S. M. Dudek, E. T. Chiang, and J. G. N. Garcia, “Regulation of sphingosine 1-phosphate-induced endothelial cytoskeletal rearrangement and barrier enhancement by SIP1 receptor, PI3 kinase, Tiam1/Rac1, and α -actinin,” *FASEB Journal*, vol. 19, no. 12, pp. 1646–1656, 2005.
- [43] T. Jung, D. Castellana, P. Klingbeil et al., “CD44v6 dependence of premetastatic niche preparation by exosomes,” *Neoplasia*, vol. 11, no. 10, pp. 1093–1105, 2009.
- [44] A. Stoeck, S. Keller, S. Riedle et al., “A role for exosomes in the constitutive and stimulus-induced ectodomain cleavage of L1 and CD44,” *The Biochemical Journal*, vol. 393, no. 3, pp. 609–618, 2006.
- [45] P. A. Singleton, L. Moreno-Vinasco, S. Sammani, S. L. Wanderling, J. Moss, and J. G. N. Garcia, “Attenuation of vascular permeability by methylglucuronide: role of mOP-R and SIP3 transactivation,” *American Journal of Respiratory Cell and Molecular Biology*, vol. 37, no. 2, pp. 222–231, 2007.
- [46] M. Das and D. K. Das, “Caveolae, caveolin, and cavins: potential targets for the treatment of cardiac disease,” *Annals of Medicine*, vol. 44, no. 6, pp. 530–541, 2012.
- [47] M. Drab, P. Verkade, M. Elger et al., “Loss of caveolae, vascular dysfunction, and pulmonary defects in caveolin-1 gene-disrupted mice,” *Science*, vol. 293, no. 5539, pp. 2449–2452, 2001.
- [48] G. Racchetti, R. D’Alessandro, and J. Meldolesi, “Astrocyte stellation, a process dependent on Rac1 is sustained by the regulated exocytosis of enlargeosomes,” *Glia*, vol. 60, no. 3, pp. 465–475, 2012.
- [49] J. Meldolesi, “Neurite outgrowth: this process, first discovered by Santiago Ramon y Cajal, is sustained by the exocytosis of two distinct types of vesicles,” *Brain Research Reviews*, vol. 66, no. 1–2, pp. 246–255, 2011.
- [50] F. Colombo, G. Racchetti, and J. Meldolesi, “Neurite outgrowth induced by NGF or LICAM via activation of the TrkA receptor is sustained also by the exocytosis of enlargeosomes,” *Proceedings of the National Academy of Sciences of the United States of America*, vol. 111, no. 47, pp. 16943–16948, 2014.
- [51] L. Y. W. Bourguignon, “Hyaluronan-mediated CD44 activation of RhoGTPase signaling and cytoskeleton function promotes tumor progression,” *Seminars in Cancer Biology*, vol. 18, no. 4, pp. 251–259, 2008.
- [52] R. Stern, “Hyaluronidases in cancer biology,” *Seminars in Cancer Biology*, vol. 18, no. 4, pp. 275–280, 2008.
- [53] M. Fabbri, C. M. Croce, and G. A. Calin, “MicroRNAs,” *Cancer Journal*, vol. 14, no. 1, pp. 1–6, 2008.
- [54] S. Fichtlscherer, A. M. Zeiher, and S. Dimmeler, “Circulating microRNAs: biomarkers or mediators of cardiovascular diseases?” *Arteriosclerosis, Thrombosis, and Vascular Biology*, vol. 31, no. 11, pp. 2383–2390, 2011.
- [55] A. Markou, Y. Liang, and E. Lianidou, “Prognostic, therapeutic and diagnostic potential of microRNAs in non-small cell lung cancer,” *Clinical Chemistry and Laboratory Medicine*, vol. 49, no. 10, pp. 1591–1603, 2011.
- [56] O. G. de Jong, M. C. Verhaar, Y. Chen et al., “Cellular stress conditions are reflected in the protein and RNA content of endothelial cell-derived exosomes,” *Journal of Extracellular Vesicles*, vol. 1, 2012.
- [57] A. Kalani, P. K. Kamat, P. Chaturvedi, S. C. Tyagi, and N. Tyagi, “Curcumin-primed exosomes mitigate endothelial cell dysfunction during hyperhomocysteinemia,” *Life Sciences*, vol. 107, no. 1–2, pp. 1–7, 2014.
- [58] W. Zhou, M. Y. Fong, Y. Min et al., “Cancer-secreted miR-105 destroys vascular endothelial barriers to promote metastasis,” *Cancer Cell*, vol. 25, no. 4, pp. 501–515, 2014.

Review Article

The Rise and Fall of Hyaluronan in Respiratory Diseases

Mark E. Lauer,^{1,2} Raed A. Dweik,^{3,4} Stavros Garantziotis,⁵ and Mark A. Aronica^{3,6}

¹*Pediatric Institute, Cleveland Clinic, Cleveland, OH 44195, USA*

²*Department of Biomedical Engineering, Cleveland Clinic, Cleveland, OH 44195, USA*

³*Department of Pathobiology, Cleveland Clinic, Cleveland, OH 44195, USA*

⁴*Department of Pulmonary and Critical Care Medicine, Cleveland Clinic, Cleveland, OH 44195, USA*

⁵*National Institute of Environmental Health Sciences, Research Triangle Park, NC 27709, USA*

⁶*Respiratory Institute, Cleveland Clinic, Cleveland, OH 44195, USA*

Correspondence should be addressed to Mark E. Lauer; lauerml@ccf.org

Received 13 October 2014; Revised 11 February 2015; Accepted 3 May 2015

Academic Editor: Arnoud Sonnenberg

Copyright © 2015 Mark E. Lauer et al. This is an open access article distributed under the Creative Commons Attribution License, which permits unrestricted use, distribution, and reproduction in any medium, provided the original work is properly cited.

In normal airways, hyaluronan (HA) matrices are primarily located within the airway submucosa, pulmonary vasculature walls, and, to a lesser extent, the alveoli. Following pulmonary injury, elevated levels of HA matrices accumulate in these regions, and in respiratory secretions, correlating with the extent of injury. Animal models have provided important insight into the role of HA in the onset of pulmonary injury and repair, generally indicating that the induction of HA synthesis is an early event typically preceding fibrosis. The HA that accumulates in inflamed airways is of a high molecular weight (>1600 kDa) but can be broken down into smaller fragments (<150 kDa) by inflammatory and disease-related mechanisms that have profound effects on HA pathobiology. During inflammation in the airways, HA is often covalently modified with heavy chains from inter-alpha-inhibitor via the enzyme tumor-necrosis-factor-stimulated-gene-6 (TSG-6) and this modification promotes the interaction of leukocytes with HA matrices at sites of inflammation. The clearance of HA and its return to normal levels is essential for the proper resolution of inflammation. These data portray HA matrices as an important component of normal airway physiology and illustrate its integral roles during tissue injury and repair among a variety of respiratory diseases.

1. Introduction

Considerable progress has been made over the past few decades in our understanding of the role of hyaluronan (HA) in pulmonary health and disease. Once thought to be an inert molecule of the extracellular matrix, a picture has emerged of HA as an important regulator of inflammation, airway hyperresponsiveness (AHR), edema, and fibrosis in the lung. This image has been made clearer by a significant number of investigations into a wide variety of different pulmonary diseases, environmental effects, and animal models of lung injury, which are summarized in this review (Figure 1).

HA is a major component of extracellular matrices (ECM) in every major organ system [1, 2]. It is a very large (>2500 kDa), unsulfated glycosaminoglycan, unattached to a core protein, though associated with several HA binding proteins and receptors that expand its repertoire of functions [3, 4]. HA is extruded from the cell surface by

three membrane-bound HA synthases (HAS1, HAS2, and HAS3) that utilize cytosolic UDP-N-acetyl-D-glucosamine (UDP-GlcNAc) and UDP-D-glucuronate (UDP-GlcUA) as substrates to form the repeating disaccharide unit β 1,3-N-GlcNAc linked β 1,4 to GlcUA [5]. The turnover of HA varies from tissue to tissue and is mediated by a family of hydrolytic, lysosomal enzymes known as hyaluronidases [6]. As murine knockout models of airway injury have shown, the clearance of HA, and its return to normal levels, is critical for the resolution of inflammation [7]. Under normal conditions, HA is synthesized as a high molecular weight (HMW) polysaccharide but can be degraded into smaller bioactive fragments during inflammatory and pathological processes [8, 9]. The only covalent modification known to occur on HA is a transesterification reaction with a C-terminal aspartate residue (Asp⁷⁰²) of an inter-alpha-inhibitor heavy chain to the 6th hydroxyl of GlcNAc on HA via the enzyme tumor-necrosis-factor-stimulated-gene-6

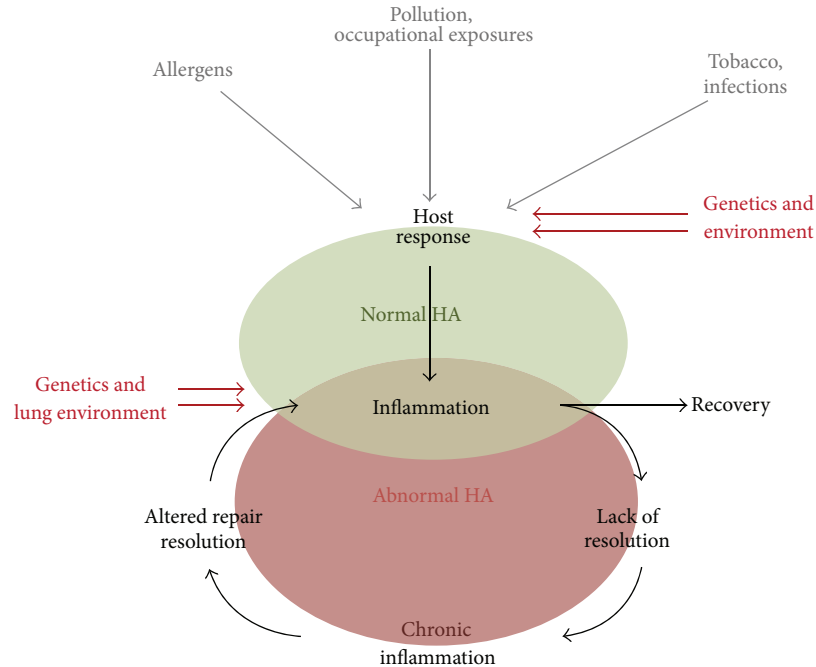


FIGURE 1: Overview of hyaluronan in respiratory disease: the lung is continuously exposed to external stimuli which can then impact HA synthesis and turnover. Factors such as type of stimuli, genetics, and the lung environment itself determine if resolution or persistent inflammation and HA changes persist.

(TSG-6) [10–14]. This reaction occurs during pathological and developmental processes and has been found in inflamed and remodeling lungs [15–17].

The present review provides a survey of HA-related data in the area of pulmonary pathobiology with an emphasis upon its expression, distribution, and turnover in a variety of respiratory disorders and conditions from both human subjects and animal models. The review is divided into three major headings: (a) environmental and occupational exposure, (b) human respiratory diseases, and (c) animal models of pulmonary injury. For a review of HA receptors and binding proteins in lung pathobiology the reader is advised to consult the review by Lennon and Singleton [18]. This review, and another [19], includes an overview of the therapeutic applications of HA in the lung. Whenever possible, actual concentrations of HA and p values were listed from the original sources. Units of measurement, such as $\mu\text{g/L}$ of HA in bronchoalveolar lavage fluid (BAL), were standardized throughout the text. The type of assay used to quantify HA was noted in most instances, and specific information on the assay was stated when possible (i.e., sandwich versus competitive ELISA-like assays). The most common methods presented in this review are radiometric or ELISA-like assays involving an HA binding protein derived from cartilage. For an overview and comparison of the sensitivity, specificity, and molecular weight accuracy of commercially available ELISA-like assays for HA analysis please see our review [20]. It should be noted that methods utilizing an HA binding protein do not distinguish between HA modified with heavy chains and HA without this modification. At times, data had

to be estimated from graphs. In such instances, the data was presented as an approximation (i.e., $\sim 10 \mu\text{g/L}$).

2. Environmental and Occupational Exposure

2.1. Farmer's Lung. Farmer's Lung is a type of alveolitis caused by a type III hypersensitivity reaction induced by the inhalation of mold derived from plant material in the agricultural industry [21]. Inflammation occurs in the alveolar wall in response to an IgG-allergen mediated immune response, causing edema and loss of pulmonary function in severe cases. Bjermer et al. examined ten patients during acute episodes of farmer's lung [21]. Impaired diffusion capacity (on average 51% of predicted) was associated with elevated levels of HA (mean concentration $547 \mu\text{g/L}$) in bronchoalveolar lavage (BAL) fluid compared to healthy controls ($15 \mu\text{g/L}$) (as determined by a radiometric assay using an HA binding protein labeled with iodine-125). HA levels declined ($154 \mu\text{g/L}$) during the 4–10-week recovery phase, nearly to normal levels at clinical remission 14 months after admission, though slightly elevated concentrations of HA were observed in about half of the subjects. Similar findings were observed in a separate study [22], and HA in BAL fluid (radiometric assay) was found to distinguish farmers with allergic alveolitis from farmers with asymptomatic alveolitis [23]. These data demonstrated that the accumulation of HA in farmer's lung was associated with the progression of the disease, suggesting the possibility that HA in the smaller airways may contribute to edema and impaired gas exchange by its relatively high hydration capacity.

2.2. Swine Confinement Workers. Larsson et al. tested the hypothesis that swine confinement workers have signs of airway inflammation, alterations of lung function, and bronchial responsiveness [24]. These workers are exposed to dust containing feed, fecal, and dander particles and develop airway symptoms, including cough, phlegm, wheeze, tightness of chest, and slight decreases in FEV₁, which had been reported [25, 26]. In Larsson's study, lung function, bronchial reactivity, and several tests for inflammation were performed on 20 randomly selected nonsmoking swine confinement workers who regarded themselves as healthy. While lung function and bronchial reactivity were not different from the urban reference group, inflammatory markers, such as elevated BAL leukocyte counts, elevated antibodies against swine dander, dust and feed, and elevated BAL levels of HA (37 µg/L compared to 27 µg/L in the reference group) were observed ($p < 0.01$) (radiometric assay). The authors concluded that signs of airway inflammation could be altered in pig farmers without alteration in lung function or bronchial reactivity. HA in BAL was found to be within normal limits in a similar study of asymptomatic dairy farmers [27] (radiometric assay).

2.3. Swedish Wood Trimmers. Workers in the logging industry are routinely exposed to mold released into the air during the harvest and transport of trees. Some of these workers develop allergic alveolitis as a result of this exposure [28]. In a study by Johard et al., signs of alveolitis were investigated in a population of Swedish wood trimmers [29]. Nineteen nonsmoking workers were subdivided into two groups, with or without serological antibodies against mold. While no difference was found in lung function (spirometry and diffusion capacity) among these subjects, BAL levels of HA were significantly elevated (42 µg/L compared to 27 µg/L in the controls) ($p < 0.001$) (radiometric assay). HA levels were not different between seropositive and seronegative workers, indicating that the elevated antibodies against mold did not predict increased risk for the development of airway inflammation. In a related rat study, this group also reported that the intratracheal instillation of sawdust, itself, resulted in increased inflammation and elevated HA levels in BAL [30] (radiometric assay).

2.4. Firefighters. Firefighters are exposed to toxic fire gases and other combustion products from their occupation which may cause acute and chronic respiratory symptoms [31, 32]. Bergström et al. tested the hypothesis that firefighters might develop inflammatory changes in their lower airways as a result of this exposure [33]. BAL was obtained from 13 nonsmoking firefighters and the results were compared to a reference group of 112 nonsmoking healthy control subjects. Elevated HA levels were observed in firefighters (27.7 µg/L) compared to the control population (10 µg/L) ($p < 0.05$) (radiometric assay). While no attempt was made to correlate the extent and timing of smoke exposure with HA levels, their data suggests that long-term occupational exposure results in inflammation that corresponds with elevated HA levels.

2.5. Asbestos. Asbestos is derived from silicate minerals and has been used to provide electrical and building insulation

due, in part, to its resistance to fire [34]. Asbestos is composed of fibrous crystals that can accumulate in the air and cause lung injury as a result of inhalation, including lung cancer, mesothelioma, pleural plaques, pleural effusion, and asbestosis [35]. In a study conducted by Cantin et al., HA concentration was measured in the BAL of 27 workers from asbestos mills and mines, 9 without asbestosis, and 18 with asbestosis [36]. Mean HA levels were found to be 53.9 µg/L in control subjects, 67.5 µg/L in asbestos-exposed workers without asbestosis, and 206 µg/L in workers with asbestosis ($p < 0.05$) (radiometric assay). This study also examined HA in the BAL of asbestos-exposed sheep. Asbestos was applied by intratracheal infusions of chrysotile at 10 mg or 100 mg doses every 10 days for 39 months. Mean HA levels were found to be 34.7 µg/L in control (PBS) sheep, 83.0 µg/L in sheep treated with the 10 mg dose, and 248.0 µg/L in the sheep treated with the 100 mg dose ($p < 0.05$). These data indicate that BAL HA levels correspond with the extent of lung damage by asbestos and with the amount of exposure to asbestos. A separate study also observed that serum HA levels corresponded to malignancies caused by asbestos exposure [37] (radiometric assay).

2.6. Flour Dust. Flour dust exposure can lead to the development of an IgE-mediated sensitization to flour proteins causing asthma and rhinitis in the baking industry in a condition known as baker's asthma [37]. Brisman et al. analyzed indices of nasal airway inflammation in bakers, seeking to relate these to nasal symptoms and exposure to airborne flour dust [38]. Twelve flour-exposed bakers participated in this study and were examined by nasal lavage, visual inspection, a test for mucociliary clearance, and nasal peak expiratory flow. A significant correlation between nasal lavage HA levels and nasal mucociliary clearance was observed (radiometric assay). Two atopic individuals had the highest levels of HA in the nasal lavage and there was a positive correlation between the cumulative dose of flour dust and HA nasal lavage levels. Furthermore, HA nasal lavage levels correlated with the number of years the subjects worked as bakers. These data indicate that a baker's occupational exposure of flour dust can cause nasal mucosal inflammation that is associated with elevated levels of HA in nasal secretions.

2.7. Conclusions. These studies indicate that (i) elevated levels of HA in BAL fluid are associated with a variety of environmental and occupational airway injuries. (ii) HA levels correspond to the extent of exposure and lung injury. And (iii) elevated HA levels in BAL may be present even in the absence of obvious lung disease. As shown in Figure 1, one of the host responses of the airways to occupational and environmental exposures is the production of HA in the lung tissue and pulmonary secretions. If the exposure continues, and inflammation fails to resolve, abnormal matrix remodeling occurs, including the chronic synthesis of HA, its modification with the heavy chains of inter-alpha-inhibitor, and the production of proinflammatory HA fragments which exacerbates the inflammatory and fibrotic stimuli [9, 39–45] (Figure 2). It should be noted that the role of heavy chain

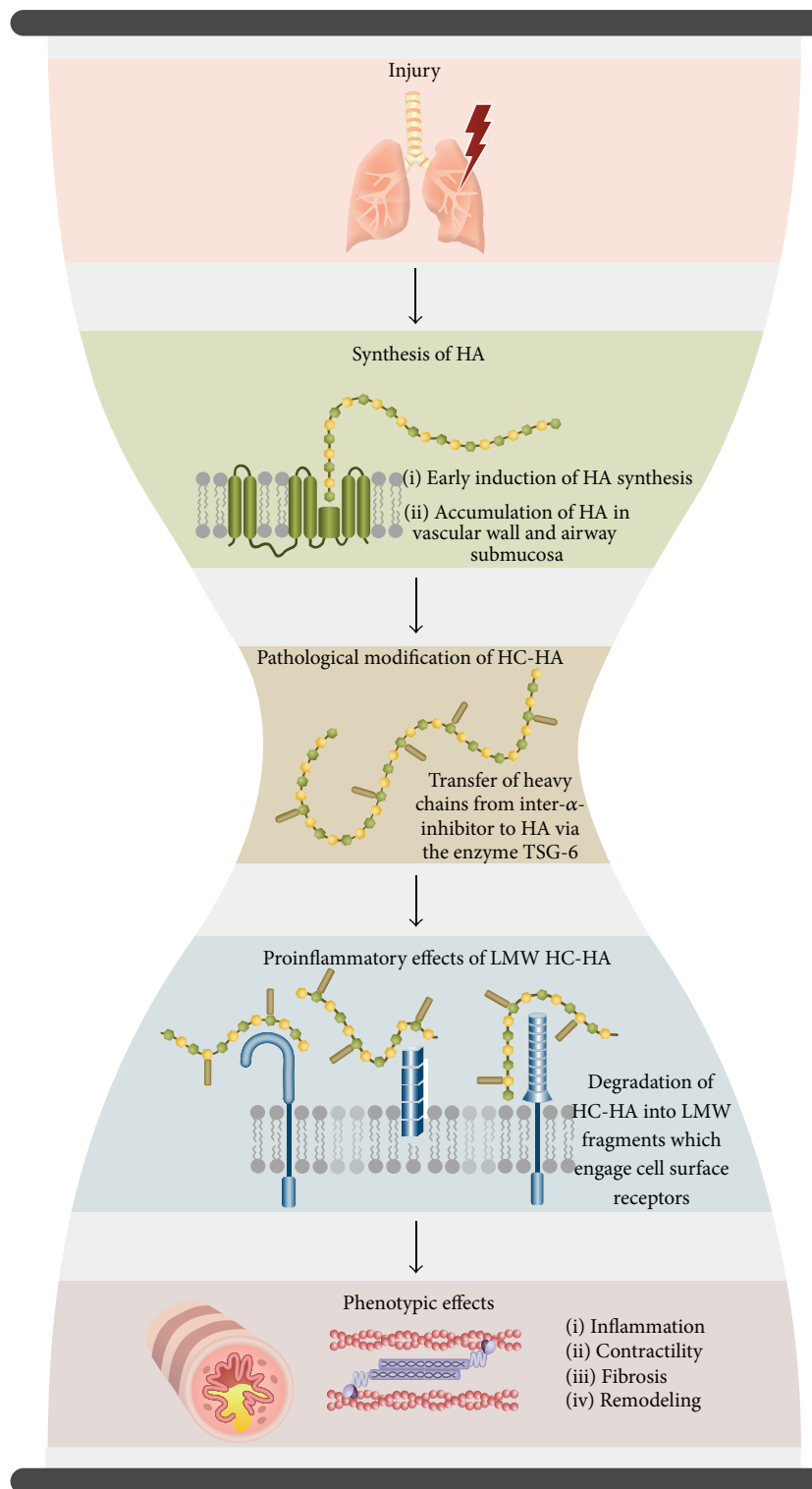


FIGURE 2: Mechanistic role of HA in the response to lung injury: lung injury leads to the synthesis of HA that accumulates in the peribronchial and perivascular spaces. The ongoing inflammation leads to the generation of heavy-chain-HA (HC-HA) complexes mediated via TSG-6 which is a bottleneck in the pathological transformation of HA matrices. These HC-HA complexes can be degraded into smaller LMW fragments which engage cell receptors such as CD44, TLR4, and TLR2 and create downstream biological effects like fibrosis, AHR, and inflammation.

modified HA fragments in directing inflammatory events has not yet been elucidated.

3. Human Respiratory Diseases

3.1. Smoking. Tobacco smoking is a major risk factor for the development of several lung diseases most notably lung cancer as well as chronic obstructive pulmonary disease (COPD) which includes emphysema and chronic bronchitis. One of the early findings, by McDevitt et al. [46], was that the gas phase of cigarette smoke, introduced into solutions of HA by the method of Kew et al. [47], led to a marked reduction in HA viscosity and size in a time-dependent manner. Dimethyl sulfoxide, a scavenger of hydroxyl radicals, inhibited this degradation, suggesting that oxidative damage by free radicals in the gas phase of cigarette smoke was the mechanism by which HA was degraded. Bracke et al. confirmed these observations in a mouse model of cigarette smoke-exposed mice [42] (see animal model section below for more information). In a study conducted by Sköld et al. [48], smoking cessation was found to result in a transient induction of HA accumulation in the BAL 1 month (38.8 $\mu\text{g/L}$), 3 months (34.0 $\mu\text{g/L}$), and 6 months (37.5 $\mu\text{g/L}$) following smoking cessation, compared to smokers before cessation (28.6 $\mu\text{g/L}$) and nonsmokers (10.0 $\mu\text{g/L}$) ($p < 0.01$ to 0.001) (radiometric assay). This data implies that the induction of HA following smoking cessation may have a reparative effect on lung pathology caused by smoke injury, while smoking itself can degrade HA into LMW forms that may promote inflammation [9].

3.2. COPD. Chronic obstructive pulmonary disease (COPD) is a progressive lung disease characterized by fixed airway obstruction that results in shortness of breath, cough, and sputum production and is typically caused by tobacco smoking [49]. In one study, COPD patients had elevated ($\sim 27 \mu\text{g/L}$) levels of HA in the BAL compared to normal nonsmokers ($\sim 17 \mu\text{g/L}$) ($p < 0.01$) [50] (radiometric assay). Additionally, COPD patients with lower pulmonary function measurements had higher levels of HA in BAL than COPD patients with relatively normal pulmonary function. Similarly, in a separate study, HA levels were higher in the sputum of COPD patients (234 $\mu\text{g/L}$) than healthy smokers (66 $\mu\text{g/L}$) ($p < 0.005$) [51] (ELISA-like assay). Furthermore, COPD patients with higher levels of sputum HA had lower FEV₁, and higher inflammatory markers, than COPD patients with moderate levels of HA. These data indicate that there is a relationship between HA levels in COPD sputum and BAL that corresponds with disease severity.

3.3. Asthma. Asthma is a chronic inflammatory disease characterized by bronchial wall basement membrane thickening, airway smooth muscle hypertrophy, mucous gland hypertrophy, vascular dilation, and airway epithelial damage [52]. The original report of HA in human asthma found HA to be the only glycosaminoglycan present in the pulmonary secretions (BAL) from 4 patients with severe asthma [53]. Later, it was determined that HA levels in BAL were significantly increased in patients with persistent asthma who were

atopic (32 $\mu\text{g/L}$) and nonatopic (21 $\mu\text{g/L}$) in comparison to control subjects (0 $\mu\text{g/L}$) and patients with mild intermittent asthma (0.5 $\mu\text{g/L}$) ($p < 0.001$) [54] (radiometric assay). Liang et al. isolated and cultured fibroblasts from endobronchial biopsies of 21 asthmatics, and 25 healthy controls, and examined the cells for HA production [43]. Baseline (unstimulated) HA production by airway fibroblasts was significantly ($p < 0.05$) higher in the asthmatic population ($\sim 900 \mu\text{g/L}$) compared to healthy controls ($\sim 200 \mu\text{g/L}$) (ELISA-like assay). Furthermore, the average HA size was lower in MW for the asthmatic ($\sim 800 \text{kDa}$) population than controls ($\sim 1500 \text{kDa}$). This was accompanied by a marked increase in HAS2 gene expression in asthmatic (~ 18 -fold) compared to control (~ 3 -fold) fibroblasts ($p < 0.05$). In another study by Ayars et al., patients with severe, steroid-dependent asthma received either mepolizumab (anti-IL-5 antibody) or placebo in a randomized, double-blind, placebo-controlled study [55]. Sputum HA was measured after 16 weeks of treatment. A significant decrease in sputum HA was observed in the mepolizumab treatment group (97 $\mu\text{g/L}$) compared to the placebo group (266 $\mu\text{g/L}$) ($p = 0.007$), which correlated with improvements in percent forced expiratory volume in 1 s (FEV₁%) ($p = 0.001$) (competitive ELISA-like assay). In summary, HA is an important component of airway secretions, and cultured fibroblasts, from asthmatics that corresponds to disease severity and pulmonary function.

3.4. Sarcoidosis. The pulmonary manifestation of sarcoidosis is the accumulation of granulomas in the interstitium, including the alveoli, small airways, and blood vessels [56]. The disease progresses to fibrosis in a small percentage (5–15%) of cases. Hallgren et al. found HA (16 $\mu\text{g/L}$) in the BAL of 23 patients with sarcoidosis, though it was undetectable in smoking or nonsmoking healthy volunteers [57] (radiometric assay). Serum HA levels were normal, but patients with abnormal lung function (spirometry) had HA BAL concentrations six times higher than patients with normal vital capacity. In a separate study, Eklund et al. found HA BAL levels from 23 sarcoidosis patients at 12 $\mu\text{g/L}$ on average [58] (radiometric assay). HA levels positively correlated with the numbers of BAL leukocytes. Bjermer et al. identified a strong correlation between BAL HA and mast cell levels which correlated inversely with lung volume [59] (radiometric assay). Macrophages and granulocyte counts were not related to BAL HA levels or indicators of lung disease, though lymphocyte counts were significantly ($p < 0.001$) elevated and corresponded to mast cells and HA levels. Blaschke et al. demonstrated that elevated levels of other extracellular matrix components, including fibronectin and type III procollagen peptide, correlated with elevated levels of HA (39 $\mu\text{g/L}$) compared to control values of 25 $\mu\text{g/L}$) in the BAL of patients with sarcoidosis ($p < 0.001$) [60] (radiometric assay). In summary, HA BAL levels are elevated in patients with sarcoidosis and correspond to decreased lung function, increased leukocyte counts, and increased extracellular matrix components.

3.5. Idiopathic Pulmonary Fibrosis. Idiopathic pulmonary fibrosis is a disease of the lung interstitium that involves fibrosis within alveolar tissue, small airways, and blood vessels [61]. Bjermer et al. found elevated levels of HA (46 $\mu\text{g/L}$) in the BAL fluid of 22 patients with idiopathic pulmonary fibrosis compared to 21 control subjects (9 $\mu\text{g/L}$) ($p < 0.001$) [62] (radiometric assay). Serum HA levels were normal, but elevated neutrophil and lymphocyte counts correlated with the increased levels of HA. Patients with deterioration of lung function and radiographic progression had higher BAL levels of HA than in patients whose disease was stable ($p < 0.01$). This study was largely substantiated by a separate study conducted by Milman et al. who expanded it to include correlations with procollagen type III aminoterminal peptide [63]. In a histological examination of HA by Garantziotis et al., HA was found to colocalize with inter-alpha-inhibitor in fibroblastic foci of patients with usual interstitial pneumonitis, implying that the HA present in these regions is likely to be covalently modified by heavy chains from inter-alpha-inhibitor [17].

3.6. Idiopathic Pulmonary Hypertension. Idiopathic pulmonary arterial hypertension (IPAH) is a progressive disease that leads to deterioration in cardiopulmonary function and premature death from right ventricular failure [64]. The pathogenesis of IPAH includes cell proliferation, vascular remodeling, and inflammatory cell recruitment. Papakonstantinou et al. investigated total glycosaminoglycan content between IPAH and control donor lungs and found that only HA had elevated levels associated with IPAH [65]. The relative HA levels in IPAH lung tissue (78.6 μg) were greater than the amount of HA in control donor lung tissue (43.2 μg) ($p < 0.01$), consistent with the observation that HAS1 gene and protein expression was elevated in the IPAH cohort while Hyal1 gene expression was significantly decreased ($p < 0.05$) (ELISA-like assay). HAS1 protein localized to pulmonary arterial smooth muscle cells in IPAH lung tissue and increased HA deposition was observed in remodeled pulmonary arteries. In a separate study, Aytikin et al. demonstrated that plasma HA levels were markedly elevated in IPAH (325 $\mu\text{g/L}$) compared with controls (28 $\mu\text{g/L}$) ($p = 0.02$) [66] (competitive ELISA-like assay). Cultured, and unstimulated, pulmonary arterial smooth muscle cells from IPAH patients secreted higher levels of HA into conditioned media (12 $\mu\text{g/mL}$) compared to control cells (6 $\mu\text{g/mL}$) ($p = 0.04$). This HA was in the form of "cable" structures that promoted the adhesion of mononuclear cells, comparing their adhesion to pulmonary arterial smooth muscle cells from IPAH (9.5×10^4 cells bound) and control subjects (3.0×10^4 cells bound) ($p = 0.01$). This same group also observed that the HA in IPAH lungs is a pathological form of HA covalently modified with heavy chains from inter-alpha-inhibitor [16]. Heavy chain modified HA (HC-HA) was found within regions of vascular modeling, including plexogenic lesions. Inflammatory cells colocalized within these matrices in regions of vascular pathology in IPAH lung tissue, raising the possibility that HC-HA may direct inflammatory events that cause vascular remodeling in IPAH.

3.7. Lung Transplant. Rao et al. investigated HA BAL and plasma levels from 57 lung transplant recipients as a marker of early posttransplantation infection and acute cellular rejection [67]. Mean BAL HA levels in recipients with clinically stable conditions was 33.5 $\mu\text{g/L}$ (radiometric assay). Mild rejection did not result in significant BAL HA levels, though it was slightly higher with infection (51.10 $\mu\text{g/L}$) ($p = 0.036$). Moderate to severe rejection resulted in significantly elevated BAL HA levels (295.0 $\mu\text{g/L}$) ($p = 0.0001$) and the highest levels were found in patients with diffuse alveolar damage (392 $\mu\text{g/L}$). Mean plasma HA levels in clinically stable recipients were 59.60 $\mu\text{g/L}$ and were elevated in severe rejection (112.0 $\mu\text{g/L}$) and diffuse alveolar damage (169.20 $\mu\text{g/L}$) and even higher in recipients with acute respiratory infection (191.0 $\mu\text{g/L}$). These observations were substantiated and expanded by Riise et al. [68, 69].

3.8. Bronchiolitis Obliterans. One of the major causes of lung transplant rejection is the onset of bronchiolitis obliterans syndrome (BOS) which is characterized by irreversible limitations of airflow associated with small airway fibrosis [70]. Todd et al. found elevated levels of HA within the intraluminal fibrous tissue of patients with BOS [71]. This corresponded with elevated expression (2-3-fold) of HAS1-3 in whole lung tissue from BOS compared to control subjects ($p < 0.05$). HA BAL levels were elevated in BOS subjects (107.91 $\mu\text{g/L}$) compared to controls (28.97 $\mu\text{g/L}$) ($p < 0.0001$) and remained steady between different grades of BOS. Furthermore, HA plasma levels were elevated in early or severe onset BOS subjects (90.37 $\mu\text{g/L}$) compared to patients who had remained BOS free for at least 5 years (44.42 $\mu\text{g/L}$) ($p = 0.03$) (sandwich ELISA-like assay).

3.9. Conclusions. (i) In normal tissues, HA matrices are primarily located within (a) the airway submucosa, (b) the walls of pulmonary vasculature, (c) and to a lesser extent, alveoli. (ii) During pulmonary injury and repair, there is increased synthesis of HA matrices in these regions that colocalizes with inflammatory cells and likely influences their activation. (iii) The HA that accumulates in these regions is often covalently modified with heavy chains from inter-alpha-inhibitor which significantly promotes leukocyte adhesion to HA matrices [15–17, 72, 73] (Figure 2). (iv) Elevated HA BAL levels correspond with the extent of lung injury while HA serum levels do not always correlate with lung injury.

4. Animal Models of Pulmonary Injury

4.1. Asthma. HA deposition and correlation with inflammation have been described in the ovalbumin [74], cockroach antigen [75], and *Aspergillus fumigatus* [76] murine models of allergic inflammation. In the ovalbumin model described by Cheng et al., the accumulation of HA within BAL was a relatively early event, occurring within the first 24 hrs after allergen challenge (~25 $\mu\text{g/L}$ compared to ~10 $\mu\text{g/L}$ in naive controls) (sandwich ELISA-like assay). HA BAL levels peaked at day 8 (~125 $\mu\text{g/L}$), corresponding with elevated inflammatory cell counts in the BAL. Induction of whole lung HAS1

and HAS2 gene induction peaked (~20-fold above naïve values) within the first 2–4 hrs and steadily declined to almost normal levels by the end of 24 hrs. The accumulation of HA in the lung tissue was evident 12 hrs after allergen challenge (~140 $\mu\text{g/g}$ dry weight compared to ~75 $\mu\text{g/g}$ in naïve controls), peaked at 6 days (~375 $\mu\text{g/g}$), and steadily declined to lower levels 6 weeks later (~150 $\mu\text{g/g}$) (Fluorophore-Assisted-Carbohydrate-Electrophoresis (FACE) analysis). Elevated peribronchial distribution of HA was apparent 12 hrs after allergen challenge and colocalized with eosinophil distribution 2 days later (HABP fluorescence microscopy). Similar results were confirmed and expanded in cockroach [75] and fungal models of allergic airway inflammation [76]. The HA that accumulated in murine lungs following ovalbumin challenge was covalently modified with heavy chains from inter-alpha-inhibitor [15]. TSG-6 $-/-$ mice, which lack the ability to transfer heavy chains to HA, developed less inflammation, lower AHR, and lower levels of HA in response to allergen challenge, implying that HC-HA is an important factor in allergic inflammation [15]. Lower levels of lung HA in TSG-6 $-/-$ mice (FACE and HABP fluorescence microscopy) subjected to allergen induced asthma may be caused by the ability of TSG-6 to not only transfer heavy chains to HA but also regulate HA accumulation [77].

4.2. Bleomycin. The bleomycin model of pulmonary fibrosis is based upon a side-effect of its use as a chemotherapeutic agent for the treatment of several cancers [78]. Bleomycin exerts its antibiotic and tumorigenic effect by inducing DNA strand breaks, though the mechanism whereby it induces lung injury is not fully understood [79]. In rodents, bleomycin induces acute alveolitis with interstitial edema and fibrosis. Using a biotinylated HA binding protein to probe rat lung tissue sections, Nettelblatt et al. observed that HA accumulated in the edematous alveolar septa 4 days after the intratracheal administration of bleomycin [80]. Lymphocytes were present in the interstitial cellular infiltrate. In control rat lungs, HA was not seen in the alveolar tissue but was confined to peribronchial and perivascular spaces. Ten and twenty days after administration of bleomycin, macrophage infiltration was observed, as well as proliferating fibroblasts and collagen deposition in the alveolar tissue. At these later time points, HA deposition became less prominent in the alveolar interstitial tissue but more distinctly located around proliferating fibroblasts. The authors noted increased lung water content that peaked 4 days after bleomycin treatment and speculated that increased levels of HA might contribute to the water accumulation. This same group also noted that the accumulation of HA in the BAL of rats treated with bleomycin was relatively small ($0.2\text{--}0.3 \times 10^6$ Daltons) and did not respond to high-dose corticosteroid treatment [81]. In a separate study in hamsters, Bray et al. observed that total lung HA levels peaked 6 days after administration of bleomycin and was 14.6-fold higher than untreated levels (autoradiography) [82]. These levels sharply dropped on day 7 and steadily declined to approximately double control values by day 17. Total levels of lysosomal hyaluronidases were increased (673 units compared to 506 units in control lungs) in the injured lungs, even at the peak of HA accumulation on

day 6, indicating active turnover of HA. It was also observed that maximal HA content occurred prior to the rise in collagen and elastin biosynthesis, suggesting that HA acts as an acute phase molecule that may direct subsequent fibrotic events. Further evidence for an early role of HA during bleomycin-induced alveolitis was obtained by Nettelblatt et al. who demonstrated that HA induction was apparent within 24 hrs of bleomycin treatment, much earlier than the fibrotic stage that occurs several days later (radiometric assay) [83]. Garantziotis et al. observed that bikunin $-/-$ mice, deficient in their ability to covalently modify HA with heavy chains from inter-alpha-inhibitor, demonstrated deficient lung angiogenesis after bleomycin exposure [17]. Teder et al. observed that CD44 $-/-$ mice succumbed to unremitting inflammation following bleomycin lung injury, characterized by the accumulation of HA fragments at the site of tissue injury and impaired clearance of macrophages, neutrophils, and lymphocytes [84]. Dygai et al. observed that the intranasal application of hyaluronidase, immobilized on polyethyleneoxide, did not modify the inflammatory process or deposition of collagen fibrils in the lung parenchyma [85]. Studies by others have substantiated, and expanded, these observations [86–92].

4.3. Elastase. The intratracheal administration of elastase remains a common and convenient method for the induction of emphysema-like airway pathology, including the augmentation of airspaces, inflammatory cell influx into the lungs, and systemic inflammation [93]. In two early studies, Moczar et al. demonstrated that cultured lung explants from hamsters, intratracheally injected with elastase, demonstrated significantly enhanced incorporation of ^{14}C -glucosamine into HA [94]. In a separate study by Cantor et al., coadministration of hyaluronidase with elastase resulted in significantly greater airspace enlargement than hamsters treated with elastase alone [95]. Rescue by the intratracheal administration of HA immediately after elastase instillation resulted in a marked decrease in airspace enlargement. When HA was administered 1 or 2 hrs before elastase administration, rescue of airspace enlargement was retained [96]. When HA was administered 1 or 2 hrs after elastase administration, rescue was compromised. Scuri et al. demonstrated a protective effect on bronchoconstriction of inhaled HA against elastase-induced injury in sheep, where 200 kDa HA had significantly greater protective effect than 70 kDa HA [97]. This protective effect was also observed in the 150–300 kDa range which was found to be more dependent upon dosage rather than MW [98]. Studies by others have substantiated and expanded these observations [99–101].

4.4. Hyperoxia. Preterm birth by cesarean section often results in an imbalance of fluid secretion and absorption in the lungs that results in interstitial edema which is treated by oxygen supplementation and/or ventilator support which can exacerbate pulmonary fluid retention [102]. Juul et al. demonstrated that the HA content of untreated neonatal rat pups decreased over the first 10 days of life while pups housed under hyperoxic conditions exhibited a time-dependent

increase in both lung HA and lung weight [103]. This HA accumulated in the perivascular regions of medium sized arteries and in the alveolar walls. A similar study by Johnsson et al. confirmed and expanded these observations in rabbit pups, delivered by cesarean section 1 or 2 days before term [104]. Though this report did not observe a time-dependent decrease in HA content of pups housed under room air conditions, continuous exposure to hyperoxia resulted in significantly elevated levels of lung HA concentration 6 days after term. This increase was accompanied by significantly elevated wet/dry lung weight ratios. Increased HA deposition was observed in alveoli, arterioles, and bronchiole of pups housed under hyperoxic conditions. The extent to which the elevated HA levels, induced by hyperoxia, contribute to edema is not yet known.

4.5. Cigarette. Tobacco smoke contains >7000 chemicals, including cyanide, benzene, formaldehyde, methanol, acetylene, and ammonia [105]. At least 70 of these chemicals are known carcinogens and many of them cause heart and lung diseases in addition to cancer [106]. Mice exposed to cigarette smoke for 4 weeks (subacute) or 24 weeks (chronic) demonstrated higher levels of staining for HA in alveolar walls for both time points [42]. This was in contrast to the deposition of collagen and fibronectin which were only elevated at the chronic time point. A modest (~25%) increase of HA levels in total lung tissue was observed in the smoke-exposed mice at 4- and 24-week time points. The size of this HA was significantly smaller (average MW about 70 kDa) than HA without smoke exposure (broad range of 250–1000 kDa), though it remains to be determined whether the MW redistribution was caused by oxidative damage from smoke exposure itself or from downstream inflammatory effects. Cigarette smoke induced HAS3 gene expression (~40%) and decreased HAS1 expression (~30%) while not significantly effecting HAS2 gene expression. Two separate studies demonstrated a therapeutic effect for inhaled aerosolized HA (150 and 1600 kDa) in a mouse and rat model of cigarette smoke exposure [107, 108]. These therapeutic effects included significantly less neutrophil infiltration, lung edema, airway apoptosis, and mucus plugging.

4.6. Ozone. Ozone exposure leads to oxidative stress-induced inflammation of the airways, epithelial injury, and AHR which peaks at 24 hours after exposure. In a study conducted by Garantziotis et al., ozone exposed mice demonstrated enhanced AHR associated with elevated levels (~40 $\mu\text{g}/\text{L}$) compared to undetectable levels in normal air exposed mice) of HA in BAL [39] (ELISA-like assay). CD44 $-/-$ (a major receptor for HA) and bikunin $-/-$ (unable to make HC-HA) mice showed even higher levels of elevated HA in response to ozone exposure (~100 $\mu\text{g}/\text{L}$) but had significantly lower levels of AHR compared to WT mice. Mice pretreated with HA binding protein were protected from developing ozone-induced AHR. LMW HA exacerbated AHR in response to ozone treatment while HMW HA alleviated it. An allergic model of asthma was also found to exacerbate AHR and HA BAL levels in response to ozone treatment [109]. Other

studies have substantiated and expanded these observations [40, 110–112].

4.7. Radiation. The pathological effect of radiation on the respiratory system is complex, involving the death of lung cells and the mounting of an inflammatory response [113]. The two major functional outcomes of radiation damage on the respiratory system include radiation pneumonitis and radiation fibrosis [113]. In a rat model of bilateral radiation-induced lung disease, Rosenbaum et al. found elevated levels of HA in serum (5.5-fold) and BAL (1.5-fold) 4 weeks after irradiation, during peak alveolitis [114]. Elevated levels of HA were not observed at earlier (2 weeks) or later (6–20 weeks) time points; thus serum HA levels appear to be a poor predictive indicator of radiation-induced pneumonitis. Histological staining demonstrated that HA accumulated in the intra-alveolar edema fluid but not the alveolar walls. Administration of methylprednisolone significantly decreased alveolitis and HA levels in the alveolar space and serum but did not affect fibrosis. In a separate study by Li et al., irradiation to the lower portion of the right lung of rats induced an accumulation of HA in BAL that was significantly elevated (152.8 $\mu\text{g}/\text{L}$) 6 weeks after irradiation compared to untreated controls (5.5 $\mu\text{g}/\text{L}$) [115]. Interestingly, HA BAL levels were not elevated at earlier (2 and 4 weeks) or later (8 and 10 weeks) time points. HAS2 gene expression was elevated at 4, 6, and 10 weeks of irradiation while Hyal2 expression decreased concomitantly. In a third study by Iwakawa et al. histological analysis of HA lung levels at sites of inflammation was evident within 12 hrs of radiation exposure and resolved 2 weeks later [116].

4.8. Ventilation. Early respiratory distress syndrome (RDS) in premature infants is characterized by lung edema ultimately leading to fibrosis or bronchopulmonary dysplasia [117]. Testing the hypothesis that increased HA levels in the alveolar interstitium would be associated with severe RDS; Juul et al. subjected 34 preterm delivered *Macaca nemestrina* monkeys to ventilation and found that HA levels were elevated (86.3 $\mu\text{g}/\text{g}$ lung wet weight) in lung extracts with progressively more severe RDS compared to animals without RDS (19.6 $\mu\text{g}/\text{g}$) ($p < 0.001$) (radiometric assay) [117]. As the severity of RDS increased, HA was increasingly associated with the microvasculature in the interalveolar spaces, and in the most severe cases, HA was present in the alveolar walls. In a separate study by Bai et al., HAS3 $-/-$ mice demonstrated reduced neutrophil infiltration, macrophage inflammatory protein-2 production, and lung microvascular leakage in response to ventilator-induced lung injury [118]. The HA produced by WT mice in response to ventilator-induced injury contained both HMW (1600 kDa) and LMW (<360 kDa) HA while only HMW HA was observed in HAS3 $-/-$ mice. Wang et al. described a therapeutic improvement in ventilated premature piglets when surfactant treatment was supplemented with HA [119].

4.9. Bacterial Infection. Bacteria colonize the respiratory tract by multiplying in or on the airway epithelial mucosa, causing inflammation, increased mucus secretion, and

impaired mucociliary clearance [120]. In one report by Juul et al., neonatal piglet lung HA levels decreased 4 hrs after inoculation with group B streptococcus (27 $\mu\text{g/g}$ wet weight) and atelectasis plus pneumonia (10 $\mu\text{g/g}$) compared to control piglets (51 $\mu\text{g/g}$) ($p < 0.005$) (radiometric assay) [121]. Later time points were not examined. In a study conducted by van der Windt et al., enhanced pulmonary inflammation was associated with decreased *Klebsiella pneumoniae* growth in CD44 $-/-$ mice compared to WT mice [122]. Lethal dosage with this bacterium did not impact the survival of CD44 $-/-$ mice compared to WT mice, though resolution of lung inflammation was delayed. Other studies confirmed and expanded some of these observations [123, 124]. Marion et al. provided evidence that *Streptococcus pneumoniae* have the capacity to utilize HA as a carbon source during colonization [125]. Intranasal exposure of staphylococcal enterotoxin B induced elevated levels of HA in BAL (~40 pg/mL) compared to control mice (~18 pg/mL) (ELISA-like assay) [126] and treatment with an inhibitor of HA synthesis (4-methylumbelliferone) had a protective effect on lung injury caused by this toxin [127]. Chang et al. demonstrated that intratracheal inoculation with *Escherichia coli* caused a rapid (2 hr) induction of HAS1 and HAS2 gene expression associated with increased histological staining for HA in the lungs [128].

4.10. Conclusions. These studies indicate the following. (i) The induction of HA synthesis in the lung is an early event following lung injury, occurring within hours of the original stimulus. (ii) HA synthesis precedes pulmonary fibrosis, and HA levels continue at elevated levels throughout the initial stages of fibrosis. (iii) The clearance of HA matrices following pulmonary injury is necessary for the proper resolution of inflammation. (iv) The size of HA is affected by the stage of disease and can exacerbate respiratory symptoms following injury (Figure 2). (v) The covalent modification of HA with heavy chains from inter- α -inhibitor, by the enzyme TSG-6, plays a key role in the development of airway inflammation [15–17, 72, 73] (Figure 2).

5. Overall Summary and Conclusions

The rise and fall of HA levels in the injured lung are essential for its repair and return to homeostasis (Figure 1). The data reviewed in this paper present a model whereby HA synthesis in the airways can be induced by either an acute injury (i.e., an asthma exacerbation) or a series of chronic insults (i.e., exposure to environmental irritants, smoking, lung transplant, genetic diseases, etc.). The induction of HA synthesis in lung tissue following an acute injury can be relatively rapid, occurring within the first 24 hrs of injury [74]. Once induced by injury, lung HA levels can remain elevated for several weeks [74]. Chronic conditions induce a low-level, long-term injury that leads to the accumulation of abnormally high levels of HA in the lung tissue. Following both acute and chronic pulmonary injury, two modifications happen to HA that regulate its pathobiology: (i) the covalent transfer of heavy chains from inter- α -inhibitor to the C6 hydroxyl of an N-acetylglucosamine residue on HA and

(ii) its degradation into LMW fragments (Figure 2). The former is a process regulated by the enzyme TSG-6 [14, 15, 17] while the latter is regulated by the activity of hyaluronidases and the production of free radicals at the site of injury [6, 9].

Clearly there is a connection between elevated HA levels and its regional distribution with inflammatory cell infiltration. Leukocytes are typically found embedded within HA matrices of the airway submucosa and in perivascular regions. The covalent modification of HA with heavy chains from inter- α -inhibitor has been shown to promote leukocyte adhesion to HA matrices [77, 129], and this modification has been described in several respiratory disorders [15–17, 72, 73]. The effect that this modification has on leukocyte pathobiology remains to be established and both proinflammatory and anti-inflammatory data have been reported [1, 2, 15, 130].

While the induction of HA synthesis is clearly triggered by pulmonary injury, its role in directing fibrotic events remains to be defined and the signals that orchestrate its turnover and degradation following injury are not fully understood. The production of HA fragments, as a result of matrix remodeling and tissue damage by free radicals, is one of the signals that mediates inflammation and fibrosis [3, 45]. These HA “danger signals” operate via TLR4, MyD88, and TIRAP signaling pathways in the airways where they regulate AHR and the production of proinflammatory cytokines [111]. Intratracheal instillation of LMW HA fragments induces CD44-dependent AHR while instillation of HMW HA is protective [39]. Thus, in the airways, and other biological systems, the size of HA is one of the mechanisms whereby this relatively simple polysaccharide directs inflammatory and fibrotic events.

A variety of stimuli have been found to induce the accumulation of HA in respiratory secretions, reaching levels between 27 and 547 $\mu\text{g/L}$ in BAL fluid. This is in contrast to the relatively low levels of HA found in the respiratory secretions of healthy controls which ranged from 0 to 53 $\mu\text{g/L}$ in the BAL fluid reported in this review. The variation of HA levels in the BAL of healthy controls cannot be explained by difference in analytical techniques since no trend was observed between these techniques in that regard. It is more likely that the selection criteria of a particular healthy control patient cohort and/or the volume of BAL fluid instilled and collected may be responsible for the range of HA levels observed in healthy controls. The cellular source of HA found in respiratory secretions includes the airway epithelium [131], and the serous epithelial cells of the submucosal glands [132, 133], while it appears to be a minor component of goblet and mucous gland cell secretions [133]. The contribution that HA makes to respiratory secretions is not fully understood, though its large hydrodynamic volume is likely to contribute to mucus hydration and its viscoelastic properties.

While elevated levels of HA promote pulmonary wound healing in acute injury, it is less clear whether elevated levels of HA promote wound healing in a chronic state. In allergic asthma, where the respiratory system mounts an immune response against a relatively inert “invader,” it is not clear whether the induction of HA has beneficial or harmful effects. If HA is exerting a beneficial effect in a specific respiratory disease, then therapeutic strategies to enhance

this effect might accelerate and improve the healing process. Indeed, several reports have described beneficial effects in the administration of HA, itself, as a therapy for several pulmonary conditions [19, 95, 97, 98, 107, 108, 119, 134–150], though the mechanisms whereby these beneficial effects occur remain to be defined. If HA is exerting a negative effect, such as might be the case in a chronic or allergic condition, then therapeutic strategies that antagonize HA synthesis, binding proteins, receptors, and so forth would be more effective.

In summary, these data present HA as a unique polysaccharide matrix which contributes to the homeostasis, maintenance, and repair of the injured lung (Figure 2). The biochemical and biophysical properties of HA endow this polysaccharide with protective and regenerative effects that contributes to edema and the regulation of AHR. The accumulation of HA at sites of pulmonary injury and repair provides an essential microenvironment that directs inflammatory events and fibrosis. The failure to mount an effective immune response, the inability to resolve inflammation, and/or the development of irreversible fibrosis in the respiratory system is, in part, influenced by the regulation of this relatively simple glycosaminoglycan.

Conflict of Interests

The authors declare that there is no conflict of interests regarding the publication of this paper.

Acknowledgments

This work was in part supported by the Division of Intramural Research, National Institute of Environmental Health Sciences, the National Institute of Allergy and Infectious Disease, and the National Heart Lung and Blood Institute AI067816, HL081064, HL103453, HL113325, and HL107147.

References

- [1] A. C. Petrey and C. A. de la Motte, "Hyaluronan, a crucial regulator of inflammation," *Frontiers in Immunology*, vol. 5, article 101, 2014.
- [2] A. Wang, C. de la Motte, M. Lauer, and V. Hascall, "Hyaluronan matrices in pathobiological processes," *FEBS Journal*, vol. 278, no. 9, pp. 1412–1418, 2011.
- [3] H. Frey, N. Schroeder, T. Manon-Jensen, R. V. Iozzo, and L. Schaefer, "Biological interplay between proteoglycans and their innate immune receptors in inflammation," *The FEBS Journal*, vol. 280, no. 10, pp. 2165–2179, 2013.
- [4] T. N. Wight, I. Kang, and M. J. Merrilees, "Versican and the control of inflammation," *Matrix Biology*, vol. 35, pp. 152–161, 2014.
- [5] D. Vigetti, E. Karousou, M. Viola, S. Deleonibus, G. de Luca, and A. Passi, "Hyaluronan: biosynthesis and signaling," *Biochimica et Biophysica Acta—General Subjects*, vol. 1840, pp. 2452–2459, 2014.
- [6] R. Stern, G. Kogan, M. J. Jedrzejewski, and L. Šoltés, "The many ways to cleave hyaluronan," *Biotechnology Advances*, vol. 25, no. 6, pp. 537–557, 2007.
- [7] D. Jiang, J. Liang, and P. W. Noble, "Hyaluronan as an immune regulator in human diseases," *Physiological Reviews*, vol. 91, no. 1, pp. 221–264, 2011.
- [8] D. Jiang, J. Liang, and P. W. Noble, "Hyaluronan in tissue injury and repair," *Annual Review of Cell and Developmental Biology*, vol. 23, pp. 435–461, 2007.
- [9] R. Stern, A. A. Asari, and K. N. Sugahara, "Hyaluronan fragments: an information-rich system," *European Journal of Cell Biology*, vol. 85, no. 8, pp. 699–715, 2006.
- [10] H.-G. Wisniewski and J. Vilček, "TSG-6: an IL-1/TNF-inducible protein with anti-inflammatory activity," *Cytokine and Growth Factor Reviews*, vol. 8, no. 2, pp. 143–156, 1997.
- [11] E. Fries and A. Kaczmarczyk, "Inter- α -inhibitor, hyaluronan and inflammation," *Acta Biochimica Polonica*, vol. 50, no. 3, pp. 735–742, 2003.
- [12] C. M. Milner and A. J. Day, "TSG-6: a multifunctional protein associated with inflammation," *Journal of Cell Science*, vol. 116, no. 10, pp. 1863–1873, 2003.
- [13] C. M. Milner, V. A. Higman, and A. J. Day, "TSG-6: a pluripotent inflammatory mediator?" *Biochemical Society Transactions*, vol. 34, no. 3, pp. 446–450, 2006.
- [14] C. M. Milner, W. Tongsoongnoen, M. S. Rugg, and A. J. Day, "The molecular basis of inter-alpha-inhibitor heavy chain transfer on to hyaluronan," *Biochemical Society Transactions*, vol. 35, no. 4, pp. 672–676, 2007.
- [15] S. Swaidani, G. Cheng, M. E. Lauer et al., "TSG-6 protein is crucial for the development of pulmonary hyaluronan deposition, eosinophilia, and airway hyperresponsiveness in a murine model of asthma," *The Journal of Biological Chemistry*, vol. 288, no. 1, pp. 412–422, 2013.
- [16] M. E. Lauer, M. Aytakin, S. A. Comhair et al., "Modification of hyaluronan by heavy chains of inter- α -inhibitor in idiopathic pulmonary arterial hypertension," *Journal of Biological Chemistry*, vol. 289, no. 10, pp. 6791–6798, 2014.
- [17] S. Garantziotis, E. Zudaire, C. S. Trempus et al., "Serum inter- α -trypsin inhibitor and matrix hyaluronan promote angiogenesis in fibrotic lung injury," *American Journal of Respiratory and Critical Care Medicine*, vol. 178, no. 9, pp. 939–947, 2008.
- [18] F. E. Lennon and P. A. Singleton, "Role of hyaluronan and hyaluronan-binding proteins in lung pathobiology," *The American Journal of Physiology—Lung Cellular and Molecular Physiology*, vol. 301, no. 2, pp. L137–L147, 2011.
- [19] J. O. Cantor, "Potential therapeutic applications of hyaluronan in the lung," *International Journal of Chronic Obstructive Pulmonary Disease*, vol. 2, pp. 283–288, 2007.
- [20] S. Haserodt, A. Metin, and R. A. Dweik, "A comparison of the sensitivity, specificity, and molecular weight accuracy of three different commercially available hyaluronan ELISA-like assays," *Glycobiology*, vol. 21, no. 2, pp. 175–183, 2011.
- [21] L. Bjermer, A. Engström-Laurent, R. Lundgren, L. Rosenhall, and R. Hällgren, "Hyaluronate and type III procollagen peptide concentrations in bronchoalveolar lavage fluid as markers of disease activity in farmer's lung," *British Medical Journal*, vol. 295, no. 6602, pp. 803–806, 1987.
- [22] Y. Cormier, M. Laviolette, A. Cantin, G. M. Tremblay, and R. Bégin, "Fibrogenic activities in bronchoalveolar lavage fluid of farmer's lung," *Chest*, vol. 104, no. 4, pp. 1038–1042, 1993.
- [23] K. Larsson, A. Eklund, P. Malmberg, L. Bjermer, R. Lundgren, and L. Belin, "Hyaluronic acid (hyaluronan) in BAL fluid distinguishes farmers with allergic alveolitis from farmers with asymptomatic alveolitis," *Chest*, vol. 101, no. 1, pp. 109–114, 1992.

- [24] K. Larsson, A. Eklund, P. Malmberg, and L. Belin, "Alterations in bronchoalveolar lavage fluid but not in lung function and bronchial responsiveness in swine confinement workers," *Chest*, vol. 101, no. 3, pp. 767–774, 1992.
- [25] R. Brouwer, K. Biersteker, P. Bongers, B. Remijn, and D. Houthuijs, "Respiratory symptoms, lung function, and IgG4 levels against pig antigens in a sample of Dutch pig farmers," *The American Journal of Industrial Medicine*, vol. 10, no. 3, pp. 283–285, 1986.
- [26] M. Iversen, R. Dahl, J. Korsgaard, T. Hallas, and E. J. Jensen, "Respiratory symptoms in Danish farmers: an epidemiological study of risk factors," *Thorax*, vol. 43, no. 11, pp. 872–877, 1988.
- [27] K. Larsson, P. Malmberg, A. Eklund, L. Belin, and E. Blaschke, "Exposure to microorganisms, airway inflammatory changes and immune reactions in asymptomatic dairy farmers. Bronchoalveolar lavage evidence of macrophage activation and permeability changes in the airways," *International Archives of Allergy and Applied Immunology*, vol. 87, no. 2, pp. 127–133, 1988.
- [28] K. Wimander and L. Belin, "Recognition of allergic alveolitis in the trimming department of a Swedish sawmill," *European Journal of Respiratory Diseases. Supplement*, vol. 107, pp. 163–167, 1980.
- [29] U. Johard, A. Eklund, M. Dahlqvist et al., "Signs of alveolar inflammation in non-smoking Swedish wood trimmers," *British Journal of Industrial Medicine*, vol. 49, no. 6, pp. 428–434, 1992.
- [30] U. Johard, A. Eklund, J. Hed et al., "Sawdust-induced inflammatory changes in rat lung: effects on alveolar and interstitial cells in relation to time," *Inflammation*, vol. 18, no. 5, pp. 547–563, 1994.
- [31] D. Sparrow, R. Bossé, B. Rosner, and S. T. Weiss, "The effect of occupational exposure on pulmonary function. A longitudinal evaluation of fire fighters and nonfire fighters," *American Review of Respiratory Disease*, vol. 125, no. 3, pp. 319–322, 1982.
- [32] P. W. Brandt-Rauf, B. Cosman, L. F. Fallon Jr., T. Tarantini, and C. Idema, "Health hazards of firefighters: acute pulmonary effects after toxic exposures," *British Journal of Industrial Medicine*, vol. 46, no. 3, pp. 209–211, 1989.
- [33] C. E. Bergström, A. Eklund, M. Sköld, and G. Tornling, "Bronchoalveolar lavage findings in firefighters," *American Journal of Industrial Medicine*, vol. 32, no. 4, pp. 332–336, 1997.
- [34] J. E. Alleman and B. T. Mossman, "Asbestos revisited," *Scientific American*, vol. 277, pp. 54–57, 1997.
- [35] E. Jamrozik, N. de Klerk, and A. W. Musk, "Asbestos-related disease," *Internal Medicine Journal*, vol. 41, no. 5, pp. 372–380, 2011.
- [36] A. M. Cantin, P. Larivée, M. Martel, and R. Bégin, "Hyaluronan (hyaluronic acid) in lung lavage of asbestos-exposed humans and sheep," *Lung*, vol. 170, no. 4, pp. 211–220, 1992.
- [37] E. Pluygers, P. Baldewyns, P. Minette, M. Beauduin, P. Gourdin, and P. Robinet, "Biomarker assessments in asbestos-exposed workers as indicators for selective prevention of mesothelioma or bronchogenic carcinoma: rationale and practical implementations," *European Journal of Cancer Prevention*, vol. 1, no. 1, pp. 57–68, 1991.
- [38] J. Brisman, K. Torén, L. Lillienberg, G. Karlsson, and S. Ahlstedt, "Nasal symptoms and indices of nasal inflammation in flour-dust-exposed bakers," *International Archives of Occupational and Environmental Health*, vol. 71, no. 8, pp. 525–532, 1998.
- [39] S. Garantziotis, Z. Li, E. N. Potts et al., "Hyaluronan mediates ozone-induced airway hyperresponsiveness in mice," *The Journal of Biological Chemistry*, vol. 284, no. 17, pp. 11309–11317, 2009.
- [40] S. Garantziotis, Z. Li, E. N. Potts et al., "TLR4 is necessary for hyaluronan-mediated airway hyperresponsiveness after ozone inhalation," *American Journal of Respiratory and Critical Care Medicine*, vol. 181, no. 7, pp. 666–675, 2010.
- [41] M. L. Ormiston, G. R. D. Slaughter, Y. Deng, D. J. Stewart, and D. W. Courtman, "The enzymatic degradation of hyaluronan is associated with disease progression in experimental pulmonary hypertension," *The American Journal of Physiology—Lung Cellular and Molecular Physiology*, vol. 298, no. 2, pp. L148–L157, 2010.
- [42] K. R. Bracke, M. A. Dentener, E. Papakonstantinou et al., "Enhanced deposition of low-molecular-weight hyaluronan in lungs of cigarette smoke—exposed mice," *American Journal of Respiratory Cell and Molecular Biology*, vol. 42, no. 6, pp. 753–761, 2010.
- [43] J. Liang, D. Jiang, Y. Jung et al., "Role of hyaluronan and hyaluronan-binding proteins in human asthma," *Journal of Allergy and Clinical Immunology*, vol. 128, no. 2, pp. 403.e3–411.e3, 2011.
- [44] L. Eldridge, A. Moldobaeva, and E. M. Wagner, "Increased hyaluronan fragmentation during pulmonary ischemia," *The American Journal of Physiology: Lung Cellular and Molecular Physiology*, vol. 301, no. 5, pp. L782–L788, 2011.
- [45] M. T. Kuipers, T. van der Poll, M. J. Schultz, and C. W. Wieland, "Bench-to-bedside review: damage-associated molecular patterns in the onset of ventilator-induced lung injury," *Critical Care*, vol. 15, article 235, 2011.
- [46] C. A. McDevitt, G. J. Beck, M. J. Ciunga, and J. O'Brien, "Cigarette smoke degrades hyaluronic acid," *Lung*, vol. 167, no. 1, pp. 237–245, 1989.
- [47] R. R. Kew, B. Ghebrehiwet, and A. Janoff, "Cigarette smoke can activate the alternative pathway of complement in vitro by modifying the third component of complement," *The Journal of Clinical Investigation*, vol. 75, no. 3, pp. 1000–1007, 1985.
- [48] C. M. Sköld, E. Blaschke, and A. Eklund, "Transient increases in albumin and hyaluronan in bronchoalveolar lavage fluid after quitting smoking: possible signs of reparative mechanisms," *Respiratory Medicine*, vol. 90, no. 9, pp. 523–529, 1996.
- [49] M. Decramer, W. Janssens, and M. Miravittles, "Chronic obstructive pulmonary disease," *The Lancet*, vol. 379, no. 9823, pp. 1341–1351, 2012.
- [50] W. D. Song, A. C. Zhang, Y. Y. Pang et al., "Fibronectin and hyaluronan in bronchoalveolar lavage fluid from young patients with chronic obstructive pulmonary diseases," *Respiration*, vol. 62, no. 3, pp. 125–129, 1995.
- [51] M. A. Dentener, J. H. J. Vernooy, S. Hendriks, and E. F. M. Wouters, "Enhanced levels of hyaluronan in lungs of patients with COPD: relationship with lung function and local inflammation," *Thorax*, vol. 60, no. 2, pp. 114–119, 2005.
- [52] J. A. Elias, C. G. Lee, T. Zheng, B. Ma, R. J. Homer, and Z. Zhu, "New insights into the pathogenesis of asthma," *The Journal of Clinical Investigation*, vol. 111, no. 3, pp. 291–297, 2003.
- [53] S. Sahu and W. S. Lynn, "Hyaluronic acid in the pulmonary secretions of patients with asthma," *Biochemical Journal*, vol. 173, no. 2, pp. 565–568, 1978.
- [54] A. M. Vignola, P. Chanez, A. M. Campbell et al., "Airway inflammation in mild intermittent and in persistent asthma," *The American Journal of Respiratory and Critical Care Medicine*, vol. 157, no. 2, pp. 403–409, 1998.
- [55] A. G. Ayars, L. C. Altman, S. Potter-Perigo, K. Radford, T. N. Wight, and P. Nair, "Sputum hyaluronan and versican in

- severe eosinophilic asthma," *International Archives of Allergy and Immunology*, vol. 161, no. 1, pp. 65–73, 2013.
- [56] D. Valeyre, A. Prasse, H. Nunes, Y. Uzunhan, P.-Y. Brillet, and J. Müller-Quernheim, "Sarcoidosis," *The Lancet*, vol. 383, no. 9923, pp. 1155–1167, 2014.
- [57] R. Hallgren, A. Eklund, A. Engstrom-Laurent, and B. Schmekel, "Hyaluronate in bronchoalveolar lavage fluid: a new marker in sarcoidosis reflecting pulmonary disease," *British Medical Journal*, vol. 290, no. 6484, pp. 1778–1781, 1985.
- [58] A. Eklund, R. Hällgren, E. Blaschke, A. Engström-Laurent, U. Persson, and B. Svane, "Hyaluronate in bronchoalveolar lavage fluid in sarcoidosis and its relationship to alveolar cell populations," *European Journal of Respiratory Diseases*, vol. 71, no. 1, pp. 30–36, 1987.
- [59] L. Bjermer, A. Engstrom-Laurent, M. Thunell, and R. Hallgren, "Hyaluronic acid in bronchoalveolar lavage fluid in patients with sarcoidosis: relationship to lavage mast cells," *Thorax*, vol. 42, no. 12, pp. 933–938, 1987.
- [60] E. Blaschke, A. Eklund, and R. Hernbrand, "Extracellular matrix components in bronchoalveolar lavage fluid in sarcoidosis and their relationship to signs of alveolitis," *American Review of Respiratory Disease*, vol. 141, no. 4 I, pp. 1020–1025, 1990.
- [61] P. J. Wolters, H. R. Collard, and K. D. Jones, "Pathogenesis of idiopathic pulmonary fibrosis," *Annual Review of Pathology*, vol. 9, pp. 157–179, 2014.
- [62] L. Bjermer, R. Lundgren, and R. Hallgren, "Hyaluronan and type III procollagen peptide concentrations in bronchoalveolar lavage fluid in idiopathic pulmonary fibrosis," *Thorax*, vol. 44, no. 2, pp. 126–131, 1989.
- [63] N. Milman, M. S. Kristensen, and K. Bentsen, "Hyaluronan and procollagen type III aminoterminal peptide in serum and bronchoalveolar lavage fluid from patients with pulmonary fibrosis," *APMIS*, vol. 103, no. 10, pp. 749–754, 1995.
- [64] Z. W. Ghamra and R. A. Dweik, "Primary pulmonary hypertension: an overview of epidemiology and pathogenesis," *Cleveland Clinic Journal of Medicine*, vol. 70, no. 1, pp. S2–S8, 2003.
- [65] E. Papakonstantinou, F. M. Kouri, G. Karakiulakis, I. Klagas, and O. Eickelberg, "Increased hyaluronic acid content in idiopathic pulmonary arterial hypertension," *European Respiratory Journal*, vol. 32, no. 6, pp. 1504–1512, 2008.
- [66] M. Aytakin, S. A. A. Comhair, C. de la Motte et al., "High levels of hyaluronan in idiopathic pulmonary arterial hypertension," *The American Journal of Physiology—Lung Cellular and Molecular Physiology*, vol. 295, no. 5, pp. L789–L799, 2008.
- [67] P. N. Rao, A. Zeevi, J. Snyder et al., "Monitoring of acute lung rejection and infection by bronchoalveolar lavage and plasma levels of hyaluronic acid in clinical lung transplantation," *Journal of Heart and Lung Transplantation*, vol. 13, no. 6, pp. 958–962, 1994.
- [68] G. C. Riise, C. Kjellström, W. Ryd et al., "Inflammatory cells and activation markers in BAL during acute rejection and infection in lung transplant recipients: a prospective, longitudinal study," *European Respiratory Journal*, vol. 10, no. 8, pp. 1742–1746, 1997.
- [69] G. C. Riise, H. Scherstén, F. Nilsson, W. Ryd, and B. A. Andersson, "Activation of eosinophils and fibroblasts assessed by eosinophil cationic protein and hyaluronan in BAL: association with acute rejection in lung transplant recipients," *Chest*, vol. 110, no. 1, pp. 89–96, 1996.
- [70] M. Estenne, J. R. Maurer, A. Boehler et al., "Bronchiolitis obliterans syndrome 2001: an update of the diagnostic criteria," *Journal of Heart and Lung Transplantation*, vol. 21, no. 3, pp. 297–310, 2002.
- [71] J. L. Todd, X. Wang, S. Sugimoto et al., "Hyaluronan Contributes to Bronchiolitis Obliterans Syndrome and Stimulates Lung Allograft Rejection through Activation of Innate Immunity," *American Journal of Respiratory and Critical Care Medicine*, vol. 189, no. 5, pp. 556–566, 2014.
- [72] J. E. Adair, V. Stober, M. Sobhany et al., "Inter- α -trypsin inhibitor promotes bronchial epithelial repair after injury through vitronectin binding," *The Journal of Biological Chemistry*, vol. 284, no. 25, pp. 16922–16930, 2009.
- [73] S. Garantziotis, J. W. Hollingsworth, R. B. Ghanayem et al., "Inter-alpha-trypsin inhibitor attenuates complement activation and complement-induced lung injury," *The Journal of Immunology*, vol. 179, no. 6, pp. 4187–4192, 2007.
- [74] G. Cheng, S. Swaidani, M. Sharma, M. E. Lauer, V. C. Hascall, and M. A. Aronica, "Hyaluronan deposition and correlation with inflammation in a murine ovalbumin model of asthma," *Matrix Biology*, vol. 30, no. 2, pp. 126–134, 2011.
- [75] G. Cheng, S. Swaidani, M. Sharma, M. E. Lauer, V. C. Hascall, and M. A. Aronica, "Correlation of hyaluronan deposition with infiltration of eosinophils and lymphocytes in a cockroach-induced murine model of asthma," *Glycobiology*, vol. 23, no. 1, pp. 43–58, 2013.
- [76] S. Ghosh, A. E. Samarasinghe, S. A. Hoselton, G. P. Dorsam, and J. M. Schuh, "Hyaluronan deposition and co-localization with inflammatory cells and collagen in a murine model of fungal allergic asthma," *Inflammation Research*, vol. 63, no. 6, pp. 475–484, 2014.
- [77] M. E. Lauer, G. Cheng, S. Swaidanis, M. A. Aronica, P. H. Weigel, and V. C. Hascall, "Tumor necrosis factor-stimulated gene-6 (TSG-6) amplifies hyaluronan synthesis by airway smooth muscle cells," *Journal of Biological Chemistry*, vol. 288, no. 1, pp. 423–431, 2013.
- [78] F. Chua, J. Gaudie, and G. J. Laurent, "Pulmonary fibrosis: searching for model answers," *American Journal of Respiratory Cell and Molecular Biology*, vol. 33, no. 1, pp. 9–13, 2005.
- [79] R. T. Dorr, "Bleomycin pharmacology: mechanism of action and resistance, and clinical pharmacokinetics," *Seminars in Oncology*, vol. 19, no. 2, pp. 3–8, 1992.
- [80] O. Nettelbladt, J. Bergh, M. Schenholm, A. Tengblad, and R. Hallgren, "Accumulation of hyaluronic acid in the alveolar interstitial tissue in bleomycin-induced alveolitis," *American Review of Respiratory Disease*, vol. 139, no. 3, pp. 759–762, 1989.
- [81] O. Nettelbladt, A. Tengblad, and R. Hallgren, "High-dose corticosteroids during bleomycin-induced alveolitis in the rat do not suppress the accumulation of hyaluronan (hyaluronic acid) in lung tissue," *European Respiratory Journal*, vol. 3, no. 4, pp. 421–428, 1990.
- [82] B. A. Bray, P. M. Sampson, M. Osman, A. Giandomenico, and G. M. Turino, "Early changes in lung tissue hyaluronan (hyaluronic acid) and hyaluronidase in bleomycin-induced alveolitis in hamsters," *American Review of Respiratory Disease*, vol. 143, no. 2, pp. 284–288, 1991.
- [83] O. Nettelbladt, A. Scheynius, J. Bergh, A. Tengblad, and R. Hällgren, "Alveolar accumulation of hyaluronan and alveolar cellular response in bleomycin-induced alveolitis," *European Respiratory Journal*, vol. 4, no. 4, pp. 407–414, 1991.
- [84] P. Teder, R. W. Vandivier, D. Jiang et al., "Resolution of lung inflammation by CD44," *Science*, vol. 296, no. 5565, pp. 155–158, 2002.
- [85] A. M. Dygai, E. G. Skurikhin, N. N. Ermakova et al., "Antifibrotic activity of hyaluronidase immobilized on polyethylenoxide under conditions of bleomycin-induced pneumofibrosis,"

- Bulletin of Experimental Biology and Medicine*, vol. 154, no. 3, pp. 388–392, 2013.
- [86] O. Nettelbladt, K. Lundberg, A. Tengblad, and R. Hällgren, “Accumulation of hyaluronan in bronchoalveolar lavage fluid is independent of iron-, complement- and granulocyte-depletion in bleomycin-induced alveolitis in the rat,” *European Respiratory Journal*, vol. 3, no. 7, pp. 765–771, 1990.
- [87] J. Hernnas, O. Nettelbladt, L. Bjermer, B. Sarnstrand, A. Malmstrom, and R. Hällgren, “Alveolar accumulation of fibronectin and hyaluronan precedes bleomycin-induced pulmonary fibrosis in the rat,” *European Respiratory Journal*, vol. 5, no. 4, pp. 404–410, 1992.
- [88] A. Zaman, Z. Cui, J. P. Foley et al., “Expression and role of the hyaluronan receptor RHAMM in inflammation after bleomycin injury,” *American Journal of Respiratory Cell and Molecular Biology*, vol. 33, no. 5, pp. 447–454, 2005.
- [89] R. C. Savani, G. Hou, P. Liu et al., “A role for hyaluronan in macrophage accumulation and collagen deposition after bleomycin-induced lung injury,” *The American Journal of Respiratory Cell and Molecular Biology*, vol. 23, no. 4, pp. 475–484, 2000.
- [90] H.-W. Zhao, L. Ü. Chang-Jun, and R.-J. Yu, “An increase in hyaluronan by lung fibroblasts: a biomarker for intensity and activity of interstitial pulmonary fibrosis?” *Respirology*, vol. 4, no. 2, pp. 131–138, 1999.
- [91] P. Teder, O. Nettelbladt, and P. Heldin, “Characterization of the mechanism involved in bleomycin-induced increased hyaluronan production in rat lung,” *American Journal of Respiratory Cell and Molecular Biology*, vol. 12, no. 2, pp. 181–189, 1995.
- [92] I. N. Zelko and R. J. Folz, “Extracellular superoxide dismutase attenuates release of pulmonary hyaluronan from the extracellular matrix following bleomycin exposure,” *FEBS Letters*, vol. 584, no. 13, pp. 2947–2952, 2010.
- [93] M. A. Antunes and P. R. M. Rocco, “Elastase-induced pulmonary emphysema: insights from experimental models,” *Anais da Academia Brasileira de Ciencias*, vol. 83, no. 4, pp. 1385–1395, 2011.
- [94] M. Moczar, C. Lafuma, F. Lange, J. Bignon, L. Robert, and E. Moczar, “Glycosaminoglycans in elastase induced emphysema,” *Bulletin Européen de Physiopathologie Respiratoire*, vol. 16, supplement, pp. 99–104, 1980.
- [95] J. O. Cantor, J. M. Cerreta, S. Keller, and G. M. Turino, “Modulation of airspace enlargement in elastase-induced emphysema by intratracheal instillation of hyaluronidase and hyaluronic acid,” *Experimental Lung Research*, vol. 21, no. 3, pp. 423–436, 1995.
- [96] J. O. Cantor, J. M. Cerreta, G. Armand, and G. M. Turino, “Further investigation of the use of intratracheally administered hyaluronic acid to ameliorate elastase-induced emphysema,” *Experimental Lung Research*, vol. 23, no. 3, pp. 229–244, 1997.
- [97] M. Scuri, W. M. Abraham, Y. Botvinnikova, and R. Forteza, “Hyaluronic acid blocks porcine pancreatic elastase (PPE)-induced bronchoconstriction in sheep,” *American Journal of Respiratory and Critical Care Medicine*, vol. 164, no. 10, pp. 1855–1859, 2001.
- [98] M. Scuri and W. M. Abraham, “Hyaluronan blocks human neutrophil elastase (HNE)-induced airway responses in sheep,” *Pulmonary Pharmacology and Therapeutics*, vol. 16, no. 6, pp. 335–340, 2003.
- [99] M. Scuri, J. R. Sabater, and W. M. Abraham, “Hyaluronan blocks porcine pancreatic elastase-induced mucociliary dysfunction in allergic sheep,” *Journal of Applied Physiology*, vol. 102, no. 6, pp. 2324–2331, 2007.
- [100] D. Negrini, A. Passi, G. De Luca, and G. Miserocchi, “Proteoglycan involvement during development of lesional pulmonary edema,” *American Journal of Physiology—Lung Cellular and Molecular Physiology*, vol. 274, no. 2, pp. L203–L211, 1998.
- [101] A. Passi, D. Negrini, R. Albertini, G. de Luca, and G. Miserocchi, “Involvement of lung interstitial proteoglycans in development of hydraulic- and elastase-induced edema,” *The American Journal of Physiology—Lung Cellular and Molecular Physiology*, vol. 275, no. 3, pp. L631–L635, 1998.
- [102] R. D. Bland, “Edema formation in the lungs and its relationship to neonatal respiratory distress,” *Acta Paediatrica*, vol. 72, supplement 305, pp. 92–99, 1983.
- [103] S. E. Juul, R. C. Krueger Jr., L. Scofield, M. B. Hershenson, and N. B. Schwartz, “Hyperoxia alone causes changes in lung proteoglycans and hyaluronan in neonatal rat pups,” *American Journal of Respiratory Cell and Molecular Biology*, vol. 13, no. 6, pp. 629–638, 1995.
- [104] H. Johnsson, L. Eriksson, A. Jonzon, T. C. Laurent, and G. Sedin, “Lung hyaluronan and water content in preterm and term rabbit pups exposed to oxygen or air,” *Pediatric Research*, vol. 44, no. 5, pp. 716–722, 1998.
- [105] R. L. Stedman, “The chemical composition of tobacco and tobacco smoke,” *Chemical Reviews*, vol. 68, no. 2, pp. 153–207, 1968.
- [106] R. Vassallo and J. H. Ryu, “Smoking-related interstitial lung diseases,” *Clinics in Chest Medicine*, vol. 33, no. 1, pp. 165–178, 2012.
- [107] J. O. Cantor, J. M. Cerreta, M. Ochoa, S. Ma, M. Liu, and G. M. Turino, “Therapeutic effects of hyaluronan on smoke-induced elastic fiber injury: does delayed treatment affect efficacy?” *Lung*, vol. 189, no. 1, pp. 51–56, 2011.
- [108] P.-M. Huang, O. Syrkina, L. Yu et al., “High MW hyaluronan inhibits smoke inhalation-induced lung injury and improves survival,” *Respirology*, vol. 15, no. 7, pp. 1131–1139, 2010.
- [109] A. Bao, L. Liang, F. Li, M. Zhang, and X. Zhou, “Effects of acute ozone exposure on lung peak allergic inflammation of mice,” *Frontiers in Bioscience*, vol. 18, no. 3, pp. 838–851, 2013.
- [110] F. Feng, Z. Li, E. N. Potts-Kant et al., “Hyaluronan activation of the Nlrp3 inflammasome contributes to the development of airway hyperresponsiveness,” *Environmental Health Perspectives*, vol. 120, no. 12, pp. 1692–1698, 2012.
- [111] Z. Li, E. N. Potts-Kant, S. Garantziotis, W. M. Foster, and J. W. Hollingsworth, “Hyaluronan signaling during ozone-induced lung injury requires TLR4, MyD88, and TIRAP,” *PLoS ONE*, vol. 6, no. 11, Article ID e27137, 2011.
- [112] Z. Li, E. N. Potts, C. A. Piantadosi, W. M. Foster, and J. W. Hollingsworth, “Hyaluronan fragments contribute to the ozone-primed immune response to lipopolysaccharide,” *The Journal of Immunology*, vol. 185, no. 11, pp. 6891–6898, 2010.
- [113] R. P. Hill, “Radiation effects on the respiratory system,” *BJR Supplement*, vol. 27, pp. 75–81, 2005.
- [114] D. Rosenbaum, S. Peric, M. Holecek, and H. E. Ward, “Hyaluronan in radiation-induced lung disease in the rat,” *Radiation Research*, vol. 147, no. 5, pp. 585–591, 1997.
- [115] Y. Li, M. Rahmanian, C. Widström, G. Lepperdinger, G. I. Frost, and P. Heldin, “Irradiation-induced expression of hyaluronan (HA) synthase 2 and hyaluronidase 2 genes in rat lung tissue accompanies active turnover of HA and induction of types I and III collagen gene expression,” *American Journal of Respiratory Cell and Molecular Biology*, vol. 23, no. 3, pp. 411–418, 2000.

- [116] M. Iwakawa, S. Noda, T. Ohta et al., "Strain dependent differences in a histological study of CD44 and collagen fibers with an expression analysis of inflammatory response-related genes in irradiated murine lung," *Journal of Radiation Research*, vol. 45, no. 3, pp. 423–433, 2004.
- [117] S. E. Juul, M. G. Kinsella, J. C. Jackson, W. E. Truog, T. A. Standaert, and W. A. Hodson, "Changes in hyaluronan deposition during early respiratory distress syndrome in premature monkeys," *Pediatric Research*, vol. 35, no. 2, pp. 238–243, 1994.
- [118] K. J. Bai, A. P. Spicer, M. M. Mascarenhas et al., "The role of hyaluronan synthase 3 in ventilator-induced lung injury," *American Journal of Respiratory and Critical Care Medicine*, vol. 172, no. 1, pp. 92–98, 2005.
- [119] X. Wang, Z. Sun, L. Qian et al., "Effects of hyaluronan-fortified surfactant in ventilated premature piglets with respiratory distress," *Biology of the Neonate*, vol. 89, no. 1, pp. 15–24, 2006.
- [120] S. Baron, Ed., *Medical Microbiology*, University of Texas Medical Branch at Galveston, Galveston, Tex, USA, 1996, <http://www.ncbi.nlm.nih.gov/books/NBK7627/>.
- [121] S. E. Juul, M. G. Kinsella, W. E. Truog, R. L. Gibson, and G. J. Redding, "Lung hyaluronan decreases during Group B Streptococcal pneumonia in neonatal piglets," *American Journal of Respiratory and Critical Care Medicine*, vol. 153, no. 5, pp. 1567–1570, 1996.
- [122] G. J. W. van der Windt, S. Florquin, A. F. de Vos et al., "CD44 deficiency is associated with increased bacterial clearance but enhanced lung inflammation during gram-negative pneumonia," *The American Journal of Pathology*, vol. 177, no. 5, pp. 2483–2494, 2010.
- [123] G. J. W. van der Windt, A. J. Hoogendijk, A. F. de vos, M. E. Kerver, S. Florquin, and T. Van Der Poll, "The role of CD44 in the acute and resolution phase of the host response during pneumococcal pneumonia," *Laboratory Investigation*, vol. 91, no. 4, pp. 588–597, 2011.
- [124] Z. Hasan, K. Palani, M. Rahman, and H. Thorlacius, "Targeting CD44 expressed on neutrophils inhibits lung damage in abdominal sepsis," *Shock*, vol. 35, no. 6, pp. 567–572, 2011.
- [125] C. Marion, J. M. Stewart, M. F. Tazi et al., "Streptococcus pneumoniae can utilize multiple sources of hyaluronic acid for growth," *Infection and Immunity*, vol. 80, no. 4, pp. 1390–1398, 2012.
- [126] O. N. Uchakina, C. M. Castillejo, C. C. Bridges, and R. J. McKallip, "The role of hyaluronic acid in SEB-induced acute lung inflammation," *Clinical Immunology*, vol. 146, no. 1, pp. 56–69, 2013.
- [127] R. J. McKallip, H. F. Hagele, and O. N. Uchakina, "Treatment with the hyaluronic acid synthesis inhibitor 4-methylumbelliferone suppresses SEB-induced lung inflammation," *Toxins*, vol. 5, no. 10, pp. 1814–1826, 2013.
- [128] M. Y. Chang, Y. Tanino, V. Vidova et al., "Reprint of: a rapid increase in macrophage-derived versican and hyaluronan in infectious lung disease," *Matrix Biology*, vol. 35, pp. 162–173, 2014.
- [129] L. Zhuo, A. Kanamori, R. Kannagi et al., "SHAP potentiates the CD44-mediated leukocyte adhesion to the hyaluronan substratum," *The Journal of Biological Chemistry*, vol. 281, no. 29, pp. 20303–20314, 2006.
- [130] H. He, S. Zhang, S. Tighe, J. Son, and S. C. G. Tseng, "Immobilized heavy chain-hyaluronic acid polarizes lipopolysaccharide-activated macrophages toward m2 phenotype," *The Journal of Biological Chemistry*, vol. 288, no. 36, pp. 25792–25803, 2013.
- [131] M. E. Monzon, S. Casalino-Matsuda, and R. M. Forteza, "Identification of glycosaminoglycans in human airway secretions," *The American Journal of Respiratory Cell and Molecular Biology*, vol. 34, no. 2, pp. 135–141, 2006.
- [132] C. B. Basbaum and W. E. Finkbeiner, "Airway secretion: a cell-specific analysis," *Hormone and Metabolic Research*, vol. 20, no. 11, pp. 661–667, 1988.
- [133] J. N. Baraniuk, T. Shizari, M. Sabol, M. Ali, and C. B. Underhill, "Hyaluronan is exocytosed from serous, but not mucous cells, of human nasal and tracheobronchial submucosal glands," *Journal of Investigative Medicine*, vol. 44, no. 2, pp. 47–52, 1996.
- [134] J. O. Cantor, J. M. Cerreta, G. Armand, and G. M. Turino, "Aerosolized hyaluronic acid decreases alveolar injury induced by human neutrophil elastase," *Proceedings of the Society for Experimental Biology and Medicine*, vol. 217, no. 4, pp. 471–475, 1998.
- [135] J. O. Cantor and G. M. Turino, "Can exogenously administered hyaluronan improve respiratory function in patients with pulmonary emphysema?" *Chest*, vol. 125, no. 1, pp. 288–292, 2004.
- [136] P. P. Nadkarni, G. S. Kulkarni, J. M. Cerreta, S. Ma, and J. O. Cantor, "Dichotomous effect of aerosolized hyaluronan in a hamster model of endotoxin-induced lung injury," *Experimental Lung Research*, vol. 31, no. 9–10, pp. 807–818, 2005.
- [137] J. O. Cantor, J. M. Cerreta, M. Ochoa et al., "Aerosolized hyaluronan limits airspace enlargement in a mouse model of cigarette smoke-induced pulmonary emphysema," *Experimental Lung Research*, vol. 31, no. 4, pp. 417–430, 2005.
- [138] G. Petrigli and L. Allegra, "Aerosolised hyaluronic acid prevents exercise-induced bronchoconstriction, suggesting novel hypotheses on the correction of matrix defects in asthma," *Pulmonary Pharmacology & Therapeutics*, vol. 19, no. 3, pp. 166–171, 2006.
- [139] C. Sondrup, Y. Liu, X. Z. Shu, G. D. Prestwich, and M. E. Smith, "Cross-linked hyaluronan-coated stents in the prevention of airway stenosis," *Otolaryngology—Head and Neck Surgery*, vol. 135, no. 1, pp. 28–35, 2006.
- [140] H. W. Taeusch, E. Dybbro, and K. W. Lu, "Pulmonary surfactant adsorption is increased by hyaluronan or polyethylene glycol," *Colloids and Surfaces B: Biointerfaces*, vol. 62, no. 2, pp. 243–249, 2008.
- [141] Y.-Y. Liu, C.-H. Lee, R. Dedaj et al., "High-molecular-weight hyaluronan—a possible new treatment for sepsis-induced lung injury: a preclinical study in mechanically ventilated rats," *Critical Care*, vol. 12, no. 4, article R102, 2008.
- [142] P. Buonpensiero, F. de Gregorio, A. Sepe et al., "Hyaluronic acid improves 'pleasantness' and tolerability of nebulized hypertonic saline in a cohort of patients with cystic fibrosis," *Advances in Therapy*, vol. 27, no. 11, pp. 870–878, 2010.
- [143] J.-M. Zahm, M. Milliot, A. Bresin, C. Coraux, and P. Birembaut, "The effect of hyaluronan on airway mucus transport and airway epithelial barrier integrity: potential application to the cytoprotection of airway tissue," *Matrix Biology*, vol. 30, no. 7–8, pp. 389–395, 2011.
- [144] L. M. Carro, A. L. Ferreira, M. R. de Valbuena Máiz, C. W. Struwing, G. G. Álvarez, and L. S. Cortina, "Tolerance of two inhaled hypertonic saline solutions in patients with cystic fibrosis," *Medicina Clinica*, vol. 138, no. 2, pp. 57–59, 2012.
- [145] M. L. Furnari, L. Termini, G. Traverso et al., "Nebulized hypertonic saline containing hyaluronic acid improves tolerability in patients with cystic fibrosis and lung disease compared with nebulized hypertonic saline alone: a prospective, randomized,

double-blind, controlled study," *Therapeutic Advances in Respiratory Disease*, vol. 6, no. 6, pp. 315–322, 2012.

- [146] A. Macchi, P. Terranova, E. Digilio, and P. Castelnovo, "Hyaluronan plus saline nasal washes in the treatment of rhino-sinusal symptoms in patients undergoing functional endoscopic sinus surgery for rhino-sinusal remodeling," *International Journal of Immunopathology and Pharmacology*, vol. 26, no. 1, pp. 137–145, 2013.
- [147] F. Cresta, A. Naselli, F. Favilli, and R. Casciaro, "Inhaled hypertonic saline+hyaluronic acid in cystic fibrosis with asthma-like symptoms: a new therapeutic chance," *BMJ Case Reports*, vol. 2013, 2013.
- [148] K. W. Lu, H. W. Taeusch, and J. A. Clements, "Hyaluronan with dextran added to therapeutic lung surfactants improves effectiveness in vitro and in vivo," *Experimental Lung Research*, vol. 39, no. 4-5, pp. 191–200, 2013.
- [149] A. Macchi, P. Castelnovo, P. Terranova, and E. Digilio, "Effects of sodium hyaluronate in children with recurrent upper respiratory tract infections: results of a randomised controlled study," *International Journal of Immunopathology and Pharmacology*, vol. 26, no. 1, pp. 127–135, 2013.
- [150] M. Ros, R. Casciaro, F. Lucca et al., "Hyaluronic acid improves the tolerability of hypertonic saline in the chronic treatment of cystic fibrosis patients: a multicenter, randomized, controlled clinical trial," *Journal of Aerosol Medicine and Pulmonary Drug Delivery*, vol. 27, no. 2, pp. 133–137, 2014.

Review Article

Size Matters: Molecular Weight Specificity of Hyaluronan Effects in Cell Biology

Jaime M. Cyphert, Carol S. Trempus, and Stavros Garantziotis

Laboratory of Respiratory Biology, Department of Intramural Research, National Institute of Environmental Health Sciences, Research Triangle Park, NC 27709, USA

Correspondence should be addressed to Stavros Garantziotis; garantziotis@niehs.nih.gov

Received 7 October 2014; Accepted 5 January 2015

Academic Editor: Hans Hermann Gerdes

Copyright © 2015 Jaime M. Cyphert et al. This is an open access article distributed under the Creative Commons Attribution License, which permits unrestricted use, distribution, and reproduction in any medium, provided the original work is properly cited.

Hyaluronan signaling properties are unique among other biologically active molecules, that they are apparently not influenced by postsynthetic molecular modification, but by hyaluronan fragment size. This review summarizes the current knowledge about the generation of hyaluronan fragments of different size and size-dependent differences in hyaluronan signaling as well as their downstream biological effects.

1. Hyaluronan: A Simple Sugar with Multifaceted Biological Effects

If there were ever a competition for the most simply designed, yet most versatile biological molecule in nature, hyaluronan (HA) would be a strong contender. Built of simple disaccharide sequences (D-glucuronic acid and D-N-acetylglucosamine, bound through alternating β -1,4 and β -1,3 glycosidic bonds), and with no known postsynthetic modification, HA was long mistaken for an inert filler of the extracellular space. In the past decades, however, it has become evident that HA possesses manifold signaling properties. A fascinating, if perhaps vexing, insight has also been that HA will often demonstrate opposing actions: it can have pro- or anti-inflammatory properties, promote or inhibit cell migration, activate, or stop cell division and differentiation. It appears that three main factors dictate the effect of HA: one is cell-specific (receptor expression, signaling pathways, and cell cycle); two are HA-related (size and location). This review will focus on HA sizes and their effect on HA signaling and biological effects.

Size dependency of signaling raises interesting questions. Why would a larger or smaller molecule of identical, monotonous molecular structure have different effects? Presumably HA receptors need a minimal molecular size to engage the ligand, but further size increase should have

no effect on receptor recognition. Two concepts which help explain this observation have gathered experimental support. The first concept suggests that HA size may influence affinity to receptors; also, receptor complexes may cluster differently depending on HA size. The second concept, less well understood, is that size may affect HA uptake by the cell, and HA intracellular signaling may also modulate biological responses.

An additional impediment on the elucidation of size-dependent HA signaling and biological effects is the confusing language that is used in scientific publications. While everyone seems to agree on designating HA over 1 million Da “high molecular weight,” the nomenclature of smaller-size HA is nebulous. Different papers use interchangeably terms such as “short-fragment HA,” “low molecular weight HA,” and “HA oligosaccharides” to describe HA molecules from a few disaccharides up to over 700 kDa. For this review we are using the following nomenclature, for expediency's sake: HA of approximately 20 monosaccharide length or less (the minimum that differentiates between monovalent and divalent interactions with CD44 [1]) are “HA oligosaccharides (oHA)”; HA of over 1 million Da (the minimum that is thought to be native HA [2]) is “high molecular weight (HMW-HA)”; everything in between is “low molecular weight (LMW-HA)”. For scientific papers it may be better to simply define the size or range of sizes the investigators

are working with, until a clear mechanistic understanding of fragment size classification emerges.

In the following we will provide brief overviews of the mechanisms of HA synthesis and degradation, which lead to the generation of different fragment sizes; the current state of knowledge on HA size-dependent signaling; and a conclusive discussion of implications and future directions.

2. Hyaluronan Synthesis

HA is uniquely synthesized at the plasma membrane rather than in the Golgi apparatus as is typical of other glycosaminoglycans (GAGs) [3]. Synthesis of mammalian HA is accomplished by a family of membrane-bound glycosyltransferases composed of three isozymes, hyaluronan synthases (HAS) 1, 2, and 3. HAS enzymes are evolutionarily conserved and are highly homologous (55–70% protein identity) [4, 5], and they catalyze the addition of UDP-D-glucuronic acid (GlcA) and UDP-N-acetyl-D-glucosamine (GlcNAc) monomers in an alternating assembly to form HA polymers [6, 7]. Although the three HAS isoforms are similar and synthesize an identical product, they exhibit differences in half-life and stability, the rate of HA synthesis, and affinity for HA substrates, all of which potentially affect the regulation of HA synthesis and biological function [8]. Of particular interest is the finding that the three HAS enzymes synthesized HA of varying molecular masses. In general, HAS3 synthesized the shortest HA polymer sizes (1×10^5 to 1×10^6 Da), while HAS1 and HAS2 synthesized larger polymers (2×10^5 to 2×10^6 Da), although the major population of HA produced by HAS2 tended to be concentrated on the longer end of the spectrum ($>2 \times 10^6$ Da) compared to HAS1, which generated a wider range of HA polymers [8]. Because of the biological differences exhibited by HA of differing polymer lengths, the innate biochemical and synthetic capabilities of the HAS enzymes may serve an important regulatory role in development, injury, and disease.

The HAS genes exhibit different temporal patterns of expression during morphogenesis [4]. HAS2 is expressed throughout all stages of embryogenesis [9] and is considered to be the major hyaluronan synthase during development. Camenisch et al. determined that, of the three HAS isoenzymes, only HAS2 was indispensable, with embryonic lethality due to severe cardiac and vascular defects at midgestation in HAS2^{-/-} mice [10]. HAS1 and HAS3 expressions, on the other hand, are restricted to early and late stages of development, respectively, although expression overlaps with HAS2 [9]. HAS1 and 3 deficient mice as well as HAS1 and 3 double knockouts are both viable and fertile [9].

At the tissue level, HAS gene expression and subsequent HA synthesis is regulated by a wide range of cytokines and growth factors (reviewed in [2, 11]). All three HAS genes may respond similarly to a particular signal, or there may be a differential response, as demonstrated by TGF- β 1-mediated downregulation of HAS3 but upregulation of HAS1 expression, seen in a dose-dependent manner in human fibroblast-like synoviocytes [12]. Dysregulation of HAS gene expression plays important roles in disease and injury, consistent with

the biological roles of HA in disease progression, wound healing, and tissue regeneration. In cancer, overexpression of hyaluronan synthases influences tumor growth, metastatic potential, and progression in several malignancies, including prostate, colon, breast, and endometrial cancers (reviewed in [13]). Ectopic expression of HAS genes may also functionally alter the biological responses of cells to injury *in vivo* [14, 15] (reviewed more extensively below). Taken together, available studies suggest that HA synthases are critical mediators in development, injury, and disease.

3. Degradation of Hyaluronan by Hyaluronidases

The mechanism of HA removal or turnover is facilitated in part by hyaluronidases (HYALs), which, in mammals, consists of a family of enzymes including hyaluronidases 1–4 (HYAL1–4), PH20, and HYALP1 [16, 17]. HYALs are also found in lower organisms, like bacteria, which catabolize HA to generate primarily disaccharides and in part facilitate mobility within tissue [2], and in leeches and crustaceans, which produce predominately tetra- and hexasaccharide fragments [18]. HYALs as a class are highly homologous endoglycosidases, and in terms of HA catabolism, they specifically hydrolyze the β -1,4 linkage of the HA molecule, which is a linear polysaccharide composed of repeating β -1,4-linked D-glucuronic acid (GlcA) and β -1,3-linked N-acetyl-D-glucosamine (GlcNAc) disaccharide units [17–19]. The range of activity of mammalian HYALs is not strictly limited to HA as they can also degrade chondroitin sulfates, although prokaryotic HYALs specifically act on HA [17, 20]. HYALs can be further broken down into distinct groups; for example, HYAL1–HYAL3 are primarily active at an acidic pH, while PH20 has optimum activity at a neutral pH [16, 21].

Of the 6 HYAL family members, HYAL1 and HYAL2 are the predominant isoforms functioning to catabolize HA in somatic tissues. Triggs-Raine et al. [22] detailed a broad mRNA expression pattern for HYAL2 (heart, skeletal muscle, colon, spleen, kidney, liver, placenta, and lung), while HYAL1 is more limited in scope but is high in liver (which is a primary location of HA degradation) and is less strongly expressed in heart, spleen, kidney, and lung; the HYAL1 protein is also found in plasma and urine. HYAL3 is even more limited in its expression pattern, with low levels in brain, liver, testis, and bone marrow [22]. PH20/SPAM1 is specific to sperm and has a role in fertilization [16]. Finally, HYAL4 is a chondroitinase with no evidence of HA catabolic activity [23], with expression in the placenta and skeletal muscle [16], and HYALP1 is an expressed pseudogene [16, 17].

HA degradation into smaller fragments is accomplished by HYAL1 and HYAL2 acting in concert to catabolize HA into tetrasaccharides. HMW-HA is anchored to the cell surface through CD44 and HYAL2 and localized to lipid rafts in the cell membrane. The acidic environment necessary for HYAL2 activity is provided by NHE2 [24], facilitating the generation of HA polymers of approximately 20 kDa (or 50 disaccharide units). In this model, 20 kDa fragments are internalized and transported first to endosome and then to

lysosomes, where lysosomal HYAL1 further degrades the HA into tetrasaccharide units (reviewed in [20]). Experimental details and confirmation of this model are still outstanding. The significance of HYAL-mediated degradation of HA is demonstrated in mucopolysaccharide hyaluronidase deficiency, first described by [25]. This disorder is characterized by elevated HA levels in the plasma (>38–90-fold increase over normal plasma levels) concomitant with lack of hyaluronidase activity [25]. This lysosomal storage disorder is now termed mucopolysaccharidosis IX [22], and subsequent characterization revealed that hyaluronidase activity is specifically abrogated through mutations in HYAL1. The disease has a relatively mild phenotype, limited to specific cell types (fibroblasts and histiocytes) and characterized by accumulation of HA, short stature, and multiple soft tissue masses in the joints. A further demonstration of how HYALs contribute to developmental processes was shown with a mouse model of HYAL2 deficiency, which, similar to mucopolysaccharidosis IX in humans, was characterized by increased plasma concentrations of HA, and a relatively mild phenotype, in this case with mild craniofacial and hematological defects [26]. Interactions with other genetic loci are suspected, as HYAL2 deficiency in an outbred mouse resulted in much more severe cardiopulmonary pathology and early mortality compared to HYAL2 deficiency in an inbred genetic background [27]. Increased HYAL levels have also been found in several carcinomas, including prostate and bladder, as well as breast and head and neck cancer, and tend to correlate with more invasive and metastatic phenotypes (reviewed in [21]). Cumulatively, this suggests that HYALs have distinctive roles in developmental and disease processes through the regulation of HA metabolism.

Although many diverse biological responses have been attributed to HA and its various size polymers, interpretation of experimental findings, both *in vivo* and *in vitro*, may be complicated by, for example, low levels of bacterial contamination, which may independently activate key HA receptors. Recently, Muto et al. [28] developed mouse lines overexpressing HYAL1, in an attempt to generate HA fragments *in vivo* independently of other mitigating factors. Using models of constitutive overexpression of HYAL1 in mouse skin (K14/HYAL1) and tamoxifen-inducible expression localized to the epidermis (K14CreERT/HYAL1), they determined that HA catabolism in the absence of injury *in vivo* initiated dendritic cell (DC) migration and maturation, which in turn muted the response to contact hypersensitization (CHS). Interestingly, HYAL1-mediated catabolism of HMW-HA into size ranging between 0.5 and 27 kDa (tetrasaccharides to 68 mer disaccharides) did not result in any phenotypic or inflammatory changes, so in the absence of any specific injury or challenge, catabolism of HA to smaller polymers by HYAL1 did not alone induce an immune response in these models. These results were recapitulated by injection of tetrasaccharide oHA into the skin of wild type mice, resulting in increased migration of DCs out of the skin and functionally, a diminished CHS response. Finally, they also showed that, in this context, HYAL1 or oHA function is dependent upon TLR4. While HYAL1 overexpression or

oHA injection in a TLR4^{-/-} background resulted in HA fragmentation, there was no change in cutaneous DC levels in either case. This effect was not seen with HYAL1 on a CD44 deficient background, demonstrating specificity for TLR4 in this process [28]. HYAL1 is only active at a low pH, which is unlikely to have been present in the uninflamed skin of these mice. Therefore, the exact mechanism of HYAL1 activity in this case and in inflammation generally is still far from completely understood. However, it should be noted that much is unknown about hyaluronidase activity and function *in vivo*, and it is possible that posttranslational processing or other factors (association with proteins or salts) substantially change activity and specificity from what is found *in vitro* [29, 30].

4. Degradation of Hyaluronan by Nonspecific Pathways

Aside from the specific enzymatic degradation pathways described above, HMW-HA can be fragmented by nonspecific pathways as well. Reactive oxygen species (ROS), including superoxide, hydrogen peroxide, nitric oxide and peroxynitrite, and hypohalous acids (reviewed in [31]), are generated during the inflammatory response in sepsis, tissue inflammation, and ischemia-reperfusion injury and can degrade HA [31]. The most direct evidence for this has been accumulated in the synovial fluid, where inflammatory oxidation leads to degradation of native HMW-HA with resulting decrease in synovial fluid viscosity and cartilage degeneration, and in the airways, where ROS can degrade luminal epithelial HA [32]. It should also be mentioned that nonenzymatically produced, ambient ROS can also generate HMW-HA breakdown products. This may be most relevant in environmental lung injury; for example, inhaled ozone and chlorine gas can generate LMW-HA from HMW-HA *in vitro*. No matter the origin, it seems clear that excessive generation of ROS contributes to a proinflammatory status by the oxidative degradation of hyaluronan. The corollary to this is that neutralization of ROS, for example, through superoxide dismutase, decreases HMW-HA degradation and inflammation [33–35]. Finally, the possibility may be entertained that ROS scavenging is in fact one of the physiological functions of HMW-HA as was proposed recently [36]; however, no experimental support for this hypothesis exists at this point. Beyond this hypothesis, it should also be noted that degradation of HMW-HA by ROS may also have salutary effects, such as the promotion of ciliary beating in the airways [37]. Thus, ROS may engage hyaluronan in a fine-tuned interaction rather than a monolithic response, and in fact hyaluronan may be involved in the emerging signaling pathway for these molecules [32, 38].

5. Effects of Hyaluronan Size on Cell Receptor Signaling

As part of the extracellular matrix (ECM), HA plays an important role in the maintenance of appropriate cell-cell communication. When ECM homeostasis is disrupted

during pathological conditions (tumor invasion, inflammation, tissue remodeling, etc.) endogenous HMW-HA can be degraded by hyaluronidases [39] and reactive oxygen species [31] into LMW-HA, which can be further depolymerized to oHA. HA and its degradation products bind several cell surface receptors such as CD44, RHAMM, HARE, LYVE1, layilin, TLR2, and TLR4 [15, 40–49], where the size of HA can have a significant influence on receptor activation and its downstream signaling. One theory proposes that signal transduction by HA is dependent on multivalent and cooperative interactions and/or the ability of HA to cluster the receptors on the membrane [15, 50]. For example the interaction of CD44 and HA is strongly influenced by cell-specific factors, cell type, state of activation, and HA size. Different sizes of HA have distinct effects on CD44 clustering: HMW-HA increases clustering strength while oHA has no apparent effect. However, sequential addition of oHA following HMW-HA reduces the clustering strength induced by HMW-HA [51]. Long chains of HA possess multivalent sites for CD44 binding while oHA have only 1 or 2 binding sites [1, 52] suggesting that oHA binding can act as an antagonist by replacing these interactions with low affinity, low valency interactions [50].

HA of different sizes can also signal through toll-like receptors (TLRs), either independently or in concert with other HA receptors. LMW-HA has been shown to engage in a unique receptor complex of CD44 and TLRs to induce cytokine release [53] and airway hyperresponsiveness (AHR) [54, 55] in macrophages and naïve mice, respectively. However, in a model of bleomycin-induced acute lung injury LMW-HA required both TLR2 and TLR4, along with MyD88, to stimulate chemokine expression, which was independent of CD44. HMW-HA was protective in this model and also required TLR2, TLR4, and MyD88 [15]. Short oHA have also been shown to transmit various “danger signals” and to signal through TLRs [56]. Interestingly, receptor binding and activation by oHA can even differ depending on the number of disaccharides present. For example, 4-mer oHA interacts with TLR2 and TLR4, but not CD44, while 6-mer oHA can bind to TLR2, TLR4, and CD44 [41, 57–59]. Additionally, 6- to 18-mer oHA bind monovalently to CD44, whereas larger polymers bind multivalently [60], which can affect clustering and signaling of this receptor. Furthermore, <6-mer oHA have low affinity for TSG-6, which is required for HA transfer to the inter-alpha-trypsin inhibitor (I α I) heavy chain and optimal signaling [61]. Conversely, 8- to 21-mer oHA induce an irreversible transfer of TSG-6 to the HA moiety and thus can compete with HA signaling by removing TSG-6 from the binding pool [62].

Size-dependent HA signaling can also differ according to cell type. LMW-HA induces activation and maturation of dendritic cells via TLR4, independently of RHAMM, CD44, and TLR2, to induce phosphorylation of p38/p42/44 MAPK and NF- κ B [41]. Conversely, LMW-HA stimulates macrophages independently of CD44 and TLR4 via the TLR2/MyD88 pathway, and HMW-HA can act as a competitive inhibitor of this response [63]. Oligosaccharide HA can activate TLR4 and CD44 pathways in chondrocytes [57, 64, 65], while in synovial fibroblasts it activates TLR2 and

TLR4, but not CD44 [66], and in vascular endothelial cells it activates RHAMM [67]. In aggregate, available evidence suggests that HA size influences receptor complex formation in a size-specific manner and thus modifies downstream signaling cascades.

6. Intracellular HA Signaling

HA is normally produced by synthases which reside at the cell membrane and is immediately extruded to the extracellular space without need for shuttling or exocytosis. Thus, most HA resides extracellularly and exerts its function in that space. However, HA has also been detected intracellularly, where it associates with the mitotic spindle, microtubules, and the receptor RHAMM [68, 69]. Two possible mechanisms by which HA may be localized intracellularly and potentially to contribute to signaling activity have been identified: intracellular (physiological or aberrant) production of HA and uptake of extracellular HA.

HA synthesis can deviate from the normal pattern, especially in malignancy and cell injury. Various hematologic malignancies such as monoclonal gammopathy of undetermined significance, multiple myeloma and Waldenström's macroglobulinemia as well as solid cancers such as bladder cancer feature cells with aberrant splice variants of HAS1, which are associated with cancer diagnosis, relapse and poor outcome (reviewed in [70]). Accumulating evidence has led to the hypothesis that HAS1 in these cancer cells may produce intracellular HA which competes with the mitotic apparatus for RHAMM binding and thus protect the cells from RHAMM-mediated mitotic arrest [70]. In conditions of endoplasmic reticulum (ER) stress, injured cells also produce HA cables that appear to emanate from a perinuclear region and protrude through the cytoplasm into the extracellular space [71]. This intracellular HA directly communicates with the extracellular space and allows inflammatory cells to congregate into the inflammatory site [71].

Uptake of extracellular HA seems to be directly tied to its digestion. HA of higher molecular weight can be digested by a variety of enzymatic and nonenzymatic [18, 29, 32, 72, 73] pathways to 50–100 long saccharide polymers and then be taken up by the cell either through receptor binding (CD44, RHAMM, LYVE-1, HARE) [74, 75] or through pinocytosis [76]. Much (or most) of the endocytosed HA is localized to the endosome and lysosome [68], where it is digested to oligosaccharides by hyaluronidases 1 and 2, and probably further by β -D-glucuronidase and β -N-acetyl-D-hexosaminidase [77]. The activities of at least HYAL1 and the extracellular β -hexosaminidase appear to be partly redundant [78]. However the regulation of HA catabolism and the fate of these fragments are unclear. They could be recycled for the generation of glycosaminoglycans, they could be exocytosed and engage extracellular HA receptors, or they could also engage intracellular HA receptors. The presence of HA receptors (notably RHAMM) in the cytoplasm strongly suggests that intracellular HA can have signaling activity. Evanko et al. have shown that intracellular HA, RHAMM, and microtubules colocalize in the cytoplasm and the nucleus [68]

and may affect the mitotic apparatus and directly or indirectly modulate RHAMM-mediated signaling [68].

7. Size Dependence of HA Biological Effects

Although the specific mechanisms involved in the diverse signaling of HA are still poorly understood, it is known that HA can modulate many biological effects including cell adhesion, cell migration, morphogenesis, tumorigenesis, cell survival, apoptosis, and inflammation and that these biological effects can differ depending on HA size. Endogenous HMW-HA has been shown to be anti-inflammatory and antiangiogenic [11]. Interestingly, depending on cellular localization, endogenous HMW-HA can either protect from epithelial apoptosis in lung injury [15] or promote an invasive fibroblast phenotype and the fibrotic process [14]. Treatment with HMW-HA can also inhibit inflammatory response in several disease models, such as in HMW-HA attenuated inflammation and lung injury in a sepsis model of ventilated rats [79], as well as ozone-induced AHR [54, 55, 80, 81]. Based on recent data, HMW-HA is emerging as a viable therapeutic option in inflammatory airway disease, due to its anti-inflammatory and antiproliferative properties. Lingering concerns however will have to be addressed, such as the potential of degradation of HMW-HA into LMW-HA and thus exacerbation of the inflammatory process. It is worth noting that inhaled HMW-HA has been used for several years in Europe, with a remarkably good safety profile [82–85].

Certain environmental exposures and disease states have been shown to lead to breaking-down of HMW-HA into fragments (LMW-HA) that can stimulate expression of proinflammatory cytokines, chemokines, and growth factors [86] and increase AHR [54]. Increased levels of LMW-HA have been found in many lung disorders including asthma, pulmonary fibrosis, COPD, allergic alveolitis, interstitial lung disease, sarcoidosis, and pulmonary hypertension (reviewed in [87]) and another article in this edition (Lauer et al.), as well as other inflammatory diseases like rheumatoid arthritis [88]. LMW-HA can also induce angiogenesis and tumor progression [50, 89]. In aggregate, the effect of LMW-HA in tissue injury seems to be proinflammatory and rather deleterious, and attempts to block LMW-HA signaling in disease may constitute novel treatments.

Interestingly, oHA of different sizes (4–16 mers) have been shown to both stimulate and inhibit inflammatory responses depending on cell type and disease model. HA oligosaccharides have been shown to increase angiogenesis during wound healing [67], stimulate proinflammatory effects in synovial fibroblasts [66], and promote cell adhesion [51]. Conversely, there are many studies that show oHA to have beneficial effects such as reducing poly(I:C)/TLR3-induced inflammation [90], modulating the onset and course of inflammatory demyelinating disease by interfering with lymphocyte-vascular endothelial cell slow rolling [91], inhibiting HA-CD44 activation of kinases, and causing disassembly of large signaling complexes [92, 93], as well as retarding the growth of several tumor types and sensitizing resistant cancer cells to various drugs [50].

Finally, it is worth mentioning that, unlike some experimental conditions, cells and tissues in situ are exposed to a variety of HA sizes at once. It is possible that the effects of exposure to a HA size mix may be more than the sum of its separate size effects, as has been demonstrated experimentally (de la Motte C, personal communication).

8. Conclusion

Much is still unknown about the biological effects of HA in tissue homeostasis and the response to injury, and crucial insights into these effects will be gained by understanding the size dependence of HA signaling. Mechanistically, we need to understand how HA size may affect receptor clustering and affinity to receptors (especially receptor variant forms); whether there is a relation between HA size and the localization of HA (intra- versus extracellular, as well as cellular compartments); how simultaneous engagement of different HA sizes may modulate signaling; and the role of intracellular HA in cell behavior. Undoubtedly, we can look forward to exciting developments in the field of HA biology which will help fuel translational applications and medical advances.

Conflict of Interests

The authors declare that there is no conflict of interests regarding the publication of this paper.

Authors' Contribution

Jaime M. Cyphert and Carol S. Trempus contributed equally as first authors.

References

- [1] J. Lesley, V. C. Hascall, M. Tammi, and R. Hyman, "Hyaluronan binding by cell surface CD44," *Journal of Biological Chemistry*, vol. 275, no. 35, pp. 26967–26975, 2000.
- [2] D. Jiang, J. Liang, and P. W. Noble, "Hyaluronan in tissue injury and repair," *Annual Review of Cell and Developmental Biology*, vol. 23, pp. 435–461, 2007.
- [3] T. C. Laurent and J. R. E. Fraser, "Hyaluronan," *The FASEB Journal*, vol. 6, no. 7, pp. 2397–2404, 1992.
- [4] K. T. Dicker, L. A. Gurski, S. Pradhan-Bhatt, R. L. Witt, M. C. Farach-Carson, and X. Jia, "Hyaluronan: a simple polysaccharide with diverse biological functions," *Acta Biomaterialia*, vol. 10, no. 4, pp. 1558–1570, 2014.
- [5] A. P. Spicer and J. A. McDonald, "Characterization and molecular evolution of a vertebrate hyaluronan synthase gene family," *The Journal of Biological Chemistry*, vol. 273, no. 4, pp. 1923–1932, 1998.
- [6] P. Prehm, "Hyaluronate is synthesized at plasma membranes," *Biochemical Journal*, vol. 220, no. 2, pp. 597–600, 1984.
- [7] P. Prehm, "Identification and regulation of the eukaryotic hyaluronate synthase," *Ciba Foundation Symposium*, vol. 143, pp. 21–40, 1989.
- [8] N. Itano, T. Sawai, M. Yoshida et al., "Three isoforms of mammalian hyaluronan synthases have distinct enzymatic properties," *Journal of Biological Chemistry*, vol. 274, no. 35, pp. 25085–25092, 1999.

- [9] J. Y. L. Tien and A. P. Spicer, "Three vertebrate hyaluronan synthases are expressed during mouse development in distinct spatial and temporal patterns," *Developmental Dynamics*, vol. 233, no. 1, pp. 130–141, 2005.
- [10] T. D. Camenisch, A. P. Spicer, T. Brehm-Gibson et al., "Disruption of hyaluronan synthase-2 abrogates normal cardiac morphogenesis and hyaluronan-mediated transformation of epithelium to mesenchyme," *Journal of Clinical Investigation*, vol. 106, no. 3, pp. 349–360, 2000.
- [11] D. Jiang, J. Liang, and P. W. Noble, "Hyaluronan as an immune regulator in human diseases," *Physiological Reviews*, vol. 91, no. 1, pp. 221–264, 2011.
- [12] K. M. Stuhlmeier and C. Pollaschek, "Differential effect of transforming growth factor β (TGF- β) on the genes encoding hyaluronan synthases and utilization of the p38 MAPK pathway in TGF- β -induced hyaluronan synthase 1 activation," *Journal of Biological Chemistry*, vol. 279, no. 10, pp. 8753–8760, 2004.
- [13] S. Adamia, P. M. Pilarski, A. R. Belch, and L. M. Pilarski, "Aber- rant splicing, hyaluronan synthases and intracellular hyaluro- nan as drivers of oncogenesis and potential drug targets," *Current Cancer Drug Targets*, vol. 13, no. 4, pp. 347–361, 2013.
- [14] Y. Li, D. Jiang, J. Liang et al., "Severe lung fibrosis requires an invasive fibroblast phenotype regulated by hyaluronan and CD44," *Journal of Experimental Medicine*, vol. 208, no. 7, pp. 1459–1471, 2011.
- [15] D. Jiang, J. Liang, J. Fan et al., "Regulation of lung injury and repair by Toll-like receptors and hyaluronan," *Nature Medicine*, vol. 11, no. 11, pp. 1173–1179, 2005.
- [16] A. B. Csoka, G. I. Frost, and R. Stern, "The six hyaluronidase- like genes in the human and mouse genomes," *Matrix Biology*, vol. 20, no. 8, pp. 499–508, 2001.
- [17] R. Stern and M. J. Jedrzejewski, "Hyaluronidases: their genomics, structures, and mechanisms of action," *Chemical Reviews*, vol. 106, no. 3, pp. 818–839, 2006.
- [18] R. Stern, "Hyaluronan catabolism: a new metabolic pathway," *European Journal of Cell Biology*, vol. 83, no. 7, pp. 317–325, 2004.
- [19] K. Meyer, "Chemical structure of hyaluronic acid," *Federation Proceedings*, vol. 17, no. 4, pp. 1075–1077, 1958.
- [20] M. Erickson and R. Stern, "Chain gangs: new aspects of hyaluronan metabolism," *Biochemistry Research International*, vol. 2012, Article ID 893947, 9 pages, 2012.
- [21] V. B. Lokeshwar and M. G. Selzer, "Hyaluronidase: both a tumor promoter and suppressor," *Seminars in Cancer Biology*, vol. 18, no. 4, pp. 281–287, 2008.
- [22] B. Triggs-Raine, T. J. Salo, H. Zhang, B. A. Wicklow, and M. R. Natowicz, "Mutations in *HYAL1*, a member of a tandemly distributed multigene family encoding disparate hyaluronidase activities, cause a newly described lysosomal dis- order, mucopolysaccharidosis IX," *Proceedings of the National Academy of Sciences of the United States of America*, vol. 96, no. 11, pp. 6296–6300, 1999.
- [23] T. Kaneiwa, S. Mizumoto, K. Sugahara, and S. Yamada, "Identifi- cation of human hyaluronidase-4 as a novel chondroitin sulfate hydrolase that preferentially cleaves the galactosaminidic link- age in the trisulfated tetrasaccharide sequence," *Glycobiology*, vol. 20, no. 3, pp. 300–309, 2009.
- [24] L. Y. W. Bourguignon, P. A. Singleton, F. Diedrich, R. Stern, and E. Gilad, "CD44 interaction with Na^+ - H^+ exchanger (NHE1) creates acidic microenvironments leading to hyaluronidase-2 and cathepsin B activation and breast tumor cell invasion," *Journal of Biological Chemistry*, vol. 279, no. 26, pp. 26991–27007, 2004.
- [25] M. R. Natowicz, M. P. Short, Y. Wang et al., "Clinical and biochemical manifestations of hyaluronidase deficiency," *The New England Journal of Medicine*, vol. 335, no. 14, pp. 1029–1033, 1996.
- [26] L. Jadin, X. Wu, H. Ding et al., "Skeletal and hematolog- ical anomalies in *HYAL2*-deficient mice: a second type of mucopolysaccharidosis IX?" *The FASEB Journal*, vol. 22, no. 12, pp. 4316–4326, 2008.
- [27] B. Chowdhury, R. Hemming, S. Hombach-Klonisch, B. Flamion, and B. Triggs-Raine, "Murine hyaluronidase 2 deficiency results in extracellular hyaluronan accumulation and severe cardiopulmonary dysfunction," *The Journal of Biological Chemistry*, vol. 288, no. 1, pp. 520–528, 2013.
- [28] J. Muto, Y. Morioka, K. Yamasaki et al., "Hyaluronan digestion controls DC migration from the skin," *The Journal of Clinical Investigation*, vol. 124, no. 3, pp. 1309–1319, 2014.
- [29] R. Stern, G. Kogan, M. J. Jedrzejewski, and L. Šoltés, "The many ways to cleave hyaluronan," *Biotechnology Advances*, vol. 25, no. 6, pp. 537–557, 2007.
- [30] M. Oettl, J. Hoehstetter, I. Asen, G. Bernhardt, and A. Buschauer, "Comparative characterization of bovine testicu- lar hyaluronidase and a hyaluronate lyase from *Streptococcus agalactiae* in pharmaceutical preparations," *European Journal of Pharmaceutical Sciences*, vol. 18, no. 3-4, pp. 267–277, 2003.
- [31] L. Šoltés, R. Mendichi, G. Kogan, J. Schiller, M. Stankovská, and J. Arnhold, "Degradative action of reactive oxygen species on hyaluronan," *Biomacromolecules*, vol. 7, no. 3, pp. 659–668, 2006.
- [32] M. E. Monzon, N. Fregien, N. Schmid et al., "Reactive oxygen species and hyaluronidase 2 regulate airway epithelial hyaluro- nan fragmentation," *The Journal of Biological Chemistry*, vol. 285, no. 34, pp. 26126–26134, 2010.
- [33] F. Gao, J. R. Koenitzer, J. M. Tobolewski et al., "Extracellular superoxide dismutase inhibits inflammation by preventing oxidative fragmentation of hyaluronan," *Journal of Biological Chemistry*, vol. 283, no. 10, pp. 6058–6066, 2008.
- [34] G. M. Campo, A. Avenoso, A. D'Ascola et al., "Inhibition of hyaluronan synthesis reduced inflammatory response in mouse synovial fibroblasts subjected to collagen-induced arthritis," *Archives of Biochemistry and Biophysics*, vol. 518, no. 1, pp. 42–52, 2012.
- [35] G. M. Campo, A. Avenoso, A. D'Ascola et al., "The SOD mimic MnTM-2-PyP(5+) reduces hyaluronandegradation-induced inflammation in mouse articular chondrocytes stimulated with Fe (II) plus ascorbate," *International Journal of Biochemistry and Cell Biology*, vol. 45, no. 8, pp. 1610–1619, 2013.
- [36] I. Juranek, R. Stern, and L. Šoltés, "Hyaluronan peroxidation is required for normal synovial function: an hypothesis," *Medical Hypotheses*, vol. 82, no. 6, pp. 662–666, 2014.
- [37] D. Manzanares, M.-E. Monzon, R. C. Savani, and M. Salathe, "Apical oxidative hyaluronan degradation stimulates airway ciliary beating via RHAMM and RON," *The American Journal of Respiratory Cell and Molecular Biology*, vol. 37, no. 2, pp. 160–168, 2007.
- [38] S. M. Casalino-Matsuda, M. E. Monzon, G. E. Conner, M. Salathe, and R. M. Forteza, "Role of hyaluronan and reactive oxygen species in tissue kallikrein-mediated epidermal growth factor receptor activation in human airways," *Journal of Biolog- ical Chemistry*, vol. 279, no. 20, pp. 21606–21616, 2004.
- [39] K. S. Girish and K. Kemparaju, "The magic glue hyaluronan and its eraser hyaluronidase: a biological overview," *Life Sciences*, vol. 80, no. 21, pp. 1921–1943, 2007.

- [40] C. Hardwick, K. Hoare, R. Owens et al., "Molecular cloning of a novel hyaluronan receptor that mediates tumor cell motility," *The Journal of Cell Biology*, vol. 117, no. 6, pp. 1343–1350, 1992.
- [41] C. Termeer, F. Benedix, J. Sleeman et al., "Oligosaccharides of hyaluronan activate dendritic cells via Toll-like receptor 4," *Journal of Experimental Medicine*, vol. 195, no. 1, pp. 99–111, 2002.
- [42] R. M. Forteza, S. M. Casalino-Matsuda, N. S. Falcon, M. V. Gattas, and M. E. Monzon, "Hyaluronan and layilin mediate loss of airway epithelial barrier function induced by cigarette smoke by decreasing," *Journal of Biological Chemistry*, vol. 287, no. 50, pp. 42288–42298, 2012.
- [43] P. Bono, K. Rubin, J. M. G. Higgins, and R. O. Hynes, "Layilin, a novel integral membrane protein, is a hyaluronan receptor," *Molecular Biology of the Cell*, vol. 12, no. 4, pp. 891–900, 2001.
- [44] C. M. Carreira, S. M. Nasser, E. di Tomaso et al., "LYVE-1 is not restricted to the lymph vessels: expression in normal liver blood sinusoids and down-regulation in human liver cancer and cirrhosis," *Cancer Research*, vol. 61, no. 22, pp. 8079–8084, 2001.
- [45] R. Prevo, S. Banerji, D. J. P. Ferguson, S. Clasper, and D. G. Jackson, "Mouse LYVE-1 is an endocytic receptor for hyaluronan in lymphatic endothelium," *Journal of Biological Chemistry*, vol. 276, no. 22, pp. 19420–19430, 2001.
- [46] S. Banerji, J. Ni, S.-X. Wang et al., "LYVE-1, a new homologue of the CD44 glycoprotein, is a lymph-specific receptor for hyaluronan," *The Journal of Cell Biology*, vol. 144, no. 4, pp. 789–801, 1999.
- [47] J. A. Weigel, R. C. Raymond, C. McGary, A. Singh, and P. H. Weigel, "A blocking antibody to the hyaluronan receptor for endocytosis (HARE) inhibits hyaluronan clearance by perfused liver," *Journal of Biological Chemistry*, vol. 278, no. 11, pp. 9808–9812, 2003.
- [48] J. A. Weigel, R. C. Raymond, and P. H. Weigel, "The hyaluronan receptor for endocytosis (HARE) is not CD44 or CD54 (ICAM-1)," *Biochemical and Biophysical Research Communications*, vol. 294, no. 4, pp. 918–922, 2002.
- [49] B. Zhou, J. A. Weigel, L. Fauss, and P. H. Weigel, "Identification of the hyaluronan receptor for endocytosis (HARE)," *Journal of Biological Chemistry*, vol. 275, no. 48, pp. 37733–37741, 2000.
- [50] B. P. Toole, S. Ghatak, and S. Misra, "Hyaluronan oligosaccharides as a potential anticancer therapeutic," *Current Pharmaceutical Biotechnology*, vol. 9, no. 4, pp. 249–252, 2008.
- [51] C. Yang, M. Cao, H. Liu et al., "The high and low molecular weight forms of hyaluronan have distinct effects on CD44 clustering," *The Journal of Biological Chemistry*, vol. 287, no. 51, pp. 43094–43107, 2012.
- [52] P. M. Wolny, S. Banerji, C. Gounou et al., "Analysis of CD44-hyaluronan interactions in an artificial membrane system: insights into the distinct binding properties of high and low molecular weight hyaluronan," *Journal of Biological Chemistry*, vol. 285, no. 39, pp. 30170–30180, 2010.
- [53] K. R. Taylor, K. Yamasaki, K. A. Radek et al., "Recognition of hyaluronan released in sterile injury involves a unique receptor complex dependent on toll-like receptor 4, CD44, and MD-2," *The Journal of Biological Chemistry*, vol. 282, no. 25, pp. 18265–18275, 2007.
- [54] S. Garantziotis, Z. Li, E. N. Potts et al., "Hyaluronan mediates ozone-induced airway hyperresponsiveness in mice," *The Journal of Biological Chemistry*, vol. 284, no. 17, pp. 11309–11317, 2009.
- [55] S. Garantziotis, Z. Li, E. N. Potts et al., "TLR4 is necessary for hyaluronan-mediated airway hyperresponsiveness after ozone inhalation," *The American Journal of Respiratory and Critical Care Medicine*, vol. 181, no. 7, pp. 666–675, 2010.
- [56] J. D. Powell and M. R. Horton, "Threat matrix: low-molecular-weight hyaluronan (HA) as a danger signal," *Immunologic Research*, vol. 31, no. 3, pp. 207–218, 2005.
- [57] G. M. Campo, A. Avenoso, S. Campo, A. D'Ascola, G. Nastasi, and A. Calatroni, "Small hyaluronan oligosaccharides induce inflammation by engaging both toll-like-4 and CD44 receptors in human chondrocytes," *Biochemical Pharmacology*, vol. 80, no. 4, pp. 480–490, 2010.
- [58] K. R. Taylor, J. M. Trowbridge, J. A. Rudisill, C. C. Termeer, J. C. Simon, and R. L. Gallo, "Hyaluronan fragments stimulate endothelial recognition of injury through TLR4," *The Journal of Biological Chemistry*, vol. 279, no. 17, pp. 17079–17084, 2004.
- [59] C. C. Termeer, J. Hennies, U. Voith et al., "Oligosaccharides of hyaluronan are potent activators of dendritic cells," *Journal of Immunology*, vol. 165, no. 4, pp. 1863–1870, 2000.
- [60] R. Schmits, J. Filmus, N. Gerwin et al., "CD44 regulates hematopoietic progenitor distribution, granuloma formation, and tumorigenicity," *Blood*, vol. 90, no. 6, pp. 2217–2233, 1997.
- [61] V. A. Higman, D. C. Briggs, D. J. Mahoney et al., "A refined model for the TSG-6 link module in complex with hyaluronan: use of defined oligosaccharides to probe structure and function," *Journal of Biological Chemistry*, vol. 289, no. 9, pp. 5619–5634, 2014.
- [62] M. E. Lauer, T. T. Glant, K. Mikecz et al., "Irreversible heavy chain transfer to hyaluronan oligosaccharides by tumor necrosis factor-stimulated gene-6," *The Journal of Biological Chemistry*, vol. 288, no. 1, pp. 205–214, 2013.
- [63] K. A. Scheibner, M. A. Lutz, S. Boodoo, M. J. Fenton, J. D. Powell, and M. R. Horton, "Hyaluronan fragments act as an endogenous danger signal by engaging TLR2," *Journal of Immunology*, vol. 177, no. 2, pp. 1272–1281, 2006.
- [64] G. M. Campo, A. Avenoso, S. Campo, A. D'Ascola, P. Traina, and A. Calatroni, "Differential effect of molecular size HA in mouse chondrocytes stimulated with PMA," *Biochimica et Biophysica Acta—General Subjects*, vol. 1790, no. 10, pp. 1353–1367, 2009.
- [65] G. M. Campo, A. Avenoso, A. D'Ascola et al., "Hyaluronan differently modulates TLR-4 and the inflammatory response in mouse chondrocytes," *BioFactors*, vol. 38, no. 1, pp. 69–76, 2012.
- [66] G. M. Campo, A. Avenoso, A. D'Ascola et al., "4-mer hyaluronan oligosaccharides stimulate inflammation response in synovial fibroblasts in part via TAK-1 and in part via p38-MAPK," *Current Medicinal Chemistry*, vol. 20, no. 9, pp. 1162–1172, 2013.
- [67] F. Gao, C. X. Yang, W. Mo, Y. W. Liu, and Y. Q. He, "Hyaluronan oligosaccharides are potential stimulators to angiogenesis via RHAMM mediated signal pathway in wound healing," *Clinical and Investigative Medicine*, vol. 31, no. 3, pp. E106–E116, 2008.
- [68] S. P. Evanko, T. Parks, and T. N. Wight, "Intracellular hyaluronan in arterial smooth muscle cells: association with microtubules, RHAMM, and the mitotic spindle," *Journal of Histochemistry and Cytochemistry*, vol. 52, no. 12, pp. 1525–1535, 2004.
- [69] S. P. Evanko and T. N. Wight, "Intracellular localization of hyaluronan in proliferating cells," *Journal of Histochemistry and Cytochemistry*, vol. 47, no. 10, pp. 1331–1342, 1999.
- [70] S. Adamia, J. Kriangkum, A. R. Belch, and L. M. Pilarski, "Aberant posttranscriptional processing of hyaluronan synthase 1 in malignant transformation and tumor progression," in *Advances in Cancer Research*, vol. 123, pp. 67–94, Elsevier, New York, NY, USA, 2014.

- [71] V. C. Hascall, A. K. Majors, C. A. de la Motte et al., "Intracellular hyaluronan: a new frontier for inflammation?" *Biochimica et Biophysica Acta*, vol. 1673, no. 1-2, pp. 3-12, 2004.
- [72] R. Stern, "Hyaluronidases in cancer biology," *Seminars in Cancer Biology*, vol. 18, no. 4, pp. 275-280, 2008.
- [73] G. M. Campo, A. Avenoso, A. D'Ascola et al., "The inhibition of hyaluronan degradation reduced pro-inflammatory cytokines in mouse synovial fibroblasts subjected to collagen-induced arthritis," *Journal of Cellular Biochemistry*, vol. 113, no. 6, pp. 1852-1867, 2012.
- [74] E. N. Harris, S. V. Kyosseva, J. A. Weigel, and P. H. Weigel, "Expression, processing, and glycosaminoglycan binding activity of the recombinant human 315-kDa hyaluronic acid receptor for endocytosis (HARE)," *The Journal of Biological Chemistry*, vol. 282, no. 5, pp. 2785-2797, 2007.
- [75] Q. Hua, C. B. Knudson, and W. Knudson, "Internalization of hyaluronan by chondrocytes occurs via receptor-mediated endocytosis," *Journal of Cell Science*, vol. 106, part 1, pp. 365-375, 1993.
- [76] H. J. Greyner, T. Wiraszka, L.-S. Zhang, W. M. Petroll, and M. E. Mummert, "Inducible macropinocytosis of hyaluronan in B16-F10 melanoma cells," *Matrix Biology*, vol. 29, no. 6, pp. 503-510, 2010.
- [77] L. Rodén, P. Campbell, J. R. Fraser, T. C. Laurent, H. Pertoft, and J. N. Thompson, "Enzymic pathways of hyaluronan catabolism.," *Ciba Foundation symposium*, vol. 143, pp. 60-76, 1989.
- [78] L. Gushulak, R. Hemming, D. Martin, V. Seyrantepe, A. Pshezhetsky, and B. Triggs-Raine, "Hyaluronidase 1 and β -hexosaminidase have redundant functions in hyaluronan and chondroitin sulfate degradation," *The Journal of Biological Chemistry*, vol. 287, no. 20, pp. 16689-16697, 2012.
- [79] Y.-Y. Liu, C.-H. Lee, R. Dedaj et al., "High-molecular-weight hyaluronan—a possible new treatment for sepsis-induced lung injury: a preclinical study in mechanically ventilated rats," *Critical Care*, vol. 12, no. 4, article R102, 2008.
- [80] Z. Li, E. N. Potts-Kant, S. Garantziotis, W. M. Foster, and J. W. Hollingsworth, "Hyaluronan signaling during ozone-induced lung injury requires TLR4, MyD88, and TIRAP," *PLoS ONE*, vol. 6, no. 11, Article ID e27137, 2011.
- [81] F. Feng, Z. Li, E. N. Potts-Kant et al., "Hyaluronan activation of the Nlrp3 inflammasome contributes to the development of airway hyperresponsiveness," *Environmental Health Perspectives*, vol. 120, no. 12, pp. 1692-1698, 2012.
- [82] A. Varricchio, M. Capasso, F. Avvisati et al., "Inhaled hyaluronic acid as ancillary treatment in children with bacterial acute rhinopharyngitis," *Journal of Biological Regulators and Homeostatic Agents*, vol. 28, no. 3, pp. 537-43, 2014.
- [83] M. Ros, R. Casciaro, F. Lucca et al., "Hyaluronic acid improves the tolerability of hypertonic saline in the chronic treatment of cystic fibrosis patients: a multicenter, randomized, controlled clinical trial," *Journal of Aerosol Medicine and Pulmonary Drug Delivery*, vol. 27, no. 2, pp. 133-137, 2014.
- [84] F. Cresta, A. Naselli, F. Favilli, and R. Casciaro, "Inhaled hypertonic saline+hyaluronic acid in cystic fibrosis with asthma-like symptoms: a new therapeutic chance," *BMJ Case Reports*, vol. 2013, 2013.
- [85] M. L. Furnari, L. Termini, G. Traverso et al., "Nebulized hypertonic saline containing hyaluronic acid improves tolerability in patients with cystic fibrosis and lung disease compared with nebulized hypertonic saline alone: a prospective, randomized, double-blind, controlled study," *Therapeutic Advances in Respiratory Disease*, vol. 6, no. 6, pp. 315-322, 2012.
- [86] M. R. Horton, C. M. McKee, C. Bao et al., "Hyaluronan fragments synergize with interferon- γ to induce the C-X-C chemokines mig and interferon-inducible protein-10 in mouse macrophages," *The Journal of Biological Chemistry*, vol. 273, no. 52, pp. 35088-35094, 1998.
- [87] F. E. Lennon and P. A. Singleton, "Role of hyaluronan and hyaluronan-binding proteins in lung pathobiology," *The American Journal of Physiology—Lung Cellular and Molecular Physiology*, vol. 301, no. 2, pp. L137-L147, 2011.
- [88] A. R. Poole, J. Witter, N. Roberts et al., "Inflammation and cartilage metabolism in rheumatoid arthritis: studies of the blood markers hyaluronic acid, orosomucoid, and keratan sulfate," *Arthritis and Rheumatism*, vol. 33, no. 6, pp. 790-799, 1990.
- [89] B. P. Toole, A. Zoltan-Jones, S. Misra, and S. Ghatak, "Hyaluronan: a critical component of epithelial-mesenchymal and epithelial-carcinoma transitions," *Cells Tissues Organs*, vol. 179, no. 1-2, pp. 66-72, 2005.
- [90] M. Y. Kim, J. Muto, and R. L. Gallo, "Hyaluronic acid oligosaccharides suppress TLR3-dependent cytokine expression in a TLR4-dependent manner," *PLoS ONE*, vol. 8, no. 8, Article ID e72421, 2013.
- [91] C. W. Winkler, S. C. Foster, A. Itakura et al., "Hyaluronan oligosaccharides perturb lymphocyte slow rolling on brain vascular endothelial cells: implications for inflammatory demyelinating disease," *Matrix Biology*, vol. 32, no. 3-4, pp. 160-168, 2013.
- [92] S. Ghatak, S. Misra, and B. P. Toole, "Hyaluronan constitutively regulates ErbB2 phosphorylation and signaling complex formation in carcinoma cells," *The Journal of Biological Chemistry*, vol. 280, no. 10, pp. 8875-8883, 2005.
- [93] S. Misra, B. P. Toole, and S. Ghatak, "Hyaluronan constitutively regulates activation of multiple receptor tyrosine kinases in epithelial and carcinoma cells," *The Journal of Biological Chemistry*, vol. 281, no. 46, pp. 34936-34941, 2006.

Research Article

Hyaluronan Synthase 3 Null Mice Exhibit Decreased Intestinal Inflammation and Tissue Damage in the DSS-Induced Colitis Model

Sean P. Kessler, Dana R. Obery, and Carol de la Motte

Department of Pathobiology, Lerner Research Institute Cleveland Clinic, 9500 Euclid Avenue, Cleveland, OH 44195, USA

Correspondence should be addressed to Sean P. Kessler; kessles@ccf.org

Received 6 October 2014; Revised 19 January 2015; Accepted 20 January 2015

Academic Editor: Arnoud Sonnenberg

Copyright © 2015 Sean P. Kessler et al. This is an open access article distributed under the Creative Commons Attribution License, which permits unrestricted use, distribution, and reproduction in any medium, provided the original work is properly cited.

Hyaluronan (HA) overproduction is a hallmark of multiple inflammatory diseases, including inflammatory bowel disease (IBD). Hyaluronan can act as a leukocyte recruitment molecule and in the most common mouse model of intestinal inflammation, the chemically induced dextran sodium sulfate (DSS) experimental colitis model, we previously determined that changes in colon distribution of HA occur before inflammation. Therefore, we hypothesized that, during a pathologic challenge, HA promotes inflammation. In this study, we tested the progression of inflammation in mice null for the hyaluronan synthase genes (HAS1, HAS3, or both HAS1 and HAS3) in the DSS-colitis model. Our data demonstrate that both the HAS1/HAS3 double and the HAS3 null mice are protected from colitis, compared to wild-type and HAS1 null mice, as determined by measurement of weight loss, disease activity, serum IL-6 levels, histologic scoring, and immunohistochemistry. Most notable is the dramatic increase in submucosal microvasculature, hyaluronan deposition, and leukocyte infiltration in the inflamed colon tissue of wild-type and HAS1 null mice. Our data suggest, HAS3 plays a crucial role in driving gut inflammation. Developing a temporary targeted therapeutic intervention of HAS3 expression or function in the microcirculation may emerge as a desirable strategy toward tempering colitis in patients undergoing flares of IBD.

1. Introduction

HA is a ubiquitous carbohydrate polymer produced by a wide variety of cell types and is present in the extracellular matrix of healthy and inflamed tissues. This glycosaminoglycan is produced as a long, straight chain polymer of up to 10^4 disaccharide units of alternating N-acetyl glucosamine and glucuronic acid without a protein core or any postsynthesis decoration or chemical modification [1]. Regulated hyaluronan production occurs at the cytoplasmic membrane surface by one or more hyaluronan synthase (HAS1, HAS2, or HAS3) enzymes before being extruded into the extracellular matrix as a space-filling, supportive anionic molecule [2]. Temporally and spatially controlled production of hyaluronan is critical in heart development as supported by the observation that the HAS2 null mutation in mice is embryonically lethal due to malformation of the heart tissue [3] and HAS3 null mice display altered neuronal activity and seizures [4]. HAS2

production of hyaluronan in skin fibroblasts is important for protecting skin from environmental stress that can induce apoptosis [5, 6]. Hyaluronan is found in almost every tissue and is especially abundant in the vitreous of the eye [7], synovial fluid in joints [8], proximal tubules of the kidney [9], the mucosal layer of the colon [10, 11], and vertebrate breast milk [12]. HA is even present in platelets and their megakaryocyte precursors; however, in these cells it accumulates in the intracellular space [13]. Hyaluronan degradation and cellular turnover are governed largely by the hyaluronidase family of enzymes, (e.g., HYAL 1 and HYAL 2) in a CD44-dependent [14] or, as recently described in a KIA1199 protein dependent, CD44-independent fashion [15].

Our lab has been investigating the role of HA in intestinal inflammation, especially as it relates to IBD. IBD encompasses human diseases Crohn's colitis and ulcerative colitis, conditions that exhibit increased HA deposition during flares, or periods of inflammation [10]. In addition, we have

shown that viral infections, ER stress, and inflammatory cytokines (especially the IBD associated factor, TNF α) cause formation of an HA rich leukocyte adhesive matrix around intestinal smooth muscle cells [10, 16] and on intestinal microvascular endothelial cells [11]. This HA matrix binds mononuclear leukocytes, including monocytes and lymphocytes and potentially contributes to inflammatory infiltrate recruitment during colitis [17].

The experimental DSS-induced murine colitis model is a well-established and consistent method to study profound inflammatory changes that occur in the gut during disease progression [18]. We previously demonstrated that hyaluronan deposition precedes inflammation and immune cell influx into damaged gut tissue in this model [11]. In addition, we observed that leukocyte adhesive, cable-like hyaluronan structures are produced at the microvessel surface and into the lumen of DSS-treated mice. Similar HA structures are observed in the microvasculature of colon tissue sections derived from IBD patients and importantly on *in vitro* grown human intestinal microvessel endothelial cells (HIMECs) isolated from colon when treated with the inflammatory cytokine, TNF α [13]. Interestingly, we discovered that, exclusively, HAS3 mRNA expression increased in HIMECs after TNF α exposure, suggesting that HAS3 is the enzyme chiefly responsible for generating luminal HA during disease [13]. Proinflammatory leukocytes [17] and platelets [13] home on these cable structures, degrading them into smaller-size proinflammatory signaling molecules which may perpetuate the inflammation cycle [13]. Based on these observations, we have proposed that increased production of HA during pathologic events, particularly HA in the microvasculature produced by HAS3, may be a key player in driving the unending cycle of inflammation experienced by IBD patients [13].

We experimentally tested whether disrupting HA production affects the inflammation process that occurs in the murine DSS-colitis model, using HAS1 null, HAS3 null, and HAS1/HAS3 double null mice. We compared the disease progression and histological changes in the colon over the ten-day time course of disease and found that mice that carried the HAS3 null mutation had much less severe colitis by every means of analysis. Weight loss, disease activity, colitis scoring, circulating IL-6 levels, and histology/immunostaining were all ameliorated in HAS3 null mice experiencing colitis. Our data suggest that controlling HAS3 expression in the microvasculature of IBD patients may be a significant target site for therapeutic drug intervention.

2. Materials and Methods

2.1. Mice. All experiments were performed under an animal welfare protocol approved by the Lerner Research Institute's Institutional Animal Care and Use Committee (IACUC). All mice were at adult age and c57Bl/6 background strain housed and bred in specific pathogen-free (SPF) microisolator cages on standard Teklad irradiated chow in the AALAC certified LRI Biological Resource Unit and acidified water. Wild-type mice (c57Bl/6J Stock number 000664) used for experiments and breeding with HAS1/3 double null mice were purchased

from Jackson Labs, Bar Harbor, ME. HAS1/HAS3 double null mice, created by crossing single null mice [19, 20], were a generous gift from Dr. Vincent Hascall in the Biomedical Engineering Department at the Lerner Research Institute [5]. HAS1KO and HAS3KO single null mice were generated by breeding the double null mice with wild-type c57Bl/6J mice and then interbreeding for the desired null allele from a dihybrid cross. Genotypes were confirmed by PCR using Qiagen (Alameda, CA) prepared genomic DNA and an Epicentre Technologies (Madison, WI) PCR Kit in a Thermo Scientific HyBaid PCR Express machine (Wilmington, DE) with the following run parameters: 95°C for 30 sec, 65°C for 30 sec, and 72°C for 1 min, 35 cycles. The amplified PCR products generated by each primer set are as follows: 341 bp HAS1 wild-type allele (mHAS1s: 5'gacgttctggccttggtctac 3' and mHAS1as: 5'gggctctactgctgctggagg 3') and 320 bp HAS3 wild-type allele (mHAS3s: 5'ggaagcagcataggtagccttg 3' and mHAS3as: 5'tgatcgccaccttaccaccag 3'). The null allele specific anti-sense primer (PGKpromAS-1: 5'gaggccactgtgtagcccaag 3') was used with the sense primers above to verify single (HAS1KO 331 bp, HAS3KO 320 bp) and double null mouse genotypes. Adult mice of the same sex and genotype were cohoused in groups of not more than 5 mice per SPF microisolator cage in the LRI Biological Resource Unit with 12-hour light/dark cycles and constantly monitored temperature and humidity conditions with husbandry performed by the LRI BRU staff.

2.2. DSS Colitis. The dextran sodium sulfate experimental mouse model was performed as previously described [11]. Briefly, mice received irradiated Harlan Teklad standard chow and acidified in-house water ad libitum in water bottles without or with the addition of 2.5% dextran sodium sulfate (number 160110) (MP Biomedicals, Solon, OH). Mice were weighed and monitored daily for signs of colitis. Mice ($n \geq 6$ per genotype) were sacrificed following IACUC approved methods on days 0, 3, 5, 7, and 10. Serum was collected by cardiac bleeding. Colons were removed, measured for length (cm) from the rectum to the cecum, and then fixed in ten times tissue volume of molecular biology grade Histochoice (AMRESCO, Solon, OH) prior to processing by LRI Histology Core Service Department.

2.3. Disease Activity Index Scoring. During the administration of DSS, all mice were observed for outward signs of colitis using a scoring system based on previous studies [21]. Points were recorded according to the following scale with minimum of 0 points and maximum total of 11 points. Weight change was calculated as (current day weight – starting weight)/starting weight \times 100: (0) 0–5%, (1) 6–10%, (2) 11–15%, (3) 15–20%, and (4) >20%. Posture was observed as (0) normal, (1) hunched. Coat fur was observed as (0) normal, (1) ruffled. Stool texture and consistency was observed as (0) normal, (1) soft, (2) soft with blood, and (3) liquid, bloody. Rectal prolapse was observed as (0) none, (1) 1 mm, and (2) 2 mm.

2.4. Colitis Scoring. On the day of sacrifice (day 0, 3, 5, 7, and 10), 1 cm rectal sections from all mice were removed

and fixed in Histochoice for 24 hours at 25°C. Subsequently, tissue was processed and cut at 2.5 µm cross-sections before staining with hematoxylin and eosin by the Lerner Research Institute Histology Core. Rectal sections from all mice were scored based on previous rating systems with a minimum score of 5 and a maximum score of 20 [22, 23]. Epithelium integrity was observed as (1) intact and well-defined crypt structure, (2) intact epithelium with reduced crypt structure, (3) breaks in epithelium layer and reduced crypt structure, and (4) loss of epithelium and crypt structure. Infiltration of leukocytes was observed as (1) none, (2) sparse, (3) moderate, and (4) fulminant. Submucosal swelling below the muscularis mucosae was observed as (1) none, (2) minor, (3) moderate, and (4) severe. Hyperplasia of the muscularis mucosa was observed as (1) none, (2) minor, (3) moderate, and (4) severe. Changes in angiogenesis were recorded, noting an increase in the number, size, and thickness of blood vessels during colitis: (1) none, (2) minor, (3) moderate, and (4) severe.

2.5. Histology and Immunohistochemistry of Rectal Sections. Hematoxylin and eosin stained rectal section images were captured with a 10x objective lens on a Leica Digital Microscope using Leica DFC425C camera and Leica Application Suite software (Leica Corp, Buffalo Grove, IL). Disease-associated changes in hyaluronan abundance and location were observed by immunostaining following previously published methods [24]. Briefly, rectal sections were deparaffinized by repeated dipping in the following solutions: Clear-Rite 3 (2 × 3 min), Flex 100 (2 min, 1 min), Flex 95 (2 min, 1 min) (Richard Allan-Thermo Scientific, Kalamazoo, MI), and tap water. Tissue was encircled with a Pap-Pen (Research Products International, Mt. Prospect, IL) before blocking for 30 min in 2% Fetal Bovine Serum-Hank's buffered saline (2% FBS-HBSS). The biotinylated hyaluronan binding protein (HABP) (Calbiochem-EMD Millipore, Billerica, MA) was diluted (1:100) in 2% FBS-HBSS and applied overnight at 4°C. Subsequently, slides were washed 3 times in HBSS before applying streptavidin-488 (1:500) (Life Technologies, Grand Island, NY) in 2% FBS-HBSS for 45 minutes in the dark at 25°C. Slides were washed 3 times in HBSS prior to mounting under cover glass with Vectashield + DAPI (Vector Labs, Burlingame, CA) and sealing with nail polish. Stained tissues were imaged at 10x magnification with a Leica microscope using ImageProPlus and Photoshop software. Scale bars = 200 µm. Semiquantitative measurement of submucosal swelling in the histology images and semiquantitative densitometry analysis of HA deposition in the immunohistochemistry images were performed with ImageProPlus software.

2.6. Serum IL-6. Serum was collected from all mice in Microtainer serum separator tubes (Becton Dickinson, Franklin Lakes, NJ), centrifuged at 4100 rpm and stored at -80°C. Twenty microliters of serum were tested in duplicate at all time points in the BioLegend Mouse IL-6 ELISA Max platform (BioLegend, San Diego, CA) according to manufacturer's instructions. The serum was also measured for protein concentration using the Bio-Rad Bradford assay system (Bio-Rad, Hercules, CA). Both assay plates were read with the

SpectraMax 340PC384 (Molecular Devices Corp., Sunnyvale, CA). The concentration of IL-6 (ng/µL) was then normalized to total protein in the serum (µg/µL) to determine the ng IL-6/µg total protein using Microsoft Office 2010 Excel followed by graphing with GraphPad Prism 5 software.

2.7. Statistics. All data was analyzed with GraphPad Prism 5 software. The data collected from each group of mice of the same genotype at the same time point was plotted as an average with error bars signifying the standard error of the mean (SEM). A one-tailed unpaired student *t*-test or a Mann-Whitney *t*-test for nonparametric data at 95% confidence was then applied to compare a mutant strain to wild-type strain for the indicated parameter or a one-factor ANOVA test of significance was applied when comparing multiple groups to each other.

3. Results

To test our hypothesis that HA is a key molecule that drives inflammation in the gut during intestinal inflammation, we treated mice that were null for either HAS1 or HAS3 or both HAS1/HAS3 in the experimental DSS-colitis model. Weight loss is a reliable and accepted measure of disease activity in this model [22, 25]. Figure 1 illustrates that all genotypes, except the HAS1 null mice, gain a small amount (1–3%) of body weight during the first three days of DSS treatment. Continued exposure to DSS, however, causes dramatic weight loss in the wild-type group between day 5 and day 7 but is less severe in the three HAS null groups, on these days. While all three null groups were protected from weight loss at all time points compared to wild-type mice, the HAS3 null group lost significantly ($P < 0.0001$) less body weight by day 7 (Figure 1(b)). Although the mean weight loss measured between HAS3 and HA1 null groups is notable, it approached but did not fully reach statistical significance at day 7 time point. HAS3 null mice lost an average of less than 5% bodyweight compared to the average loss of 11% by the wild-type group. We focused on day 7 time point because this is the time point where the most dramatic changes in disease progression occur, although the animals continue to lose weight through day 10 and are variably distressed.

In addition to weight loss, 2.5% DSS-treated c57B/6 background strain wild-type mice typically exhibit rectal bleeding between day 5 and day 7 with stools becoming soft and loose to the point of being liquid by day 10. At day 10, mouse fur can take on a ruffled appearance as the mice display reduced motility and adopt a hunched posture. We therefore noted this disease activity (DAI) by assigning points by following a previously reported scoring index as described in the methods section, based on weight loss, ruffled fur, hunched posture, rectal bleeding, bloody stools, and rectal prolapse [21]. Our data revealed that the HAS3 null mice displayed the lowest disease activity score at all time points (Figure 2(a)) compared to the other three groups. Comparing the DAI at day 7, we observed that HAS1 mice were more severely affected compared to wild-type mice ($P < 0.05$) while both HAS3 and HAS1/HAS3 null mice were significantly more protected ($P < 0.002$ and $P < 0.05$, resp.)

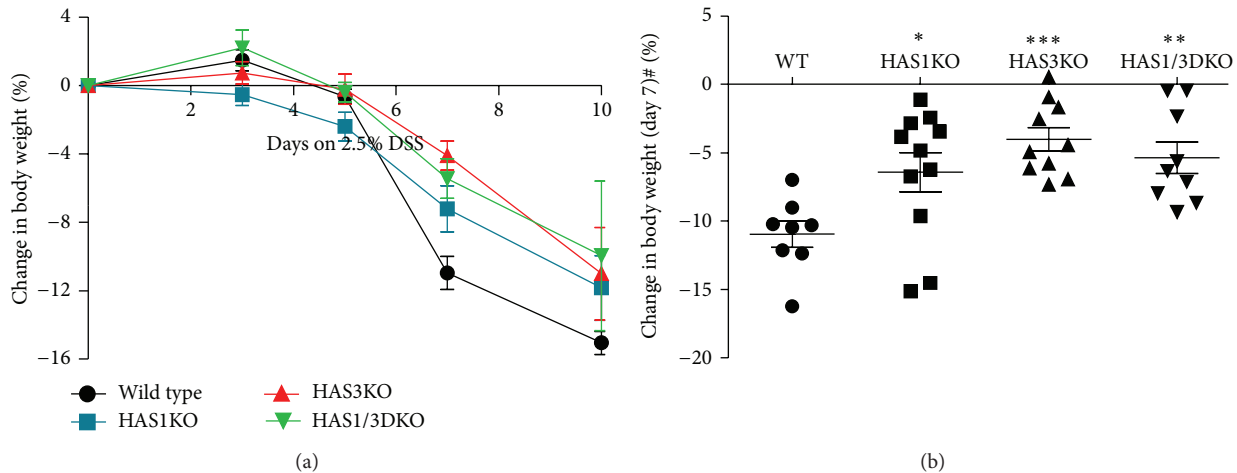


FIGURE 1: Change in body weight during DSS-induced colitis. (a) Groups of 6 or more adult mice of each indicated genotype were provided with 2.5% DSS in their drinking water for up to 10 days. Body weight measured at days 3, 5, 7, and 10 was compared to starting weight at day 0 for each mouse. The data points reflect the average change in body weight with error bars representing \pm SEM. (b) Significance of day 7 weight loss of genotypes compared to the wild-type group: *** $P < 0.0001$, ** $P < 0.005$, and * $P < 0.05$ in Student's unpaired t -test, 95% confidence. One-way ANOVA test for the mean weight loss compared for all groups $^{\#}P < 0.005$.

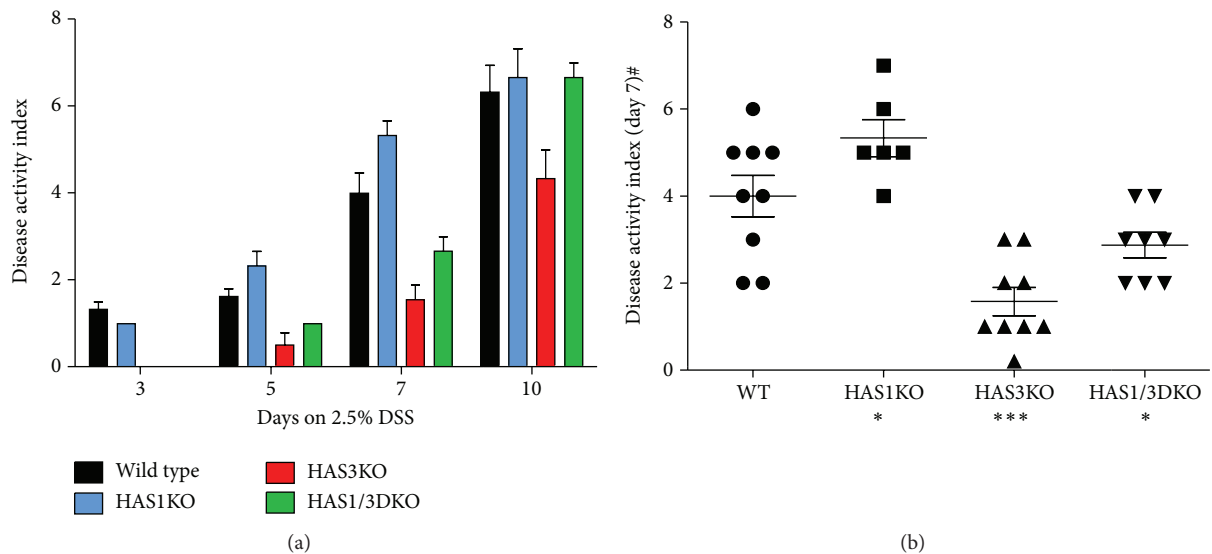


FIGURE 2: Disease activity index (DAI) during DSS-induced colitis. (a) All mice were observed for outward signs of disease including weight loss, hunched posture, ruffled fur, bloody stools, and rectum prolapse. Data bars reflect the average of six or more mice per time point for each genotype with error bars set at the \pm SEM. (b) DAI at day 7. Significance of day 7 weight loss of genotypes compared to the wild-type groups: *** $P < 0.002$ and * $P < 0.05$ in a Mann-Whitney nonparametric unpaired t -test, 95% confidence.

(Figure 2(b)). Another associated marker of colitis scoring for this model is colon shortening. During the progression of disease, overall colon length shortens from 9.5–10 cm in untreated mice to approximately 5.5–6 cm in wild-type mice treated with DSS for 10 days. Figure 3 illustrates the shortening of the colon in all genotypes over the course of the DSS treatment with HAS3 null mice retaining the most colon length at day 7 ($P < 0.05$) and day 10 ($P < 0.001$) time points, respectively.

Elevated levels of the inflammatory cytokine IL-6 have been documented in IBD patients and in experimental mice

treated with DSS [26, 27]. To test whether the decreased DAI and retention of body weight observed in HAS3 null mice were also accompanied by a change in circulating IL-6 levels, we collected serum from all mice on the day of sacrifice by cardiac puncture. Serum IL-6 levels, measured in an ELISA format and normalized for total protein concentration, are presented in Figure 4. We observed that the HAS3 null mice possessed the lowest amount of circulating IL-6 at all time points we tested, but especially at day 7, compared to wild-type mice ($P < 0.005$). At day 7, IL-6 levels in the HAS3 null mice were barely detectable, whereas wild-type, HAS1 null,

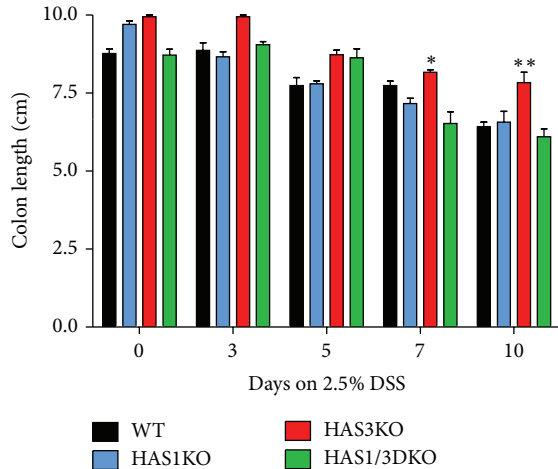


FIGURE 3: Decrease in colon length of DSS-treated mice. Colons removed from mice sacrificed at the indicated time points were measured for distance (cm) from the distal end of the cecum to the rectum. Bars represent the average of 6 or more mice from each indicated genotype at the noted time point. Error bars reflect the \pm SEM. The significant decrease of colon length at day 7 for the HAS3 null mice is indicated; * $P < 0.05$, ** $P < 0.01$.

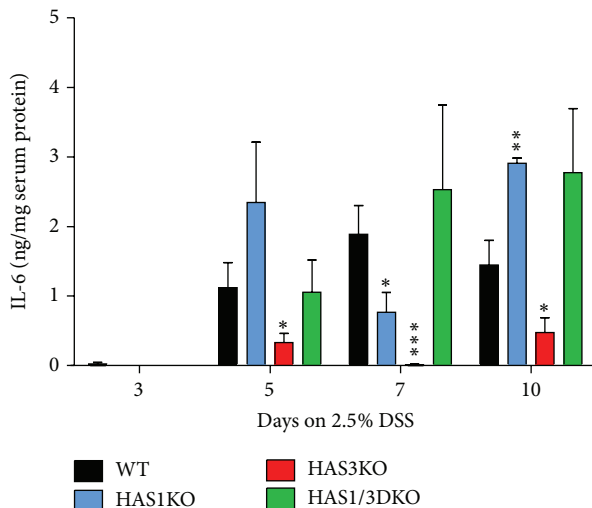


FIGURE 4: Serum IL-6 in DSS-treated mice. Serum isolated from all mice was tested for IL-6 in an ELISA format, normalized by protein concentration in the serum sample by Bradford assay to determine the ng IL-6/ μ g total serum protein. Bars represent the average of mice of the same genotype at the indicated time point. Error bars reflect \pm SEM. Comparison of null mice to wild-type mice at the indicated time point: * $P < 0.05$, ** $P < 0.01$, and *** $P < 0.005$ at 95% confidence.

and HAS1/3 double null mice all have elevated circulating IL-6 in the 1.0–2.5 ng/mg range. Interestingly, the HAS1/HAS3 null mice had the highest level of IL-6, even surpassing levels found in wild-type mice at each time point.

Histological analysis, utilizing a scoring system described previously [22, 23], is a valuable tool to semi-quantitatively

assess the damage in the colon tissue during experimentally induced colitis events as it is to assess the extent of tissue injury observed in tissues surgically removed from IBD patients. Hematoxylin and eosin (H&E) stained rectal sections (the site where colitis begins in this model) from mice sacrificed at each time point were observed and scored for epithelial erosion/crypt damage, submucosal swelling, leukocyte infiltration, muscularis mucosae hyperplasia, and increased angiogenesis using the point system described in the methods. Representative tissue sections are presented in Figure 6. As the length of time mice exposed to DSS increased, the average colitis scores for all genotype groups also increased (Figure 5(a)). However, a distinct and dramatic separation occurs when comparing the HAS3 null group (colitis score 10.5) to wild-type mice (colitis score 16.5) at day 7 ($P < 0.005$), while there is no difference in the mean score comparison between wild-type and HAS1 null mice at day 7 (Figure 5(b)). The HAS1/3 null group score is lower than the wild-type group score and approaches but does not fully meet statistical significance at this day 7 time point. At day 10 time point, the difference is even more pronounced and demonstrates the decrease in colitis severity when the HAS3 enzyme is absent, both in the HAS3 null and the HAS1/3 null groups (Figure 5(a)).

The profound changes that occur in the mouse distal colon over the 10 days of DSS-induced colitis can be seen in Figure 6. Distal colon (rectal) sections were selected for specific analysis since this model is bacterially driven and the rectal area has the highest microbe burden. Once the epithelial layers have been effaced and crypt damage ensues due to continuous chemical exposure, direct microbe interaction with host immune cells occurs. Similar pathological changes are routinely observed in human IBD patient intestinal tissue after repeated flares of inflammation. While submucosal swelling and epithelial damage commence at day 3 in wild-type and the HAS1 null groups, this effect is delayed or dramatically reduced in both HAS1/3 and HAS3 null mouse groups even at 10 days of treatment (Figure 6). In addition, leukocyte infiltration, muscularis mucosae hyperplasia, and increased angiogenesis are all evident in day 7 and day 10 in the wild-type and HAS1 null groups but not in HAS1/3 or HAS3 null mice. To determine the extent of submucosal expansion in the longitudinal rectal folds in each tissue over the course of the experimental colitis in Figure 6(a), we measured the area of swelling using imaging software (Figure 6(b)). The representative submucosal region measured is indicated in the untreated wild-type mouse. Both the H&E images and the expansion measurements indicate the dramatic changes in the submucosal region of wild-type and HAS1 null mice, especially at day 7 and day 10, compared to the HAS3 null and HAS1/3 null mice. Immunostaining of these adjacent matched rectal sections for hyaluronan deposition and clearance over the 10-day time course also reveals distinctly different HA staining patterns in the mice lacking the intact HAS3 allele. Figure 7 demonstrates that in all groups there is increased deposition of hyaluronan at day 3 in the submucosa and mucosal/lamina propria regions of the colon. By day 5, in the wild-type and HAS1 null groups, submucosal swelling is very pronounced, whereas

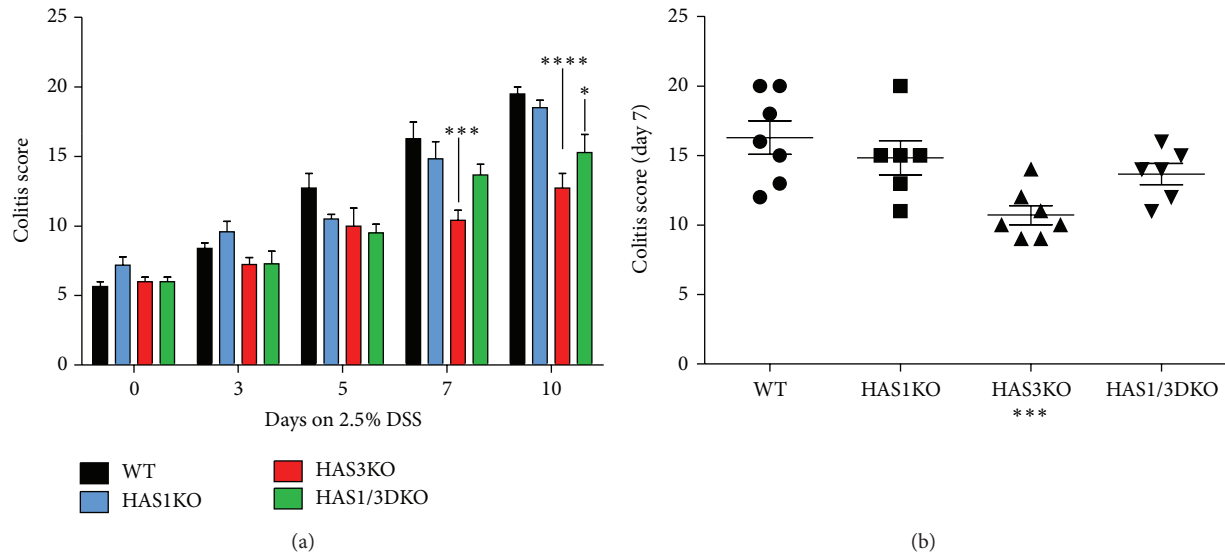


FIGURE 5: Histological colitis scores for DSS-treated mice. Hematoxylin and eosin stained rectal cross-sections from DSS-treated mice were scored for pathology changes including erosion of the epithelium layer, leukocyte infiltration, submucosal swelling, muscularis mucosae hyperplasia, and increased vascularization as described in methods. (a) Bars represent the average scores of groups of mice of the same genotype at the indicated time points with error bars reflecting \pm SEM. Comparison of null mice to wild-type mice at the indicated time point: * $P < 0.05$, *** $P < 0.005$, and **** $P < 0.001$ at 95% confidence. (b) The colitis score at day 7 is presented with significance of HAS3 null compared to wild-type mice at 95% confidence noted *** $P < 0.005$.

this swelling did not occur in animals with HAS3 deletion. At days 7 and 10, the mice that possess HAS3 (the wild-type and HAS1 null groups) exhibit a very noticeable persistence and increase in hyaluronan deposition in the damaged mucosa as well as around the highly vascularized areas in the submucosa. Semiquantitative densitometric analysis of the HA staining in the longitudinal folds of the lamina propria and submucosal regions was performed to track the changes in hyaluronan in both compartments in each genotype over the course of the colitis (Figure 7(b)). The regions measured for each subcompartment of the rectal fold are illustrated as yellow masked areas on the image from the untreated wild-type mouse. In unchallenged animals, homeostatic levels of HA in the lamina propria extracellular matrix of distal colon tissue are typically decreased with deletion of enzymes HAS1 (~50%) and especially HAS3 (~75%) compared to wild type. In the submucosa, overall lower levels of HA are produced per area, but the relationship of decreased levels of HA with deletion of HAS1 and HAS3 is also observed. Unexpectedly, HA levels in the HAS3 null tissue are lower than in the HAS1/HAS3 double deletion intestinal tissue.

Similar HA analysis was performed on sections obtained from mice undergoing DSS treatment. With DSS challenge, wild-type HA levels in the lamina propria remain relatively constant until day 5 when the HA levels decrease, corresponding to the time that leukocyte infiltration and crypt destruction are evident. Paradoxically, HAS1 null mice have the highest levels of HA at day 3 (1.8-fold compared to wild-type mice) and the higher HA level is maintained throughout the course of disease, reaching 5-fold wild-type levels at day 7 when the disease has reached its pathologic peak. In comparison, HAS3 null animals maintain near wild-type mice levels

of HA in the lamina propria throughout the time course, and the HAS1/HAS3 double null animals showed intermediate expression compared to HAS1 null and HAS3 null tissue. The HA content of submucosal tissue also changes during DSS colitis, with wild-type animals showing a great increase in distal colon connective tissue HA at 7 days, the time point when the submucosal inflammatory infiltrate is most evident (Figure 6(a)). Similar to the lamina propria, the HAS1 mice show higher submucosal expression throughout the DSS time course, and the HAS3 mice exhibit normal to low expression. Of note, neither mutant genotype nor the double null peaked at day 7 or exhibited the submucosal inflammation of the wild-type mouse colon. This data provides snapshots of the presence of HA in intestine and how it changes owing to HAS enzyme mutation. However, a causal relationship between HAS expression and HA deposition from this data is not possible to assess since in the inflammation model the cellular makeup of the tissue changes drastically during the disease. Independent of HAS expression, loss of epithelium leads to HA loss from the lamina propria (especially evident on day 10, Figure 6(a)) and the infiltrating leukocytes and platelets have the ability to degrade HA. Additionally, reactive oxygen species generated during inflammation can mediate depolymerization of HA.

Enlargements of the images from 7-day DSS treatment of wild-type and HAS3 null mice are presented in Figure 8 and they display strikingly different tissue structure. Firstly, observing from the intestinal lumen downward, the lamina propria (Lp) of wild-type animals has lost all epithelium (E) as well as crypt architecture, and infiltrating leukocytes are prevalent in this tissue area (Figure 8(a)). In the HAS3 null section (Figure 8(c)), the epithelium and crypt architecture

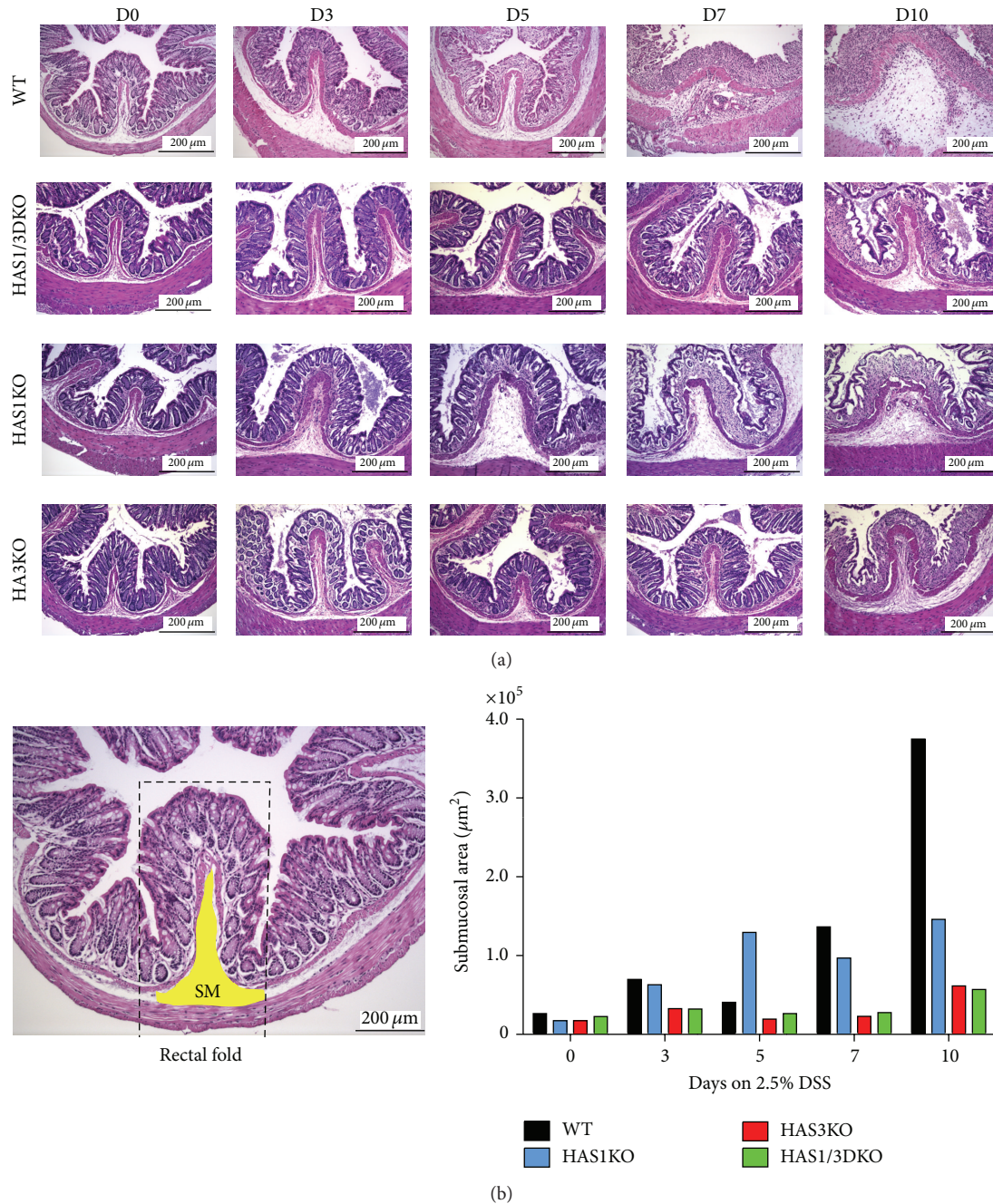
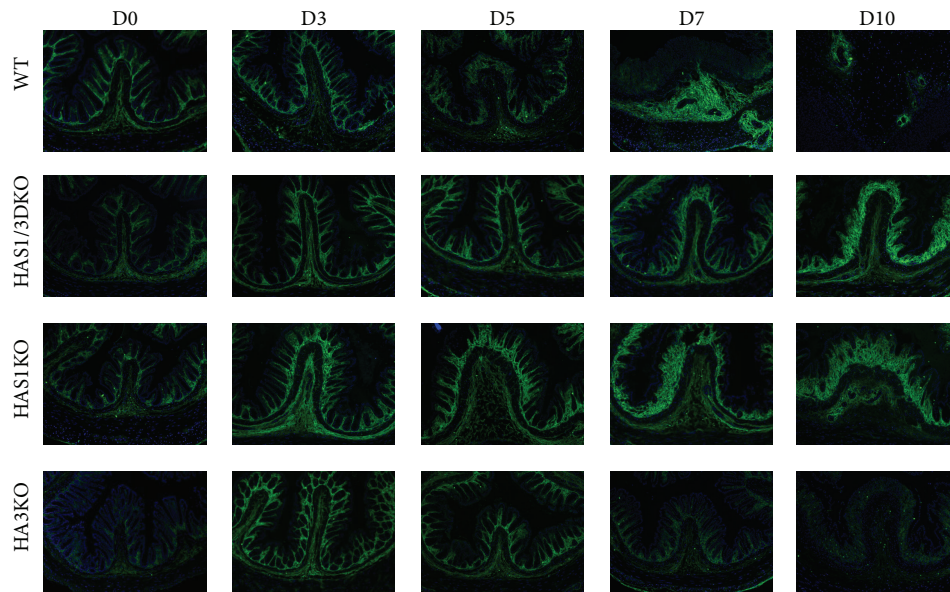


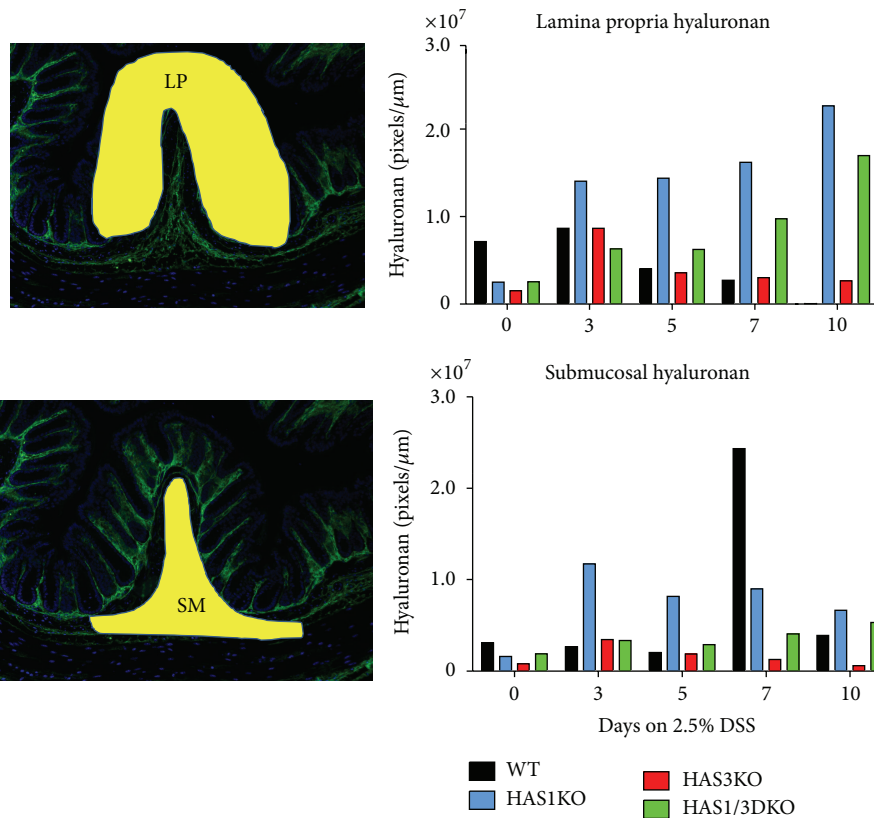
FIGURE 6: Histology of rectal sections from DSS-treated mice. (a) Representative rectal images of hematoxylin and eosin stained cross-sections from mice of each genotype sacrificed on the indicated DSS treatment time point at 10x magnification (scale bar = 200 μm). Images captured with a Leica digital brightfield microscope and the Leica application software (LAS). (b) Submucosal swelling of the rectal longitudinal folds (dashed line) in the images presented in panel (a) was measured (area μm²) using ImageProPlus software. The untreated wild-type rectal section illustrates the region measured (yellow).

are largely maintained in the lamina propria, and very little increase in the population of infiltrating leukocytes is noted. Secondly, while the muscularis mucosa (Mm) is slightly expanded in the HAS3 null animals, it does not achieve the overall thickness observed in the wild-type group. Thirdly, the submucosa (Sm) of the wild-type mouse colon is vastly expanded compared to the HAS3 null tissue and contains

many more and thicker walled blood vessels (V). Strikingly, there is also a much greater presence of infiltrating leukocytes (L) in the submucosal space of the wild-type mouse colon than in the HAS3 null tissue (Figure 8(a) versus Figure 8(c)). HA deposition within the inflamed and highly vascularized submucosa region of the wild-type sections is tremendously increased compared to either day 7 treated HAS3 null section



(a)



(b)

FIGURE 7: Immunohistochemistry of DSS-treated mice. (a) Adjacent rectal sections to the H&E stained tissues presented in Figure 6 were stained for hyaluronan (green) with the biotinylated hyaluronan binding protein (HABP) and Alexa Fluor streptavidin-488. Nuclei were stained with DAPI (blue). Images are 10x magnification captured with a Leica digital fluorescent microscope and ImageProPlus software. (b) Semi-quantitative densitometric analysis of HA staining in longitudinal folds in the images presented in panel (a). The untreated wild-type rectal section illustrates the regions measured (yellow). Lamina propria HA staining (LP) is the region above the muscularis mucosae while submucosa HA staining (SM) is the area below the muscularis mucosae and above the muscularis externa.

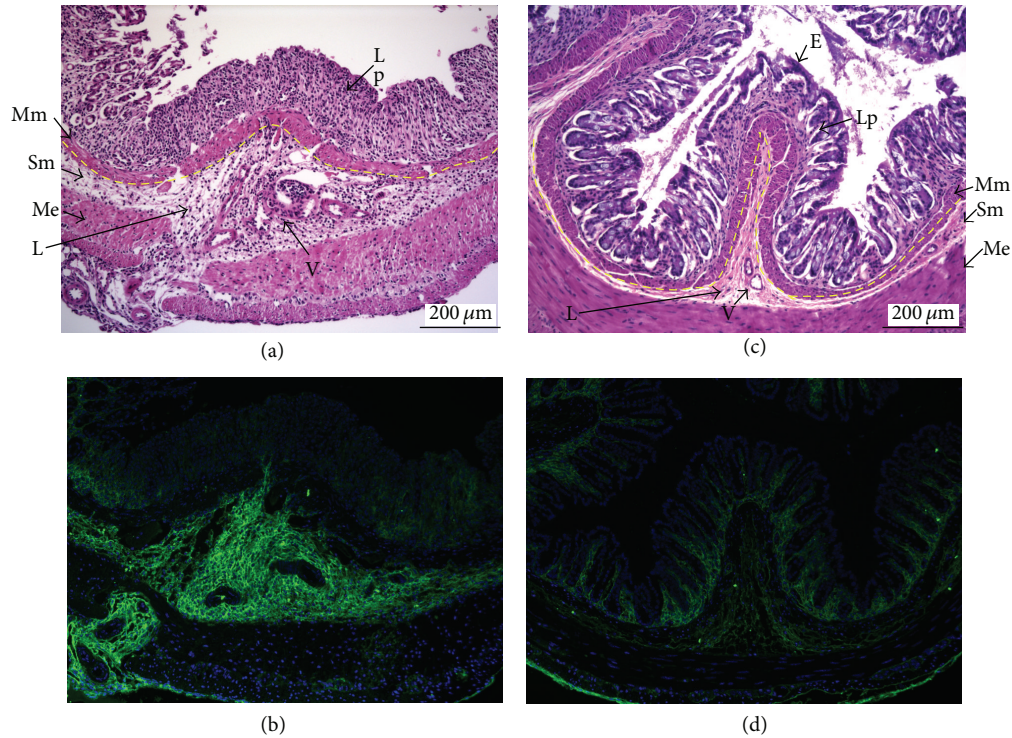


FIGURE 8: Histology and immunohistochemistry of day 7 DSS-treated wild-type and HAS3 null rectal sections. Cross-section images from Figures 6 and 7 were enlarged to show detail with the following tissue regions marked as follows: (E) epithelium, (Lp) lamina propria, (Mm) muscularis mucosae, (Sm) submucosae, (V) blood vessels, (Me) muscularis externa, and (L) leukocytes. The luminal muscularis mucosae and submucosae boundary are marked in yellow dashed line.

(Figure 8(b) versus Figure 8(d)) or the untreated wild-type control (Figure 7). The absence of numerous expanded blood vessels and reduced hyaluronan deposition in the HAS3 null submucosa may explain why a leukocyte infiltrate is minor in these mice at day 7.

4. Discussion

Hyaluronan can be found in almost every tissue location in the vertebrate body. An adult human turns over an estimated 15 grams of HA every day through balanced tissue specific synthesis by hyaluronan synthase enzymes (HAS1, HAS2, and HAS3) and controlled degradation by hyaluronidase enzymes (HYAL1, HYAL2) [28]. Misregulated HA metabolism has serious physiological consequences in human patients and can be recapitulated in knockout mouse models. Altered HAS enzymes function has been implicated in multiple myeloma (HAS1) [29], in renal-controlled fluid balance, heart formation, long bone/spine development, wound healing (HAS2) [3, 6, 9, 30–33], and seizures (HAS3) [4]. Ablation of hyaluronidase enzyme function results in mucopolysaccharidosis lysosomal storage disorder (HYAL1) [34, 35], craniofacial bone disorders, heart valve defects and thrombocytopenia (HYAL2) [36, 37], and lung carcinoma (HYAL3) [38]. We were therefore surprised that HAS1 null, HAS3 null, and HAS1/HAS3 double null mice had no obvious physical, developmental, or reproductive defects. This

finding, together with the data that HAS2 null animals are embryologically lethal, indicates that HAS2 is the crucial HA generator in the body. HAS2 is thought to be the major inducible synthase in mesenchymal cells including fibroblasts and smooth muscle cells [39, 40]. The data presented here showing HA staining of the colon (Figure 7) support this idea. The HA content in unchallenged HAS1/HAS3 null (only HAS2 expressing) colons is not dramatically different than in wild-type mouse tissues that express all three isoenzymes. The question then arises: why are there three enzymes that make the same HA product when HAS2 seems to be sufficient. We hypothesized that HAS1 and HAS3 may play a role during times of stress and tested this notion in a chemically induced, bacterially driven model of inflammation.

In our previous experimental DSS-induced colitis studies and studies reported by others, there is a direct correlation between outward signs of disease and pathological changes that take place in the gut tissues [11, 21]. Interestingly, Zheng et al. have previously reported that both HAS2 and HAS3 mRNA are upregulated in mouse colon tissue during DSS colitis [41]. Histological staining of rectal sections of wild-type mice reveals a very consistent pattern of intestinal damage including epithelial cell and crypt loss; areas of submucosal swelling which contain increased hyaluronan deposition; increased vascularization; and inflammatory cell infiltration into the damaged site. To determine whether perturbing HA production could change the course of colitis,

we outbred the HAS1/3 double null mice with wild-type, background matched c57B/6 mice to generate the single HAS1 or HAS3 null strains used in the current DSS-colitis model study. Testing all four genotypes revealed that HAS1 null mice and wild-type mice, both of which retain the HAS3 gene, are equally adversely affected by DSS administration on all points of analysis. The HAS3 null group, similar to the HAS1/3 double null cohort, was far less affected by DSS-induced colitis. In fact, our data indicates that the HAS3 mice are even more resistant than the HAS1/3 group. The HAS3 null mice have the lowest DAI, the lowest colitis score, and the lowest circulating levels of the proinflammatory cytokine IL-6, compared to the wild-type, HAS1 null, and HAS1/3 null groups. IL-6 is a cytokine that drives inflammation and is an accepted marker of inflammatory changes, especially in gastrointestinal disorders [42, 43]. Previous reports by others have indicated a strong compensation for the loss of both HAS1 and HAS3 by greater induction of HAS2 [6]. Perhaps this accounts for the small discrepancy between the higher levels of protection observed in the HAS3 null group compared to the HAS1/3 nulls.

Overall, our laboratory focuses on investigating the role of HA in the initiation and perpetuation of the inflammatory cycle observed in patients suffering with IBD. Since we have previously recognized: (1) that HA is present at higher levels in inflamed IBD colon tissue compared to non-inflamed IBD tissue as well as non-IBD controls [10]; (2) that HA can act as a leukocyte adhesion molecule on activated human intestinal smooth muscle cells [17] and microvessel endothelial cells [11] *in vitro*; and (3) that changes in HA remodeling happen prior to inflammation *in vivo* in models of colitis, we asked whether disruption of normal HA production *in vivo* would alter the course of induced intestinal inflammation. In the current work we found that deletion of one of the HA synthesizing enzymes, specifically HAS3, but not HAS1, significantly reduced the course of colitis in mice. Leukocyte infiltration, epithelial loss, blood vessel expansion and tissue damage were all reduced in the absence of HAS3. This suggests that the HA produced by HAS3 expressing cells is critical to mounting an inflammatory response, and that the HAS3 gene is somehow important for responding to challenge. The next question is how does HAS3 accomplish this function? At least three possible explanations are plausible: the HA product is somehow different, the location of expression is different, or the factors that regulate HAS3 gene expression are different, compared to HAS2 especially.

Data supporting the idea that the three HA synthases make different sized products has been put forth; HAS1 and HAS2 in membrane preparations synthesize very large HA chains (average molecular mass $2 \times 10^5 \sim 2 \times 10^6$ Da) while HAS3 produces a smaller HA size range ($1 \times 10^5 \sim 1 \times 10^6$ Da) [44]. A possible reason HAS3 appears to contribute so significantly to inflammation may be due to the routine production of smaller sized HA that is known to signal pro-inflammatory, pro-angiogenic responses through Toll-like receptors 4 and 2 [45–47]. However, Brinck and Heldin showed using whole cells expressing the different singular HAS enzymes, that HA size was not substantially different [48]. This differential size

distinction theory, in any case, is somewhat difficult to accept in the tissue setting where hyaluronan degrading enzymes and cellular clearance mechanisms are operative and likely to alter all HA sizes even further.

Our previous data provide support that both location of expression and inciting stimulus may be important for the specific HAS3 (versus HAS2) participation in inflammation. We have demonstrated that HAS3 is important for increasing HA on microvascular endothelium under inflammatory conditions (i.e., the presence of TNF α), and that the HA produced is leukocyte adhesive [11]. In contrast, intestinal smooth muscle cells produce increased HA, predominantly through regulation of HAS2 (unpublished) and do not produce a leukocyte adhesive matrix in response to TNF α [17]. In addition, we have determined that human platelets, when activated, have the ability to fragment the HA on endothelial surfaces using the enzyme HYAL2 [13, 49]. Therefore, our new and previously reported data suggest a scenario in the microvessels of the intestine to partially explain the pathological changes in DSS colitis and human IBD; the HA produced by HAS3 is both a leukocyte recruitment molecule which aids in extravasation into the intestinal tissue, and additionally is a substrate for platelets to create HA fragments that drive cell activation and angiogenesis. Further experiments using vascular specific deletions of HAS3 may be useful in determining if this scenario is correct.

In addition to the concept that disease progression is due to the HAS gene expression, HA size and location of deposition, one cannot rule out the possible role of the activity of the HAS enzymes as they function to polymerize HA cables. Previous studies have demonstrated that HAS1 and HAS2 enzymes can multimerize into a complex HA generating molecular machine [50, 51]. Inactive HAS2 mutant proteins were shown to dimerize with wild-type HAS2 and consequently blocked HA production. Our data suggests that HAS1 may act as a negative regulator of HA synthesis by HAS2 since both HAS1 null and HAS1/3 double null mutants displayed higher levels of HA deposition during colitis. Definitive confirmation of the role of HAS1 as a spoiler will require the generation of the appropriate tagged enzymes for *in vitro* analysis or the generation of new transgenic mice.

Current regimens utilized to combat inflammation in colitis include anti-TNF [52] and anti-IL-6 [26] therapies. However, some patients stop responding to these therapies. Recently, several groups have reported the use of RNAi therapeutic liposomes [53] or nano-particle molecules [54] to selectively knockdown genes driving angiogenesis in tumor vessels *in vivo*, without causing off-target silencing in other larger blood vessels. Since HAS3 is expressed in the microvasculature, it might one day be possible to selectively target RNAi of HAS3 expression, especially in these patients that no longer respond positively to traditional drug therapies.

5. Conclusion

Our data suggest HAS3 plays a crucial role in driving gut inflammation while HAS1 may act to repress the hyaluronan synthesis of the other HAS enzymes. HAS3 null mice exhibit decreased intestinal inflammation and tissue damage in the

DSS-induced colitis model compared to wild-type, HAS1 null, and HAS1/3 double null mice while mice lacking HAS1 exhibit heightened HA deposition in both the lamina propria and submucosa during induced colitis. We suggest that future studies aimed at controlling HAS3 expression in the intestinal microvasculature may reveal new therapeutic intervention strategies for patients suffering from IBD.

Conflict of Interests

The authors declare that there is no conflict of interests regarding the publication of this paper.

Acknowledgments

The authors gratefully acknowledge research funding for this project from the Eunice Kennedy Shriver National Institute of Child Health and Human Development NIH/NICHD Grant 5R01 HD061918-03 to Carol de la Motte and the funding support from the Programs of Excellence in Glycoscience NIH/NHLBI Grant 1P01 HLI07147-01 to Carol de la Motte. They also thank the LRI Image Core and histology staff, Eric Diskin, Cassandra Rogers, and Diane Maholovic for imaging technical assistance and tissue processing. They thank the entire LRI Biological Resource Staff for their superior care of the animals in this study. They thank the members of the de la Motte lab for helpful discussion.

References

- [1] A. J. Day and J. K. Sheehan, "Hyaluronan: polysaccharide chaos to protein organisation," *Current Opinion in Structural Biology*, vol. 11, no. 5, pp. 617–622, 2001.
- [2] P. H. Weigel, V. C. Hascall, and M. Tammi, "Hyaluronan synthases," *The Journal of Biological Chemistry*, vol. 272, no. 22, pp. 13997–14000, 1997.
- [3] T. D. Camenisch, A. P. Spicer, T. Brehm-Gibson et al., "Disruption of hyaluronan synthase-2 abrogates normal cardiac morphogenesis and hyaluronan-mediated transformation of epithelium to mesenchyme," *The Journal of Clinical Investigation*, vol. 106, no. 3, pp. 349–360, 2000.
- [4] A. M. Arranz, K. L. Perkins, F. Irie et al., "Hyaluronan deficiency due to Has3 knock-out causes altered neuronal activity and seizures via reduction in brain extracellular space," *The Journal of Neuroscience*, vol. 34, no. 18, pp. 6164–6176, 2014.
- [5] J. A. MacK, R. J. Feldman, N. Itano et al., "Enhanced inflammation and accelerated wound closure following tetraphorbol ester application or full-thickness wounding in mice lacking hyaluronan synthases Has1 and Has3," *The Journal of Investigative Dermatology*, vol. 132, no. 1, pp. 198–207, 2012.
- [6] Y. Wang, M. E. Lauer, S. Anand, J. A. Mack, and E. V. Maytin, "Hyaluronan synthase 2 protects skin fibroblasts against apoptosis induced by environmental stress," *Journal of Biological Chemistry*, vol. 289, no. 46, pp. 32253–32265, 2014.
- [7] J. G. Hollyfield, M. E. Rayborn, M. Tammi, and R. Tammi, "Hyaluronan in the interphotoreceptor matrix of the eye: species differences in content, distribution, ligand binding and degradation," *Experimental Eye Research*, vol. 66, no. 2, pp. 241–248, 1998.
- [8] J. R. Fraser and T. C. Laurent, "Turnover and metabolism of hyaluronan," *Ciba Foundation Symposium*, vol. 143, pp. 41–53, 1989.
- [9] D. R. Michael, A. O. Phillips, A. Krupa et al., "The human hyaluronan synthase 2 (HAS2) gene and its natural antisense RNA exhibit coordinated expression in the renal proximal tubular epithelial cell," *The Journal of Biological Chemistry*, vol. 286, no. 22, pp. 19523–19532, 2011.
- [10] C. A. de la Motte, V. C. Hascall, J. Drazba, S. K. Bandyopadhyay, and S. A. Strong, "Mononuclear leukocytes bind to specific hyaluronan structures on colon mucosal smooth muscle cells treated with polyinosinic acid: polycytidylic acid. Inter- α -trypsin inhibitor is crucial to structure and function," *The American Journal of Pathology*, vol. 163, no. 1, pp. 121–133, 2003.
- [11] S. Kessler, H. Rho, G. West, C. Fiocchi, J. Drazba, and C. de la Motte, "Hyaluronan (HA) deposition precedes and promotes leukocyte recruitment in intestinal inflammation," *Clinical and Translational Science*, vol. 1, no. 1, pp. 57–61, 2008.
- [12] D. R. Hill, H. K. Rho, S. P. Kessler et al., "Human milk hyaluronan enhances innate defense of the intestinal epithelium," *The Journal of Biological Chemistry*, vol. 288, no. 40, pp. 29090–29104, 2013.
- [13] C. De La Motte, J. Nigro, A. Vasanji et al., "Platelet-derived hyaluronidase 2 cleaves hyaluronan into fragments that trigger monocyte-mediated production of proinflammatory cytokines," *The American Journal of Pathology*, vol. 174, no. 6, pp. 2254–2264, 2009.
- [14] H. Harada and M. Takahashi, "CD44-dependent intracellular and extracellular catabolism of hyaluronic acid by hyaluronidase-1 and -2," *The Journal of Biological Chemistry*, vol. 282, no. 8, pp. 5597–5607, 2007.
- [15] H. Yoshida, A. Nagaoka, S. Nakamura, Y. Sugiyama, Y. Okada, and S. Inoue, "Murine homologue of the human KIAA1199 is implicated in hyaluronan binding and depolymerization," *FEBS Open Bio*, vol. 3, pp. 352–356, 2013.
- [16] A. K. Majors, R. C. Austin, C. A. de La Motte et al., "Endoplasmic reticulum stress induces hyaluronan deposition and leukocyte adhesion," *The Journal of Biological Chemistry*, vol. 278, no. 47, pp. 47223–47231, 2003.
- [17] C. A. de La Motte, V. C. Hascall, A. Calabro, B. Yen-Lieberman, and S. A. Strong, "Mononuclear leukocytes preferentially bind via CD44 to hyaluronan on human intestinal mucosal smooth muscle cells after virus infection or treatment with poly(I-C)," *The Journal of Biological Chemistry*, vol. 274, no. 43, pp. 30747–30755, 1999.
- [18] F. Rieder, S. Kessler, M. Sans, and C. Fiocchi, "Animal models of intestinal fibrosis: new tools for the understanding of pathogenesis and therapy of human disease," *The American Journal of Physiology—Gastrointestinal and Liver Physiology*, vol. 303, no. 7, pp. G786–G801, 2012.
- [19] K. J. Bai, A. P. Spicer, M. M. Mascarenhas et al., "The role of hyaluronan synthase 3 in ventilator-induced lung injury," *The American Journal of Respiratory and Critical Care Medicine*, vol. 172, no. 1, pp. 92–98, 2005.
- [20] N. Kobayashi, S. Miyoshi, T. Mikami et al., "Hyaluronan deficiency in tumor stroma impairs macrophage trafficking and tumor neovascularization," *Cancer Research*, vol. 70, no. 18, pp. 7073–7083, 2010.
- [21] S. N. S. Murthy, H. S. Cooper, H. Shim, R. S. Shah, S. A. Ibrahim, and D. J. Sedergran, "Treatment of dextran sulfate sodium-induced murine colitis by intracolonic cyclosporin," *Digestive Diseases and Sciences*, vol. 38, no. 9, pp. 1722–1734, 1993.

- [22] M. Mähler, I. J. Bristol, E. H. Leiter et al., "Differential susceptibility of inbred mouse strains to dextran sulfate sodium-induced colitis," *American Journal of Physiology—Gastrointestinal and Liver Physiology*, vol. 274, no. 3, pp. G544–G551, 1998.
- [23] E. J. Shin, M. J. Sung, H. J. Yang, M. S. Kim, and J.-T. Hwang, "Boehmeria nivea attenuates the development of dextran sulfate sodium-induced experimental colitis," *Mediators of Inflammation*, vol. 2014, Article ID 231942, 7 pages, 2014.
- [24] C. A. de la Motte and J. A. Drazba, "Viewing hyaluronan: imaging contributes to imagining new roles for this amazing matrix polymer," *Journal of Histochemistry and Cytochemistry*, vol. 59, no. 3, pp. 252–257, 2011.
- [25] I. Okayasu, S. Hatakeyama, M. Yamada, T. Ohkusa, Y. Inagaki, and R. Nakaya, "A novel method in the induction of reliable experimental acute and chronic ulcerative colitis in mice," *Gastroenterology*, vol. 98, no. 3, pp. 694–702, 1990.
- [26] M. Allocca, M. Jovani, G. Fiorino, S. Schreiber, and S. Danese, "Anti-IL-6 treatment for inflammatory bowel diseases: next cytokine, next target," *Current Drug Targets*, vol. 14, no. 12, pp. 1508–1521, 2013.
- [27] S. L. S. Yan, J. Russell, and D. N. Granger, "Platelet activation and platelet-leukocyte aggregation elicited in experimental colitis are mediated by interleukin-6," *Inflammatory Bowel Diseases*, vol. 20, no. 2, pp. 353–362, 2014.
- [28] R. Stern, "Hyaluronan catabolism: a new metabolic pathway," *European Journal of Cell Biology*, vol. 83, no. 7, pp. 317–325, 2004.
- [29] S. Adamia, A. A. Reichert, H. Kuppasamy et al., "Inherited and acquired variations in the hyaluronan synthase 1 (HAS1) gene may contribute to disease progression in multiple myeloma and Waldenstrom macroglobulinemia," *Blood*, vol. 112, no. 13, pp. 5111–5121, 2008.
- [30] A.-E. Declèves, N. Caron, V. Voisin et al., "Synthesis and fragmentation of hyaluronan in renal ischaemia," *Nephrology Dialysis Transplantation*, vol. 27, no. 10, pp. 3771–3781, 2012.
- [31] P. Moffatt, E. R. Lee, B. St-Jacques, K. Matsumoto, Y. Yamaguchi, and P. J. Roughley, "Hyaluronan production by means of Has2 gene expression in chondrocytes is essential for long bone development," *Developmental Dynamics*, vol. 240, no. 2, pp. 404–412, 2011.
- [32] P. J. Roughley, L. Lamplugh, E. R. Lee, K. Matsumoto, and Y. Yamaguchi, "The role of hyaluronan produced by Has2 gene expression in development of the spine," *Spine*, vol. 36, no. 14, pp. E914–E920, 2011.
- [33] X. Zhu, X. Deng, G. Huang et al., "A novel mutation of Hyaluronan synthase 2 gene in Chinese children with ventricular septal defect," *PLoS ONE*, vol. 9, no. 2, Article ID e87437, 2014.
- [34] D. C. Martin, V. Atmuri, R. J. Hemming et al., "A mouse model of human mucopolysaccharidosis IX exhibits osteoarthritis," *Human Molecular Genetics*, vol. 17, pp. 1904–1915, 2008.
- [35] B. Triggs-Raine, T. J. Salo, H. Zhang, B. A. Wicklow, and M. R. Natowicz, "Mutations in HYAL1, a member of a tandemly distributed multigene family encoding disparate hyaluronidase activities, cause a newly described lysosomal disorder, mucopolysaccharidosis IX," *Proceedings of the National Academy of Sciences of the United States of America*, vol. 96, no. 11, pp. 6296–6300, 1999.
- [36] B. Chowdhury, R. Hemming, S. Hombach-Klonisch, B. Flammion, and B. Triggs-Raine, "Murine hyaluronidase 2 deficiency results in extracellular hyaluronan accumulation and severe cardiopulmonary dysfunction," *The Journal of Biological Chemistry*, vol. 288, no. 1, pp. 520–528, 2013.
- [37] L. Jadin, X. Wu, H. Ding et al., "Skeletal and hematological anomalies in HYAL2-deficient mice: a second type of mucopolysaccharidosis IX?" *FASEB Journal*, vol. 22, no. 12, pp. 4316–4326, 2008.
- [38] R.-X. Zhang, J.-H. Zhu, J. Fan, and X.-Q. Ji, "Analysis of HYAL3 gene mutations in Chinese lung squamous cell carcinoma patients," *Tumori*, vol. 99, no. 1, pp. 108–112, 2013.
- [39] A. Jacobson, J. Brinck, M. J. Briskin, A. P. Spicer, and P. Heldin, "Expression of human hyaluronan synthases in response to external stimuli," *The Biochemical Journal*, vol. 348, no. 1, pp. 29–35, 2000.
- [40] A. D. Recklies, C. White, L. Melching, and P. J. Roughley, "Differential regulation and expression of hyaluronan synthases in human articular chondrocytes, synovial cells and osteosarcoma cells," *The Biochemical Journal*, vol. 354, no. 1, pp. 17–24, 2001.
- [41] L. Zheng, T. E. Riehl, and W. F. Stenson, "Regulation of colonic epithelial repair in mice by Toll-like receptors and hyaluronic acid," *Gastroenterology*, vol. 137, no. 6, pp. 2041–2051, 2009.
- [42] F. Rieder, L. Cheng, K. M. Harnett et al., "Gastroesophageal reflux disease-associated esophagitis induces endogenous cytokine production leading to motor abnormalities," *Gastroenterology*, vol. 132, no. 1, pp. 154–165, 2007.
- [43] S. A. Strong, T. T. Pizarro, J. S. Klein, F. Cominelli, and C. Fiocchi, "Proinflammatory cytokines differentially modulate their own expression in human intestinal mucosal mesenchymal cells," *Gastroenterology*, vol. 114, no. 6, pp. 1244–1256, 1998.
- [44] N. Itano, T. Sawai, M. Yoshida et al., "Three isoforms of mammalian hyaluronan synthases have distinct enzymatic properties," *The Journal of Biological Chemistry*, vol. 274, no. 35, pp. 25085–25092, 1999.
- [45] K. A. Scheibner, M. A. Lutz, S. Boodoo, M. J. Fenton, J. D. Powell, and M. R. Horton, "Hyaluronan fragments act as an endogenous danger signal by engaging TLR2," *Journal of Immunology*, vol. 177, no. 2, pp. 1272–1281, 2006.
- [46] R. Stern, A. A. Asari, and K. N. Sugahara, "Hyaluronan fragments: an information-rich system," *European Journal of Cell Biology*, vol. 85, no. 8, pp. 699–715, 2006.
- [47] K. R. Taylor, K. Yamasaki, K. A. Radek et al., "Recognition of hyaluronan released in sterile injury involves a unique receptor complex dependent on toll-like receptor 4, CD44, and MD-2," *The Journal of Biological Chemistry*, vol. 282, no. 25, pp. 18265–18275, 2007.
- [48] J. Brinck and P. Heldin, "Expression of recombinant hyaluronan synthase (HAS) isoforms in CHO cells reduces cell migration and cell surface CD44," *Experimental Cell Research*, vol. 252, no. 2, pp. 342–351, 1999.
- [49] S. Albeiroti, K. Ayasoufi, D. R. Hill, B. Shen, and C. A. de la Motte, "Platelet hyaluronidase-2: an enzyme that translocates to the surface upon activation to function in extracellular matrix degradation," *Blood*, 2014.
- [50] A. Ghosh, H. Kuppasamy, and L. M. Pilarski, "Aberrant splice variants of HAS1 (hyaluronan synthase 1) multimerize with and modulate normally spliced HAS1 protein," *The Journal of Biological Chemistry*, vol. 284, no. 28, pp. 18840–18850, 2009.
- [51] E. Karousou, M. Kamiryo, S. S. Skandalis et al., "The activity of hyaluronan synthase 2 is regulated by dimerization and ubiquitination," *The Journal of Biological Chemistry*, vol. 285, no. 31, pp. 23647–23654, 2010.
- [52] I. Guerra and F. Bermejo, "Management of inflammatory bowel disease in poor responders to infliximab," *Clinical and Experimental Gastroenterology*, vol. 7, pp. 359–367, 2014.

- [53] Y. Sakurai, H. Hatakeyama, Y. Sato et al., "RNAi-mediated gene knockdown and anti-angiogenic therapy of RCCs using a cyclic RGD-modified liposomal-siRNA system," *Journal of Controlled Release*, vol. 173, no. 1, pp. 110–118, 2014.
- [54] Z. Huang, L. Dong, J. Chen et al., "Low-molecular weight chitosan/vascular endothelial growth factor short hairpin RNA for the treatment of hepatocellular carcinoma," *Life Sciences*, vol. 91, no. 23-24, pp. 1207–1215, 2012.

Research Article

Carboxymethyl Hyaluronan-Stabilized Nanoparticles for Anticancer Drug Delivery

Jessica L. Woodman,^{1,2} Min Sung Suh,³ Jianxing Zhang,⁴ Yuvabharath Kondaveeti,⁵
Diane J. Burgess,³ Bruce A. White,⁵ Glenn D. Prestwich,⁴ and Liisa T. Kuhn²

¹Department of Materials Science and Engineering, University of Connecticut, Storrs, CT 06269, USA

²Department of Reconstructive Sciences, UConn Health, Farmington, CT 06030, USA

³Department of Pharmaceutical Sciences, University of Connecticut, Storrs, CT 06269, USA

⁴Department of Medicinal Chemistry, University of Utah, Salt Lake City, UT 84108, USA

⁵Department of Cell Biology, UConn Health, Farmington, CT 06030, USA

Correspondence should be addressed to Glenn D. Prestwich; glenn.prestwich@pharm.utah.edu

Received 26 September 2014; Accepted 31 March 2015

Academic Editor: Rony Seger

Copyright © 2015 Jessica L. Woodman et al. This is an open access article distributed under the Creative Commons Attribution License, which permits unrestricted use, distribution, and reproduction in any medium, provided the original work is properly cited.

Carboxymethyl hyaluronic acid (CMHA) is a semisynthetic derivative of HA that is recognized by HA binding proteins but contains an additional carboxylic acid on some of the 6-hydroxyl groups of the N-acetyl glucosamine sugar units. These studies tested the ability of CMHA to stabilize the formation of calcium phosphate nanoparticles and evaluated their potential to target therapy resistant, CD44⁺/CD24^{-/low} human breast cancer cells (BT-474_{EMT}). CMHA stabilized particles (nCaP^{CMHA}) were loaded with the chemotherapy drug *cis*-diamminedichloroplatinum(II) (CDDP) to form nCaP^{CMHA}CDDP. nCaP^{CMHA}CDDP was determined to be poorly crystalline hydroxyapatite, 200 nm in diameter with a -43 mV zeta potential. nCaP^{CMHA}CDDP exhibited a two-day burst release of CDDP that tapered resulting in 86% release by 7 days. Surface plasmon resonance showed that nCaP^{CMHA}CDDP binds to CD44, but less effectively than CMHA or hyaluronan. nCaP^{CMHA-AF488} was taken up by CD44⁺/CD24⁻ BT-474_{EMT} breast cancer cells within 18 hours. nCaP^{CMHA}CDDP was as cytotoxic as free CDDP against the BT-474_{EMT} cells. Subcutaneous BT-474_{EMT} tumors were more reproducibly inhibited by a near tumor dose of 2.8 mg/kg CDDP than a 7 mg/kg dose nCaP^{CMHA}CDDP. This was likely due to a lack of distribution of nCaP^{CMHA}CDDP throughout the dense tumor tissue that limited drug diffusion.

1. Introduction

In the United States, over 1.6 million people were newly diagnosed with cancer in 2013 and 13.7 million people were battling cancer or were in remission [1]. Approximately 1 in 5 breast cancer survivors will have a recurrence within 10 years of adjuvant therapy [2]. While chemotherapies generally target rapidly dividing cells, relatively dormant cells exist within tumors which are resistant to chemotherapy [3–6]. Therapy-resistant breast cancer cells have a common phenotype of CD44⁺/CD24^{-/low}, in which CD44 is a transmembrane hyaluronan (HA) receptor. HA is a major glycosaminoglycan component of the extracellular matrix [7]. The expression of CD44 has been linked to cancer

progression via metastases and drug resistance [8]. The presence of CD44⁺ cells in patients with triple negative breast cancer (TNBC) is an indicator of poor outcomes and is linked with recurrence [9]. TNBC patients have limited treatment options, because their cancer does not present with hormone receptors that are effectively targeted for treatment [10]. These patients could greatly benefit from a localized high dose treatment that could reduce the tumor size prior to surgical resection, thereby reducing the incidence of recurrence. Two histological studies examining breast cancer patient tumor samples prior to and after primary systemic chemotherapy evidenced an increase in therapy-resistant CD44⁺/CD24^{-/low} cells after treatment [5, 11]. The objective of this work was to determine whether calcium phosphate nanoparticles

stabilized with a chemically modified HA could effectively target and kill therapy-resistant human TNBC cells with the CD44⁺/CD24^{low} phenotype.

Utilizing HA as a targeting moiety to deliver chemotherapeutics to cancer cells has been an ongoing area of research. One approach has been to chemically modify HA to allow attachment of carboxyl-containing drugs [12], and an HA-Paclitaxel prodrug bioconjugate has been prepared that showed selective toxicity against cancer cells overexpressing CD44 [13, 14]. Drug carrier systems modified with HA have been shown to enter the cell via CD44 mediated endocytosis [15]. Chen et al. showed mesoporous silica nanoparticles targeted with HA entered cells expressing CD44 [16]. In this study targeted calcium phosphate nanoparticles (nCaP) were synthesized as the drug carrier. Calcium phosphate is an excellent biomaterial because it is biocompatible, resorbable, and nonimmunogenic [17–19]. CaP synthesized via wet precipitation will form microcrystals, instead of nanoparticles, if crystallization and agglomeration are not halted with a stabilizer. Limiting crystal growth and agglomeration with a stabilizer is important to improve injectability of colloidal suspensions of CaP used for drug delivery. In the present studies, chemically modified HA was evaluated as a dual stabilizer/targeting ligand for nCaP. The chemically modified HA had additional carboxylate groups installed on a predetermined fraction of the N-acetylglucosamine units at the 6-hydroxyl group [20, 21]. Carboxylates interact with and stabilize calcium ions during precipitation of CaP [22]. The structure of the carboxymethyl hyaluronan (CMHA) used for these studies is shown in Figure 1.

It has been shown in our lab and others that stabilized nCaP can bind and release the chemotherapy drug *cis*-diamminedichloroplatinum (CDDP), a commonly used chemotherapeutic [23, 24]. CDDP is an effective anticancer drug but has dose limiting nephrotoxicity; thus, improved formulations with less toxicity are needed. We hypothesized that CMHA could be used to stabilize nCaP and simultaneously target CD44 expressing therapy resistant cells while delivering CDDP. The nCaP^{CMHA}CDDP was physically characterized using transmission electron microscopy (TEM), X-ray diffraction, particle size analysis, and *in vitro* drug release studies. The ability of CMHA and nCaP^{CMHA}CDDP to bind CD44 was examined using surface plasmon resonance. Cellular uptake was assessed using the CD44⁺ BT-474_{EMT} cells. Cytotoxicity of nCaP^{CMHA}CDDP and the impact of CMHA on cytotoxicity of Aq CDDP were examined *in vitro* against both CD44⁻ BT-474 and CD44⁺ BT-474_{EMT} cell types. Lastly, an *in vivo* antitumor efficacy study was performed in a model of human therapy resistant TNBC using BT-474_{EMT} cells to create tumors in immunodeficient mice.

2. Materials and Methods

2.1. Materials. Calcium lactate pentahydrate (Sigma C8356), K₂HPO₄ (Sigma S1804), Pt(NH₃)Cl₂ (CDDP, Sigma P4394), and AgNO₃ (Silver Nitrate, Sigma S6506) used to prepare the nanoparticles were all purchased from Sigma-Aldrich, (St. Louis, MO). Darvan 811 was purchased from R. T. Vanderbilt

Holding Company, Inc. (Norwalk, CT). CMHA and HA for these studies were prepared as previously described [20, 21]. Aqueated CDDP (Aq CDDP) that does not contain chloride ions is a net positive charged molecule that can bind to calcium phosphate nanoparticles and was prepared as described previously [23]. As a control, Aq CDDP was reacted with a solution of CMHA overnight to form an electrostatically bound conjugate and used to investigate the cytotoxicity of CDDP and CMHA without the calcium phosphate phase present.

BT-474 [25, 26] and BT-474_{EMT} cells were used for the cytotoxicity testing and *in vivo* tumor studies. BT-474_{EMT} were derived from human HER2-amplified epithelial BT-474 through serial mammosphere cultures over three weeks as previously described [27]. Serial mammosphere culture caused the BT-474 cells to undergo EMT and generated cells with a mesenchymal phenotype including enhanced proliferation rate, and cell surface marker expression of CD44⁺/CD24⁻ [28]. BT-474 cells were maintained in DMEM/F12 (Gibco 11330) with 10% FBS, 1% penicillin/streptomycin 10,000 U/mL (Gibco 15140), and 1% insulin (Gibco 41400). BT-474_{EMT} cells were maintained in DMEM/F12 (Gibco 11330) with 10% FBS, 1% penicillin/streptomycin 10,000 U/mL (Gibco 15140). BD Matrigel for cell injections was purchased from BD Biosciences (San Jose, CA).

J:Nu female mice were purchased from Jackson Laboratory (Bar Harbor, ME) and used for the *in vivo* tumor studies at 6–8 weeks of age. Female athymic nude mice, 6–8 weeks of age, were obtained from Charles River Laboratories International, Inc. (Wilmington, MA).

2.2. nCaP^{CMHA}CDDP Production and Physical Characterization. Synthesis of nCaP^{CMHA}CDDP was based on a previously reported method [23]. To make nCaP^{CMHA}, an equal volume of 30 mM K₂HPO₄ was added to stirred 30 mM calcium lactate and immediately followed by addition of 2% (w/v) CMHA (34 kDa) in water at 20% of the total volume of precipitation. Nanoparticles were collected after 10 min of mixing via centrifugation (12000 rpm for 45 min) and washed once with MilliQ water. The nCaP^{CMHA} was resuspended at a concentration of 4 mg particles per mL of binding solution made of 1:1 (v:v) 20 mM potassium phosphate buffer and 1 mg/mL Aq CDDP. After 20 hours of binding protected from light on a heated rocker (LAB-LINE thermorocker, Barnstead Thermolyne, Dubuque, IA) maintained at 37°C, the particles were collected via centrifugation, rinsed with 10 mM KPB, and diluted to approximately 175 mg nCaP^{CMHA}CDDP/mL MilliQ water. The suspension was injectable through a 25 gauge needle. All solutions/liquids during the synthesis process were sterile-filtered with a 0.2 μm filter in order to prepare a sterile product for cell culture and animal testing. The nCaP^{CMHA}CDDP suspension was stored at room temperature and shielded from light prior to use. Another type of nCaP stabilized with Darvan (nCaP^DCDDP) instead of CMHA was made for use as a control for bulk shift during surface plasmon resonance studies. nCaP^DCDDP was prepared as previously described [23] except that calcium

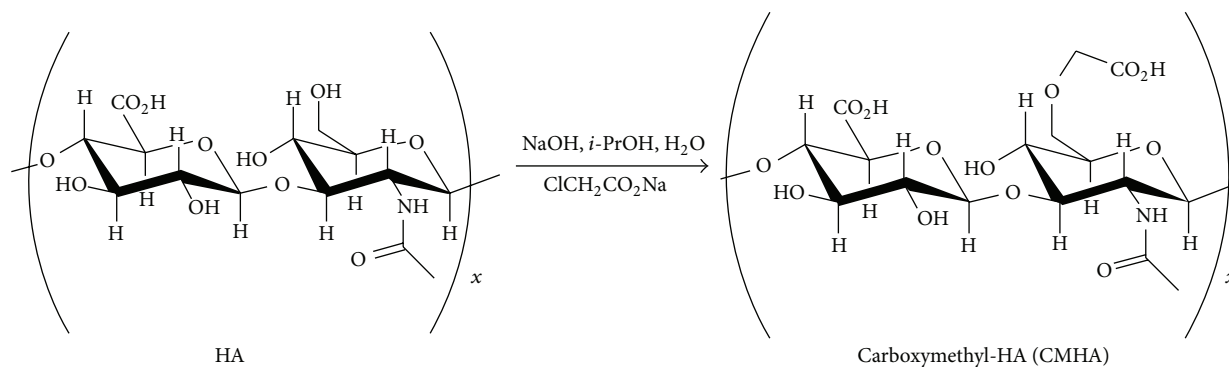


FIGURE 1: Chemical modification of hyaluronan (HA) to carboxymethyl hyaluronan (CMHA). HA was chemically modified to produce CMHA in a basic solution which modifies approximately 15–20% of the 6'-OH groups of the N-acetylglucosamine residues. This process reduces the molecular weight and introduces additional carboxyl groups for stabilization of nCaP.

lactate pentahydrate was used instead of $\text{Ca}(\text{NO}_3)_2 \cdot 4\text{H}_2\text{O}$, to match the calcium used in $\text{nCaP}^{\text{CMHA}}\text{CDDP}$.

The concentration of CDDP within the $\text{nCaP}^{\text{CMHA}}\text{CDDP}$ and $\text{nCaP}^{\text{D}}\text{CDDP}$ was determined by inductively coupled plasma-optical emission spectroscopy (ICP-OES) (Perkin Elmer Optima 5300 DV, ESIS Inc., Cromwell, CT) after dissolution of the particles in 1 N HCl. Particle size analysis (PSA) was performed via dynamic light scattering using a 90 Plus Particle Sizer (Brookhaven Instruments, NY). Samples were prepared by sonicating the particle suspension and diluting the suspension 12x in MilliQ water. The morphology and size of the particles were observed by using a Hitachi H-7650 transmission electron microscope (TEM). TEM samples were prepared by sonicating the particle suspension and diluting the suspension 26x in MilliQ water and then 10x in 70% ethanol prior to placing a $5\ \mu\text{L}$ sample on a formvar carbon coated 300 mesh Cu grid and blotting excess solution. Prior to imaging the sample was completely dried in air for 5 min. Samples were imaged at 80 kV with the TEM. X-ray diffraction (XRD) was used to determine changes in crystallinity with addition of stabilizer and to compare dry versus wet nCaP. Samples of lyophilized calcium phosphate without stabilizer (microCaP), lyophilized $\text{nCaP}^{\text{CMHA}}$, and wet $\text{nCaP}^{\text{CMHA}}$ were analyzed using a Bruker D2 Phaser.

2.3. $\text{nCaP}^{\text{CMHA}}\text{CDDP}$ In Vitro Drug Release. *In vitro* drug release studies were performed using a USP apparatus 4 (Sotax CE, Sotax, Horsham, PA) modified with a dialysis adapter with a molecular weight cut-off of 100 kD [29]. A sample of 0.4 mL of particle suspension was loaded into the dialysis adapter with $100\ \mu\text{L}$ release medium. Release medium was 10 mM PBS pH 7.4 with 0.1% sodium azide. A flow rate of 8 mL/min was used for the study with the cell temperature maintained at 37°C . Release samples were drawn at 1 h, 3 h, 5 h, 7 hr, 12 hr, 1 d, 2 d, 3 d, 4 d, 5 d, 6 d, 7 d, and 10 d. At each time point 5 mL of release solution was taken and replaced with 5 mL of fresh PBS. CDDP content in the release solution was determined by ICP-OES. Media replacement during the release study was considered in the calculation of cumulative release.

2.4. Surface Plasmon Resonance. Interaction of $\text{nCaP}^{\text{CMHA}}\text{CDDP}$, CMHA (~34 kDa), and HA (60 kDa) with CD44 were studied with surface plasmon resonance, BioRad ProteOn XPR36 with a GLC ProteOn sensor chip (BioRad, Hercules, CA). Recombinant human CD44-Fc chimera (~170 kDa) (R&D Systems, Minneapolis, MN) was immobilized on the sensor chip using amine coupling chemistry ProteOn Amine Coupling Kit. Briefly, the sensor chip surface was activated with 1:1 mixture of sulfo-N-hydroxysuccinimide (sulfo-NHS) and ethyl-3-(3-dimethylamino)propyl carbodiimide (EDC) for 7 min. CD44-Fc was dissolved in 10 mM acetate buffer pH 4 to a concentration of $5\ \mu\text{g}/\text{mL}$ and flown over the activated surface for 14 min. The remaining reactive groups were blocked with 1 M ethanolamine HCl pH 8.5. A blank flow channel (FC) was prepared by EDC/NHS activation without the CD44 receptor. Throughout all the SPR measurements PBS pH 7.4 supplemented with 0.005% Tween 20 was used as the running buffer. Samples were diluted with running buffer. CMHA and HA were diluted to concentrations of $1\ \mu\text{M}$ and $5\ \mu\text{M}$. $\text{nCaP}^{\text{X}}\text{CDDP}$ samples were diluted to a concentration of $350\ \mu\text{g}/\text{mL}$, which was found to be a good compromise between sufficient binding response and bulk refractive index shift. The samples were injected over the sensor chip surface coated with human CD44-Fc at $100\ \mu\text{L}/\text{min}$ for 150 s. The dissociation in the running buffer took place for another 600 s. After each measurement cycle the sensor chip surface was regenerated with 10 mM glycine HCl pH 2.0 at a flow rate of $200\ \mu\text{L}/\text{min}$. The responses on the blank flow cell were subtracted from the CD44-Fc coated flow cell.

2.5. Flow Cytometry. BT-474 and BT-474_{EMT} cells were analyzed for CD44 and CD24 expression using flow cytometry. Cells were washed once with phosphate-buffered saline (PBS) and then harvested with 0.05% trypsin/0.025% EDTA. Detached cells were washed with PBS that was supplemented with 0.2% (w/v) bovine serum albumin (BSA) (wash buffer) and resuspended in the wash buffer (10^6 cells/ $100\ \mu\text{L}$). Combinations of fluorochrome-conjugated monoclonal antibodies obtained from BioLegend (San Diego, CA) reactive against

human and mouse CD44 (Alexa Fluor 647) and BD Pharmingen (San Jose, CA) CD24 (PE-Cy7) or their respective isotype controls were added to the cell suspension at concentrations recommended by the manufacturer and incubated at 4°C in the dark for 30 to 40 min. The labeled cells were washed in the wash buffer and then analyzed on a MACSQuant Analyzer, MACS Miltenyi Biotec (Auburn, CA).

2.6. Cellular Uptake Studies. Fluorescently labeled nCaP^{CMHA-AF488} was made via the method described in Section 2.2, with minor modifications. Briefly, Alexa Fluor 488 labeled CMHA was incorporated into the CMHA solution at 6% the total volume of CMHA used in the precipitation. All other reaction steps to create nCaP^{CMHA} were performed the same way. BT-474_{EMT} cells were seeded at a density of 1×10^5 cells in an 8-well glass bottom plate and allowed to adhere for 24 hours after which nCaP^{CMHA-AF488} was added at the following concentrations: 200 µg/mL, 1 mg/mL, or 2 mg/mL in 500 µL complete media. After 2, 8, and 18 h after incubation, the glass slide chambers were washed 2x with PBS to remove any loose nanoparticles, and the cells were fixed 4% paraformaldehyde in PBS for 15 min. The fixed cells were washed with PBS 3x to remove the excess paraformaldehyde and then dried for 3 h. The fixed cells were stained and mounted with Prolong Gold antifade mounting media containing the nuclear stain 4',6-diamidino-2-phenylindole (DAPI) (Thermo Fisher Scientific, Waltham, MA). Microscopic analysis was performed using a Nikon AIR Spectral Confocal Microscope. Conditions of the confocal microscopic analysis were a Z-stack thickness of 11 µm, individual stack thickness of 0.35 µm, and an oil immersed 40x objective.

2.7. Cytotoxicity. Cytotoxicity experiments were conducted using BT-474 (CD44 positive) and BT-474_{EMT} (CD44 negative) cells plated in 96-well plates at 6×10^4 and 2×10^5 cells/mL, respectively, with 50 µL suspension per well. Two different seeding densities were used due to the very different growth rates of the cells during the cytotoxicity test. These cell types were selected to allow for the determination of cytotoxicity of nCaP^{CMHA}CDDP relative to CD44 expression and to elucidate if CMHA enhances cell uptake and consequently cytotoxicity. BT-474 cells are CD44 negative and were thus used as a negative control. Cells were allowed to proliferate for 24 hours and then the test samples were added in an additional 50 µL volume for a total of 100 µL per well. The following groups were examined: CDDP, Aq-CDDP, and CMHA reacted with Aq CDDP (Aq CDDP-CMHA), nCaP^{CMHA}CDDP, nCaP^{CMHA}, and CMHA. Each group was serially diluted 1:3 across the plate using PBS. Cells were assayed 48 h after drug addition using in an MTS assay (CellTiter 96 AQueous One, G3580, Promega Corp., Madison, WI), where metabolic activity was determined using a Spectramax Plus³⁸⁴ Spectrophotometer (Molecular Biosciences, Sunnyvale, CA) at an absorbance of 490 nm. To determine the IC₅₀ (50% inhibitory concentration) a nonlinear regression curve fit analysis was performed with

at least four replicates per group per concentration. All experiments shown were repeated two to three times.

2.8. BT-474_{EMT} Tumor Take Rate. To assess the growth parameters of BT-474_{EMT} tumors a tumor take rate study was performed in eight 6–8-week-old, immunocompromised athymic nude mice. Mice were given subcutaneous injections in the right rear flank via a 25-gauge needle of 5×10^5 cells in a 100 µL volume of BD Matrigel and base media (ratio of 60:40) based on the cell number utilized for a comparable transformed breast cancer cell type [30]. Animals were monitored at least every other day for normal grooming and appearance. Tumors were measured beginning at day 7 following inoculation. At this time point the Matrigel carrier has degraded allowing for a true cell-based tumor volume measurement.

2.9. nCaP^{CMHA}CDDP In Vivo Maximum Tolerable Dose Determination. Two J:Nu immunocompromised mice with established BT-474_{EMT} tumors were injected once intratumorally with 10 mg/kg nCaP^{CMHA}CDDP (80–90 µL per injection). A second study was conducted using athymic nude mice ($N = 4$), where a 7 mg/kg dose of nCaP^{CMHA}CDDP (60–70 µL) was administered once intratumorally. For both studies animals were monitored daily for weight loss and grooming and euthanized if weight loss met or exceeded 15%.

2.10. nCaP^{CMHA}CDDP In Vivo Antitumor Efficacy and Toxicity Study. An efficacy and toxicity study was performed using BT-474_{EMT} cells in J:Nu mice. The study included 24 6-week-old mice inoculated with 5×10^5 BT-474_{EMT} cells in 100 µL of a 60:40 ratio of BD Matrigel: cells in base media in the right rear flank via a 25-gauge needle. Tumors were measured daily 7 days following inoculation using digital calipers to calculate the tumor volume assuming an ellipsoid shape: $V = (W)^2 * L * 0.4$. Tumors were treated once with 2.8 mg/kg (60 µL) CDDP NT (8 mice), 60 µL of saline NT (4 mice), 60 µL of nCaP^{CMHA} NT (4 mice), or 7 mg/kg nCaP^{CMHA}CDDP NT (8 mice), when tumor volume reached $100 \pm 10 \text{ mm}^3$.

Systemic toxicity was evaluated by weight change and overall grooming/appearance. Tumor volume and mouse weight were monitored at least every other day. Mice were euthanized due to significant weight loss (>15%), a tumor length measurement greater than 2 cm, or completion of the study (day 30). At this time tumors were resected and weighed. All animal experimental procedures were approved by the Animal Care and Use Committee of the University of Connecticut Health Center (Farmington, CT).

2.11. Statistical Analysis. Statistical analysis was performed using an unpaired *t*-test (comparing two groups) or Tukey one-way ANOVA (comparing three or more test groups to a control group), as indicated in the methods. A *P* value of less than 0.05 was considered statistically significant. Data is presented as a mean value with its standard deviation indicated (mean ± SD).

TABLE 1: Average physical characteristics of nCaP^{CMHA}CDDP. Ratio of components, precipitation volume, and stabilizer final concentration remained the same from batch to batch. Yield, CDDP concentration, drug loading, particle size, polydispersity, and zeta potential represent averages and standard deviations from a minimum of three batches.

Physical characteristic	nCaP ^{CMHA} CDDP
Ca : P : Stabilizer (v : v : v)	2 : 2 : 1
Total precipitation volume (mL)	250
Stabilizer final concentration (mg/mL)	4
Yield (mg nCaP/mL precipitation)	2.3 ± 0.4
CDDP concentration (mg/mL)	4.1 ± 1.4
Drug loading (μg CDDP/mg nCaP)	140 ± 12
Particle size (nm)	204 ± 13 nm
Polydispersity	0.116
Zeta potential (mV)	-43 ± 4

3. Results and Discussion

The physical characteristics of nCaP^{CMHA}CDDP are shown in Table 1. Precipitation of nCaP^{CMHA} resulted in an efficient yield of 2.3 ± 0.4 mg per mL of precipitation solution. The CDDP concentration in the nCaP^{CMHA}CDDP suspension was 4.1 ± 1.4 mg/mL, with a drug loading of 140 ± 12 μg CDDP/mg nCaP^{CMHA}. nCaP^{CMHA}CDDP were on average 204 ± 13 nm in diameter as measured by dynamic light scattering with a polydispersity of 0.116. The zeta potential of the particles was -43 ± 4 mV, which is greater than the colloidal stability threshold of ±30 mV thereby providing evidence of enhanced stability due to surface charge prevention of aggregation [31]. XRD data showed nCaP^{CMHA} was poorly crystalline apatite based on the major peak occurring at 30° which corresponds well with hydroxyapatite. MicroCaP made without the CMHA stabilizer was more crystalline in nature resembling brushite and poorly crystalline hydroxyapatite (Figure 2(a)) [32, 33]. The introduction of CMHA clearly restricts the crystallization of CaP, as can be seen by the broad peaks of nCaP^{CMHA} XRD spectra relative to the spectra of microCaP which exhibited a crystalline pattern with major peaks of hydroxyapatite as well as brushite (calcium hydrogen phosphate dehydrate, CaHPO₄·2H₂O). Transmission electron microscopy (TEM) (Figure 2(b)) revealed that nCaP^{CMHA}CDDP in suspension forms small aggregates that correlate well with their measured particle size using DLS, 204 ± 13 nm. The addition of CMHA during precipitation of CaP resulted in successful stabilization of nCaP. TEM images revealed small 30–80 nm particles, agglomerated into larger particles, which likely accounts for the 200 nm size measured by DLS. These characteristics of the nCaP^{CMHA}CDDP resulted in a clog-free injectable nanoparticle suspension via a 25G needle.

To design an effective nanoparticle drug delivery system it is essential to optimize the physicochemical interactions of each component: the carrier, the drug, and any biological targeting moiety [34]. It was shown in previous work that sodium polyacrylate (Darvan 811, D) halts CaP crystal growth

[23]. This is due to the repeating carboxylate groups throughout the polymer. There is significant literature showing the carboxylate groups of sodium citrate (3 carboxylate groups per molecule) interact with the Ca ions during CaP precipitation acting as a surfactant to halt nucleation [22, 35–38]. Though these molecules effectively stabilize CaP, they have no biological targeting capacity. We therefore used a stabilizer that has biological targeting capability concurrent with nCaP stabilization. CMHA is a modified HA with additional carboxylate groups, thus allowing for more effective nCaP stabilization. CMHA at a degree of modification below 25% binds to HA binding proteins with comparable affinity and avidity as native HA. Importantly, cross-linked hydrogels based on thiolated CMHA improve wound healing in cutaneous and ophthalmic injuries [39], allow delivery of small molecules as well as growth factors and other macromolecules [40], and are safe and effective vehicles for cell delivery and retention [40]. Clinical products based on CMHA are in development for cell therapy [41]. Thus, CMHA was selected to enhance uptake of nCaP^{CMHA}CDDP by cells expressing CD44. After confirming that a stable calcium phosphate nanoparticle was achieved, we tested whether these nanoparticles could bind, release, and maintain biological efficacy of CDDP. The *in vitro* release of the nCaP^{CMHA}CDDP in PBS, pH 7.4, at 37°C over time can be seen in Figure 3. Under the rigorous, high speed and high volume release conditions nCaP^{CMHA}CDDP exhibited a burst release of 73% of the CDDP bound in two days which plateaued and reached a total of 86% after seven days.

Surface plasmon resonance (SPR) was performed to assess the interaction and binding of CMHA, nCaP^{CMHA}CDDP, and HA to CD44. Human CD44 chimera was immobilized on four channels of the sensor chip and two channels were amine coupled and blocked serving as a negative control for nonspecific binding. To correct for bulk shift due to the size of the nanoparticles, nCaP^DCDDP was examined as a control. As expected, HA most effectively bound to CD44 with CMHA approaching, but not equaling, the binding affinity of HA (Figure 4). nCaP^{CMHA}CDDP also binds CD44, but this binding is lower than free CMHA or HA. Importantly, this binding is specific as it overcomes any bulk interactions observed with nCaP^DCDDP. SPR analysis of targeted nanoparticles is challenging. SPR systems utilize complex microfluidics that normally transport solutions containing ligands or proteins of interest, but generally not solid materials such as nCaP. Of additional concern is the ability to correct for bulk shift due to the relatively large nanoparticles passing over the sensor. nCaP^DCDDP served as a comparably sized, nonspecific nanoparticle control. The density of the receptor (CD44) immobilized on the chip is inherently related to the response measured; therefore, we utilized a low density of CD44 on the chip surface [42]. The highest binding observed was for HA (60 kDa), followed by CMHA (34 kDa). The chemical modification of HA to create CMHA occurs at 15–20% of the repeating 6'-OH groups of the N-acetylglucosamine residues. The interaction of CD44 and HA has low affinity but high avidity. A single HA disaccharide contains an N-acetyl-D-glucosamine and

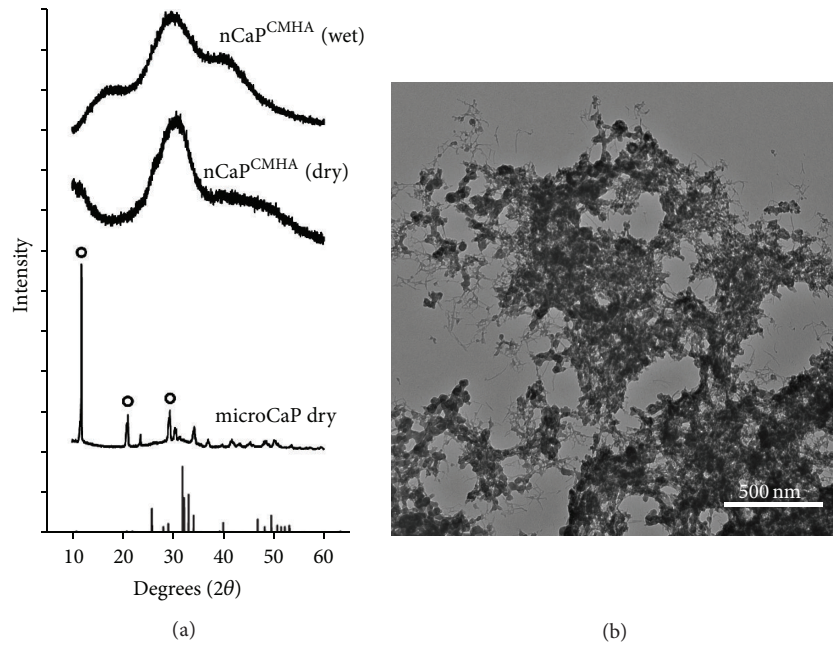


FIGURE 2: Physical characterization of $nCaP^{CMHA}$ using X-ray diffraction and transmission electron microscopy. (a) XRD spectra of $nCaP^{CMHA}$ suspension ($nCaP^{CMHA}$ wet), lyophilized $nCaP^{CMHA}$ ($nCaP^{CMHA}$ dry), and lyophilized CaP without stabilizer added during precipitation (microCaP dry). Hydroxyapatite standard (JCPDS, #09-0432, bars) is shown for comparison. $nCaP^{CMHA}$ both wet and dry has a major broad peak corresponding to the major peaks of hydroxyapatite. MicroCaP pattern has major peaks characteristic of brushite (peaks denoted by open circles). MicroCaP was precipitated without a stabilizer and has larger crystalline particles (narrow peaks). With the CMHA stabilizer present the crystallization is halted, depicted by broad peaks with little long range order. (b) TEM image of $nCaP^{CMHA}$ -CDDP showing particles 20–50 nm in diameter clustered into larger, 200 nm, particles due to drying prior to imaging.

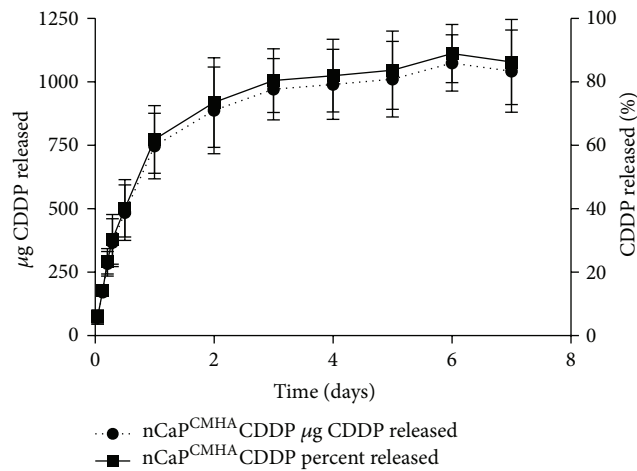


FIGURE 3: *In vitro* release testing of $nCaP^{CMHA}$ -CDDP using a modified USP Apparatus 4. Release was conducted in 10 mM PBS pH 7.4, 0.1% sodium azide at 37°C. The left axis is cumulative CDDP released with percent CDDP released on the right y-axis. The formulation provides sustained delivery of CDDP for 2 days under these infinite sink conditions. After 2 days $nCaP^{CMHA}$ -CDDP released 74% of the total CDDP bound. At day 7, $nCaP^{CMHA}$ -CDDP released an average of 86% of the total CDDP bound.

D-glucuronic acid, HA_2 . It has been shown that HA_6 is necessary for binding CD44, but HA_{10} is preferred [43]. Additionally, divalent binding occurs with HA_{20} and larger oligomers. This likely explains the slight reduction in binding of CMHA to CD44, due to an interruption of sugar residues by the added carboxylate groups of CMHA compared to HA.

Flow cytometry analysis confirmed BT-474 are 1.71% positive for both CD44 and CD24 and the majority of cells stained positively for CD24 alone, 98.3% (Figures 5(a)–5(c)). These cells were thus a good negative control for CD44 targeting. BT-474_{EMT} cells stained 99.7% positive for CD44 and negative for CD24, which corresponds well to

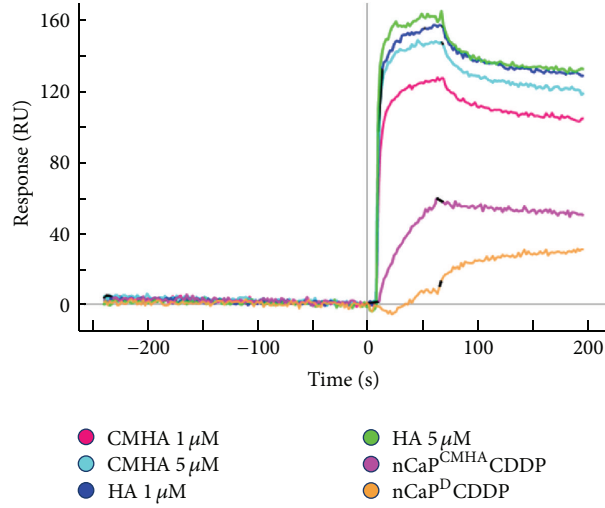


FIGURE 4: Surface plasmon resonance sensogram depicting binding of CMHA, HA, and nCaP^{CMHA}CDDP with immobilized CD44. All data shown has been corrected for nonspecific binding to blank channels of blocked NHS-EDC. nCaP^DCDDP was used as a comparable sized control, which does not have specific interactions with CD44. HA has the highest affinity for CD44, followed by CMHA then nCaP^{CMHA}CDDP.

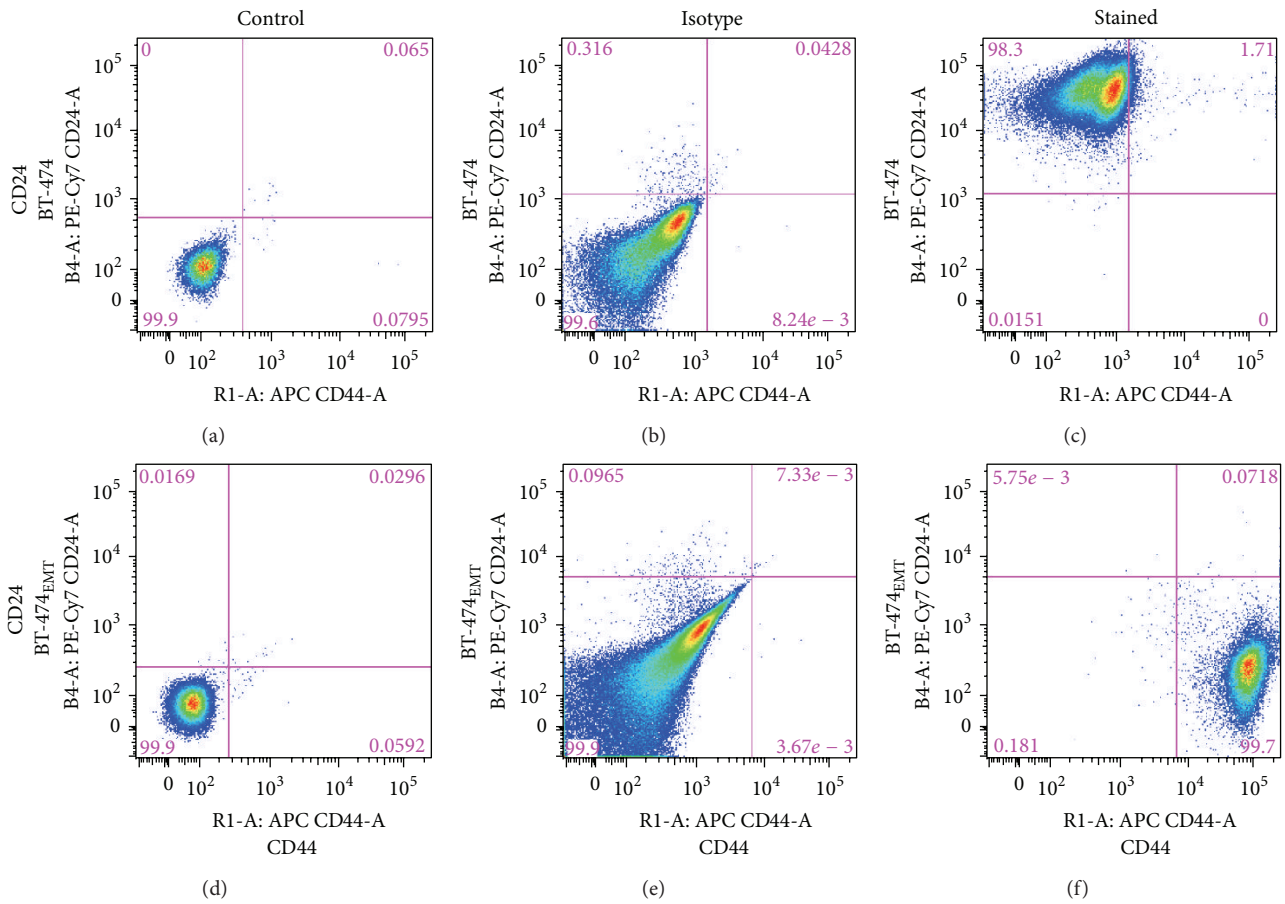


FIGURE 5: Flow cytometry data for the BT-474 and BT-474_{EMT} cells demonstrates appropriate CD44 expression for the studies. The numbers in the corner of each quadrant are the percentage of positive cells within the quadrant. (a) BT-474 unstained control, (b) BT-474 isotype control, (c) BT-474 stained cells with CD44, Alexa Fluor 647, and CD24, PE-Cy7. BT-474 cells are CD44^{low}/CD24^{high}. These cells served as the negative control for CD44 targeting, because they lack CD44 expression. (d) BT-474_{EMT} unstained control, (e) BT-474_{EMT} isotype control, (f) BT-474_{EMT} stained cells with CD44, Alexa Fluor 647, and CD24, PE-Cy7. BT-474_{EMT} cells are CD44⁺/CD24^{low}. These cells were tested to investigate CD44 targeting, as they have high CD44 expression.

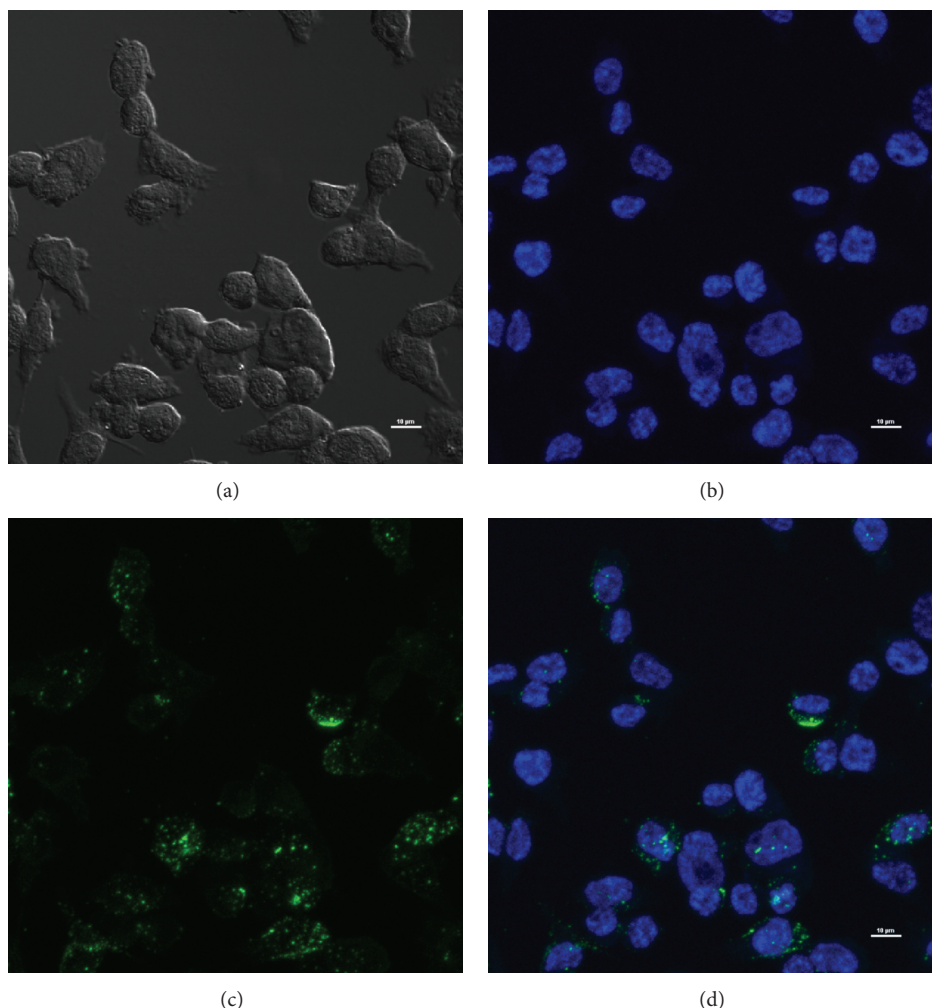


FIGURE 6: Cellular uptake study using BT-474_{EMT} cells. Cells were plated and allowed to adhere for 24 hours, after which nCaP^{CMHA-AF488} was added at a concentration of 2 mg/mL. After 18 hours, nCaP^{CMHA-AF488} can clearly be seen within cells as confirmed by Z-stack confocal images. (a) Differential interference contrast (DIC) image, (b) cells stained with DAPI, (c) cells imaged containing nCaP^{CMHA-AF488}, and (d) overlay of DAPI and AF488 images, showing nCaP^{CMHA-AF488} uptake.

the phenotype of therapy resistant breast cancer cells in the literature, CD44⁺/CD24^{low} (Figures 5(d)–5(f)) [11, 44]. BT-474_{EMT} cells were therefore used as the CD44⁺ test groups of cells to examine CD44 specificity with cellular uptake and cytotoxicity of nCaP^{CMHA-AF488}. In the cell uptake studies no significant uptake was determined for the 200 μg/mL or 1 mg/mL concentrations at any time tested (images not shown). At the 2 mg/mL dose, significant cellular uptake was determined at 18 hours posttreatment (Figures 6(a)–6(d)). Z-stack images were obtained, confirming the nCaP^{CMHA-AF488} was within the cell with nuclei counterstained with DAPI. This was a preliminary test of cellular uptake. These were insufficient to prove that nCaP^{CMHA-AF488} cellular uptake was mediated by CD44. To do so, at least two controls are necessary, a CD44⁻ cell type and a CD44⁺ cell type pretreated with HA to saturate the CD44 receptors [45] and should be included in future studies. SPR showed nCaP^{CMHA} CDDP had lower binding than CMHA, which is likely due to

two factors. Only 30% of the 4 mg/mL CMHA in the precipitation is incorporated into nCaP^{CMHA}. Additionally, nCaP^{CMHA} CDDP is stored as a suspension which allows the CaP to undergo Ostwald ripening incorporating much of the CMHA within the nCaP core [46, 47]. The exposure time required for cellular uptake of nCaP^{CMHA-AF488} was more than four times that of mesoporous silica nanoparticles targeted to CD44 via HA, where a 200 kDa HA was used [15].

The cytotoxicity of CMHA, nCaP^{CMHA}, CDDP, Aq CDDP, Aq CDDP-CMHA, and nCaP^{CMHA} CDDP was examined against BT-474 (CD44 negative) and BT-474_{EMT} (CD44 positive) cells. These studies confirmed that CMHA did not have any inherent toxicity to either cell type (Figure 7(a)). The CMHA stabilized nCaP^{CMHA} also had no cytotoxicity when tested at the concentrations which matched the amount of nCaP in the nCaP^{CMHA} CDDP test groups (Figure 7(b)). The IC₅₀ curves of CDDP, Aq CDDP, and Aq CDDP reacted with CMHA (Aq CDDP-CMHA), and nCaP^{CMHA} CDDP against

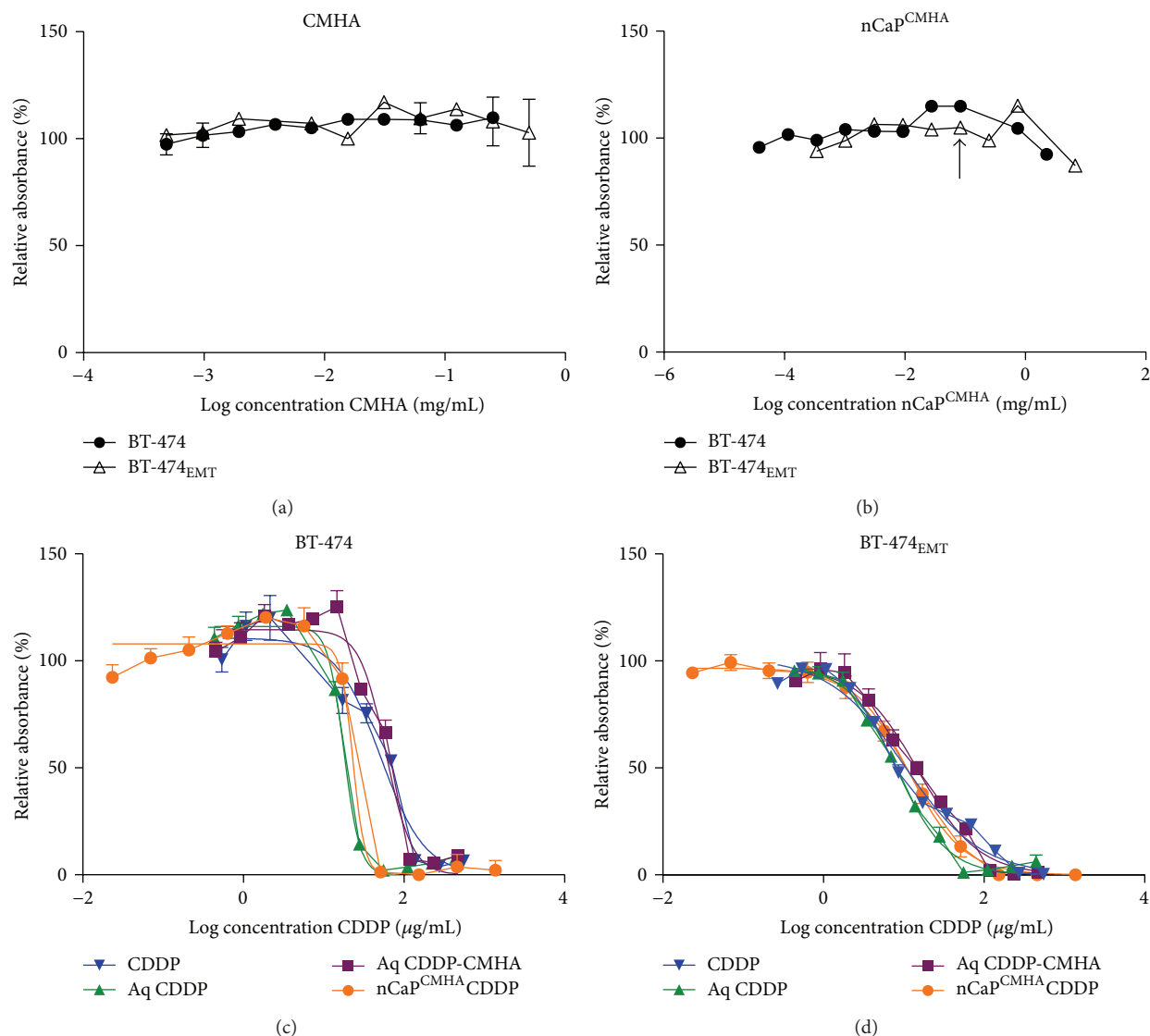


FIGURE 7: Cytotoxicity examination of CMHA, nCaP^{CMHA}, CDDP, Aq CDDP, Aq CDDP-CMHA and nCaP^{CMHA} CDDP evaluated against BT-474 and BT-474_{EMT} cells using an MTS assay. (a) Evaluation of CMHA alone against BT-474 and BT-474_{EMT} cells, showing no cytotoxicity. (b) Evaluation of nCaP^{CMHA} alone against BT-474 and BT-474_{EMT} cells, showing no cytotoxicity. (c) Cytotoxicity evaluation using BT-474 (CD44⁺) cells. CDDP, Aq CDDP, and Aq CDDP reacted with CMHA (Aq CDDP-CMHA), and nCaP^{CMHA} CDDP curves are plotted. (d) Cytotoxicity evaluation using BT-474_{EMT} (CD44⁻) cells. CDDP, Aq CDDP, and Aq CDDP reacted with CMHA (Aq CDDP-CMHA), and nCaP^{CMHA} CDDP curves are plotted.

BT-474 cells are shown in Figure 7(c). The IC₅₀ curves of CDDP, Aq CDDP, and Aq CDDP reacted with CMHA (Aq CDDP-CMHA), and nCaP^{CMHA} CDDP against BT-474_{EMT} cells are shown in Figure 7(d). The IC₅₀ values calculated from these curve fits are shown in Table 2. nCaP^{CMHA} CDDP and Aq CDDP were significantly more cytotoxic than CDDP alone against BT-474 cells and Aq CDDP-CMHA was significantly less cytotoxic ($P \leq 0.001$). nCaP^{CMHA} CDDP had comparable cytotoxicity to CDDP against BT-474_{EMT} cells. Aq CDDP-CMHA was significantly less cytotoxic ($P \leq 0.001$) and Aq CDDP was significantly more cytotoxic ($P \leq 0.05$) for BT-474_{EMT} cells.

Interestingly, nCaP^{CMHA} CDDP did not show preferential cytotoxicity to cells with high CD44 expression (BT-474_{EMT}) compared to those with negative CD44 expression (BT-474), or compared to CDDP alone. It was hypothesized nCaP^{CMHA} CDDP would target cells with high CD44 expression causing increased cytotoxicity. In related studies, mesoporous silica nanoparticles targeted with HA and carrying doxorubicin were significantly more cytotoxic than doxorubicin alone against CD44 expressing cells but were significantly less cytotoxic to CD44 negative cells [16]. Similarly, an HA Taxol prodrug was more cytotoxic than free Taxol against cells expressing CD44 and had limited to no

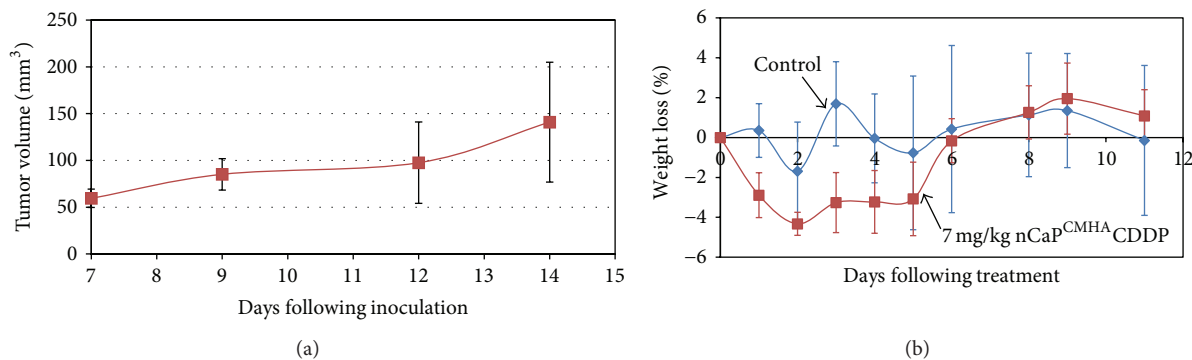


FIGURE 8: *In vivo* tumor take rate and maximum tolerable dose studies. (a) Tumor take rate study performed in athymic nude mice with 5×10^5 BT-474_{EMT} cells injected subcutaneously in right rear flank of animals. Data represents average tumor volume versus days following inoculation with standard deviations. (b) Maximum tolerable dose study conducted with athymic nude mice (6–8 weeks old) carrying BT-474_{EMT} tumors. An intratumoral 7 mg/kg dose of nCaP^{CMHA}CDDP (4 mice/group) was compared to an untreated control (4 mice/group). nCaP^{CMHA}CDDP caused minimal weight loss at 7 mg/kg and all animals recovered.

TABLE 2: Tabulated IC₅₀ values of CDDP, Aq CDDP, Aq CDDP-CMHA, and nCaP^{CMHA}CDDP examined with BT-474 and BT-474_{EMT} cells, from curves shown in Figures 7(a) and 7(b), respectively. For BT-474 cells Aq CDDP and nCaP^{CMHA}CDDP were both significantly more effective than CDDP alone and Aq CDDP-CMHA was significantly less effective than CDDP. For BT-474_{EMT} cells nCaP^{CMHA}CDDP was as cytotoxic as CDDP alone and Aq CDDP was significantly more effective while Aq CDDP-CMHA was significantly less effective.

Cell type	IC ₅₀ (μg/mL)			
	CDDP	Aq CDDP	Aq CDDP-CMHA	nCaP ^{CMHA} CDDP
BT-474	50.6 ± 3.3	17.1 ± 0.9 ^c	59.0 ± 2.7 ^c	23.1 ± 3.9 ^c
BT-474 _{EMT}	10.5 ± 1.1	8.78 ± 0.6 ^a	16.24 ± 1.5 ^c	12.1 ± 1.4

^a $P \leq 0.05$.

^c $P \leq 0.001$.

cytotoxicity against cells that did not express CD44 [13, 14]. These studies demonstrate a specific CD44 mediated uptake in the HA containing particles that allowed the drug to release intracellularly, where cells lacking CD44 did not take up the prodrug. Possible reasons for the opposite findings in our studies are as follows. While nCaP^{CMHA} was taken up by BT-474_{EMT} cells, the uptake was relatively slow compared to other HA nanoparticle formulations which were taken up after 4 hours of exposure [15, 16]. The SPR data implies that the HA presentation after adsorption to the CaP was not optimal. The future use of CMHA with greater spacing between the carboxylate groups may overcome this. Additionally it was expected that the BT-474_{EMT} cells would be chemotherapy resistant and would require a carrier to enhance effectiveness of CDDP, since comparable mesenchymal-derived MCF-7 cells were resistant to other chemotherapies (docetaxel and tamoxifen) [11, 30]. However, the cytotoxicity data shows that BT-474_{EMT} cells are sensitive to CDDP as compared to BT-474 cells without CD44. The major adducts caused by CDDP are 1,2-intrastrand cross-links that interfere with DNA replication and transcription resulting in cell death during G2 phase prior to mitosis [48]. Unexpectedly the nCaP^{CMHA}CDDP was more cytotoxic than CDDP alone against the BT-474 cells without CD44. The controlled release of CDDP from nCaP^{CMHA}CDDP allowed for prolonged

delivery of drug to the slower replicating BT-474 cells, which could explain the enhanced cytotoxicity of nCaP^{CMHA}CDDP over CDDP alone.

Importantly, the nCaP^{CMHA}CDDP had equivalent cytotoxicity to CDDP *in vitro* which means nCaP^{CMHA} had no negative impact on the biological activity of CDDP and thus these particles were suitable candidates for evaluation in an *in vivo* tumor model. The *in vivo* tumor forming capability of BT-474_{EMT} cells had not been previously studied; therefore, their ability to form tumors was first examined in a tumor take rate study. BT-474_{EMT} tumors formed after cell injections were 50 mm³ on average after 7 days. After approximately 12 days tumors were 100 mm³ (Figure 8(a)). Animals were monitored for 25 days following inoculation where tumors continued to grow steadily up to 500 mm³ without necrosis. The comparable mesenchymal-derived human MCF-7 human BC cells were also tested under the same conditions in an *in vivo* tumor model and were found to have similar growth rates as the BT-474_{EMT} with volumes reaching 500 ± 100 mm³ at 20 days following inoculation [30]. These studies confirmed that this new human breast cancer tumor model BT-474_{EMT} was not too fast growing and did not develop necrotic tumors.

A maximum tolerable dose (MTD) study was conducted in mice bearing BT-474_{EMT} tumors. Based on a small pilot

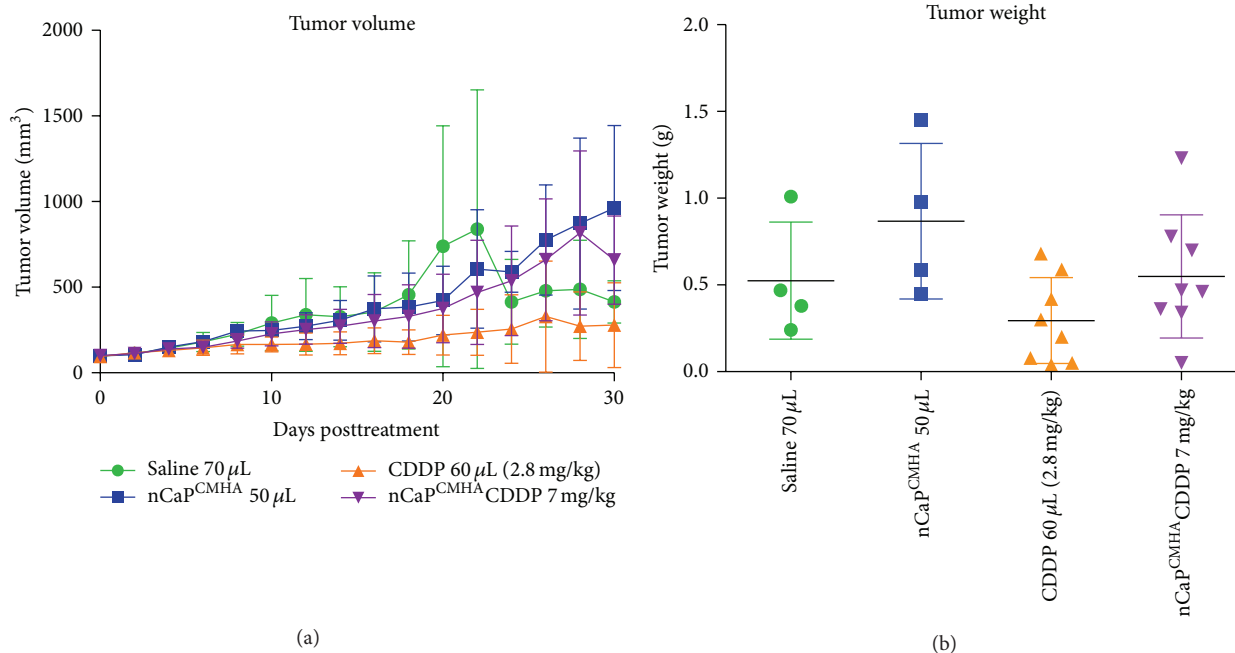


FIGURE 9: Efficacy study of nCaP^{CMHA}CDDP conducted on J:Nu mice bearing BT-474_{EMT} tumors. Animals were treated once when their tumor volume reached $100 \pm 10 \text{ mm}^3$ and were compared to 2.8 mg/kg CDDP administered near the tumor. Tumor volume, grooming, and weight loss were monitored every other day following treatment. (a) The graph depicts average tumor volume (mm^3) per group versus days posttreatment. The negative control saline IT ($70 \mu\text{L}$) had no effect on tumor growth. nCaP^{CMHA} ($60 \mu\text{L}$) had no effect on tumor growth. CDDP at 2.8 mg/kg administered near the tumor delayed tumor growth. (b) Tumor weight at the end of the study or at time of euthanasia for the efficacy study shown in (a). Tumors were resected and weighed. Animals were euthanized if tumor diameter was measured $> 2 \text{ cm}$ or at the completion of the study (day 30). No significant differences were found between groups.

study showing excessive weight loss in at least one mouse mice treated with 10 mg/kg nCaP^{CMHA}CDDP, mice were given 7 mg/kg nCaP^{CMHA}CDDP ($60\text{--}70 \mu\text{L}$) intratumorally into tumors with an average tumor volume of 170 mm^3 , 14 days following cell inoculation. The results are shown in Figure 8(b), where the maximum weight loss was 5% occurring at two to five days following treatment. This is an acceptable weight loss during treatment with chemotherapeutics; therefore, this dose was deemed tolerable and used for the antitumor studies.

To assess the antitumor efficacy of the nCaP^{CMHA}CDDP, tumors were treated once by direct injection near the tumor with one of the following treatments: 2.8 mg/kg ($60 \mu\text{L}$) CDDP (8 mice), $60 \mu\text{L}$ of saline (4 mice), $60 \mu\text{L}$ of nCaP^{CMHA} (4 mice), or 7 mg/kg nCaP^{CMHA}CDDP (8 mice), when tumor volume reached $100 \pm 10 \text{ mm}^3$. No significant differences in tumor volume or weights were found among groups (Figure 9(a)), even the positive control (CDDP only). No animal experienced weight loss greater than 2% at these doses (data not shown). At the time of euthanasia, tumors were resected and weighed to compare to volumetric measurements. The resulting tumor weights were plotted relative to treatment (Figure 9(b)). No significant differences were found between groups when analyzed according to tumor weight. No treatment caused toxicity to the animals as measured by weight loss and overall grooming/appearance.

Survival over time posttreatment was evaluated for each group (Figure 10). Mice were not actually allowed to die due to the treatments or tumor growth; instead they were euthanized if the tumors reached a tumor length measurement greater than 20 mm. In this slow growing model half of the untreated animals still had small tumors at the end point of the study making it difficult to observe large changes in tumor size due to treatment. Large standard deviations of tumor volume in the untreated group (as well as treatment group) were another problem obscuring differences between groups. In our studies with the FaDu (human head and neck squamous cell carcinoma) tumor model, it was necessary to use a larger number of cells (2×10^6 cells) to achieve reproducible growth rather than 5×10^5 cells (which was used in these studies with the BT-474_{EMT}). If a higher number of BT-474_{EMT} cells were injected, limited variability in tumor volume might have occurred enabling a more discriminating evaluation of the test groups.

At the time of resection, depots of nCaP^{CMHA}CDDP of a similar size to that injected were observed adjacent to the tumor on one or both sides indicating the nCaP was not resorbed or degraded over one month of implantation. Visual observations of the placement of the material allowed us to make a correlation between treatment placement and efficacy. The nCaP^{CMHA}CDDP had the greatest antitumor effect when it was evenly distributed around the tumor. The lack of an

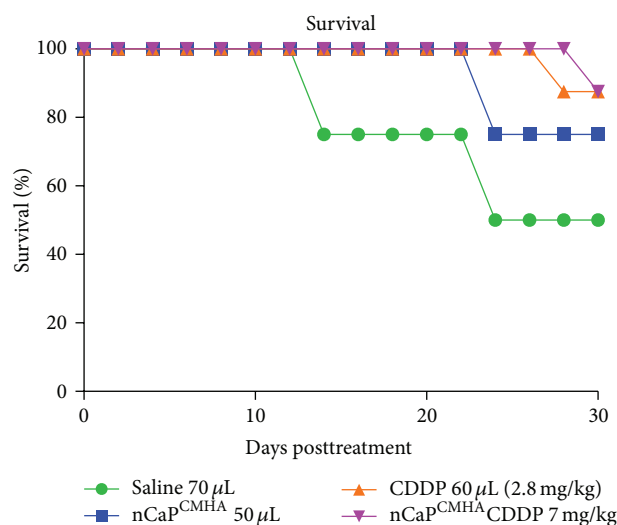


FIGURE 10: Survival was plotted for the efficacy study shown in Figure 9. The study was conducted on J:Nu mice bearing BT-474_{EMT} tumors. Animals were treated once when their tumor volume reached $100 \pm 10 \text{ mm}^3$ and compared to 2.8 mg/kg CDDP administered near tumor (NT). Tumor volume, grooming, and weight loss were monitored every other day following treatment. Survival was defined as a tumor diameter $> 2 \text{ cm}$ or inability to groom. A treatment of 7 mg/kg nCaP^{CMHA}CDDP and 2.8 mg/kg CDDP (NT) was most effective at prolonging survival compared to control treatments of saline or nCaP^{CMHA} (NT).

even distribution nCaP^{CMHA}CDDP may have contributed to the lack of antitumor efficacy observed in these animals. nCaP^{CMHA}CDDP did not freely diffuse throughout the tumor due to the density of the tumor, and therefore only the areas of the tumor proximal to the nCaP^{CMHA}CDDP depot were exposed to the CDDP. It is likely that the ability of free CDDP to diffuse throughout the tumor caused the more reproducible tumor growth inhibition observed in the CDDP alone group. Intravenous administration of the nanoparticles may allow for greater penetration of the treatment into the tumor interior with an associated increased antitumor effect. A recently published clinical trial shows that neoadjuvant CDDP intravenous treatment was effective for patients with TNBC, though this treatment has not yet been adopted clinically [49]. Therefore, continued investigations on CDDP delivery systems are warranted for TNBC.

4. Conclusions

CMHA is a novel and effective stabilizer for nCaP that can bind to CD44 receptors for potential targeting applications. Importantly, it was determined that CMHA has no negative impact on the biological activity of CDDP *in vitro*, against human breast cancer cells. nCaP^{CMHA}CDDP allowed for efficient release of CDDP. nCaP^{CMHA}CDDP had equivalent cytotoxicity to CDDP alone against CD44⁺ cells and was more cytotoxic for CD44⁻ cells. Tumors are very heterogeneous in cell surface expression and therefore cytotoxicity to both CD44⁺ and CD44⁻ cells is important *in vivo*. In

future studies, an intravenous dose of nCaP^{CMHA}CDDP at the maximum tolerable dose with optimized cell uptake and tumor infiltration should be examined *in vivo* to evaluate the targeting of therapy resistant CD44⁺ cells by chemically modified HA.

Conflict of Interests

The authors declare that there is no conflict of interests regarding the publication of this paper.

Acknowledgments

The authors would like to acknowledge financial support from the University of Connecticut's 2012 UCHC/Storrs and Regional Campus Incentive Grant (UCIG) to Drs. Diane J. Burgess and Liisa T. Kuhn.

References

- [1] American Cancer Society, *Cancer Facts & Figures*, American Cancer Society, Atlanta, Ga, USA, 2013.
- [2] A. M. Brewster, G. N. Hortobagyi, K. R. Broglio et al., "Residual risk of breast cancer recurrence 5 years after adjuvant therapy," *Journal of the National Cancer Institute*, vol. 100, no. 16, pp. 1179–1183, 2008.
- [3] M. D. Curley, L. A. Garrett, J. O. Schorge, R. Foster, and B. R. Rueda, "Evidence for cancer stem cells contributing to the pathogenesis of ovarian cancer," *Frontiers in Bioscience*, vol. 16, no. 1, pp. 368–392, 2011.
- [4] K. D. Steffensen, A. B. Alvero, Y. Yang et al., "Prevalence of epithelial ovarian cancer stem cells correlates with recurrence in early-stage ovarian cancer," *Journal of Oncology*, vol. 2011, Article ID 620523, 12 pages, 2011.
- [5] H. E. Lee, J. H. Kim, Y. J. Kim et al., "An increase in cancer stem cell population after primary systemic therapy is a poor prognostic factor in breast cancer," *British Journal of Cancer*, vol. 104, no. 11, pp. 1730–1738, 2011.
- [6] A. B. Alvero, R. Chen, H.-H. Fu et al., "Molecular phenotyping of human ovarian cancer stem cells unravel the mechanisms for repair and chemo-resistance," *Cell Cycle*, vol. 8, no. 1, pp. 158–166, 2009.
- [7] Y. Luo and G. D. Prestwich, "Synthesis and selective cytotoxicity of a hyaluronic acid-antitumor bioconjugate," *Bioconjugate Chemistry*, vol. 10, no. 5, pp. 755–763, 1999.
- [8] K. E. Miletti-González, S. Chen, N. Muthukumaran et al., "The CD44 receptor interacts with P-glycoprotein to promote cell migration and invasion in cancer," *Cancer Research*, vol. 65, no. 15, pp. 6660–6667, 2005.
- [9] A. Giatromanolaki, E. Sivridis, A. Fiska, and M. I. Koukourakis, "The CD44+/CD24- phenotype relates to 'triple-negative' state and unfavorable prognosis in breast cancer patients," *Medical Oncology*, vol. 28, no. 3, pp. 745–752, 2011.
- [10] H. van Epps, "Triple-negative breast cancer: divide and conquer," *CURE Magazine*, 2013.
- [11] X. Li, M. T. Lewis, J. Huang et al., "Intrinsic resistance of tumorigenic breast cancer cells to chemotherapy," *Journal of the National Cancer Institute*, vol. 100, no. 9, pp. 672–679, 2008.
- [12] T. Pouyani and G. D. Prestwich, "Functionalized derivatives of hyaluronic acid oligosaccharides: drug carriers and novel

- biomaterials," *Bioconjugate Chemistry*, vol. 5, no. 4, pp. 339–347, 1994.
- [13] Y. Luo, M. R. Ziebell, and G. D. Prestwich, "A hyaluronic acid-taxol antitumor bioconjugate targeted to cancer cells," *Biomacromolecules*, vol. 1, no. 2, pp. 208–218, 2000.
- [14] Y. Luo and G. D. Prestwich, "Synthesis and selective cytotoxicity of a hyaluronic acid–antitumor bioconjugate," *Bioconjugate Chemistry*, vol. 10, no. 5, pp. 755–763, 1999.
- [15] M. Yu, S. Jambhrunkar, P. Thorn, J. Chen, W. Gu, and C. Yu, "Hyaluronic acid modified mesoporous silica nanoparticles for targeted drug delivery to CD44-overexpressing cancer cells," *Nanoscale*, vol. 5, no. 1, pp. 178–183, 2013.
- [16] Z. Chen, Z. Li, Y. Lin, M. Yin, J. Ren, and X. Qu, "Biomimetic mineralization inspired surface engineering of nanocarriers for pH-responsive, targeted drug delivery," *Biomaterials*, vol. 34, no. 4, pp. 1364–1371, 2013.
- [17] M. Banik and T. Basu, "Calcium phosphate nanoparticles: a study of their synthesis, characterization and mode of interaction with salmon testis DNA," *Dalton Transactions*, vol. 43, no. 8, pp. 3244–3259, 2014.
- [18] R. Detsch, D. Hagemeyer, M. Neumann et al., "The resorption of nanocrystalline calcium phosphates by osteoclast-like cells," *Acta Biomaterialia*, vol. 6, no. 8, pp. 3223–3233, 2010.
- [19] V. Sokolova, O. Rotan, J. Klesing et al., "Calcium phosphate nanoparticles as versatile carrier for small and large molecules across cell membranes," *Journal of Nanoparticle Research*, vol. 14, article 910, 2012.
- [20] J. L. Vanderhoof, M. Alcoutlabi, J. J. Magda, and G. D. Prestwich, "Rheological properties of cross-linked hyaluronan-gelatin hydrogels for tissue engineering," *Macromolecular Bioscience*, vol. 9, no. 1, pp. 20–28, 2009.
- [21] X. Z. Shu, Y. Liu, and G. D. Prestwich, "Modified macromolecules and methods of making and using thereof," 7, 981, 2011.
- [22] W. Jiang, H. Pan, Y. Cai et al., "Atomic force microscopy reveals hydroxyapatite-citrate interfacial structure at the atomic level," *Langmuir*, vol. 24, no. 21, pp. 12446–12451, 2008.
- [23] X. Cheng and L. Kuhn, "Chemotherapy drug delivery from calcium phosphate nanoparticles," *International Journal of Nanomedicine*, vol. 2, no. 4, pp. 667–674, 2007.
- [24] B. Palazzo, M. Iafisco, M. Laforgia et al., "Biomimetic hydroxyapatite-drug nanocrystals as potential bone substitutes with antitumor drug delivery properties," *Advanced Functional Materials*, vol. 17, no. 13, pp. 2180–2188, 2007.
- [25] M. Murohashi, K. Hinohara, M. Kuroda et al., "Gene set enrichment analysis provides insight into novel signalling pathways in breast cancer stem cells," *British Journal of Cancer*, vol. 102, no. 1, pp. 206–212, 2010.
- [26] C. Sheridan, H. Kishimoto, R. K. Fuchs et al., "CD44⁺/CD24⁻ breast cancer cells exhibit enhanced invasive properties: an early step necessary for metastasis," *Breast Cancer Research*, vol. 8, no. 5, article R59, 2006.
- [27] G. Dontu, W. M. Abdallah, J. M. Foley et al., "In vitro propagation and transcriptional profiling of human mammary stem/progenitor cells," *Genes and Development*, vol. 17, no. 10, pp. 1253–1270, 2003.
- [28] Y. Kondaveeti, I. K. Reed, and B. A. White, "Epithelial-mesenchymal transition induces similar metabolic alterations in two independent breast cancer cell lines," *Cancer Letter*, vol. 364, no. 1, pp. 44–58, 2015.
- [29] U. Bhardwaj and D. J. Burgess, "A novel USP apparatus 4 based release testing method for dispersed systems," *International Journal of Pharmaceutics*, vol. 388, no. 1–2, pp. 287–294, 2010.
- [30] I. K. Guttilla, K. N. Phoenix, X. Hong, J. S. Tirnauer, K. P. Claffey, and B. A. White, "Prolonged mammosphere culture of MCF-7 cells induces an EMT and repression of the estrogen receptor by microRNAs," *Breast Cancer Research and Treatment*, vol. 132, no. 1, pp. 75–85, 2012.
- [31] R. Singh and J. W. Lillard Jr., "Nanoparticle-based targeted drug delivery," *Experimental and Molecular Pathology*, vol. 86, no. 3, pp. 215–223, 2009.
- [32] C. Andres, V. Sinani, D. Lee, Y. Gun'ko, and N. Kotov, "Anisotropic calcium phosphate nanoparticles coated with 2-carboxyethylphosphonic acid," *Journal of Materials Chemistry*, vol. 16, no. 40, pp. 3964–3968, 2006.
- [33] A. Dosen and R. F. Giese, "Thermal decomposition of brushite, CaHPO₄·2H₂O to monetite CaHPO₄ and the formation of an amorphous phase," *American Mineralogist*, vol. 96, no. 2–3, pp. 368–373, 2011.
- [34] P. Grodzinski and D. Farrell, "Future opportunities in cancer nanotechnology—NCI strategic workshop report," *Cancer Research*, vol. 74, no. 5, pp. 1307–1310, 2014.
- [35] J. L. Giocondi, B. S. El-Dasher, G. H. Nancollas, and C. A. Orme, "Molecular mechanisms of crystallization impacting calcium phosphate cements," *Philosophical Transactions of the Royal Society A: Mathematical, Physical and Engineering Sciences*, vol. 368, no. 1917, pp. 1937–1961, 2010.
- [36] Y.-Y. Hu, A. Rawal, and K. Schmidt-Rohr, "Strongly bound citrate stabilizes the apatite nanocrystals in bone," *Proceedings of the National Academy of Sciences of the United States of America*, vol. 107, no. 52, pp. 22425–22429, 2010.
- [37] M. A. Martins, C. Santos, M. M. Almeida, and M. E. V. Costa, "Hydroxyapatite micro- and nanoparticles: nucleation and growth mechanisms in the presence of citrate species," *Journal of Colloid and Interface Science*, vol. 318, no. 2, pp. 210–216, 2008.
- [38] K. Bleek and A. Taubert, "New developments in polymer-controlled, bioinspired calcium phosphate mineralization from aqueous solution," *Acta Biomaterialia*, vol. 9, no. 5, pp. 6283–6321, 2013.
- [39] G. D. Prestwich, "Clinical biomaterials for scar-free healing and localized delivery of cells and growth factors," *Advances in Wound Care*, vol. 1, pp. 394–399, 2010.
- [40] G. D. Prestwich, "Hyaluronic acid-based clinical biomaterials derived for cell and molecule delivery in regenerative medicine," *Journal of Controlled Release*, vol. 155, no. 2, pp. 193–199, 2011.
- [41] G. D. Prestwich, I. E. Erickson, T. I. Zarebinski, M. West, and W. P. Tew, "The translational imperative: making cell therapy simple and effective," *Acta Biomaterialia*, vol. 8, no. 12, pp. 4200–4207, 2012.
- [42] C. Tassa, J. L. Duffner, T. A. Lewis et al., "Binding affinity and kinetic analysis of targeted small molecule-modified nanoparticles," *Bioconjugate Chemistry*, vol. 21, no. 1, pp. 14–19, 2010.
- [43] J. Lesley, V. C. Hascall, M. Tammi, and R. Hyman, "Hyaluronan binding by cell surface CD44," *The Journal of Biological Chemistry*, vol. 275, no. 35, pp. 26967–26975, 2000.
- [44] M. Al-Hajj, M. S. Wicha, A. Benito-Hernandez, S. J. Morrison, and M. F. Clarke, "Prospective identification of tumorigenic breast cancer cells," *Proceedings of the National Academy of Sciences of the United States of America*, vol. 100, no. 7, pp. 3983–3988, 2003.

- [45] H. S. S. Qhattal and X. Liu, "Characterization of CD44-mediated cancer cell uptake and intracellular distribution of hyaluronan-grafted liposomes," *Molecular Pharmaceutics*, vol. 8, no. 4, pp. 1233–1246, 2011.
- [46] S. Kumar, X. Xu, R. Gokhale, and D. J. Burgess, "Formulation parameters of crystalline nanosuspensions on spray drying processing: a DoE approach," *International Journal of Pharmaceutics*, vol. 464, no. 1-2, pp. 34–45, 2014.
- [47] V. Sokolova and M. Epple, "Inorganic nanoparticles as carriers of nucleic acids into cells," *Angewandte Chemie—International Edition*, vol. 47, no. 8, pp. 1382–1395, 2008.
- [48] E. R. Jamieson and S. J. Lippard, "Structure, recognition, and processing of cisplatin-DNA adducts," *Chemical Reviews*, vol. 99, no. 9, pp. 2467–2498, 1999.
- [49] D. P. Silver, A. L. Richardson, A. C. Eklund et al., "Efficacy of neoadjuvant cisplatin in triple-negative breast cancer," *Journal of Clinical Oncology*, vol. 28, no. 7, pp. 1145–1153, 2010.

Review Article

Utilization of Glycosaminoglycans/Proteoglycans as Carriers for Targeted Therapy Delivery

Suniti Misra,¹ Vincent C. Hascall,² Ilia Atanelishvili,³
Ricardo Moreno Rodriguez,¹ Roger R. Markwald,¹ and Shibnath Ghatak¹

¹Department of Regenerative Medicine and Cell Biology, Medical University of South Carolina, Charleston, SC 29425, USA

²Department of Biomedical Engineering/ND20, Cleveland Clinic, Cleveland, OH, USA

³Division of Rheumatology & Immunology, Department of Medicine, Medical University of South Carolina, 114 Doughty Street, Charleston, SC 29425, USA

Correspondence should be addressed to Suniti Misra; misra@musc.edu and Shibnath Ghatak; ghatak@musc.edu

Received 20 September 2014; Revised 19 January 2015; Accepted 15 February 2015

Academic Editor: Pavel Hozak

Copyright © 2015 Suniti Misra et al. This is an open access article distributed under the Creative Commons Attribution License, which permits unrestricted use, distribution, and reproduction in any medium, provided the original work is properly cited.

The outcome of patients with cancer has improved significantly in the past decade with the incorporation of drugs targeting cell surface adhesive receptors, receptor tyrosine kinases, and modulation of several molecules of extracellular matrices (ECMs), the complex composite of collagens, glycoproteins, proteoglycans, and glycosaminoglycans that dictates tissue architecture. Cancer tissue invasive processes progress by various oncogenic strategies, including interfering with ECM molecules and their interactions with invasive cells. In this review, we describe how the ECM components, proteoglycans and glycosaminoglycans, influence tumor cell signaling. In particular this review describes how the glycosaminoglycan hyaluronan (HA) and its major receptor CD44 impact invasive behavior of tumor cells, and provides useful insight when designing new therapeutic strategies in the treatment of cancer.

1. Introduction

During development, wound healing, and malignancies, normal cells and cancer cells often have to traffic through extracellular matrices (ECMs). ECMs form the microenvironment around cells and are composed of a dynamic and complex assortment of collagens, glycoproteins, glycosaminoglycans, and proteoglycans. Many cells can only migrate and grow in cultures when they are attached to surfaces through ECM. Some studies have reported that cancer cells can only traffic through the ECM via the proteolytic cleavage of structural barriers in ECM, while other studies have also indicated that neoplastic cells can traverse the ECM without mobilizing proteases [1, 2]. Thus, the ECMs produced by epithelial cells and stromal cells provide much more than just mechanical and structural support and are involved in the regulation of cell morphology, metabolism, differentiation, and survival.

Proteoglycans (PGs) (Figures 1 and 2) are proteins with a variable number of glycosaminoglycan (GAG) side

chains [3]. The three classes of PGs with GAG chains and core proteins are (i) chondroitin/dermatan sulfate (CS/DS) PGs; (ii) heparin/heparan sulfate (Hep/HS) PGs; and (iii) keratan sulfate (KS) PGs [4, 5]. Hyaluronan (HA), a GAG, is synthesized without a core protein [6]. As indicated by their names (Figures 1 and 2), the GAGs other than HA are sulfated. GAGs have a critical role in assembling protein-protein complexes such as growth factor-receptor or enzyme-inhibitor interactions on the cell surface and in the extracellular matrix. These interactions can transduce signals by formation of ternary complexes of ligand, receptor, and PG for initiating cell signaling events or inhibiting biochemical pathways (Figure 3). Thus, GAGs can potentially sequester proteins and enzymes and present them to the appropriate site for activation. For a given high-affinity GAG-protein interaction, the positioning of the protein binding oligosaccharide motifs along the GAG chain determines if an active signaling complex is assembled at the cell surface or an inactive complex is sequestered in the matrix [7–9].

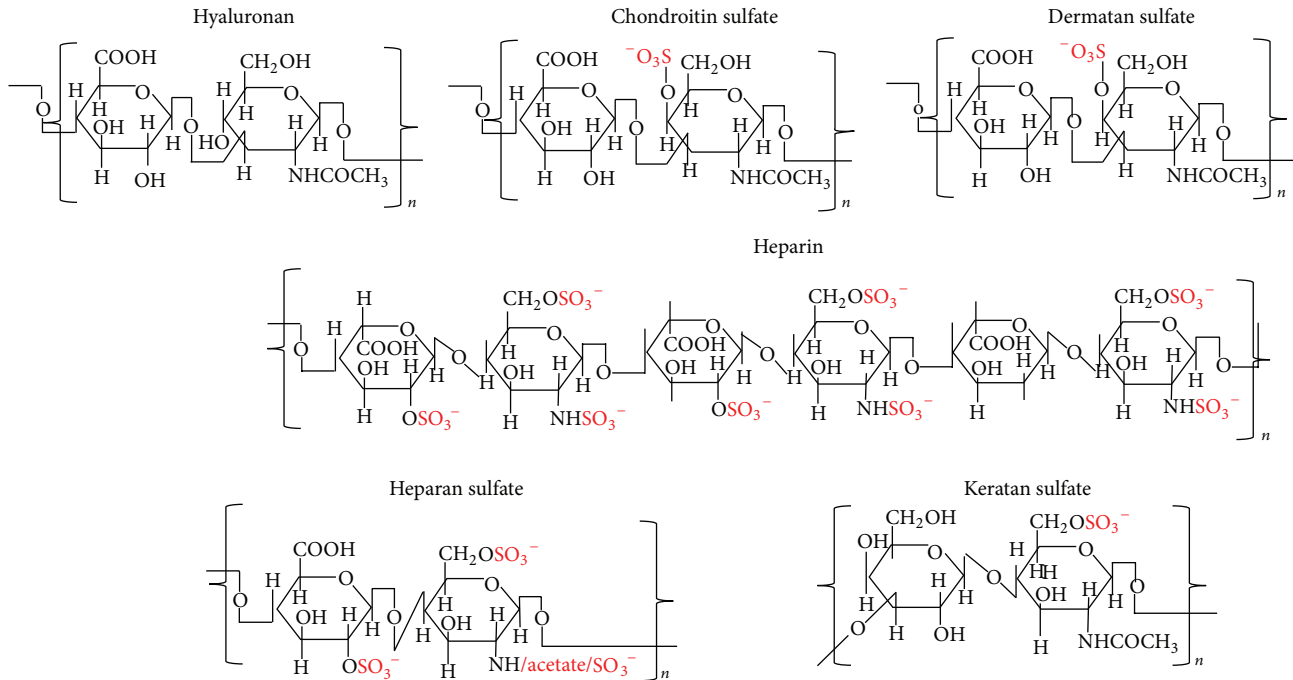


FIGURE 1: Structures of repeating disaccharides of glycosaminoglycans.

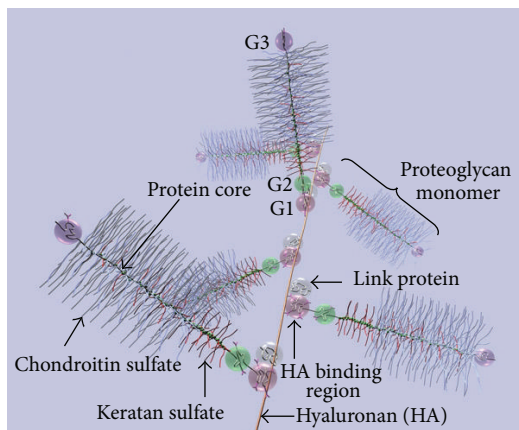


FIGURE 2: Diagram of part of an aggrecan aggregate. G1, G2, and G3 are globular, folded regions of the central core protein. Proteoglycan aggregate showing the noncovalent binding of proteoglycan to HA with the link proteins.

Overexpression of HA synthase 2 (HAS2) increases receptor tyrosine kinase-dependent signaling in breast and colon cancer cells [10–13], whereas antisense-mediated suppression of HAS2 inhibits tumorigenesis and progression of breast and prostate cancers [14, 15]. PGs and GAGs can have various physiological functions in different organs as well as roles in various pathologies. The details of these properties of GAGs and PGs are beyond the scope of this chapter. The present chapter will review the works that describe the utilization of GAGs in delivery of molecules for therapeutic purposes and highlights new possibilities for modulating HA interactions

with CD44 variants (CD44v) for therapeutic control of cancer.

2. Biology of Hyaluronan and Its Receptor CD44

2.1. Biology of HA. HA is a major component in the ECM of most mammalian tissues, and HA accumulates in sites of cell division and rapid matrix remodeling that occurs during embryonic morphogenesis, inflammation, and tumorigenesis [16–19]. HA is found in pericellular matrices attached to HA-synthesizing enzymes or its receptors and is also present in intracellular degradation compartments [18–25]. HA is omnipresent in the human body and in all vertebrates, occurring in almost all biological fluids and tissues, with the highest amounts in the vitreous of the eye, synovial fluids, and the ECM of soft connective tissues. HA has repeat disaccharides consisting of D-glucuronic acid and N-acetyl glucosamine (Figure 1) [26–28]. Native HA has a very high molar mass, usually in the order of millions of Daltons (10^5 to 10^7 Da) before being progressively degraded into smaller fragments during its catabolism and eventual lysosomal degradation [27, 29, 30]. It possesses interesting viscoelastic properties based on its polymeric and polyelectrolyte characteristics. The amount present in tissues depends on its synthesis by synthases [31], degradation by hyaluronidases [32], and clearance through lymphatics (by LYVE-1 receptors) [33] and liver (by HARE receptors) [34]. Multivalent interaction of HA with CD44 collaborates in driving numerous tumor-promoting signaling pathways and transporter activities [35]. HA regulates proliferation and motility through CD44 and

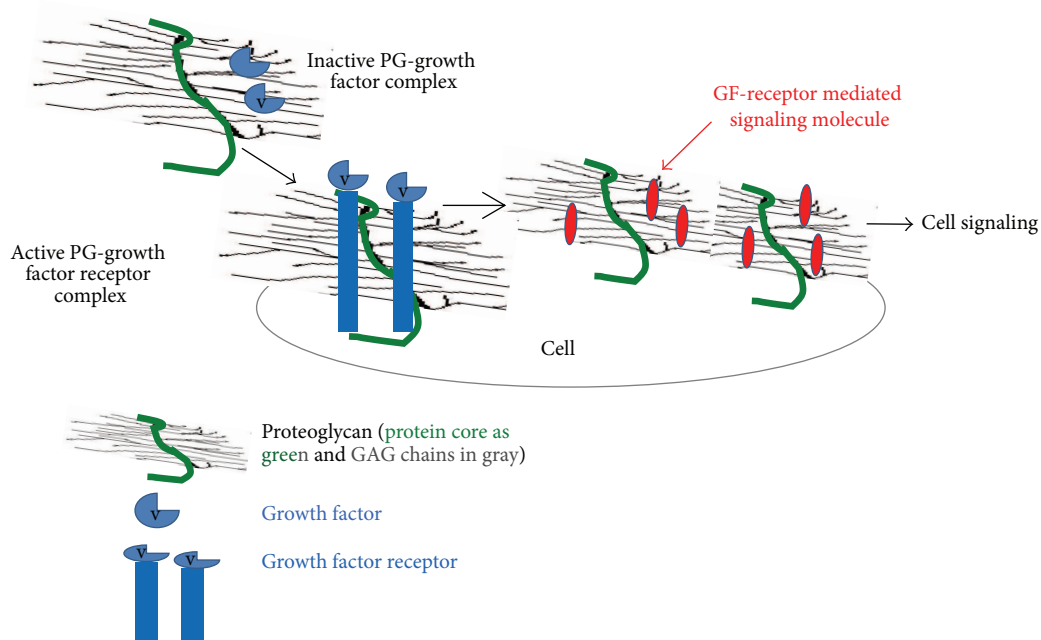


FIGURE 3: Proteoglycans act as coreceptors for growth factor receptor (GFR) signaling, thus influencing cell signaling and cell behavior. GAGs present as a part of proteoglycans on the cell surface and in ECM, bind to numerous proteins, and modulate their function.

RHAMM (Receptor for HA Mediated Motility) [36], whereas the binding of HA to Intercellular Adhesion Molecule 1 (ICAM-1) may contribute to the control of ICAM-1-mediated inflammatory activation [37]. Despite its simple structure, HA is an extraordinarily versatile GAG and is involved in several key processes, including early EMT in development and morphogenesis, cell signaling, wound repair and regeneration, matrix organization, and many inflammatory pathologies [10, 13, 18, 19, 21–25, 38–47]. During carcinogenesis, changes in both nonnative CD44v (splice variants) and native (standard) CD44s arise [48]. Downstream signals of HA-CD44v interactions have been found to promote tumorigenesis, cancer cell migration, and metastasis [46, 47, 49]. Thus, various strategies are evolving for treatments of cancer that focus on HA and CD44, including interference with the HA-CD44v signaling, by either targeting drugs to CD44v [50], targeting drugs to the HA matrix [51], or interfering with HA-CD44v interactions [52].

2.2. HA Metabolism. Increased HA synthase (HAS) activity can contribute to tumor growth. 4-Methylumbelliferone (4-MU) has been widely investigated as a HAS inhibitor and has been shown to inhibit growth and motility and to induce apoptosis of several cancer cell lines. *In vivo*, 4-MU reduces tumor microvessel density [53], suppresses development of distant metastasis [54], and sensitizes human pancreatic cancer cells to the cytotoxic drug gemcitabine [55]. Although 4-MU may serve as an interesting anticancer approach in various cancers [53–55], no clinical trials have been conducted to use it as an anticancer activity because it is not patentable.

HA-degrading enzymes, hyaluronidases (HYALs), show both cancer-promoting and suppressing properties. In several clinical trials, the addition of bovine HYAL in therapeutic protocols resulted in slowing the growth of tumors [56, 57]. However, further studies have been abandoned due to induction of inflammation or pain in the joints because of enhanced HYAL activity in normal tissues [58].

The major concentrations of HA are found within the skin and musculoskeletal system, which account for 50% of total body HA. In these tissues, the rate of HA turnover is rapid ($t_{1/2} \sim 0.5$ d) by comparison with other extracellular matrix components [29]. Surprisingly, most degradation does not occur within the skin itself; rather HA is transported through the lymphatic system to distant lymph nodes where 90% of the HA in lymph is degraded or reenters the circulation to be rapidly endocytosed by liver endothelial HA receptors [59, 60]. Hence, lymph nodes are a major outlet for HA transport from tissues such as the skin and intestine, where they extract and metabolize as much as 10% of the total body HA content within a 24 h period [61–63] through the afferent lymph pathways where its larger polymers are more rapidly removed. This turnover can be further increased after either tissue injury or sepsis. The HA from lymph nodes enters the circulation resulting in a half-life of less than 1 minute (in rats) [64] and is distributed into the liver [65], where liver endothelium is a site of uptake and degradation of HA. The role and fate of HA have been widely investigated; however, effects of size and dose of HA on its metabolism have not been well documented yet. Similarly, enhanced accumulation of the matrix HA in the cortical renal interstitium is linked to the proinflammatory events in the kidney. It has been shown that HA-synthase and hyaluronidase genes are constitutively

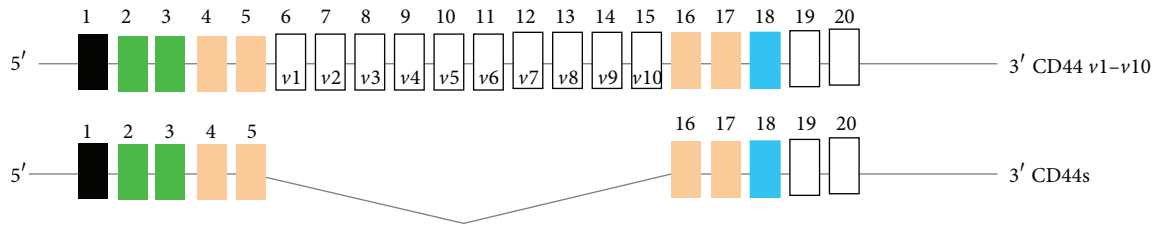


FIGURE 4: Alternative splicing in CD44 pre-mRNA. CD44 pre-mRNA is encoded by 20 exons. The common CD44s (hematopoietic) form contains no extra exons, and the protein may have a serine motif encoded in exon 5 that initiates synthesis of a chondroitin sulfate or dermatan sulfate chain. Alternative splicing of CD44 predominantly involves variable insertion of 10 extra exons with combinations of exons 6–15 and spliced in $v1$ – $v10$ into the stem region, of which $v3$ encodes a substitution site for a heparan sulfate chain. Variable numbers of the v exons can be spliced in epithelial cells, endothelial cells, and inflammatory monocytes and also upregulated commonly on neoplastic transformation depending on the tissue.

expressed in renal cells suggesting that HA synthesis as well as HA degradation occurs in these cells [66, 67]. In interstitial nephritis sites where HA is increased, HA receptor CD44 is expressed in high levels suggesting *in vivo* interaction of HA and CD44 [68, 69].

2.3. Biology of CD44. To understand the role of the HA receptor CD44 in modifying malignant properties, it is essential to recognize its structures. Due to paucity of studies regarding involvement of CD44 variants in tumor angiogenesis and cancer stem cells, we discuss its functions in tumor cells in general and how cell-specific perturbation of HA-CD44v interaction can be used to inhibit cancer growth. CD44 (Figure 4) is a transmembrane protein encoded by a single gene. Due to alternative splicing, multiple forms of CD44v are generated that are further modified by N- and O-linked glycosylations. The smallest CD44 isoform that lacks variant exons, designated CD44s, contains an N-terminal signal sequence (exon 1), a link module that binds to HA (exons 2 and 3), a stem region (exons 4, 5, 16, and 17), a single-pass transmembrane domain (exon 18), and a cytoplasmic domain (exon 20). In all forms of CD44 cDNAs, exon 19 is spliced out so that the transmembrane domain encoded by exon 18 is followed by the cytoplasmic domain encoded by exon 20, producing the 73 amino acid cytoplasmic domain. CD44s can be a proteoglycan with a potential CS or DS substitution. Insertion of the $v3$ exon includes the potential for HS chain substitution [70], which can influence ligand binding and cell behavior by allowing CD44 to be a coreceptor for HGF with *c-met* [71]. The affinity of CD44 for these GAG substitutions depends on posttranslational modifications, such as modification in glycosylation [72] during alternate splicing of variant exons, and this function depends on cell type and growth condition. Isoforms that contain a variable number of exon insertions ($v1$ – $v10$) at the proximal plasma membrane external region are expressed primarily on tumor cells [43, 70, 73].

Decades of research have shown that CD44 participates in major oncogenic signaling networks and in complexes with oncogenes that promote every aspect of tumor progression [18, 70]. Conversely, CD44 is extremely sensitive to changes in the microenvironment, and its reaction to changing

extra- and intracellular conditions is still the subject of active research. For example, it was found that, in breast cancer cells, CD44 may act as a metastatic suppressor gene when it is influenced by reactive oxygen species (ROS), as seen by decreased CD44 protein expression in the Alpha5 cell line in a compensatory response to increased MnSOD protein expression [74]. Many of the contradictory findings published to date may be due to experimental and technical differences among studies; however, a picture has emerged suggesting that CD44 may function differently at different stages of cancer progression [75, 76]. For example, mice with germline disruptions of CD44 display relatively mild phenotypes compared with mice in which tissue-specific CD44 function is disrupted at adult phases of development or in later phases. This suggests that the absence of CD44 in early development and a loss of CD44 function late in development are tolerated differently [70].

3. Targeted Drug Delivery

Drug delivery can be localized, oral, or systemic by various carriers. Drug delivery systems that combine the benefits of various approaches will be made to address the needs of specific applications. Oral drug delivery is the easiest and a convenient route for drug administration. However, anticancer drugs, docetaxel and doxorubicin, and insulin in diabetes cannot be delivered orally because of their low oral bioavailability for various reasons. Nanoscale drug-delivery systems improve drug release kinetics, regulate biodistribution, and minimize toxic side effects, which enhances the therapeutic index. Nanoparticle diameters ranging from 70 nm to 200 nm demonstrate the most prolonged circulation times [77], minimizing the risk of recognition by the reticuloendothelial system as well as clearance by the liver and the spleen [78, 79].

GAGs are utilized in nanoscale drug delivery systems or in other formats, to deliver cargo, systemically or locally, loaded with drugs or biologics for therapeutic purposes to treat a variety of disease conditions, including cancer, glaucoma, wound healing, and burn. For wound healing and burn injury, the drugs are delivered by direct application of GAGs in conjunction with drugs. Ophthalmic drugs are

also delivered locally. Systemically administered therapeutic molecules for cancer treatment enter into blood vessels of the tumors, pass the vessel wall, move through the ECM, avoid getting cleared by the lymphatics, and finally migrate through the interstitium barrier [80]. In reality, the case is not so simple. Use of intravital microscopy has revealed the complex anatomical barriers involved and has provided functional insights of their properties. These barriers can be abnormal, change with space and time, and depend on host-tumor interactions [81, 82]. The GAG carrier should have bioadhesive preference to tumor vasculature rather than to normal vasculature. Thus, the main focus of the delivery will be in the tumor vasculature. How will the drug penetrate the barrier that shields the tumor from the delivery? How can the surrounding blood vessels be targeted? How will the drug differentiate cancer cells from normal cells? How can the drug efflux following entry into cancer cells be avoided? Solutions of these and other questions are discussed below.

4. GAGs/PGs in Drug Delivery

4.1. Heparin/Heparan Sulfate in Drug Delivery. Heparin is primarily used as a blood anticoagulant due to its binding to the serine threonine protease antithrombin causing the inhibitor to inactivate thrombin [83]. Heparin was chosen as a carrier of Amphotericin B in heparin coated nanoparticles [84]. However, its use was discontinued because of its rapid clearance from blood due to heparin binding to hepatic liver sinusoids. Heparin still attracts attention due to its antiangiogenic and anticancer activities in addition to its activities on anticoagulation, deep vein thrombosis, and pulmonary embolism. Heparin is not absorbed orally because of its high molecular weight, negative charge, and hydrophilicity and therefore cannot be used in oral drug delivery [85]. By conjugating heparin with hydrophobic bile taurocholic acid (TCA), oral bioavailability of heparin was increased. For example, less water soluble docetaxel (DTX) was made orally available through conjugation with heparin and TCA, and as a result, excellent bioavailability of DTX increased [86]. In fact the conjugate is absorbed in the ileum by a bile acid transporter as well as by passive diffusion [87].

The high negative charge density of heparin has been exploited to form nanoparticles based on electrostatic interactions. Due to affinity for growth factors, heparin can potentially be a good carrier for these growth factors. Heparin nanoparticles were noncovalently assembled via electrostatic interactions between low-molecular-weight heparin (LMW-Hep) and *N,N,N*-trimethyl chitosan chloride (TMC). Vascular endothelial growth factor (VEGF) was entrapped in these LMW-Hep/TMC nanoparticles by affinity interactions with LMW-Hep. Controlled zero order release of VEGF from these nanoparticles was observed over a period of 14 days, and a total cumulative release was about 49% [88]. Heparin-Chitosan/c-PGA nanoparticles were prepared for multifunctional delivery of heparin and bFGF in ischemic tissues [89]. In addition to the physical incorporation of heparin into nanomaterials, heparin-decorated HA-based hydrogel particles were also prepared with consistent release of growth factors and bioactive HA molecules [90].

The HA was first modified with heparin and then formed into spherical nanoparticles that were used as vehicles for growth factor delivery in hydrogel matrices. For example, packing a covalently linked perlecan that contains HS chains with HA microgels was used as an injectable therapeutic agent to release BMP2 to repair cartilage matrix by intra-articular injection in a reversible animal model of osteoarthritis. The results show that a knee treated with the microgel had less damage than a control knee. The microgels act as a depot of BMP2, which is slowly released in the affected joint [91].

Depending on the type of HS-PG, the number of GAG chains varies from 1 to 100 attached to protein cores ranging from 10 to 500 kDa [92–94]. HS-PGs act as cell-surface endocytosis receptors [95]. The two major families of HS-PGs are the transmembrane syndecans and the GPI-anchored glypicans [7]. Recently, it was reported that syndecan-4, a ubiquitous transmembrane PG [96] present on the cell surface, binds and mediates the transport of a cationic cell penetrating peptide (CPP; 17 amino acids) into the cells [97]. CPP is a universal carrier that crosses the plasma membrane carrying drugs that include peptides, oligonucleotides, siRNAs, and liposomes [98–103]. The penetrating peptide can carry cargoes many times larger than its own size. Thus, application of CPPs appears to be encouraged in drug targeting and delivery, although the mechanism of translocation is largely unknown. Glypican 1 expression is upregulated in pancreatic cancer cells and surrounding fibroblasts, and the mitogenic response of pancreatic cancer cells to bFGF and HB-epidermal growth factor is abrogated by antisense attenuation of this HS-PG [104]. Similarly, perlecan expression is upregulated at sites of active angiogenesis, and the angiogenic effects of bFGF are suppressed by experimental downregulation of perlecan [105]. The HS-PGs found in the ECM (perlecan, aggrecan, and collagen XVIII) are large modular proteins that contribute to the structure, hydration, and permeability of the ECM. The capacity of HS-PGs to interact with both the matrix architecture and soluble ligands defines a unique combination of properties that enables normal cells to sense and respond to controlling influences in their environment. Cancer cells employ various mechanisms to exploit these properties to gain a survival advantage. Grubb et al. [106] used the high capacity uptake function mediated by HS-PGs to investigate if a lysosomal enzyme, beta-glucuronidase, could be taken up and transported to the lysosome as a possible way to treat lysosomal storage diseases. In these diseases, undigested GAGs collect progressively in lysosomes due to mutations that inactivate various enzymes required for complete degradation of GAGs, which leads to lysosomal dysfunction and manifestation of diseases associated with aging or other pathologies [107].

4.2. Chondroitin/Dermatan Sulfate in Drug Delivery. Use of biodegradable and nontoxic biomaterials from natural polymers has been explored to prepare materials for drug encapsulation and controlled delivery into tumors. Chondroitin sulfates have good biocompatibility and are primarily located on PGs in ECMs in tissues such as cartilage, skin, corneas, and umbilical cords. While circulating in the body during drug

delivery, the hydrodynamic and hydrophilic properties of CS prevent undesirable interactions with plasma proteins and cells. Anaerobic bacteria, *Bacteroides thetaiotaomicron* and *Bacteroides ovatus*, which are residents of the large intestine, degrade CS. This suggests that CS can be a good candidate as a drug delivery agent to intestine for treatment of cancer. The positive charge on polyethylene imine (PEI) in DNA-PEI complexes can be neutralized by coating them with the highly anionic CS. A complex consisting of 10 kDa CS, PEI, and an expression vector for granulocyte macrophage-colony stimulating factor (GM-CSF) was able to deliver the plasmid into intraperitoneal and subcutaneous tumors in a syngeneic mouse model, and the released CSF inhibited tumor growth [108]. Water solubility of CS has limited its application as a drug-functionalized solid material. Hydrophobic modification of CS by O-acetylation was then used in a nanosize delivery model that increased bioavailability for anticancer drugs together with minimum side effects [109–111]. Nanosize also increased the potential for localization in tumors thus providing better targeting through enhanced permeation and retention (EPR) [112] in tumor vasculatures. CS nanocapsules, CS nanogels, and CS functionalized mesostructured silica nanoparticles have been developed for controlled release and targeted delivery of bioactive compounds. Nanocapsules have relatively lower density, less consumption, high loading capacity, and better protection of the loaded compound. Nanogels are comprised of hydrophobic inner shell cores and hydrophilic outer shells or coronas. The hydrophobic cores determine drug loading efficiency and release. The hydrophilic coronas provide prolonged and more effective circulation of the relevant drug and can act as barriers against interactions with other cells, proteins, and body tissues [113, 114], which prevents recognition by the reticuloendothelial system.

Melanoma chondroitin sulfate proteoglycan (MCS-PG) is another example that can be a target to induce apoptotic signals in melanoma cells. MCS-PGs are expressed in 85% of melanomas [115], and they increase metastatic properties motility [116] and invasion [117] in melanoma cells and promote growth of the cells. However, they are also present in cells of the melanocyte lineage, in basal cells of the epidermis, in hair follicles, and in pericytes [115]. Therefore, the melanocytes would also be exposed to both anti-MCS-PG monoclonal antibodies and immune-toxin mediated attack strategies [118, 119]. Xi et al. [120, 121] prepared a CS nanocapsule loaded with indomethacin for delivery and demonstrated its pH responsiveness when studied *in vitro* in a pharmacological drug release model. Xi et al. [121] also prepared functionalized mesoporous silica nanoparticles (MSNs) with CS coronas (NMCS-MSN), which exhibited high drug loading capacity and pH-triggered controlled release of drug simultaneously. Typically, NMCS-MSN was mixed with test drug doxorubicin to form NMCS-MSN-Dox that was then cross-linked with bisulfate. This resulted in release of doxorubicin in a pH responsive manner that was more cytotoxic to HeLa cells than free doxorubicin. Nanogels are self-organized when a solution of acetylated CS (AC-CS) in dimethylsulfoxide (DMSO) is dialyzed in aqueous medium. DMSO is displaced by water, and nanogels are

formed. Park et al. [122] prepared doxorubicin loaded AC-CS nanogels by dialyzing a mixture of doxorubicin and AC-CS in DMSO in borate buffer. Another notable application of CS in a drug delivery vehicle is the use of folate linked CS on surfaces of Pluronic 127 nanogels [123] to target folate receptor rich cancer cells. The Pluronic 127 is an inhibitor of the drug efflux transporter. This vehicle can release the drug payload following receptor mediated entry into folate receptor rich tumors, which then blocks the efflux of the drug and retains it inside the cells.

A form of DS known as DS 435 [124] with an average molecular weight of 22.2 kDa was prepared from beef lung mucosa. It has an unusual property to target neovascular transport. It contains 2-sulfated IdoUA and 4-sulfated GalNAc (with some 4,6-di-sulfated GalNAc) disaccharide structures, which do not bind to the antithrombin III receptor present on endothelium and which have low anti-Xa anticoagulant and fibrinolytic activities. These sulfation patterns on DS 435 selectively target the neovascular system and penetrate into the tumor matrix. Its subsequent uptake by tumors is high owing to its high heparin cofactor II binding. Nanoparticles with doxorubicin cores coated with DS 435 were prepared by high pressure homogenization. The particles injected intravenously showed deeper matrix penetration than regular doxorubicin. DS-Dox demonstrated better therapeutic efficacies in a human MX-1 breast xenograft study [124]. It was concluded that DS drug combinations were transported rapidly and selectively across tumor neovascular endothelium and penetrated deeply into the tumor matrix.

4.3. Keratan Sulfate (KS) in Drug Delivery. Keratan sulfate (KS) is a linear GAG that consists of repeating disaccharides composed of galactose and N-acetylglucosamine (GlcNAc) with sulfation at the 6-O positions on the disaccharides. KS, the major GAG in cornea, is present on one of three core proteins (lumican, keratocan, or mimecan) forming KS-PGs [125]. KS has long been believed to play a central role in corneal homeostasis because it is altered when the cornea becomes opaque during injury or disease [126]. Large quantities of cell-associated KS are found in the endometrial lining during the menstrual cycle and have an important role during embryo implantation. Specifically, the antiadhesive properties of KS have important roles in both endothelial cell migration in cornea epithelium and in embryo implantation during the menstrual cycle [127–129]. Several reviews describe possible structures and functions of KS-PGs [130–132], but the role of KS-PGs in drug delivery is not known clearly. KS plays an important role in mucopolysaccharidosis IVA (MPS IVA, Morquio A disease), an inherited lysosomal storage disorder that features skeletal chondrodysplasia. In this Morquio A syndrome, serum KS increases due to deficiency of N-acetylgalactosamine-6-sulfate sulfatase (GALNS), which is required to degrade KS. Recent studies used a bone-targeting drug delivery system with E6-tagged GALNS where GALNS was bioengineered with the N-terminus extended by the hexaglutamate sequence (E6) to improve targeting to bone (E6-GALNS). The results showed improved efficacy of enzyme-replacement therapy to bone and cartilage in Morquio A disease [133].

4.4. HA in Drug Delivery

4.4.1. HA in Transdermal Delivery. Skin is the largest organ in the body (15% body weight), which contains most of the body's HA, and is a barrier against water loss and invading pathogens. The outer layer stratum corneum (15 μm) provides this barrier function. Below the stratum corneum is epidermis (130–180 μm), and next to it is the dermis (2000 μm) that contains nerves, blood vessels, nociceptors, lymph vessels, hair follicles, and sweat glands. In normal skin, HA is found in the intercellular spaces of epidermis except in the upper granular layer and in the stratum corneum. Because HA is nonantigenic, intradermal delivery of substances using HA as a vehicle will not pose any problem. HA is used as a transdermal drug delivery vehicle in various forms, including hydrogels, and as microneedles to deliver insulin and immunogens for immunization. For example, the transdermal delivery of insulin using microneedles (MNs) fabricated with 15% HA containing insulin is used in diabetes patients [134]. In diabetic rats, the microneedles applied in skin dissolved in an hour with rapid release of insulin, and the holes produced by the microneedles disappeared within 24 hours demonstrating reversible skin damage. The insulin administered by this approach was almost completely absorbed from the skin into the systemic circulation as indicated by pharmacodynamic and pharmacokinetic parameters [134]. Similarly, during vaccination, transcutaneous immunization via these micro needles can be used for easy delivery of the antigens [135–138]. Recent advancements in self-dissolving microneedles using biodegradable materials is a promising vaccination approach [139–142]. For example, in transcutaneous immunization (TCI) of tetanus toxoid (TT) and diphtheria toxoid (DT), sodium HA was mixed separately with TT and DT to form the micro needles [139–142]. TCI systems with microneedles physically penetrate the stratum corneum and directly deliver the antigen into the epidermal layer and dermis, which contain an advanced immune system with antigen-presenting cells (APCs) such as Langerhans cells (LCs) or dermal dendritic cells (dDCs). The antibody titers against the toxoids increased, and the vaccination protected the TT-vaccinated animals against tetanus toxin.

Despite the high molecular weight and hydrophilicity of HA, it is known to be delivered through the skin tissue in both mice and humans using MNs [143–145], whereas in delivery of antibodies, the HA is composed of low molecular mass of 55 kDa and of 25 kDa [146]. MNs fabricated from HA show complete dissolution within 1 h of application to rat skin *in vivo* [134], whereas the delivery time of TCI (influenza vaccination)/TT/DT fabricated with HA is 1–5 min [141].

4.4.2. HA in Burn Injury. Burn injury to skin and flesh is caused by heat or electricity. Depending on the depth of burn, injuries are classified in terms of degrees, from superficial (first-degree), to underlying layers (second-degree), and to all layers (third-degree). Burn injuries over relatively small areas are an example of an acute, local inflammatory state. Following such an initial burn injury, the affected skin/flesh progresses to tissue ischemia and necrosis [147]. The initial injury induces a zone where protein denaturation, significant

tissue loss, and cell death occur. Burned tissue is in a cytotoxic and degenerative state [148]. Thus, proinflammatory mediator levels of tumor necrosis factor alpha (TNF- α), interleukin-1 β (IL-1 β), and interleukin-6 (IL-6) increase both systemically and locally in burn areas [149]. These mediators establish the pathophysiological environment of burns. Therefore, neutralizing these targets could effectively regulate the complex inflammatory cascade. Antibodies against TNF- α or IL-1 β conjugated to high molecular weight HA diffuse slowly thus providing a sustained delivery of the antibodies in the wound [150]. Animal studies indicated that, in a partial-thickness rat burn model, HA treatment alone reduced burn progression by nearly 30%, while anti-TNF- α -HA reduced it approximately 70% and decreased macrophage infiltration into the injury site compared to controls [151].

4.4.3. HA in Ocular Drug Delivery. HA was first discovered in the vitreous body by Meyer and Palmer in 1934 [26]. HA is a component of vitreous humor, lacrimal gland, conjunctiva, corneal epithelium, and tear film [152]. Graue et al. [153] were the first to create a novel noninflammatory preparation of HMW HA on a commercial scale, and its use in ocular surgery protects the corneal endothelium. The properties of HA that have made it a first choice in ocular drug delivery are excellent moisturization properties, mucoadhesiveness, extended drug-retention time in tear fluid and drug contact time [154], bioavailability and tissue healing properties, promotion of growth of corneal epithelial cells [155, 156], and suppression of inflammation [157, 158]. Numerous topically administered preparations have been developed based on these properties of HA, including pilocarpine [159–161], tropicamide [162], timolol [160, 163], and tobramycin [163]. Recently *in situ* gel technology has been developed in which modified HA solutions with drugs can be dropped into the conjunctival sac where it is converted into a gel with increased bioavailability and duration, which is a promising approach [164]. In this method, ophthalmic drug was delivered using graft copolymers prepared by coupling mono amine-terminated poloxamer (MATP) with a HA backbone using 1-ethyl-3-(3-dimethylaminopropyl)-carbodiimide (EDC) and *N*-hydroxysuccinimide (NHS) as coupling agents. This poloxamer-graft-HA hydrogel slows down drug elimination by lacrimal flow, both by undergoing *in situ* gel formation and by interacting with the mucus. Also, this hydrogel can be used to enhance wound healing of an injured mucus layer of the eye [164]. Noncancer drug delivery applications of GAG delivery systems are presented in Table 1.

4.5. Cancer Drug Delivery Applications of GAG/HA Delivery Systems

4.5.1. Role of HA and CD44 in Drug Conjugates. Tumors often exhibit a phenomenon known as the enhanced permeability and retention effect (EPR). This is a result of two issues: increased permeability of the capillary endothelium in malignant tissues compared to that of normal tissues and the lack of tumor lymphatic drainage within the tumor interstitium that results in drug accumulation. If a therapeutic agent is

TABLE 1: Noncancer drug delivery applications of GAG delivery systems.

Application	Components	Drug	References
Transcutaneous delivery	Hyaluronic acid microneedles	Insulin	[134]
Transcutaneous immunization	Hyaluronic acid microneedles	Tetanus, Diphtheria, Malaria, and Influenza	[141, 142]
Topical delivery on burn sites	Hyaluronic acid	Anti-IL-6-hyaluronic acid conjugate. Anti-TNF- α -hyaluronic acid conjugate	[151]
Ocular delivery	Hyaluronic acid	Pilocarpine, timolol against glaucoma, tropicamide for dilation of pupil, tobramycin against bacterial infection of eye	[159–161, 163] [162, 163]
Oral delivery	Heparin is conjugated with taurocholic acid (TCA)	Docetaxel (DTX)	[86, 87]
Intra-articular injection	LMW heparin-N,N,N trimethylchitosan chloride (TMC)-nanoparticles,	Heparin, VEGF, and bFGF	[89]
	Heparin-Chitosan-nanoparticles hyaluronic acid-heparin hydrogel	Growth factor, for example, BMP2	[91]
Intracellular delivery	Cell penetrating peptide (CPP)	Peptides, oligonucleotides, siRNAs, and liposomes	[98–103, 107]

coupled to a suitable biodegradable drug carrier, then such carriers have the potential of increasing the concentration of drug distribution in the tumor tissue due to the EPR effect [44]. Administering a drug in a carrier alters its distribution profile by directing it into the tumor and by exploiting the EPR effect [18]. The therapeutic efficacy depends on a specific drug target process that has the ability to cross the cellular barrier, find the tumor, and reach the intracellular target sites to alter the tumor biology. Thus, an appropriate drug carrier would effectively transport the drugs through the cellular membrane with improved drug circulation time, solubility and stability of the drug, and would reach the cell and intracellular target sites. Several interesting smart carrier systems based on both synthetic and natural polymers have been designed and developed to achieve these goals [165].

In recent years, several features in HA prompted investigators to consider it as an important driver for drug delivery for the following reasons. (a) HA is a promising component from the pharmaceutical standpoint because it is biodegradable, biocompatible, nontoxic, hydrophilic, and nonantigenic. (b) The carboxylate on the glucuronic acid and the hydroxyls on the *N*-acetyl glucosamine can be potentially used to conjugate a drug [166], and the acetyl on the *N*-acetyl glucosamine can be removed enzymatically to expose an amino group that can also be used for drug conjugation [167]. (c) The molecular mass of HA is an important consideration while preparing the drug conjugate. For instance, a 90 kDa fluorescein-labeled HA gradually accumulated in the liver and then was distributed into endothelium, whereas 10 kDa or less HA was rapidly excreted into urine *in vivo* [168]. This indicates that HA with high average molecular weight has hepatic targeting ability. The success of HA as a carrier depends on the number of receptors available on the target cells and on the affinity between the homing ligand and the receptor. HMW HA can cross-link with a number of CD44 receptors and be endocytosed. However, it is rapidly cleared

from circulation by the liver hepatocytes [169], and any excess of the targeting compound can lead to adverse effects [170]. This rapid clearance was circumvented by choosing HA oligosaccharides long enough to bind to CD44 but too short to bind to the HARE receptor, which may permit targeting to cells that overexpress CD44. The minimum HA length required to interact with individual CD44 molecules is 6 to 10 saccharides [171] with moderate affinity. Several pre-clinical studies have shown that HA chemically conjugated to cytotoxic agents improved anticancer properties of the agent *in vitro* [50, 172, 173]. HA-drug conjugates also improve the inadequate water solubility of some anticancer agents [18, 165, 174, 175]. Targeting CD44 presents a very promising and novel approach against HA-induced tumorigenesis.

4.5.2. Approaches for Targeting HA

(i) *HA Backbone Based Conjugated Drugs*. HA conjugated drugs are more soluble in water than the drugs alone. For instance, the antimetabolic chemotherapeutic agent paclitaxel (PTX) has low water solubility. Upon conjugation to HA, water solubility of the prodrug HA-PTX significantly increased, and CD44 dependent cellular uptake increased *in vitro* [176]. The prodrug HYTAD1-p20 (HA-PTX) conjugate (renamed as ONCOFID-P by the pharmaceutical company Fidia) shows significant benefit over original PTX in terms of *in vitro* activity against bladder carcinoma cells, *in vivo* safety profile, and pharmacokinetics [177]. ONCOFID-P is in Phase II clinical study in the intravesicle therapy of patients with nonmuscle invasive cancer of the bladder (EudraCT 2009-012274-13). A phase I clinical study was initiated to investigate its maximum tolerated dose and safety profile following i.p. infusion in patients affected by intraperitoneal carcinogenesis in ovarian, breast, stomach, bladder, or colon cancers [178–180]. Luo et al. coupled PTX-N-hydroxysuccinimide

ester (PTX-NHS) with HA of molecular weight ~11 kDa [181]. PTX release from the hydrogel film was evaluated *in vitro* using selected antibacterial and anti-inflammatory drugs [181]. The pharmaceutical company Fidia prepared ONCOFID-S, another HA prodrug conjugate with SN-38, the active CPT11 (irinotecan) metabolite. The HA used had a molecular weight of ~200 kDa. *In vitro* and *in vivo* cytotoxicities were investigated using ONCOFID-S in several CD44 overexpressing cancer cells, including colon, gastric, breast, esophageal, ovarian, and human lung cancer cells [178]. The treatments reduced all parameters correlating with poor prognosis in peritoneal colorectal cancer (CRC) carcinomatosis without any myelotoxicity or mesothelial inflammation [182]. A recent *in vivo* study with HA-cisplatin reported a significant improvement in antitumor efficacy, with lower toxicity compared to standard cisplatin, in locally advanced head and neck squamous cell carcinoma [183].

(ii) *HA-Encapsulated Drugs*. Another strategy for HA-based CD44 targeting utilizes the concept that the large volume domain of HA (molecular weight > 750 kDa) can noncovalently entrap small therapeutic molecules within this matrix. HA was then used as a macromolecular carrier for the irinotecan drug along with its targeting properties [184]. The principle is that the HA-drug complex will accumulate in the microvasculature of the xenograft tumor, increase drug retention at the tumor site, and allow for active uptake of the drug by the tumor cells via HA receptors. Clinical trials of three such HA formulations (termed hyaluronic acid chemotransport technology (HyACT)) have been undertaken in Australia. Phase I clinical evaluation of two formulations based on HA (HyACT) with 5-fluorouracil (5-FU) (HyFIVETM) and on HA with Dox (HyDOXTM) demonstrated reasonable efficacy without compromising safety of these formulations [185, 186].

(iii) *HA-Tailed Drug Carriers*. These include the following HA conjugates.

- (a) Bisphosphonates (BPs) [187]: high molecular weight HA is linked via a hydrazide group to bisphosphonate (HA-BP). The hydrazide group of the HA-BP can also be used to explore hydrazone linkage of other drugs, such as doxorubicin, which could be integrated into the hydrogel matrix following treatment with aldehyde modified-HA [187]. The cytotoxicity of the HMW HA-BP was directly proportional to cell surface HA receptor levels.
- (b) Carbonates [188, 189]: Di Meo et al. proposed a bioconjugate (HA-pCB) composed of n-propyl carbonate linked to HA via an ester linkage. Its cellular uptake was evaluated *in vitro* on a variety of human tumor cells. HA-pCB produced high intracellular accumulation of boron atoms.
- (c) Chitosan [190, 191]: Jain et al. prepared chitosan-HA nanoparticles (HA-CTNPs). 5-FU loaded nanoparticles were then prepared by the ionotropic gelation method. Their surface was coupled to the carboxylic group of HA by using carbodiimide chemistry [1-ethyl-3-(3-dimethylaminopropyl) carbodiimide (EDC)] with chitosan amine groups to form amide linkages. The *in vitro* cellular uptake and cytotoxicity results suggest that the 5-FU loaded HA-CTNP formulation leads to increased uptake in comparison with chitosan nanoparticles alone (CNTPs), and that this significantly enhanced cytotoxicity compared with either CNTP or free 5-FU in HT29 colorectal cancer cell lines, which overexpress the CD44 receptor.
- (d) Gagomers (GAG-mers) [192]: GAG-mers (glycosaminoglycan cluster of particles) are composed of lipid molecules that self-assemble into particulate clusters in hydrophilic solutions, which are then covalently coated with HMW (1.2–5 MDa) HA by carbodiimide activation of carboxyl groups at a lipid: HA ratio of 10:1 (w/w). When tested in primary head and neck cancers and normal cells taken from the same patient [192], GAG-mers selectively bound only to the tumor cells.
- (e) Liposomes/lipoplexes [193–197]: HMW HA was decorated on nanosized encapsulated anticancer drugs. In a first study, mitomycin C (MMC) was encapsulated in HA-liposomes (HA-LIP), and their behaviors *in vitro* and *in vivo* were compared to those of plain liposomes. The cytotoxic activity of the drug loaded into HA-LIP was found to be ~100-fold that of free drug in cultured tumor cell lines overexpressing the HA receptors, but not in cells with low receptor expression levels. *In vivo* tumor model studies confirmed the higher antitumor activity of HA-LIP containing MMC compared with MMC alone or with unmodified liposomes. In a second study, complexes were prepared with plasmid DNA pCMV-luc and lipoplexes (conjugates), which contained HA and the amino-reactive group of a lipid, dioleoylphosphatidylethanolamine (HA-DOPE), to form cationic liposomes having negative zeta potential and a mean diameter of 250–300 nm [195]. With this approach, conjugation depends on the molecular weight of HA. The HA-LIP conjugate can be used to deliver plasmid DNA and siRNA to CD44 positive cancer cells [195, 198]. The presence of HMW HA in the lipoplexes enhanced nucleic acid protection from degradation by DNase I or RNase VI. In case of LMW HA, the HA was linked to PE to form a conjugate in which only one PE molecule is linked to a HA molecule [196, 197]. This procedure enables a controlled amount of HA to be introduced into the liposomes. The ability to target LMW HA decorated liposomes was demonstrated in an interesting approach [196]. HA oligosaccharides were attached to PE and incorporated into the liposomes, which increased their recognition, cytotoxicity, and transfection efficiency by tumor cells expressing high levels of CD44 in a temperature-dependent manner. Uptake of the liposomes was also dependent on the density of HA.

- (f) Micelles: the hydrophilic backbone of HA was first dissolved in DMSO and then conjugated via its carboxyl groups to amino functions of poly-L-histidine (PHis), or polyethylene glycol (PEG). These HA construct form nanocomplexes by self-organizing into micelles, and they can carry anticancer drugs, including paclitaxel (PTX). PTX when entrapped into the hydrophobic cores of the folic acid- (FA-) conjugated HA-C18 micelles exhibited higher cytotoxic activity compared to Taxol in MCF-7 cells that overexpress both the folate receptor and CD44. FA-HA-C18 micelles showed low cytotoxic activity compared to Taxol in A549 cells that only overexpress CD44 [199]. The HA-PTX [199], HA-DOX [200], and HA-salinomycin [201] micelles exhibited more pronounced cytotoxic effects on HA receptor overexpressing cancer cells than on receptor deficient cells.
- (g) Nanocarrier: HA when conjugated to a nanocarrier acts as a protective structural component and provides a targeting coating that influences the circulation time and biodistribution (pharmacokinetic properties) and the cell specific uptake properties of the large carriers. Cargo liposomes or nanoparticles were able to deliver anticancer drugs, including epirubicin [50], doxorubicin [196], paclitaxel [176], and mitomycin-C [50], as well as siRNA, to CD44 overexpressing cells [202].
- (h) In addition to the well-developed strategies described above, several multifunctional nanocompounds have recently been developed that combine therapeutic and diagnostic properties. These nanoparticles include quantum dots [203], carbon nanotubes [204], nanodots [205], graphene [206], gold nanoparticles [207], iron oxide nanoparticles [208], and silica nanoparticles [209], and they have been found to acquire novel characteristics after their conjugation with HA [203–210]. Cancer drug delivery applications of GAG/HA delivery systems are presented in Table 2.

4.5.3. Approaches for Targeting CD44. CD44 proteins exist in three states with respect to HA binding: nonbinding, nonbinding unless activated by physiological stimuli, and constitutive binding [171, 211, 212]. After the HA-drug conjugates are internalized via CD44 [213], the drug can be released and activated mainly by intracellular enzymatic hydrolysis [176]. CD44 is endogenously expressed at low levels on various cell types in normal tissues [214], but it requires activation before it can bind to HA. Activated CD44 is overexpressed on solid tumors, but much less, or not at all on their nontumorigenic counterparts. Cellular activation can affect HA targeted drugs by inducing transition of CD44 to a high-affinity state. For example, tumor-derived cells express CD44 in a high-affinity state that is capable of binding and internalizing HA. Transitions from the inactive, low-affinity state to the active, high-affinity state by CD44 require post-translational modifications. Posttranslational modifications of CD44 can be induced by ligation of antigen receptors [215], sulfation, or the action of cytokines [216]. Glycosylation is

required for CD44 to bind HA on certain cell types, while glycosylations rich in sialic acid decrease HA binding [72, 217]. HA induces signaling when it binds to constitutively activated CD44 variants (CD44v) [218–221]. CD44 can also react with other molecules, including collagen, fibronectin, osteopontin, growth factors, and matrix metalloproteinases (MMPs), but the functional roles of such interactions are less well known [70]. Thus, targeting drugs to CD44 are one of the appropriate strategies for cancer treatment. HA is the major CD44 ligand, and HA with innate ability as a drug carrier increases the drug concentration on CD44 overexpressing cancer cells, as well as for other pathologies [166, 172, 181, 222–227]. HA-CD44 interaction, which deserves particular attention, can initiate signal transduction pathways leading to cancer cell growth, adhesion, migration, invasion, and metastasis. Therefore, inhibiting HA-CD44 interaction has been investigated [18, 19, 44, 228–230].

A considerable number of studies indicate that CD44 isoforms correlate with bad prognosis in patients with most human cancers [231–238] except in neuroblastomas and prostate cancer [239, 240]. CD44v6 is quite likely to be a suitable target for anticancer therapy because it is (a) causally involved in metastasis of a rat pancreatic carcinoma [241]; (b) redundantly correlated with the human tumors mentioned above; and (c) correlated with oncogenic functions in colorectal cancer (CRC) both *in vitro* and *in vivo* [12, 18, 43, 232, 234, 235]. Four approaches have been proposed to target CD44: (i) targeting with anti-CD44 antibodies, (ii) interrupting HA-CD44 interaction by HA oligosaccharides (oHAs), (iii) enzymatic degradation of HA, and (iv) tissue-specific deletion of CD44 variant signaling by our validated tissue specific delivery of CD44v6shRNA into tumor cells. Therapeutic applications of disrupting the HA/GAG biological systems are presented in Table 3.

(i) Targeting with Anti-CD44 Antibodies. Anti-CD44 antibodies against highly expressed CD44v variants can effectively target drugs to cells expressing a selective CD44v, which can then inhibit and disrupt CD44 matrix interactions and alter CD44 signaling and cause apoptosis [256]. Antibodies against highly expressed variants can also be designed to selectively deliver a cytotoxic drug to cancer cells. Anti-CD44v6 conjugated with a cytotoxic drug mertansine has been used in early phase clinical trials. In head neck and squamous cell cancer (HNSCC) patients, humanized anti-CD44v6 monoclonal antibody (HAMA) labelled with technetium-99m was first tested [231]. Given the promising results of a phase I clinical study with the radionuclide-antibody conjugates [242–246], a new strategy was advanced to prepare an immunotoxin with bivatuzumab [247] and used in the next clinical trial on thirty HNSCC patients. Only three patients showed a partial response [257], and one patient died of toxic epidermal necrolysis, after which further trials were abruptly withdrawn. Later, HNSCC patients suffering from early stage breast cancer were also treated with this humanized CD44v6 antibody [258], and it accumulated in nontumor areas, indicating limitations in the use of this antibody therapy. Thus, CD44v6 remains a crucial target for tumor therapy. To address this issue, we have developed

TABLE 2: Cancer drug delivery applications of GAG/HA delivery systems.

Application	Components	Drug	References
Antimitotic delivery in bladder carcinoma cells	Hyaluronic acid (HA) 10–12 KDa	Paclitaxel	[176, 177, 181]
Anti-DNA winding delivery In CD44 overexpressing colon, breast, esophageal, and ovarian cancer	Hyaluronic acid 200 KDa	Irinotecan	[178, 182]
HA-encapsulated drug delivery for metastatic breast, prostate and colon cancer	Hyaluronic acid ~750 KDa	5-FU, doxorubicin	[185, 186]
Localized delivery in bone disease in cancer	Hyaluronic acid	Bisphosphonate	[187]
Nanoparticle delivery in colon cancer	Chitosan-hyaluronic acid	5-FU	[190, 191]
Peritumoral delivery of nanovectors in head/neck cancer (HNSCC)	Lipid-Hyaluronic acid (1.2–5 MDa)	Mitomycin C	[192]
	Hyaluronic acid	Cisplatin	[183]
Intracellular delivery of polymeric micelles for CD44 and folate receptor overexpressing breast and lung cancer and in cancer stem cells	Folic acid conjugated HA-C18 micelles	Paclitaxol, doxorubicin, salinomycin, and doxorubicin	[199–201]
	Folate linked CS on surfaces of Pluronic 127 nanogels		[123]
Intracellular delivery of CD44 overexpressing cancer (breast, colon, and HNSCC)	HA-nanocarrier	Epirubicin, doxorubicin	[50, 176, 196]
		Paclitaxel, mitomycin C, siRNAs	[202]
Intracellular delivery of nanogels in breast cancer	Doxorubicin cores coated with dextran sulfate (DS 435)-nanoparticles	Doxorubicin	[124]

TABLE 3: Therapeutic applications of disrupting the HA/GAG biological systems.

Application	Components	Drug	References
Phase I trial for maximum tolerated dose and safety profile in intraperitoneal infusion in ovarian, breast, colon, stomach, and bladder cancer	Hyaluronic acid (HA) 10–12 KDa	Paclitaxel	[177]
<i>In vivo</i> cytotoxicity in peritoneal colorectal cancer	Hyaluronic acid ~200 KDa	Irrinotecan	[182]
HA-encapsulated drug delivery for metastatic breast, prostate, and colon cancer	Hyaluronic acid ~750 KDa	5-FU, Doxorubicin	[185, 186]
Localized delivery in bone disease in cancer	Hyaluronic acid	Bisphosphonate	[187]
Nanoparticle delivery in colon cancer	Chitosan-hyaluronic acid	5-FU	[190, 191]
Peritumoral delivery of nanovectors in head/neck squamous cell cancer (HNSCC)	Lipid-hyaluronic acid (1.2–5 MDa)	Mitomycin C	[192]
	Hyaluronic acid	Cisplatin	[183]
Targeting with anti-CD44 antibodies in cancers including myeloid leukemia and HNSCC	Anti-CD44 antibody (Ab), humanized anti-CD44v6 monoclonal antibody (HAMA) labelled with technetium-99m	Anti-CD44Ab, Anti-CD44v6Ab	[231, 242–247]
Targeting <i>in vitro</i> breast cancer cells and xenograft lung tumor by interrupting HA-CD44 interaction	Small HA-oligosaccharides	6–18 saccharide units (oHAs)	[11, 13, 41, 248, 249]
Targeting enzymatic degradation of HA in EMT-6 breast cancer cells, bladder cancer cells	bovine testicular, bacterial hyaluronidases, HYALI-v1		[250, 251] [252]
Targeting leukemia cell by nonviral vectors in leukemia K562 cells	Transferrin-PEG-test luciferase plasmid-nanoparticle	test luciferase plasmid	[253, 254]
<i>In vivo</i> targeting CD44v6 by tissue specific deletion of CD44 variant in intestine/colon tumor in Apc Min/+ mice	pSico-CD44v6shRNA plus pFabpl-Cre	CD44v6shRNA	[18, 43, 44, 255]

a novel tissue specific shRNA delivery strategy by a Cre-lox system. This technology is discussed below.

(ii) *Interrupting HA-CD44 Interaction.* This approach involves substituting multivalent interaction of HA with CD44 by monovalent interaction of HA-CD44 using small HA oligosaccharides (6–18 saccharide units (oHAs)) [248, 259]. The oHAs inhibit HA-CD44 downstream cell survival and proliferation pathways, and they stimulate apoptosis and expression of phosphatase and tensin homologue (PTEN) [41]. The oHAs also sensitize cultured cancer cells to some chemotherapeutic drugs by inhibiting expression of MDRI and other ABC transporters [11, 13, 249]. While oHAs inhibit the growth of several tumors implanted as xenografts [41], they did not give consistent significant growth inhibition in adenoma growth of Apc Min/+ mice. Thus, we developed small interfering RNA (siRNA) and, even more advantageous, short hairpin RNA (shRNA), to target CD44v6 in colon cancer, showed that they can successfully interrupt HA-CD44v6 interaction and signaling (~90–95%). We then developed a novel shRNA delivery approach to target HA-CD44v6 specifically in tumor cells [18, 43, 44, 255], which is discussed in the following sections. Targeting CD44v6 with CD44v6shRNA inhibits distant tumor growth in mice, suggesting that it can also work against metastatic cancer cells. Due to its specificity for CD44v6, normal cells expressing CD44 remain unaffected [18, 43, 44, 255].

(iii) *Enzymatic Degradation of HA.* Hyaluronidases (HYALs) are a class of enzymes that predominantly degrade HA. However, HYALs can also degrade chondroitin sulfate and chondroitin [32]. They are endoglycosidases that hydrolyze the β -N-acetyl-D-glucosaminidic linkages in the HA polymer. Among the 6 HYALs present in the human genome HYAL-1, HYAL-2, and PH20 are well characterized. Recently, Lokeshwar et al. have shown that the expression of HYAL-1-v1 in bladder cancer cells that express wild type HYAL-1, induces G2-M arrest and apoptosis [252]. It has been shown that commercial bovine testicular or bacterial hyaluronidase acts as an antiadhesive compound on EMT-6 tumor spheroids [250], and hyaluronidase-disaggregated EMT-6 spheroids were shown to possess chemosensitivity to cyclophosphamide [250], and also to improve the therapeutic effectiveness of these agents, that is, by increasing the accessibility of solid tumors to the chemotherapeutic drugs. Unlike EMT-6 cells, Hyals have limitations as an antiadhesive agent for other human tumors [251].

(iv) *Tissue-Specific Deletion of CD44 Variant Signaling.* This section discusses the fundamental aspects of therapeutic cell-specific delivery addressing: (a) what to deliver (engineered therapeutic CD44v6shRNA delivery for *in situ*), (b) how to deliver (delivery strategies, in particular nonviral transferrin-(Tf-) coated PEG-PEI (Tf-PEG-PEI-nanoparticles) for *in situ* cell specific therapy), and (c) where to deliver (tumor-cell targets, in particular colon tumor cells for *in situ* cell-specific therapy). The technique of using shRNA in an expression vector is an alternative strategy to stably suppress selected gene expression, which suggests that the use of shRNA

expression vectors holds potential promise for therapeutic approaches for silencing disease causing genes [260]. There are two ways to deliver shRNA in cancer cells, either using a viral vector or a nonviral vector. Viral vectors have been used to achieve proof of principle in animal models and, in selected cases, in human clinical trials [261]. Systemic targeting by viral vectors towards the desired tissue is difficult because the host immune responses activate viral clearance. Systemic administration of a large amount of adenovirus (e.g., into the liver) can also be a serious health hazard and even caused the death of one patient [261]. Nevertheless, there has been considerable interest in developing nonviral vectors for gene therapy. In this regard, nonviral vectors, such as positively charged polyethyleneimine- (PEI-) complexes shielded with polyethylene glycol (PEG), can be used safely to avoid the nonspecific interactions with nontarget cells and blood components [253].

Figures 5 and 6 illustrate the model for the uptake of Tf-PEG-PEI-nanoparticles carrying multiple functional domains. Nonviral vectors were once limited for their low gene transfer efficiency. However, the incorporation of various ligands, such as peptides, growth factors, and proteins, or antibodies for targets highly expressed on cancer cells, circumvented this obstacle [254]. Also, enhanced permeability due to aberrant vasculature in solid tumors and retention of ligand coated vectors around the receptors of tumor cells can increase chances for high probability of interaction with the cancer cells [43]. Thus, the nonviral vectors can acquire high gene transfer efficiency [43]. This concept was tested by preparing nonviral vector Tf-PEG-PEI-nanoparticles with plasmids packed inside an outer PEG-PEI layer coated with transferrin (Tf), an iron transporting protein [43, 254] that binds with Tf-receptors (Tf-R) with high affinity (depicted in the model in Figures 5 and 6). The Tf-R is present at much higher levels on the tumor cells [43] than on phenotypically normal epithelial cells. Association of transferrin with the Tf-PEG-PEI-nanoparticles significantly enhances transfection efficiency of shRNA generator-plasmids by promoting the internalization of Tf-PEG-PEI-nanoparticles in dividing and nondividing cells through receptor-mediated endocytosis [254]. The uptake of Tf-PEG-PEI-nanoparticles carrying multiple functional domains (surface shielding particles Tf-PEG-PEI, shRNA generator plasmids, tissue specific promoter driven-Cre-recombinase plasmids, and conditionally silenced plasmid) can overcome the intracellular barriers for successful delivery of the shRNA.

This shRNA plasmid delivery approach was tested for transfection of pSV- β -gal/Tf-PEG-PEI-nanoparticles in cellular models (Figure 7). Following this experiment, we successfully demonstrated that the CD44v6shRNA is localized into the colon tumor cells by an end-point assay of CD44v6 expression and by perturbation of HA-CD44v6 interaction as reflected in the reduction in the number of tumors [43] (Figure 8). The tissue specific shRNA delivery was made possible by the use of Cre-recombinase produced in response to a colon tissue specific promoter, which deletes the interruption between the U6 promoter and the CD44v6shRNA oligonucleotide. The newly developed cell-specific shRNA delivery approach by Misra et al. [43] confirmed that targeting

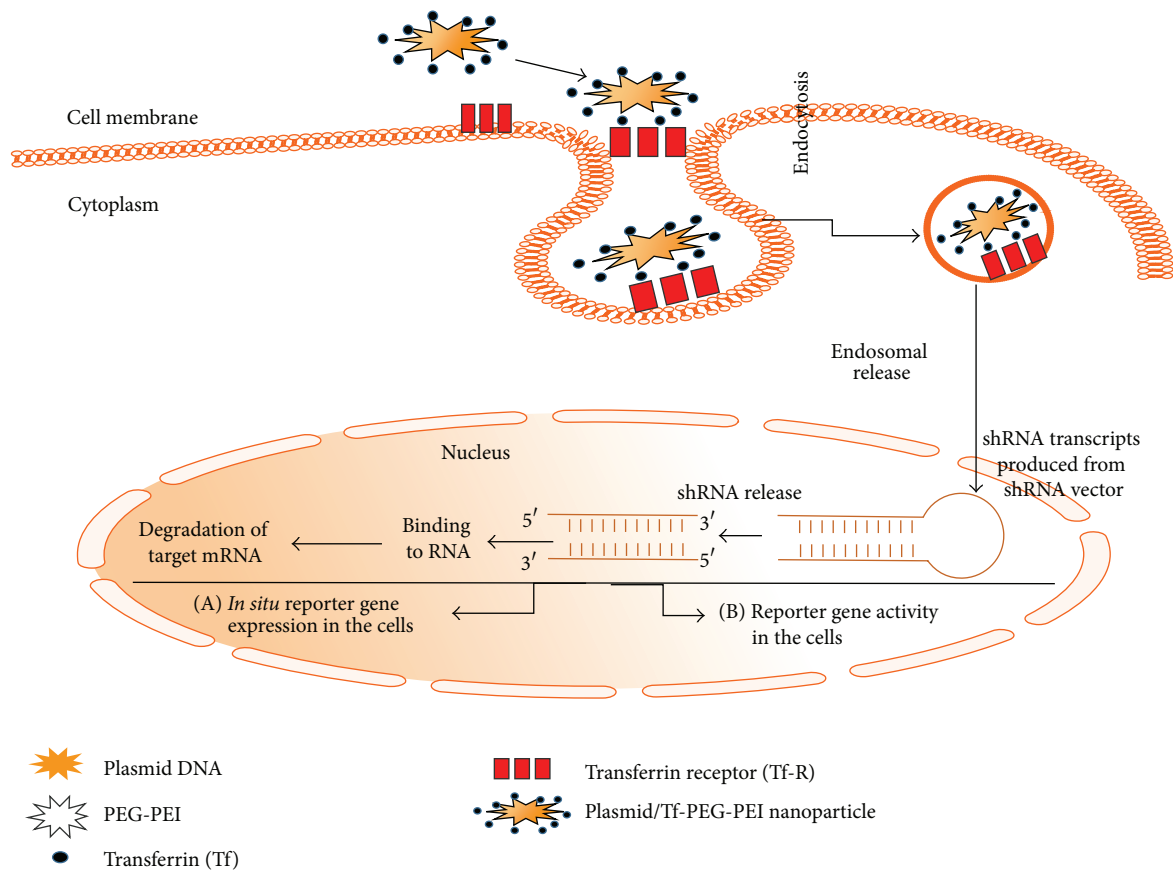


FIGURE 5: Schematic illustration of cellular uptake of plasmid DNA/Tf-PEG-PEI (nanoparticles) polyplexes, their shielding from nonspecific interaction, and the mechanism of action of shRNA (adapted from [43]). Internalization of PEG-shielded and Tf-R-targeted polyplexes into target cells occurs by receptor-mediated endocytosis after association of polyplex ligand Tf to Tf-R present on the target cell plasma membrane. Internalized particles are trafficked to endosomes followed by endosomal release of the particles and/or the nucleic acid into cytoplasm. Released siRNA will form a RNA-induced silencing complex and will be guided for cleavage of complementary target mRNA in the cytoplasm. siRNA (antisense) guide strand will direct the targeted RNAs to be cleaved by RNA endonuclease. Finally plasmid/Tf-PEG-PEI-nanoparticles delivery in the target cell shows reporter gene expression and activity.

the signaling pathways induced by HA-CD44v6 interaction inhibited distant colon tumor growth in *Apc Min/+* mice. Our recent unpublished *in vivo* studies with the C57Bl/6 mice have now shown that systemic delivery of a mixture of two plasmids in Tf-PEG-PEI-nanoparticles (pARR₂-Probasin-Cre/Tf-PEG-PEI-nanoparticles and floxed pSico-CD44v9shRNA/Tf-PEG-PEI-nanoparticles) can target both localized and metastatic prostate cancer cells. This novel approach opens up new ways to combat cancer and to understand tumorigenesis *in vivo* for the following reasons.

- (1) Cell specific shRNA to CD44 variant (CD44vshRNA) is released by applying a tissue specific promoter driven Cre-lox mechanism.
- (2) This shRNA silences the expression of the selected CD44 variant in the target tissue cancer cells.
- (3) This shRNA does not affect the normal target tissue cells, which rely on the standard CD44s and do not express the targeted CD44 variant and therefore are not affected by the plasmids.

- (4) The target CD44vshRNA will not be expressed in other types of cells because the tissue specific promoter only unlocks the Cre-recombinase in the targeted tissue cells thereby reducing potential side effects [43].
- (5) The Tf-PEG-PEI-nanoparticles that carry plasmids are biodegradable and cleared from the system.
- (6) This method inhibits the pathophysiological role of HA-CD44v interactions in cancer.
- (7) It can establish diagnostic markers for the targeted cancer, including CD44 variants, soluble CD44, and HA.
- (8) It can identify HA-CD44v interactions as innovative novel therapeutic targets against cancer progression.

Thus, the conditional suppression of gene expression by the use of an CD44vshRNA expressing plasmid holds potential promise for therapeutic approaches for silencing HA-CD44 variant signaling and downstream signaling pathways that promote disease causing genes [260].

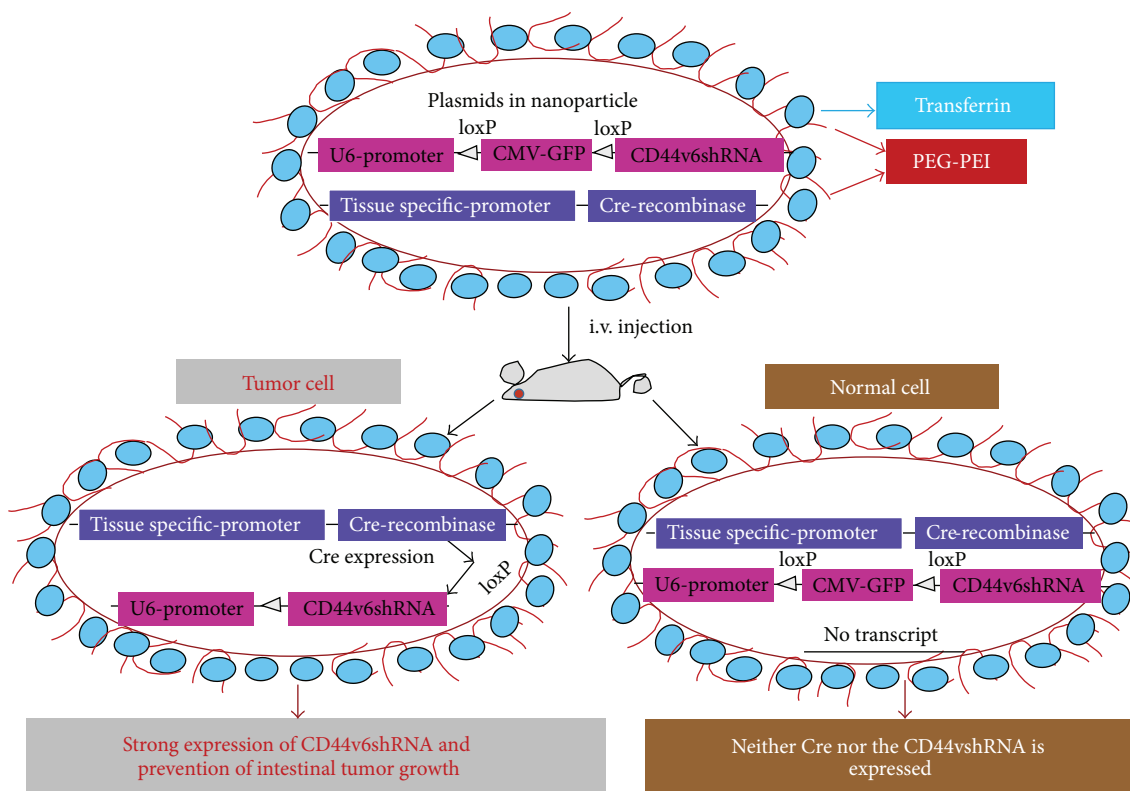


FIGURE 6: Model for delivery of shRNA (adapted from [18]). This illustration depicts cellular uptake of plasmid Tf-PEG-PEI nanoparticles and the mechanism of action of shRNA. First, a pSico vector containing a U6 promoter-loxP-CMV-GFP-STOP signal-loxP-CD44vshRNA (gene of interest) is made. Second, an expression vector with the Cre-recombinase gene controlled by the tissue specific promoter is created. Third, the two vectors are packaged in transferrin (Tf) coated-PEG-PEI nanoparticles that bind with Tf-receptors (Tf-R) present at high levels in the targeted tumor cells. Delivery of the vectors in normal and malignant cells from the targeted tissue results in deletion of the Stop signal and transcription of Cre-recombinase driven by the tissue specific promoter. The target gene (CD44vshRNA) is then unlocked and transcribed through the strong U6 promoter for high expression. The normal tissue cells are not affected because they do not make the targeted CD44 variant. Tf-PEG-PEI nanoparticle coated plasmids (pSico-CD44v6shRNA/pFabpl-Cre) circulating in blood accumulate at tumor regions enhanced by the EPR effect. Endocytosis mediated by ligand-receptor interactions occurs because the nanoparticles are coated with the Tf-ligand for the Tf-R receptor on the tumor cell surface.

5. Conclusions

Among various GAGs and PGs, much research has demonstrated the ability of HA to target cancer cells overexpressing the HA receptor CD44, in particular its variants, and that HA interaction with CD44v augments cancer pathobiology (Figure 9). Thus, interference with the function of HA-CD44 can inhibit the malignant process at multiple stages. This can be accomplished by perturbation of HA-CD44 signaling pathways and disruption of the HA matrix with hyaluronidases to facilitate passive carrier uptake, targeting the HA tumor matrix and providing sustained source of drug to the tumor site or by targeting CD44 receptor by CD44 blocking antibody or tissue specific targeting of specific variants of CD44 that are overexpressed in tumors. Cancer is a disease of the organism and is the subject of intense research around the world, but many questions about how the disease works remain unanswered. However, the multifaceted functions of GAGs and PGs require

careful, context-dependent therapeutic applications because they have dual functions; and targeting ECM GAGs and PGs may promote escape of tumor cells from the primary tumor by inhibiting cancer cell attachment and increasing distant metastatic migration of tumor cells. Alternative viable and beneficial approaches are targeting the tumor ECM to disrupt HA-CD44v signaling pathways, keeping the function of CD44s intact. Thus, our validated tumor specific delivery of CD44 variant-shRNA has considerable advantage versus other therapeutic strategies. First, this technique avoids multiple chemical steps to prepare HA conjugated cytotoxic drugs and conjugation to nanocarriers. Second, it abolishes the CD44v variants in the cancer cells only. Third, a number of cell types in normal tissues that express CD44s or the hematopoietic form will not be affected because these are not activated. Fourth, although inflammation-associated cancers accumulate activated immune cells with upregulated transferrin receptors and CD44 variants and may take up the Tf-PEG-PEI-nanoparticles, there will be no deletion

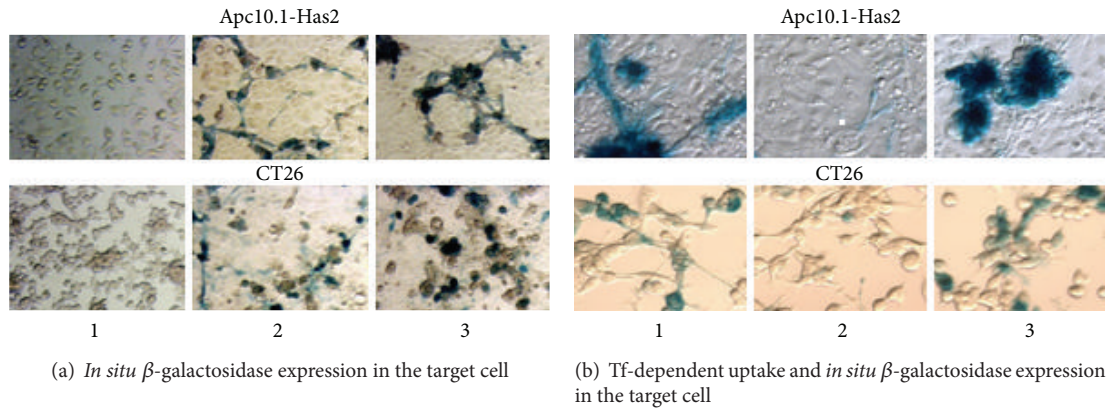
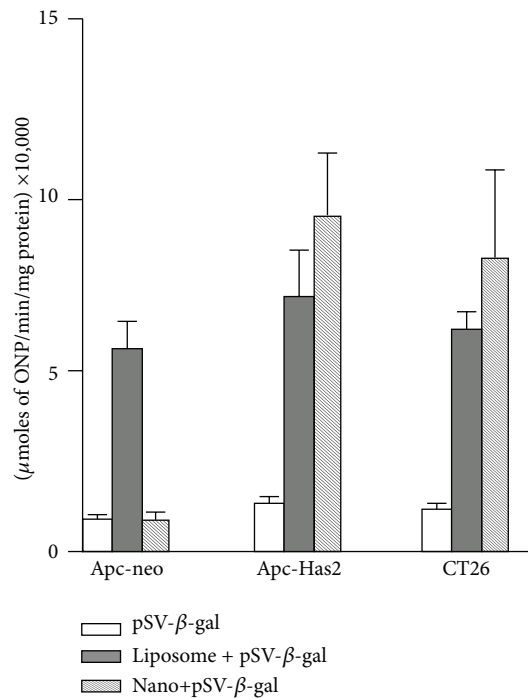
(a) *In situ* β -galactosidase expression in the target cell(b) Tf-dependent uptake and *in situ* β -galactosidase expression in the target cell(c) β -galactosidase enzyme activity in the target cell

FIGURE 7: Uptake of pSV- β -galactosidase/Tf-PEG-PEI (nanoparticles) into target cell. Delivery of pSV- β -gal nanoparticles in colon cancer cells (adapted from [43]). (a) *In situ* β -galactosidase expression in the target cell. The *Apc10.1-HAS2* clone and the CT26 cells were treated for 48 h with the pSV- β -gal alone (panel 1), with the pSV- β -gal with liposome (panel 2), or with the pSV- β -gal/nanoparticles (35 nm average diameter, 8 μ g of pSV- β -gal/mL) (panel 3). The average size of the pSV- β -gal/nanoparticles is ~ 35 nm \pm 20 nm. The transfected cells were fixed in 0.2% glutaraldehyde in PBS and washed twice in PBS. The cells were treated with a β -galactosidase staining solution and digitally photographed. (b) Transferrin-dependent uptake and *in situ* β -galactosidase expression in the target cell. The *Apc 10.1-HAS2* cells were transfected with the pSV- β -gal with liposome (panel 1), treated with Tf-R antibody and followed by transfection with the pSV- β -gal/nanoparticles (8 μ g pSV- β -gal/mL) (panel 2), or treated with the pSV- β -gal/nanoparticles (8 μ g pSV- β -gal/mL) alone (panel 3). The transfected cells were fixed in 0.2% glutaraldehyde in PBS and washed twice in PBS. β -galactosidase expressions in the cells were digitally photographed. (c) Cell-free extracts of parallel cultures were prepared in 10 mM CHAPS buffer and assayed for β -galactosidase activity using *o*-nitrophenyl β -D-galactopyranoside as substrate. The results are expressed as micromoles of *o*-nitrophenol formed per min/mg protein and represent \pm S.D. of triplicate assays from the untransfected, liposome-transfected, or nanoparticles-treated cultures for each cell type.

of CD44 variant because the promoter is not lymphocyte specific. To target activated lymphocytes, specific lymphocyte promoter driven-Cre plasmids would have to be used. Fifth, accumulation of antibody in nontumor areas is a major limitation of anti-CD44 antibody therapy. Experiments so far have not shown any such effect in shRNA delivery.

The HA-CD44 interaction system is illustrated in Figure 9 where we specify alternatives for cancer therapeutical aspects (discussed in this review) that specifically perturb HA-CD44 signaling pathways.

In conclusion, CD44 is the most prevalent cell surface marker of cancer stem cells (CSCs) [230, 262–264]. CD44

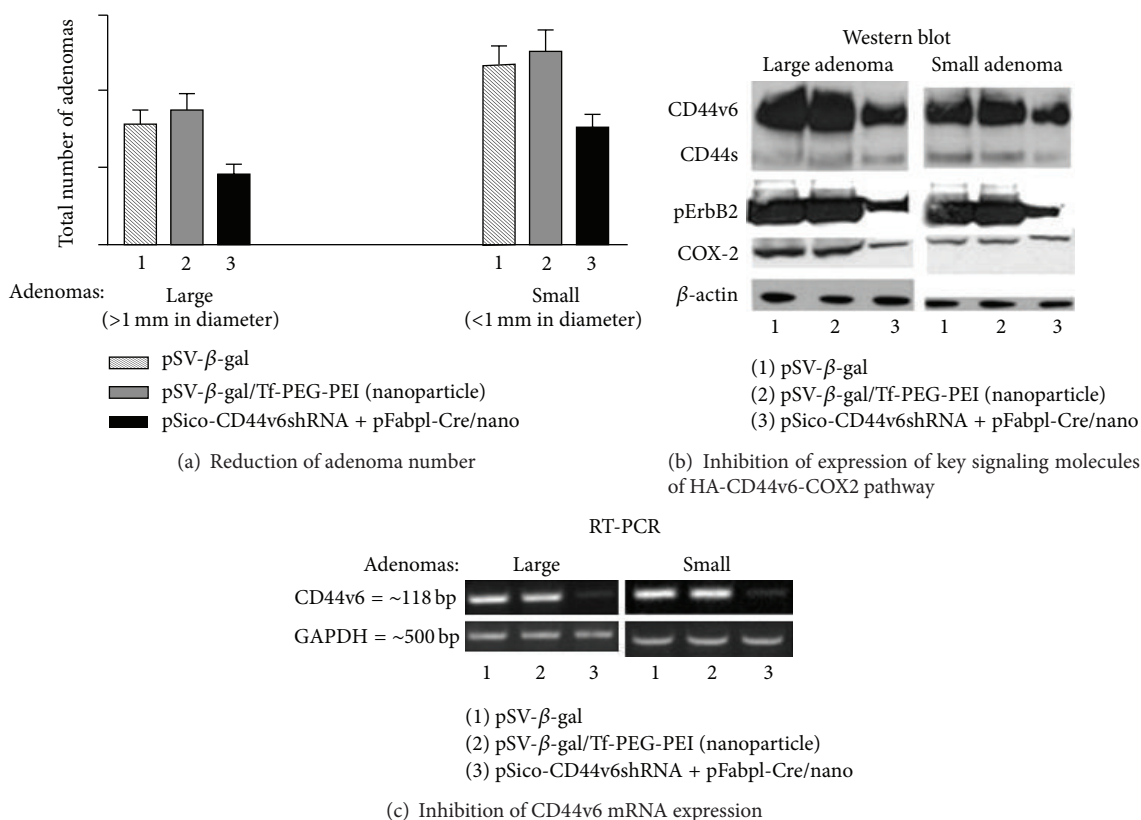


FIGURE 8: Systemic application of pSicoCD44v6shRNA plasmid in *Apc Min/+* mice. Effect of plasmid/nanoparticle treatment on protein expression, RT-PCR analysis, and number of adenomas in *Apc Min/+* mice (adapted from [43]). Thirty *Apc Min/+* mice were randomly divided into three groups. Group 1 received pSV- β -galactosidase (100 μ g/100 μ L, intraperitoneally (i.p.)) alone, Group 2 received pSV- β -gal nanoparticles (100 μ g/100 μ L, i.p.) targeted to the Tf-R, and Group 3 received pSico-CD44v6shRNA (75 μ g) plus pFabpl-Cre (25 μ g)/nanoparticles i.p. every other day. 10 days after beginning treatment, the animals were sacrificed, and the large (>1 mm) and small (<1 mm) adenomas were counted (a). The tumor and adjacent normal tissues were subsequently processed for (b) western blots for CD44, pErbB2, TERB2, COX-2, and β -actin and (c) RT-PCR analyses for CD44 variants from total RNA. Total ErbB2 remained unchanged in all the treatment groups (data not shown).

transcripts undergo complex alternative splicing of CD44 precursor mRNA under the influence of epithelial splicing regulatory protein 1 (ESRP1) [18, 70], giving rise to functionally different CD44 variant isoforms (CD44v1-v10), encoded by one single gene. Importantly, ablation of CD44v6 or ESRP1 with our CD44vshRNA/Tf-PEG-PEI-nanoparticles or ESRP1shRNA/Tf-PEG-PEI-nanoparticles will have important potential to reduce tumor growth that involves overexpression of CD44v or ESRP1, indicating the importance of tissue specific delivery of shRNA/nanoparticle technology.

Abbreviations

GAG:	Glycosaminoglycan
PG:	Proteoglycan
HA:	Hyaluronan
ECM:	Extracellular matrix
HAS:	Hyaluronan synthase
HYALS:	Hyaluronidases
shRNA:	Short hairpin RNA
Tf:	Transferrin

TfR:	Transferrin receptor
Plasmids/Tf-PEG-PEI:	Plasmids/Transferrin-polyethylene glycol-polyethylene imine.

Conflict of Interests

The authors have no conflict of interests.

Authors' Contribution

Shibnath Ghatak and Suniti Misra wrote the review. Dr. Vincent C. Hascall reviewed the draft and final paper. Dr. Roger R. Markwald edited the final paper. Ricardo Moreno Rodriguez and Ilia Atanelishvili helped to draw the figures.

Acknowledgments

This work was supported by 1R03CA167722-01A1 (to Suniti Misra and Shibnath Ghatak), P20RR021949 (to Shibnath Ghatak), P20RR016434 (to Suniti Misra, Shibnath Ghatak, and Roger R. Markwald), P20RR16461-05 (to Shibnath

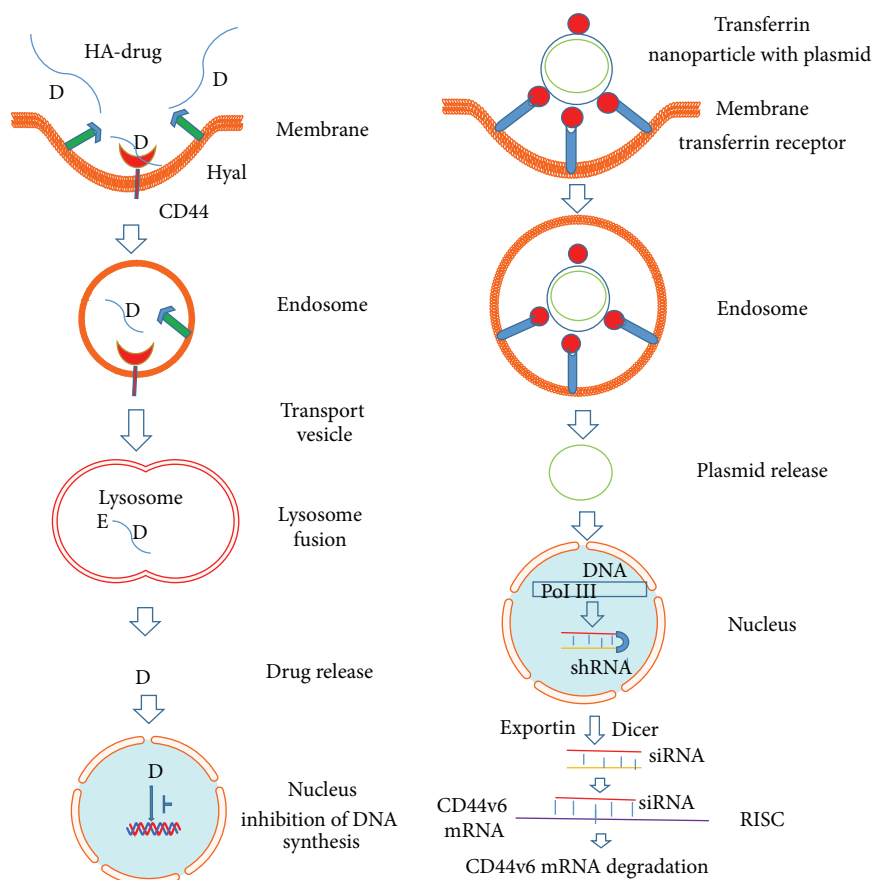


FIGURE 9: Exploitation of HA-CD44 interaction for anticancer therapy. Left panel represents the internalization of HA-drug conjugate that ultimately releases the drug that inhibits DNA synthesis of cancer cells. CD44 on the cell membrane binds the HA-drug conjugate and is internalized by endocytosis. The endosome formed is moved to the lysosome and fused. Here the HA in the conjugate is degraded first by hyaluronidase 1 (Hyal-1) into small HA oligosaccharides and next by lysosomal glycosidases to monosaccharides followed by release of the drug. The drug inhibits the DNA synthesis in the nucleus. Right panel exemplifies the steps that target the CD44v6mRNA in cancer cells by CD44v6shRNA. Plasmids producing CD44v6shRNA are coated with transferrin nanoparticles to target transferrin receptors of the cells. The particles are then internalized and form an endosome from which the plasmids are released to the nucleus where activation of DNA pol III occurs that results in CD44v6shRNA production. Through exportin, the newly produced CD44v6shRNA come out into cytoplasm where it is converted into CD44v6siRNA by dicer enzyme. One of the strands of siRNA will bind to CD44v6mRNA and forms RNA-induced silencing complex (RISC) which is ultimately degraded.

Ghatak and Roger R. Markwald), RO1-HL033756-24 (to Suniti Misra, Shibnath Ghatak, and Roger R. Markwald), P01HL107147 and 1P30AR050953 (to Vincent C. Hascall), EPS 0903795 (to Suniti Misra).

References

- [1] K. Wolf, Y. I. Wu, Y. Liu et al., "Multi-step pericellular proteolysis controls the transition from individual to collective cancer cell invasion," *Nature Cell Biology*, vol. 9, no. 8, pp. 893–904, 2007.
- [2] F. Sabeh, R. Shimizu-Hirota, and S. J. Weiss, "Protease-dependent versus-independent cancer cell invasion programs: three-dimensional amoeboid movement revisited," *The Journal of Cell Biology*, vol. 185, no. 1, pp. 11–19, 2009.
- [3] T. E. Hardingham and A. J. Fosang, "Proteoglycans: many forms and many functions," *The FASEB Journal*, vol. 6, no. 3, pp. 861–870, 1992.
- [4] B. Mulloy and C. C. Rider, "Cytokines and proteoglycans: an introductory overview," *Biochemical Society Transactions*, vol. 34, no. 3, pp. 409–413, 2006.
- [5] J. R. Bishop, M. Schuksz, and J. D. Esko, "Heparan sulphate proteoglycans fine-tune mammalian physiology," *Nature*, vol. 446, no. 7139, pp. 1030–1037, 2007.
- [6] K. Mythreya and G. C. Blobe, "Proteoglycan signaling co-receptors: roles in cell adhesion, migration and invasion," *Cellular Signalling*, vol. 21, no. 11, pp. 1548–1558, 2009.
- [7] M. Bernfield, M. Götte, P. W. Park et al., "Functions of cell surface heparan sulfate proteoglycans," *Annual Review of Biochemistry*, vol. 68, pp. 729–777, 1999.
- [8] J. Yang, M. A. Price, C. L. Neudauer et al., "Melanoma chondroitin sulfate proteoglycan enhances FAK and ERK activation by distinct mechanisms," *Journal of Cell Biology*, vol. 165, no. 6, pp. 881–891, 2004.
- [9] C. C. Reed, A. Waterhouse, S. Kirby et al., "Decorin prevents metastatic spreading of breast cancer," *Oncogene*, vol. 24, no. 6, pp. 1104–1110, 2005.

- [10] S. Ghatak, S. Misra, and B. P. Toole, "Hyaluronan constitutively regulates ErbB2 phosphorylation and signaling complex formation in carcinoma cells," *Journal of Biological Chemistry*, vol. 280, no. 10, pp. 8875–8883, 2005.
- [11] S. Misra, S. Ghatak, and B. P. Toole, "Regulation of MDR1 expression and drug resistance by a positive feedback loop involving hyaluronan, phosphoinositide 3-kinase, and ErbB2," *The Journal of Biological Chemistry*, vol. 280, no. 21, pp. 20310–20315, 2005.
- [12] S. Misra, L. M. Obeid, Y. A. Hannun et al., "Hyaluronan constitutively regulates activation of COX-2-mediated cell survival activity in intestinal epithelial and colon carcinoma cells," *Journal of Biological Chemistry*, vol. 283, no. 21, pp. 14335–14344, 2008.
- [13] S. Misra, B. P. Toole, and S. Ghatak, "Hyaluronan constitutively regulates activation of multiple receptor tyrosine kinases in epithelial and carcinoma cells," *Journal of Biological Chemistry*, vol. 281, no. 46, pp. 34936–34941, 2006.
- [14] M. A. Simpson, C. M. Wilson, and J. B. McCarthy, "Inhibition of prostate tumor cell hyaluronan synthesis impairs subcutaneous growth and vascularization in immunocompromised mice," *The American Journal of Pathology*, vol. 161, no. 3, pp. 849–857, 2002.
- [15] L. Udabage, G. R. Brownlee, M. Waltham et al., "Antisense-mediated suppression of hyaluronan synthase 2 inhibits the tumorigenesis and progression of breast cancer," *Cancer Research*, vol. 65, no. 14, pp. 6139–6150, 2005.
- [16] T. D. Camenisch, J. A. Schroeder, J. Bradley, S. E. Klewer, and J. A. McDonald, "Heart-valve mesenchyme formation is dependent on hyaluronan-augmented activation of ErbB2-ErbB3 receptors," *Nature Medicine*, vol. 8, no. 8, pp. 850–855, 2002.
- [17] T. D. Camenisch, A. P. Spicer, T. Brehm-Gibson et al., "Disruption of hyaluronan synthase-2 abrogates normal cardiac morphogenesis and hyaluronan-mediated transformation of epithelium to mesenchyme," *Journal of Clinical Investigation*, vol. 106, no. 3, pp. 349–360, 2000.
- [18] S. Misra, P. Heldin, V. C. Hascall et al., "Hyaluronan-CD44 interactions as potential targets for cancer therapy," *FEBS Journal*, vol. 278, no. 9, pp. 1429–1443, 2011.
- [19] S. Misra, V. Hascall, N. Karamanos, R. A. Markwald, and S. Ghatak, *Targeting Tumor Microenvironment in Cancer Progression*, DeGruyter, Berlin, Germany, 2012.
- [20] V. C. Hascall and T. Laurent, *Hyaluronan: Structure and Physical Properties*, 1997, <http://www.glycoforum.gr.jp>.
- [21] V. C. Hascall, A. K. Majors, C. A. De La Motte et al., "Intracellular hyaluronan: a new frontier for inflammation?" *Biochimica et Biophysica Acta—General Subjects*, vol. 1673, no. 1-2, pp. 3–12, 2004.
- [22] A. P. Spicer and J. Y. L. Tien, "Hyaluronan and morphogenesis," *Birth Defects Research Part C: Embryo Today*, vol. 72, no. 1, pp. 89–108, 2004.
- [23] P. Heldin and H. Pertoft, "Synthesis and assembly of the hyaluronan-containing coats around normal human mesothelial cells," *Experimental Cell Research*, vol. 208, no. 2, pp. 422–429, 1993.
- [24] S. P. Evanko, T. Parks, and T. N. Wight, "Intracellular hyaluronan in arterial smooth muscle cells: association with microtubules, RHAMM, and the mitotic spindle," *Journal of Histochemistry & Cytochemistry*, vol. 52, no. 12, pp. 1525–1535, 2004.
- [25] B. P. Toole, "Hyaluronan: from extracellular glue to pericellular cue," *Nature Reviews Cancer*, vol. 4, no. 7, pp. 528–539, 2004.
- [26] K. Meyer and J. W. Palmer, "The polysaccharide of the vitreous humor," *Journal of Biological Chemistry*, vol. 107, pp. 629–634, 1934.
- [27] P. Olczyk, K. Komosińska-Vassev, K. Winsz-Szczotka, K. Kuźnik-Trocha, and K. Olczyk, "Hyaluronan: structure, metabolism, functions, and role in wound healing," *Postępy Higieny i Medycyny Doświadczalnej*, vol. 62, pp. 651–659, 2008.
- [28] N. S. Gandhi and R. L. Mancera, "The structure of glycosaminoglycans and their interactions with proteins," *Chemical Biology and Drug Design*, vol. 72, no. 6, pp. 455–482, 2008.
- [29] T. C. Laurent and J. R. E. Fraser, "Hyaluronan," *The FASEB Journal*, vol. 6, no. 7, pp. 2397–2404, 1992.
- [30] W. Y. J. Chen and G. Abatangelo, "Functions of hyaluronan in wound repair," *Wound Repair and Regeneration*, vol. 7, no. 2, pp. 79–89, 1999.
- [31] P. H. Weigel and P. L. DeAngelis, "Hyaluronan synthases: a decade-plus of novel glycosyltransferases," *The Journal of Biological Chemistry*, vol. 282, no. 51, pp. 36777–36781, 2007.
- [32] R. Stern and M. J. Jedrzejak, "Hyaluronidases: their genomics, structures, and mechanisms of action," *Chemical Reviews*, vol. 106, no. 3, pp. 818–839, 2006.
- [33] S. Banerji, J. Ni, S. X. Wang et al., "LYVE-1, a new homologue of the CD44 glycoprotein, is a lymph-specific receptor for hyaluronan," *Journal of Cell Biology*, vol. 144, no. 4, pp. 789–801, 1999.
- [34] B. Zhou, J. A. Weigel, L. Fauss, and P. H. Weigel, "Identification of the hyaluronan receptor for endocytosis (HARE)," *The Journal of Biological Chemistry*, vol. 275, no. 48, pp. 37733–37741, 2000.
- [35] B. P. Toole, A. Zoltan-Jones, S. Misra, and S. Ghatak, "Hyaluronan: a critical component of epithelial-mesenchymal and epithelial-carcinoma transitions," *Cells Tissues Organs*, vol. 179, no. 1-2, pp. 66–72, 2005.
- [36] L. M. Pilarski, A. Masellis-Smith, A. R. Belch, B. Yang, R. C. Savani, and E. A. Turley, "RHAMM, a receptor for hyaluronan-mediated motility, on normal human lymphocytes, thymocytes and malignant B cells: a mediator in B cell malignancy?" *Leukemia and Lymphoma*, vol. 14, no. 5-6, pp. 363–374, 1994.
- [37] Y. Wang, H. Du, and G. Zhai, "Recent advances in active hepatic targeting drug delivery system," *Current Drug Targets*, vol. 15, no. 6, pp. 573–599, 2014.
- [38] S. Ghatak, G. S. Bogatkevich, I. Atelishvili et al., "Overexpression of c-Met and CD44v6 receptors contributes to autocrine TGF- β 1 signaling in interstitial lung disease," *Journal of Biological Chemistry*, vol. 289, no. 11, pp. 7856–7872, 2014.
- [39] S. Ghatak, V. C. Hascall, R. R. Markwald, and S. Misra, "Stromal hyaluronan interaction with epithelial CD44 variants promotes prostate cancer invasiveness by augmenting expression and function of hepatocyte growth factor and androgen receptor," *Journal of Biological Chemistry*, vol. 285, no. 26, pp. 19821–19832, 2010.
- [40] S. Ghatak, S. Misra, R. A. Norris et al., "Periostin induces intracellular cross-talk between kinases and hyaluronan in atrioventricular valvulogenesis," *The Journal of Biological Chemistry*, vol. 289, no. 12, pp. 8545–8561, 2014.
- [41] S. Ghatak, S. Misra, and B. P. Toole, "Hyaluronan oligosaccharides inhibit anchorage-independent growth of tumor cells by suppressing the phosphoinositide 3-kinase/Akt cell survival pathway," *Journal of Biological Chemistry*, vol. 277, no. 41, pp. 38013–38020, 2002.

- [42] S. Misra, V. C. Hascall, F. G. Berger, R. R. Markwald, and S. Ghatak, "Hyaluronan, CD44, and cyclooxygenase-2 in colon cancer," *Connective Tissue Research*, vol. 49, no. 3-4, pp. 219-224, 2008.
- [43] S. Misra, V. C. Hascall, C. De Giovanni, R. R. Markwald, and S. Ghatak, "Delivery of CD44 shRNA/nanoparticles within cancer cells. Perturbation of hyaluronan/CD44v6 interactions and reduction in adenoma growth in Apc Min/+mice," *Journal of Biological Chemistry*, vol. 284, no. 18, pp. 12432-12446, 2009.
- [44] S. Misra, V. C. Hascall, N. K. Karamanos, R. R. Markwald, and S. Ghatak, *Delivery Systems Targeting Cancer at the Level of ECM*, DeGruyter, Berlin, Germany, 2012.
- [45] L. Y. W. Bourguignon, K. Peyrollier, W. Xia, and E. Gilad, "Hyaluronan-CD44 interaction activates stem cell marker Nanog, Stat-3-mediated MDR1 gene expression, and ankyrin-regulated multidrug efflux in breast and ovarian tumor cells," *The Journal of Biological Chemistry*, vol. 283, no. 25, pp. 17635-17651, 2008.
- [46] L. Y. W. Bourguignon, P. A. Singleton, H. Zhu, and F. Diedrich, "Hyaluronan-mediated CD44 interaction with RhoGEF and Rho kinase promotes Grb2-associated binder-1 phosphorylation and phosphatidylinositol 3-kinase signaling leading to cytokine (macrophage-colony stimulating factor) production and breast tumor progression," *Journal of Biological Chemistry*, vol. 278, no. 32, pp. 29420-29434, 2003.
- [47] L. Y. W. Bourguignon, K. Peyrollier, E. Gilad, and A. Brightman, "Hyaluronan-CD44 interaction with neural Wiskott-Aldrich syndrome protein (N-WASP) promotes actin polymerization and ErbB2 activation leading to beta-catenin nuclear translocation, transcriptional up-regulation, and cell migration in ovarian tumor cells," *The Journal of Biological Chemistry*, vol. 282, no. 2, pp. 1265-1280, 2007.
- [48] D. Naor, S. Nedvetzki, I. Golan, L. Melnik, and Y. Faitelson, "CD44 in cancer," *Critical Reviews in Clinical Laboratory Sciences*, vol. 39, no. 6, pp. 527-579, 2002.
- [49] L. Y. W. Bourguignon, H. Zhu, L. Shao, and Y. W. Chen, "CD44 interaction with tiam1 promotes Rac1 signaling and hyaluronic acid-mediated breast tumor cell migration," *The Journal of Biological Chemistry*, vol. 275, no. 3, pp. 1829-1838, 2000.
- [50] K. Akima, H. Ito, Y. Iwata et al., "Evaluation of antitumor activities of hyaluronate binding antitumor drugs: synthesis, characterization and antitumor activity," *Journal of Drug Targeting*, vol. 4, no. 1, pp. 1-8, 1996.
- [51] J. I. Park, L. Cao, V. M. Platt et al., "Antitumor therapy mediated by 5-fluorocytosine and a recombinant fusion protein containing TSG-6 hyaluronan binding domain and yeast cytosine deaminase," *Molecular Pharmaceutics*, vol. 6, no. 3, pp. 801-812, 2009.
- [52] M.-S. Sy, Y.-J. Guo, and I. Stamenkovic, "Inhibition of tumor growth in vivo with a soluble CD44-immunoglobulin fusion protein," *The Journal of Experimental Medicine*, vol. 176, no. 2, pp. 623-627, 1992.
- [53] V. B. Lokeshwar, L. E. Lopez, D. Munoz et al., "Antitumor activity of hyaluronic acid synthesis inhibitor 4-methylumbelliferone in prostate cancer cells," *Cancer Research*, vol. 70, no. 7, pp. 2613-2623, 2010.
- [54] E. Arai, Y. Nishida, J. Wasa et al., "Inhibition of hyaluronan retention by 4-methylumbelliferone suppresses osteosarcoma cells *in vitro* and lung metastasis *in vivo*," *British Journal of Cancer*, vol. 105, no. 12, pp. 1839-1849, 2011.
- [55] H. Nakazawa, S. Yoshihara, D. Kudo et al., "4-methylumbelliferone, a hyaluronan synthase suppressor, enhances the anticancer activity of gemcitabine in human pancreatic cancer cells," *Cancer Chemotherapy and Pharmacology*, vol. 57, no. 2, pp. 165-170, 2006.
- [56] J. Klocker, H. Sabitzer, W. Raunik, S. Wieser, and J. Schumer, "Hyaluronidase as additive to induction chemotherapy in advanced squamous cell carcinoma of the head and neck," *Cancer Letters*, vol. 131, no. 1, pp. 113-115, 1998.
- [57] K. Pillwein, R. Fuiko, I. Slavc et al., "Hyaluronidase additional to standard chemotherapy improves outcome for children with malignant brain tumors," *Cancer Letters*, vol. 131, no. 1, pp. 101-108, 1998.
- [58] C. J. Whatcott, H. Han, R. G. Posner, G. Hostetter, and D. D. Von Hoff, "Targeting the tumor microenvironment in cancer: why hyaluronidase deserves a second look," *Cancer Discovery*, vol. 1, no. 4, pp. 291-296, 2011.
- [59] J. R. E. Fraser, W. G. Kimpton, T. C. Laurent, R. N. P. Cahill, and N. Vakakis, "Uptake and degradation of hyaluronan in lymphatic tissue," *Biochemical Journal*, vol. 256, no. 1, pp. 153-158, 1988.
- [60] J. R. Fraser and T. C. Laurent, "Turnover and metabolism of hyaluronan," *Ciba Foundation Symposium*, vol. 143, pp. 41-53, 1989.
- [61] G. Ostgaard and R. K. Reed, "Hyaluronan turnover in the rat small intestine," *Acta Physiologica Scandinavica*, vol. 149, no. 2, pp. 237-244, 1993.
- [62] G. Ostgaard and R. K. Reed, "Intravenous saline infusion in rat increases hyaluronan efflux in intestinal lymph by increasing lymph flow," *Acta Physiologica Scandinavica*, vol. 147, no. 3, pp. 329-335, 1993.
- [63] G. Ostgaard and R. K. Reed, "Increased lymphatic hyaluronan output and preserved hyaluronan content of the rat small intestine in prolonged hypoproteinaemia," *Acta Physiologica Scandinavica*, vol. 152, no. 1, pp. 51-56, 1994.
- [64] L. B. Dahl, T. C. Laurent, and B. Smedsrød, "Preparation of biologically intact radioiodinated hyaluronan of high specific radioactivity: coupling of ¹²⁵I-tyramine-cellobiose to amino groups after partial N-deacetylation," *Analytical Biochemistry*, vol. 175, no. 2, pp. 397-407, 1988.
- [65] J. R. E. Fraser, T. C. Laurent, H. Pertoft, and E. Baxter, "Plasma clearance, tissue distribution and metabolism of hyaluronic acid injected intravenously in the rabbit," *Biochemical Journal*, vol. 200, no. 2, pp. 415-424, 1981.
- [66] E. Feusi, L. Sun, A. Sibalic, B. Beck-Schimmer, B. Oertli, and R. P. Wüthrich, "Enhanced hyaluronan synthesis in the MRL-Fas^{lpr} kidney: role of cytokines," *Nephron*, vol. 83, no. 1, pp. 66-73, 1999.
- [67] L.-K. Sun, E. Feusi, A. Sibalic, B. Beck-Schimmer, and R. P. Wüthrich, "Expression profile of hyaluronidase mRNA transcripts in the kidney and in renal cells," *Kidney and Blood Pressure Research*, vol. 21, no. 6, pp. 413-418, 1998.
- [68] V. Sibalic, X. Fan, J. Loffing, and R. P. Wüthrich, "Upregulated renal tubular CD44, hyaluronan, and osteopontin in kdkd mice with interstitial nephritis," *Nephrology Dialysis Transplantation*, vol. 12, no. 7, pp. 1344-1353, 1997.
- [69] P. S. Benz, X. Fan, and R. P. Wüthrich, "Enhanced tubular epithelial CD44 expression in MRL-lpr lupus nephritis," *Kidney International*, vol. 50, no. 1, pp. 156-163, 1996.
- [70] H. Ponta, L. Sherman, and P. A. Herrlich, "CD44: from adhesion molecules to signalling regulators," *Nature Reviews Molecular Cell Biology*, vol. 4, no. 1, pp. 33-45, 2003.

- [71] R. van der Voort, T. E. I. Taher, V. J. M. Wielenga et al., "Heparan sulfate-modified CD44 promotes hepatocyte growth factor/scatter factor-induced signal transduction through the receptor tyrosine kinase c-Met," *The Journal of Biological Chemistry*, vol. 274, no. 10, pp. 6499–6506, 1999.
- [72] T. P. Skelton, C. Zeng, A. Nocks, and I. Stamenkovic, "Glycosylation provides both stimulatory and inhibitory effects on cell surface and soluble CD44 binding to hyaluronan," *Journal of Cell Biology*, vol. 140, no. 2, pp. 431–446, 1998.
- [73] D. Naor, S. B. Wallach-Dayana, M. A. Zahalka, and R. V. Sionov, "Involvement of CD44, a molecule with a thousand faces, in cancer dissemination," *Seminars in Cancer Biology*, vol. 18, no. 4, pp. 260–267, 2008.
- [74] C. Echiburú-Chau, D. Roy, and G. M. Calaf, "Metastatic suppressor CD44 is related with oxidative stress in breast cancer cell lines," *International Journal of Oncology*, vol. 39, no. 6, pp. 1481–1489, 2011.
- [75] J. M. V. Louderbough, J. A. Brown, R. B. Nagle, and J. A. Schroeder, "CD44 promotes epithelial mammary gland development and exhibits altered localization during cancer progression," *Genes and Cancer*, vol. 2, no. 8, pp. 771–781, 2011.
- [76] J. M. V. Louderbough and J. A. Schroeder, "Understanding the dual nature of CD44 in breast cancer progression," *Molecular Cancer Research*, vol. 9, no. 12, pp. 1573–1586, 2011.
- [77] S. V. Vinogradov, T. K. Bronich, and A. V. Kabanov, "Nanosized cationic hydrogels for drug delivery: preparation, properties and interactions with cells," *Advanced Drug Delivery Reviews*, vol. 54, no. 1, pp. 135–147, 2002.
- [78] L. Y. Qiu and Y. H. Bae, "Polymer architecture and drug delivery," *Pharmaceutical Research*, vol. 23, no. 1, pp. 1–30, 2006.
- [79] S. Svenson and D. A. Tomalia, "Dendrimers in biomedical applications—reflections on the field," *Advanced Drug Delivery Reviews*, vol. 57, no. 15, pp. 2106–2129, 2005.
- [80] U. Häcker, K. Nybakken, and N. Perrimon, "Heparan sulphate proteoglycans: the sweet side of development," *Nature Reviews Molecular Cell Biology*, vol. 6, no. 7, pp. 530–541, 2005.
- [81] R. K. Jain, L. L. Munn, and D. Fukumura, "Dissecting tumour pathophysiology using intravital microscopy," *Nature Reviews Cancer*, vol. 2, no. 4, pp. 266–276, 2002.
- [82] V. P. Chauhan, T. Stylianopoulos, Y. Boucher, and R. K. Jain, "Delivery of molecular and nanoscale medicine to tumors: transport barriers and strategies," *Annual Review of Chemical and Biomolecular Engineering*, vol. 2, pp. 281–298, 2011.
- [83] R. J. Linhardt, "2003 Claude S. Hudson award address in carbohydrate chemistry. Heparin: structure and activity," *Journal of Medicinal Chemistry*, vol. 46, no. 13, pp. 2551–2564, 2003.
- [84] K. V. Clemons, D. F. Ranney, and D. A. Stevens, "A novel heparin-coated hydrophilic preparation of amphotericin B hydrosomes," *Current Opinion in Investigational Drugs*, vol. 2, no. 4, pp. 480–487, 2001.
- [85] D. Y. Lee, Z. Khatun, J.-H. Lee, Y.-K. Lee, and I. In, "Blood compatible graphene/heparin conjugate through noncovalent chemistry," *Biomacromolecules*, vol. 12, no. 2, pp. 336–341, 2011.
- [86] Z. Khatun, M. Nurunnabi, G. R. Reeck, K. J. Cho, and Y.-K. Lee, "Oral delivery of taurocholic acid linked heparin-docetaxel conjugates for cancer therapy," *Journal of Controlled Release*, vol. 170, no. 1, pp. 74–82, 2013.
- [87] Z. Khatun, M. Nurunnabi, K. J. Cho, Y. Byun, Y. H. Bae, and Y.-K. Lee, "Oral absorption mechanism and anti-angiogenesis effect of taurocholic acid-linked heparin-docetaxel conjugates," *Journal of Controlled Release*, vol. 177, no. 1, pp. 64–73, 2014.
- [88] H. Tan, Q. Shen, X. Jia, Z. Yuan, and D. Xiong, "Injectable nanohybrid scaffold for biopharmaceuticals delivery and soft tissue engineering," *Macromolecular Rapid Communications*, vol. 33, no. 23, pp. 2015–2022, 2012.
- [89] D.-W. Tang, S.-H. Yu, Y.-C. Ho, F.-L. Mi, P.-L. Kuo, and H.-W. Sung, "Heparinized chitosan/poly(γ -glutamic acid) nanoparticles for multi-functional delivery of fibroblast growth factor and heparin," *Biomaterials*, vol. 31, no. 35, pp. 9320–9332, 2010.
- [90] X. Xu, A. K. Jha, R. L. Duncan, and X. Jia, "Heparin-decorated, hyaluronic acid-based hydrogel particles for the controlled release of bone morphogenetic protein 2," *Acta Biomaterialia*, vol. 7, no. 8, pp. 3050–3059, 2011.
- [91] P. P. Srinivasan, S. Y. McCoy, A. K. Jha et al., "Injectable perlecan domain I-hyaluronan microgels potentiate the cartilage repair effect of BMP2 in a murine model of early osteoarthritis," *Biomedical Materials*, vol. 7, no. 2, Article ID 024109, 2012.
- [92] A. R. Poole, "Proteoglycans in health and disease: structures and functions," *Biochemical Journal*, vol. 236, no. 1, pp. 1–14, 1986.
- [93] K. Prydz and K. T. Dalen, "Synthesis and sorting of proteoglycans," *Journal of Cell Science*, vol. 113, part 2, pp. 193–205, 2000.
- [94] M. Bernfield, R. Kokenyesi, M. Kato et al., "Biology of the syndecans: a family of transmembrane heparan sulfate proteoglycans," *Annual Review of Cell Biology*, vol. 8, pp. 365–393, 1992.
- [95] H. C. Christianson and M. Belting, "Heparan sulfate proteoglycan as a cell-surface endocytosis receptor," *Matrix Biology*, vol. 35, pp. 51–55, 2014.
- [96] Y.-M. Guo, M. Liu, J.-L. Yang et al., "Intercellular imaging by a polyarginine derived cell penetrating peptide labeled magnetic resonance contrast agent, diethylenetriamine pentaacetic acid gadolinium," *Chinese Medical Journal*, vol. 120, no. 1, pp. 50–55, 2007.
- [97] T. Letohto, A. Keller-Pintér, E. Kusz et al., "Cell-penetrating peptide exploited syndecans," *Biochimica et Biophysica Acta*, vol. 1798, no. 12, pp. 2258–2265, 2010.
- [98] J. Wang, Z. Lu, M. G. Wientjes, and J. L.-S. Au, "Delivery of siRNA therapeutics: barriers and carriers," *AAPS Journal*, vol. 12, no. 4, pp. 492–503, 2010.
- [99] F. Said Hassane, A. F. Saleh, R. Abes, M. J. Gait, and B. Lebleu, "Cell penetrating peptides: overview and applications to the delivery of oligonucleotides," *Cellular and Molecular Life Sciences*, vol. 67, no. 5, pp. 715–726, 2010.
- [100] N. A. Brooks, D. S. Pouniotis, K. C. Sheng, V. Apostolopoulos, and G. A. Pietersz, "A membrane penetrating multiple antigen peptide (MAP) incorporating ovalbumin CD8 epitope induces potent immune responses in mice," *Biochimica et Biophysica Acta—Biomembranes*, vol. 1798, no. 12, pp. 2286–2295, 2010.
- [101] N. A. Brooks, D. S. Pouniotis, C.-K. Tang, V. Apostolopoulos, and G. A. Pietersz, "Cell-penetrating peptides: application in vaccine delivery," *Biochimica et Biophysica Acta*, vol. 1805, no. 1, pp. 25–34, 2010.
- [102] M. M. Fretz and G. Storm, "TAT-peptide modified liposomes: preparation, characterization, and cellular interaction," *Methods in Molecular Biology*, vol. 605, pp. 349–359, 2010.
- [103] L. N. Patel, J. Wang, K.-J. Kim, Z. Borok, E. D. Crandall, and W.-C. Shen, "Conjugation with cationic cell-penetrating peptide increases pulmonary absorption of insulin," *Molecular Pharmaceutics*, vol. 6, no. 2, pp. 492–503, 2009.
- [104] J. Kleeff, T. Ishiwata, A. Kumbasar et al., "The cell-surface heparan sulfate proteoglycan glypican-1 regulates growth factor action in pancreatic carcinoma cells and is overexpressed in human pancreatic cancer," *Journal of Clinical Investigation*, vol. 102, no. 9, pp. 1662–1673, 1998.

- [105] B. Sharma, M. Handler, I. Eichstetter, J. M. Whitelock, M. A. Nugent, and R. V. Iozzo, "Antisense targeting of perlecan blocks tumor growth and angiogenesis in vivo," *The Journal of Clinical Investigation*, vol. 102, no. 8, pp. 1599–1608, 1998.
- [106] J. H. Grubb, C. Vogler, and W. S. Sly, "New strategies for enzyme replacement therapy for lysosomal storage diseases," *Rejuvenation Research*, vol. 13, no. 2-3, pp. 229–236, 2010.
- [107] J. E. Wraith, "Lysosomal disorders," *Seminars in Neonatology*, vol. 7, no. 1, pp. 75–83, 2002.
- [108] K. Hamada, C. Yoshihara, T. Ito et al., "Antitumor effect of chondroitin sulfate-coated ternary granulocyte macrophage-colony-stimulating factor plasmid complex for ovarian cancer," *Journal of Gene Medicine*, vol. 14, no. 2, pp. 120–127, 2012.
- [109] Z. Liu, Y. Jiao, Y. Wang, C. Zhou, and Z. Zhang, "Polysaccharides-based nanoparticles as drug delivery systems," *Advanced Drug Delivery Reviews*, vol. 60, no. 15, pp. 1650–1662, 2008.
- [110] V. R. Sinha and R. Kumria, "Polysaccharides in colon-specific drug delivery," *International Journal of Pharmaceutics*, vol. 224, no. 1-2, pp. 19–38, 2001.
- [111] K. S. Soppimath, T. M. Aminabhavi, A. R. Kulkarni, and W. E. Rudzinski, "Biodegradable polymeric nanoparticles as drug delivery devices," *Journal of Controlled Release*, vol. 70, no. 1-2, pp. 1–20, 2001.
- [112] S. Mitra, U. Gaur, P. C. Ghosh, and A. N. Maitra, "Tumour targeted delivery of encapsulated dextran-doxorubicin conjugate using chitosan nanoparticles as carrier," *Journal of Controlled Release*, vol. 74, no. 1–3, pp. 317–323, 2001.
- [113] C.-T. Lee, C.-P. Huang, and Y.-D. Lee, "Preparation of amphiphilic poly(L-lactide)-graft-chondroitin sulfate copolymer self-aggregates and its aggregation behavior," *Biomacromolecules*, vol. 7, no. 4, pp. 1179–1186, 2006.
- [114] G. Mocanu, D. Mihai, L. Picton, D. LeCerf, and G. Muller, "Associative pullulan gels and their interaction with biological active substances," *Journal of Controlled Release*, vol. 83, no. 1, pp. 41–51, 2002.
- [115] M. R. Campoli, C.-C. Chang, T. Kageshita, X. Wang, J. B. McCarthy, and S. Ferrone, "Human high molecular weight-melanoma-associated antigen (HMW-MAA): a melanoma cell surface chondroitin sulfate proteoglycan (MSCP) with biological and clinical significance," *Critical Reviews in Immunology*, vol. 24, no. 4, pp. 267–296, 2004.
- [116] J. Yang, M. A. Price, Y. L. Gui et al., "Melanoma proteoglycan modifies gene expression to stimulate tumor cell motility, growth, and epithelial-to-mesenchymal transition," *Cancer Research*, vol. 69, no. 19, pp. 7538–7547, 2009.
- [117] J. Iida, K. L. Wilhelmson, J. Ng et al., "Cell surface chondroitin sulfate glycosaminoglycan in melanoma: role in the activation of pro-MMP-2 (pro-gelatinase A)," *Biochemical Journal*, vol. 403, no. 3, pp. 553–563, 2007.
- [118] C.-C. Chang, M. Campoli, W. Luo, W. Zhao, K. S. Zaenker, and S. Ferrone, "Immunotherapy of melanoma targeting human high molecular weight melanoma-associated antigen: potential role of nonimmunological mechanisms," *Annals of the New York Academy of Sciences*, vol. 1028, pp. 340–350, 2004.
- [119] M. Schwenkert, K. Birkholz, M. Schwemmlin et al., "A single chain immunotoxin, targeting the melanoma-associated chondroitin sulfate proteoglycan, is a potent inducer of apoptosis in cultured human melanoma cells," *Melanoma Research*, vol. 18, no. 2, pp. 73–84, 2008.
- [120] J. Xi, L. Zhou, and Y. Fei, "Preparation of chondroitin sulfate nanocapsules for use as carries by the interfacial polymerization method," *International Journal of Biological Macromolecules*, vol. 50, no. 1, pp. 157–163, 2012.
- [121] J. Xi, J. Qin, and L. Fan, "Chondroitin sulfate functionalized mesostructured silica nanoparticles as biocompatible carriers for drug delivery," *International Journal of Nanomedicine*, vol. 7, pp. 5235–5247, 2012.
- [122] W. Park, S.-J. Park, and K. Na, "Potential of self-organizing nanogel with acetylated chondroitin sulfate as an anti-cancer drug carrier," *Colloids and Surfaces B: Biointerfaces*, vol. 79, no. 2, pp. 501–508, 2010.
- [123] S.-J. Huang, S.-L. Sun, T.-H. Feng, K.-H. Sung, W.-L. Lui, and L.-F. Wang, "Folate-mediated chondroitin sulfate-Pluronic 127 nanogels as a drug carrier," *European Journal of Pharmaceutical Sciences*, vol. 38, no. 1, pp. 64–73, 2009.
- [124] G. Mascellani, L. Liverani, P. Bianchini et al., "Structure and contribution to the heparin cofactor II-mediated inhibition of thrombin of naturally oversulphated sequences of dermatan sulphate," *Biochemical Journal*, vol. 296, no. 3, pp. 639–648, 1993.
- [125] K. Meyer, A. Linker, E. A. Davidson, and B. Weissmann, "The mucopolysaccharides of bovine cornea," *The Journal of Biological Chemistry*, vol. 205, no. 2, pp. 611–616, 1953.
- [126] J. R. Hassell, D. A. Newsome, J. H. Krachmer, and M. M. Rodrigues, "Macular corneal dystrophy: failure to synthesize a mature keratan sulfate proteoglycan," *Proceedings of the National Academy of Sciences of the United States of America*, vol. 77, no. 6, pp. 3705–3709, 1980.
- [127] T. C. Li, J. D. Aplin, A. Warren, R. A. Graham, P. Dockery, and I. D. Cooke, "Endometrial responses to three different progestins in artificial cycles: a prospective, crossover study," *Fertility and Sterility*, vol. 62, no. 1, pp. 191–193, 1994.
- [128] R. A. Graham, T. C. Li, I. D. Cooke, and J. D. Aplin, "Keratan sulphate as a secretory product of human endometrium: cyclic expression in normal women," *Human Reproduction*, vol. 9, no. 5, pp. 926–930, 1994.
- [129] J. L. Funderburgh, "Keratan sulfate: structure, biosynthesis, and function," *Glycobiology*, vol. 10, no. 10, pp. 951–958, 2000.
- [130] J. L. Funderburgh, M. L. Funderburgh, M. M. Mann, and G. W. Conrad, "Physical and biological properties of keratan sulphate proteoglycan," *Biochemical Society Transactions*, vol. 19, no. 4, pp. 871–876, 1991.
- [131] V. C. Hascall, "Structure and biosynthesis of proteoglycans with keratan sulfate," *Progress in Clinical and Biological Research*, vol. 110, pp. 3–15, 1982.
- [132] H. Greiling, "Structure and biological functions of keratan sulfate proteoglycans," *EXS*, vol. 70, pp. 101–122, 1994.
- [133] S. Tomatsu, A. M. Montão, V. C. Dung et al., "Enhancement of drug delivery: enzyme-replacement therapy for murine Morquio A syndrome," *Molecular Therapy*, vol. 18, no. 6, pp. 1094–1102, 2010.
- [134] S. Liu, M.-N. Jin, Y.-S. Quan et al., "The development and characteristics of novel microneedle arrays fabricated from hyaluronic acid, and their application in the transdermal delivery of insulin," *Journal of Controlled Release*, vol. 161, no. 3, pp. 933–941, 2012.
- [135] A. R. Mathers and A. T. Larregina, "Professional antigen-presenting cells of the skin," *Immunologic Research*, vol. 36, no. 1–3, pp. 127–136, 2006.
- [136] K. Sugita, K. Kabashima, K. Atarashi, T. Shimauchi, M. Kobayashi, and Y. Tokura, "Innate immunity mediated by epidermal keratinocytes promotes acquired immunity involving Langerhans cells and T cells in the skin," *Clinical & Experimental Immunology*, vol. 147, no. 1, pp. 176–183, 2007.

- [137] C. L. Berger, J. G. Vasquez, J. Shofner, K. Mariwalla, and R. L. Edelson, "Langerhans cells: mediators of immunity and tolerance," *International Journal of Biochemistry and Cell Biology*, vol. 38, no. 10, pp. 1632–1636, 2006.
- [138] N. Romani, B. E. Clausen, and P. Stoitzner, "Langerhans cells and more: langerin-expressing dendritic cell subsets in the skin," *Immunological Reviews*, vol. 234, no. 1, pp. 120–141, 2010.
- [139] J.-H. Park, M. G. Allen, and M. R. Prausnitz, "Biodegradable polymer microneedles: fabrication, mechanics and transdermal drug delivery," *Journal of Controlled Release*, vol. 104, no. 1, pp. 51–66, 2005.
- [140] J. W. Lee, J.-H. Park, and M. R. Prausnitz, "Dissolving microneedles for transdermal drug delivery," *Biomaterials*, vol. 29, no. 13, pp. 2113–2124, 2008.
- [141] S. P. Sullivan, D. G. Koutsonanos, M. del Pilar Martin et al., "Dissolving polymer microneedle patches for influenza vaccination," *Nature Medicine*, vol. 16, no. 8, pp. 915–920, 2010.
- [142] K. Matsuo, S. Hirobe, Y. Yokota et al., "Transcutaneous immunization using a dissolving microneedle array protects against tetanus, diphtheria, malaria, and influenza," *Journal of Controlled Release*, vol. 160, no. 3, pp. 495–501, 2012.
- [143] F. J. Verbaan, S. M. Bal, D. J. van den Berg et al., "Assembled microneedle arrays enhance the transport of compounds varying over a large range of molecular weight across human dermatomed skin," *Journal of Controlled Release*, vol. 117, no. 2, pp. 238–245, 2007.
- [144] T. J. Brown, D. Alcorn, and J. R. E. Fraser, "Absorption of hyaluronan applied to the surface of intact skin," *Journal of Investigative Dermatology*, vol. 113, no. 5, pp. 740–746, 1999.
- [145] M. B. Brown and S. A. Jones, "Hyaluronic acid: a unique topical vehicle for the localized delivery of drugs to the skin," *Journal of the European Academy of Dermatology and Venereology*, vol. 19, no. 3, pp. 308–318, 2005.
- [146] J. J. Skehel and M. D. Waterfield, "Studies on the primary structure of the influenza virus hemagglutinin," *Proceedings of the National Academy of Sciences of the United States of America*, vol. 72, no. 1, pp. 93–97, 1975.
- [147] J. W. Shupp, T. J. Nasabzadeh, D. S. Rosenthal, M. H. Jordan, P. Fidler, and J. C. Jeng, "A review of the local pathophysiologic bases of burn wound progression," *Journal of Burn Care and Research*, vol. 31, no. 6, pp. 849–873, 2010.
- [148] G. Arturson, "Pathophysiology of the burn wound and pharmacological treatment. The Rudi Hermans Lecture, 1995," *Burns*, vol. 22, no. 4, pp. 255–274, 1996.
- [149] M. G. Schwacha, B. M. Thobe, T. Daniel, and W. J. Hubbard, "Impact of thermal injury on wound infiltration and the dermal inflammatory response," *Journal of Surgical Research*, vol. 158, no. 1, pp. 112–120, 2010.
- [150] M. S. Pandey, B. A. Baggenstoss, J. Washburn, E. N. Harris, and P. H. Weigel, "The hyaluronan receptor for endocytosis (HARE) activates NF- κ B-mediated gene expression in response to 40–400-kDa, but not smaller or larger, hyaluronans," *Journal of Biological Chemistry*, vol. 288, no. 20, pp. 14068–14079, 2013.
- [151] L. T. Sun, E. Friedrich, J. L. Heuslein et al., "Reduction of burn progression with topical delivery of (antitumor necrosis factor- α)-hyalurononic acid conjugates," *Wound Repair and Regeneration*, vol. 20, no. 4, pp. 563–572, 2012.
- [152] C. Le Boultais, L. Acar, H. Zia, P. A. Sado, T. Needham, and R. Leverage, "Ophthalmic drug delivery systems—recent advances," *Progress in Retinal and Eye Research*, vol. 17, no. 1, pp. 33–58, 1998.
- [153] E. L. Graue, F. M. Polack, and E. A. Balazs, "The protective effect of Na-hyaluronate to corneal endothelium," *Experimental Eye Research*, vol. 31, no. 1, pp. 119–127, 1980.
- [154] R. Gurny, J. E. Ryser, C. Tabatabay, M. Martenet, P. Edman, and O. Camber, "Precorneal residence time in humans of sodium hyaluronate as measured by gamma scintigraphy," *Graefes Archive for Clinical and Experimental Ophthalmology*, vol. 228, no. 6, pp. 510–512, 1990.
- [155] J. A. P. Gomes, R. Amankwah, A. Powell-Richards, and H. S. Dua, "Sodium hyaluronate (hyaluronic acid) promotes migration of human corneal epithelial cells in vitro," *British Journal of Ophthalmology*, vol. 88, no. 6, pp. 821–825, 2004.
- [156] E. Tani, C. Katakami, and A. Negi, "Effects of various eye drops on corneal wound healing after superficial keratectomy in rabbits," *Japanese Journal of Ophthalmology*, vol. 46, no. 5, pp. 488–495, 2002.
- [157] T. C. Laurent, U. B. G. Laurent, and J. R. E. Fraser, "The structure and function of hyaluronan: an overview," *Immunology & Cell Biology*, vol. 74, no. 2, pp. A1–A7, 1996.
- [158] M. F. Saettone, D. Monti, M. T. Torracca, and P. Chetoni, "Mucoadhesive ophthalmic vehicles: evaluation of polymeric low-viscosity formulations," *Journal of Ocular Pharmacology*, vol. 10, no. 1, pp. 83–92, 1994.
- [159] O. Camber, P. Edman, and R. Gurny, "Influence of sodium hyaluronate on the meiotic effect of pilocarpine in rabbits," *Current Eye Research*, vol. 6, no. 6, pp. 779–784, 1987.
- [160] C. Bucolo and P. Mangiafico, "Pharmacological profile of a new topical pilocarpine formulation," *Journal of Ocular Pharmacology and Therapeutics*, vol. 15, no. 6, pp. 567–573, 1999.
- [161] C. Bucolo, S. Mangiafico, and A. Spadaro, "Methylprednisolone delivery by Hyalobend corneal shields and its effects on rabbit ocular inflammation," *Journal of Ocular Pharmacology and Therapeutics*, vol. 12, no. 2, pp. 141–149, 1996.
- [162] R. Herrero-Vanrell, A. Fernandez-Carballido, G. Frutos, and R. Cadorniga, "Enhancement of the mydriatic response to tropicamide by bioadhesive polymers," *Journal of Ocular Pharmacology and Therapeutics*, vol. 16, no. 5, pp. 419–428, 2000.
- [163] S. A. Gandolfi, A. Massari, and J. G. Orsoni, "Low-molecular-weight sodium hyaluronate in the treatment of bacterial corneal ulcers," *Graefes Archive for Clinical and Experimental Ophthalmology*, vol. 230, no. 1, pp. 20–23, 1992.
- [164] K. Y. Cho, T. W. Chung, B. C. Kim et al., "Release of ciprofloxacin from poloxamer-graft-hyaluronic acid hydrogels in vitro," *International Journal of Pharmaceutics*, vol. 260, no. 1, pp. 83–91, 2003.
- [165] K. Y. Choi, G. Saravanakumar, J. H. Park, and K. Park, "Hyaluronic acid-based nanocarriers for intracellular targeting: interfacial interactions with proteins in cancer," *Colloids and Surfaces B: Biointerfaces*, vol. 99, pp. 82–94, 2012.
- [166] T. Pouyani and G. D. Prestwich, "Functionalized derivatives of hyaluronic acid oligosaccharides: drug carriers and novel biomaterials," *Bioconjugate Chemistry*, vol. 5, no. 4, pp. 339–347, 1994.
- [167] M. B. Duncan, M. Liu, C. Fox, and J. Liu, "Characterization of the N-deacetylase domain from the heparan sulfate N-deacetylase/N-sulfotransferase 2," *Biochemical and Biophysical Research Communications*, vol. 339, no. 4, pp. 1232–1237, 2006.
- [168] S. Mochizuki, A. Kano, N. Shimada, and A. Maruyama, "Uptake of enzymatically-digested hyaluronan by liver endothelial cells in vivo and in vitro," *Journal of Biomaterials Science, Polymer Edition*, vol. 20, no. 1, pp. 83–97, 2009.

- [169] E. N. Harris, S. V. Kyosseva, J. A. Weigel, and P. H. Weigel, "Expression, processing, and glycosaminoglycan binding activity of the recombinant human 315-kDa Hyaluronic Acid Receptor for Endocytosis (HARE)," *The Journal of Biological Chemistry*, vol. 282, no. 5, pp. 2785–2797, 2007.
- [170] E. Ruoslahti, S. N. Bhatia, and M. J. Sailor, "Targeting of drugs and nanoparticles to tumors," *The Journal of Cell Biology*, vol. 188, no. 6, pp. 759–768, 2010.
- [171] J. Lesley, V. C. Hascall, M. Tammi, and R. Hyman, "Hyaluronan binding by cell surface CD44," *Journal of Biological Chemistry*, vol. 275, no. 35, pp. 26967–26975, 2000.
- [172] Y. Luo and G. D. Prestwich, "Synthesis and selective cytotoxicity of a hyaluronic acid-antitumor bioconjugate," *Bioconjugate Chemistry*, vol. 10, no. 5, pp. 755–763, 1999.
- [173] D. Coradini, C. Pellizzaro, G. Miglierini, M. G. Daidone, and A. Perbellini, "Hyaluronic acid as drug delivery for sodium butyrate: improvement of the anti-proliferative activity on a breast-cancer cell line," *International Journal of Cancer*, vol. 81, no. 3, pp. 411–416, 1999.
- [174] J. Gaffney, S. Matou-Nasri, M. Grau-Olivares, and M. Slevin, "Therapeutic applications of hyaluronan," *Molecular BioSystems*, vol. 6, no. 3, pp. 437–443, 2010.
- [175] V. M. Platt and F. C. Szoka Jr., "Anticancer therapeutics: targeting macromolecules and nanocarriers to hyaluronan or CD44, a hyaluronan receptor," *Molecular Pharmaceutics*, vol. 5, no. 4, pp. 474–486, 2008.
- [176] Y. Luo, M. R. Ziebell, and G. D. Prestwich, "A hyaluronic acid—taxol antitumor bioconjugate targeted to cancer cells," *Biomacromolecules*, vol. 1, no. 2, pp. 208–218, 2000.
- [177] A. Rosato, A. Banzato, G. de Luca et al., "HYTAD1-p20: a new paclitaxel-hyaluronic acid hydrosoluble bioconjugate for treatment of superficial bladder cancer," *Urologic Oncology*, vol. 24, no. 3, pp. 207–215, 2006.
- [178] A. Serafino, M. Zonfrillo, F. Andreola et al., "CD44-targeting for antitumor drug delivery: a new SN-38-hyaluronan bioconjugate for locoregional treatment of peritoneal carcinomatosis," *Current Cancer Drug Targets*, vol. 11, no. 5, pp. 572–585, 2011.
- [179] P. F. Bassi, A. Volpe, D. D'Agostino et al., "Paclitaxel-hyaluronic acid for intravesical therapy of bacillus Calmette-Guerin refractory carcinoma in situ of the bladder: results of a phase I study," *Journal of Urology*, vol. 185, no. 2, pp. 445–449, 2011.
- [180] I. M. Montagner, A. Banzato, G. Zuccolotto et al., "Paclitaxel-hyaluronan hydrosoluble bioconjugate: mechanism of action in human bladder cancer cell lines," *Urologic Oncology*, vol. 31, no. 7, pp. 1261–1269, 2013.
- [181] Y. Luo, K. R. Kirker, and G. D. Prestwich, "Cross-linked hyaluronic acid hydrogel films: new biomaterials for drug delivery," *Journal of Controlled Release*, vol. 69, no. 1, pp. 169–184, 2000.
- [182] G. Tringali, F. Bettella, M. C. Greco, M. Campisi, D. Renier, and P. Navarra, "Pharmacokinetic profile of Oncofid-S after intraperitoneal and intravenous administration in the rat," *Journal of Pharmacy and Pharmacology*, vol. 64, no. 3, pp. 360–365, 2012.
- [183] S. M. Cohen, N. Rockefeller, R. Mukerji et al., "Efficacy and toxicity of peritumoral delivery of nanoconjugated cisplatin in an *in vivo* murine model of head and neck squamous cell carcinoma," *JAMA Otolaryngology: Head and Neck Surgery*, vol. 139, no. 4, pp. 382–387, 2013.
- [184] T. J. Brown, "The development of hyaluronan as a drug transporter and excipient for chemotherapeutic drugs," *Current Pharmaceutical Biotechnology*, vol. 9, no. 4, pp. 253–260, 2008.
- [185] M. A. Rosenthal, P. Gibbs, T. J. Brown et al., "Phase I and pharmacokinetic evaluation of intravenous hyaluronic acid in combination with doxorubicin or 5-fluorouracil," *Chemotherapy*, vol. 51, no. 2-3, pp. 132–141, 2005.
- [186] P. Gibbs, T. J. Brown, R. Ng et al., "A pilot human evaluation of a formulation of irinotecan and hyaluronic acid in 5-fluorouracil-refractory metastatic colorectal cancer patients," *Chemotherapy*, vol. 55, no. 1, pp. 49–59, 2009.
- [187] O. P. Varghese, W. Sun, J. Hilborn, and D. A. Ossipov, "In situ cross-linkable high molecular weight hyaluronan-bisphosphonate conjugate for localized delivery and cell-specific targeting: a hydrogel linked prodrug approach," *Journal of the American Chemical Society*, vol. 131, no. 25, pp. 8781–8783, 2009.
- [188] C. Di Meo, L. Panza, D. Capitani et al., "Hyaluronan as carrier of carboranes for tumor targeting in boron neutron capture therapy," *Biomacromolecules*, vol. 8, no. 2, pp. 552–559, 2007.
- [189] C. di Meo, L. Panza, F. Campo et al., "Novel types of carborane-carrier hyaluronan derivatives via 'click chemistry,'" *Macromolecular Bioscience*, vol. 8, no. 7, pp. 670–681, 2008.
- [190] A. Jain and S. K. Jain, "In vitro and cell uptake studies for targeting of ligand anchored nanoparticles for colon tumors," *European Journal of Pharmaceutical Sciences*, vol. 35, no. 5, pp. 404–416, 2008.
- [191] A. Jain, S. K. Jain, N. Ganesh, J. Barve, and A. M. Beg, "Design and development of ligand-appended polysaccharidic nanoparticles for the delivery of oxaliplatin in colorectal cancer," *Nanomedicine: Nanotechnology, Biology, and Medicine*, vol. 6, no. 1, pp. e179–e190, 2010.
- [192] G. Bachar, K. Cohen, R. Hod et al., "Hyaluronan-grafted particle clusters loaded with Mitomycin C as selective nanovectors for primary head and neck cancers," *Biomaterials*, vol. 32, no. 21, pp. 4840–4848, 2011.
- [193] D. Peer and R. Margalit, "Loading mitomycin C inside long circulating hyaluronan targeted nano-liposomes increases its antitumor activity in three mice tumor models," *International Journal of Cancer*, vol. 108, no. 5, pp. 780–789, 2004.
- [194] D. Peer and R. Margalit, "Tumor-targeted hyaluronan nanoliposomes increase the antitumor activity of liposomal doxorubicin in syngeneic and human xenograft mouse tumor models," *Neoplasia*, vol. 6, no. 4, pp. 343–353, 2004.
- [195] C. Surace, S. Arpicco, A. Dufay-Wojcicki et al., "Lipoplexes targeting the CD44 hyaluronic acid receptor for efficient transfection of breast cancer cells," *Molecular Pharmaceutics*, vol. 6, no. 4, pp. 1062–1073, 2009.
- [196] R. E. Eliaz and F. C. Szoka Jr., "Liposome-encapsulated doxorubicin targeted to CD44: a strategy to kill CD44-overexpressing tumor cells," *Cancer Research*, vol. 61, no. 6, pp. 2592–2601, 2001.
- [197] D. Ruhela, K. Riviere, and F. C. Szoka Jr., "Efficient synthesis of an aldehyde functionalized hyaluronic acid and its application in the preparation of hyaluronan-lipid conjugates," *Bioconjugate Chemistry*, vol. 17, no. 5, pp. 1360–1363, 2006.
- [198] A. Dufay Wojcicki, H. Hillaireau, T. L. Nascimento et al., "Hyaluronic acid-bearing lipoplexes: physico-chemical characterization and in vitro targeting of the CD44 receptor," *Journal of Controlled Release*, vol. 162, no. 3, pp. 545–552, 2012.
- [199] Y. Liu, J. Sun, W. Cao et al., "Dual targeting folate-conjugated hyaluronic acid polymeric micelles for paclitaxel delivery," *International Journal of Pharmaceutics*, vol. 421, no. 1, pp. 160–169, 2011.

- [200] L. Qiu, Z. Li, M. Qiao et al., "Self-assembled pH-responsive hyaluronic acid-g-poly(l-histidine) copolymer micelles for targeted intracellular delivery of doxorubicin," *Acta Biomaterialia*, vol. 10, no. 5, pp. 2024–2035, 2014.
- [201] Y. Zhang, H. Zhang, X. Wang, J. Wang, X. Zhang, and Q. Zhang, "The eradication of breast cancer and cancer stem cells using octreotide modified paclitaxel active targeting micelles and salinomycin passive targeting micelles," *Biomaterials*, vol. 33, no. 2, pp. 679–691, 2012.
- [202] H. Lee, H. Mok, S. Lee, Y.-K. Oh, and T. G. Park, "Target-specific intracellular delivery of siRNA using degradable hyaluronic acid nanogels," *Journal of Controlled Release*, vol. 119, no. 2, pp. 245–252, 2007.
- [203] T. Pellegrino, S. Kudera, T. Liedl, A. M. Javier, L. Manna, and W. J. Parak, "On the development of colloidal nanoparticles towards multifunctional structures and their possible use for biological applications," *Small*, vol. 1, no. 1, pp. 48–63, 2005.
- [204] R. Tenne, "Inorganic nanotubes and fullerene-like nanoparticles," *Nature Nanotechnology*, vol. 1, no. 2, pp. 103–111, 2006.
- [205] S. N. Baker and G. A. Baker, "Luminescent carbon nanodots: emergent nanolights," *Angewandte Chemie*, vol. 49, no. 38, pp. 6726–6744, 2010.
- [206] A. K. Geim, "Graphene: status and prospects," *Science*, vol. 324, no. 5934, pp. 1530–1534, 2009.
- [207] M.-Y. Lee, J.-A. Yang, H. S. Jung et al., "Hyaluronic acid-gold nanoparticle/interferon α complex for targeted treatment of hepatitis C virus infection," *ACS Nano*, vol. 6, no. 11, pp. 9522–9531, 2012.
- [208] A. Kumar, B. Sahoo, A. Montpetit, S. Behera, R. F. Lockey, and S. S. Mohapatra, "Development of hyaluronic acid-Fe₂O₃ hybrid magnetic nanoparticles for targeted delivery of peptides," *Nanomedicine: Nanotechnology, Biology, and Medicine*, vol. 3, no. 2, pp. 132–137, 2007.
- [209] J. Lu, M. Liang, Z. Li, J. I. Zink, and F. Tamanoi, "Biocompatibility, biodistribution, and drug-delivery efficiency of mesoporous silica nanoparticles for cancer therapy in animals," *Small*, vol. 6, no. 16, pp. 1794–1805, 2010.
- [210] H.-J. Cho, H. Y. Yoon, H. Koo et al., "Self-assembled nanoparticles based on hyaluronic acid-ceramide (HA-CE) and Pluronic for tumor-targeted delivery of docetaxel," *Biomaterials*, vol. 32, no. 29, pp. 7181–7190, 2011.
- [211] J. Lesley, N. English, C. Charles, and R. Hyman, "The role of the CD44 cytoplasmic and transmembrane domains in constitutive and inducible hyaluronan binding," *European Journal of Immunology*, vol. 30, no. 1, pp. 245–253, 2000.
- [212] J. Lesley and R. Hyman, "CD44 can be activated to function as a hyaluronic acid receptor in normal murine T cells," *European Journal of Immunology*, vol. 22, no. 10, pp. 2719–2723, 1992.
- [213] M. Culty, H. A. Nguyen, and C. B. Underhill, "The hyaluronan receptor (CD44) participates in the uptake and degradation of hyaluronan," *The Journal of Cell Biology*, vol. 116, no. 4, pp. 1055–1062, 1992.
- [214] J. Cichy and E. Puré, "The liberation of CD44," *Journal of Cell Biology*, vol. 161, no. 5, pp. 839–843, 2003.
- [215] M. Allouche, R. S. Charrad, A. Bettaieb, C. Greenland, C. Grignon, and F. Smadja-Joffe, "Ligation of the CD44 adhesion molecule inhibits drug-induced apoptosis in human myeloid leukemia cells," *Blood*, vol. 96, no. 3, pp. 1187–1190, 2000.
- [216] S. Legras, J.-P. Lévesque, R. Charrad et al., "CD44-mediated adhesiveness of human hematopoietic progenitors to hyaluronan is modulated by cytokines," *Blood*, vol. 89, no. 6, pp. 1905–1914, 1997.
- [217] S. Katoh, Z. Zheng, K. Oritani, T. Shimozato, and P. W. Kincade, "Glycosylation of CD44 negatively regulates its recognition of hyaluronan," *Journal of Experimental Medicine*, vol. 182, no. 2, pp. 419–429, 1995.
- [218] Q. He, J. Lesley, R. Hyman, K. Ishihara, and P. W. Kincade, "Molecular isoforms of murine CD44 and evidence that the membrane proximal domain is not critical for hyaluronate recognition," *Journal of Cell Biology*, vol. 119, no. 6, pp. 1711–1719, 1992.
- [219] J. Sleeman, W. Rudy, M. Hofmann, J. Moll, P. Herrlich, and H. Ponta, "Regulated clustering of variant CD44 proteins increases their hyaluronate binding capacity," *Journal of Cell Biology*, vol. 135, no. 4, pp. 1139–1150, 1996.
- [220] J. P. Sleeman, S. Arming, J. F. Moll et al., "Hyaluronate-independent metastatic behavior of CD44 variant-expressing pancreatic carcinoma cells," *Cancer Research*, vol. 56, no. 13, pp. 3134–3141, 1996.
- [221] J. P. Sleeman, K. Kondo, J. Moll, H. Ponta, and P. Herrlich, "Variant exons v6 and v7 together expand the repertoire of glycosaminoglycans bound by CD44," *The Journal of Biological Chemistry*, vol. 272, no. 50, pp. 31837–31844, 1997.
- [222] K. P. Vercruyse, G. D. Prestwich, and J.-W. Kuo, "Hyaluronate derivatives in drug delivery," *Critical Reviews in Therapeutic Drug Carrier Systems*, vol. 15, no. 5, pp. 513–555, 1998.
- [223] S. Jaracz, J. Chen, L. V. Kuznetsova, and I. Ojima, "Recent advances in tumor-targeting anticancer drug conjugates," *Bioorganic and Medicinal Chemistry*, vol. 13, no. 17, pp. 5043–5054, 2005.
- [224] T. Pouyani and G. D. Prestwich, "Biotinylated hyaluronic acid: a new tool for probing hyaluronate-receptor interactions," *Bioconjugate Chemistry*, vol. 5, no. 4, pp. 370–372, 1994.
- [225] G. D. Prestwich, D. M. Marecak, J. F. Marecek, K. P. Vercruyse, and M. R. Ziebell, "Controlled chemical modification of hyaluronic acid: synthesis, applications, and biodegradation of hydrazide derivatives," *Journal of Controlled Release*, vol. 53, no. 1–3, pp. 93–103, 1998.
- [226] Y.-H. Liao, S. A. Jones, B. Forbes, G. P. Martin, and M. B. Brown, "Hyaluronan: pharmaceutical characterization and drug delivery," *Drug Delivery*, vol. 12, no. 6, pp. 327–342, 2005.
- [227] A. K. Yadav, P. Mishra, and G. P. Agrawal, "An insight on hyaluronic acid in drug targeting and drug delivery," *Journal of Drug Targeting*, vol. 16, no. 2, pp. 91–107, 2008.
- [228] N. Afratis, C. Gialeli, D. Nikitovic et al., "Glycosaminoglycans: key players in cancer cell biology and treatment," *FEBS Journal*, vol. 279, no. 7, pp. 1177–1197, 2012.
- [229] V. Orian-Rousseau, "CD44, a therapeutic target for metastasizing tumours," *European Journal of Cancer*, vol. 46, no. 7, pp. 1271–1277, 2010.
- [230] M. Zöller, "CD44: can a cancer-initiating cell profit from an abundantly expressed molecule?" *Nature Reviews Cancer*, vol. 11, no. 4, pp. 254–267, 2011.
- [231] K.-H. Heider, H. Kuthan, G. Stehle, and G. Munzert, "CD44v6: a target for antibody-based cancer therapy," *Cancer Immunology, Immunotherapy*, vol. 53, no. 7, pp. 567–579, 2004.
- [232] J. Zeilstra, S. P. J. Joosten, H. van Andel et al., "Stem cell CD44v isoforms promote intestinal cancer formation in Apc(min) mice downstream of Wnt signaling," *Oncogene*, vol. 33, no. 5, pp. 665–670, 2014.
- [233] R. Stauder, W. Eisterer, J. Thaler, and U. Gunthert, "CD44 variant isoforms in non-Hodgkin's lymphoma: a new independent prognostic factor," *Blood*, vol. 85, no. 10, pp. 2885–2899, 1995.

- [234] M. Todaro, M. P. Alea, A. B. di Stefano et al., "Colon cancer stem cells dictate tumor growth and resist cell death by production of interleukin-4," *Cell Stem Cell*, vol. 1, no. 4, pp. 389–402, 2007.
- [235] W. Guo and P. S. Frenette, "Alternative CD44 splicing in intestinal stem cells and tumorigenesis," *Oncogene*, vol. 33, no. 5, pp. 537–538, 2014.
- [236] C. Kainz, P. Kohlberger, G. Sliutz et al., "Splice variants of CD44 in human cervical cancer stage IB to IIB," *Gynecologic Oncology*, vol. 57, no. 3, pp. 383–387, 1995.
- [237] C. Kainz, P. Kohlberger, C. Tempfer et al., "Prognostic value of CD44 splice variants in human stage III cervical cancer," *European Journal of Cancer Part A: General Topics*, vol. 31, no. 10, pp. 1706–1709, 1995.
- [238] H.-F. Hsieh, J.-C. Yu, L.-I. Ho, S.-C. Chiu, and H.-J. Harn, "Molecular studies into the role of CD44 variants in metastasis in gastric cancer," *Journal of Clinical Pathology: Molecular Pathology*, vol. 52, no. 1, pp. 25–28, 1999.
- [239] E. Shtivelman and J. M. Bishop, "Expression of CD44 is repressed in neuroblastoma cells," *Molecular and Cellular Biology*, vol. 11, no. 11, pp. 5446–5453, 1991.
- [240] A. M. de Marzo, C. Bradshaw, J. Sauvageot, J. I. Epstein, and G. J. Miller, "CD44 and CD44v6 downregulation in clinical prostatic carcinoma: relation to Gleason grade and cytoarchitecture," *The Prostate*, vol. 34, no. 3, pp. 162–168, 1998.
- [241] S. Seiter, R. Arch, S. Reber et al., "Prevention of tumor metastasis formation by anti-variant CD44," *Journal of Experimental Medicine*, vol. 177, no. 2, pp. 443–455, 1993.
- [242] D. R. Colnot, A. J. Wilhelm, J. Cloos et al., "Evaluation of limited blood sampling in a preceding 99mTc-labeled diagnostic study to predict the pharmacokinetics and myelotoxicity of 186Re-cMab U36 radioimmunotherapy," *Journal of Nuclear Medicine*, vol. 42, no. 9, pp. 1364–1367, 2001.
- [243] R. De Bree, J. C. Roos, J. J. Quak, W. Den Hollander, G. B. Snow, and G. A. M. S. Van Dongen, "Radioimmunoscintigraphy and biodistribution of technetium-99m-labeled monoclonal antibody U36 in patients with head and neck cancer," *Clinical Cancer Research*, vol. 1, no. 6, pp. 591–598, 1995.
- [244] R. de Bree, J. C. Roos, J. J. Quak et al., "Biodistribution of radiolabeled monoclonal antibody E48 IgG and F(ab')₂ in patients with head and neck cancer," *Clinical Cancer Research*, vol. 1, no. 3, pp. 277–286, 1995.
- [245] P. K. E. Börjesson, E. J. Postema, J. C. Roos et al., "Phase I therapy study with 186Re-labeled humanized monoclonal antibody BIWA 4 (Bivatuzumab) in patients with head and neck squamous cell carcinoma," *Clinical Cancer Research*, vol. 9, no. 10, part 2, pp. 3961S–3972S, 2003.
- [246] D. R. Colnot, J. C. Roos, R. de Bree et al., "Safety, biodistribution, pharmacokinetics, and immunogenicity of ^{99m}Tc-labeled humanized monoclonal antibody BIWA 4 (bivatuzumab) in patients with squamous cell carcinoma of the head and neck," *Cancer Immunology, Immunotherapy*, vol. 52, no. 9, pp. 576–582, 2003.
- [247] B. M. Tjink, J. Buter, R. de Bree et al., "A phase I dose escalation study with anti-CD44v6 bivatuzumab mertansine in patients with incurable squamous cell carcinoma of the head and neck or esophagus," *Clinical Cancer Research*, vol. 12, no. 20, part 1, pp. 6064–6072, 2006.
- [248] H. Urakawa, Y. Nishida, W. Knudson et al., "Therapeutic potential of hyaluronan oligosaccharides for bone metastasis of breast cancer," *Journal of Orthopaedic Research*, vol. 30, no. 4, pp. 662–672, 2012.
- [249] S. Misra, S. Ghatak, A. Zoltan-Jones, and B. P. Toole, "Regulation of multidrug resistance in cancer cells by hyaluronan," *The Journal of Biological Chemistry*, vol. 278, no. 28, pp. 25285–25288, 2003.
- [250] B. St. Croix, J. W. Rak, S. Kapitain, C. Sheehan, C. H. Graham, and R. S. Kerbel, "Reversal by hyaluronidase of adhesion-dependent multicellular drug resistance in mammary carcinoma cells," *Journal of the National Cancer Institute*, vol. 88, no. 18, pp. 1285–1296, 1996.
- [251] B. St. Croix, S. Man, and R. S. Kerbel, "Reversal of intrinsic and acquired forms of drug resistance by hyaluronidase treatment of solid tumors," *Cancer Letters*, vol. 131, no. 1, pp. 35–44, 1998.
- [252] V. B. Lokeshwar, V. Estrella, L. Lopez et al., "HYAL1-v1, an alternatively spliced variant of HYAL1 hyaluronidase: a negative regulator of bladder cancer," *Cancer Research*, vol. 66, no. 23, pp. 11219–11227, 2006.
- [253] M. Kursa, G. F. Walker, V. Roessler et al., "Novel shielded transferrin-polyethylene glycol-polyethylenimine/DNA complexes for systemic tumor-targeted gene transfer," *Bioconjugate Chemistry*, vol. 14, no. 1, pp. 222–231, 2003.
- [254] N. C. Bellocq, S. H. Pun, G. S. Jensen, and M. E. Davis, "Transferrin-containing, cyclodextrin polymer-based particles for tumor-targeted gene delivery," *Bioconjugate Chemistry*, vol. 14, no. 6, pp. 1122–1132, 2003.
- [255] S. Ghatak, V. C. Hascall, F. G. Berger et al., "Tissue-Specific shRNA delivery: a novel approach for gene therapy in cancer," *Connective Tissue Research*, vol. 49, no. 3-4, pp. 265–269, 2008.
- [256] G. Song, X. Liao, L. Zhou, L. Wu, Y. Feng, and Z. C. Han, "HI44a, an anti-CD44 monoclonal antibody, induces differentiation and apoptosis of human acute myeloid leukemia cells," *Leukemia Research*, vol. 28, no. 10, pp. 1089–1096, 2004.
- [257] H. Riechelmann, A. Sauter, W. Golze et al., "Phase I trial with the CD44v6-targeting immunoconjugate bivatuzumab mertansine in head and neck squamous cell carcinoma," *Oral Oncology*, vol. 44, no. 9, pp. 823–829, 2008.
- [258] M. Koppe, F. van Schaijk, J. Roos et al., "Safety, pharmacokinetics, immunogenicity, and biodistribution of 186Re-labeled humanized monoclonal antibody BIWA 4 (Bivatuzumab) in patients with early-stage breast cancer," *Cancer Biotherapy and Radiopharmaceuticals*, vol. 19, no. 6, pp. 720–729, 2004.
- [259] B. P. Toole, S. Ghatak, and S. Misra, "Hyaluronan oligosaccharides as a potential anticancer therapeutic," *Current Pharmaceutical Biotechnology*, vol. 9, no. 4, pp. 249–252, 2008.
- [260] C. P. Paul, P. D. Good, I. Winer, and D. R. Engelke, "Effective expression of small interfering RNA in human cells," *Nature Biotechnology*, vol. 20, no. 5, pp. 505–508, 2002.
- [261] S. E. Raper, N. Chirmule, F. S. Lee et al., "Fatal systemic inflammatory response syndrome in a ornithine transcarbamylase deficient patient following adenoviral gene transfer," *Molecular Genetics and Metabolism*, vol. 80, no. 1-2, pp. 148–158, 2003.
- [262] L. E. Ailles and I. L. Weissman, "Cancer stem cells in solid tumors," *Current Opinion in Biotechnology*, vol. 18, no. 5, pp. 460–466, 2007.
- [263] N. A. Lobo, Y. Shimono, D. Qian, and M. F. Clarke, "The biology of cancer stem cells," *Annual Review of Cell and Developmental Biology*, vol. 23, pp. 675–699, 2007.
- [264] P. Dalerba, R. W. Cho, and M. F. Clarke, "Cancer stem cells: models and concepts," *Annual Review of Medicine*, vol. 58, pp. 267–284, 2007.

Research Article

Selective Activation of Cancer Stem Cells by Size-Specific Hyaluronan in Head and Neck Cancer

Marisa Shiina and Lilly Y. W. Bourguignon

San Francisco Veterans Affairs Medical Center and Department of Medicine, University of California at San Francisco and Endocrine Unit (111N2), 4150 Clement Street, San Francisco, CA 94121, USA

Correspondence should be addressed to Lilly Y. W. Bourguignon; lilly.bourguignon@ucsf.edu

Received 24 September 2014; Revised 12 March 2015; Accepted 18 March 2015

Academic Editor: Hirofumi Sawai

Copyright © 2015 M. Shiina and L. Y. W. Bourguignon. This is an open access article distributed under the Creative Commons Attribution License, which permits unrestricted use, distribution, and reproduction in any medium, provided the original work is properly cited.

We determined that human head and neck cancer cells (HSC-3 cell line) contain a subpopulation displaying cancer stem cell (CSC) properties and are very tumorigenic. Specifically, we investigated whether different sizes of hyaluronan (HA) (e.g., 5 kDa, 20 kDa, 200 kDa, or 700 kDa-HA-sizes) play a role in regulating these CSCs. First, we observed that 200 kDa-HA (but not other sizes of HA) preferentially induces certain stem cell marker expression resulting in self-renewal and clonal formation of these cells. Further analyses indicate that 200 kDa-HA selectively stimulates the expression of a panel of microRNAs (most noticeably miR-10b) in these CSCs. Survival protein (cIAP-1) expression was also stimulated by 200 kDa-HA in these CSCs leading to cisplatin resistance. Furthermore, our results indicate that the anti-miR-10 inhibitor not only decreases survival protein expression, but also increases chemosensitivity of the 200 kDa-HA-treated CSCs. These findings strongly support the contention that 200 kDa-HA plays a pivotal role in miR-10 production leading to survival protein upregulation and chemoresistance in CSCs. Together, our findings suggest that selective activation of oncogenic signaling by certain sizes of HA (e.g., 200 kDa-HA) may be instrumental in the formation of CSC functions leading to tumor cell survival and chemoresistance in head and neck cancer progression.

1. Introduction

Human head and neck squamous cell carcinoma (HNSCC) is the sixth most common cancer worldwide and is also one of the most deadly cancers [1]. The three-year survival rate for patients with advanced-stage HNSCC and treated with standard therapy is only 30 to 50% [1]. This deadly disease includes cancers of the lip, oral cavity, pharynx, hypopharynx, larynx, nose, nasal, sinuses, neck, ears, and salivary glands [1]. Nearly 40 to 60% of HNSCC patients subsequently develop recurrences or distant metastases [1]. Thus, there is currently a great need to clarify the key mechanisms of tumor initiation and progression underlying the clinical behavior of HNSCC.

Accumulating evidence indicates that most tumors contain a small population of cells which persistently initiate tumor growth and promote tumor progression. These “cancer stem cells (CSCs)” [also called “tumor-initiating cells (TICs)”] share several of the hallmarks of normal stem cells [2, 3]. For example, CSCs undergo self-renewal, maintain

quiescence, display multipotentiality, and express survival protein/antiapoptosis proteins [2, 3]. Another well-known property of CSCs is their ability to expand the stem cell population by undergoing cell proliferation/survival and/or clone formation and differentiation [2, 3]. A number of studies have identified specific molecules expressed in CSCs that correlate with both stem cell properties and tumor cell behaviors. Among such molecules is CD44 which is a multifunctional transmembrane glycoprotein expressed in many cells and tissues including HNSCC cells and other carcinoma tissues [2, 3]. CD44 is commonly expressed in various isoforms generated by alternative mRNA splicing of variant exons inserted into an extracellular membrane-proximal site [4]. CD44 is expressed in both normal and cancer stem cells (CSCs) and serves as an important stem cell marker [2, 3].

Hyaluronan (HA) is a major component in the extracellular matrix (ECM) of most mammalian tissues. HA is a nonsulfated, unbranched glycosaminoglycan consisting of

repeating disaccharide units, D-glucuronic acid, and N-acetyl-D-glucosamine [5, 6]. Under physiological conditions, HA is synthesized by several HA synthases [7] and HA fragments of low molecular mass are produced by hyaluronidases or oxidation [8]. One general concept which has emerged from these studies is that HA fragments (small- versus mid-size-HAs) and their larger precursor molecules (i.e., intact HA) may be involved in distinct biological activities [9, 10]. In addition, the formation of biologically active HA fragments from the large HA in the ECM occurs during periods of proliferation, migration, differentiation, and development as well as injury-related repairs [9, 10]. A number of studies indicate that large size-HA promotes transcriptional activation and differentiation, whereas small-size-HA induces cell proliferation and migration [9, 10]. HA is enriched in many types of tumors [11, 12] and also has been found to be increased in stem cell niches [13, 14]. Furthermore, the unique HA-enriched microenvironment appears to be involved in both self-renewal and differentiation of normal human stem cells [13, 14].

All CD44 isoforms contain a HA-binding site in their extracellular domain and thereby serve as a major cell surface receptor for HA [5, 6]. The fact that both CD44 and HA are overexpressed at tumor attachment sites and that HA binding to CD44 stimulates a variety of tumor cell-specific functions and tumor progression [11, 12] suggests that the HA-CD44 interaction is a critical requirement for tumor progression. However, the cellular and molecular mechanisms underlying HA's ability to regulate CD44-positive CSCs by different sizes of HA during HNSCC progression remain poorly understood. Furthermore, the oncogenic mechanism(s) occurring during activation of CSCs by size-specific HAs during head and neck cancer progression remain(s) to be unknown.

In this study we have investigated the effects of different sizes of HA (ranging from 5 kDa to 700 kDa) on CSC signaling and function in head and neck cancer cells. Our results indicate that 200 kDa-HA (and to a much lesser extent 5 kDa-HA, 20 kDa-HA, and 700 kDa-HA) plays an important role in the selective activation of pluripotency factor (stem cell marker) expression, microRNA signaling and CSC functions required for tumor cell behaviors lead to head and neck cancer progression.

2. Materials and Methods

2.1. Cell Culture. Tumor-derived HSC-3 cell line (from human squamous carcinoma cells of mouth), was kindly provided from Dr. Randy Kramer (University of California, San Francisco, CA). Cells were grown in DMEM/F12 medium (Corning, NY) supplemented with 10% fetal bovine serum.

2.2. Antibodies and Reagents. Rabbit anti-CD44v3 antibody was obtained from EMD Chemicals (Gibbstown, NJ). Other immunoreagents such as rabbit anti-cIAP1 antibody were from Abcam (Cambridge, MA) and rabbit anti-actin antibody was purchased from Cell Signaling (Beverly, MA),

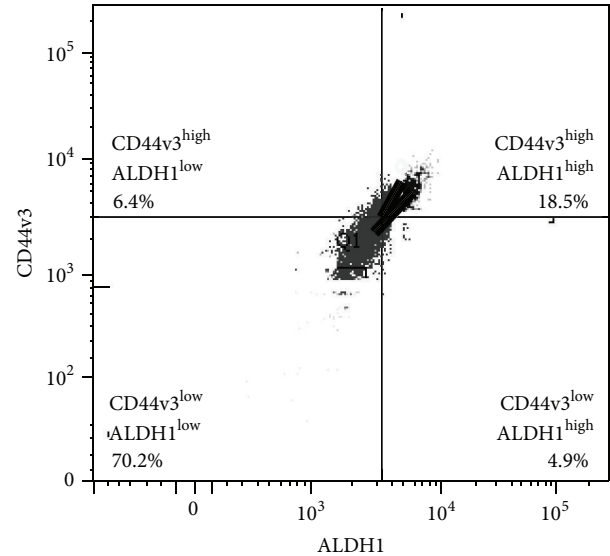


FIGURE 1: Isolation of cancer stem cell-like population from tumor-derived HNSCC (HSC-3 cells) using multicolor fluorescence-activated cell sorter (FACS). Tumor-derived human HNSCC (HSC-3 cells) were incubated with both ALDEFLUOR kit (to measure an ALDH1 enzymatic activity) and allophycocyanin- (APC-) labeled anti-CD44v3 antibody (recognizing the v3-specific domain of CD44) followed by FACS and cell sorting (Figure 1). Flow cytometry analyses of HSC-3 tumor cell populations including CD44v3^{high}ALDH1^{high} (top right quad, 18.5%) or CD44v3^{high}ALDH1^{low} (top left quad, 6.4%) or CD44v3^{low}ALDH1^{high} (bottom right quad, 4.9%) or CD44v3^{low}ALDH1^{low} (bottom left quad, 70.2%). Live tumor cell sorting was then done using a FACS-fluorescence-activated cell sorter to isolate CD44v3^{high}ALDH1^{high} cells or CD44v3^{low}ALDH1^{low} for the study.

respectively. Cisplatin was obtained from Millipore (Darmstadt, Germany). Different sizes of research grade HA fragments (e.g., 5 kDa, 20 kDa, 200 kDa, and 700 kDa) were purchased from Lifecore Biomedical (Chaska, MN).

2.3. Sorting Tumor-Derived HSC-3 Cell Populations by Multicolor Fluorescence-Activated Cell Sorter (FACS). The identification of aldehyde dehydrogenase-1 (ALDH1) activity from tumor-derived HSC-3 cells was conducted using the ALDEFLUOR kit (StemCell Technologies, Durham, NC). Specifically, tumor cells were suspended in ALDEFLUOR assay buffer containing ALDH1 substrate (BAAA, 1 mol/L per 1×10^6 cells) and incubated for 30 min at 37°C. As a negative control, HSC-3 cells were treated with a specific ALDH1 inhibitor, 50 mmol/L diethylaminobenzaldehyde (DEAB) (50 mmol/L).

Next, for labeling cell surface marker, tumor-derived HSC-3 cells were resuspended in 100 μ L ALDEFLUOR buffer followed by incubating with 20 μ L allophycocyanin- (APC-) labeled anti-CD44v3 antibody (recognizing the v3-specific domain of CD44) or APC-labeled normal mouse IgG (as a control) (BD Bioscience, San Jose, CA) for 15 min at 4°C. For FACS sorting, tumor cells were resuspended in PBS buffer followed by FACS (BD FACS Aria II, BD Bioscience, San Jose,

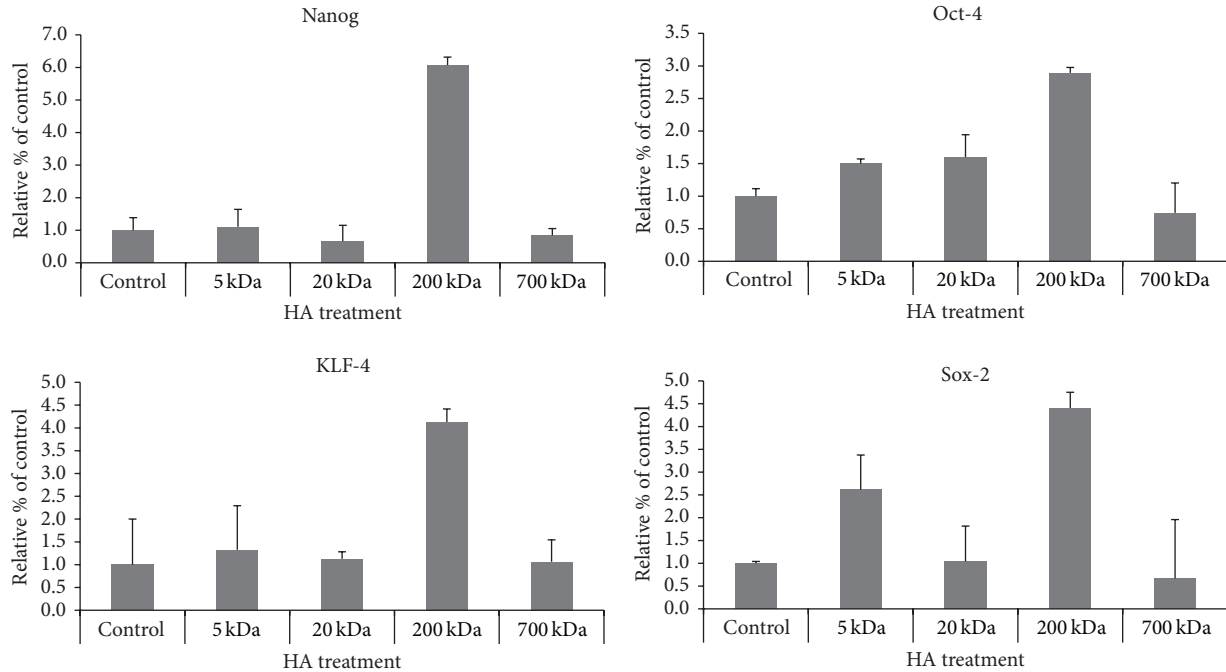


FIGURE 2: Effects of various sizes of HA on stimulating stem cell marker (Nanog, Oct4, Sox2, and KLF-4) expression in CD44v3^{high} ALDH1^{high} cells using Q-PCR analyses.

CA) sorting using dual-wavelength analysis. Subsequently, CD44v3^{high} ALDH1^{high} tumor cell population was collected and used for various experiments described in this study.

2.4. Tumorigenicity Assay. Nonobese, diabetic/severe combined immunodeficient (NOD/SCID) immunocompromised mice (5-week-old female mice) were purchased from Charles River Laboratories International, Inc. (Wilmington, MA) and maintained in microisolator cages. Specifically, these NOD/SCID were injected subcutaneously and/or submucosally in the floor of the mouth with sorted CD44v3^{high} ALDH1^{high} cells or unsorted HSC-3 cells (suspended in 0.1 mL Matrigel Basement Membrane Matrix) ranging from 50, 500, to 5,000 cells. These mice were then monitored twice weekly for palpable tumor formation and euthanized 4 or 8 weeks after transplantation to assess tumor formation. Tumors were measured using a Vernier caliper, weight, and photographed. A portion of the subcutaneous tumors and/or submucosa tumors was collected. Some tumors were cut into small fragments with sterile scissors and miced with a sterile scalpel, rinsed with Hans' balanced salt solution containing 2% heat-inactivated calf serum (Invitrogen), and centrifuged for 5 min at 1,000 rpm. The resulting tissue specimen was placed in a solution of DMED F-12 containing 300 U/mL collagenase and 100 U/mL hyaluronidase (StemCell Technologies, Durham, NC). The mixture was incubated at 37°C to dissociate cells. The digestion was arrested with the addition of FBS and the cells were filtered through a 40 μm nylon sieve. The cells were washed twice with Hans' balanced salt solution plus 2% heat-inactivated calf serum for FACS as described above.

2.5. Quantitative PCR (Q-PCR). Total RNA was isolated from CD44v3^{high} ALDH1^{high} cells (pretreated with no HA or 5 kDa-HA or 20 kDa-HA or 200 kDa-HA or 700 kDa-HA for 24 h) using Tripure Isolation Reagent kits (Roche Applied Science, Indianapolis, IN). First-stranded cDNAs were synthesized from RNA using Superscript First-Strand Synthesis system (Invitrogen, Carlsbad, CA). Gene expression was quantified using probe-based Sybr Green PCR Master Mix kits, ABI PRISM 7900HT sequence detection system, and SDS software (Applied Biosystems, Foster City, CA). A cycle threshold (minimal PCR cycles required for generating a fluorescent signal exceeding a preset threshold) was determined for each gene of interest and normalized to a cycle threshold for a housekeeping gene (36B4) determined in parallel. The 36B4 is a human acidic ribosomal phosphoprotein PO whose expression was not changed in tumor cells. The Q-PCR primers used for detecting gene expression of Oct4, Sox2, Nanog, and KLF-4 were as follows: specifically, two Oct4-specific primers (the sense primer 5'-GGTATTCAG-CCAAACGACCA-3' and the antisense primer 5'-CAC-ACTCGGACCACATCCTT-3'); two Sox2-specific primers (the sense primer 5'-GACAGTTACGCGCACATGAA-3' and the antisense primer 5'-TAGGTCTGCGAGCTGGTC-AT-3'); and two Nanog-specific primers (the sense primer 5'-GTGATTTGTGGCCTGAAGA-3' and the antisense primer 5'-ACACAGCTGGGTGGAAGAGA-3'); two KLF4-specific primers (the sense primer 5'-CACCATGGACCC-GGGCGTGGCTGCCAGAAA and the antisense primer 5'-TTAGGCTGTTCTTTCCGGGGCCACGA) were used. The Q-PCR primers used for detecting gene expression of various miRNAs were as follows: specifically, two

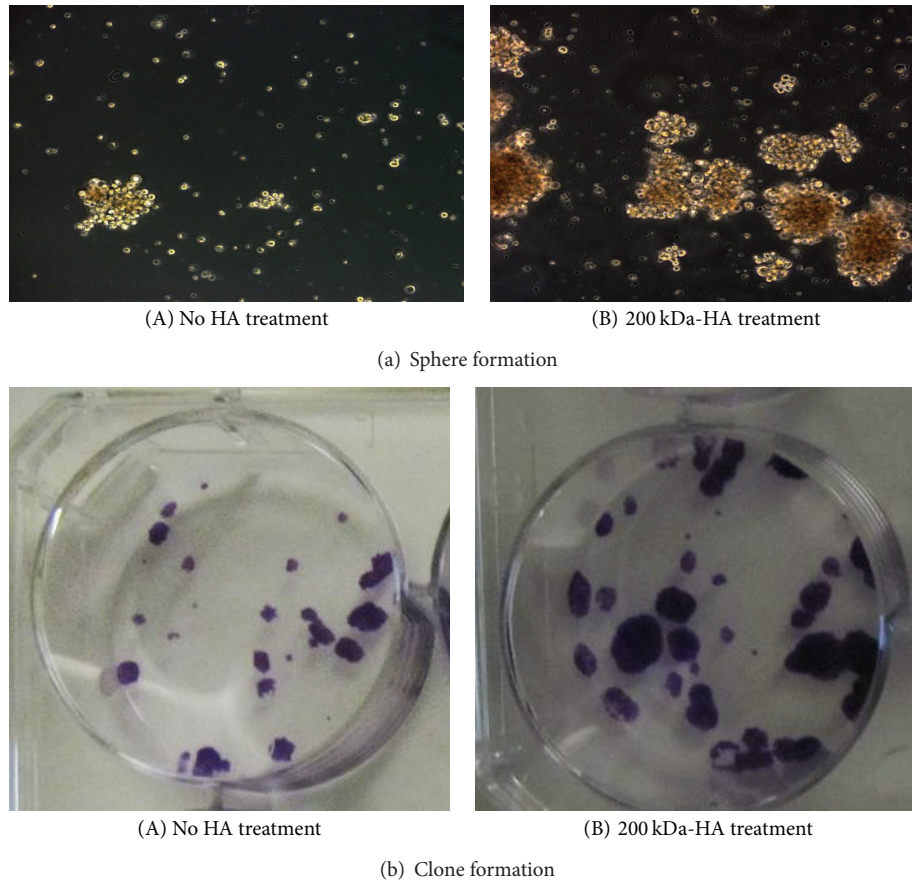


FIGURE 3: Measurement of sphere formation (a) and clone formation (b) CD44v3^{high}ALDH1^{high} (CSC) cells. (a) Sphere formation of CD44v3^{high}ALDH1^{high} cells [treated with no HA (A) or with 200 kDa-HA (B)] in a mixture of 5 mg/mL of matrigel (Corning) and defined medium (RPMI-1640 medium containing EGF and bFGF without serum) for 3 weeks (21 days) as described in Section 2. (b) Clone formation (differentiation) of CD44v3^{high}ALDH1^{high} cells pretreated with no HA (A) or with 200 kDa-HA (B). Specifically, clone formation and differentiation were induced by incubating CD44v3^{high}ALDH1^{high} cells (dissociated from spheres treated with 200 kDa-HA or without HA for 10 days as described above). After the removal of 200 kDa-HA from the cells, these sphere-derived CD44v3^{high}ALDH1^{high} cells were then incubated in RPMI 1640 complete culture and 10% fetal bovine serum for ~7–10 days. After most cell clones expand to >50–100 cells, they were fixed with methanol followed by staining with crystal violet to visualize clone formation as described in Section 2.

miR-10b-specific primers (the sense primer 5'-GGATAC-CCTGTAGAACCGAA and the antisense primer 5'-CAG-TGCGTGTCTGGAGT); two 23b-27b-specific primers (the sense primer 5'-TCACATTGCCAGGGATTACCA and the antisense primer 5'-TGCACCTGTTCTCCAATCTGC); two miR-373 primers (the sense primer 5'-CCTTCAACA-GCTCATCAAGGGCT and the antisense primer 5'-TAC-CCGCCCTCACCCAATCAA); two miR-34a primers (the sense primer 5'-TGCGAGTGTCTTAGCTGGTTG and the antisense primer 5'-GGCAGTATACTTGCTGATTGCTT); two miR-145 primers (the sense primer 5'-GGTCCA-GTTTTCCAGG and the antisense primer 5'-CAGTGC-GTGTCGTGGAGT); two miR-181a (the sense primer 5'-AACATTCAACGCTGTCGGT and the antisense primer 5'-CAGTCAACGGTCAGTGGTTT). Finally, for detecting 36B4 gene expression, two 36B4-specific primers (the sense primer 5'-GCGACCTGGAAGTCCAACACTAC-3' and the antisense primer 5'-ATCTGCTGCATCTGCTTGG-3') were used.

2.6. Immunoblotting Techniques. RIPA buffer-solubilized cell lysate of untransfected CD44v3^{high}ALDH1^{high} cells (pre-treated with no HA or 5 kDa-HA or 20 kDa-HA or 200 kDa-HA for 3 days) or CD44v3^{high}ALDH1^{high} cells transfected with anti-miR-10b inhibitor or miRNA-negative control followed by 200 kDa-HA (50 μ g/mL) addition (or no HA addition) for 3 days at 37°C were immunoblotted using various immunoreagents [e.g., mouse anti-cIAP-1 (2 μ g/mL) or goat anti-actin (2 μ g/mL) (as a loading control), resp.].

2.7. Spheroid Formation and Self-Renewal Assays. CD44v3^{high}ALDH1^{high} cells were analyzed for spheroid formation and self-renewal using the methods described previously [15].

2.8. Clone Formation and Differentiation Assays. For analyzing the clone formation (differentiation) properties, CD44v3^{high}ALDH1^{high} cells (treated with 200 kDa-HA or no

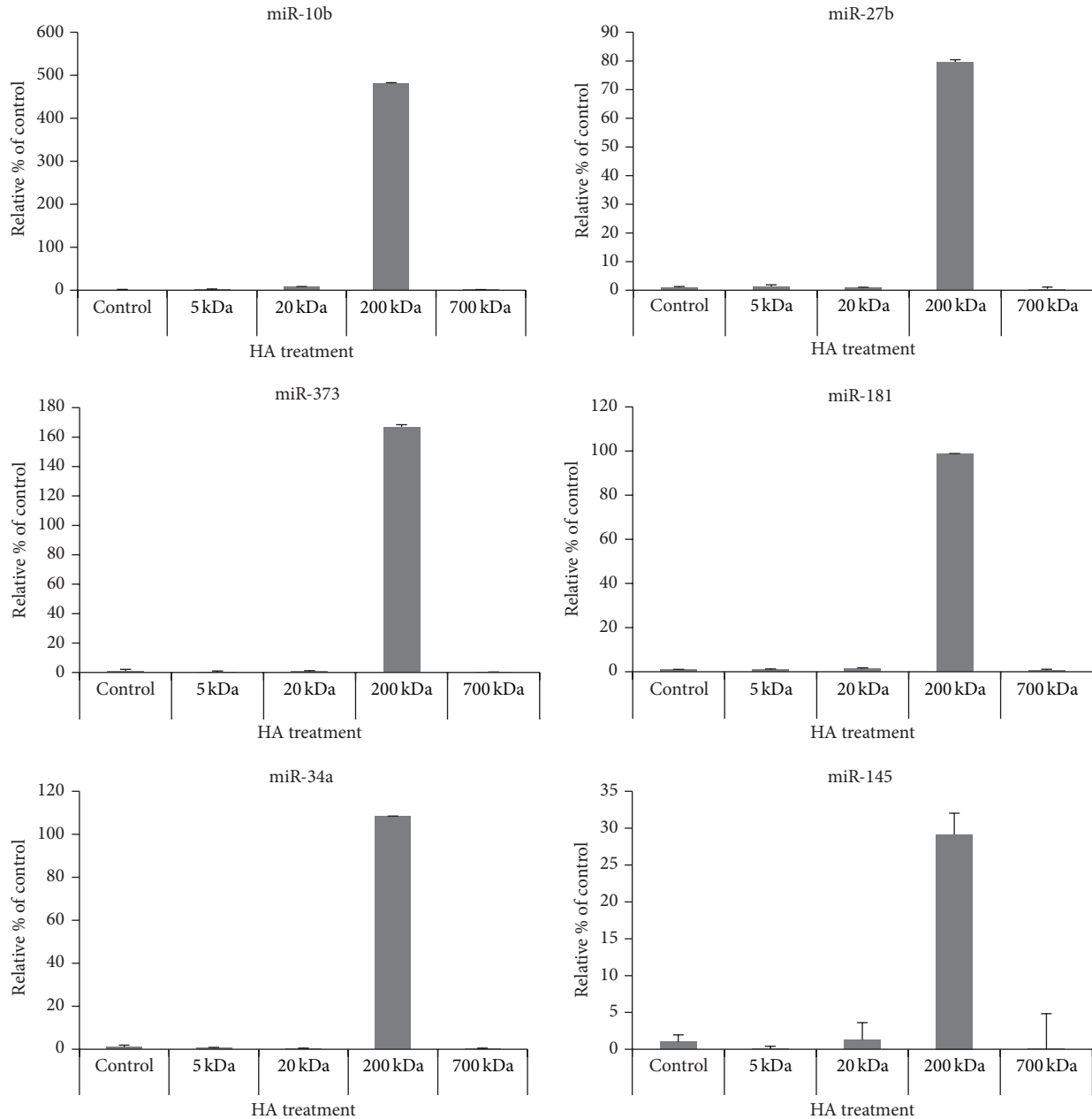


FIGURE 4: Detection of various miRNA expressions in CD44v3^{high}ALDH^{high} cells treated with different sizes of HA. Detection of miR-10b, miR-27b, miR-373, miR-181, miR-34a, and miR-145 production in CD44v3^{high}ALDH^{high} cells following the treatment with different sizes of HA (e.g., 5 kDa-HA, 20 kDa-HA, 200 kDa-HA, 700 kDa-HA, and no HA) and analyzing by Q-PCR as described in Section 2.

HA) were dissociated from spheres and inoculated to 6-well plates at a density of 200 cells per well in six-well plates, and cultured with DMEM/F12 plus 10% serum for ~21 days. After most cell clones expand to >50–100 cells, they were fixed with methanol followed by staining with crystal violet. The clone formation efficiency (CFE) was expressed as the ratio of the clone number to the planted cell number.

2.9. Tumor Cell Growth Assays. Sphere-derived CD44v3^{high}ALDH1^{high} cells (5×10^3 cells/well) were incubated in basal medium with B27 plus 200 kDa-HA (50 μ g/mL) or no HA.

Medium were replenished every 3 days. Twenty-on (21) days after plating, total cell growth was then counted under a microscope at low magnification.

In some cases, these sphere-derived CD44v3^{high}ALDH1^{high} cells (transfected with anti-10b inhibitor or miRNA-negative control) were also incubated with various concentrations of cisplatin (0–20 μ M) with no HA or with 200 kDa-HA (50 μ g/mL). After 7-day incubation at 37°C, CellTiter-Glo Luminescent Cell Viability Assays (Promega, Madison, WI) were analyzed as described previously [15]. The percentage of absorbance relative to untreated controls

TABLE 1: Analyses of tumor formation by CD44v3^{high} ALDH1^{high} cells, CD44v3^{low} ALDH1^{low} cells, CD44v3^{low} ALDH1^{high} cells, or unsorted cells subcutaneously injected into NOD/SCID mice.

Cell populations	Tumor formation*		
	5,000 cells injected (8 weeks)	500 cells injected (8 weeks)	50 cells injected (8 weeks)
CD44v3 ^{high} ALDH1 ^{high} cells	20/20	18/20	16/20
CD44v3 ^{low} ALDH1 ^{high} cells	3/20	1/20	0/20
CD44v3 ^{low} ALDH1 ^{low} cells	1/20	0/20	0/20
Unsorted cells	2/20	0/20	0/20

*For the tumor cell injection, each mouse was subcutaneously inoculated with CD44v3^{high} ALDH1^{high} cells or CD44v3^{low} ALDH1^{high} cells or CD44v3^{low} ALDH1^{low} cells or unsorted cells with 5,000 cells, 500 cells, or 50 cells as described in the Section 2. The values expressed in the Table 1 represent the number of animals developed tumors/total number of animals used in the study. The tumor formation assay was performed on at least 5 different experiments with a standard deviation less than $\pm 5\%$.

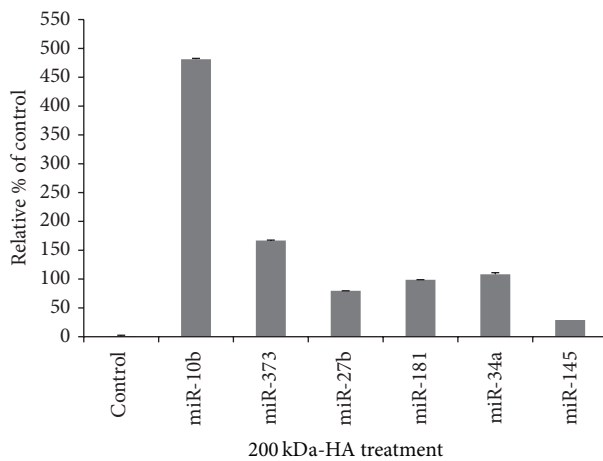


FIGURE 5: Comparison of miR-10b expression with various other miRNA productions in CD44v3^{high} ALDH1^{high} cells following the treatment with different sizes of HA (e.g., 5 kDa-HA, 20 kDa-HA, 200 kDa-HA, 700 kDa-HA, and no HA) and analyzing by Q-PCR as described in Section 2.

(i.e., cells treated with neither HA nor chemotherapeutic drugs) was plotted as a linear function of drug concentration. The 50% inhibitory concentration (IC_{50}) was identified as a concentration of drug required to achieve a 50% growth inhibition relative to untreated controls.

3. Results and Discussion

3.1. Isolation of CD44v3^{high} ALDH1^{high} Cells [Cancer Stem Cell- (CSC-) Like Cells] from Human HNSCC Cell Lines. Overexpression of CD44v3 has been shown to be closely associated with HNSCC development and progression. Aldehyde dehydrogenase-1 (ALDH1), a detoxifying enzyme responsible for the oxidation of intracellular aldehydes, is also considered to be a common marker for both normal stem cells and malignant cancer stem cells (CSCs) from HNSCC [15–17]. In this study we isolated CD44v3^{high} ALDH1^{high} subpopulations from tumor-derived human HNSCC cells (HSC-3) using FACS-fluorescence-activated cell sorting procedures (Figure 1). Our results indicate that CD44v3^{high} ALDH1^{high} cells (to a much lesser extent

CD44v3^{high} ALDH1^{low}, CD44v3^{low} ALDH1^{high}, CD44v3^{low} ALDH1^{low}, or unsorted cells) were capable of forming large size tumors in NOD/SCID mice injected with as few as 50 CD44v3^{high} ALDH1^{high} cells (Table 1). These findings indicate that CD44v3^{high} ALDH1^{high} cells display cancer stem cell- (CSC-) like properties by exhibiting very high tumor initiation potential. However, the cellular and molecular mechanisms that produce CSC-like properties of CD44v3^{high} ALDH1^{high} cells were not known and, therefore, they are the focus of this investigation.

3.2. Analyses of Stemness Marker (Nanog, Oct4, Sox2, and KLF-4) Expression, Cell Growth/Self-Renewal, and Clone Formation (Differentiation) in CD44v3^{high} ALDH1^{high} (CSC-Like) Cells following Different Sizes of HA Treatment. Identification of the extracellular matrix (ECM) components [e.g., hyaluronan (HA)] contributing to CSC-like properties will enable us to gain a better understanding regarding the role of the microenvironment in initiating and maintaining CSC properties. The question of whether different sizes of HA fragments (ranging from 5 kDa to 700 kDa) regulate CSC signaling and function in head and neck cancer cells has not been fully addressed and therefore is the focus of this study.

There is compelling evidence showing that certain stem cell markers such as Nanog, Oct, Sox2, and KLF-4 are known to form a self-organized core of transcription factors that maintain pluripotency and self-renewal of human embryonic stem cells [18–21]. In this study we found that the expressions of Nanog, Oct, Sox2, and KLF-4 are significantly increased in CD44v3^{high} ALDH1^{high} cells treated with 200 kDa-HA based on Q-PCR analyses (Figure 2). There is only a low level of stem cell marker expression detected with other sizes of HAs (e.g., 5 kDa-HA, 20 kDa-HA or 700 kDa-HA, or no HA treatment) (Figure 2). These findings clearly indicate that the stem cell markers (Nanog, Oct4, Sox2, and KLF-4) are upregulated in the CD44v3^{high} ALDH1^{high} cell subpopulation isolated from HNSCC (HSC-3) following 200 kDa-HA treatment.

To determine whether 200 kDa-HA-treated CD44v3^{high} ALDH1^{high} cells (overexpressing stem cell markers, Nanog, Oct4, Sox2, and KLF-4) are capable of undergoing self-renewal and long-term tumor cell growth, we assessed the ability of these tumorigenic CD44v3^{high} ALDH1^{high} cells

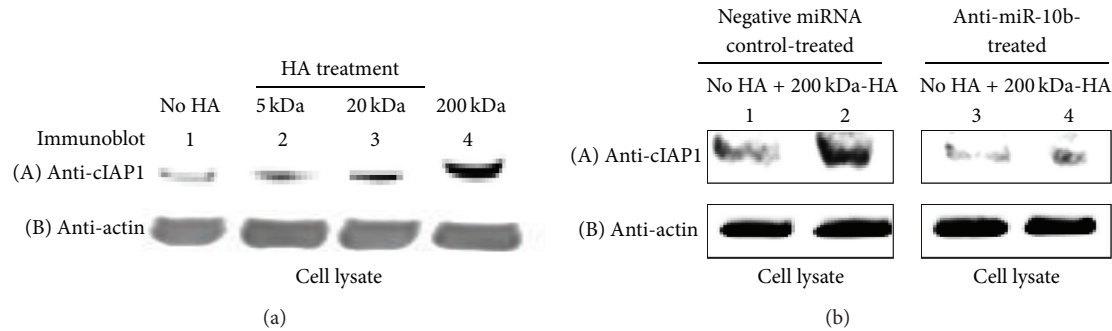


FIGURE 6: Analyses of 200 kDa-HA-mediated survival protein (cIAP1) expression in CD44v3^{high} ALDH1^{high} cells. (a) Detection of the expression of cIAP1 by anti-cIAP1-mediated immunoblotting using cell lysate isolated from CD44v3^{high} ALDH1^{high} cells treated with different sizes of HA [e.g., no HA ((A), lane 1), 5 kDa-HA ((A), lane 2), 20 kDa-HA ((A), lane 3), and 200 kDa-HA ((A), lane 4)] for 3 days. (b) Detection of the expression of cIAP1 by anti-cIAP1-mediated immunoblotting using cell lysate isolated from CD44v3^{high} ALDH1^{high} cells transfected with negative miRNA control [treated with no HA ((A), lane 1) or with 200 kDa-HA for 24 h ((A), lane 2)] or treated with anti-miR-10b inhibitor with no HA ((A), lane 3) or with 200 kDa HA addition for 3 days ((A), lane 4). The amount of actin detected by anti-actin-mediated immunoblot ((a): (B), lane 1–4; (b): (B), lane 1–4) in each gel lane was used as a loading control.

to grow in a “sphere forming” culture by incubating them in serum-free spheroid medium containing 200 kDa-HA (or no HA). After 14 days of incubating these cells in the serum-free medium, we observed that the 200 kDa-HA-treated CD44v3^{high} ALDH1^{high} cells form large numbers of spheres (Figure 3(a)-(B)), ranging from 50 to 100 cells per spheroid (Figure 3(a)-(B)). In contrast, only a very small number of spheres were detected in those cells that were not treated with HA (Figure 3(a)-(B)). Therefore, it appears that sphere formation with CD44v3^{high} ALDH1^{high} cells involves the binding of 200 kDa-HA.

To further test the ability of these CD44v3^{high} ALDH1^{high} cells (untreated or pretreated with 200 kDa-HA followed by dissociation from spheres after a serial passage of 1st, 2nd, and 3rd generation of sphere formation) to undergo clone formation and differentiation, we conducted clone formation assay (Figure 3(b)). Our data showed that the level of clone formation appears to be significantly higher in these 200 kDa-HA-treated CD44v3^{high} ALDH1^{high} cells (Figure 3(b)-(B)) as compared to those detected in CD44v3^{high} ALDH1^{high} cells with no HA treatment (Figure 3(b)-(A)). These observations suggest that CD44v3^{high} ALDH1^{high} cells are capable of displaying cancer stem cell-like properties (e.g., sphere formation, cell growth/self-renewal, and clone formation/differentiation) in a 200 kDa-HA-specific manner.

3.3. Analyses of microRNA Production in CD44v3^{high} ALDH1^{high} (CSC-Like) Cells following Different Sizes of HA Treatment. Accumulating evidence now indicates that noncoding microRNAs (miRNAs, approximately 22 nucleotides) are involved in head and neck cancer development [22–25]. Our previous study demonstrated that certain oncogenic microRNAs promote the cancer stem cell functions of CD44v3^{high} ALDH1^{high} (CSC-like) subpopulation from HNSCC (HSC-3) [15]. In this study we found that a panel of stem cell-related miRNAs including miR-10b, miR-27b, miR-373, miR-181, miR-34a,

and miR-145 is preferentially upregulated by 200 kDa-HA. In contrast, the other sizes of HA (e.g., 5 kDa-HA, 20 kDa-HA, and 700 kDa-HA) fail to induce various miRNA productions in the CD44v3^{high} ALDH1^{high} (CSC-like) cell subpopulation (Figure 4). Most noticeably, miR-10 appears to undergo the highest level of stimulation by 200 kDa-HA (Figure 5). In order to verify whether the 200 kDa-HA-induced miRNA-10b contributes to malignancy in the head and neck cancer cells, the following miR-10-regulated functional events were performed.

3.4. Detection of Survival Protein Expression and Chemotherapy Resistance. Survival proteins such as inhibitors of apoptosis proteins (IAPs) are frequently upregulated in CSCs following HA treatment [15]. Importantly, high levels of IAPs in CSCs increase cell survival due to the binding of IAPs to caspases and the suppression of apoptosis [26]. Here, we found that the expression of IAPs such as c-IAP-1 significantly increased in CD44v3^{high} ALDH1^{high} cells treated with 200 kDa-HA based on anti-c-IAP-1-mediated immunoblot analyses (Figure 6). There is only a relatively low level of c-IAP-1 expression detected with other sizes of HAs (e.g., 5 kDa-HA, 20 kDa-HA, or no HA treatment) (Figure 6(a)). These findings clearly indicate that the survival proteins such as c-IAP-1 are upregulated in the CD44v3^{high} ALDH1^{high} cell subpopulation isolated from HNSCC (HSC-3) following 200 kDa-HA treatment.

Our present data also demonstrate that downregulation of miR-10b by treating CD44v3^{high} ALDH1^{high} cells with an anti-miR-10b inhibitor (but not a negative-control miRNA) results in the downregulation of cIAP-1 (Figure 6(b), lane 3 and lane 4 versus lane 1 and 2) in the presence of 200 kDa-HA. Together, these results indicate that the signaling network containing miR-10b is functionally coupled to the stimulation of survival protein production in CSCs. These specific effects may facilitate the CSC-mediated HNSCC progression following HA treatment.

TABLE 2: Effects of anti-miR-10b on cisplatin-induced cell growth inhibition in CD44v3^{high}ALDH1^{high} cells following 200 kDa-HA treatment.

Treatments	Cisplatin-induced tumor cell growth inhibition IC ₅₀ (μM) [*] (% of control)
Negative miRNA control-treated cells (control) (No HA)	2.00 ± 0.15 (100.00%)
Negative miRNA control-treated cells (+200 kDa-HA)	5.75 ± 0.14 (288.00%)
Anti-miR-10-treated cells (No HA)	1.58 ± 0.22 (0.79%)
Anti-miR-10b-treated cells (+200 kDa-HA)	1.58 ± 0.23 (0.79%)

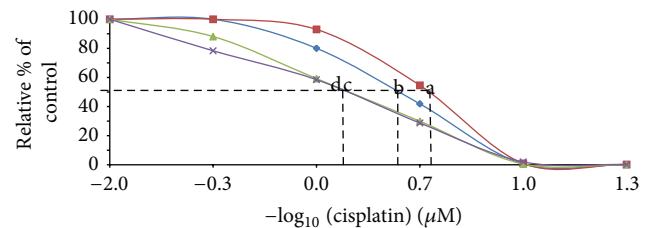
^{*}Tumor cell growth inhibition (IC₅₀) is designated as “the μM concentration of chemotherapeutic drug (e.g., cisplatin treatment) that causes 50% inhibition of tumor cell growth” using CellTiter-Glo Luminescent Cell Viability Assay as described in Section 2. IC₅₀ values are presented as the means ± standard deviation. All assays consisted of at least six replicates and were performed on at least 3–5 different experiments.

Further analyses indicate that the addition of 200 kDa-HA in negative miRNA-treated CD44v3^{high}ALDH1^{high} cells significantly decreases the ability of cisplatin to induce tumor cell death (Figure 7(a) versus Figure 7(b); Table 2). These observations strongly suggest that 200 kDa-HA causes both a decrease in tumor cell death and an increase in tumor cell survival leading to the enhancement of chemoresistance (Figure 7(a) versus Figure 7(b); Table 2). Moreover, down-regulation of miR-10b by treating CD44v3^{high}ALDH1^{high} HNSCC cells with an anti-miR-10b inhibitor (but not negative miRNA control-treated samples) effectively attenuates 200 kDa-HA-mediated tumor CD44v3^{high}ALDH1^{high} cell survival (Figure 7(c) versus Figure 7(d); Table 2) and enhances cisplatin sensitivity in CD44v3^{high}ALDH1^{high} cells (Table 2). These findings clearly indicate that downregulation of the 200 kDa-HA-induced miR-10b function (by anti-miR-10b treatment) may represent a new target for therapeutic agents designed to cause head and neck cancer CSCs to undergo cell death and remain chemotherapy sensitive.

4. Conclusion

Advanced head and neck squamous cell carcinoma (HNSCC) is an aggressive disease and a deadly cancer. Thus, clarification of key aspects of tumor cell functions underlying the clinical behavior of HNSCC is greatly needed. Cancer stem cells (CSCs) found in head and neck cancer have been implicated in the initiation/development of malignancy [27]. Because little is known regarding the molecular basis underlying CSC signaling and function, it is important to identify molecule(s) which can be used for predicting the oncogenic potential and possible drug targets for head and neck cancer-derived CSCs.

Hyaluronan (HA) is well-known as one of the major components in extracellular matrices (ECM). HA is often bound to CD44, a ubiquitous, abundant, and functionally important cell surface receptor. Different sizes of HA are known to bind to CD44; and our studies show that they influence a variety of cellular functions. However, our understanding of CD44 interaction with different sizes of HA fragments in cancer stem cells (CSCs) from HNSCC is lacking. In this study we found that size-specific HA (in particular, 200 kDa-HA) plays a pivotal role in the selective activation of CD44v3^{high}ALDH1^{high} (CSC-like) functions and microRNA signaling (in particular, miR-10b) required for tumor cell



Treatment	IC ₅₀ (cisplatin, μM)
(a) Negative miRNA control (+200 kDa-HA)	5.75 ± 0.15
(b) Negative miRNA control (No HA)	2.00 ± 0.14
(c) Anti-miRNA-10b (+200 kDa HA)	1.58 ± 0.22
(d) Anti-miRNA-10b (No HA)	1.58 ± 0.23

FIGURE 7: Effects of anti-miR-10b on cisplatin-induced cell growth inhibition in CD44v3^{high}ALDH1^{high} cells following 200 kDa-HA treatment. Effects of cisplatin-induced cell growth inhibition in CD44v3^{high}ALDH1^{high} cells transfected with negative miRNA control plus 200 kDa-HA addition (a) or with no HA addition (b) or transfected with anti-miR-10b inhibitor plus 200 kDa HA addition (c) or with no HA addition (d) for 7 days. Tumor cell growth inhibition (IC₅₀) is designated as “the μM concentration of chemotherapeutic drug (e.g., cisplatin treatment) that causes 50% inhibition of tumor cell growth” using CellTiter-Glo Luminescent Cell Viability Assay as described in the Section 2. IC₅₀ values are presented as the means ± standard deviation.

survival, chemoresistance, and head and neck cancer progression. Thus, silencing or inhibiting 200 kDa-HA-activated miRNA-10b may provide important new therapeutic targets to block matrix HA-associated CSC behaviors (e.g., tumor cell survival and chemoresistance) in head and neck cancer.

As summarized in Figure 8, we propose that the binding of 200 kDa-HA (step 1) to CD44v3^{high}ALDH1^{high} cells promotes specific target gene expression (step 2), including stem cell marker (Nanog, Oct4, Sox2, and KLF-4) expression (step 3-a). The resultant stem cell marker expression then induces spheres/self-renewal properties and clone formation (differentiation) (step 4-a) contributing to cancer stem cell functions and highly tumorigenic properties (step 5-a). At the same time, the binding of 200 kDa-HA to

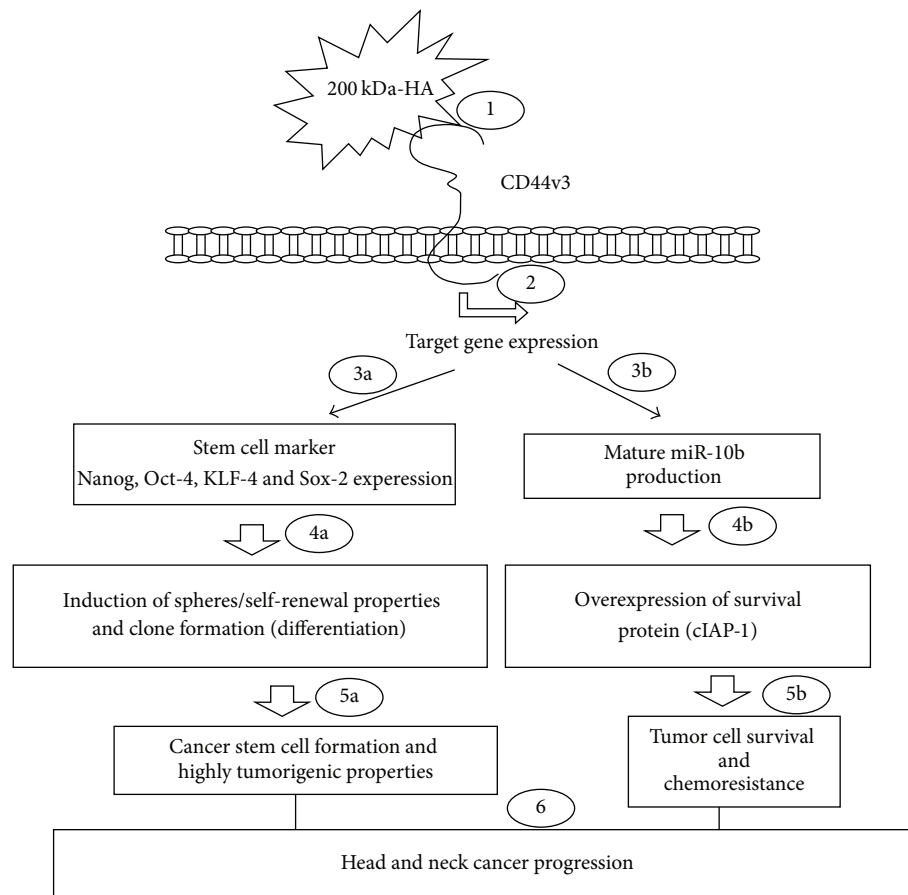


FIGURE 8: A proposed model for oncogenic signaling induced by 200 kDa-HA in the regulation of miRNA-10 production and cancer stem cell (CSC) functions in CD44v3^{high} ALDH1^{high} cells. The binding of 200 kDa-HA (step 1) to CD44v3^{high} ALDH1^{high} cells promotes specific target gene expression (step 2), including stem cell marker (Nanog, Oct-4, KLF-4 and Sox-2) expression (step 3-a). The resultant stem cell marker expression then induces spheres/self-renewal properties and clone formation (differentiation) (step 4-a) contributing to cancer stem cell formation and highly tumorigenic properties (step 5-a). At the same time, the binding of 200 kDa-HA to CD44v3^{high} ALDH1^{high} cells also stimulates miR-10b gene expression/mature miR-10b production (step 3-b) which then stimulates survival protein, IAP (c-IAP1) expression (step 4-b), and HNSCC cell antiapoptosis/survival as well as chemoresistance (step 5-b). Taken together, these findings suggest that HA- (in particular, 200 kDa-HA-) mediated cancer stem cell (CSC) pathways and miR-10b function play a critical role in promoting tumor formation and chemoresistance leading to head and neck cancer progression (step 6).

CD44v3^{high}ALDH1^{high} cells also stimulates miR-10b gene expression/mature miR-10b production (step 3-b) which then stimulates survival protein, IAP (c-IAP1) expression (step 4-b), and HNSCC cell anti-apoptosis/survival as well as chemoresistance (step 5-b). Taken together, these findings suggest that HA- (in particular, 200 kDa-HA-) mediated cancer stem cell (CSC) pathways and miR-10b function play a critical role in promoting tumor formation and chemoresistance leading to head and neck cancer progression (step 6).

Disclosure

Lilly Y. W. Bourguignon is a VA Senior Research Career Scientist.

Conflict of Interests

All authors declare no conflict of interests.

Acknowledgments

The authors gratefully acknowledge the assistance of Dr. Gerard J. Bourguignon in the preparation and review of this paper. This work was supported by Veterans Affairs (VA) Merit Review Awards (RR & D-II01 RX000601 and BLR & D-5I01 BX000628), United States Public Health grants (R01 CA66163), and DOD grant.

References

- [1] D. M. Parkin, F. Bray, J. Ferlay, and P. Pisani, "Global cancer statistics, 2002," *Ca: A Cancer Journal for Clinicians*, vol. 55, no. 2, pp. 74–108, 2005.
- [2] P. Dalerba, R. W. Cho, and M. F. Clarke, "Cancer stem cells: models and concepts," *Annual Review of Medicine*, vol. 58, pp. 267–284, 2007.

- [3] A. Schulenburg, H. Ulrich-Pur, D. Thurnher et al., "Neoplastic stem cells: a novel therapeutic target in clinical oncology," *Cancer*, vol. 107, no. 10, pp. 2512–2520, 2006.
- [4] G. R. Screaton, M. V. Bell, D. G. Jackson, F. B. Cornelis, U. Gerth, and J. I. Bell, "Genomic structure of DNA encoding the lymphocyte homing receptor CD44 reveals at least 12 alternatively spliced exons," *Proceedings of the National Academy of Sciences of the United States of America*, vol. 89, no. 24, pp. 12160–12164, 1992.
- [5] T. C. Laurent and J. R. E. Fraser, "Hyaluronan," *The FASEB Journal*, vol. 6, no. 7, pp. 2397–2404, 1992.
- [6] J. Y. Lee and A. P. Spicer, "Hyaluronan: a multifunctional, megaDalton, stealth molecule," *Current Opinion in Cell Biology*, vol. 12, no. 5, pp. 581–586, 2000.
- [7] P. H. Weigel, V. C. Hascall, and M. Tammi, "Hyaluronan synthases," *The Journal of Biological Chemistry*, vol. 272, no. 22, pp. 13997–14000, 1997.
- [8] R. Stern and M. J. Jedrzejas, "Hyaluronidases: their genomics, structures, and mechanisms of action," *Chemical Reviews*, vol. 106, no. 3, pp. 818–839, 2006.
- [9] L. Y. W. Bourguignon, G. Wong, W. Xia, M.-Q. Man, W. M. Holleran, and P. M. Elias, "Selective matrix (hyaluronan) interaction with CD44 and RhoGTPase signaling promotes keratinocyte functions and overcomes age-related epidermal dysfunction," *Journal of Dermatological Science*, vol. 72, no. 1, pp. 32–44, 2013.
- [10] L. Y. Bourguignon, "Matrix hyaluronan-activated CD44 signaling promotes keratinocyte activities and improves abnormal epidermal functions," *The American Journal of Pathology*, vol. 184, no. 7, pp. 1912–1919, 2014.
- [11] W. Knudson, C. Biswas, X. Q. Li, R. E. Nemecek, and B. P. Toole, "The role and regulation of tumour-associated hyaluronan," *Ciba Foundation symposium*, vol. 143, pp. 150–159, 1989.
- [12] B. P. Toole, T. N. Wight, and M. I. Tammi, "Hyaluronan-cell interactions in cancer and vascular disease," *The Journal of Biological Chemistry*, vol. 277, no. 7, pp. 4593–4596, 2002.
- [13] D. N. Haylock and S. K. Nilsson, "The role of hyaluronic acid in hemopoietic stem cell biology," *Regenerative Medicine*, vol. 1, no. 4, pp. 437–445, 2006.
- [14] L. Astachov, R. Vago, M. Aviv, and Z. Nevo, "Hyaluronan and mesenchymal stem cells: from germ layer to cartilage and bone," *Frontiers in Bioscience*, vol. 16, no. 1, pp. 261–276, 2011.
- [15] L. Y. W. Bourguignon, G. Wong, C. Earle, and L. Chen, "Hyaluronan-CD44v3 interaction with Oct4-Sox2-Nanog promotes miR-302 expression leading to self-renewal, clonal formation, and cisplatin resistance in cancer stem cells from head and neck squamous cell carcinoma," *The Journal of Biological Chemistry*, vol. 287, no. 39, pp. 32800–32824, 2012.
- [16] Y. C. Chen, Y. W. Chen, H. S. Hsu et al., "Aldehyde dehydrogenase 1 is a putative marker for cancer stem cells in head and neck squamous cancer," *Biochemical and Biophysical Research Communications*, vol. 385, no. 3, pp. 307–313, 2009.
- [17] M. R. Clay, M. Tabor, J. H. Owen et al., "Single-marker identification of head and neck squamous cell carcinoma cancer stem cells with aldehyde dehydrogenase," *Head and Neck*, vol. 32, no. 9, pp. 1195–1201, 2010.
- [18] L. A. Boyer, I. L. Tong, M. F. Cole et al., "Core transcriptional regulatory circuitry in human embryonic stem cells," *Cell*, vol. 122, no. 6, pp. 947–956, 2005.
- [19] W. Herr and M. A. Cleary, "The POU domain: versatility in transcriptional regulation by a flexible two-in-one DNA-binding domain," *Genes and Development*, vol. 9, no. 14, pp. 1679–1693, 1995.
- [20] I. Chambers, D. Colby, M. Robertson et al., "Functional expression cloning of Nanog, a pluripotency sustaining factor in embryonic stem cells," *Cell*, vol. 113, no. 5, pp. 643–655, 2003.
- [21] K. Mitsui, Y. Tokuzawa, H. Itoh et al., "The homeoprotein nanog is required for maintenance of pluripotency in mouse epiblast and ES cells," *Cell*, vol. 113, no. 5, pp. 631–642, 2003.
- [22] S. S. Chang, W. J. Wei, I. Smith et al., "MicroRNA alterations in head and neck squamous cell carcinoma," *International Journal of Cancer*, vol. 123, no. 12, pp. 2791–2797, 2008.
- [23] S. Volinia, G. A. Calin, C.-G. Liu et al., "A microRNA expression signature of human solid tumors defines cancer gene targets," *Proceedings of the National Academy of Sciences of the United States of America*, vol. 103, no. 7, pp. 2257–2261, 2006.
- [24] L. Y. W. Bourguignon, "Hyaluronan-CD44 interaction promotes microRNA signaling and RhoGTPase activation leading to tumor progression," *Small GTPases*, vol. 3, no. 1, pp. 53–59, 2012.
- [25] L. Y. W. Bourguignon, C. Earle, G. Wong, C. C. Spevak, and K. Krueger, "Stem cell marker (Nanog) and Stat-3 signaling promote MicroRNA-21 expression and chemoresistance in hyaluronan/CD44-activated head and neck squamous cell carcinoma cells," *Oncogene*, vol. 31, no. 2, pp. 149–160, 2012.
- [26] A. M. Hunter, E. C. LaCasse, and R. G. Korneluk, "The inhibitors of apoptosis (IAPs) as cancer targets," *Apoptosis*, vol. 12, no. 9, pp. 1543–1568, 2007.
- [27] L. Y. Bourguignon, M. Shiina, and J. J. Li, "Chapter ten—Hyaluronan-CD44 interaction promotes oncogenic signaling, microRNA functions, chemoresistance, and radiation resistance in cancer stem cells leading to tumor progression," in *Advances in Cancer Research*, vol. 123, pp. 255–275, 2014.

Review Article

Roles of Proteoglycans and Glycosaminoglycans in Wound Healing and Fibrosis

Shibnath Ghatak,¹ Edward V. Maytin,² Judith A. Mack,² Vincent C. Hascall,²
Ilia Atanelishvili,³ Ricardo Moreno Rodriguez,¹ Roger R. Markwald,¹ and Suniti Misra¹

¹Department of Regenerative Medicine and Cell Biology, Medical University of South Carolina, Charleston, SC 29425, USA

²Department of Biomedical Engineering, Cleveland Clinic, Cleveland, OH 44195, USA

³Division of Rheumatology & Immunology, Department of Medicine, Medical University of South Carolina, 114 Doughty Street, Charleston, SC 29425, USA

Correspondence should be addressed to Shibnath Ghatak; ghatak@musc.edu and Suniti Misra; misra@musc.edu

Received 20 September 2014; Accepted 1 April 2015

Academic Editor: Arnoud Sonnenberg

Copyright © 2015 Shibnath Ghatak et al. This is an open access article distributed under the Creative Commons Attribution License, which permits unrestricted use, distribution, and reproduction in any medium, provided the original work is properly cited.

A wound is a type of injury that damages living tissues. In this review, we will be referring mainly to healing responses in the organs including skin and the lungs. *Fibrosis* is a process of dysregulated extracellular matrix (ECM) production that leads to a dense and functionally abnormal connective tissue compartment (dermis). In tissues such as the skin, the repair of the dermis after wounding requires not only the *fibroblasts* that produce the ECM molecules, but also the overlying epithelial layer (*keratinocytes*), the *endothelial cells*, and *smooth muscle cells* of the blood vessel and white blood cells such as *neutrophils* and *macrophages*, which together orchestrate the cytokine-mediated signaling and paracrine interactions that are required to regulate the proper extent and timing of the repair process. This review will focus on the importance of extracellular molecules in the microenvironment, primarily the proteoglycans and glycosaminoglycan hyaluronan, and their roles in wound healing. First, we will briefly summarize the physiological, cellular, and biochemical elements of wound healing, including the importance of cytokine cross-talk between cell types. Second, we will discuss the role of proteoglycans and hyaluronan in regulating these processes. Finally, approaches that utilize these concepts as potential therapies for fibrosis are discussed.

1. Introduction

Our understanding of the biology of wound healing has advanced significantly in recent years. A major goal is to determine what are the biochemical/physiological factors in the wound that can reconstruct the damaged parts more effectively. Wound healing is a dynamic interactive process involving many precisely interrelated phases that overlap in time and lead to the restitution of tissue integrity. The healing process reflects the complex and coordinated body response to tissue injury resulting from the interactions of different cell types and extracellular matrix components. Failure of coordinated regulation can result in tissue fibrosis with excessive collagen production and, if highly progressive, the fibrotic process may eventually lead to organ malfunction and death. Most chronic wounds are associated with fibrosis of various

organs, ischemia, or diabetes mellitus and affect from 3 to 6 million people in the USA, with older persons (>65) accounting for 85% of these events. Nonhealing wounds result in enormous health care expenditures, with the total cost estimated to be more than \$3 billion *per year* [1].

The importance of the ECM in the complex processes of wound healing is that it provides architectural support for the tissues and a platform for cells and molecules that regulate inter- and intracellular signaling. ECMs are secreted molecules that constitute the cell microenvironment and are composed of a dynamic and complex array of glycoproteins, collagens, glycosaminoglycans (GAGs), and proteoglycans (PGs). Among these, the GAG hyaluronan (HA) and the PGs such as versican and aggrecan are all partners in the control of the wound healing process. It is now well accepted that the ECM not only provides architectural support for resting

tissues, but also undergoes important alterations after injury that are essential for directing cell behavior during the wound healing process. The function of the ECM facilitates repair of the wound either directly by modulating important aspects of cell behavior such as adhesion, migration, proliferation, metabolism, differentiation, and survival, or indirectly by modulating extracellular protease secretion/activation, or by modulating growth factor activity or bioavailability. Cells have specific transmembrane receptors that recognize ECM components and interact with the intracellular cytoskeleton and signaling pathways [2]. Classic examples of ECM interactions with cells that fulfill the criteria of anchoring and adhesion to receptors that modulate intracellular signaling pathways involve cell surface receptors such as integrins and the HA receptor CD44 [3–5]. Receptors on ECM are involved in many pathological processes, including inflammation, fibrosis diseases, and cancer [6–8]. Although it is clear that a cascade of ECM molecules, including GAGs, PGs, connective tissue glycoproteins, and cell surface adhesion receptors, are involved in wound healing, we will primarily address the problem of wound healing with abnormal fibrosis by focusing on the role of the cell-adhesion molecule CD44 and its principal ligand HA in wound healing and tissue fibrosis.

2. Biochemical and Physiological Characteristics of Wound Healing

2.1. Wound Healing and Fibrosis. Wounds are injuries to a living tissue. The cellular, molecular, biochemical, and physiological events associated with wound healing permit living tissue to repair tissue injury. This process consists of a highly orchestrated sequence of events that require the collaborative efforts of many different cell types, including blood cells, epithelial and connective tissue cells, inflammatory cells, and many soluble factors, such as coagulation factors, growth factors, and cytokines. The behaviour of each of the participating cell types during the phases of proliferation, migration, matrix synthesis, and contraction, as well as the soluble factor and matrix signals present at a wound site, is crucial for repairing the tissue injury. It is a dynamic and strongly regulated process that starts immediately after the initial lesion, and it will last until complete closure of the wound and regeneration of the tissue as functional as possible occurs. Fibroblasts are the principal biosynthetic cells producing interstitial collagens, fibronectins, and other matrix components. They also differentiate into myofibroblasts, a specialized contractile cell type responsible for closure of the wound. In the setting of repetitive trauma or certain pathological states, increased ECM deposition of abnormal matrix (scarring; fibrosis) occurs in a variety of fibrotic diseases in tissues, including liver [9], kidney [10], lung [11], and heart [12, 13], and in scleroderma [14, 15]. Collagen deposition in the matrix is a requisite and, typically, reversible part of wound healing. However, in fibrosis, normal tissue repair can evolve into a progressively irreversible fibrotic response with fibroblast differentiation to excessive numbers of myofibroblasts and increased collagen deposition.

2.2. Sequence of Processes in Wound Healing. Wound healing involves integrated and overlapping phases: (a) haemostasis, (b) inflammation, (c) proliferation, and (d) remodelling (Figure 1).

2.2.1. The Homeostasis of Wound Healing. Immediately after the injury, vascular constriction and platelet aggregation at the injury site form a fibrin clot, which reduces leakage of blood from damaged blood vessels in the wound. The fibrin clot is a temporary shield containing many important molecules: fibronectin (FN), SPARC (Secreted Protein, Acidic and Rich in Cysteine), thrombospondin, vitronectin, and growth factors such as transforming growth factor- β (TGF- β), platelet-derived growth factor (PDGF), fibroblast growth factor (FGF), epidermal growth factor (EGF), and insulin-like growth factor-1 (IGF-1) released by platelets and monocytes [16]. Components of the fibrin clot also bind to cells and to other ECM proteins simultaneously [17]. The clot then provides a provisional matrix for migration of the cells to pass over and through during the wound repair process [16, 18].

2.2.2. The Inflammation Phase. Once the bleeding is controlled, sequential infiltration of inflammatory cells, such as neutrophils, macrophages, and lymphocytes into the wound (chemotaxis) promote the inflammatory phase [19–21]. A critical function of neutrophils is the clearance of invading microbes and cellular debris in the wound area, although these cells also produce substances such as proteases and reactive oxygen species (ROS), which can cause additional damage. Unless a wound is grossly infected, the neutrophil infiltration terminates within a few days, and expended neutrophils will be phagocytosed by tissue macrophages, which then degrade nonviable tissue and dead bacteria. Inflammation lasts as long as there is debris in the wound. However, inflammation can lead to the damage of tissue if it lasts too long. Thus, the reduction of inflammation is frequently a goal in therapeutic settings.

2.2.3. The Proliferation and Migratory Phase. By clearing the apoptotic cells, macrophages help the resolution of inflammation, and they undergo a phenotypic transition to a reparative state that stimulates keratinocytes, fibroblasts, and angiogenesis to promote tissue regeneration [22, 23]. T-lymphocytes migrate into wounds following the inflammatory cells and macrophages, and they peak during the late-proliferative/early-remodelling phase. Although the role of T-lymphocytes is not completely understood, studies have reported that CD4+ cells (T-helper cells) have a stimulatory role while CD8+ cells (T-suppressor-cytotoxic cells) have an inhibitory role in wound healing [24, 25]. Blood factors are released into the wound that cause the migration and division of cells, which prepares them for the proliferative phase. In this way, macrophages promote the transition to the proliferative phase of healing.

2.2.4. The Reparative Phase and Remodeling. The *reparative phase and remodeling* is characterized by the formation of

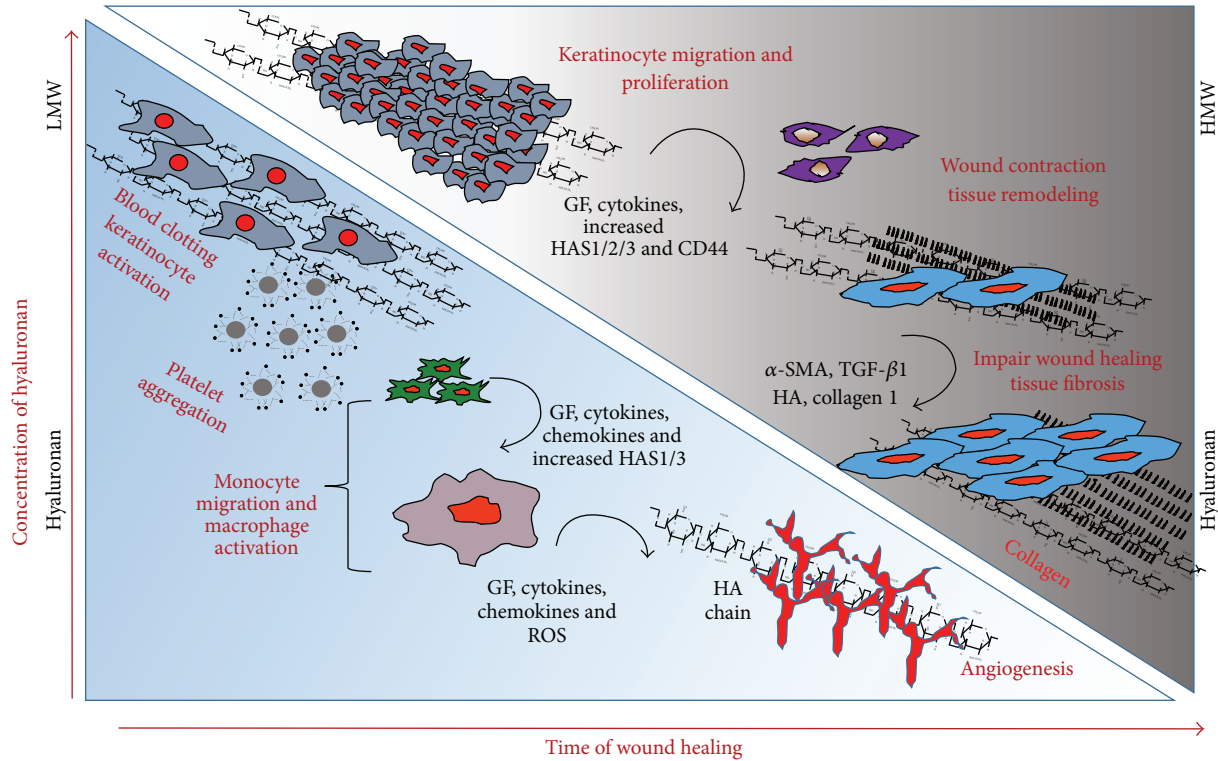


FIGURE 1: Schematic presentation of changes in hyaluronan synthesis/molecular size and cellular events and matrix events during the course of wound healing and fibrosis. Many of the biological processes mediated by HA are crucial for wound healing and fibrosis. After injury, wound healing follows a tightly regulated sequence of events. These phases are inflammation, granulation tissue formation, proliferation, reepithelization, and remodelling. In the early phases, high molecular HA is degraded by reactive oxygen species from activated granulocytes and by hyaluronidases secreted from platelets. Then monocytes secrete inflammatory mediators, which attract additional inflammatory cells. Keratinocytes become activated to migrate, proliferate, and to synthesize HA. As a result the LMW degradation products are active inducers of angiogenesis and inflammation. At later stages the interim matrix becomes supplemented with newly synthesized HMW HA, which contributes to tissue remodelling. During repetitive injury, the repairing processes are hindered, and the *keratinocytes*, the endothelial cells, and *smooth muscle cells* of the blood vessel, *neutrophils*, and *macrophages* together orchestrate the increased cytokine-mediated signaling and augment HA-CD44 signaling and excess collagen production that results in fibrosis.

the granulation tissue that fills the wound before reepithelialization where epithelial cells migrate across the new tissue to form a barrier between the wound and the environment. Granulation tissue contains fibroblasts and endothelial cells in an ECM that contains GAGs and PGs [26], which supports capillary growth, fibronectin, and collagen formation at the site of injury so that vascular density of the wound can return to normal. Thus, following robust proliferation and ECM synthesis, wound healing enters the final remodelling phase, where the wound also undergoes physical contraction mediated by contractile fibroblasts (myofibroblasts) that appear in the wound [20, 21] (Figure 1).

3. Modulators of Fibrosis in Wound Healing

3.1. Soluble Mediators in the ECM during Wound Healing and Fibrosis. The time-dependent sequence of events in wound healing includes regulation of cell-ECM interactions that are controlled by soluble mediators that act synergistically to direct wound remodelling by regulating ECM synthesis and degradation. Subsequently, the myofibroblast population is also expanded as a result of epithelial cells undergoing

epithelial-to-mesenchymal transition (EMT) and of the activation of resident fibroblasts that leads to ECM deposition and tissue remodeling. The types of soluble mediators released during tissue injury are described below.

Following tissue injury, platelets aggregate and release platelet-derived growth factor-AB (PDGF-AB) from the granules. Consequent infiltration of macrophages provides an additional source of PDGF-AB. PDGFs are potent mitogens and chemoattractants for many cells, including fibroblasts, smooth muscle cells, mesenchymal cells, neutrophils, and monocytes, and they upregulate fibronectin, procollagen, and collagen activities. PDGFs have crucial roles in fibrotic disorders such as kidney, lung, and skin fibrosis [10, 27–29]. Healing of the wounds involves increased infiltration of inflammatory cells and fibroblasts followed by a marked increase in collagen deposition at the wound site. TGF-β1 influences collagen degradation by stimulating tissue inhibitor of metalloproteinase (TIMP), which inhibits protease activity and decreases degradation of newly synthesized collagen [30–33]. We and others showed that blocking TGF-β1 decreases ECM deposition, scar formation, and fibrosis [14, 34]. Like PDGF, the fibrogenic potential of TGF-β1 makes

it a prime candidate for drug therapy in settings of tissue fibrosis [35].

FGFs are strongly mitogenic for endothelial cells and are involved in angiogenesis, directing endothelial cell migration, proliferation, and plasminogen activator synthesis [36]. IGFs are produced by several cell types including macrophages and fibroblasts [37, 38], and they have the potential to activate fibroblasts by either stimulating replication or increasing the production of connective tissue components such as collagen, elastin, and PGs, including versican [39, 40]. EGF acts as a mitogenic factor for cells including fibroblasts, keratinocytes, smooth muscle cells, and epithelial cells [41–44] and increases skin wounds [45]. However, exaggeration of this process of repair and the subsequent increased reorganization of the tissue matrix can lead to the development of fibrotic scar tissue that is characterized by excessive accumulation of ECM components, including fibronectin, PGs, HA, and interstitial collagens.

3.2. Proteoglycans in Wound Healing. PGs have core proteins or glycoproteins with large GAG side-chains (Figure 2), and they participate in cell-cell and cell-matrix interactions, cell proliferation, and migration, and in cytokine and growth factor signaling associated with wound healing. Small leucine-rich PGs (SLRPs) and the chondroitin sulfate PG versican are found in the dermis of wounds, the PG perlecan in the basement membrane, and the heparan sulfate PGs, syndecans, and glypicans on the cell surfaces. The versican-v3 isoform promotes transition of normal dermal fibroblasts to myofibroblasts [46, 47]. Perlecan regulates wound healing through induction of angiogenesis [48]. Increased expression of syndecans-1 and syndecans-4 in wounds [49] stimulates keratinocyte [50] and endothelial cell migration and angiogenesis in mice [51]. Decorin, a member of the SLRP family, negatively regulates TGF- β 1 [52] and demonstrates effects of antifibrosis in various tissues, including kidney [53], muscle [54], and lung [55]. GAG chains covalently bound to the core protein of PGs dominate their physical properties. PGs can maintain the ECM in a hydrated condition, exclude other macromolecules, and allow permeability of low molecular weight solutes. Thus, by interacting with other ECM components, PGs are critical to organize the matrix [56, 57].

3.3. Glycosaminoglycans in Wound Healing. Of the various ECM macromolecules, the GAG side-chains of PGs are very important players in wound healing. GAG chains (Figure 3) exhibit considerable structural diversity resulting from a complex biosynthesis that is tightly regulated in biological systems, enabling the modified GAGs to selectively interact with a variety of ligands in a spatially and temporally controlled manner [56, 57]. During the proliferation phase of wound healing, fibroblasts and other mesenchymal cells enter the inflammatory site of the wound in response to growth factors that are necessary for stimulation of cell proliferation [58]. The fibroblasts synthesize collagen and PGs, which continues for several weeks with proportional increases of collagen. During this time, endothelial cells form capillaries, and the GAGs (HA, chondroitin sulfate (CS), and dermatan

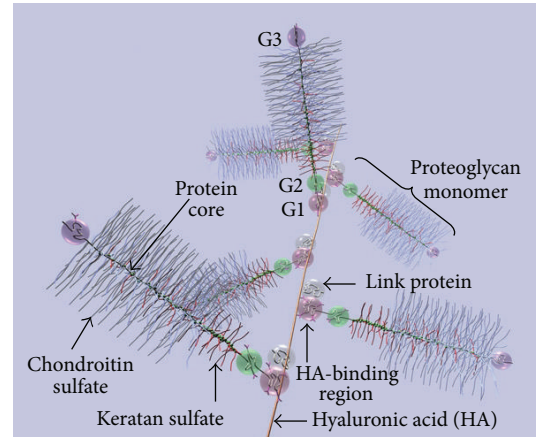


FIGURE 2: Diagram of part of an aggrecan aggregate. G1, G2, and G3 are globular, folded regions of the central core protein. Proteoglycan aggrecan showing the noncovalent binding of proteoglycan to HA with the link proteins.

sulfate (DS)) also change in their levels. Initially, HA is synthesized in large amounts by the fibroblasts for 2 weeks [26], followed by increased levels of DS and CS PGs [59]. Gradually, when the proliferation of cells reaches a plateau, heparan sulfate (HS) PGs are elevated in the wound. Sulfated PGs with CS and DS assist in collagen polymerization [60], and HS PGs on cells can create anchors to surrounding matrix [61]. PG degradation by proteases in the wounds can release GAG-peptide fragments, which may modulate the wound healing process [62]. For instance, CS and DS can regulate growth factor activity and may stimulate nitric oxide production, which, in turn, can modulate angiogenesis, whereas HS can stimulate the release of IL-1, IL-6, PGE2, and TGF- β and contribute to the modulation of its proangiogenic effects in the tissues [63, 64]. Studies have demonstrated colocalization of the large CS PG versican with HA in cables in smooth muscle cells [65] and in an epithelial cell system [66]. Of the GAGs, HA has a key role in each phase of wound healing as well as in regulating ECM organization and metabolism [67].

3.4. HA in Wound Healing and Fibrosis

3.4.1. Structure of Hyaluronan. HA is omnipresent in the human body and in all vertebrates, occurring in almost all biological fluids and tissues, with the highest amounts in the ECM of soft connective tissues. HA is a linear, naturally occurring, nonsulfated GAG of the ECM (Figure 3). HA has a repeat of disaccharides consisting of D-glucuronic acid and N-acetylglucosamine [68–70]. Native HA has a very high molar mass, usually in the order of millions of Daltons, (10^5 to 10^7 Da) before being progressively degraded into smaller fragments in the ECM [14, 67, 70, 71]. It possesses interesting viscoelastic properties based on its polymeric and polyelectrolyte characteristics. Despite its relatively simple structure, HA is an extraordinarily versatile GAG and is involved in several key processes, including early EMT in development and morphogenesis, cell signaling, wound repair and regeneration, matrix organization and pathobiology.

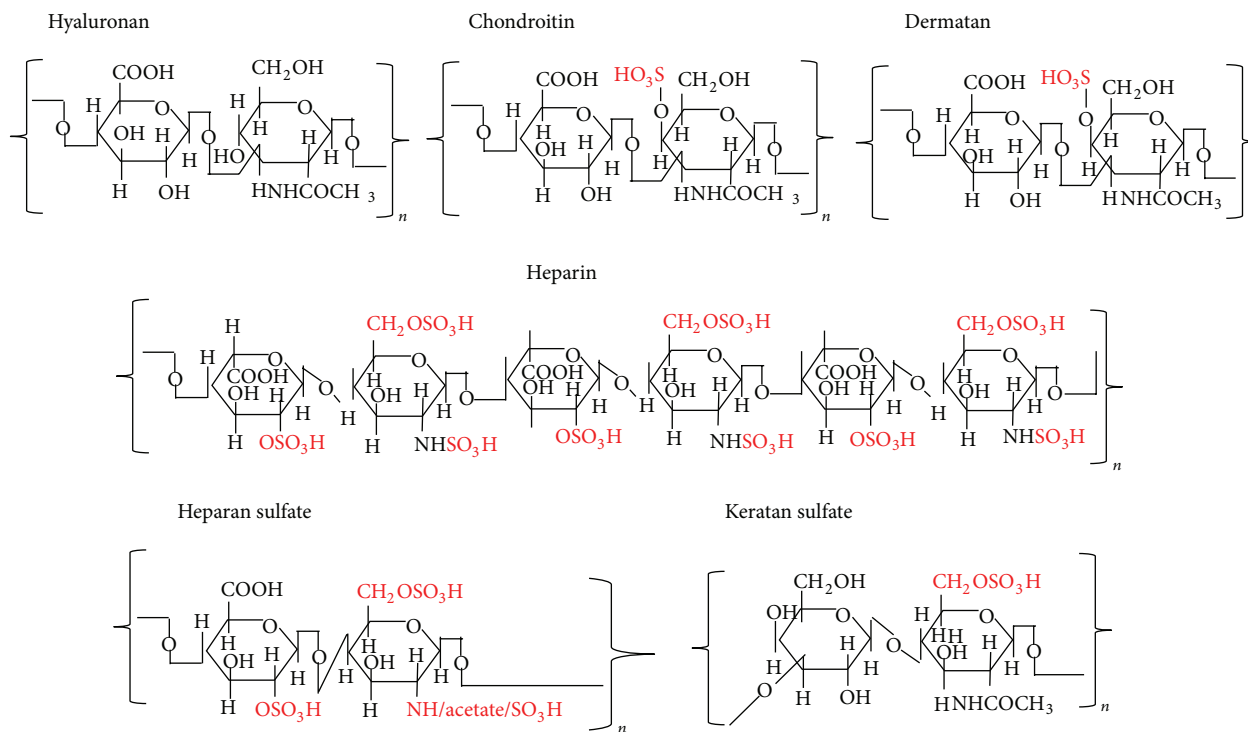


FIGURE 3: Structures of repeating disaccharides of glycosaminoglycans.

3.4.2. HA during Inflammation in Tissue Injury and Fibrosis.

A pattern has emerged; following tissue injury, inflammatory cells, keratinocytes, fibroblasts, endothelial cells, and pluripotent stem cells undergo interactions with ECM macromolecules or their fragments to heal the wound. During the inflammatory phase of wound healing, HA accumulates in the wound bed and acts as a regulator of early inflammation. The major functions of HA in this phase are to modulate inflammatory cell and fibroblast cell migration, proinflammatory cytokine synthesis, and the phagocytosis of invading microbes [67]. In this inflammatory phase, HA degradation products (low-MW HA presumably $\sim 2.5 \times 10^5$ Da) can promote early inflammation. At sites of inflammation and tissue injury, these low-MW HA fragments that accumulate from degradation of high molecular weight HA can initiate toll-receptor-2 and toll-receptor-4 (TL-R2 and TL-R4) induction of proinflammatory cytokines IL-6, TNF- α , and IL-1 β [72]. These cytokines, in turn, induce HA production *in vitro* by various cell types, including endothelial cells [73], dendritic cells [74], and fibroblasts [75]. The proliferative phase overlaps with the remodeling phase where keratinocytes differentiate to fibroblasts. During these events, the growth factors and cytokines released by the inflammatory cells induce fibroblast and keratinocyte migration and proliferation. Furthermore, the levels of HA synthesized by both fibroblasts and keratinocytes are elevated during reepithelialization where epithelial cells migrate across the new tissue to form a barrier between the wound and the environment [26] (Figure 1).

The levels of HA and its degradation products are abundant in patients with scleroderma fibrosis and in the animal models of bleomycin-induced lung injury [76, 77].

The excessive production of HA is one of the major events in scleroderma fibrosis [78, 79]. Furthermore, increased HA levels are observed in bronchoalveolar lavage (BAL) fluid and/or plasma from patients with pulmonary fibrosis [80], interstitial lung disease [81], and idiopathic pulmonary injury [82]. However, failure to remove HA fragments from the site of tissue injury contributes to the unremitting inflammation and destruction observed in tissue fibrosis [83]. Clearance of HA fragments depends both on its receptor CD44 [84] and on recognition by the host via TL-R2 and TL-R4 [85] (Figure 1).

3.4.3. HA Synthases and Tissue Injury.

Most cells synthesize HA at some point during their life cycles implicating its function for fundamental biological processes. Unlike all of the sulfated GAGs, biosynthesis of HA does not require a core protein and is not done in the cell's Golgi networks. HA is naturally synthesized by a class of integral membrane proteins called HA synthases, of which vertebrates have three types: HAS1, HAS2, and HAS3 [86–88]. The expression of various HAS isozymes is likely to be a fine control system critical for the effective mediation of different cell behaviors. While HAS1 and HAS2 are able to produce large-sized HA (up to 2000 kDa), HA produced by HAS3 is of a lower molecular mass (100–1000 kDa) [89–91]. HAS2 is dynamically regulated at several levels. For example, a number of studies have defined the details of transcriptional regulation of the HAS2 gene promoter in response to a variety of cytokines and growth factors that are released as a result of wounding [92, 93]. Some of the most dramatic effects of cytokines on HA regulation occur in epidermal keratinocytes of the skin, in which HA production is boosted many-fold by exposure

to a variety of growth factors including EGFR [94, 95]. Interestingly, wounding of keratinocytes releases HB-EGF, which itself has been shown to upregulate HA synthesis in neighboring cells [96, 97], an example of the paracrine effects (cell-cell cross-talk) that now appear to have a central role in mechanisms of fibrosis (discussed more below). HAS2 activity can also be governed by posttranslational pathways, such as regulation of O-GlcNAcylation. Once in circulation, HA is very effectively removed by hepatic endothelial cells. This efficient process recovers the sugars by internalization and transport to lysosomes [98]. Most cells do not have this option but do have a metabolically active pericellular matrix (glycocalyx). (Figure 4) For example, keratinocytes catabolize hyaluronan by a mechanism that involves the CD44 HA receptor [86, 99] and a hyaluronidase, most likely GPI-anchored hyaluronidase 2 [100]. The presence of a protease, such as ADAMTS5 (aggrecanase) is likely also involved in order to remove associated proteoglycans (aggrecan and versican) [47]. CD44 rapidly transports ($t_{1/2}$ of ~15 min) the fragmented HA (20–30 kDa) with any remaining bound proteins into an endosomal compartment distinct from coated pits and pinocytotic uptake pathways. The fragments are then transported to lysosomes for complete degradation ($t_{1/2}$ of ~3 h) (Figure 4) [86, 99]. Therefore, distinct sites for biosynthesis and catabolism of HA on the surface of cells could effectively cooperate in controlling its dynamic metabolism. The stability of cytosolic HAS2 is significantly increased when serine 221 on Has2 is O-GlcNAcylated [86, 101]. Recent studies from our laboratory indicate that the matricellular protein periostin regulates HAS2 activation at a serine residue in embryonic heart valve remodelling [102]. It is possible that O-GlcNAcylation of this serine is a key for regulating whether or not HAS2 remains inactivated in response to periostin during development of the heart valve [102], which would allow the enzyme to migrate to the cell surface after its synthesis in the ER. There is increasing evidence that phosphorylation of serine and threonine residues in HAS2 to control hyaluronan synthesis whether or not it is activated [86, 103]. The phosphoserine increases when HA synthesis increases and phosphothreonine increases when HA synthesis decreases, as it is expected from the data discussed by Hascall's group [86].

HA, either alone or more often through its interaction with its binding partner CD44 on the cell membrane, is crucial for the tissue morphogenesis. For example, while the HAS1 and HAS3 null mice are developmentally normal, HAS2 deletion results in lethal defects in cardiac development and vascular abnormalities. TGF- β 2-induced HAS2 expression and subsequent HA-CD44 signaling are required for endocardial cushion formation in HAS2-null mice [104–107]. Recent studies demonstrate that the balance of HA produced by distinct HAS enzymes is important for regulating inflammatory responses and wound contraction in the skin after injury [108]. At physiological pH, HA is a highly polyanionic molecule associated with counter ions, such as Na⁺, K⁺, Ca²⁺, and Mg²⁺. HA is characterized by its ability to occupy large hydrophilic solvent domains due to its very large size, which helps maintain the extracellular space and facilitates the transport of small molecular weight solutes through its

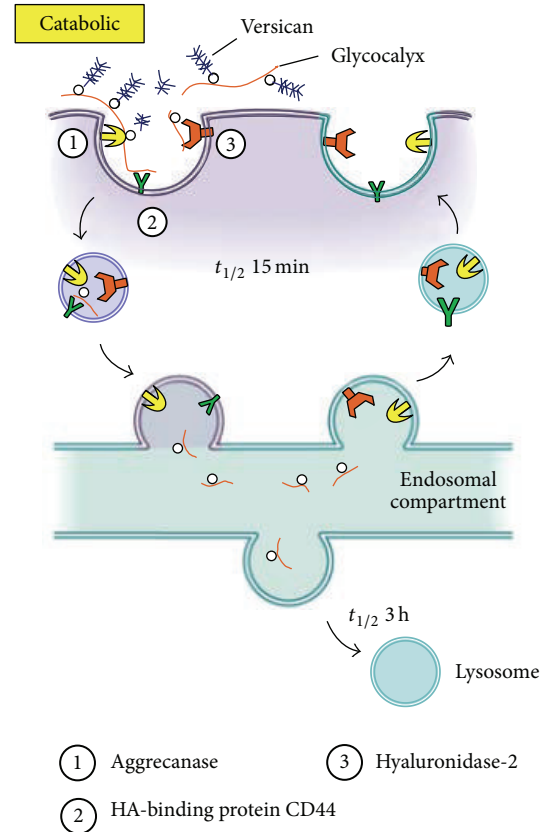


FIGURE 4: Model for catabolism of pericellular hyaluronan glyco-lycocalyx matrices (adapted from [86] with the permission from Dr. Hascall).

domain. Solutions of high molecular mass HA exhibit time-dependent viscoelasticity because of polymer chain entanglement [109]. During rapid growth and tissue remodelling, the viscoelastic properties of HA depend on its molecular weight. The hydrated domain and the viscoelastic properties of HA are relevant for the application of HA in tissue repair as has been known for decades. In addition to the physicochemical effects of HA, HA also mediates the migration of fibroblasts to the wound site [110, 111]. *In vitro* studies have demonstrated that, in the presence of specific growth factors, the higher the levels of HA, the greater the cell migration in cell cultures [14, 102, 112–116]. Most of the effects of HA upon cell behavior are mediated via interactions between HA and the HA receptors, CD44 [7, 14, 111, 113, 117–120] and RHAMM [121–124], through which intracellular signalling pathways are activated.

In skin wound healing, the differentiation of fibroblasts to myofibroblasts is very important for the closure of wounds and for the formation of the collagen-rich scar. In this regard, various studies have pointed to an important role of HA and HAS enzymes in regulating fibroblast-to-myofibroblast conversion. Work by the group of Steadman and Phillips has shown that the pericellular HA coat that surrounds human dermal fibroblasts appears to regulate profibrotic behavior of

these fibroblasts, such that inhibition of HA synthesis significantly reduces TGF- β -driven fibroblast proliferation [125] and transformation to myofibroblasts [126]. Furthermore, the mechanism by which HA regulates TGF- β signaling effects in the fibroblasts appears to involve changes in colocalization of the HA receptor (CD44) and the epidermal growth factor receptor (EGFR), both of which interact in the plasma membrane within lipid rafts [127–129]. Strong evidence for an important link between HA, CD44, and fibrotic processes is also found in the lung (as discussed later in Section 4.2.1). At another level, HA in the skin appears to regulate cytokine production and secretion in healing wounds by regulating the influx of leukocytes into the wound area. For example, selective loss of Has1 and Has3 (in Has1/Has3 double knockout mice) leads to a proinflammatory milieu that favors recruitment of neutrophils and macrophages in the connective tissue (dermis) [108]. In the Has1/Has3 double knockout mice, the rate of wound closure is accelerated (rather than inhibited), despite loss of HA-synthetic capacity in the skin epithelium and a reduction in overall HA levels in the dermis [108]. One possible explanation for this rapid wound closure is the observation that neutrophils and macrophages are recruited in greater numbers from small cutaneous vessels at the wound sites [108]. The abundant leukocytes secrete higher amounts of cytokines (e.g., TGF- β 1), which probably activate local fibroblasts, making them more contractile and promoting their transformation into myofibroblasts, which thereby contracts the wounded [108]. The mechanism for robust neutrophil/macrophage recruitment in the Has1/Has3 mice is currently unknown. In a third example of how HA is important in fibrosis, overactive fibroblast behavior contributes to the pathogenesis of progressive fibrotic disorders such as scleroderma [71, 130–132]. Recent studies have shown that a critical element in the etiology of scleroderma is the presence of abnormal paracrine signaling involving signal-amplification loops between skin fibroblasts and the overlying keratinocytes. When keratinocytes from scleroderma patient skin are cocultured with fibroblasts, the fibroblasts were stimulated to produce more ECM due to dysregulated paracrine signaling involving IL-1 and TGF- β [130]. Given the importance of HA in regulating fibroblast responses to TGF- β and other cytokines, the potential for involvement of HA and CD44 in fibrotic processes of the skin appears to be ripe for future investigation.

In the lung, Has-mediated HA synthesis also has a vital role in repair after tissue injury. In the human disease *idiopathic pulmonary arterial hypertension*, increased HAS1 and decreased HAS2 levels are observed in pulmonary artery smooth muscle cells isolated from the patients, in whom total lung HA concentrations are also increased [82]. In a mouse model of *asthma*, expression of HAS1 and HAS2 is increased in lung tissue [133]. Conditional deletion of HAS2 in mesenchymal cells in α -smooth muscle actin (α -SMA)-HAS2 transgenic mice abrogated the invasive fibroblast phenotype, impeded myofibroblast accumulation, and inhibited the development of lung fibrosis [83].

3.4.4. HA Degradation. High molecular weight HA has many crucial structural and physiological functions in wound

repair following injury on the basis of its molecular weight and accessibility to various HA-binding proteins (HABPs) [67]. HA synthesis and degradation are tightly regulated during embryonic development and homeostatic processes. HA is removed from the ECM as a consequence of local catabolism. In mammals, the enzymatic degradation of HA results from the action of 5 functional hyaluronidases (Hyal), of which Hyal1 and Hyal2 are the two most common and ubiquitously important [71]. Hyal1 and Hyal2 are considered to be the main active HAases in tissues in almost all somatic tissues [134]. No HAase activity for human Hyal3 has been shown [127], and, in mice, Hyal3 does not seem to have a major role in constitutive HA degradation [135]. Recently, a novel HAase (KIAA1199) has been described, which is also detectable in human skin [136]. The larger isoform of Hyal1 is often secreted by the cell, while the smaller isoform is retained in acidic intracellular vesicles and lysosomes [137]. Hyal2 is often found as a glycosylphosphatidylinositol- (GPI-) anchored form, tethered to the extracellular side of the plasma membrane [138, 139]. By catalyzing the hydrolysis of HA, a major constituent of the interstitial barrier, Hyals lower the viscosity of HA, thereby increasing tissue permeability. Hyal1 has the maximal HA-degrading activity at pH 3.5–3.8 and cleaves HA to small oligosaccharides, which is consistent with its role of activity within lysosomes [140]. Hyal2 shows optimal activity at pH 6.0–7.0 and cleaves high molecular weight HA into intermediate size fragments of ~20 kDa [127].

HA degradation products stimulate endothelial cell proliferation, migration, and tube formation following activation of specific HA receptors, in particular CD44 and RHAMM [141]. HA fragments are implicated in the progression of lung diseases [142], and Hyals are elevated in scleroderma, a fibrotic lung disease [138, 143]. Furthermore, reactive oxygen species (ROS) can fragment HA under oxidative conditions [144]. HA catabolism by Hyals and ROS creates products that have biological activities distinct from native high molecular weight HA. HA fragments less than 20 disaccharides have been shown to be angiogenic [145]. Low and intermediate molecular weight HA (2×10^4 – 4.5×10^5 Da) can stimulate gene expression in macrophages, endothelial cells, eosinophils, and certain epithelial cells [146–149]. HA at ~200 kDa represents an interesting therapeutic strategy as it promotes reconstruction of a functional epithelium monolayer *in vitro* [150]. On the other hand, excessive HA degradation products also promote fibrotic scar tissue formation [151, 152].

3.4.5. HA Receptor Interaction Induces Signaling in Wound Healing and Fibrosis. HA is involved in embryogenesis, wound repair, and tissue regeneration [142]. Skin wounds on early mammalian embryos heal perfectly with no signs of scarring and with complete restitution of the normal skin architecture [153], and the wound fluid HA is of high molecular weight [154]. During tissue injury and inflammation, HA that is normally present as high molecular weight (>1000 kDa) is modified into monocyte-adhesive matrices that stimulate immune cells at the injury site to express inflammatory genes through interactions with cell surface

receptors. This leads to the release of enzymes and free radicals, which break the long chain molecules to lower molecular weight forms that have extraordinarily wide-ranging and often opposing biological functions, owing to the activation of different signal transduction pathways [155]. Studies have shown that HA fragments of lower molecular weight (~50–200 kDa) are proinflammatory, immunostimulatory, and proangiogenic, and they competitively bind to HA receptors on cell surfaces [156] (Figure 4).

While HA fragments may be important in initiating the inflammatory response, removal of these fragments is also critical for the resolution of the repair process [157]. Initial studies indicated that signaling initiated by HA degradation products involves CD44 primarily. However, studies of CD44-null macrophages indicate that there are other signaling pathways, notably through toll-like receptors, TL-R2 and TL-R4 [85]. Biological functions of HA and HA fragments are manifested through its interactions with a large number of HA-binding proteins (HABPs or hyaladherins) that exhibit significant differences in their tissue expression, specificity, affinity, and regulation [4, 7, 84, 118, 158–163]. A number of HBP bind HA through binding motifs, known as the link module, which consists of a span of ~100 amino acids that binds HA when oriented in the correct tertiary structure [164]. HABPs are constituents of the ECM, stabilize its integrity, and are involved in cellular signal transduction dependent on the molecular weight of HA and the cell phenotype [165].

Generally, HABPs interact with a minimum of 6–10 sugar residues of HA [142]. Therefore, a single chain of high molecular weight HA can theoretically accommodate on the order of 1000 HABPs [166]. The HBP link module family includes the link proteins, the PGs aggrecan, versican, brevican and neurocan, CD44 standard and variants, tumor necrosis factor- α stimulated gene 6 (TSG-6), and lymphatic vessel endothelial receptor 1 (LYVE-1) [167–169]. Studies have shown that, in response to HA of 40–400 kDa, the NF- κ B-mediated gene expression is activated by HA binding with HA receptor for endocytosis (HARE) [170]. The RHAMM receptor is an unrelated HA-binding protein with a HA-binding site peptide motif (B(X7) B) of minimal size of interaction with HA. CD44 and RHAMM are well-studied receptors associated with tissue injury, repair, cancer cell growth, and metastasis [4, 14, 159, 163, 171–173]. In addition, the binding of HA to intracellular adhesion molecule (ICAM-1) may affect its binding to other receptors at early stages of inflammatory activation [174].

3.4.6. CD44 in Wound Healing and Fibrosis. The constitutive expression of CD44 and HA by a wide variety of cells implies that the interaction between these molecules is regulated. CD44 is the best characterized transmembrane HA receptor and because of its wide distribution it is considered to be the major HA receptor on most cell types [169]. CD44 is a structurally variable and multifunctional cell surface glycoprotein encoded by a single gene [175] (Figure 5). The genomic structure of CD44 consists of 21 exons [175] and the CD44 gene expression varies in size due to insertion of alternatively spliced variable exons derived from

exon6–exon14 to form CD44v1–CD44v10 that are located in the membrane-proximal extracellular CD44 domains [176], approximately where N-terminal sequence homology between CD44 molecules from different species ends. The standard CD44 (CD44s) has a molecular weight ~90 kDa and exhibits extensive N-linked and O-linked glycosylation of the extracellular region, emphasizing the glycoprotein nature of CD44. CD44 can be induced to bind HA in cells activated with inflammatory stimuli, including cytokines, such as TNF- α , IL- α , IL-1 β , IL-3, granulocyte-macrophage colony stimulating factor (GM-CSH), and interferon- γ (IFN γ) [84, 177, 178]. The molecular mechanisms underlying the induction of CD44-mediated HA binding include increased expression, variable glycosylation, receptor clustering, GAG attachment, phosphorylation, and inclusion of variant exons in the receptor [6, 7, 177, 179–184].

The bioactivity of the HA fragments strongly depends on their molecular weight. We and others have shown that malignant cells produce HA in order to activate their tumorigenic functions [7, 113, 117, 119, 120, 182, 185–190], while smaller oligosaccharides (~2–3 kDa) can ameliorate these effects *in vitro* [191, 192]. The variant 6 isoform, CD44v6, is of particular interest because it is overexpressed in many cancers, and HA-CD44v6 promotes growth [6, 7, 118, 193–198], which has a significant role in disease onset and progression. An increase in serum soluble CD44v6 due to MMP cleavage, along with serum HGF and HA levels, may serve as companion biomarkers for the presence of tumors and their responsiveness to CD44v6 [199–205]. We have shown that HA-CD44v6 signaling promotes tumor cell survival and tumor growth [182]. In addition, HA binding to CD44v6 is more avid than to CD44s and results in altered signaling [206–208]. In addition, CD44v6 mediates cross-talk between CD44v6 and receptor tyrosine kinases (RTKs), including c-Met [14, 209]. We also demonstrated that periostin, a fibrogenic extracellular matrix protein, also activates HAS2 thus releasing free HA [102], which interacts with CD44 to regulate phenotypic transitions of lung fibroblasts to an invasive “myofibroblastic” phenotype, characterized by the overexpression of CD44, collagen 1, and α -SMA [14] (Figure 1). Overexpression of HAS2 by α -SMA positive myofibroblasts produced fatal lung fibrosis, whereas conditional knockout of HAS2 in myofibroblasts reduced the development of lung fibrosis. Moreover, CD44 contributed to the progressive fibrotic phenotype because lung fibrosis was reduced by either crossing the α -SMA-HAS2 transgenic mouse with the CD44 deficient mouse or by treatment with a blocking antibody to CD44.

All the functional effects of HA in inflammation and fibrosis may not be mediated by CD44. The role of CD44 in HA binding and signaling has recently been investigated in hematopoietic cells from CD44-null mice [210]. CD44-null mice develop normally and exhibit minor abnormalities in hematopoiesis and lymphocyte recirculation [210], indicating that the lack of CD44 can be compensated for in CD44-null mice. The induction of inflammatory gene expression in response to HA was observed in the CD44-null bone marrow cultures and in dendritic cells. It has been shown in wound healing or tissue injury that there is a potent mechanism for clearing HA following the injury. However, CD44-null mice

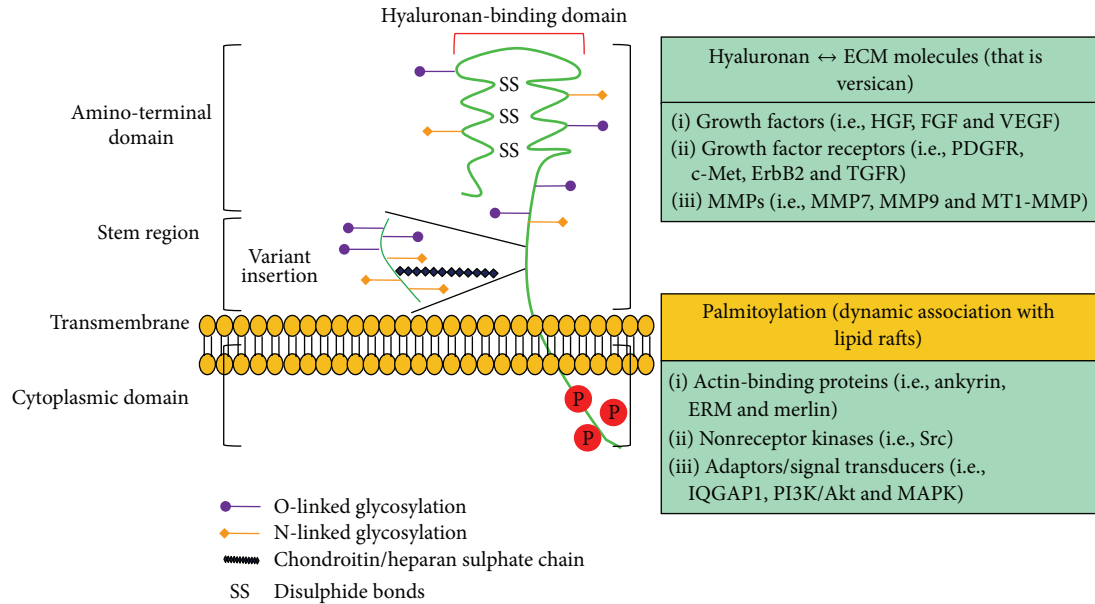


FIGURE 5: Structure, binding domains, and interactions of CD44 (Adapted from [7]). The ectodomain of CD44 contains HA-binding motifs and can contain chondroitin sulfate or heparan sulfate chains that can affect its HA-binding capacity and enable its interactions with growth factors and growth factor receptors, and its interaction with matrix metalloproteinases (MMPs). Transmembrane and cytoplasmic domains undergo multiple posttranslational modifications, including palmitoylation and phosphorylation on cysteine and serine residues, respectively, promoting the binding of proteins with crucial functions in cytoskeletal organization and signaling. ErbB2: epidermal growth factor receptor-2; ERM: ezrin–radixin–moesin; FGF: fibroblast growth factor; HGF: hepatocyte growth factor; IQGAP1: IQ motif containing GTPase activating protein 1; MAPK: mitogen-activated protein kinase; PDGFR: platelet-derived growth factor receptor; PI3K: phosphoinositide 3-kinase; TGFR: transforming growth factor receptor; VEGF: vascular endothelial growth factor.

challenged with bleomycin in an experimental model of lung injury accumulate extensive HA matrix that is not removed by the recruited macrophages with the resulting compromise of oxygen exchange, which results in death [83]. This suggests that CD44 may have evolved as a defence mechanism required for survival. Studies with the CD44-null mice and tissues have discovered the differential effects of CD44 in the predominant cell types that mediate host injury, suggesting potential roles for CD44 in mediating pathogenesis of host injury [172, 211]. For example, administration of IL-2 to wild-type mice triggered a significant vascular leak syndrome (VLS) in the lungs and liver. In contrast, in CD44-null mice, VLS induced by IL-2 was markedly reduced in the lungs and liver [211]. CD44-null mice exhibit enhanced hepatitis in a ConA-induced hepatocellular injury model [212]. Future studies in CD44-null mice will elucidate the importance of HA homeostasis and provide new insights into the role of CD44 *in vivo* and in the tissue/cell models required to study the mechanisms of action of CD44 at the cellular and molecular levels of tissue injury and repair.

4. Therapeutic Approaches Relevant to Hyaluronan and CD44 in Wound Healing and Fibrosis

4.1. Therapeutic Approaches for Wound Healing

4.1.1. Exogenous Application of Hyaluronan in Wound Healing. The viscoelastic and hydrated domain properties of HA are

relevant for exogenous application of HA in tissue repair and regeneration processes. Exogenous application of HA accelerates skin wound healing in various animal models, including rats and hamsters [213–215]. Corneal epithelial wound healing by exogenously applied HA has been known for decades [216]. Laurent et al. [217] showed that exogenous HA can promote scarless healing in tympanic membranes, and Balasz and Denlinger [218] hypothesized that HA rich matrices can inhibit fibrous scars. Later, it was shown that *in utero* scarless fetal tissue repair is associated with high overall levels of HA for longer periods, indicating that high levels of HA may in part reduce collagen matrix deposition and contribute to scarless tissue repair [219]. In the older (late gestation) fetus and in adults, a reduction in HA levels is associated with fibrotic scarring [151]. Mack et al. demonstrated scarless healing in adults in an animal model, Hoxb13 knockout mice, in which HA levels remain elevated in adult skin [220]. Conversely, when Hoxb13 is overexpressed in the epidermis, HA levels are suppressed *in vitro* [221] and the skin behaves as a profibrotic wound-healing environment *in vivo* [222]. Although older findings in the literature regarding HA levels and wound healing were rather difficult to interpret in the past, newer ideas about the role of HA in regulating cytokine receptor signaling at the individual target cell level may help to reconcile the role of HA in fibrosis and healing in the future, as discussed further below.

4.1.2. Proteins Associated with Hyaluronan Are Critical Determinants of Tissue Remodeling [223]. The effects of different

HA preparations in the following studies are attributed to differences in growth factor and cytokine presentation to HA, and to HA receptor mediated molecular organization. The identification of the biological activities of various growth factors and cytokines in wound healing suggest that cells in injury models can respond to peptide factors for the long-term repair processes. Several growth factors derived from fibroblasts affect HA production [224]. For example, fibroblasts derived TGF- β 1, b-FGF, PDGF, and EGF stimulate HA synthesis synergistically, and their effects on cell proliferation are through HA-initiated pathways, indicating the benefits of exogenous application of HA on ECM remodelling. It has been shown that fetal and adult fibroblast cells react differently to HA [151]. The former produce more ECM protein when HA is added to the culture, show greater migration to HA *in vitro*, and are insensitive to the applied PDGF, b-FGF, and EGF [225]. PDGF induces expression of TGF- β 1 in adult wounds, which suggests that some of the longer term effects of PDGF are achieved indirectly by activation of TGF- β 1 by fibroblasts within granulation tissue [226]. Clinical studies have also demonstrated that exogenous application of PDGF-AB together with other growth factors to chronic wounds can accelerate their closure [227, 228]. Application of EGF to organotypic cultures of epidermal cells leads to increased HAS with increased proliferation and migration, and TGF- β 1 inhibits this response, a finding that shows why scarring wounds heal slowly [95]. Fetal and adult wound healing also differ with respect to the participation of various cytokines, particularly members of the TGF- β family. Increased canonical Wnt signaling occurs during postnatal wound repair but not during fetal cutaneous wound repair [229]. In this regard, TGF- β 1 and TGF- β 2 have been detected in adult wounds, while TGF- β 3 is the principal isoform found in fetal wounds in response to rWnt3a protein [229]. Moreover, increased levels of macromolecular HA lead to decreased scarring in fetal life, whereas adult fibroblasts increased scarring due to increased HA breakdown products [230]. In addition, rapid wound closure is reported in HAS1/HAS3 double knockout mice, which have decreased amounts of HA in the skin, and wounding is accompanied by increased efflux of neutrophils into the tissue and by an earlier onset of myofibroblast differentiation [108]. In this case, increased inflammation might compensate for the decreased HA. Thus, in clinical settings, HA-protein (growth factor/cytokine) complexes may ameliorate the scarring [231]. It is likely that addition or removal of combinations of growth factors, or other agents such as protease inhibitors, will be more beneficial in some clinical circumstances.

We have shown that manipulating HA concentrations and HA-CD44 interactions can alter signaling pathways with many regulatory and adaptor molecules, including Src kinases, Rho-GTPases, PI3kinase, ankyrin, and ezrin [7, 118]. The engagement of CD44 with HA can modify cell survival and proliferation by changing intracellular engagement of ERM proteins [192, 232]. Additionally, HA may activate several receptor tyrosine kinases and HA-CD44 may promote clustering [233] and cooperate with other growth factor receptors [188, 190]. Additionally, we have shown that silencing variant 6 (CD44v6) inhibits tumor growth *in vitro* and

in vivo [117, 182]. Moreover, blocking CD44v6 inhibits fibrogenesis of fibroblasts in scleroderma lung fibrosis [14], and blocking HA-CD44v6 downregulates fibroblast contractility [102]. Therefore, HA-CD44 variant interactions may modify several signaling pathways not directly related to CD44, but to other receptors that may interact with CD44 [234]. Thus, in clinical settings, increased HA in response to TNF- α , IL- α , IL-1 β , IL-3, GM-CSH, and IFN γ [84, 177, 178] may promote HA-CD44 clustering and synergize with the cytokine receptor signaling pathways to induce fibrotic responses. This could explain how small HA fragments not capable of bridging receptors can alter these responses.

4.1.3. ECM Remodeling by Manipulating the Interaction of HA with Other Matrix Molecules. Based on the studies above, there is now increasing evidence that HA can be used in biomedical applications for beneficial effects in wound healing. Bioengineered material used in research generally contains ECM molecules, including collagen and HA. The collagen matrix was developed by Bell et al. [235] and is commercially available as Apligraf. Later, a matrix containing collagen and CS has been available as Integra [236]. Coculture of Apligraf with neonatal foreskin fibroblasts and keratinocytes significantly alters the composition of the matrices produced [237]. The problem with these matrices is that the collagen used is xenogeneic bovine collagen.

Identification of HA for its ability to augment keratinocyte proliferation, fibroblast migration, and endothelial cell angiogenic responses in the wound bed makes it a useful biopolymer for wound healing, and pretreatment of HA matrices with fibroblasts has been applied to human wounds [238]. In contrast to collagen, HA is identical between species and has been used to make biomaterials by stable chemical modifications that have been used for wound healing. Furthermore, the degradation of HA matrix can have many effects on the regenerating wound, including water homeostasis, enhancement of angiogenesis, and collagen deposition and organization, which can benefit epithelial regeneration. HA also has free-radical scavenging properties. For example, benzyl esters of HA (HYAFF p80 and HYAFF p100), with differing degradation profiles, were used with a Laserskin method to treat both chronic and acute wounds, which showed excellent results in promoting angiogenesis in the wound bed and epithelial engraftment after 14 days and wound healing without contraction [239]. HA scaffolding material, including thiol-functionalized derivative HA-DTPH, has already been shown to be completely biocompatible in tissue engineering and implantation to provide three-dimensional templates that can improve cell growth and growth factor presentation [240–243]. Application of a cross-linked HA derivative (polyethylene glycol diacrylate-(PEGDA-) cross-linked HA-DTPH (HA-DTPH-PEGDA)) strongly inhibited contraction of a collagen matrix, whereas high molecular weight HA (HMW HA) facilitated collagen gel contraction. This suggests that manipulating the interaction of HA with other matrix molecules can alter ECM remodeling in wound healing [244]. HA is known to have a very short half-life of several hours in the body, which

should be overcome for tissue augmentation applications. The residence time of HA can be prolonged by cross-linking HA in cosmetic fillers by the chemical modification of carboxyl groups of HA [245, 246] because they are in recognition sites of hyaluronidase (Hyal2) [247] and HA receptors [248, 249].

4.2. Therapeutic Approaches for Fibrosis. Fibrosis is the accumulation of ECM components in organs or tissues and is a fundamental feature of systemic sclerosis (SSc) [250, 251]. We are studying wound healing in SSc, which affects the skin and many internal organs, including the lungs, the gastrointestinal tract, and the heart. We will discuss a few therapeutic strategies and possible agents designed to inhibit pathologic mesenchymal phenotypes in SSc fibrosis, including treatment approaches that modulate inflammatory pathways, inhibit profibrotic growth factors, modulate epigenetic codes, and interfere with mesenchymal phenotype.

4.2.1. Role of HA-CD44 Interaction on Profibrotic Growth Factors and Cytokines. As discussed in previous sections, many cytokines are involved in tissue repair, PDGF, EGF, FGF, and IGF1, and they can have many different roles in the healing process, ranging from regulation of cell proliferation, differentiation, and chemotaxis to directing wound remodeling by regulating ECM synthesis and degradation. These proteins may be locally synthesized and released as polypeptide growth factors and cytokines, which then have key roles in regulating cell and tissue functions.

Besides these, TGF- β 1 is a fundamental component of tissue regeneration and repair. It increases profibrotic signals that promote biosynthesis of important components of the ECM, including collagens, CTGF, collagen receptor integrins, decorin, and TIMPs [252]. TGF- β 1 is secreted at sites of injury by platelets and monocytes as well as by other cells, which promotes autocrine and paracrine interactions. We showed that TGF- β 1 autocrine signaling in SSc fibroblasts induces a sustained expression of CD44v6, which interacts with HA and activates cell cycle progression and α -SMA production via Erk activation that increases collagen matrix synthesis. Inhibition of TGF- β 1, or blocking CD44v6 by CD44v6siRNA, reduces these functions of SSc fibroblasts significantly [14]. We postulated that when TGF- β 1 stimulation of fibroblasts is inappropriate, that is, too much TGF- β 1 or heightened sensitivity to TGF- β 1 due to autocrine signaling, pathologic fibrosis ensues with sustained HA-CD44v6 that will eventually overwhelm the system in favor of profibrotic effects [14]. In addition, we postulated that the increase in antifibrotic hepatocyte growth factor (HGF) expression at the onset of chronic injury may initially compensate and support a regenerative process [14, 253], whereas repetitive lung injury results in overexpression of TGF- β 1 that leads to the profibrogenic effects. Therefore, the balance between TGF- β 1 and HGF appears to have a critical role in determining whether the injured tissues undergo recovery or fibrogenesis [14]. Fresolimumab is a human monoclonal antibody that inactivates all forms of TGF- β . In Phase I trials, fresolimumab was safe and well tolerated in patients with primary focal segmental glomerulosclerosis, IPF, and renal cancer. Similarly, Phase

II trials of a human monoclonal antibody for CTGF (FG 3019) for patients with liver fibrosis (due to chronic hepatitis B infection) and pulmonary fibrosis are promising. Imatinib mesylate, used for the treatment of chronic myelogenous leukemia (CML), blocks both profibrotic TGF- β 1 signaling and suppresses activity of the PDGF receptor [254, 255]. In SSc, however, the results are still inconclusive.

4.2.2. Role of HA-CD44 Interaction in Mesenchymal Cell Activation. The mechanisms that regulate fibroblast to myofibroblast differentiation in SSc remain poorly understood. As many profibrotic pathways are linked to TGF- β 1 signaling, novel antifibrotic therapies that target other pathways may indirectly act via suppression of TGF- β 1. For example, peroxisome proliferator-activated receptor- γ (PPAR- γ) can suppress TGF- β 1-dependent cell activation and collagen production in fibroblasts and inhibit the development of fibrosis in murine models [256]. Recent studies also suggest that NADPH oxidase 4 (NOX4) is essential for TGF- β -induced differentiation of fibroblasts to myofibroblasts *in vitro* and for bleomycin-induced pulmonary fibrosis *in vivo* [257]. The development of small molecule inhibitors and/or other strategies targeting NOX4 or the use of PPAR- γ agonists may abrogate fibrosis through antifibrotic mechanisms. Studies suggest that the RhoA/ROCK pathway is a critical regulator of contractility of mesenchymal cells, including lung fibroblasts from SSc patients [258–260]. Fasudil, a small molecule inhibitor of ROCK, has recently been studied in US populations for other disease indications (<https://www.clinicaltrials.gov/>). It also reduces myofibroblast activation in lung fibrosis in an animal model [260], suggesting a potential use of this compound for treatment of fibrotic diseases.

Finally, the profibrotic pathway linked to TGF- β 1 signaling may directly act through a profibrotic mechanism through the augmentation of a HA-CD44 pathway. For example, HA can promote a profibrogenic activity in fibroblasts cells, as shown by changes in cellular behavior due to HA-CD44 interaction that induces biological processes. When hyaluronan synthase 2 (HAS2) was transgenically overexpressed by myofibroblasts *in vivo*, a severe fibrotic phenotype followed bleomycin-induced lung injury, presumably due to HA-CD44 function [83]. Mesenchymal fibroblasts that are derived from HAS2-deficient mice, or are treated with a CD44 blocking antibody, fail to show the same degree of fibrogenic function as do wild-type mice [83]. Our recent study [14] showed that sustained CD44v6-induced signals regulate myofibroblast proliferation, activation, and matrix deposition in SSc fibroblasts in response to autocrine TGF- β 1 stimulation. This indicates that tissue specific blocking of HA-CD44 signaling by silencing CD44 using specific siRNA can be a viable approach to attenuate profibrogenic functions.

5. Conclusion

Together these studies address components of wound healing processes and describe a number of different mechanisms that have been implicated in the pathogenesis of defective wound healing that leads to progressive fibrosis disorders.

Concepts relating wound healing to fibrogenic mechanisms have converged on a model of inflammation that coordinates with ECM components, soluble mediators that induce wound healing, and failure of tissue regeneration leading to fibrosis. HA-based novel therapeutic mechanisms that can use HA-biomaterials and antagonists to HA-CD44 signaling pathways are beginning to produce promising results in *in vitro* and *in vivo* models of both wound healing and fibrosis. Considering that promising studies sometimes do not translate into patient benefit under different biological conditions and disease states, care must be taken to ensure the long-term safety of using advanced engineering strategies and well-conducted and controlled clinical trials need to be evaluated before the therapeutic agents, or HA-based biomaterials can be recommended for defective wound healing. Our future studies will focus on determining the mechanisms by which HA-CD44 regulates impaired wound healing, with particular emphasis on microRNAs that regulate HA synthesis and CD44 biology in normal and pathological wound healing.

Abbreviations

GAG: Glycosaminoglycan
 PG: Proteoglycan
 HA: Hyaluronan
 ECM: Extracellular matrix
 HAS: Hyaluronan synthase
 Hyals: Hyaluronidases.

Conflict of Interests

The authors declare that there is no conflict of interests regarding the publication of this paper.

Authors' Contribution

Suniti Misra and Shibnath Ghatak wrote the review. Dr. Vincent C. Hascall reviewed the draft and final paper. Dr. Roger R. Markwald edited the final paper. Dr. Edward V. Maytin and Judith A. Mack reviewed the abstract and Introduction. Ricardo Moreno Rodriguez and Ilia Atanelishvili helped to draw the figures.

Acknowledgments

This work was supported by 1R03CA167722-01A1 (to Suniti Misra and Shibnath Ghatak), P20RR021949 (to Shibnath Ghatak), P20RR016434 (to Suniti Misra, Shibnath Ghatak, and Roger R. Markwald), P20RR16461-05 (to Shibnath Ghatak and Roger R. Markwald), RO1-HL033756-24 (to Suniti Misra, Shibnath Ghatak, and Roger R. Markwald), P01HL107147 and 1P30AR050953 (to Vincent C. Hascall), and EPS 0903795 (to Suniti Misra).

References

[1] N. B. Menke, K. R. Ward, T. M. Witten, D. G. Bonchev, and R. F. Diegelmann, "Impaired wound healing," *Clinics in Dermatology*, vol. 25, no. 1, pp. 19–25, 2007.

- [2] M. J. Bissell, H. G. Hall, and G. Parry, "How does the extracellular matrix direct gene expression?" *Journal of Theoretical Biology*, vol. 99, no. 1, pp. 31–68, 1982.
- [3] R. O. Hynes, "Integrins: bidirectional, allosteric signaling machines," *Cell*, vol. 110, no. 6, pp. 673–687, 2002.
- [4] H. Ponta, L. Sherman, and P. A. Herrlich, "CD44: from adhesion molecules to signalling regulators," *Nature Reviews Molecular Cell Biology*, vol. 4, no. 1, pp. 33–45, 2003.
- [5] R. V. Sionov and D. Naor, "Hyaluronan-independent lodgment of CD44+ lymphoma cells in lymphoid organs," *International Journal of Cancer*, vol. 71, no. 3, pp. 462–469, 1997.
- [6] S. Misra, V. C. Hascall, N. K. Karamanos, R. R. Markwald, and S. Ghatak, *Delivery Systems Targeting Cancer at the Level of ECM*, DeGruyter, Berlin, Germany, 2012.
- [7] S. Misra, P. Heldin, V. C. Hascall et al., "Hyaluronan-CD44 interactions as potential targets for cancer therapy," *The FEBS Journal*, vol. 278, no. 9, pp. 1429–1443, 2011.
- [8] M. Shimaoka and T. A. Springer, "Therapeutic antagonists and conformational regulation of integrin function," *Nature Reviews: Drug Discovery*, vol. 2, no. 9, pp. 703–716, 2003.
- [9] J. P. Iredale, "Tissue inhibitors of metalloproteinases in liver fibrosis," *International Journal of Biochemistry and Cell Biology*, vol. 29, no. 1, pp. 43–54, 1997.
- [10] A. M. El Nahas, E. C. Muchaneta-Kubara, M. Essawy, and O. Soylemezoglu, "Renal fibrosis: insights into pathogenesis and treatment," *International Journal of Biochemistry and Cell Biology*, vol. 29, no. 1, pp. 55–62, 1997.
- [11] R. P. Marshall, R. J. McAnulty, and G. J. Laurent, "The pathogenesis of pulmonary fibrosis: Is there a fibrosis gene?" *International Journal of Biochemistry and Cell Biology*, vol. 29, no. 1, pp. 107–120, 1997.
- [12] K. T. Weber, Y. Sun, and L. C. Katwa, "Myofibroblasts and local angiotensin II in rat cardiac tissue repair," *International Journal of Biochemistry and Cell Biology*, vol. 29, no. 1, pp. 31–42, 1997.
- [13] K. T. Weber, Y. Sun, L. C. Katwa, and J. P. M. Cleutjens, "Tissue repair and angiotensin II generated at sites of healing," *Basic Research in Cardiology*, vol. 92, no. 2, pp. 75–78, 1997.
- [14] S. Ghatak, G. S. Bogatkevich, I. Atanelishvili et al., "Overexpression of c-Met and CD44v6 receptors contributes to autocrine TGF- β 1 signaling in interstitial lung disease," *The Journal of Biological Chemistry*, vol. 289, no. 11, pp. 7856–7872, 2014.
- [15] M. B. Kahaleh, "The role of vascular endothelium in fibroblast activation and tissue fibrosis, particularly in scleroderma (systemic sclerosis) and pachydermoperiostosis (primary hypertrophic osteoarthropathy)," *Clinical and Experimental Rheumatology*, vol. 10, supplement 7, pp. 51–56, 1992.
- [16] R. A. F. Clark, J. M. Lanigan, P. DellaPelle, E. Manseau, H. F. Dvorak, and R. B. Colvin, "Fibronectin and fibrin provide a provisional matrix for epidermal cell migration during wound reepithelialization," *Journal of Investigative Dermatology*, vol. 79, no. 5, pp. 264–269, 1982.
- [17] K. M. Yamada and R. A. F. Clark, *Provisional Matrix*, Plenum Press, New York, NY, USA, 1996.
- [18] R. A. F. Clark, *Wound Repair: Overview and General Considerations*, Plenum Press, 1996.
- [19] G. Broughton II, J. E. Janis, and C. E. Attinger, "The basic science of wound healing," *Plastic and Reconstructive Surgery*, vol. 117, no. 7, pp. 12S–34S, 2006.
- [20] A. C. L. Campos, A. K. Groth, and A. B. Branco, "Assessment and nutritional aspects of wound healing," *Current Opinion in Clinical Nutrition and Metabolic Care*, vol. 11, no. 3, pp. 281–288, 2008.

- [21] A. Gosain and L. A. DiPietro, "Aging and wound healing," *World Journal of Surgery*, vol. 28, no. 3, pp. 321–326, 2004.
- [22] A. J. Meszaros, J. S. Reichner, and J. E. Albina, "Macrophage-induced neutrophil apoptosis," *Journal of Immunology*, vol. 165, no. 1, pp. 435–441, 2000.
- [23] D. M. Mosser and J. P. Edwards, "Exploring the full spectrum of macrophage activation," *Nature Reviews. Immunology*, vol. 8, no. 12, pp. 958–969, 2008.
- [24] J. E. Park and A. Barbul, "Understanding the role of immune regulation in wound healing," *American Journal of Surgery*, vol. 187, no. 5, 2004.
- [25] M. E. Swift, A. L. Burns, K. L. Gray, and L. A. DiPietro, "Age-related alterations in the inflammatory response to dermal injury," *Journal of Investigative Dermatology*, vol. 117, no. 5, pp. 1027–1035, 2001.
- [26] R. A. F. Clark, *Overview and General Consideration of Wound Repair*, Plenum, New York, NY, USA, 1988.
- [27] T. Iwayama and L. E. Olson, "Involvement of PDGF in fibrosis and scleroderma: recent insights from animal models and potential therapeutic opportunities," *Current Rheumatology Reports*, vol. 15, no. 2, 2013.
- [28] A. Leask, "Possible strategies for anti-fibrotic drug intervention in scleroderma," *Journal of Cell Communication and Signaling*, vol. 5, no. 2, pp. 125–129, 2011.
- [29] M. Trojanowska, "Role of PDGF in fibrotic diseases and systemic sclerosis," *Rheumatology*, vol. 47, pp. v2–4, 2008.
- [30] M. Eastwood, R. Porter, U. Khan, G. McGrouther, and R. Brown, "Quantitative analysis of collagen gel contractile forces generated by dermal fibroblasts and the relationship to cell morphology," *Journal of Cellular Physiology*, vol. 166, no. 1, pp. 33–42, 1996.
- [31] R. J. McAnulty, J. S. Campa, A. D. Cambrey, and G. J. Laurent, "The effect of transforming growth factor beta on rates of procollagen synthesis and degradation in vitro," *Biochimica et Biophysica Acta—Molecular Cell Research*, vol. 1091, no. 2, pp. 231–235, 1991.
- [32] A. B. Roberts, K. C. Flanders, U. I. Heine et al., "Transforming growth factor-beta: multifunctional regulator of differentiation and development," *Philosophical Transactions of the Royal Society of London, Series B: Biological Sciences*, vol. 327, no. 1239, pp. 145–154, 1990.
- [33] A. B. Roberts, U. I. Heine, K. C. Flanders, and M. B. Sporn, "Transforming growth factor- β . Major role in regulation of extracellular matrix," *Annals of the New York Academy of Sciences*, vol. 580, pp. 225–232, 1990.
- [34] M. Shah, D. M. Foreman, and M. W. J. Ferguson, "Neutralisation of TGF-beta 1 and TGF-beta 2 or exogenous addition of TGF-beta 3 to cutaneous rat wounds reduces scarring," *Journal of Cell Science*, vol. 108, no. 3, pp. 985–1002, 1995.
- [35] T. J. Franklin, "Therapeutic approaches to organ fibrosis," *International Journal of Biochemistry and Cell Biology*, vol. 29, no. 1, pp. 79–89, 1997.
- [36] J. Folkman and M. Klagsbrun, "Angiogenic factors," *Science*, vol. 235, no. 4787, pp. 442–447, 1987.
- [37] P. R. Atkison, E. R. Weidman, B. Bhaumick, and R. M. Bala, "Release of somatomedin-like activity by cultured WI-38 human fibroblasts," *Endocrinology*, vol. 106, no. 6, pp. 2006–2012, 1980.
- [38] W. N. Rom, P. Basset, G. A. Fells, T. Nukiwa, B. C. Trapnell, and R. G. Crystal, "Alveolar macrophages release an insulin-like growth factor I-type molecule," *Journal of Clinical Investigation*, vol. 82, no. 5, pp. 1685–1693, 1988.
- [39] R. H. Goldstein, C. F. Poliks, P. F. Pilch, B. D. Smith, and A. Fine, "Stimulation of collagen formation by insulin and insulin-like growth factor I in cultures of human lung fibroblasts," *Endocrinology*, vol. 124, no. 2, pp. 964–970, 1989.
- [40] N. K. Harrison, A. D. Cambrey, A. R. Myers et al., "Insulin-like growth factor-I is partially responsible for fibroblast proliferation induced by bronchoalveolar lavage fluid from patients with systemic sclerosis," *Clinical Science*, vol. 86, no. 2, pp. 141–148, 1994.
- [41] M. Laato, V. M. Kähäri, J. Niinikoski, and E. Vuorio, "Epidermal growth factor increases collagen production in granulation tissue by stimulation of fibroblast proliferation and not by activation of procollagen genes," *Biochemical Journal*, vol. 247, no. 2, pp. 385–388, 1987.
- [42] J.-P. Pienimäki, K. Rilla, C. Fülöp et al., "Epidermal growth factor activates hyaluronan synthase 2 in epidermal keratinocytes and increases pericellular and intracellular hyaluronan," *The Journal of Biological Chemistry*, vol. 276, no. 23, pp. 20428–20435, 2001.
- [43] J. G. Rheinwald and H. Green, "Epidermal growth factor and the multiplication of cultured human epidermal keratinocytes," *Nature*, vol. 265, no. 5593, pp. 421–424, 1977.
- [44] A. B. Schreiber, M. E. Winkler, and R. Derynck, "Transforming growth factor- α : a more potent angiogenic mediator than epidermal growth factor," *Science*, vol. 232, no. 4755, pp. 1250–1253, 1986.
- [45] G. L. Brown, L. B. Nanney, J. Griffen et al., "Enhancement of wound healing by topical treatment with epidermal growth factor," *The New England Journal of Medicine*, vol. 321, no. 2, pp. 76–79, 1989.
- [46] S. Cattaruzza and R. Perris, "Proteoglycan control of cell movement during wound healing and cancer spreading," *Matrix Biology*, vol. 24, no. 6, pp. 400–417, 2005.
- [47] N. Hattori, D. A. Carrino, M. E. Lauer et al., "Pericellular versican regulates the fibroblast-myofibroblast transition: a role for ADAMTS5 protease-mediated proteolysis," *The Journal of Biological Chemistry*, vol. 286, no. 39, pp. 34298–34310, 2011.
- [48] Z. Zhou, J. Wang, R. Cao et al., "Impaired angiogenesis, delayed wound healing and retarded tumor growth in Perlecan heparan sulfate-deficient mice," *Cancer Research*, vol. 64, no. 14, pp. 4699–4702, 2004.
- [49] K. Elenius, S. Vainio, M. Laato, M. Salmivirta, I. Thesleff, and M. Jalkanen, "Induced expression of syndecan in healing wounds," *Journal of Cell Biology*, vol. 114, no. 3, pp. 585–595, 1991.
- [50] M. A. Stepp, H. E. Gibson, P. H. Gala et al., "Defects in keratinocyte activation during wound healing in the syndecan-1-deficient mouse," *Journal of Cell Science*, vol. 115, no. 23, pp. 4517–4531, 2002.
- [51] F. Echtermeyer, M. Streit, S. Wilcox-Adelman et al., "Delayed wound repair and impaired angiogenesis in mice lacking syndecan-4," *The Journal of Clinical Investigation*, vol. 107, no. 2, pp. R9–R14, 2001.
- [52] Y. Yamaguchi, D. M. Mann, and E. Ruoslahti, "Negative regulation of transforming growth factor- β by the proteoglycan decorin," *Nature*, vol. 346, no. 6281, pp. 281–284, 1990.
- [53] Y. Isaka, D. K. Brees, K. Ikegaya et al., "Gene therapy by skeletal muscle expression of decorin prevents fibrotic disease in rat kidney," *Nature Medicine*, vol. 2, no. 4, pp. 418–423, 1996.
- [54] K. Fukushima, N. Badlani, A. Usas, F. Riano, F. H. Fu, and J. Huard, "The use of an antifibrosis agent to improve muscle recovery after laceration," *The American Journal of Sports Medicine*, vol. 29, no. 4, pp. 394–402, 2001.

- [55] M. Kolb, P. J. Margetts, P. J. Sime, and J. Gaudie, "Proteoglycans decorin and biglycan differentially modulate TGF- β -mediated fibrotic responses in the lung," *The American Journal of Physiology—Lung Cellular and Molecular Physiology*, vol. 280, no. 6, pp. L1327–L1334, 2001.
- [56] J. R. Couchman and C. A. Pataki, "An introduction to proteoglycans and their localization," *Journal of Histochemistry and Cytochemistry*, vol. 60, no. 12, pp. 885–897, 2012.
- [57] K. Prydz and K. T. Dalen, "Synthesis and sorting of proteoglycans," *Journal of Cell Science*, vol. 113, no. 2, pp. 193–205, 2000.
- [58] P. Martin, "Wound healing—aiming for perfect skin regeneration," *Science*, vol. 276, no. 5309, pp. 75–81, 1997.
- [59] J. Latterra, R. Ansbacher, and L. A. Culp, "Glycosaminoglycans that bind cold-insoluble globulin in cell-substratum adhesion sites of murine fibroblasts," *Proceedings of the National Academy of Sciences of the United States of America*, vol. 77, no. 11, pp. 6662–6666, 1980.
- [60] T. N. Wight, D. K. Heinegard, and V. C. Hascall, *Proteoglycans: Structure and Function*, Plenum Press, New York, NY, USA, 1991.
- [61] M. W. Lark and L. A. Culp, *Cell-Matrix Interaction: Biochemistry of Close and Tight-Focal Adhesive Contacts of Fibroblasts to Extracellular Matrices*, MerceL Decker, New York, NY, USA, 1987.
- [62] P. V. Peplow, "Glycosaminoglycan: a candidate to stimulate the repair of chronic wounds," *Thrombosis and Haemostasis*, vol. 94, no. 1, pp. 4–16, 2005.
- [63] N. Ortéga, F. E. L'Faqihi, and J. Plouët, "Control of vascular endothelial growth factor angiogenic activity by the extracellular matrix," *Biology of the Cell*, vol. 90, no. 5, pp. 381–390, 1998.
- [64] K. R. Taylor and R. L. Gallo, "Glycosaminoglycans and their proteoglycans: host-associated molecular patterns for initiation and modulation of inflammation," *The FASEB Journal*, vol. 20, no. 1, pp. 9–22, 2006.
- [65] C. A. de La, V. C. Motte, and J. Drazba, "Poly I:C induces mononuclear leukocyte-adhesive hyaluronan structures on colon smooth muscle cells: α 1 and versican facilitate adhesion," in *Hyaluronan 2000*, Woodhead Publishing, Wrexham, Wales, 2000.
- [66] V. C. Hascall, A. K. Majors, C. A. de la Motte et al., "Intracellular hyaluronan: a new frontier for inflammation?" *Biochimica et Biophysica Acta—General Subjects*, vol. 1673, no. 1–2, pp. 3–12, 2004.
- [67] W. Y. J. Chen and G. Abatangelo, "Functions of hyaluronan in wound repair," *Wound Repair and Regeneration*, vol. 7, no. 2, pp. 79–89, 1999.
- [68] N. S. Gandhi and R. L. Mancera, "The structure of glycosaminoglycans and their interactions with proteins," *Chemical Biology and Drug Design*, vol. 72, no. 6, pp. 455–482, 2008.
- [69] K. Meyer and J. W. Palmer, "The polysaccharide of the vitreous humor," *The Journal of Biological Chemistry*, vol. 107, no. 3, pp. 629–634, 1934.
- [70] P. Olczyk, K. Komosińska-Vashev, K. Winsz-Szczotka, K. Kuźnik-Trocha, and K. Olczyk, "Hyaluronan: structure, metabolism, functions, and role in wound healing," *Postępy Higieny i Medycyny Doświadczalnej*, vol. 62, pp. 651–659, 2008.
- [71] T. C. Laurent and J. R. E. Fraser, "Hyaluronan," *The FASEB Journal*, vol. 6, no. 7, pp. 2397–2404, 1992.
- [72] G. M. Campo, A. Avenoso, S. Campo, A. D'Ascola, G. Nastasi, and A. Calatroni, "Molecular size hyaluronan differently modulates toll-like receptor-4 in LPS-induced inflammation in mouse chondrocytes," *Biochimie*, vol. 92, no. 2, pp. 204–215, 2010.
- [73] M. Mohamadzadeh, H. DeGrendele, H. Arizpe, P. Estess, and M. Siegelman, "Proinflammatory stimuli regulate endothelial hyaluronan expression and CD44/HA-dependent primary adhesion," *Journal of Clinical Investigation*, vol. 101, no. 1, pp. 97–108, 1998.
- [74] P. L. Bollyky, S. P. Evanko, R. P. Wu et al., "Th1 cytokines promote T-cell binding to antigen-presenting cells via enhanced hyaluronan production and accumulation at the immune synapse," *Cellular and Molecular Immunology*, vol. 7, no. 3, pp. 211–220, 2010.
- [75] T. S. Wilkinson, S. Potter-Perigo, C. Tsoi, L. C. Altman, and T. N. Wight, "Pro- and anti-inflammatory factors cooperate to control hyaluronan synthesis in lung fibroblasts," *American Journal of Respiratory Cell and Molecular Biology*, vol. 31, no. 1, pp. 92–99, 2004.
- [76] M. A. Dentener, J. H. J. Vernooy, S. Hendriks, and E. F. M. Wouters, "Enhanced levels of hyaluronan in lungs of patients with COPD: relationship with lung function and local inflammation," *Thorax*, vol. 60, no. 2, pp. 114–119, 2005.
- [77] O. Nettelbladt and R. Hallgren, "Hyaluronan (hyaluronic acid) in bronchoalveolar lavage fluid during the development of bleomycin-induced alveolitis in the rat," *American Review of Respiratory Disease*, vol. 140, no. 4, pp. 1028–1032, 1989.
- [78] J. P. Freitas, P. Filipe, I. Emerit, P. Meunier, C. F. Manso, and F. Guerra Rodrigo, "Hyaluronic acid in progressive systemic sclerosis," *Dermatology*, vol. 192, no. 1, pp. 46–49, 1996.
- [79] H. Levesque, N. Baudot, B. Delpéch, M. Vayssairat, A. Gancel, and H. Courtois, "Clinical correlations and prognosis based on hyaluronic acid serum levels in patients with progressive systemic sclerosis," *British Journal of Dermatology*, vol. 124, no. 5, pp. 423–428, 1991.
- [80] E. S. Bensadoun, A. K. Burke, J. C. Hogg, and C. R. Roberts, "Proteoglycan deposition in pulmonary fibrosis," *American Journal of Respiratory and Critical Care Medicine*, vol. 154, no. 6, part 1, pp. 1819–1828, 1996.
- [81] A. M. Cantin, P. Larivee, M. Martel, and R. Begin, "Hyaluronan (hyaluronic acid) in lung lavage of asbestos-exposed humans and sheep," *Lung*, vol. 170, no. 4, pp. 211–220, 1992.
- [82] E. Papakonstantinou, F. M. Kouri, G. Karakioulakis, I. Klagas, and O. Eickelberg, "Increased hyaluronic acid content in idiopathic pulmonary arterial hypertension," *European Respiratory Journal*, vol. 32, no. 6, pp. 1504–1512, 2008.
- [83] Y. Li, D. Jiang, J. Liang et al., "Severe lung fibrosis requires an invasive fibroblast phenotype regulated by hyaluronan and CD44," *Journal of Experimental Medicine*, vol. 208, no. 7, pp. 1459–1471, 2011.
- [84] E. Puré and C. A. Cuff, "A crucial role for CD44 in inflammation," *Trends in Molecular Medicine*, vol. 7, no. 5, pp. 213–221, 2001.
- [85] D. Jiang, J. Liang, J. Fan et al., "Regulation of lung injury and repair by Toll-like receptors and hyaluronan," *Nature Medicine*, vol. 11, no. 11, pp. 1173–1179, 2005.
- [86] V. C. Hascall, A. Wang, M. Tammi et al., "The dynamic metabolism of hyaluronan regulates the cytosolic concentration of UDP-GlcNAc," *Matrix Biology*, vol. 35, pp. 14–17, 2014.
- [87] J. Y. Lee and A. P. Spicer, "Hyaluronan: a multifunctional, megaDalton, stealth molecule," *Current Opinion in Cell Biology*, vol. 12, no. 5, pp. 581–586, 2000.
- [88] R. H. Tammi, A. G. Passi, K. Rilla et al., "Transcriptional and post-translational regulation of hyaluronan synthesis," *FEBS Journal*, vol. 278, no. 9, pp. 1419–1428, 2011.

- [89] N. Itano and K. Kimata, "Mammalian hyaluronan synthases," *IUBMB Life*, vol. 54, no. 4, pp. 195–199, 2002.
- [90] N. Itano, T. Sawai, M. Yoshida et al., "Three isoforms of mammalian hyaluronan synthases have distinct enzymatic properties," *The Journal of Biological Chemistry*, vol. 274, no. 35, pp. 25085–25092, 1999.
- [91] P. H. Weigel, V. C. Hascall, and M. Tammi, "Hyaluronan synthases," *The Journal of Biological Chemistry*, vol. 272, no. 22, pp. 13997–14000, 1997.
- [92] J. Monslow, J. D. Williams, C. A. Guy et al., "Identification and analysis of the promoter region of the human hyaluronan synthase 2 gene," *The Journal of Biological Chemistry*, vol. 279, no. 20, pp. 20576–20581, 2004.
- [93] K. Saavalainen, S. Pasonen-Seppänen, T. W. Dunlop, R. Tammi, M. I. Tammi, and C. Carlberg, "The human hyaluronan synthase 2 gene is a primary retinoic acid and epidermal growth factor responding gene," *The Journal of Biological Chemistry*, vol. 280, no. 15, pp. 14636–14644, 2005.
- [94] S. Karvinen, S. Pasonen-Seppänen, J. M. T. Hyttinen et al., "Keratinocyte growth factor stimulates migration and hyaluronan synthesis in the epidermis by activation of keratinocyte hyaluronan synthases 2 and 3," *The Journal of Biological Chemistry*, vol. 278, no. 49, pp. 49495–49504, 2003.
- [95] S. Pasonen-Seppänen, S. Karvinen, K. Törrönen et al., "EGF upregulates, whereas TGF- β downregulates, the hyaluronan synthases Has2 and Has3 in organotypic keratinocyte cultures: correlations with epidermal proliferation and differentiation," *Journal of Investigative Dermatology*, vol. 120, no. 6, pp. 1038–1044, 2003.
- [96] J. Monslow, N. Sato, J. A. MacK, and E. V. Maytin, "Wounding-induced synthesis of hyaluronic acid in organotypic epidermal cultures requires the release of heparin-binding EGF and activation of the EGFR," *Journal of Investigative Dermatology*, vol. 129, no. 8, pp. 2046–2058, 2009.
- [97] S. M. Pasonen-Seppänen, E. V. Maytin, K. J. Törrönen et al., "All-trans retinoic acid-induced hyaluronan production and hyperplasia are partly mediated by EGFR signaling in epidermal keratinocytes," *Journal of Investigative Dermatology*, vol. 128, no. 4, pp. 797–807, 2008.
- [98] M. S. Pandey, E. N. Harris, J. A. Weigel, and P. H. Weigel, "The cytoplasmic domain of the hyaluronan receptor for endocytosis (hare) contains multiple endocytic motifs targeting coated pit-mediated internalization," *The Journal of Biological Chemistry*, vol. 283, no. 31, pp. 21453–21461, 2008.
- [99] R. Tammi, K. Rilla, J.-P. Pienimäki et al., "Hyaluronan enters keratinocytes by a novel endocytic route for catabolism," *The Journal of Biological Chemistry*, vol. 276, no. 37, pp. 35111–35122, 2001.
- [100] B. Andre, C. Duterme, K. Van Moer, J. Mertens-Strijthagen, M. Jadot, and B. Flamion, "Hyal2 is a glycosylphosphatidylinositol-anchored, lipid raft-associated hyaluronidase," *Biochemical and Biophysical Research Communications*, vol. 411, no. 1, pp. 175–179, 2011.
- [101] D. Vigetti, S. Deleonibus, P. Moretto et al., "Role of UDP-N-acetylglucosamine (GlcNAc) and O-GlcNAcylation of hyaluronan synthase 2 in the control of chondroitin sulfate and hyaluronan synthesis," *The Journal of Biological Chemistry*, vol. 287, no. 42, pp. 35544–35555, 2012.
- [102] S. Ghatak, S. Misra, R. A. Norris et al., "Periostin induces intracellular cross-talk between kinases and hyaluronan in atrioventricular valvulogenesis," *The Journal of Biological Chemistry*, vol. 289, no. 12, pp. 8545–8561, 2014.
- [103] D. Vigetti, M. Viola, E. Karousou, G. de Luca, and A. Passi, "Metabolic control of hyaluronan synthases," *Matrix Biology*, vol. 35, pp. 8–13, 2014.
- [104] T. D. Camenisch, J. A. Schroeder, J. Bradley, S. E. Klewer, and J. A. McDonald, "Heart-valve mesenchyme formation is dependent on hyaluronan-augmented activation of ErbB2-ErbB3 receptors," *Nature Medicine*, vol. 8, no. 8, pp. 850–855, 2002.
- [105] T. D. Camenisch, A. P. Spicer, T. Brehm-Gibson et al., "Disruption of hyaluronan synthase-2 abrogates normal cardiac morphogenesis and hyaluronan-mediated transformation of epithelium to mesenchyme," *Journal of Clinical Investigation*, vol. 110, no. 3, pp. 349–360, 2000.
- [106] E. A. Craig, A. F. Austin, R. R. Vaillancourt, J. V. Barnett, and T. D. Camenisch, "TGF β 2-mediated production of hyaluronan is important for the induction of epicardial cell differentiation and invasion," *Experimental Cell Research*, vol. 316, no. 20, pp. 3397–3405, 2010.
- [107] J. McDonald, V. C. Hascall, K. Meyer, and J. W. Palmer, "Hyaluronan minireview series," *The Journal of Biological Chemistry*, vol. 277, no. 7, pp. 4575–4579, 2002.
- [108] J. A. Mack, R. J. Feldman, N. Itano et al., "Enhanced inflammation and accelerated wound closure following tetraborbor ester application or full-thickness wounding in mice lacking hyaluronan synthases Has1 and Has3," *Journal of Investigative Dermatology*, vol. 132, no. 1, pp. 198–207, 2012.
- [109] P. Gribbon, B. C. Heng, and T. E. Hardingham, "The molecular basis of the solution properties of hyaluronan investigated by confocal fluorescence recovery after photobleaching," *Biophysical Journal*, vol. 77, no. 4, pp. 2210–2216, 1999.
- [110] I. Ellis, J. Banyard, and S. L. Schor, "Differential response of fetal and adult fibroblasts to cytokines: cell migration and hyaluronan synthesis," *Development*, vol. 124, no. 8, pp. 1593–1600, 1997.
- [111] I. R. Ellis and S. L. Schor, "Differential effects of TGF- β 1 on hyaluronan synthesis by fetal and adult skin fibroblasts: Implications for cell migration and wound healing," *Experimental Cell Research*, vol. 228, no. 2, pp. 326–333, 1996.
- [112] J. A. Brown, "The role of hyaluronic acid in wound healing's proliferative phase," *Journal of Wound Care*, vol. 13, no. 2, pp. 48–51, 2004.
- [113] S. Ghatak, V. C. Hascall, N. K. Karamanos, R. R. Markwald, and S. Misra, *Targeting the Tumor Microenvironment in Cancer Progression*, DeGruyter, Berlin, Germany, 2012.
- [114] S. Ghatak, V. C. Hascall, R. R. Markwald, and S. Misra, "Stromal hyaluronan interaction with epithelial CD44 variants promotes prostate cancer invasiveness by augmenting expression and function of hepatocyte growth factor and androgen receptor," *The Journal of Biological Chemistry*, vol. 285, no. 26, pp. 19821–19832, 2010.
- [115] K. Rilla, M. J. Lammi, R. Sironen et al., "Changed lamellipodial extension, adhesion plaques, and migration in epidermal keratinocytes containing constitutively expressed sense and antisense hyaluronan synthase 2 (Has2) genes," *Journal of Cell Science*, vol. 115, no. 18, pp. 3633–3643, 2002.
- [116] B. P. Toole, "Hyaluronan in morphogenesis," *Seminars in Cell & Developmental Biology*, vol. 12, no. 2, pp. 79–87, 2001.
- [117] S. Misra, S. Ghatak, N. Patil et al., "Novel dual cyclooxygenase and lipoxygenase inhibitors targeting hyaluronan-CD44v6 pathway and inducing cytotoxicity in colon cancer cells," *Bioorganic and Medicinal Chemistry*, vol. 21, no. 9, pp. 2551–2559, 2013.

- [118] S. Misra, V. Hascall, N. Karamanos, R. A. Markwald, and S. Ghatak, *Targeting Tumor Microenvironment in Cancer Progression*, De Gruyter, 2012.
- [119] S. Misra, V. C. Hascall, F. G. Berger, R. R. Markwald, and S. Ghatak, "Hyaluronan, CD44, and cyclooxygenase-2 in colon cancer," *Connective Tissue Research*, vol. 49, no. 3-4, pp. 219–224, 2008.
- [120] S. Misra, L. M. Obeid, Y. A. Hannun et al., "Hyaluronan constitutively regulates activation of COX-2-mediated cell survival activity in intestinal epithelial and colon carcinoma cells," *The Journal of Biological Chemistry*, vol. 283, no. 21, pp. 14335–14344, 2008.
- [121] C. A. Maxwell, J. J. Keats, M. Crainie et al., "RHAMM is a centrosomal protein that interacts with dynein and maintains spindle pole stability," *Molecular Biology of the Cell*, vol. 14, no. 6, pp. 2262–2276, 2003.
- [122] C. A. Maxwell, J. McCarthy, and E. Turley, "Cell-surface and mitotic-spindle RHAMM: moonlighting or dual oncogenic functions?" *Journal of Cell Science*, vol. 121, part 7, pp. 925–932, 2008.
- [123] E. A. Turley, "Hyaluronan and cell locomotion," *Cancer and Metastasis Reviews*, vol. 11, no. 1, pp. 21–30, 1992.
- [124] E. A. Turley, P. W. Noble, and L. Y. Bourguignon, "Signaling properties of hyaluronan receptors," *The Journal of Biological Chemistry*, vol. 277, no. 7, pp. 4589–4592, 2002.
- [125] S. Meran, D. W. Thomas, P. Stephens et al., "Hyaluronan facilitates transforming growth factor-beta1-mediated fibroblast proliferation," *The Journal of Biological Chemistry*, vol. 283, no. 10, pp. 6530–6545, 2008.
- [126] S. Meran, D. Thomas, P. Stephens et al., "Involvement of hyaluronan in regulation of fibroblast phenotype," *The Journal of Biological Chemistry*, vol. 282, no. 35, pp. 25687–25697, 2007.
- [127] H. Harada and M. Takahashi, "CD44-dependent intracellular and extracellular catabolism of hyaluronic acid by hyaluronidase-1 and -2," *The Journal of Biological Chemistry*, vol. 282, no. 8, pp. 5597–5607, 2007.
- [128] S. Meran, D. D. Luo, R. Simpson et al., "Hyaluronan facilitates transforming growth factor-beta1-dependent proliferation via CD44 and epidermal growth factor receptor interaction," *The Journal of Biological Chemistry*, vol. 286, no. 20, pp. 17618–17630, 2011.
- [129] A. C. Midgley, M. Rogers, M. B. Hallett et al., "Transforming growth factor-beta1 (TGF-beta1)-stimulated fibroblast to myofibroblast differentiation is mediated by hyaluronan (HA)-facilitated epidermal growth factor receptor (EGFR) and CD44 colocalization in lipid rafts," *The Journal of Biological Chemistry*, vol. 288, no. 21, pp. 14824–14838, 2013.
- [130] N. Aden, A. Nuttall, X. Shiwen et al., "Epithelial cells promote fibroblast activation via IL-1alpha in systemic sclerosis," *Journal of Investigative Dermatology*, vol. 130, no. 9, pp. 2191–2200, 2010.
- [131] A. Ghaffari, R. T. Kilani, and A. Ghahary, "Keratinocyte-conditioned media regulate collagen expression in dermal fibroblasts," *Journal of Investigative Dermatology*, vol. 129, no. 2, pp. 340–347, 2009.
- [132] P. Shephard, G. Martin, S. Smola-Hess, G. Brunner, T. Krieg, and H. Smola, "Myofibroblast differentiation is induced in keratinocyte-fibroblast co-cultures and is antagonistically regulated by endogenous transforming growth factor-beta, and interleukin-1," *American Journal of Pathology*, vol. 164, no. 6, pp. 2055–2066, 2004.
- [133] G. Cheng, S. Swaidani, M. Sharma, M. E. Lauer, V. C. Hascall, and M. A. Aronica, "Hyaluronan deposition and correlation with inflammation in a murine ovalbumin model of asthma," *Matrix Biology*, vol. 30, no. 2, pp. 126–134, 2011.
- [134] A. B. Csóka, S. W. Scherer, and R. Stern, "Expression analysis of six paralogous human hyaluronidase genes clustered on chromosomes 3p21 and 7q31," *Genomics*, vol. 60, no. 3, pp. 356–361, 1999.
- [135] V. Atmuri, D. C. Martin, R. Hemming et al., "Hyaluronidase 3 (HYAL3) knockout mice do not display evidence of hyaluronan accumulation," *Matrix Biology*, vol. 27, no. 8, pp. 653–660, 2008.
- [136] H. Yoshida, A. Nagaoka, A. Kusaka-Kikushima et al., "KIAA1199, a deafness gene of unknown function, is a new hyaluronan binding protein involved in hyaluronan depolymerization," *Proceedings of the National Academy of Sciences of the United States of America*, vol. 110, no. 14, pp. 5612–5617, 2013.
- [137] T. B. Csóka, G. I. Frost, T. Wong, and R. Stern, "Purification and microsequencing of hyaluronidase isozymes from human urine," *FEBS Letters*, vol. 417, no. 3, pp. 307–310, 1997.
- [138] G. Lepperdinger, B. Strobl, and G. Kreil, "HYAL2, a human gene expressed in many cells, encodes a lysosomal hyaluronidase with a novel type of specificity," *The Journal of Biological Chemistry*, vol. 273, no. 35, pp. 22466–22470, 1998.
- [139] S. K. Rai, F.-M. Duh, V. Vigdorovich, A. Danilkovitch-Miagkova, M. I. Lerman, and A. D. Miller, "Candidate tumor suppressor HYAL2 is a glycosylphosphatidylinositol (GPI)-anchored cell-surface receptor for jaagsiekte sheep retrovirus, the envelope protein of which mediates oncogenic transformation," *Proceedings of the National Academy of Sciences of the United States of America*, vol. 98, no. 8, pp. 4443–4448, 2001.
- [140] G. Kreil, "Hyaluronidases—a group of neglected enzymes," *Protein Science*, vol. 4, no. 9, pp. 1666–1669, 1995.
- [141] M. Slevin, J. Krupinski, J. Gaffney et al., "Hyaluronan-mediated angiogenesis in vascular disease: uncovering RHAMM and CD44 receptor signaling pathways," *Matrix Biology*, vol. 26, no. 1, pp. 58–68, 2007.
- [142] R. Stern, A. A. Asari, and K. N. Sugahara, "Hyaluronan fragments: an information-rich system," *European Journal of Cell Biology*, vol. 85, no. 8, pp. 699–715, 2006.
- [143] B. A. Neudecker, R. Stern, and M. K. Connolly, "Aberrant serum hyaluronan and hyaluronidase levels in scleroderma," *British Journal of Dermatology*, vol. 150, no. 3, pp. 469–476, 2004.
- [144] J. D. McNeil, O. W. Wiebkin, W. H. Betts, and L. G. Cleland, "Depolymerisation products of hyaluronic acid after exposure to oxygen-derived free radicals," *Annals of the Rheumatic Diseases*, vol. 44, no. 11, pp. 780–789, 1985.
- [145] D. C. West, I. N. Hampson, F. Arnold, and S. Kumar, "Angiogenesis induced by degradation products of hyaluronic acid," *Science*, vol. 228, no. 4705, pp. 1324–1336, 1985.
- [146] C. M. McKee, C. J. Lowenstein, M. R. Horton et al., "Hyaluronan fragments induce nitric-oxide synthase in murine macrophages through a nuclear factor kappaB-dependent mechanism," *The Journal of Biological Chemistry*, vol. 272, no. 12, pp. 8013–8018, 1997.
- [147] C. M. McKee, M. B. Penno, M. Cowman et al., "Hyaluronan (HA) fragments induce chemokine gene expression in alveolar macrophages: the role of HA size and CD44," *Journal of Clinical Investigation*, vol. 98, no. 10, pp. 2403–2413, 1996.
- [148] B. Oertli, B. Beck-Schimmer, X. Fan, and R. P. Wüthrich, "Mechanisms of hyaluronan-induced up-regulation of ICAM-1 and VCAM-1 expression by murine kidney tubular epithelial cells: hyaluronan triggers cell adhesion molecule expression through a mechanism involving activation of nuclear factor-kappaB and activating protein-1," *The Journal of Immunology*, vol. 161, no. 7, pp. 3431–3437, 1998.

- [149] M. Slevin, J. Krupinski, S. Kumar, and J. Gaffney, "Angiogenic oligosaccharides of hyaluronan induce protein tyrosine kinase activity in endothelial cells and activate a cytoplasmic signal transduction pathway resulting in proliferation," *Laboratory Investigation*, vol. 78, no. 8, pp. 987–1003, 1998.
- [150] K. Ghazi, U. Deng-Pichon, J. M. Warnet, and P. Rat, "Hyaluronan fragments improve wound healing on in vitro cutaneous model through P2X7 purinoreceptor basal activation: role of molecular weight," *PLoS ONE*, vol. 7, no. 11, Article ID e48351, 2012.
- [151] D. C. West, D. M. Shaw, P. Lorenz, N. S. Adzick, and M. T. Longaker, "Fibrotic healing of adult and late gestation fetal wounds correlates with increased hyaluronidase activity and removal of hyaluronan," *International Journal of Biochemistry and Cell Biology*, vol. 29, no. 1, pp. 201–210, 1997.
- [152] D. C. West and M. Yaqoob, "Serum hyaluronan levels follow disease activity in vasculitis," *Clinical Nephrology*, vol. 48, no. 1, pp. 9–15, 1997.
- [153] D. J. Whitby and M. W. J. Ferguson, "The extracellular matrix of lip wounds in fetal, neonatal and adult mice," *Development*, vol. 112, no. 2, pp. 651–668, 1991.
- [154] T. Sawai, N. Usui, K. Sando et al., "Hyaluronic acid of wound fluid in adult and fetal rabbits," *Journal of Pediatric Surgery*, vol. 32, no. 1, pp. 41–43, 1997.
- [155] D. Jiang, J. Liang, and P. W. Noble, "Hyaluronan in tissue injury and repair," *Annual Review of Cell and Developmental Biology*, vol. 23, pp. 435–461, 2007.
- [156] D. C. West and S. Kumar, "Hyaluronan and angiogenesis," *Ciba Foundation Symposium*, vol. 143, pp. 187–201, 1989.
- [157] P. Teder, R. W. Vandivier, D. Jiang et al., "Resolution of lung inflammation by CD44," *Science*, vol. 296, no. 5565, pp. 155–158, 2002.
- [158] C. B. Knudson and W. Knudson, "Hyaluronan-binding proteins in development, tissue homeostasis, and disease," *The FASEB Journal*, vol. 7, no. 13, pp. 1233–1241, 1993.
- [159] D. Naor, S. Nedvetzki, I. Golan, L. Melnik, and Y. Faitelson, "CD44 in cancer," *Critical Reviews in Clinical Laboratory Sciences*, vol. 39, no. 6, pp. 527–579, 2002.
- [160] D. Naor, S. B. Wallach-Dayana, M. A. Zahalka, and R. V. Sionov, "Involvement of CD44, a molecule with a thousand faces, in cancer dissemination," *Seminars in Cancer Biology*, vol. 18, no. 4, pp. 260–267, 2008.
- [161] D. Naor, R. V. Sionov, and D. Ish-Shalom, "CD44: structure, function, and association with the malignant process," *Advances in Cancer Research*, vol. 71, pp. 241–319, 1997.
- [162] E. A. Turley, L. Austen, K. Vandelig, and C. Clary, "Hyaluronan and a cell-associated hyaluronan binding protein regulate the locomotion of ras-transformed cells," *The Journal of Cell Biology*, vol. 112, no. 5, pp. 1041–1047, 1991.
- [163] M. Zöller, "CD44: can a cancer-initiating cell profit from an abundantly expressed molecule?" *Nature Reviews Cancer*, vol. 11, no. 4, pp. 254–267, 2011.
- [164] D. Kohda, C. J. Morton, A. A. Parkar et al., "Solution structure of the link module: a hyaluronan-binding domain involved in extracellular matrix stability and cell migration," *Cell*, vol. 86, no. 5, pp. 767–775, 1996.
- [165] K. T. Dicker, L. A. Gurski, S. Pradhan-Bhatt, R. L. Witt, M. C. Farach-Carson, and X. Jia, "Hyaluronan: a simple polysaccharide with diverse biological functions," *Acta Biomaterialia*, vol. 10, no. 4, pp. 1558–1570, 2014.
- [166] A. J. Day and C. A. de la Motte, "Hyaluronan cross-linking: a protective mechanism in inflammation?" *Trends in Immunology*, vol. 26, no. 12, pp. 637–643, 2005.
- [167] S. Banerji, J. Ni, S.-X. Wang et al., "LYVE-1, a new homologue of the CD44 glycoprotein, is a lymph-specific receptor for hyaluronan," *The Journal of Cell Biology*, vol. 144, no. 4, pp. 789–801, 1999.
- [168] J. D. Kahmann, R. O'Brien, J. M. Werner et al., "Localization and characterization of the hyaluronan-binding site on the link module from human TSG-6," *Structure*, vol. 8, no. 7, pp. 763–774, 2000.
- [169] G. Tzircotis, R. F. Thorne, and C. M. Isacke, "Chemotaxis towards hyaluronan is dependent on CD44 expression and modulated by cell type variation in CD44-hyaluronan binding," *Journal of Cell Science*, vol. 118, no. 21, pp. 5119–5128, 2005.
- [170] M. S. Pandey, B. A. Baggenstoss, J. Washburn, E. N. Harris, and P. H. Weigel, "The hyaluronan receptor for endocytosis (HARE) activates NF-kappaB-mediated gene expression in response to 40–400-kDa, but not smaller or larger, hyaluronans," *The Journal of Biological Chemistry*, vol. 288, no. 20, pp. 14068–14079, 2013.
- [171] T. Ahrens, V. Assmann, C. Fieber et al., "CD44 is the principal mediator of hyaluronic-acid-induced melanoma cell proliferation," *Journal of Investigative Dermatology*, vol. 116, no. 1, pp. 93–101, 2001.
- [172] P. W. Noble, "Hyaluronan and its catabolic products in tissue injury and repair," *Matrix Biology*, vol. 21, no. 1, pp. 25–29, 2002.
- [173] B. P. Toole and V. C. Hascall, "Hyaluronan and tumor growth," *American Journal of Pathology*, vol. 161, no. 3, pp. 745–747, 2002.
- [174] M. W. Makgoba, M. E. Sanders, G. E. Ginther Luce et al., "ICAM-1 a ligand for LFA-1-dependent adhesion of B, T and myeloid cells," *Nature*, vol. 331, no. 6151, pp. 86–88, 1988.
- [175] G. R. Screaton, M. V. Bell, D. G. Jackson, F. B. Cornelis, U. Gerth, and J. I. Bell, "Genomic structure of DNA encoding the lymphocyte homing receptor CD44 reveals at least 12 alternatively spliced exons," *Proceedings of the National Academy of Sciences of the United States of America*, vol. 89, no. 24, pp. 12160–12164, 1992.
- [176] K. W. Lynch, "Consequences of regulated pre-mRNA splicing in the immune system," *Nature Reviews Immunology*, vol. 4, no. 12, pp. 931–940, 2004.
- [177] J. Cichy and E. Puré, "Oncostatin M and transforming growth factor-beta 1 induce post-translational modification and hyaluronan binding to CD44 in lung-derived epithelial tumor cells," *The Journal of Biological Chemistry*, vol. 275, no. 24, pp. 18061–18069, 2000.
- [178] A. Maiti, G. Maki, and P. Johnson, "TNF-alpha induction of CD44-mediated leukocyte adhesion by sulfation," *Science*, vol. 282, no. 5390, pp. 941–943, 1998.
- [179] L. E. Esford, A. Maiti, S. A. Bader, F. Tufaro, and P. Johnson, "Analysis of CD44 interactions with hyaluronan in murine L cell fibroblasts deficient in glycosaminoglycan synthesis: a role for chondroitin sulfate," *Journal of Cell Science*, vol. 111, part 7, pp. 1021–1029, 1998.
- [180] S. Katoh, Z. Zheng, K. Oritani, T. Shimozato, and P. W. Kincade, "Glycosylation of CD44 negatively regulates its recognition of hyaluronan," *Journal of Experimental Medicine*, vol. 182, no. 2, pp. 419–429, 1995.
- [181] J. Lesley, N. English, A. Perschl, J. Gregoroff, and R. Hyman, "Variant cell lines selected for alterations in the function of the hyaluronan receptor CD44 show differences in glycosylation,"

- Journal of Experimental Medicine*, vol. 182, no. 2, pp. 431–437, 1995.
- [182] S. Misra, V. C. Hascall, C. de Giovanni, R. R. Markwald, and S. Ghatak, “Delivery of CD44 shRNA/nanoparticles within cancer cells: perturbation of hyaluronan/CD44v6 interactions and reduction in adenoma growth in Apc Min/+ MICE,” *The Journal of Biological Chemistry*, vol. 284, no. 18, pp. 12432–12446, 2009.
- [183] E. Puré, R. L. Camp, D. Peritt, R. A. Panettieri Jr., A. L. Lazaar, and S. Nayak, “Defective phosphorylation and hyaluronate binding of CD44 with point mutations in the cytoplasmic domain,” *Journal of Experimental Medicine*, vol. 181, no. 1, pp. 55–62, 1995.
- [184] T. P. Skelton, C. Zeng, A. Nocks, and I. Stamenkovic, “Glycosylation provides both stimulatory and inhibitory effects on cell surface and soluble CD44 binding to hyaluronan,” *The Journal of Cell Biology*, vol. 140, no. 2, pp. 431–446, 1998.
- [185] L. Y. W. Bourguignon, P. A. Singleton, H. Zhu, and F. Diedrich, “Hyaluronan-mediated CD44 interaction with RhoGEF and Rho kinase promotes Grb2-associated binder-1 phosphorylation and phosphatidylinositol 3-kinase signaling leading to cytokine (macrophage-colony stimulating factor) production and breast tumor progression,” *The Journal of Biological Chemistry*, vol. 278, no. 32, pp. 29420–29434, 2003.
- [186] L. Y. W. Bourguignon, H. Zhu, L. Shao, and Y. W. Chen, “CD44 interaction with Tiam1 promotes Rac1 signaling and hyaluronic acid-mediated breast tumor cell migration,” *The Journal of Biological Chemistry*, vol. 275, no. 3, pp. 1829–1838, 2000.
- [187] L. Y. W. Bourguignon, H. Zhu, L. Shao, and Y.-W. Chen, “CD44 interaction with c-Src kinase promotes cortactin-mediated cytoskeleton function and hyaluronic acid-dependent ovarian tumor cell migration,” *The Journal of Biological Chemistry*, vol. 276, no. 10, pp. 7327–7336, 2001.
- [188] S. Misra, S. Ghatak, and B. P. Toole, “Regulation of MDRI expression and drug resistance by a positive feedback loop involving hyaluronan, phosphoinositide 3-kinase, and ErbB2,” *The Journal of Biological Chemistry*, vol. 280, no. 21, pp. 20310–20315, 2005.
- [189] S. Misra, S. Ghatak, A. Zoltan-Jones, and B. P. Toole, “Regulation of multidrug resistance in cancer cells by hyaluronan,” *Journal of Biological Chemistry*, vol. 278, no. 28, pp. 25285–25288, 2003.
- [190] S. Misra, B. P. Toole, and S. Ghatak, “Hyaluronan constitutively regulates activation of multiple receptor tyrosine kinases in epithelial and carcinoma cells,” *The Journal of Biological Chemistry*, vol. 281, no. 46, pp. 34936–34941, 2006.
- [191] S. Ghatak, S. Misra, and B. P. Toole, “Hyaluronan oligosaccharides inhibit anchorage-independent growth of tumor cells by suppressing the phosphoinositide 3-kinase/Akt cell survival pathway,” *The Journal of Biological Chemistry*, vol. 277, no. 41, pp. 38013–38020, 2002.
- [192] S. Ghatak, S. Misra, and B. P. Toole, “Hyaluronan constitutively regulates ErbB2 phosphorylation and signaling complex formation in carcinoma cells,” *The Journal of Biological Chemistry*, vol. 280, no. 10, pp. 8875–8883, 2005.
- [193] K.-H. Heider, M. Hofmann, E. Hors et al., “A human homologue of the rat metastasis-associated variant of CD44 is expressed in colorectal carcinomas and adenomatous polyps,” *Journal of Cell Biology*, vol. 120, no. 1, pp. 227–233, 1993.
- [194] T. Ishida, “Immunohistochemical expression of the CD44 variant 6 in colorectal adenocarcinoma,” *Surgery Today*, vol. 30, no. 1, pp. 28–32, 2000.
- [195] R. Neumayer, H. R. Rosen, A. Reiner et al., “CD44 expression in benign and malignant colorectal polyps,” *Diseases of the Colon and Rectum*, vol. 42, no. 1, pp. 50–55, 1999.
- [196] V. J. M. Wielenga, K.-H. Heider, G. J. A. Offerhaus et al., “Expression of CD44 variant proteins in human colorectal cancer is related to tumor progression,” *Cancer Research*, vol. 53, no. 20, pp. 4754–4756, 1993.
- [197] V. J. M. Wielenga, R. van der Neut, G. J. A. Offerhaus, and S. T. Pals, “CD44 Glycoproteins in colorectal cancer: expression, function, and prognostic value,” *Advances in Cancer Research*, vol. 77, pp. 169–187, 2000.
- [198] V. J. M. Wielenga, R. van der Voort, J. W. R. Mulder et al., “CD44 splice variants as prognostic markers in colorectal cancer,” *Scandinavian Journal of Gastroenterology*, vol. 33, no. 1, pp. 82–87, 1998.
- [199] S. M. Chang, R. D. Xing, F. M. Zhang, and Y. Q. Duan, “Serum soluble CD44v6 levels in patients with oral and maxillofacial malignancy,” *Oral Diseases*, vol. 15, no. 8, pp. 570–572, 2009.
- [200] B. Delpuch, B. Chevallier, N. Reinhardt et al., “Serum hyaluronan (hyaluronic acid) in breast cancer patients,” *International Journal of Cancer*, vol. 46, no. 3, pp. 388–390, 1990.
- [201] A. Josefsson, H. Adamo, P. Hammarsten et al., “Prostate cancer increases hyaluronan in surrounding nonmalignant stroma, and this response is associated with tumor growth and an unfavorable outcome,” *The American Journal of Pathology*, vol. 179, no. 4, pp. 1961–1968, 2011.
- [202] T. Jung, W. Gross, and M. Zöller, “CD44v6 coordinates tumor matrix-triggered motility and apoptosis resistance,” *The Journal of Biological Chemistry*, vol. 286, no. 18, pp. 15862–15874, 2011.
- [203] Q. Xie, R. Bradley, L. Kang et al., “Hepatocyte growth factor (HGF) autocrine activation predicts sensitivity to MET inhibition in glioblastoma,” *Proceedings of the National Academy of Sciences of the United States of America*, vol. 109, no. 2, pp. 570–575, 2011.
- [204] R. D. Xing, S. M. Chang, Y. Q. Duan, F. M. Zhang, and F. S. Dong, “Examination of serum hyaluronic acid level in patients with oral and maxillofacial malignancy,” *Hua Xi Kou Qiang Yi Xue Za Zhi*, vol. 22, no. 4, pp. 309–311, 2004.
- [205] Q. Yu and I. Stamenkovic, “Localization of matrix metalloproteinase 9 to the cell surface provides a mechanism for CD44-mediated tumor invasion,” *Genes and Development*, vol. 13, no. 1, pp. 35–48, 1999.
- [206] M. C. Levesque and B. F. Haynes, “In vitro culture of human peripheral blood monocytes induces hyaluronan binding and up-regulates monocyte variant CD44 isoform expression,” *Journal of Immunology*, vol. 156, no. 4, pp. 1557–1565, 1996.
- [207] Y. Matsubara, S. Katoh, H. Taniguchi, M. Oka, J. Kadota, and S. Kohno, “Expression of CD44 variants in lung cancer and its relationship to hyaluronan binding,” *Journal of International Medical Research*, vol. 28, no. 2, pp. 78–90, 2000.
- [208] J. P. Sleeman, S. Arming, J. F. Moll et al., “Hyaluronate-independent metastatic behavior of CD44 variant-expressing pancreatic carcinoma cells,” *Cancer Research*, vol. 56, no. 13, pp. 3134–3141, 1996.
- [209] V. Orian-Rousseau, L. Chen, J. P. Sleeman, P. Herrlich, and H. Ponta, “CD44 is required for two consecutive steps in HGF/c-Met signaling,” *Genes and Development*, vol. 16, no. 23, pp. 3074–3086, 2002.
- [210] U. Protin, T. Schweighoffer, W. Jochum, and F. Hilberg, “CD44-deficient mice develop normally with changes in subpopulations and recirculation of lymphocyte subsets,” *Journal of Immunology*, vol. 163, no. 9, pp. 4917–4923, 1999.

- [211] A. Q. Rafi-Janajreh, D. Chen, R. Schmits et al., "Evidence for the involvement of CD44 in endothelial cell injury and induction of vascular leak syndrome by IL-2," *Journal of Immunology*, vol. 163, no. 3, pp. 1619–1627, 1999.
- [212] D. Chen, R. J. McKallip, A. Zeytun et al., "CD44-Deficient mice exhibit enhanced hepatitis after concanavalin A injection: evidence for involvement of CD44 in activation-induced cell death," *Journal of Immunology*, vol. 166, no. 10, pp. 5889–5897, 2001.
- [213] G. Abatangelo, M. Martelli, and P. Vecchia, "Healing of hyaluronic acid-enriched wounds: histological observations," *Journal of Surgical Research*, vol. 35, no. 5, pp. 410–416, 1983.
- [214] D. Foschi, F. Castoldi, E. Radaelli et al., "Hyaluronic acid prevents oxygen free-radical damage to granulation tissue: a study in rats," *International Journal of Tissue Reactions*, vol. 12, no. 6, pp. 333–339, 1990.
- [215] S. R. King, W. L. Hickerson, and K. G. Proctor, "Beneficial actions of exogenous hyaluronic acid on wound healing," *Surgery*, vol. 109, no. 1, pp. 76–84, 1991.
- [216] M. Nakamura, M. Hikida, and T. Nakano, "Concentration and molecular weight dependency of rabbit corneal epithelial wound healing on hyaluronan," *Current Eye Research*, vol. 11, no. 10, pp. 981–986, 1992.
- [217] C. Laurent, S. Hellstrom, and L.-E. Stenfors, "Hyaluronic acid reduces connective tissue formation in middle ears filled with absorbable gelatin sponge: an experimental study," *The American Journal of Otolaryngology: Head and Neck Medicine and Surgery*, vol. 7, no. 3, pp. 181–186, 1986.
- [218] E. A. Balasz and J. L. Denlinger, *Clinical Uses of Hyaluronan*, John Wiley & Sons, 1989.
- [219] M. T. Longaker, E. S. Chiu, N. S. Adzick, M. Stern, M. R. Harrison, and R. Stern, "Studies in fetal wound healing. V. A prolonged Presence of hyaluronic acid characterizes fetal wound fluid," *Annals of Surgery*, vol. 213, no. 4, pp. 292–296, 1991.
- [220] J. A. Mack, S. R. Abramson, Y. Ben et al., "Hoxb13 knockout adult skin exhibits high levels of hyaluronan and enhanced wound healing," *The FASEB Journal*, vol. 17, no. 10, pp. 1352–1354, 2003.
- [221] J. A. Mack, L. Li, N. Sato, V. C. Hascall, and E. V. Maytin, "Hoxb13 up-regulates transglutaminase activity and drives terminal differentiation in an epidermal organotypic model," *The Journal of Biological Chemistry*, vol. 280, no. 33, pp. 29904–29911, 2005.
- [222] J. A. MacK and E. V. Maytin, "Persistent inflammation and angiogenesis during wound healing in K14-directed hoxb13 transgenic mice," *Journal of Investigative Dermatology*, vol. 130, no. 3, pp. 856–865, 2010.
- [223] D. A. R. Burd, R. M. Greco, S. Regauer, M. T. Longaker, J. W. Siebert, and H. G. Garg, "Hyaluronan and wound healing: a new perspective," *British Journal of Plastic Surgery*, vol. 44, no. 8, pp. 579–584, 1991.
- [224] P. Heldin, T. C. Laurent, and C.-H. Heldin, "Effect of growth factors on hyaluronan synthesis in cultured human fibroblasts," *Biochemical Journal*, vol. 258, no. 3, pp. 919–922, 1989.
- [225] B. A. Mast, R. F. Diegelmann, T. M. Krummel, and I. K. Cohen, "Hyaluronic acid modulates proliferation, collagen and protein synthesis of cultured fetal fibroblasts," *Matrix*, vol. 13, no. 6, pp. 441–446, 1993.
- [226] G. F. Pierce, T. A. Mustoe, J. Lingelbach et al., "Platelet-derived growth factor and transforming growth factor-beta enhance tissue repair activities by unique mechanisms," *The Journal of Cell Biology*, vol. 109, no. 1, pp. 429–440, 1989.
- [227] S. E. Lynch, J. C. Nixon, R. B. Colvin, and H. N. Antoniades, "Role of platelet-derived growth factor in wound healing: synergistic effects with other growth factors," *Proceedings of the National Academy of Sciences of the United States of America*, vol. 84, no. 21, pp. 7696–7700, 1987.
- [228] G. F. Pierce, J. E. Tarpley, J. Tseng et al., "Detection of platelet-derived growth factor (PDGF)-AA in actively healing human wounds treated with recombinant PDGF-BB and absence of PDGF in chronic nonhealing wounds," *The Journal of Clinical Investigation*, vol. 96, no. 3, pp. 1336–1350, 1995.
- [229] A. L. Carre, A. W. James, L. MacLeod et al., "Interaction of wingless protein (Wnt), transforming growth factor-beta, and hyaluronan production in fetal and postnatal fibroblasts," *Plastic and Reconstructive Surgery*, vol. 125, no. 1, pp. 74–88, 2010.
- [230] M. David-Raoudi, F. Tranchepain, B. Deschrevel et al., "Differential effects of hyaluronan and its fragments on fibroblasts: relation to wound healing," *Wound Repair and Regeneration*, vol. 16, no. 2, pp. 274–287, 2008.
- [231] R. C. Cabera, J. W. Siebert, Y. Eidelman, L. I. Gold, M. T. Longaker, and H. G. Garg, "The in vivo effect of hyaluronan associated protein-collagen complex on wound repair," *Biochemistry and Molecular Biology International*, vol. 37, no. 1, pp. 151–158, 1995.
- [232] H. Morrison, L. S. Sherman, J. Legg et al., "The NF2 tumor suppressor gene product, merlin, mediates contact inhibition of growth through interactions with CD44," *Genes and Development*, vol. 15, no. 8, pp. 968–980, 2001.
- [233] S. P. Thankamony and W. Knudson, "Acylation of CD44 and its association with lipid rafts are required for receptor and hyaluronan endocytosis," *The Journal of Biological Chemistry*, vol. 281, no. 45, pp. 34601–34609, 2006.
- [234] P. Heldin, *Growth Factor Regulation of Hyaluronan Metabolism in Tumor Progression*, 2011.
- [235] E. Bell, B. Ivarsson, and C. Merrill, "Production of a tissue-like structure by contraction of collagen lattices by human fibroblasts of different proliferative potential in vitro," *Proceedings of the National Academy of Sciences of the United States of America*, vol. 76, no. 3, pp. 1274–1278, 1979.
- [236] I. V. Yannas, E. Lee, D. P. Orgill, E. M. Skrabut, and G. F. Murphy, "Synthesis and characterization of a model extracellular matrix that induces partial regeneration of adult mammalian skin," *Proceedings of the National Academy of Sciences of the United States of America*, vol. 86, no. 3, pp. 933–937, 1989.
- [237] S. R. Slivka, L. K. Landeen, F. Zeigler, M. P. Zimber, and R. L. Bartel, "Characterization, barrier function, and drug metabolism of an in vitro skin model," *Journal of Investigative Dermatology*, vol. 100, no. 1, pp. 40–46, 1993.
- [238] G. Galassi, P. Brun, M. Radice et al., "In vitro reconstructed dermis implanted in human wounds: degradation studies of the HA-based supporting scaffold," *Biomaterials*, vol. 21, no. 21, pp. 2183–2191, 2000.
- [239] D. A. Hollander, C. Soranzo, S. Falk, and J. Windolf, "Extensive traumatic soft tissue loss: reconstruction in severely injured patients using cultured hyaluronan-based three-dimensional dermal and epidermal autografts," *Journal of Trauma—Injury, Infection and Critical Care*, vol. 50, no. 6, pp. 1125–1136, 2001.
- [240] Y. Liu, A. Skardal, X. Z. Shu, and G. D. Prestwich, "Prevention of peritendinous adhesions using a hyaluronan-derived hydrogel film following partial-thickness flexor tendon injury," *Journal of Orthopaedic Research*, vol. 26, no. 4, pp. 562–569, 2008.
- [241] G. D. Prestwich, "Engineering a clinically-useful matrix for cell therapy," *Organogenesis*, vol. 4, no. 1, pp. 42–47, 2008.

- [242] G. D. Prestwich, "Evaluating drug efficacy and toxicology in three dimensions: using synthetic extracellular matrices in drug discovery," *Accounts of Chemical Research*, vol. 41, no. 1, pp. 139–148, 2008.
- [243] X. Z. Shu, Y. Liu, Y. Luo, M. C. Roberts, and G. D. Prestwich, "Disulfide cross-linked hyaluronan hydrogels," *Biomacromolecules*, vol. 3, no. 6, pp. 1304–1311, 2002.
- [244] T. D. Mehra, K. Ghosh, X. Z. Shu, G. D. Prestwich, and R. A. F. Clark, "Molecular stenting with a crosslinked hyaluronan derivative inhibits collagen gel contraction," *Journal of Investigative Dermatology*, vol. 126, no. 10, pp. 2202–2209, 2006.
- [245] J.-W. Kuo, D. A. Swann, and G. D. Prestwich, "Chemical modification of hyaluronic acid by carbodiimides," *Bioconjugate Chemistry*, vol. 2, no. 4, pp. 232–241, 1991.
- [246] E. J. Oh, S. W. Kang, B. S. Kim, G. Jiang, H. C. Il, and K. H. Sei, "Control of the molecular degradation of hyaluronic acid hydrogels for tissue augmentation," *Journal of Biomedical Materials Research—Part A*, vol. 86, no. 3, pp. 685–693, 2008.
- [247] K. L. Chao, L. Muthukumar, and O. Herzberg, "Structure of human hyaluronidase-1, a hyaluronan hydrolyzing enzyme involved in tumor growth and angiogenesis," *Biochemistry*, vol. 46, no. 23, pp. 6911–6920, 2007.
- [248] J. Entwistle, C. L. Hall, and E. A. Turley, "HA receptors: regulators of signalling to the cytoskeleton," *Journal of Cellular Biochemistry*, vol. 61, no. 4, pp. 569–577, 1996.
- [249] H. Lee, H. Mok, S. Lee, Y.-K. Oh, and T. G. Park, "Target-specific intracellular delivery of siRNA using degradable hyaluronic acid nanogels," *Journal of Controlled Release*, vol. 119, no. 2, pp. 245–252, 2007.
- [250] A. Gabrielli, E. V. Avvedimento, and T. Krieg, "Scleroderma," *The New England Journal of Medicine*, vol. 360, no. 19, pp. 1989–2003, 2009.
- [251] J. Varga and D. Abraham, "Systemic sclerosis: a prototypic multisystem fibrotic disorder," *The Journal of Clinical Investigation*, vol. 117, no. 3, pp. 557–567, 2007.
- [252] M. S. Anscher, W. P. Peters, H. Reisenbichler, W. P. Petros, and R. L. Jirtle, "Transforming growth factor beta as a predictor of liver and lung fibrosis after autologous bone marrow transplantation for advanced breast cancer," *The New England Journal of Medicine*, vol. 328, no. 22, pp. 1592–1598, 1993.
- [253] K. Matsumoto and T. Nakamura, "Hepatocyte growth factor: renotropic role and potential therapeutics for renal diseases," *Kidney International*, vol. 59, no. 6, pp. 2023–2038, 2001.
- [254] A. Akhmetshina, P. Venalis, C. Dees et al., "Treatment with imatinib prevents fibrosis in different preclinical models of systemic sclerosis and induces regression of established fibrosis," *Arthritis and Rheumatism*, vol. 60, no. 1, pp. 219–224, 2009.
- [255] J. H. W. Distler, A. Jüngel, L. C. Huber et al., "Imatinib mesylate reduces production of extracellular matrix and prevents development of experimental dermal fibrosis," *Arthritis and Rheumatism*, vol. 56, no. 1, pp. 311–322, 2007.
- [256] H. A. Burgess, L. E. Daugherty, T. H. Thatcher et al., "PPAR γ agonists inhibit TGF- β induced pulmonary myofibroblast differentiation and collagen production: implications for therapy of lung fibrosis," *The American Journal of Physiology: Lung Cellular and Molecular Physiology*, vol. 288, no. 6, pp. L1146–L1153, 2005.
- [257] L. Hecker, J. Cheng, and V. J. Thannickal, "Targeting NOX enzymes in pulmonary fibrosis," *Cellular and Molecular Life Sciences*, vol. 69, no. 14, pp. 2365–2371, 2012.
- [258] K. Burridge and M. Chrzanowska-Wodnicka, "Focal adhesions, contractility, and signaling," *Annual Review of Cell and Developmental Biology*, vol. 12, pp. 463–519, 1996.
- [259] M. Chrzanowska-Wodnicka and K. Burridge, "Rho-stimulated contractility drives the formation of stress fibers and focal adhesions," *Journal of Cell Biology*, vol. 133, no. 6, pp. 1403–1415, 1996.
- [260] Y. Zhou, X. Huang, L. Hecker et al., "Inhibition of mechanosensitive signaling in myofibroblasts ameliorates experimental pulmonary fibrosis," *Journal of Clinical Investigation*, vol. 123, no. 3, pp. 1096–1108, 2013.

Review Article

Hyaluronan Synthase: The Mechanism of Initiation at the Reducing End and a Pendulum Model for Polysaccharide Translocation to the Cell Exterior

Paul H. Weigel

Department of Biochemistry & Molecular Biology, The Oklahoma Center for Medical Glycobiology, University of Oklahoma Health Sciences Center, Oklahoma City, OK 73190, USA

Correspondence should be addressed to Paul H. Weigel; paul-weigel@ouhsc.edu

Received 2 October 2014; Accepted 14 January 2015

Academic Editor: Howard Beverley Osborne

Copyright © 2015 Paul H. Weigel. This is an open access article distributed under the Creative Commons Attribution License, which permits unrestricted use, distribution, and reproduction in any medium, provided the original work is properly cited.

Hyaluronan (HA) biosynthesis has been studied for over six decades, but our understanding of the biochemical details of how HA synthase (HAS) assembles HA is still incomplete. Class I family members include mammalian and streptococcal HASs, the focus of this review, which add new intracellular sugar-UDPs at the reducing end of growing hyaluronyl-UDP chains. HA-producing cells typically create extracellular HA coats (capsules) and also secrete HA into the surrounding space. Since HAS contains multiple transmembrane domains and is lipid-dependent, we proposed in 1999 that it creates an intraprotein HAS-lipid pore through which a growing HA-UDP chain is translocated continuously across the cell membrane to the exterior. We review here the evidence for a synthase pore-mediated polysaccharide translocation process and describe a possible mechanism (the Pendulum Model) and potential energy sources to drive this ATP-independent process. HA synthases also synthesize chitin oligosaccharides, which are created by cleavage of novel oligo-chitosyl-UDP products. The synthesis of chitin-UDP oligomers by HAS confirms the reducing end mechanism for sugar addition during HA assembly by streptococcal and mammalian Class I enzymes. These new findings indicate the possibility that HA biosynthesis is initiated by the ability of HAS to use chitin-UDP oligomers as self-primers.

1. Introduction and Overview of HA Biosynthesis

Cell-free biosynthesis of HA was demonstrated in 1959 using *Streptococcus* membranes [1]. The enzyme responsible, HA synthase (HAS), is a membrane protein that requires only Mg^{+2} and two sugar-UDP substrates (GlcUA-UDP and GlcNAc-UDP) to polymerize HA chains. (To be consistent in using the standard convention of showing the reducing end of any glycan or saccharide to the right, we do not use the normal convention for nucleotide-sugars (e.g., UDP-GlcNAc); instead HA-UDP, GlcNAc-UDP, and GlcUA-UDP are abbreviated to show their reducing ends to the right.) No one was able to identify any streptococcal or eukaryotic HA synthase gene until 1993 when the *hasA* gene was identified and cloned, and the *S. pyogenes* HAS protein was expressed [2–4]. Identification of the *hasA* gene and the biochemical

demonstration that only the HAS protein was required to synthesize HA [5] then led to the identification of *hasA* genes in *S. equisimilis* [6] and *S. uberis* [7] and vertebrate homologues of these HAS genes in many species [8–10]. The first active HAS was purified when the recombinant enzymes from Group A (SpHAS) and Group C (SeHAS) *Streptococcus* were overexpressed in *E. coli* SURE cells [11].

Mammalian genomes have three different HAS genes (HAS1, HAS2, and HAS3) that are expressed at specific times and specific tissues during development, aging, wound healing, and under normal or pathologic conditions or in diseases such as cancer [12, 13]. HA, which is found in only some prokaryotes but is a general ubiquitous extracellular matrix component in vertebrates [14, 15], is a linear heteropolysaccharide composed of the repeating disaccharide: (-3)- β -D-N-acetylglucosamine- β (1,4)-D-glucuronic acid- β (1-). This unsulfated glycosaminoglycan is a major component in

cartilage and dermis, and in synovial and vitreous fluids. HA plays an important role during fertilization, embryogenesis, development, and differentiation [16, 17] and is also involved in many diverse cellular functions and behaviors, such as cell migration, phagocytosis, and proteoglycan assembly [18]. Additionally, HA plays important roles during wound healing and is used as a drug delivery vehicle, a cosmetic ingredient, and an analgesic device [19–21].

All known HASs, except one, are related structurally, show high sequence identity or similarity, share similar multi-membrane-domain organizations (with 6–8 membrane domains), predicted topologies, and processive mechanisms, and constitute a large family, the Class I HASs [10, 22]. The only known Class II HAS, from *Pasteurella multocida*, is different from Class I HASs in membrane attachment (having a single membrane domain), gene and protein sequence, domain organization, and having a distributive (nonprocessive) mechanism. This review focuses on the characteristics of Class I streptococcal and mammalian HASs.

Streptococcal and mammalian HASs in membranes [23–26] or as purified enzymes [27] elongate HA at the reducing end and do not require an exogenous primer to begin HA synthesis. HAS initiates biosynthesis using just the two sugar-UDP substrates, although we now know that the enzyme makes a self-primer using only GlcNAc-UDP (described below). HAS is an unusual enzyme in that it uses four substrates (i.e., two sugar-nucleotides and two types of HA-UDP chains, with either GlcUA or GlcNAc at the reducing end) and two glycosyltransferase activities within the same protein. DNA and RNA polymerases utilize template molecules to direct synthesis of products with only one type of bond between monomers. Heteropolysaccharide synthases, such as HAS (which makes a $[\text{GlcNAc}(\beta 1,4)\text{GlcUA}(\beta 1,3)]_n$ -UDP polymer), create *de novo* two different glycoside linkages in an alternating manner. The HA product after each sugar addition then becomes a substrate for the next sugar addition. In the presence of exogenous precursors, membrane-bound HASs use at least seven binding or catalytic functions (Figure 1) to synthesize disaccharide units at the reducing end of a growing HA-UDP chain. Class I HAS enzymes are processive; they do not rebind and extend HA chains once they are released.

SpHAS, the only Class I HAS whose topology has been determined experimentally [28], has the N- and C-terminus and majority of the SpHAS protein inside the cell (Figure 2). StrepHASs have six membrane domains (MDs), four of which pass through the membrane giving two small loops of the protein exposed to the extracellular side. The other two MDs, one within the large central catalytic domain and one in the C-terminal one-third of the protein, interact with the membrane as amphipathic helices or reentrant loops but do not appear to span the membrane. The presence of two MDs in HAS that are amphipathic and do not cross the membrane is intriguing because these might be particularly well suited for the formation of an intraprotein pore. Vertebrate HASs contain an additional C-terminal region of ~130–160 aa with two trans-MDs. The amino ~75% of the larger eukaryotic HAS family members is homologous to SpHAS with the same predicted domain organization, so the overall topological

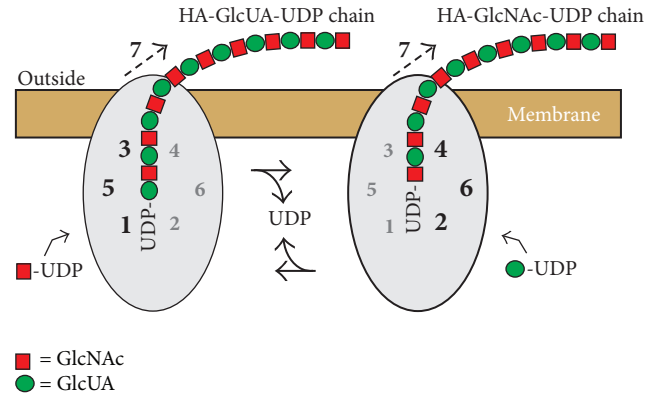


FIGURE 1: Schematic model of HAS showing the functions needed for HA chain growth at the reducing end and transfer to the cell surface. HAS uses multiple discrete functions (numbers 1–7) to assemble each HA disaccharide (red squares are GlcNAc and green circles are GlcUA). The same HAS protein is indicated in two different situations, at sequential times, as it alternately adds HA-GlcUA-UDP to a new GlcNAc-UDP, using functions 1, 3, and 5 (left), and then adds HA-GlcNAc-UDP to a new GlcUA-UDP, using functions 2, 4, and 6 (right). In this example (variant 1; Table 1) the sugar-UDPs are sequentially added in a continuous alternating manner and each cohort of needed functions cycles between being active (larger black numbers) and inactive (smaller gray numbers) within the active site domains (gray ovals). The functions required to add GlcNAc-UDP to HA-GlcUA-UDP are (left): 1, GlcNAc-UDP acceptor binding; 3, HA-GlcUA-UDP donor binding; 5, HA-GlcUA-UDP: GlcNAc-UDP, $\beta 1,3$ (HA-GlcUA-) transferase; and 7, HA translocation through the membrane. The functions required to add GlcUA-UDP to HA-GlcNAc-UDP are (right): 2, GlcUA-UDP acceptor binding; 4, HA-GlcNAc-UDP donor binding; 6, HA-GlcNAc-UDP: GlcUA-UDP, $\beta 1,4$ (HA-GlcNAc-) transferase; and 7, HA translocation.

TABLE 1: Three variations of the Pendulum hypothesis.

Variant	Disaccharide assembly	Glycosyl-UDP sites
1	Sequential	Four independent sites
2	Simultaneous	Three independent sites
3	Alternating	Two or three dependent sites

The mechanism for adding sugars to the reducing end of HA could entail polymerization of a disaccharide unit by either a sequential (i.e., one sugar at a time) or a concerted (i.e., simultaneous) mechanism. For the sequential assembly of a disaccharide unit (variant 1), the enzyme would need two glycosyl-UDP binding sites for addition of each sugar, one for a HA-UDP and one for a sugar-UDP. Since there are two types of HA-UDP species, the enzyme would need four glycosyl-UDP binding sites to assemble each disaccharide unit. For disaccharide assembly at the reducing end in a concerted way (variant 2), HAS would require three glycosyl-UDP binding sites, one each for GlcNAc-UDP, GlcUA-UDP, and a specific HA-UDP donor chain (i.e., HA-GlcUA-UDP or HA-GlcNAc-UDP), depending on which of the two possible HA disaccharide units was assembled. Another variation is that HAS contains only one donor and one acceptor glycosyl-UDP binding site, whose specificities alternate as the two sugars are assembled one at a time (variant 3). If there is a single donor binding site, its specificity would alternately recognize HA-GlcUA-UDP and HA-GlcNAc-UDP. There could be two separate sugar-UDP sites, but if there is a single acceptor binding site, its specificity would also alternate in a reciprocal fashion with the HA-UDP site to bind GlcUA-UDP or GlcNAc-UDP.

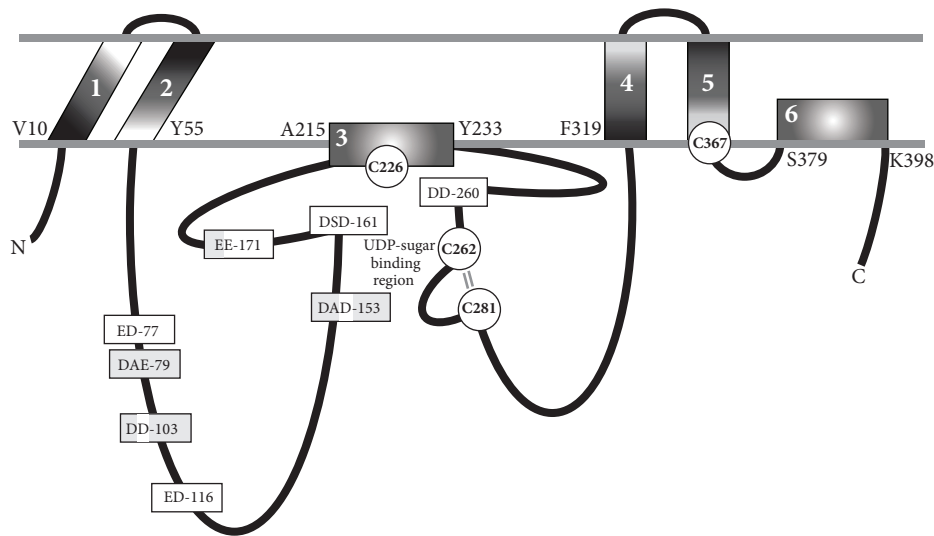


FIGURE 2: Membrane organization of HAS domains and conserved potential glycosyl-UDP binding regions. The experimentally determined topology of SpHAS [28] is modified to incorporate the discovery [46] that all four Cys residues of SeHAS (white circles) are at the membrane-protein interface and are located in or very near to the sugar-UDP binding sites. These four Cys residues are positionally conserved in the Class I HAS family. The SeHAS numbering shows the amino acids at the cytoplasmic junctions of the six MDs (white numbers 1–6). The parallel lines (gray) between C262 and C281 indicate the close proximity (~ 5 Å) of these residues; they are not disulfide bonded. Eight “DXD”- or “XDD”-equivalent motifs in SeHAS, potential glycosyl-UDP binding sites (rectangle boxes), are either conserved just among the streptococcal enzymes (light gray) or also among the eukaryotic HASs (white); a few exceptions are discussed in the text. In some motifs, a streptococcal acidic residue is shaded white to indicate its conservation in the HAS family.

organization of all the Class I HASs is predicted to be similar [10].

2. HAS Activity Is Regulated by Its Lipid Environment

Radiation inactivation studies [29] showed that the “active unit” mass of SeHAS or SpHAS is ~ 23 kDa more than a monomer, but smaller than a HAS dimer. The additional 23 kDa was identified as phospholipid (CL). The active streptococcal enzymes are HAS protein monomers in complex with 14–18 molecules of CL or other phospholipids. Similarly, active XIHAS1 is a monomer of ~ 69 kDa with an additional ~ 20 kDa of unknown components [30], probably phospholipid although this was not confirmed. Kinetic characterization of purified StrepHASs [31] and human HAS2 [32] confirmed that activity of these enzymes is regulated by, or dependent on, lipids. Purified StrepHASs have low activity without lipid and are activated ~ 10 -fold by exogenous CL [11, 33], with high specificity for particular fatty acyl chains [34]. SeHAS is highly activated by oleoyl (C18:1) CL, but almost completely inactive with myristyl (C14:0) CL. The activity of purified human HAS2 in reconstituted liposomes is greatly influenced by cholesterol and the available lipids [32] and manipulating plasma membrane cholesterol content in different cell types causes them to make less HA [35, 36]. Thus, Class I HASs are either lipid-dependent or regulated by their lipid and cholesterol microenvironment. Strong positive modulation by cholesterol might also serve to minimize intracellular HA synthesis, which could be detrimental to many cellular pathways and functions if in excess.

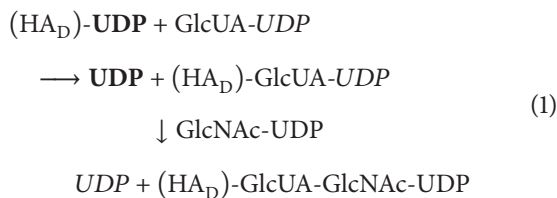
3. Mammalian HAS Activity Is Regulated by Precursor Availability, Posttranslational Modifications and Protein-Protein Interactions

In streptococcal [37], *B. subtilis* [38], or mammalian [39] cells expressing HAS and making HA, the consumption of the two precursor sugar-UDPs is extraordinarily high compared to cells not making HA. To enable HA synthesis cells must have greater expression levels of the biosynthetic enzymes and greater flux rates in the precursor metabolic pathways; this often results in higher steady-state precursor concentrations, but a more important factor is that the rate of precursor synthesis supports the high rate of HAS precursor use. HAS regulation in mammalian cells is more complicated than in bacteria and several groups have identified a range of different mechanisms, including transcriptional and posttranslational control [40, 41]. Mammalian HAS2 has been studied the most and is regulated posttranslationally by phosphorylation [42], O-GlcNAcylation, and GlcNAc-UDP levels [43, 44], and by ubiquitination and dimerization [45]. It is not known if any of these regulatory mechanisms alters HAS monosaccharide assembly activity or HA translocation activity, but since these two functions are coupled, altering one activity is expected to alter both.

4. HA Synthases Elongate HA at the Reducing End

Stoolmiller and Dorfman [47] reported that the SpHAS adds new sugars to the nonreducing end, but other studies with

membranes from streptococci [24] or eukaryotic cells [23, 26] show that HA synthesis occurs at the reducing end. Purified SeHAS and SpHAS [27] or SpHAS in crude membranes [25] also add sugar-UDP units at the reducing end. The mechanism for polysaccharide biosynthesis is different if chain growth is from the reducing or nonreducing end. When a sugar is added from a sugar-nucleotide (making it the donor) to the nonreducing end of a polysaccharide (the acceptor), the nucleotide (e.g., UDP) is released. However, for reducing end elongation, the growing polymer chain is always attached to UDP. Reaction (1) shows the reaction for HA disaccharide assembly (D = disaccharide units). During HA synthesis, the UDP released at each transfer step comes from the HA-UDP intermediate formed by addition of the previous sugar. In each cycle of monosaccharide addition, the released UDP is derived from the last monosaccharide added:



The donor HA-UDP transfers a hyaluronyl- (HA-) chain to the new sugar-UDP (acceptor) without cleavage of the latter high-energy linkage to UDP; the UDP released is from the HA-UDP donor. This situation is analogous to that for protein and fatty acid synthesis [48].

The IUBMB nomenclature for HAS glycosyltransferase activities (EC 2.4.1.212) is different compared to that for typical glycosyltransferases (Figure 1). An enzyme that utilizes GlcNAc-UDP to add to the nonreducing end of GlcUA would create a GlcNAc(β 1,4)GlcUA linkage, whereas the HAS transferase activity adding GlcNAc-UDP at the reducing end creates the GlcUA(β 1,3)GlcNAc linkage. Systematic naming of a transferase activity specifies the *donor: acceptor, group transferred*. Thus, addition of a GlcUA residue to a GlcNAc at the reducing end of the growing HA chain is catalyzed by an activity that adds a hyaluronyl chain from HA-GlcNAc-UDP to GlcUA-UDP. This is a HA-GlcNAc(α 1 \rightarrow)UDP:GlcUA(α 1 \rightarrow)UDP, β (1,4) hyaluronyltransferase. Similarly, an activity adding GlcNAc-UDP to a HA-GlcUA-UDP chain is a HA-GlcUA(α 1 \rightarrow)UDP:GlcNAc(α 1 \rightarrow)UDP, β (1,3) hyaluronyltransferase.

5. HA Translocation to the Cell Exterior Is Mediated by the HAS Protein Itself

The active sites of HAS and the sugar-UDP substrates are inside cells [28], so how do the large HA products (e.g., >40,000 sugars long; >8 MDa) reach the surface or extracellular space? Only the exogenous HAS protein (gene) and sufficient GlcNAc-UDP and GlcUA-UDP are required for HA biosynthesis and secretion by heterologous cells that cannot normally make HA, including *E. faecalis* [3], *B. subtilis* [38] and *D. melanogaster* [49]. Based on these findings and the lipid dependence and the topology of HAS, we proposed that HAS must have the ability to translocate the growing HA

chain across the cell membrane into the extracellular space [11]. An alternative proposal was that an ABC transport system is required for the appearance of extracellular HA [50, 51], as for many bacterial polysaccharides [52]; HAS would synthesize intracellular HA that, while still being assembled, would be exported by a nearby membrane-bound ABC transport system.

It seemed unlikely that an ABC transport system was involved in HA translocation for several reasons: (i) It is unexpected that ABC polysaccharide transporters in *E. faecalis*, *B. subtilis*, and fruit flies would have such low specificity for their normal substrate that they would effectively transport HA. (ii) Since multiple MDs are not needed for just HA synthesis (e.g., the Class II *P. multocida* HAS contains one membrane anchor and, unlike Class I HASs, can be expressed as an active soluble truncated protein [53]), the topological organization of HAS enzymes, containing 6–8 membrane domains, is more consistent with a translocation function [54]. (iii) HAS activity is lipid-dependent or modulated by its lipid environment, consistent with an inherently intimate organization within the membrane bilayer, as expected for an HA translocation function, but not the independent ABC transport model. (iv) The sugar-UDP binding sites of Strep and mammalian HASs are at the inner membrane surface [46], which better fits a model in which the HA-UDP chain is extended near or within the membrane and translocated through the enzyme to the exterior (Figure 2). (v) Class I HASs are processive enzymes, meaning they do not release their HA-UDP chains during synthesis; dissociation of HA from HAS does not occur [5, 55]. This characteristic strongly supports a Pore model. HA-UDP that is bound by weak HA-HAS interactions would be released, moved, and elongated continuously within the enzyme, while still being retained by the topological constraint of being within a pore. In the ABC model, HA-HAS interactions are reversible, as for the nonprocessive PmHAS, which dissociates from and then rebinds HA after every sugar addition [53].

The strong biochemical logic supporting a Pore Translocation Model was confirmed by multiple studies showing that an ABC transporter Model for HA translocation is not correct. Thomas and Brown [56] found that ABC transporters are not involved in HA translocation by breast cancer cells and Medina et al. [57] showed that purified SeHAS mediates luminal dye efflux when added to liposomes, demonstrating the presence of an intraprotein pore. Hubbard et al. [58] found that SeHAS, incorporated into liposomes, delivers HA directly to the internal lumen, demonstrating that HAS possesses the predicted HA translocation function.

Misra et al. [59] showed that ABC transporter MDRI expression is regulated by changes in the pericellular HA coat. Coordinately regulated expression of ABC transporters and HAS provides an alternative interpretation of studies implicating a role for transporters in HA transfer. Two independent cellular protective mechanisms (provided by pericellular HA coats and ABC multidrug transporters) may have coevolved in vertebrates to be coordinately regulated in a complex manner in response to environmental cues; this could explain why HAS and extracellular HA levels are lower in cells treated with inhibitors of multidrug transporter function [50]. Another

explanation for inhibition of HA translocation by ABC transporter inhibitors is that these inhibitors alter uridine uptake or salvage pathways and change uridine nucleotide pools, which inhibits HAS (e.g., controls were not preformed to verify that substrate sugar-UDP levels did not decrease or that the potent HAS inhibitor UDP did not increase).

Finally, the finding that a bacterial cellulose synthase creates an intraprotein pore, in which the product cellulose is synthesized and translocated [60], confirms the principle we proposed in 1999 [11] that glycosyltransferases such as HA and cellulose synthases can mediate both polysaccharide synthesis and translocation.

6. HAS Synthesizes Chitin and Chitosyl-UDP Oligosaccharides

SeHAS synthesizes chitin oligomers, $(\text{GlcNAc-}\beta\text{1,4})_n$ [61], as reported for XIHAS1 [62] and MmHAS1 [63]. More importantly, however, and consistent with reducing end sugar addition, we found that SeHAS also makes novel chitin oligomers attached to $\text{-GlcNAc}(\alpha\text{1}\rightarrow)\text{UDP}$ at the reducing end [61]. SeHAS incubated with only GlcNAc-UDP makes a series of $(\text{GlcNAc-}\beta\text{1,4})_n\text{-GlcNAc}(\alpha\text{1}\rightarrow)\text{UDP}$ oligomers (for $n = 2\text{--}15$) corresponding to $(\text{GlcNAc})_2\text{-UDP}$ through $(\text{GlcNAc})_7\text{-UDP}$ products. SeHAS membranes incubated without substrate or with only GlcUA-UDP show no signals in this region. Product identifications were confirmed by MS-MS fragmentation and digestion with jack bean $\beta\text{-N-acetylglucosaminidase}$ (e.g., all species ultimately yielded GlcNAc-UDP). For example, tri- and tetraoligomers were confirmed to contain $\beta\text{1,4}$ -linked GlcNAc residues attached to GlcNAc-UDP because treatment with jack bean hexosaminidase converted almost all the initial oligomers to GlcNAc-UDP or $(\text{GlcNAc})_2\text{-UDP}$ (Figure 3). Thus, HAS synthesizes $(\text{GlcNAc-}\beta\text{1,4})_{1\text{--}7}\text{-GlcNAc}(\alpha\text{1}\rightarrow)\text{UDP}$ oligomers. These unusual sugar-nucleotide species, activated by α -attachment to UDP, are unstable and readily cleaved to yield chitin oligomers, explaining the ability of Class I HASs to make chitin.

Although HAS does not require an exogenous primer to make HA, these novel self-made $(\text{GlcNAc})_n\text{-UDP}$ products could potentially serve as endogenous primers that enable HAS to initiate HA chain assembly. In this proposed scenario (Figure 4), the nonreducing end of all HA chains retains this initial chitin oligomer primer, and all HA molecules have a novel non-HA structure (a chitin oligosaccharide cap) at their nonreducing end. Ongoing studies support this hypothesis [64], including HAS-dependent m/z signals indicating hybrid chitin-HA species such as $\text{GlcNAc}_6(\text{GlcUA-GlcNAc})_2$ in ovine testicular hyaluronidase-digested samples (Figure 5(b)). Empty vector membranes without HAS (Figure 5(a)) or SeHAS membranes incubated without substrate (not shown) show no signals in this region. The hybrid chitin-HA digestion fragments can be affinity purified, fractionated by TLC or PAGE, and shown to contain multiple nonreducing GlcNAc residues that are releasable by treatment with jack bean hexosaminidase, as in Figure 3. Since we studied chitin-UDP oligomer products *in vitro* only,

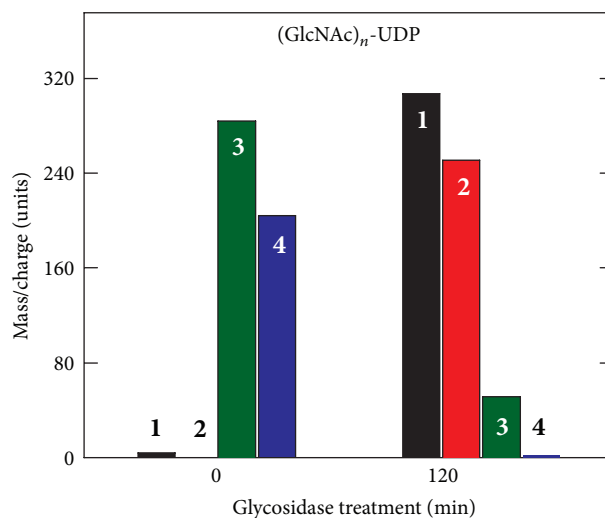


FIGURE 3: Glycosidase treatment converts larger $(\text{GlcNAc})_n\text{-UDP}$ oligomers to GlcNAc-UDP . SeHAS membranes were incubated for 30 min with UDP-GlcNAc alone, Folch extracted, fractionated over a size exclusion column, and samples were either untreated (0 min) or treated (120 min) with jack bean hexosaminidase. The samples were then analyzed by MALDI-TOF MS to identify and quantify m/z signals of candidate oligomeric chitin-UDP fragments corresponding to $n = 1\text{--}4$ (boldface white or black numbers). The presence of chitin linkages was confirmed by the ability of glycosidase treatment to shift species with 3 or 4 sugars to products with 1 (GlcNAc-UDP) or 2 sugars. Additional MS/MS analysis of the starting sample ions (not shown) revealed smaller members of the expected oligomer series, including GlcNAc-UDP .

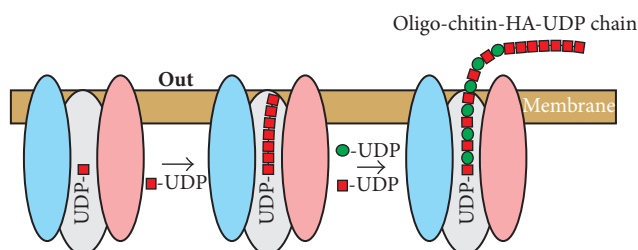


FIGURE 4: HAS initiation of HA synthesis using a self-made oligo-chitosyl-UDP primer results in HA chains with a chitin oligosaccharide cap at the nonreducing end. HAS makes chitin oligomers when incubated with GlcNAc-UDP (red squares) alone. We found that the enzyme first makes chitin oligomers linked to UDP at the reducing end [61], consistent with the mechanism of addition at the reducing end, and that these molecules could then serve as self-primers for HA disaccharide synthesis (GlcUA ; green circles).

under conditions (e.g., exposure to a single sugar-UDP) that may not normally be encountered in cells, it remains to be demonstrated if these interesting products are also made *in vivo*. Studies are in progress to determine if HA molecules made by streptococcal and mammalian Class I HASs contain a nonreducing end chitin oligosaccharide cap. The presence of a chitin cap would have important physiologic implications for the polarity of HA chains and the potential ability of chitin-like binding proteins in the biomatrix or

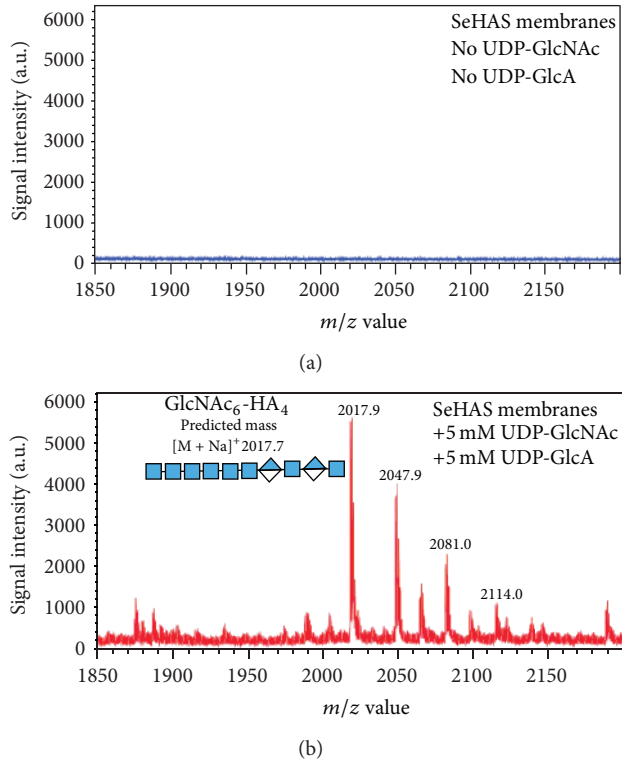


FIGURE 5: Mass spectral evidence for chitin-HA in HA made by SeHAS. Empty vector (a) or SeHAS (b) membranes were preincubated for 30 min with UDP-GlcNAc, UDP-GlcUA was added, and incubation proceeded for several minutes. The membranes were heated to release HA and subjected to two cycles of Folch extraction. Extracted HA products were speed vacuum concentrated, digested with ovine testicular hyaluronidase, and the resulting oligomers were subjected to affinity selection over carbograph. Eluted material was surveyed by MALDI-TOF MS to identify “hybrid” fragments corresponding to a chitin oligomer cap linked to HA disaccharides, such as the GlcNAc₆-(GlcUA-GlcNAc)₂ species shown.

on cell surfaces to orient, align, and organize individual HA polymers into bundles; for example, cables or fibers [65].

7. Class I HAS Performs Multiple Binding and Catalytic Function in Order to Synthesize HA

We noted above the seven functions that all Class I HAS enzymes possess in order to catalyze the steady-state assembly of GlcNAc(β 1,3)GlcUA(β 1,4) disaccharides during HA synthesis. The recent discovery that HASs are also able to make oligo-chitosyl-UDP species and that these can serve as self-primers for subsequent HA assembly means that this enzyme family also possesses more binding site and catalysis functions than previously recognized. These functions are summarized in Box 1, using the standard transferase nomenclature, and listed in order of use in the initiation and assembly of HA. The synthesis of chitin-UDP species requires three binding sites with different structural specificities and two transferase activities (Box 1(A), functions 1–5). Initiation of

HA synthesis requires making the first disaccharide using a non-HA substrate, so an acceptor site for the GlcUA to be added and a unique transferase activity (used only once for each HA molecule synthesized) are needed (Box 1(B), functions 6 and 7). Subsequent steady-state HA disaccharide synthesis requires seven functions, using two binding sites noted in (A) and (B) (functions 2 and 6), two additional hyaluronyl-UDP species binding sites, and two additional corresponding transferase activities (Box 1(C), functions 8–11). The final function is the translocation activity of HAS, which acts in a continuous manner during HA chain elongation but is listed separately to emphasize its novel and separate nature, as a “spatial” rather than chemical catalytic process (Box 1(D), function 12). Thus, an astounding 12 discrete functions are attributable to Class I HASs in order for these enzymes to initiate, assemble, and transfer the oligo-chitosyl-HA-UDP polysaccharide to the cell exterior; it is not known if released HA chains are still attached to UDP at their reducing ends or if chains are released because this group has been lost and elongation has therefore stopped, resulting in HA release.

8. A Pendulum Model for Polysaccharide Translocation

We proposed a novel mechanism in 2004 [37] by which a single membrane-bound HAS-lipid complex could simultaneously extend a polymer chain at its reducing end and extrude the growing chain through the membrane (Figures 6 and 7), in a process not requiring other proteins or ATP. The model also applies to other membrane polysaccharide synthases that use two transferase sites to make hetero- or homopolysaccharides (e.g., cellulose). The model involves continuous “swinging” movement by enzyme domains (pendulum-like) and has variations (three of which are noted in Table 1), depending on whether the catalytic mechanism utilizes independent glycosyl-UDP binding sites (e.g., variants 1 and 2) or one site with alternating specificity (e.g., variant 3). Disaccharide assembly in variant 1 or 2 is sequential or simultaneous, respectively, whereas assembly would necessarily be one sugar at a time in a variant 3 mechanism. Key features of the Pendulum Model are presented below to describe Pendulum Model variant 1, but similar central points and considerations apply to variant 2.

(i) *HAS Has Two Functional Domains That Act as “Arms.”* Each arm contains an active site for one of the glycosyltransferase functions, a binding site for one of the acceptor sugar-UDPs, and a binding site for one of the donor HA-UDP species (Figure 6(a)). The right arm (pink) contains the GlcNAc-UDP acceptor binding site, the HA-GlcNAc-UDP donor binding site, and the (1,4) hyaluronyltransferase activity that makes the GlcNAc- β (1,4)-GlcUA linkage. Some residues participating in interactions (e.g., binding) needed for each function might be in either arm or in other HAS domains not shown in Figures 6 and 7.

(ii) *Only One Arm Is Active at a Time and Their Activities Are Reciprocal.* When one arm is active as a transferase, the other

Functions and activities of Class I HA synthases needed for HA synthesis.

(A) Synthesis of (GlcNAc)_n-UDP Self Primer

- (1) Donor site for: GlcNAc(α1 →)UDP
 (2) Acceptor site for: GlcNAc(α1 →)UDP
 (3) Transferase activity: GlcNAc(α1 →)UDP: GlcNAc(α1 →)UDP, GlcNAc(β1,4)
 (4) Donor site for: [GlcNAc(β1,4)]_n(α1 →)UDP
 (5) Transferase activity: [GlcNAc(β1,4)]_n(α1 →)UDP: GlcNAc(α1 →)UDP, [GlcNAc(β1,4)]_n
- $$\text{GlcNAc}(\alpha 1 \rightarrow)\text{UDP} + \text{GlcNAc}(\alpha 1 \rightarrow)\text{UDP} \xrightarrow{(3)} \text{UDP} + \text{GlcNAc}(\beta 1,4)\text{GlcNAc}(\alpha 1 \rightarrow)\text{UDP}$$
- $$\text{GlcNAc}(\beta 1,4)\text{GlcNAc}(\beta 1,4)\text{GlcNAc}(\alpha 1 \rightarrow)\text{UDP} + \text{UDP} \xrightarrow{(5) \checkmark} \text{GlcNAc}(\alpha 1 \rightarrow)\text{UDP}$$
- $$[\text{GlcNAc}(\beta 1,4)]_{n+2}\text{GlcNAc}(\alpha 1 \rightarrow)\text{UDP} + n \text{UDP} \xrightarrow{(5) \checkmark n} [\text{GlcNAc}(\alpha 1 \rightarrow)\text{UDP}]$$

(B) Synthesis of first HA disaccharide

- (6) Acceptor site for: GlcUA(α1 →)UDP
 (7) Transferase: [GlcNAc(β1,4)]_nGlcNAc(α1 →)UDP: GlcUA(α1 →)UDP, [GlcNAc(β1,4)]_n
 [GlcNAc(β1,4)]_nGlcNAc(α1 →)UDP + GlcUA(α1 →)UDP $\xrightarrow{(7)}$ [GlcNAc(β1,4)]_nGlcNAc(β1,4)GlcUA(α1 →)UDP + UDP

(C) Steady-state synthesis of HA

- (8) Donor site for: Hyaluronyl-GlcUA(β1,3)GlcNAc(α1 →)UDP
 (9) Donor site for: Hyaluronyl-GlcNAc(β1,4)GlcUA(α1 →)UDP
 (10) Transferase: Hyaluronyl-GlcNAc(α1 →)UDP: UDP(α1 →)GlcUA, hyaluronyl-GlcNAc(β1,4)
 (11) Transferase: Hyaluronyl-GlcUA(α1 →)UDP: UDP-GlcNAc, hyaluronyl-GlcUA(β1,3)
 (HA)_D-UDP + UDP-GlcUA + UDP-GlcNAc $\xrightarrow{(10)\&(11)}$ (HA)_{D+1}-UDP + UDP + UDP

(D) Steady-state extrusion of HA-UDP across the membrane through a HAS pore

- (12) Hyaluronyl-UDP translocation activity

Box 1: Summary of HAS functions required for HA biosynthesis. At least twelve discrete binding and catalytic function are required for Class I HA synthases to create a (GlcNAc)_n-UDP self-primer (A, functions 1–5), to initiate HA disaccharide synthesis (B, functions 6 and 7), and to then assemble HA disaccharide units in a continuous manner (C, functions 8–11), while the growing HA-UDP chain is also continuously translocated through the HAS-lipid complex pore to the cell surface or exterior (D, function 12). Two functions for steady-state HA disaccharide synthesis (C) are also used to make (GlcNAc)_n-UDP (#2) or the first HA disaccharide (#6).

serves as an acceptor binding site. Each arm can “swing” to one of three functionally different positions (Figure 6(b)) that correspond to conformations in which it is active as a donor binding site and transferase, inactive, and active as an acceptor binding site. For example, the right (pink) arm can be active as a donor binding site for HA-GlcNAc-UDP and the (β1,4) transferase (Figure 6(b), left), inactive (Figure 6(b), center), or active as an acceptor binding site for GlcNAc-UDP (Figure 6(b), right). In the same relative positions, the left arm is similarly active as an acceptor binding site for GlcUA-UDP (Figure 6(b), left), inactive (Figure 6(b), center), or active as the (β1,3) transferase and donor binding site for HA-GlcUA-UDP (Figure 6(b), right). The relationship of the arms in a neutral inactive conformation (Figure 6(b), center) creates misalignment of glycosyl-UDP acceptor and donor sites that is not suitable for glycosyl binding or transfer. In contrast, when the arms have moved to either the left or the right position, the alignment of glycosyl-UDP donor and acceptor are favorable for the respective transferase activity to function. In either of the two functional positions, in which transferase activities add sugar-UDP to the growing HA-UDP chain, there is only one appropriate active arrangement of all

the binding and catalytic sites (Figure 6(c)). Even if binding of the alternate acceptor and donor could occur, the active sites would not be aligned for functional sugar transfer (Figure 6(c), left).

(iii) *HA-UDP Translocation Is Coupled to Sugar Addition.* As each arm moves from one side to the other through a sugar addition cycle, the HA chain is extruded through the enzyme and lipid bilayer (each row in Figure 7) one sugar at a time (or two at a time if concerted disaccharide synthesis occurs). With each new sugar-UDP addition, the bound HA-UDP chain is passed from one HAS arm to the other (e.g., like a person pulling up a rope, hand-over-hand) and as the arms swing, the nonreducing end of bound HA-UDP is simultaneously moved away from the intracellular active sites. The synchronized arm movement provides the force needed to move the bound HA-chain through the protein pore and cell membrane to the cell exterior. The bound HA-chain does not dissociate from HAS during continuous elongation because it is always bound to one arm or the other as it cycles between the two arms and it is always topologically constrained by being within the HAS-lipid pore.

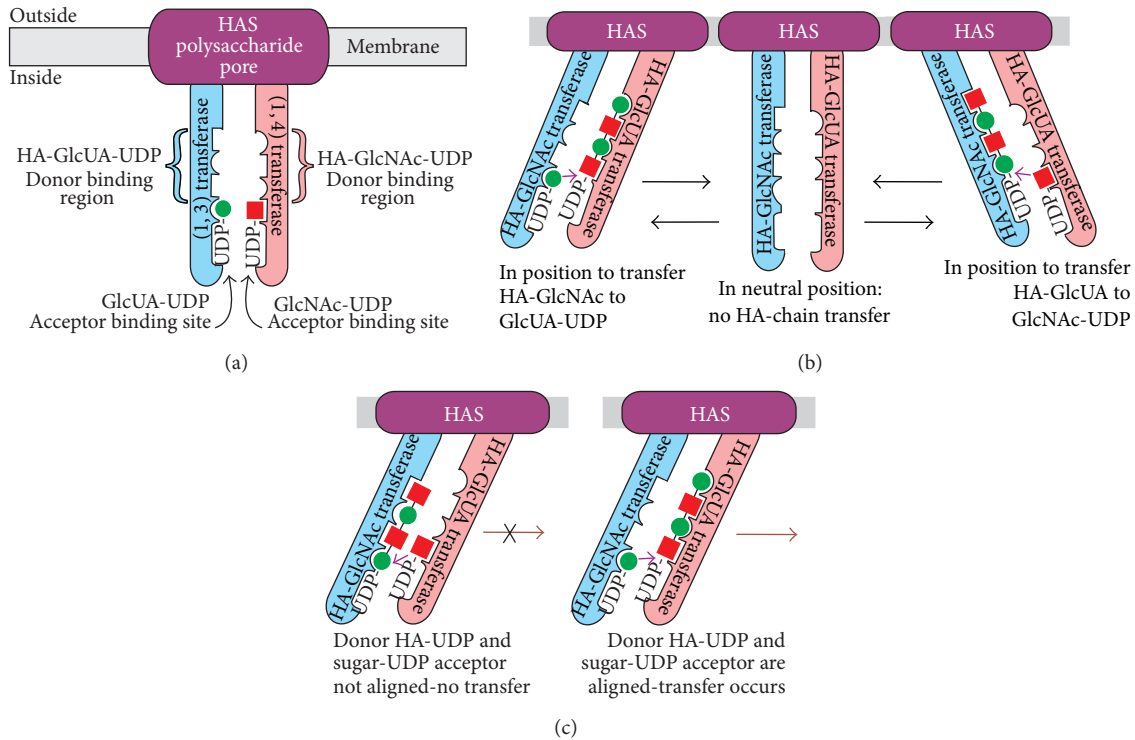


FIGURE 6: The Pendulum Model for HAS Translocation of HA. (a) Organization of hyaluronyl transferase domains and glycosyl-UDP binding sites within HAS. The scheme shows the cell membrane (gray) and three overall domains of the HAS-lipid complex: a pore region (purple) containing HAS MDs through which a growing HA chain is passed to the exterior, and two catalytic domains that behave as swinging arms (blue and pink). Each arm contains one of the two functional hyaluronyl transferase activities and binding sites needed to add either an HA-GlcUA-UDP donor chain to GlcNAc-UDP [left arm (blue); the $\beta(1,3)$ -hyaluronyl transferase] or an HA-GlcNAc-UDP donor chain to GlcUA-UDP [right arm (pink); the $\beta(1,4)$ -hyaluronyl transferase]. The figure also illustrates that an individual sugar-UDP binding site is part of the HA-UDP binding site on each arm. (b) The interactions between the glycosyl-UDP binding sites and hyaluronyl transferase domains change as the domain arms move. The three positions, from left to right, indicate three conformations in which HAS is either able to create the GlcNAc $\beta(1,4)$ GlcUA bond, unable to perform either transferase function, or able to create the GlcUA $\beta(1,3)$ GlcNAc bond. The left and right positions also illustrate that when the enzyme is in position to catalyze one of the transferase reactions, the growing HA chain is bound primarily to one arm, whereas the sugar-UDP substrate is bound to the other arm. In the central panel, a neutral or inactive position, the individual sugar binding sites in the HA-binding region on each arm are “misaligned” so that they are unable to bind HA at the same time. (c) HAS hyaluronyl transferase activities require correct alignment between the glycosyl-UDP binding sites on opposite domain arms. Transferase function depends on how the two arms are aligned with respect to the ability to bind substrates or to perform catalysis. The relative positioning of HA-UDP and sugar-UDP binding sites are shown with the complementary glycosyl-UDP substrates bound incorrectly and not aligned for creating a glycoside bond (left) or with the right substrates bound and aligned correctly for successful -GlcNAc- $\beta(1,4)$ -GlcUA-bond formation (right).

(iv) *Other Variants of the Pendulum Model.* The general scheme for other variants of the Pendulum Model is slightly different compared to that for variant 1 (Table 1). In variant 2 the three glycosyl-UDP binding sites might be in one arm, but the transferase sites and the HA-binding sites for moving the chain could be on the other arm or both arms. The glycosyl-UDP binding sites could be on two arms in variant 3, and simultaneous disaccharide assembly could occur in swinging from one position to the other. Release of UDP products could occur as the arms swing to the other position, transfer (and translocate) the HA-UDP chain, and “reload” for another round of disaccharide assembly. An alternating specificity mechanism (variant 3) involving fewer sites, whose glycosyl-UDP binding specificity cycles between two species (e.g., HA-GlcNAc-UDP and HA-GlcUA-UDP),

is intrinsically more complicated and may thus be less likely, especially given the large number of potential glycosyl-UDP binding sites in the Class I HAS family (Figure 2 and Section 10 below).

A key mechanistic feature to consider for concerted addition of a disaccharide unit to HA-UDP by adding both UDP-sugars simultaneously is that HAS would use only one of the two possible HA-UDP donors, either HA-GlcUA-UDP or HA-GlcNAc-UDP and thus make only one of the two possible HA disaccharide units (i.e., HA-GlcUA($\beta(1,3)$)GlcNAc-UDP versus HA-GlcNAc($\beta(1,4)$)GlcUA-UDP, resp.). Although no data currently support one mechanism over another, the presence of a chitin cap at the nonreducing end defines the first HA disaccharide made (Box 1) as GlcNAc($\beta(1,4)$)GlcUA and makes it likely that subsequent coordinated disaccharide

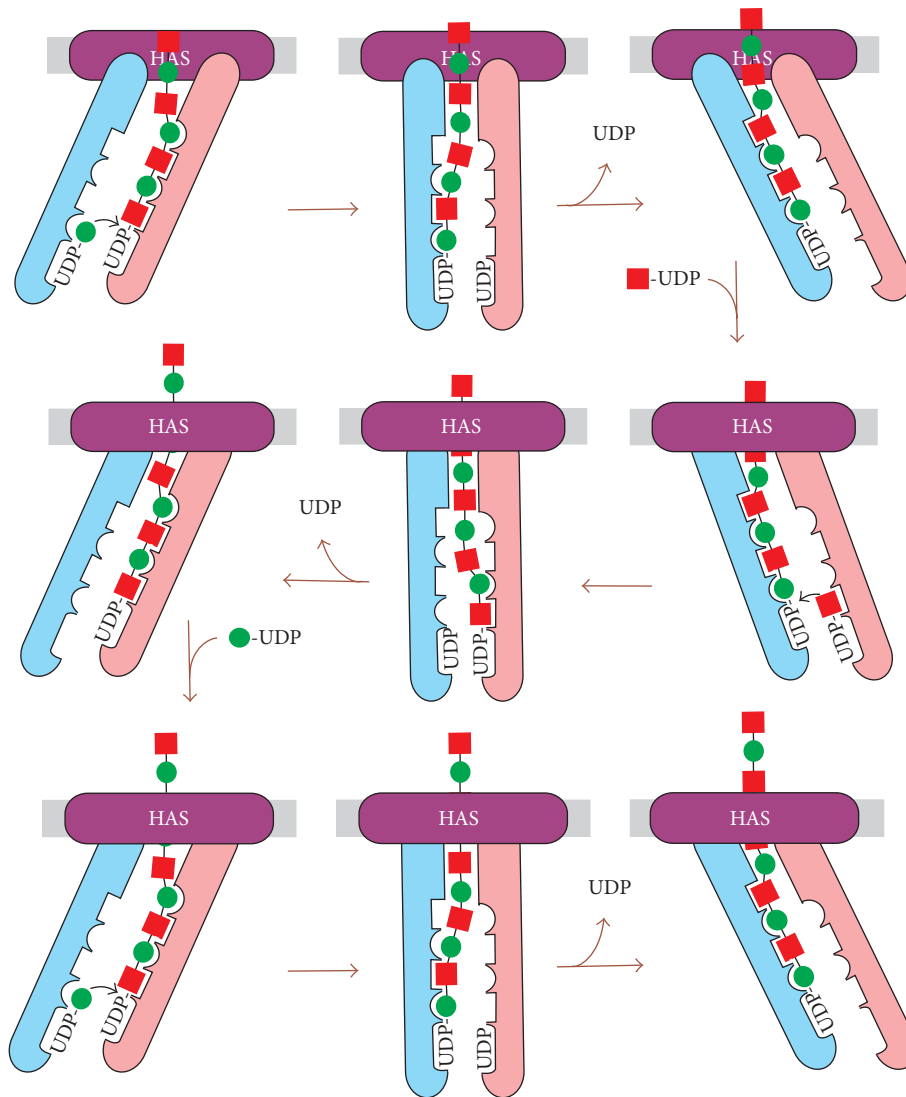
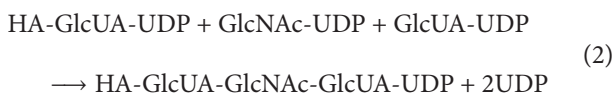


FIGURE 7: The Pendulum Model: Arm movement and HA transfer between arms drives HA chain translocation through the HAS-lipid complex to the cell exterior. The changing alignment of the HA-binding regions on the two arms in the two extreme positions (left and right) creates the ability of the enzyme to move the HA chain from one arm to the other (shown in each row). When the arms swing from one extreme position to the other, the HA chain is transferred from the first arm to the other arm as the HA-binding site alignments move out of (neutral position) and then back into register. A “time-lapse” of HAS action is illustrated in the nine panels as the enzyme adds three new sugars to an HA-UDP chain of seven sugars. The enzyme goes through three stages of arm movement (in each row) to add each new sugar. After assembly of each disaccharide, the enzyme arms are in the same starting position (e.g., the left panels in top and bottom rows). The sugars “crossing” the membrane are shown outside of the enzyme in the top row to help orient the reader, and then within the intraprotein pore in the middle and bottom rows. An animation of this process showing chain translocation through assembly of an HA 10-mer is at http://www.glycoforum.gr.jp/science/hyaluronan/HA06a/Pendulum_Hypothesis_Anima.files/slide0001.htm.

assembly would utilize the three bound substrates indicated in reaction (2), so that donor HA-GlcUA-UDP will be covalently linked to GlcNAc-UDP, as it in turn is linked to GlcUA-UDP in sequential coupled reactions that would be essentially simultaneous:



9. The Bioenergetics of HA Translocation

Any mechanism of HA translocation by HAS must account for several potential bioenergetic obstacles: (i) the energy barrier associated with transfer of a hydrophilic HA chain across a hydrophobic membrane lipid bilayer, (ii) the energy required to move an HA molecule might become progressively greater as it elongates to larger mass and hydrodynamic volume [66], and (iii) the energy to cause conformational changes and movement of domains within the enzyme that

could be physically responsible for rapid chain movement across the membrane without releasing the chain. For perspective, an 8 MDa HA chain proportionally enlarged to human scale would be equivalent to a 1 mm wide thread >30 m long.

(i) *How Does HAS Overcome the Hydrophobic Membrane Barrier?* Membrane transporters, such as lac permease with 12 MDs [67], mediate sugar transfer through an intraprotein pore created by interactions among many MDs. HASs appear to compensate for not having enough MDs to form such an intraprotein pore by their interactions with phospholipids [11, 32]. HAS-lipid interactions could allow the enzyme to create a larger pore-like passage within the enzyme, through which the growing HA chain could pass [11, 57, 68]. HAS-lipid complexes would present exterior hydrophobic interactions with fatty acyl groups in the bilayer, while engaging HA on the interior pore surface with hydrophilic interactions; thus, an HA chain moving through a HAS-lipid pore could effectively bypass the hydrophobic membrane barrier.

(ii) *How Could HAS Move HA Chains with Masses That Get Progressively Greater?* Intuitively, one might expect that the energy needed to overcome the inertia of, and move, a long HA-UDP chain (e.g., 4 MDa) would be much greater than the energy needed to move a short HA oligosaccharyl-UDP chain (e.g., 4 kDa). However, two factors may make this apparent “molecular weight-lifting” less difficult than it appears.

(a) *HA Segmentation.* The segmented, semi-independent movement of discrete portions (roughly 100 sugars long) of a large HA chain [69–71] could create an upper limit for the “apparent” mass of HA that HAS would need to “move” to translocate a discrete section. If segments of ~100 sugars behave semi-independently for brief periods (e.g., msec), during which translocation is favored, then the apparent mass of HA against which HAS needs to generate a translocation force would only be ~20 kDa. As a chain was initiated and elongated, HAS might initially translocate it rapidly and then progressively more slowly until the segmental length was approached, and a steady-state translocation rate was then reached. The observed kinetic profile for how HA mass increases during synthesis begins very rapidly and then becomes slower [55].

(b) *Increased Release Forces.* The net forces generated by Brownian motion may tend to pull the HA chain away from the enzyme and thus facilitate the translocation action of HAS. A possible chain release mechanism, in fact, could be the balance between the Brownian and other forces acting to release the HA and the HA-binding forces mediated by sites within the enzyme acting to retain the HA [66]. In contrast, cells with a pericellular HA coat might effectively stabilize and stop HA synthesis, because the presence of nearby HAS-HA complexes could augment and increase the forces favoring HA retention. As HA chain density

increased at the cell surface, the network of interacting chains would diminish the effects of Brownian-generated forces acting to release the HA, thus resulting in a stabilized gel-like cell surface coat still anchored to multiple HAS molecules. In the extreme of this scenario, HA synthesis would slow or stop as forces generated by the HA coat network increased, finally providing too much resistance for HAS to translocate HA.

(iii) *What Are the Energy Sources for HA Translocation?* At least three possible energy sources could contribute to an HA translocation mechanism (Figure 8), as estimated below: glycosyl-UDP hydrolysis [4–8 kJ/mol], H-bond formation [12–24 kJ/mol], and ion-pair reactions and the potential energy of electrochemical gradients [4–8 kJ/mol]. If these energy sources contribute to the HA translocation mechanism, a conservative estimate of the total free energy change for HA translocation is ~30 kJ/mol or ~7 kcal/mol (1 kcal = 4.18 kJ) of HA disaccharide units moved across the membrane. This is equivalent to 1 ATP and would be a favorable bioenergetic situation, explaining how an ATP-independent translocation process is feasible.

(a) *UDP-Sugar Hydrolysis.* The free energy for Glc-UDP hydrolysis is 7.3–7.6 kcal/mol and the difference between Glc-UDP hydrolysis and glucoside bond formation is ~0.6–1.0 kcal/mol [72]. Values for hydrolysis of GlcNAc-UDP and GlcUA-UDP are not available but are presumably somewhat greater, due to destabilizing repulsive and steric factors. Free energy differences between sugar-UDP hydrolysis and glycoside bond formation for GlcNAc and GlcUA are likely similar to Glc, ~0.6–1.0 kcal/mol. Thus, the available “excess” free energy to perform additional work beyond creating two glycoside bonds could be ~1–2 kcal/mol (~4–8 kJ/mol) of HA disaccharide units (Figure 8, #1).

(b) *Electrochemical Gradients or External Ion Reactions May Provide Additional Energy.* HA translocation to the cell exterior must necessarily be associated with one or more electrochemical gradients that could provide additional energy for the translocation process. HAS might recognize only one of ≥ 4 possible UDP-GlcUA species as the correct substrate during catalysis, depending on the state of the carboxyl group. The carboxyl group could be dissociated and free (i.e., an anion) or neutral and bound to either H^+ , Na^+ , or K^+ (Mg^{+2} is also a possibility). In most of these cases, a favorable energetic situation would occur when newly added GlcUA is transferred to the exterior: protonated carboxyl groups would readily dissociate releasing H^+ , negatively charged carboxyl groups would bind to extracellular cations (e.g., Na^+), and bound K^+ ions would exchange with Na^+ ions, which are in excess. Such ion-pair reactions would yield energy (that is difficult to estimate) and tend to increase (pull) the equilibrium for translocation, in a manner similar to removal of a reaction product.

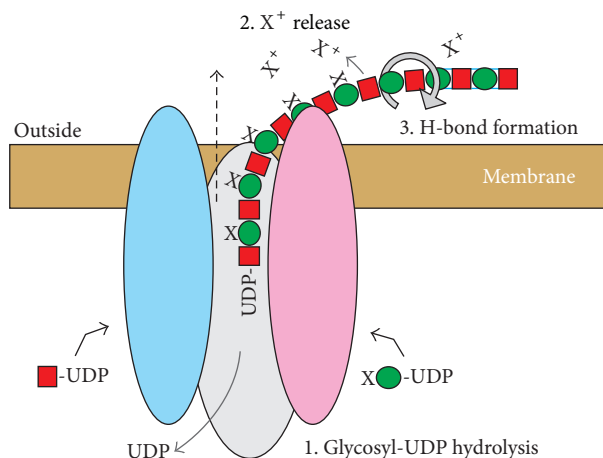


FIGURE 8: Three energy sources may drive the HAS-mediated translocation of HA-UDP. The diagram illustrates three sources of energy (numbers 1–3) that could contribute to an overall favorable free energy change to drive translocation (dashed black arrow), equivalent to ~ 1 ATP per disaccharide, as discussed in the text. 1. Two HA-UDP bonds are hydrolyzed to make two glycoside bonds per disaccharide. 2. Energy can be captured by extracellular release of a cation (X^+ ; bound to the intracellular GlcUA-UDP substrate and incorporated into HA by HAS) as the GlcUA is released from HAS and any associated restraints on the $-\text{CO}_2X$ group by the translocation process. Subsequent reactions in the extracellular environment (e.g., ion-pair association, dissociation, or exchange) and the coupling of a released ion, such as K^+ , to a cellular electrochemical gradient (potential) would provide favorable energetics. 3. Up to four H-bonds (blue lines between sugars at far right) could be formed as each new GlcNAc-GlcUA disaccharide (red squares and green circles, resp.) is released to the exterior, free of constraints imposed by being bound to HAS. For example, two H-bonds between the released disaccharide GlcNAc and GlcUA and two H-bonds between the GlcUA in the disaccharide released during the previous synthetic cycle and the new disaccharide GlcNAc. The gray circular arrow indicates a glycosidic bond that rotates (e.g., so that the N-acetyl and carboxyl group of adjacent sugars are on the same side of the chain) allowing the formation of new H-bonds.

The situation with bound K^+ might be particularly favorable because HA translocation would also then be coupled to the cellular K^+ ion gradient (high intracellular and low outside), providing an additional energy source for overall HA synthesis and translocation [73]. Given the intracellular abundance of K^+ , ion composition and pH, the K^+ -GlcUA-UDP species is likely the most abundant form of GlcUA-UDP and, thus, likely to be the normal HAS substrate. Consistent with this, purified SeHAS is more active in the presence of K^+ than Na^+ ions [33]. The energy available if one K^+ per disaccharide is transferred to the extracellular environment is ~ 1 – 2 kcal/mol (4 – 8 kJ/mol) of HA disaccharides (Figure 8, #2). This value, as noted above, is likely underestimated because it lacks the contributions from associated ion-pair reactions.

(c) *H-Bond formation*. Experimental and modeling studies [69, 71, 74, 75] indicate that HA forms multiple

intrachain H-bonds, by creating up to two H-bonds between adjacent sugars (similar to H-bonds between amino acids to form protein α -helices). Additional energy could be captured for chain translocation if HAS couples the formation of several new H-bonds with HA chain movement and the rotation of alternate newly added sugars occurring within or just external to the HAS pore (Figure 8, #3). Assuming an average value of ~ 6 kJ/mol (~ 1.5 kcal/mol) for intra-HA H-bonds, then translocation could yield up to 12 – 24 kJ/mol (3 – 6 kcal/mol) associated with the formation of 2 – 4 H-bonds per mol HA disaccharides.

10. Class I HASs Contain Multiple Potential Glycosyl-UDP Binding Sites

HASs contain only one conserved “DXD” motif (DSD¹⁶¹ in SeHAS; Figure 2), typically found in the active sites of many glycosyltransferases and whose carboxyl groups are coordinated with Mg^{+2} and the phosphoryl groups of a nucleotide-sugar [76]. However, the same “DXD” function can be mediated by essentially any cluster in which two of three contiguous residues are Asp or Glu [77]. StrepHASs also contain a second DAD¹⁵³ motif, which is conserved in the HAS family, except for chicken HAS2 and chlorella HAS (Asp¹⁵³ is conserved in all HASs). A DAE⁷⁹ motif in SeHAS and SpHAS, but not in SuHAS, is present in 10 of 13 eukaryotic HASs. Related “XDD” motifs are also present in all HASs at multiple positions: for example, SeHAS GDD²⁶⁰; ED⁷⁷ (EN in *Chlorella* HAS); ED¹¹⁶ (conserved positionally as EE, EXE, DE, or EXD). Five of the seven “XDD” motifs conserved in the StrepHASs are conserved positionally (i.e., within ≤ 6 residues) in all HASs, with the exception of XIHAS1 (in which 3 of the 5 motifs are conserved, but five others are also present). Thus, all Class I HASs except XIHAS1 contain at least six conserved DXD or XDD motifs and, therefore, all HASs potentially have enough glycosyl-UDP binding sites to assemble a disaccharide unit in either a coordinated or simultaneous manner (Table 1).

11. HAS as a Glycosyltransferase Family Member and Consequent Structural Predictions

HAS is a member of the GT2 family [78–80] in the CAZy database (<http://www.cazy.org/>) and catalyzes an inverted mechanism (i.e., creating a β -linked glycoside from the α -linked precursor). These family members require a divalent metal ion and contain at least one DXD motif and a GT-A fold (related to the Rossmann fold), consisting of a seven-stranded β -sheet flanked by α -helices. The active site in GT-2 proteins is created by the association of the large β -sheet with a smaller β -sheet. Present in perhaps $>5,000$ proteins, a basic GT-A fold provides a versatile “platform” for creating a variety of catalytic situations.

HAS is an exceptional GT2 family member due to its multiple MDs, which might create inherent topologic constraints

in regions of homology to the GT-A fold (making modeling essentially impossible). Based on extensive sequence similarity through a ~260 aa region between MD2 and MD4 (Figure 2), the HAS catalytic domain might adopt an overall fold similar to other GT2 family members, including cellulose synthase [81]. Similarities between HA and cellulose synthases include N-terminal nucleotide binding motifs, a putative catalytic base, a QxxRW motif associated with processivity, and that both proteins create an intraprotein pore for their products [58, 60]. The GT2 family model predicts that the N-terminal subdomain binds the sugar-UDP donor and the C-terminal subdomain binds the acceptor. For enzymes such as HAS that add to the reducing end the normal designation of donor and acceptor binding sites may be switched. Thus, in HAS an N-terminal subdomain binding site for sugar-UDP could be an acceptor site. Alternatively, if this was conserved as a donor site, then it would accommodate an HA-UDP substrate. The ultimate answers to many of the molecular and mechanistic questions posed here will likely only be revealed when the structure of HAS is ultimately determined at sufficient atomic resolution.

12. Conclusions

Since the first HAS gene was cloned in 1993, the field has progressed and answered important questions about the molecular basis of HA synthesis. In particular, there is a growing consensus that membrane-bound Class I HAS enzymes are lipid-dependent and active as both protein monomers or HAS multimers associated with specific lipids (and cholesterol) and that the Strep and mammalian HASs assemble HA at the reducing end. It is now resolved that HAS uses intracellular precursors and couples HA synthesis with HA translocation to the cell surface or biomatrix. Elucidation of this multifunctional process will surely reveal more surprises and unexpected intricacies about the complicated orchestration of molecular processes employed by a single enzyme protein to assemble and simultaneously translocate one of the largest single biomolecules made in the animal or microbial kingdoms. Future structural studies will reveal whether the general principles of the Pendulum Model are able to explain the mechanism of how HAS couples HA synthesis with translocation. Understanding how these enzymes work to synthesize and translocate HA will likely provide opportunities to identify therapeutics and to better understand how HASs are involved in normal human health and in tumorigenesis, metastasis, and inflammatory diseases such as arthritis.

Abbreviations

CL:	Cardiolipin
GlcNAc-UDP:	The nucleotide-sugar with the reducing end at the right
GlcUA-UDP:	The nucleotide-sugar with the reducing end at the right
HA:	Hyaluronic acid, hyaluronate, and hyaluronan
HA-:	A hyaluronyl group

HA-UDP:	A hyaluronyl group with α -linked UDP at the reducing end
HAS:	HA synthase
MD:	Membrane domain
SeHAS:	<i>Streptococcus equisimilis</i> HAS
SpHAS:	<i>Streptococcus pyogenes</i> HAS
StrepHAS:	Streptococcal HA synthases
SuHAS:	<i>Streptococcus uberis</i> HAS
XIHAS:	<i>Xenopus laevis</i> .

Conflict of Interests

The author declares that there is no conflict of interests regarding the publication of this paper.

Acknowledgments

Research from the author's laboratory was supported by the National Institutes of Health Grant GM35978 from the Institute of General Medical Sciences. The author also thanks Dr. Christopher West for very helpful discussions and input.

References

- [1] A. Markovitz, J. A. Cifonelli, and A. Dorfman, "The biosynthesis of hyaluronic acid by group A *Streptococcus*. VI. Biosynthesis from uridine nucleotides in cell-free extracts," *The Journal of Biological Chemistry*, vol. 234, pp. 2343–2350, 1959.
- [2] P. L. DeAngelis, J. Papaconstantinou, and P. H. Weigel, "Molecular cloning, identification, and sequence of the hyaluronan synthase gene from group A *Streptococcus pyogenes*," *The Journal of Biological Chemistry*, vol. 268, no. 26, pp. 19181–19184, 1993.
- [3] P. L. DeAngelis, J. Papaconstantinou, and P. H. Weigel, "Isolation of a *Streptococcus pyogenes* gene locus that directs hyaluronan biosynthesis in acapsular mutants and in heterologous bacteria," *Journal of Biological Chemistry*, vol. 268, no. 20, pp. 14568–14571, 1993.
- [4] B. A. Dougherty and I. van de Rijn, "Molecular characterization of *hasA* from an operon required for hyaluronic acid synthesis in group A streptococci," *Journal of Biological Chemistry*, vol. 269, no. 1, pp. 169–175, 1994.
- [5] P. L. DeAngelis and P. H. Weigel, "Immunochemical confirmation of the primary structure of streptococcal hyaluronan synthase and synthesis of high molecular weight product by the recombinant enzyme," *Biochemistry*, vol. 33, no. 31, pp. 9033–9039, 1994.
- [6] K. Kumari and P. H. Weigel, "Molecular cloning, expression, and characterization of the authentic hyaluronan synthase from group C *Streptococcus equisimilis*," *The Journal of Biological Chemistry*, vol. 272, no. 51, pp. 32539–32546, 1997.
- [7] P. N. Ward, T. R. Field, W. G. F. Ditcham, E. Maguin, and J. A. Leigh, "Identification and disruption of two discrete loci encoding hyaluronic acid capsule biosynthesis genes *hasA*, *hasB*, and *hasC* in *Streptococcus uberis*," *Infection and Immunity*, vol. 69, no. 1, pp. 392–399, 2001.
- [8] P. L. DeAngelis, "Hyaluronan synthases: fascinating glycosyltransferases from vertebrates, bacterial pathogens, and algal viruses," *Cellular and Molecular Life Sciences*, vol. 56, no. 7–8, pp. 670–682, 1999.
- [9] A. P. Spicer and J. A. McDonald, "Characterization and molecular evolution of a vertebrate hyaluronan synthase gene family,"

- Journal of Biological Chemistry*, vol. 273, no. 4, pp. 1923–1932, 1998.
- [10] P. H. Weigel and P. L. DeAngelis, “Hyaluronan synthases: a decade-plus of novel glycosyltransferases,” *Journal of Biological Chemistry*, vol. 282, no. 51, pp. 36777–36781, 2007.
- [11] V. L. Tlapak-Simmons, B. A. Baggenstoss, T. Clyne, and P. H. Weigel, “Purification and lipid dependence of the recombinant hyaluronan synthases from *Streptococcus pyogenes* and *Streptococcus equisimilis*,” *The Journal of Biological Chemistry*, vol. 274, no. 7, pp. 4239–4245, 1999.
- [12] J. Y. L. Tien and A. P. Spicer, “Three vertebrate hyaluronan synthases are expressed during mouse development in distinct spatial and temporal patterns,” *Developmental Dynamics*, vol. 233, no. 1, pp. 130–141, 2005.
- [13] K. Törrönen, K. Nikunen, R. Kärnä, M. Tammi, R. Tammi, and K. Rilla, “Tissue distribution and subcellular localization of hyaluronan synthase isoenzymes,” *Histochemistry and Cell Biology*, vol. 141, no. 1, pp. 17–31, 2014.
- [14] C. B. Knudson and W. Knudson, “Hyaluronan-binding proteins in development, tissue homeostasis, and disease,” *FASEB Journal*, vol. 7, no. 13, pp. 1233–1241, 1993.
- [15] J. R. E. Fraser, T. C. Laurent, and U. B. G. Laurent, “Hyaluronan: its nature, distribution, functions and turnover,” *Journal of Internal Medicine*, vol. 242, no. 1, pp. 27–33, 1997.
- [16] B. A. Fenderson, I. Stamenkovic, and A. Aruffo, “Localization of hyaluronan in mouse embryos during implantation, gastrulation and organogenesis,” *Differentiation*, vol. 54, no. 2, pp. 85–98, 1993.
- [17] B. P. Toole, “Hyaluronan in morphogenesis,” *Journal of Internal Medicine*, vol. 242, no. 1, pp. 35–40, 1997.
- [18] E. A. Turley, P. Bowman, and M. A. Kytryk, “Effects of hyaluronate and hyaluronate binding proteins on cell motile and contact behaviour,” *Journal of Cell Science*, vol. 78, pp. 133–145, 1985.
- [19] E. A. Balazs, “Analgesic effect of elastoviscous hyaluronan solutions and the treatment of arthritic pain,” *Cells Tissues Organs*, vol. 174, no. 1–2, pp. 49–62, 2003.
- [20] E. A. Balazs and J. L. Denlinger, “Viscosupplementation: a new concept in the treatment of osteoarthritis,” *Journal of Rheumatology*, vol. 20, no. 39, pp. 3–9, 1993.
- [21] K. L. Goa and P. Benfield, “Hyaluronic acid—a review of its pharmacology and use as a surgical aid in ophthalmology, and its therapeutic potential in joint disease and wound healing,” *Drugs*, vol. 47, no. 3, pp. 536–566, 1994.
- [22] N. Itano and K. Kimata, “Mammalian hyaluronan synthases,” *IUBMB Life*, vol. 54, no. 4, pp. 195–199, 2002.
- [23] P. Prehm, “Biosynthesis of hyaluronan: direction of chain elongation,” *Biochemical Journal*, vol. 398, no. 3, pp. 469–473, 2006.
- [24] P. Prehm, “Synthesis of hyaluronate in differentiated teratocarcinoma cells. Mechanism of chain growth,” *Biochemical Journal*, vol. 211, no. 1, pp. 191–198, 1983.
- [25] S. Bodevin-Authelet, M. Kusche-Gullberg, P. E. Pummill, P. L. DeAngelis, and U. Lindahl, “Biosynthesis of hyaluronan: direction of chain elongation,” *The Journal of Biological Chemistry*, vol. 280, no. 10, pp. 8813–8818, 2005.
- [26] T. Asplund, J. Brinck, M. Suzuki, M. J. Briskin, and P. Heldin, “Characterization of hyaluronan synthase from a human glioma cell line,” *Biochimica et Biophysica Acta—General Subjects*, vol. 1380, no. 3, pp. 377–388, 1998.
- [27] V. L. Tlapak-Simmons, C. A. Baron, R. Gotschall, D. Haque, W. M. Canfield, and P. H. Weigel, “Hyaluronan biosynthesis by class I streptococcal hyaluronan synthases occurs at the reducing end,” *The Journal of Biological Chemistry*, vol. 280, no. 13, pp. 13012–13018, 2005.
- [28] C. Heldermon, P. L. DeAngelis, and P. H. Weigel, “Topological organization of the hyaluronan synthase from *Streptococcus pyogenes*,” *The Journal of Biological Chemistry*, vol. 276, no. 3, pp. 2037–2046, 2001.
- [29] V. L. Tlapak-Simmons, E. S. Kempner, B. A. Baggenstoss, and P. H. Weigel, “The active streptococcal hyaluronan synthases (HASS) contain a single HAS monomer and multiple cardiolipin molecules,” *The Journal of Biological Chemistry*, vol. 273, no. 40, pp. 26100–26109, 1998.
- [30] P. E. Pummill, E. S. Kempner, and P. L. DeAngelis, “Functional molecular mass of a vertebrate hyaluronan synthase as determined by radiation inactivation analysis,” *Journal of Biological Chemistry*, vol. 276, no. 43, pp. 39832–39835, 2001.
- [31] V. L. Tlapak-Simmons, B. A. Baggenstoss, K. Kumari, C. Heldermon, and P. H. Weigel, “Kinetic characterization of the recombinant hyaluronan synthases from *Streptococcus pyogenes* and *Streptococcus equisimilis*,” *Journal of Biological Chemistry*, vol. 274, no. 7, pp. 4246–4253, 1999.
- [32] P. Ontong, Y. Hatada, S. Taniguchi, I. Kakizaki, and N. Itano, “Effect of a cholesterol-rich lipid environment on the enzymatic activity of reconstituted hyaluronan synthase,” *Biochemical and Biophysical Research Communications*, vol. 443, no. 2, pp. 666–671, 2014.
- [33] V. L. Tlapak-Simmons, C. A. Baron, and P. H. Weigel, “Characterization of the purified hyaluronan synthase from *Streptococcus equisimilis*,” *Biochemistry*, vol. 43, no. 28, pp. 9234–9242, 2004.
- [34] P. H. Weigel, Z. Kyosseva, and L. C. Torres, “Phospholipid dependence and liposome reconstitution of purified hyaluronan synthase,” *Journal of Biological Chemistry*, vol. 281, no. 48, pp. 36542–36551, 2006.
- [35] S. W. Sakr, S. Potter-Perigo, M. G. Kinsella et al., “Hyaluronan accumulation is elevated in cultures of low density lipoprotein receptor-deficient cells and is altered by manipulation of cell cholesterol content,” *The Journal of Biological Chemistry*, vol. 283, no. 52, pp. 36195–36204, 2008.
- [36] A. Kultti, R. Kärnä, K. Rilla et al., “Methyl-beta-cyclodextrin suppresses hyaluronan synthesis by down-regulation of hyaluronan synthase 2 through inhibition of Akt,” *The Journal of Biological Chemistry*, vol. 285, no. 30, pp. 22901–22910, 2010.
- [37] P. H. Weigel, “The bacterial hyaluronan synthases—an update,” in *Science of Hyaluronan Today*, V. C. Hascall and M. Yanagishita, Eds., 2004.
- [38] B. Widner, R. Behr, S. von Dollen et al., “Hyaluronic acid production in *Bacillus subtilis*,” *Applied and Environmental Microbiology*, vol. 71, no. 7, pp. 3747–3752, 2005.
- [39] M. Viola, D. Vignetti, A. Genasetti et al., “Molecular control of the hyaluronan biosynthesis,” *Connective Tissue Research*, vol. 49, no. 3–4, pp. 111–114, 2008.
- [40] R. H. Tammi, A. G. Passi, K. Rilla et al., “Transcriptional and post-translational regulation of hyaluronan synthesis,” *FEBS Journal*, vol. 278, no. 9, pp. 1419–1428, 2011.
- [41] D. Vignetti and A. Passi, “Hyaluronan synthases posttranslational regulation in cancer,” in *Hyaluronan Signaling and Turnover*, vol. 123 of *Advances in Cancer Research*, chapter 4, pp. 95–119, Elsevier, New York, NY, USA, 2014.

- [42] D. Vigetti, M. Clerici, S. Deleonibus et al., "Hyaluronan synthesis is inhibited by adenosine monophosphate-activated protein kinase through the regulation of HAS2 activity in human aortic smooth muscle cells," *The Journal of Biological Chemistry*, vol. 286, no. 10, pp. 7917–7924, 2011.
- [43] V. C. Hascall, A. Wang, M. Tammi et al., "The dynamic metabolism of hyaluronan regulates the cytosolic concentration of UDP-GlcNAc," *Matrix Biology*, vol. 35, pp. 14–17, 2014.
- [44] T. A. Jokela, K. M. Makkonen, S. Oikari et al., "Cellular content of UDP-N-acetylhexosamines controls hyaluronan synthase 2 expression and correlates with O-linked N-acetylglucosamine modification of transcription factors YY1 and SP1," *The Journal of Biological Chemistry*, vol. 286, no. 38, pp. 33632–33640, 2011.
- [45] E. Karousou, M. Kamiryo, S. S. Skandalis et al., "The activity of hyaluronan synthase 2 is regulated by dimerization and ubiquitination," *The Journal of Biological Chemistry*, vol. 285, no. 31, pp. 23647–23654, 2010.
- [46] K. Kumari and P. H. Weigel, "Identification of a membrane-localized cysteine cluster near the substrate-binding sites of the *Streptococcus equisimilis* hyaluronan synthase," *Glycobiology*, vol. 15, no. 5, pp. 529–539, 2005.
- [47] A. C. Stoolmiller and A. Dorfman, "The biosynthesis of hyaluronic acid by *Streptococcus*," *Journal of Biological Chemistry*, vol. 244, no. 2, pp. 236–246, 1969.
- [48] P. W. Robbins, D. Bray, M. Dankert, and A. Wright, "Direction of chain growth in polysaccharide synthesis," *Science*, vol. 158, no. 3808, pp. 1536–1542, 1967.
- [49] S. Takeo, M. Fujise, T. Akiyama et al., "In vivo hyaluronan synthesis upon expression of the mammalian hyaluronan synthase gene in drosophila," *Journal of Biological Chemistry*, vol. 279, no. 18, pp. 18920–18925, 2004.
- [50] P. Prehm and U. Schumacher, "Inhibition of hyaluronan export from human fibroblasts by inhibitors of multidrug resistance transporters," *Biochemical Pharmacology*, vol. 68, no. 7, pp. 1401–1410, 2004.
- [51] G. Ouskova, B. Spellerberg, and P. Prehm, "Hyaluronan release from *Streptococcus pyogenes*: export by an ABC transporter," *Glycobiology*, vol. 14, no. 10, pp. 931–938, 2004.
- [52] M. J. Fath and R. Kolter, "ABC transporters: bacterial exporters," *Microbiological Reviews*, vol. 57, no. 4, pp. 995–1017, 1993.
- [53] W. Jing and P. L. de Angelis, "Dissection of the two transferase activities of the *Pasteurella multocida* hyaluronan synthase: two active sites exist in one polypeptide," *Glycobiology*, vol. 10, no. 9, pp. 883–889, 2000.
- [54] K. Kumari, B. A. Baggenstoss, A. L. Parker, and P. H. Weigel, "Mutation of two intramembrane polar residues conserved within the hyaluronan synthase family alters hyaluronan product size," *The Journal of Biological Chemistry*, vol. 281, no. 17, pp. 11755–11760, 2006.
- [55] B. A. Baggenstoss and P. H. Weigel, "Size exclusion chromatography-multiangle laser light scattering analysis of hyaluronan size distributions made by membrane-bound hyaluronan synthase," *Analytical Biochemistry*, vol. 352, no. 2, pp. 243–251, 2006.
- [56] N. K. Thomas and T. J. Brown, "ABC transporters do not contribute to extracellular translocation of hyaluronan in human breast cancer in vitro," *Experimental Cell Research*, vol. 316, no. 7, pp. 1241–1253, 2010.
- [57] A. P. Medina, J. Lin, and P. H. Weigel, "Hyaluronan synthase mediates dye translocation across liposomal membranes," *BMC Biochemistry*, vol. 13, no. 1, article 2, 2012.
- [58] C. Hubbard, J. T. McNamara, C. Azumaya, M. S. Patel, and J. Zimmer, "The hyaluronan synthase catalyzes the synthesis and membrane translocation of hyaluronan," *Journal of Molecular Biology*, vol. 418, no. 1–2, pp. 21–31, 2012.
- [59] S. Misra, S. Ghatak, and B. P. Toole, "Regulation of MDRI expression and drug resistance by a positive feedback loop involving hyaluronan, phosphoinositide 3-kinase, and ErbB2," *The Journal of Biological Chemistry*, vol. 280, no. 21, pp. 20310–20315, 2005.
- [60] J. L. W. Morgan, J. Strumillo, and J. Zimmer, "Crystallographic snapshot of cellulose synthesis and membrane translocation," *Nature*, vol. 493, no. 7431, pp. 181–186, 2013.
- [61] P. H. Weigel, C. M. West, P. Zhao, L. Wells, B. A. Baggenstoss, and J. L. Washburn, "Hyaluronan synthase assembles chitin oligomers with -GlcNAc(α 1 \rightarrow)UDP at the reducing end," *Glycobiology*, vol. 25, no. 6, pp. 632–643, 2015.
- [62] C. E. Semino and P. W. Robbins, "Synthesis of 'Nod'-like chitin oligosaccharides by the *Xenopus* developmental protein DG42," *Proceedings of the National Academy of Sciences of the United States of America*, vol. 92, no. 8, pp. 3498–3501, 1995.
- [63] M. Yoshida, N. Itano, Y. Yamada, and K. Kimata, "In vitro synthesis of hyaluronan by a single protein derived from mouse HAS1 gene and characterization of amino acid residues essential for the activity," *The Journal of Biological Chemistry*, vol. 275, no. 1, pp. 497–506, 2000.
- [64] C. L. Feasley, B. A. Baggenstoss, and P. H. Weigel, "(GlcNAc)n-UDP oligomer synthesis by class I hyaluronan synthase and its role as a self priming initiator for hyaluronan synthesis," in *Proceedings of the 9th International Conference on Hyaluronan (Hyaluronan '13)*, p. 21, Oklahoma City, Okla, USA, June 2013, http://www.ishas.org/images/2013_Conference/ISHAS.2013_Book_of_Abstracts.pdf.
- [65] C. A. De la Motte, V. C. Hascall, J. Drazba, S. K. Bandyopadhyay, and S. A. Strong, "Mononuclear leukocytes bind to specific hyaluronan structures on colon mucosal smooth muscle cells treated with polyinosinic acid: polycytidylic acid. Inter- α -trypsin inhibitor is crucial to structure and function," *American Journal of Pathology*, vol. 163, no. 1, pp. 121–133, 2003.
- [66] P. H. Weigel and B. A. Baggenstoss, "Hyaluronan synthase polymerizing activity and control of product size are discrete enzyme functions that can be uncoupled by mutagenesis of conserved cysteines," *Glycobiology*, vol. 22, no. 10, pp. 1302–1310, 2012.
- [67] J. Abramson, I. Smirnova, V. Kasho, G. Verner, H. R. Kaback, and S. Iwata, "Structure and mechanism of the lactose permease of *Escherichia coli*," *Science*, vol. 301, no. 5633, pp. 610–615, 2003.
- [68] H. Palsdottir and C. Hunte, "Lipids in membrane protein structures," *Biochimica et Biophysica Acta—Biomembranes*, vol. 1666, no. 1–2, pp. 2–18, 2004.
- [69] J. E. Scott and F. Heatley, "Biological properties of hyaluronan in aqueous solution are controlled and sequestered by reversible tertiary structures, defined by NMR spectroscopy," *Biomacromolecules*, vol. 3, no. 3, pp. 547–553, 2002.
- [70] D. A. Gabriel and M. E. Carr Jr., "Calcium destabilizes and causes conformational changes in hyaluronic acid," *The American Journal of the Medical Sciences*, vol. 298, no. 1, pp. 8–14, 1989.
- [71] P. Dais, E. Tylianakis, J. Kanetakis, and F. R. Taravel, "¹³C nuclear magnetic relaxation study of segmental dynamics of hyaluronan in aqueous solutions," *Biomacromolecules*, vol. 6, no. 3, pp. 1397–1404, 2005.

- [72] G. Avigad, "Sucrose-uridine diphosphate glucosyltransferase from Jerusalem artichoke tubers," *The Journal of Biological Chemistry*, vol. 239, pp. 3613–3618, 1964.
- [73] D. Hagenfeld, B. Borkenhagen, T. Schulz, H. Schillers, U. Schumacher, and P. Prehm, "Hyaluronan export through plasma membranes depends on concurrent K^+ efflux by K_{ir} channels," *PLoS ONE*, vol. 7, no. 6, Article ID e39096, 2012.
- [74] J. E. Scott and F. Heatley, "Hyaluronan forms specific stable tertiary structures in aqueous solution: A ^{13}C NMR study," *Proceedings of the National Academy of Sciences of the United States of America*, vol. 96, no. 9, pp. 4850–4855, 1999.
- [75] A. Almond, J. K. Sheehan, and A. Brass, "Molecular dynamics simulations of the two disaccharides of hyaluronan in aqueous solution," *Glycobiology*, vol. 7, no. 5, pp. 597–604, 1997.
- [76] C. Breton and A. Imberty, "Structure/function studies of glycosyltransferases," *Current Opinion in Structural Biology*, vol. 9, no. 5, pp. 563–571, 1999.
- [77] S. Gulberti, S. Fournel-Gigleux, G. Mulliert et al., "The functional glycosyltransferase signature sequence of the human β 1,3-glucuronosyltransferase is a XDD motif," *Journal of Biological Chemistry*, vol. 278, no. 34, pp. 32219–32226, 2003.
- [78] I. M. Saxena, R. M. Brown Jr., M. Fevre, R. A. Geremia, and B. Henrissat, "Multidomain architecture of β -glycosyl transferases: implications for mechanism of action," *Journal of Bacteriology*, vol. 177, no. 6, pp. 1419–1424, 1995.
- [79] J. Liu and A. Mushegian, "Three monophyletic superfamilies account for the majority of the known glycosyltransferases," *Protein Science*, vol. 12, no. 7, pp. 1418–1431, 2003.
- [80] C. Breton, L. Šnajdrová, C. Jeanneau, J. Koča, and A. Imberty, "Structures and mechanisms of glycosyltransferases," *Glycobiology*, vol. 16, no. 2, pp. 29R–37R, 2006.
- [81] I. M. Saxena, R. M. Brown Jr., and T. Dandekar, "Structure—function characterization of cellulose synthase: relationship to other glycosyltransferases," *Phytochemistry*, vol. 57, no. 7, pp. 1135–1148, 2001.

Review Article

Hyperglycemia-Induced Changes in Hyaluronan Contribute to Impaired Skin Wound Healing in Diabetes: Review and Perspective

Sajina Shakya,¹ Yan Wang,¹ Judith A. Mack,^{1,2} and Edward V. Maytin^{1,2}

¹Department of Biomedical Engineering, Lerner Research Institute, Cleveland Clinic, 9500 Euclid Avenue, Cleveland, OH 44195, USA

²Department of Dermatology, Dermatology & Plastic Surgery Institute, Cleveland Clinic, 9500 Euclid Avenue, Cleveland, OH 44195, USA

Correspondence should be addressed to Edward V. Maytin; maytine@ccf.org

Received 17 December 2014; Accepted 1 July 2015

Academic Editor: Paul H. Weigel

Copyright © 2015 Sajina Shakya et al. This is an open access article distributed under the Creative Commons Attribution License, which permits unrestricted use, distribution, and reproduction in any medium, provided the original work is properly cited.

Ulcers and chronic wounds are a particularly common problem in diabetics and are associated with hyperglycemia. In this targeted review, we summarize evidence suggesting that defective wound healing in diabetics is causally linked, at least in part, to hyperglycemia-induced changes in the status of hyaluronan (HA) that resides in the pericellular coat (glycocalyx) of endothelial cells of small cutaneous blood vessels. Potential mechanisms through which exposure to high glucose levels causes a loss of the glycocalyx on the endothelium and accelerates the recruitment of leukocytes, creating a proinflammatory environment, are discussed in detail. Hyperglycemia also affects other cells in the immediate perivascular area, including pericytes and smooth muscle cells, through exposure to increased cytokine levels and through glucose elevations in the interstitial fluid. Possible roles of newly recognized, cross-linked forms of HA, and interactions of a major HA receptor (CD44) with cytokine/growth factor receptors during hyperglycemia, are also discussed.

1. Introduction

Diabetes, which affects ~24 million people or 8% of the U.S. population [1], is a disease in which abnormal glucose metabolism plays a central role. Hyperglycemia (defined as high glucose levels in the bloodstream) results from loss of pancreatic insulin-producing cells in type 1 diabetes, or loss of normal insulin-responsiveness of target cells such as muscle and fat cells in type 2 diabetes, and leads to severe clinical complications over time [2]. These complications include renal failure, retinopathy, atherosclerosis, peripheral vascular disease, loss of peripheral sensory nerve function (neuropathy), and impaired wound-healing ability. The combined effects of neuropathy and poor wound healing lead to formation of nonhealing skin ulcers of the feet and lower limbs, a particularly common problem in diabetics. Nearly 15% of diabetic individuals will develop a foot ulcer, and many eventually lose a limb to amputation, at an overall healthcare cost of at least \$10.9 billion per year in the U.S.

[3]. Recent evidence suggests that impaired wound healing in diabetic patients is directly related to poorly regulated serum glucose levels. For example, a recent clinical study in diabetics showed that high levels of hemoglobin A1c, an indicator of poor hyperglycemic control, correlate directly with delayed wound healing [4]. Unfortunately, despite improved methods for providing proper insulin delivery and glucose control, nonhealing wounds and chronic ulcers remain a persistent problem.

Hyaluronan (HA) is a glycosaminoglycan, present in all mammalian tissues, that is composed entirely of two sugar subunits, glucuronic acid and N-acetylglucosamine [5]. Very abundant in skin and many other tissues, HA is structurally simple yet functionally complex [6]. Here, we review evidence that impairments in wound healing in diabetics are mechanistically linked to hyperglycemia through altered synthesis and degradation of hyaluronan (HA). After providing a short wound healing-orientation, we will summarize evidence from the literature showing that hyperglycemia leads to

degradation of HA in the glycocalyx (pericellular coat) of endothelial cells, thereby increasing leukocyte recruitment and creating a proinflammatory microenvironment that adversely affects not only blood vessel function, but also adjacent pericytes, smooth muscle cells, and fibroblasts.

In the skin, inflammation and fibrosis (scar formation) are prominent features during normal wound healing, as reviewed in more detail in this HA special issue [7]. Wound healing is a very complex process involving three overlapping phases that comprise the *inflammatory phase*, ~days 1–3; *tissue regenerative (proliferative) phase*, ~days 3–10; and *remodeling phase*, ~2 weeks to 3 months [8, 9]. On days 1–3, a wave of neutrophils is recruited from the bloodstream. Responding to local cytokine gradients, the neutrophils adhere to the luminal wall of small postcapillary venules, traverse the endothelium, and migrate into the dermal tissue. On day 3, a second wave of leukocytes (monocyte/macrophages) arrive to engulf and remove the dead neutrophils that have released their granules and undergone apoptosis. Both neutrophils and macrophages secrete large amounts of cytokines including transforming growth factor beta (TGF- β), the major cytokine that stimulates fibroblasts to differentiate into activated, contractile myofibroblasts. Myofibroblasts are the cells that produce most of the collagen and other matrix molecules that comprise the new extracellular matrix (ECM), or scar. Scar tissue is gradually remodeled over many months, approaching but never quite reproducing the original architecture; thus, healed adult wounds typically attain only ~70% of the tensile breaking strength of unwounded skin. The overall sequence of events during wound healing implies that inflammation and fibrosis are closely linked. Excessive or prolonged presence of inflammatory cells in a wound will drive myofibroblast conversion, increase fibrosis (with imperfect macromolecular assembly of collagen and GAG elements), and result in functionally impaired scar tissue.

In diabetes, wound healing is delayed [10]. A major reason for this appears to be chronic, enhanced inflammation, which disrupts the timing of ECM synthesis and ultimately reduces the quality of the restored collagen architecture. Diabetic patients with poor hyperglycemic control appear to be in a heightened inflammatory state, even in the absence of wounding or infection. This important concept was convincingly demonstrated by a clinical study in which 108 diabetic patients and 36 healthy controls were followed prospectively for ~2 years [11]. At study initiation, patients were ulcer-free, but foot ulceration developed in nearly one-third (29%) of the diabetic patients over time. At the first study visit, all patients underwent blood sampling and forearm skin biopsy for measurements of serum protein markers and skin histopathology. Remarkably, the levels of many cytokines and proteins associated with inflammation (interleukins IL-6 and IL-8; tumor necrosis factor alpha, TNF- α ; C-reactive protein; fibrinogen) were significantly elevated in the diabetic patients at baseline. In biopsies from forearm (unwounded) skin, diabetics had a higher number of cells overall, and the number of inflammatory cells around blood vessels (a strong indicator of inflammation) was higher. The diabetic subjects also had higher expression of CD31 (in proliferating vessels) and MMP-9 (in leukocytes and vessels) in the skin. These

findings suggest a preexisting, hyperinflammatory state. Experimental studies in diabetic animal models, including mice [12] and rabbits [13], have also clearly demonstrated baseline increases in inflammatory cytokines (IL-6, IL-8, and TNF- α) in diabetic skin in the absence of wounding.

We propose that this chronic, proinflammatory state in diabetic skin may be caused by underlying abnormalities in HA and other GAGs that form the pericellular matrix on the apical surfaces of the endothelial cells (EC). The pericellular matrix (glycocalyx) is a structure, comprising HA and various GAG-containing proteoglycans, that is present to varying degrees on most cell types [14]. In Sections 2 and 3 below, we describe data showing that the glycocalyx on the luminal surface of EC in blood vessels is altered (reduced) as a result of hyperglycemia and discuss mechanisms for how this might lead to proinflammatory consequences. In Section 4, we speculate on how hyperglycemia and proinflammatory cytokine signaling may affect perivascular cells, changing the balance between cell proliferation and cell death and altering the production of ECM.

2. Hyperglycemia Leads to Loss of the Endothelial Cell Glycocalyx in Small Vessels of the Skin

The structure and importance of the endothelial glycocalyx have been described in several reviews [14–16]. Located on the luminal side of blood vessel walls, this glycocalyx is an important structure with several critical functions, including the following: (1) serving as a reservoir for antithrombotic factors such as antithrombin III that prevent clotting and as a shield to prevent direct contact between circulating platelets and the EC which would trigger further clot formation; (2) regulating the production of nitric oxide (NO) and NO-mediated signaling in response to flow-induced shear stress; (3) modulating the permeability of macromolecules at tight junctions between endothelial cells; (4) modulating leukocyte adhesion.

A recent critical discovery is that *in response to hyperglycemia, the thickness of the glycocalyx on blood vessel endothelia is significantly reduced*, leading to loss of protective functions and other deleterious changes. In studies in humans, the thickness of the endothelial glycocalyx can be measured indirectly by comparing intravascular distribution volume of a glycocalyx permeable tracer (e.g., dextran 40) with that of an impermeable tracer (e.g., labeled erythrocytes). Nieuwdorp et al. showed that acute hyperglycemia in healthy subjects was associated with a ~50% reduction in glycocalyx volume [17]. Reduction of the glycocalyx was likely due to damage by reactive oxygen species (ROS) generated under hyperglycemic conditions, because infusion of the antioxidant N-acetylcysteine (NAC) could prevent the reduction [17]. To test this hypothesis further, glycocalyx measurements were performed in type 1 diabetic patients and in age-matched controls [18]. In addition to the indirect tracer method used above, orthogonal polarization spectral (OPS) imaging was also employed to visualize the sublingual microcirculation (blood vessels beneath the tongue). Both

the systemic glycocalyx volume and the directly measured glycocalyx thickness were reduced by 50–86% in type 1 diabetic patients relative to normal controls [18]. The same research group showed that HA is an important component of the glycocalyx and is affected in diabetes [19]. They did this by measuring the activity of hyaluronidases, HA-degrading enzymes that comprise five members in mammals (HYAL1, HYAL2, HYAL3, HYAL4, and PH20; HYAL1 and HYAL2 are the major hyaluronidases in somatic tissues) [20]. Hyaluronidase activity and circulating levels of HA were both elevated in the serum of diabetic patients [19], suggesting that hyaluronidase activity may contribute to the degradation of the endothelial glycocalyx in diabetes.

2.1. Studies on Atherosclerosis Provide Evidence That the EC Glycocalyx Is Important for Understanding Diabetic Vascular Abnormalities. Nieuwdorp et al. showed that perturbation of HA metabolism predisposes patients with type 1 diabetes mellitus to atherosclerosis [19]. These investigators performed a study to evaluate the relationship between HA and hyaluronidase with carotid intima-media thickness (cIMT), an established surrogate marker for cardiovascular disease. In type 1 diabetic patients and control subjects, the cIMT of patients' carotid arteries was measured, and multivariate regression analyses were performed to determine relationships between HA, hyaluronidase, and cIMT. Type 1 diabetics showed structural changes of the arterial wall associated with increased HA catabolism, thereby supporting altered glycosaminoglycan metabolism in type 1 diabetes as a potential mechanism involved in accelerated atherogenesis.

Hyaluronidase was also the subject of a study by Kucur et al. [21], in which 162 nondiabetic patients undergoing coronary angiography, with or without stable coronary artery disease (CAD), were examined. Hyaluronidase assays in these patients showed significantly increased serum hyaluronidase activity in patients with CAD, suggesting a role of HA degradation in the pathophysiology of atherosclerosis.

Another study examined the potential role of HA in the development of atherosclerosis by using an inhibitor of HA synthesis (4-methylumbelliferone) in atherosclerosis-prone mice [22]. That study, discussed more fully in Section 3.4, concluded that inhibition of HA synthesis interferes with the protective function of the glycocalyx and accelerates atherosclerotic progression.

In addition to HA, the glycocalyx of ECs also contains proteoglycans, comprising heparan sulfate (HS) and chondroitin sulfate (CS) chains linked to core proteins such as syndecan and versican, and all interact with HA either directly or indirectly; see the review by Reitsma et al. for a concise summary of these GAG components [14]. The importance of HS in the endothelial glycocalyx was suggested by a study in which heparanase (an enzyme that degrades HS) was microinfused into capillaries of the hamster cremaster muscle, leading to an increase in the concentration of red blood cells flowing within those capillaries [23]. If the heparanase was heat-inactivated prior to infusion, then the effect was abolished. These data suggested that HS in the endothelial glycocalyx is important for physiological responsiveness of the capillary. A study by Han et al. extended

this to diabetes, by showing that decreased amounts of HS-containing proteoglycans (HSPGs) can contribute to diabetic endothelial injury [24]. Porcine aortic ECs were cultured in normal glucose (5.5 mM), or in high glucose (30 mM), in the presence or absence of insulin. The concentrations of GAGs associated with cells or free in the culture media were determined. High glucose decreased the amount of GAGs associated with cells and increased GAGs in the medium; the addition of insulin to high glucose cultures restored the levels of GAGs toward normal. Thus, hyperglycemia induces HSPG degradation or inhibits its synthesis (likely due to EC injury), and insulin may have a direct protective effect on the endothelium, independent of its blood glucose-lowering effect.

2.2. Hyperglycemia Decreases Normal Endothelial Cell (EC) Functioning and May Lead to Lethal EC Damage. Risso et al. examined human umbilical vein endothelial cells (HUVECs) in culture and showed that intermittent high glucose enhances apoptotic cell death [25]. HUVECs cultured for 14 days in media containing glucose at 5 mM, 20 mM, or a daily alternating regimen of 5 or 20 mM showed more apoptosis in the cells exposed to intermittent high glucose. In the study, levels of Bcl-2 (apoptosis-protective) and Bax (apoptosis-promoting) proteins were examined. Continuous hyperglycemia led to a relative decrease in Bcl-2 and an increase in Bax levels; these changes were larger in magnitude during intermittent high glucose exposure. Thus, in diabetics, variability in glycemic control could be more deleterious to the endothelium than constant high glucose concentrations.

Another study, by Zuurbier et al, reinforces the idea that intermittent hyperglycemia is just as bad, if not worse, than continuous glucose elevation. Mice that were normoglycemic, transiently hyperglycemic (25 mM) for 60 min due to glucose infusion, or hyperglycemic (25 mM) for 2–4 weeks (db/db mice) were studied [26]. The glycocalyx was probed using a 40 kDa Texas Red dextran (control) known to permeate the glycocalyx under all conditions, along with 70 kDa FITC dextran which is excluded from the glycocalyx in healthy animals. Clearance of these dyes from the blood was measured. Short-term hyperglycemia caused a rapid decrease in the ability of the glycocalyx to exclude 70 kDa dextran, interpreted as a loss of barrier function of the glycocalyx; the barrier loss was just as severe as that observed with continuous hyperglycemia.

3. Potential Molecular Mechanisms for How HA May Regulate Vascular Inflammation in Diabetes

We will now discuss, in more detail, proposed molecular mechanisms that may link altered HA in the endothelial glycocalyx to inflammation and vascular complications of diabetes.

3.1. Inflammation and Thrombosis in Vessels Are Exacerbated by Platelet-Derived Hyaluronidase. The EC glycocalyx is a reservoir for various antithrombotic factors, such

as antithrombin III, and a reduction in this storage pool due to thinning of the glycocalyx in diabetes could alter the balance between pro- and anticoagulatory factors [14]. Furthermore, a reduced glycocalyx volume could encourage interactions between platelets and endothelial cell-surface receptors and promote platelet adhesion and aggregation. Also, platelets are known to promote leukocyte recruitment and adhesion, further enhancing the inflammatory milieu [27]. Platelets were recently discovered to mediate another proinflammatory mechanism, one involving HA cleavage. In 2009, de la Motte et al. demonstrated that human platelets contain exclusively HYAL2, but no HYAL1 (whereas most human cells contain both). HYAL2 is a hyaluronidase that is GPI-anchored on the cell membrane and cleaves extracellular HA into intermediate-sized fragments, whereas lysosomal HYAL1 degrades HA into very small fragments [28]. Platelet HYAL2 is stored in α -granules and upon platelet activation becomes expressed on the cell surface, where it functions to degrade extracellular HA matrix [29]. The HA fragments generated by platelet-derived HYAL2 initiate inflammatory and angiogenic signaling by stimulating mononuclear leukocytes in the immediate microenvironment to produce proinflammatory cytokines, such as IL-6 and IL-8 [28]. The critical take-home message here is that when intact HA is degraded, smaller fragments are formed that are highly angiogenic, inflammatory, and immunogenic in a size-dependent manner [30, 31] and can trigger cellular stress responses (by serving as endogenous danger signals) [32, 33].

3.2. Loss of the EC Glycocalyx in Diabetes Leads to Reduced Nitric Oxide (NO) Production. Nitric oxide (NO) is a non-polar gaseous molecule that is synthesized and released by endothelial cells and subsequently acts upon vascular smooth muscle cells to reduce vascular tone [34]. NO is synthesized by NO synthases (NOS). ECs express the endothelial form of NOS (eNOS), which can be activated by several factors including flow-related shear stress activation of stretch-operated nonselective cation channels (SOCC) in the cell membrane, leading to elevation of intracellular calcium levels, activation of eNOS, and the production of NO from L-arginine and molecular oxygen [35]. Other mechanisms by which shear stress may activate eNOS have been proposed, including phosphorylation by protein kinases associated with the intracellular cytoskeleton or through interaction with membrane receptors such as CD44 that are colocalized within lipid rafts along with other signaling molecules including eNOS [36–38].

As described in Section 2, the EC glycocalyx is reduced by hyperglycemia. Thus, one might expect that a loss of glycocalyx could affect shear-induced activation of eNOS, NO synthesis, and vasodilation, and indeed this seems to be the case. When canine femoral arteries were treated with hyaluronidase to degrade the HA glycocalyx, shear-induced NO production was impaired [39]. Heparitinase treatment also impaired NO production in bovine EC, showing that disruption of heparan sulfate in the glycocalyx could also affect NO production [40]. In fact, removal of each of the three different specific components of the glycocalyx (HA, heparan sulfate, and sialic acid, but *not* chondroitin

sulfate) was shown to significantly reduce shear-induced NO production in bovine ECs [38].

Other studies have shown that the impairment of shear-induced NO responses observed during hyperglycemia involves the cytoskeleton. Studying porcine aortic EC in a parallel flow chamber, Kemeny et al. showed that hyperglycemia impairs intracellular actin alignment and NOS activation in response to shear stress [41]. Under normal glucose conditions, the alignment of EC cytoskeletal actin fibers increased by 10% in response to shear, but in high glucose, actin fiber rearrangement increased by less than 3%. eNOS phosphorylation increased with shear stress for ECs in normal glucose but did not significantly change for cells in high glucose [41]. Chen et al. used atomic force microscopy (AFM) and laser scanning confocal microscopy (LSCM) to study the role of cytoskeletal rearrangement and NO synthesis in HUVECs [42]. Under constant high glucose (25 mM) or fluctuating high glucose (25 mM/5 mM), HUVECs released significantly less NO into the culture supernatants; the cells also exhibited decreased eNOS expression and showed mechanical stiffening of the cell membrane. A NOS enzyme inhibitor (L-NAME) elicited similar effects. Overall, the conclusion from these two studies is that hyperglycemia is associated with stiffening of endothelial cell membranes, altered cytoskeletal alignment, and decreased NO synthesis in response to flow shear stress, all of which could result in stiffer blood vessels and a reduction in vasodilatory capacity, thereby predisposing vessels to increased risk of occlusion and thrombosis.

Hypothetically, loss of HA in the EC glycocalyx during hyperglycemia could reduce shear stress-induced NO production via at least two mechanisms. HA normally binds to CD44, a receptor that resides in membrane lipid rafts that also contain eNOS, and perhaps other signaling molecules that may be necessary for eNOS activation [37]. A loss of HA:CD44 interaction might therefore reduce local eNOS activity. Alternatively, CD44 is known to interact with the cytoskeleton (via the cytoplasmic tail of CD44, described more in Section 3.3), so that theoretically a reduction in HA:CD44 signaling could affect cytoskeleton-associated protein kinases that phosphorylate eNOS and thus reduce NO production.

3.3. Hyperglycemia Impairs the Ability of the EC Glycocalyx to Regulate the Permeability of Macromolecules. The EC glycocalyx influences blood flow and presents a selective barrier to movement of macromolecules from plasma to the endothelial surface. Work by Henry and Duling advanced the notion that permeability of the endothelial glycocalyx is determined by HA [43]. Video microscopy was used to visualize microvessels in the hamster cremaster muscle, to investigate whether HA was involved in permeation properties of the glycocalyx (i.e., the ability of tracer molecules to penetrate into the apical glycocalyx). The glycocalyx thickness was visualized as a clear space between the anatomic diameter of a small blood vessel and the diameter of red blood cells within that vessel. The investigators asked whether several fluorescently tagged dextran tracers (70, 145, 580, and 2000 kDa), all normally too large to enter the glycocalyx, might do so after experimental

degradation of HA. After a 1 h treatment with hyaluronidase, increased access of the 70 and 145 kDa dextran tracers into the glycocalyx was observed (i.e., hyaluronidase appeared to create a more open matrix, enabling the smaller dextran molecules to penetrate deeper into the glycocalyx). Following hyaluronidase treatment, an infusion of a mixture of high molecular weight (MW) HA and chondroitin sulfate was able to reconstitute the glycocalyx. Thus, HA appears to be an essential component for glycocalyx barrier function.

In inflamed blood vessels, leakage of fluid and protein occurs through gaps between the ECs. Singleton et al. noted that this leakage is increased in diabetes, and they proposed a mechanism in which interactions between glycocalyx HA and CD44, a major cell-surface receptor for hyaluronan, may be involved [44, 45]. CD44, "floating" in the cell membrane, is localized in cholesterol-rich microdomains called lipid rafts, which are important regulators of vascular integrity [46]. Normally, full-length HA is bound to the extracellular portion of CD44; this ligand-receptor attachment promotes interactions between the internal (cytoplasmic) residues of CD44 and signaling molecules such as Akt/Tiam1/Rac1 and Annexin A2/protein S100, which then enhance the formation of cortical actin filaments that strengthen intercellular contacts between neighboring ECs [44, 45]. Hyperglycemia reduces the amount of HA in the glycocalyx (e.g., through degradation by hyaluronidase), leaving less HA available to bind to CD44. Loss of HA:CD44 binding reduces downstream CD44 signaling. This leads to loss of cortical actin filaments (through conversion to actin stress fibers) and permits EC to pull apart, now allowing leakage of fluid and protein to occur at intercellular junctions and thus contributing to the inflammatory microenvironment.

3.4. Changes in the EC Glycocalyx during Hyperglycemia Promote Leukocyte Adhesion. First, we will review evidence that hyperglycemic injury can lead to increased recruitment of leukocytes at sites of activated (inflamed) blood vessels in the skin. We will then discuss some current ideas about how HA may be involved in this process.

Since the reference point for studies on diabetes should always be the patient, we mention again the clinical report by Dinh et al. (discussed in the Introduction) that reported higher numbers of perivascular leukocytes associated with small cutaneous blood vessels in diabetic patients, relative to normoglycemic controls [11]. However, without experimental data, it is not possible to predict how HA specifically may affect leukocyte adhesion. For example, work by the Siegelman group in the late 1990s established that the expression of HA on cultured ECs is increased by exposure to proinflammatory cytokines (TNF α and IL-1 β) and that this HA induction is selective to ECs derived from microvasculature and not from large vessels [47]. Furthermore, lymphocytes were shown to tether and adhere to this HA glycocalyx via their CD44 receptors [48]. From these observations, one might predict that a reduced HA glycocalyx during hyperglycemia should lead to less rather than more leukocyte adhesion, whereas in most wound-healing studies the opposite is observed. Since the majority of leukocytes found in early wounds are neutrophils and macrophages,

not lymphocytes, different recruitment mechanisms amongst different leukocyte subtypes remain a distinct possibility.

To begin to investigate mechanisms for the role of the EC glycocalyx in leukocyte recruitment in an animal model *in vivo*, Constantinescu et al. employed venules of the mouse cremaster muscle to test the hypothesis that glycocalyx degradation stimulates leukocyte-endothelial cell adhesion [49]. When heparitinase was administered locally to degrade the endothelial glycocalyx, an increase in adherent leukocytes was observed. Another agent that degrades the endothelial glycocalyx is oxidized low density lipoprotein (Ox-LDL); when Ox-LDL was administered systemically into the mouse, leukocyte adhesion increased dose-dependently. Perfusion of the venules with heparan sulfate or heparin reconstituted the endothelial glycocalyx and attenuated the Ox-LDL-induced leukocyte-endothelial cell adhesion. The authors concluded that circulating heparan sulfate and heparin attach to the venule wall and attenuate Ox-LDL-induced leukocyte immobilization.

Nagy et al. examined the potential role of HA synthesis in the development of atherosclerosis in a mouse model [22]. This study in Apo E deficient mice addressed the effects of long-term pharmacological inhibition of HA synthesis on vascular function and atherosclerosis. Administration of 4-methylumbelliferone (4-MU), an inhibitor of HA synthesis, led to a marked increase of aortic plaque burden at 25 weeks. An increase in recruitment of macrophages to vascular lesions was detected after 2 and 21 weeks of 4-MU treatment. Also, severe damage of the endothelial glycocalyx after 2 and 21 weeks of 4-MU was detected by electron microscopy of the innominate artery and myocardial capillaries. The authors concluded that systemic inhibition of hyaluronan synthesis by 4-MU interferes with the protective function of the endothelial glycocalyx, thereby facilitating leukocyte adhesion, subsequent inflammation, and progression of atherosclerosis.

In our lab, we have utilized HAS1/HAS3 double-knockout (HAS1/3 null) mice as another model in which to study effects of altered HA upon leukocyte recruitment from the vasculature. In mammals, three HA synthase enzymes (HAS1, HAS2, and HAS3) are normally expressed. Deletion of the *Has2* gene is embryonic lethal in mice, due to defects in cardiac development; however, mice lacking *Has1* and/or *Has3* genes are normal and viable [50]. Interestingly, cutaneous wound healing is abnormal in the HAS1/3 null mice and is associated with increased wound inflammation due to enhanced recruitment of neutrophils at day 1 and macrophages at day 3, emanating from the cutaneous microvasculature at the wound site [50]. Compared to the normal amounts of HA in the blood vessels and surrounding dermis in wild type mouse skin (Figure 1(a)), reduced amounts of HA in the dermis and blood vessel walls (including HA associated with the EC) are observed in HAS1/3 null mice in the same vessels at which large numbers of neutrophils appear to be recruited (Figure 1(b)). Further experiments are ongoing in our laboratory to test the hypothesis that reduced HA in the endothelial glycocalyx allows leukocytes greater access to adhesion molecules such as V-CAM and I-CAM on the endothelial surface.

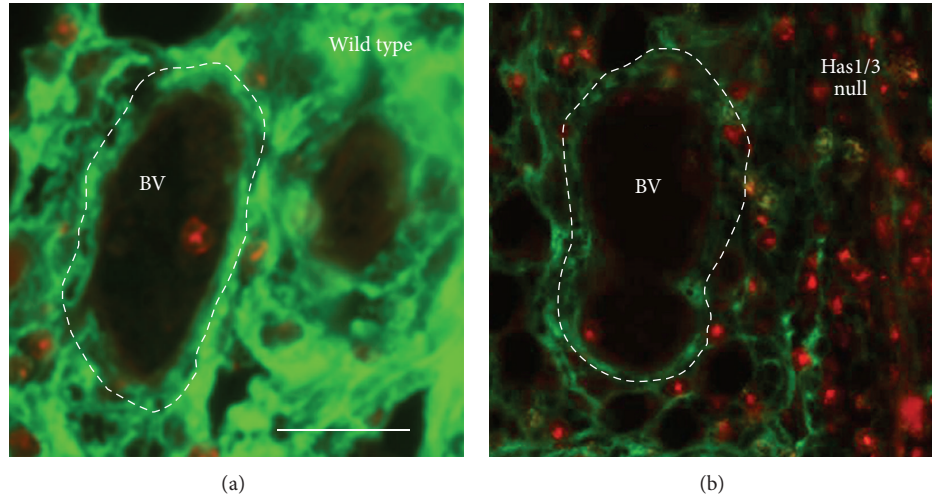


FIGURE 1: Skin biopsies from a wound edge at 24 h after wounding. Specimens from (a) normal mice (*wild type*) or (b) knockout mice lacking the genes for HAS1 and HAS3 (*Has1/3 null*) were stained with an HA binding probe to visualize HA (green) and an anti-myeloperoxidase antibody to visualize neutrophils (red). Note the marked loss of HA and increase in neutrophils extravasating from the blood vessel (BV) in the HAS1/3 deficient skin. Bar, 50 μm . From [50], used with permission.

3.5. Changes in HA Structure Play a Role in Promoting Leukocyte Adhesion. Up to now, we have discussed how HA is *quantitatively* altered during hyperglycemia; that is, its amount is reduced in the glycocalyx. However, HA can also undergo *qualitative* changes, in terms of altered structural properties, when it is synthesized by cells undergoing a stress response such as exposure to high glucose. As summarized in a recent mini review [52], cells exposed to a variety of stressful conditions produce a form of HA that is leukocyte-adhesive. This HA is “sticky,” forming aggregates in cell culture that resemble thick HA “cables” [53, 54]. Aggregation is due, at least in part, to cross-linking of HA strands via protein subunits (the heavy chains of inter-alpha-trypsin inhibitor) that are added covalently through the enzymatic action of tumor necrosis factor-stimulated gene 6 protein, TSG-6 [55–58].

Because HA is produced from intracellular glucose-derived precursors (glucuronic acid and N-acetylglucosamine), HA synthesis appears to be particularly sensitive to local concentrations of glucose in the tissue. Recent work by Wang and Hascall in renal mesangial cells showed that an important cellular mechanism for dealing with high glucose (e.g., 25 mM; normal is ~ 5 mM) is to make an aggregated form of HA (“HA cable” structure) that reflects abnormal production of HA inside the cells [52]. HA is normally made by HAS enzymes at the plasma membrane and extruded directly into the extracellular space, whereas HA produced during hyperglycemia is synthesized within intracellular compartments by HAS enzymes residing in the ER, Golgi apparatus, and transport vesicles. This internal HA is then eliminated from the cell through an autophagy mechanism in which HA-containing autophagosomes fuse with the plasma membrane and then release the aggregated form of HA into the extracellular environment. The aggregated HA cables are then removed by macrophages.

The teleological concept here is that HA serves as a kind of “glucose trap” during times of excessive cytosolic glucose influx, helping cells to eliminate glucose by incorporating it into a stable polymer via internal synthesis of HA within endoplasmic reticulum (ER) and Golgi membranes, which is then released into the extracellular space as HA cables [52]. However, elimination of internal HA comes at a price, because the HA cables are highly adhesive for leukocytes that can trigger inflammation and cause tissue destruction. This hyperglycemia-induced mechanism for producing proinflammatory HA matrices is now well established for mesangial cells of the diabetic kidney [59, 60] and more recently for adipose cells exposed to high glucose [61]. An interesting question that we plan to investigate is whether a similar autophagic HA mechanism might be operative in the EC glycocalyx of small blood vessels in diabetic skin.

4. Potential Molecular Mechanisms by Which HA, Altered in Diabetes, May Regulate Fibrosis

4.1. Diabetes and the Abnormal Production of ECM by Cells Surrounding the Blood Vessels. Glucose exchange across capillary walls is known to occur by diffusion through pores between the endothelial cells (reviewed in [62]). This free exchange is the basis for the development of new devices for continuous glucose monitoring which allow one to estimate plasma glucose concentrations from measurements of glucose concentration in the interstitial fluid of skin [63–66]. In diabetics [62, 64] and in healthy volunteers [67], interstitial glucose concentrations in the dermis reach nearly the same levels as glucose in the plasma, although with a well-described time lag in uptake kinetics. This time lag, while important for clinical glucose monitoring, is not important for the biology under consideration here, where it is sufficient

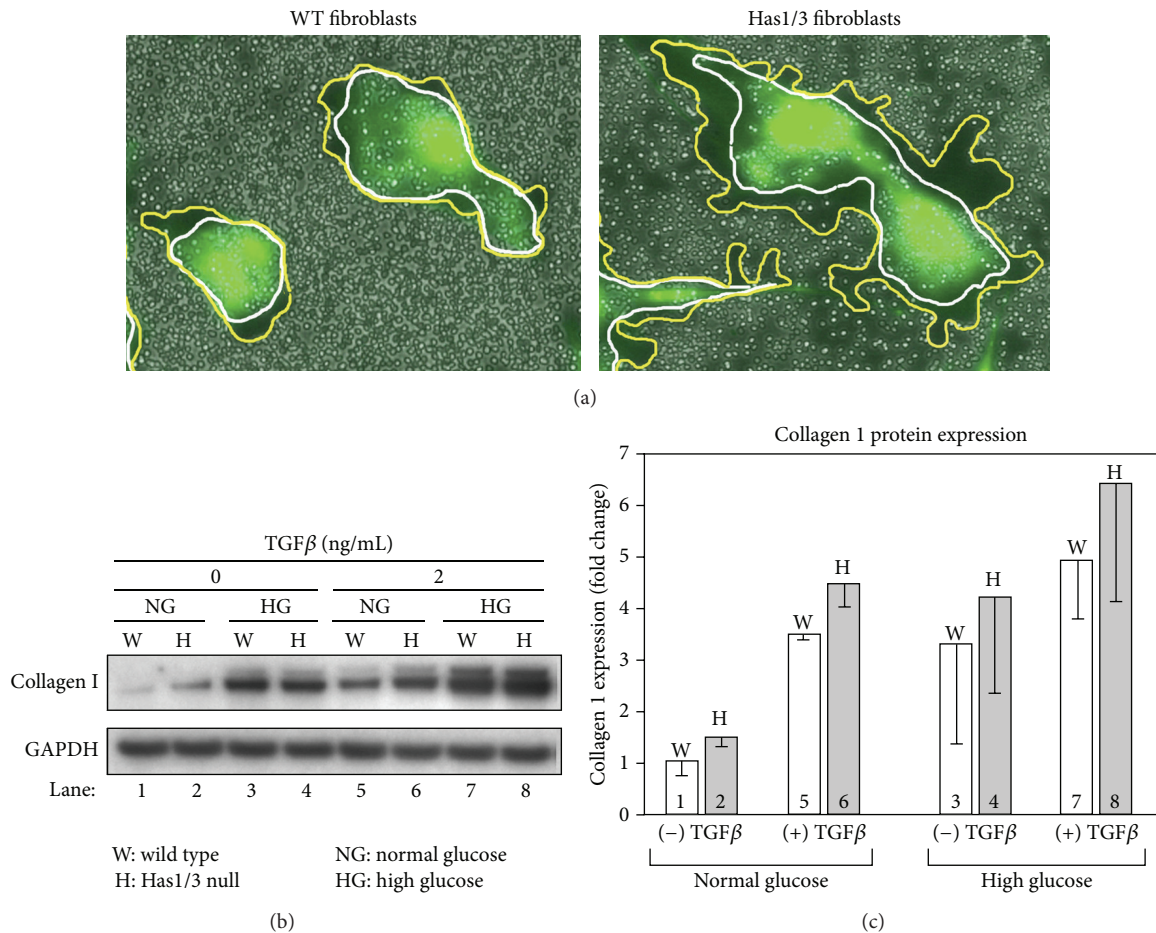


FIGURE 2: Skin fibroblasts with a larger HA glycoalyx are more responsive to TGF-β and produce more collagen when cultured in a high glucose medium. Skin fibroblasts from either wild type (WT) or Has1/3 null mice were cultured in normal glucose (1 g/L) or in high glucose (4.5 g/L) in the absence or presence of TGF-β1 (2 ng/mL) in DMEM media with 1% FBS for 48 hours. (a) Erythrocyte exclusion assay to visualize the pericellular coat on WT and Has1/3 null fibroblasts [51]. Cells were labeled with calcein to delineate the cell bodies. The HA glycoalyx is indicated between the white and yellow lines. (b) Western blot of protein from WT or Has1/3 null fibroblasts, probed with an antibody to type 1 collagen. GAPDH, loading control. (c) Quantification of protein band intensities from two independent western analysis experiments, performed under the conditions shown in panel (b) and normalized to GAPDH. *White bars*, WT fibroblasts. *Gray bars*, Has1/3 null fibroblasts. *Error bars*, mean ± half-range.

to know that cells in extravascular locations (in the dermis adjacent to the blood vessels) are intermittently exposed to high glucose concentrations and undergo hyperglycemic stress. These extravascular cells include fibroblasts, smooth muscle cells, and pericytes.

Pericytes are a particularly interesting type of cell, being very closely associated with small cutaneous blood vessels and having cytoplasmic processes that wrap around the circumference of capillaries and postcapillary venules, making contact with the ECs [68]. While relatively little is known about them, pericytes appear to play an important supportive role for EC proliferation and survival. Indeed, the loss of pericytes by apoptosis in the eye correlates with loss of retinal ECs in diabetic individuals and is a major mechanism leading to retinopathy and blindness [69]. In the skin, 3D reconstructions of electron microscopic images of capillaries showed that pericytes in diabetic skin are still

present but exhibit an abnormal morphology that consists of hypertrophy, abnormal cytoplasmic branching, and gaps in basement membranes that probably account for the known increase in vascular permeability [68]. Interestingly, the walls of these vessels are thickened by deposition of a belt of basement membrane-like material admixed with variable amounts of collagen fibrils, along with another unidentified material deposited within the vascular wall itself [68, 70]. These classical studies, while limited to morphological observation, strongly suggest that the pericyte (a mesenchymal cell type) produces increased amounts of abnormal ECM that contributes to a sclerotic or fibrotic vascular phenotype in diabetics and impairs the proper functioning of the vessel. From our earlier considerations, we postulate that increased levels of proinflammatory cytokines, exposure to high glucose levels, or both are contributing to abnormal pericyte morphology and excessive production of ECM.

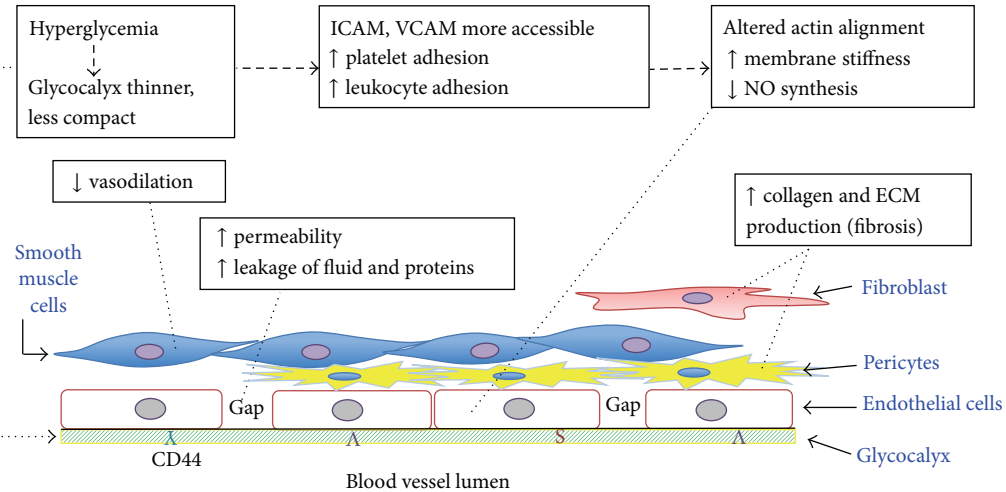


FIGURE 3: Summary of hyperglycemia-induced changes, within blood vessels and in their immediate surroundings, that involve alterations in HA.

4.2. Hyperglycemia Promotes Fibrosis by Increasing HA Synthesis and Decreasing Apoptosis in Smooth Muscle Cells and Fibroblasts. HA biology can be surprisingly cell-specific. Thus, while hyperglycemia causes problems in dermal microvessels by reducing HA in the EC glycocalyx, hyperglycemia affects dermal mesenchymal cells by increasing their HA glycocalyxes. Work from the Tammi group showed that, in vascular smooth muscle cells (SMCs), high glucose promotes HA synthesis and HAS gene expression but impairs vascular SMC function as reflected by a reduced ability to contract collagen gels; this offers a potential mechanism whereby hyperglycemia could disturb vascular remodeling and contribute to arteriosclerosis [71]. Vigezzi et al. showed that HMW-HA can protect human aortic SMCs against apoptosis induced by 4-methylumbelliferone (an HA synthesis inhibitor), suggesting that higher amounts of HA associated with SMCs increase their survival and might favor accumulation of SMCs in the vessel wall [72]. A similar relationship in which higher HA production appears to be protective against apoptosis was demonstrated in our studies of dermal fibroblasts [51]. Using HAS1/HAS3 double-knockout mice [51], we showed that fibroblasts compensate for the loss of HAS1 and HAS3 by overexpressing HAS2, resulting in an increase in HAS2 activity and synthesis of an enlarged HA glycocalyx relative to normal fibroblasts (Figure 2(a)). When exposed to apoptosis-inducing stress such as serum starvation, the HAS1/3 null cells were less likely to die [51].

We recently began to investigate how these murine fibroblasts respond to hyperglycemia. Elegant studies by the Steadman group in human lung fibroblasts have shown that CD44 (a major HA receptor) interacts with the TGF- β receptor (TGF β R) and that this interaction is obligatory for full activity of downstream TGF- β signaling, including the conversion to myofibroblasts [73, 74]. Inhibition of HA abrogates TGF- β pathway activity in their system [73, 74]. We hypothesize that a similar mechanism may apply to murine skin fibroblasts. Figures 2(b) and 2(c) provide preliminary

evidence to support this idea. In fibroblasts from HAS1/3 null mice (i.e., cells with large HA coats), collagen-synthetic responses are elevated relative to wild type fibroblasts under the following conditions: at baseline in normal glucose (lane 2); in response to 2 ng/mL of TGF- β 1 in normal glucose (lane 6); and in response to the combination of high glucose and TGF- β 1 (lane 8). These observations are consistent with the notion that the HA glycocalyx supports TGF β R-driven profibrotic processes. Work in our laboratory is ongoing to test this hypothesis further.

5. Conclusion

In this review, we have discussed current evidence regarding mechanisms by which altered hyaluronan (HA) in microvessels of the skin may lead to poor wound healing in diabetic patients. These ideas are summarized in Figure 3. The major premise is that hyperglycemia causes loss of the HA-containing glycocalyx on endothelial surfaces of cutaneous microvessels, leading to increased leukocyte adhesiveness and triggering the release of cytokines that contribute to a proinflammatory environment. Such changes are likely to increase oxidative damage, decrease proper responsiveness of vascular ECs, and impede neoangiogenesis and other repair responses during the tissue regenerative phase of wound healing. Other cell types at or near the blood vessel wall, including pericytes, smooth muscle cells, and fibroblasts, are also adversely affected by hyperglycemia and the cytokine-rich environment but through different mechanisms. One mechanism may be an enhanced sensitivity to profibrotic cytokines such as TGF- β , whose receptors interact with CD44 and with HA in the glycocalyx of the mesenchymal cells. A better understanding of hyperglycemia-related mechanisms in the skin is a worthy goal, as it may suggest new approaches to heal or prevent skin ulcers in patients with diabetes.

Conflict of Interests

The authors declare that there is no conflict of interests regarding the publication of this paper.

Acknowledgment

All authors received support from the following grant from the U.S. National Institutes of Health: P01 HL107147.

References

- [1] C. C. Cowie, K. F. Rust, E. S. Ford et al., "Full accounting of diabetes and pre-diabetes in the U.S. population in 1988–1994 and 2005–2006," *Diabetes Care*, vol. 32, no. 2, pp. 287–294, 2009.
- [2] D. M. Nathan, B. Zinman, P. A. Cleary et al., "Modern-day clinical course of type 1 diabetes mellitus after 30 years' duration: the diabetes control and complications trial/epidemiology of diabetes interventions and complications and Pittsburgh epidemiology of diabetes complications experience (1983–2005)," *Archives of Internal Medicine*, vol. 169, no. 14, pp. 1307–1316, 2009.
- [3] A. Gordoio, P. Scuffham, A. Shearer, A. Oglesby, and J. A. Tobian, "The health care costs of diabetic peripheral neuropathy in the U.S.," *Diabetes Care*, vol. 26, no. 6, pp. 1790–1795, 2003.
- [4] A. L. Christman, E. Selvin, D. J. Margolis, G. S. Lazarus, and L. A. Garza, "Hemoglobin A1C predicts healing rate in diabetic wounds," *Journal of Investigative Dermatology*, vol. 131, no. 10, pp. 2121–2127, 2011.
- [5] P. H. Weigel, V. C. Hascall, and M. Tammi, "Hyaluronan synthases," *The Journal of Biological Chemistry*, vol. 272, no. 22, pp. 13997–14000, 1997.
- [6] M. I. Tammi, A. J. Day, and E. A. Turley, "Hyaluronan and homeostasis: a balancing act," *The Journal of Biological Chemistry*, vol. 277, no. 7, pp. 4581–4584, 2002.
- [7] S. Ghatak, R. R. Markwald, V. C. Hascall et al., "Roles of proteoglycans and glycosaminoglycans in wound healing and fibrosis," *International Journal of Cell Biology*. In press.
- [8] A. J. Singer and R. A. F. Clark, "Cutaneous wound healing," *The New England Journal of Medicine*, vol. 341, no. 10, pp. 738–746, 1999.
- [9] J. Ebner and E. V. Maytin, "Cutaneous wound healing," in *Dermatologic Surgery*, A. V. Vidimos, C. T. Ammirati, and C. Poblete-Lopez, Eds., pp. 81–100, Saunders-Elsevier, 2009.
- [10] P. Velander, C. Theopold, T. Hirsch et al., "Impaired wound healing in an acute diabetic pig model and the effects of local hyperglycemia," *Wound Repair and Regeneration*, vol. 16, no. 2, pp. 288–293, 2008.
- [11] T. Dinh, F. Tecilazich, A. Kafanas et al., "Mechanisms involved in the development and healing of diabetic foot ulceration," *Diabetes*, vol. 61, no. 11, pp. 2937–2947, 2012.
- [12] P. Algenstaedt, C. Schaefer, T. Biermann et al., "Microvascular alterations in diabetic mice correlate with level of hyperglycemia," *Diabetes*, vol. 52, no. 2, pp. 542–549, 2003.
- [13] L. Pradhan, X. Cai, S. Wu et al., "Gene expression of pro-inflammatory cytokines and neuropeptides in diabetic wound healing," *Journal of Surgical Research*, vol. 167, no. 2, pp. 336–342, 2011.
- [14] S. Reitsma, D. W. Slaaf, H. Vink, M. A. M. J. van Zandvoort, and M. G. A. O. Egbrink, "The endothelial glycocalyx: composition, functions, and visualization," *Pflügers Archiv*, vol. 454, no. 3, pp. 345–359, 2007.
- [15] M. Nieuwdorp, M. C. Meuwese, H. Vink, J. B. L. Hoekstra, J. P. Kastelein, and E. S. G. Stroes, "The endothelial glycocalyx: a potential barrier between health and vascular disease," *Current Opinion in Lipidology*, vol. 16, no. 5, pp. 507–511, 2005.
- [16] F. E. Lennon and P. A. Singleton, "Hyaluronan regulation of vascular integrity," *American Journal of Cardiovascular Disease*, vol. 1, no. 3, pp. 200–213, 2011.
- [17] M. Nieuwdorp, T. W. van Haeften, M. C. L. G. Gouverneur et al., "Loss of endothelial glycocalyx during acute hyperglycemia coincides with endothelial dysfunction and coagulation activation in vivo," *Diabetes*, vol. 55, no. 2, pp. 480–486, 2006.
- [18] M. Nieuwdorp, H. L. Mooij, J. Kroon et al., "Endothelial glycocalyx damage coincides with microalbuminuria in type 1 diabetes," *Diabetes*, vol. 55, no. 4, pp. 1127–1132, 2006.
- [19] M. Nieuwdorp, F. Holleman, E. de Groot et al., "Perturbation of hyaluronan metabolism predisposes patients with type 1 diabetes mellitus to atherosclerosis," *Diabetologia*, vol. 50, no. 6, pp. 1288–1293, 2007.
- [20] R. Stern and M. J. Jedrzejewski, "Hyaluronidases: their genomics, structures, and mechanisms of action," *Chemical Reviews*, vol. 106, no. 3, pp. 818–839, 2006.
- [21] M. Kucur, B. Karadag, F. K. Isman et al., "Plasma hyaluronidase activity as an indicator of atherosclerosis in patients with coronary artery disease," *Bratislavské Lekárske Listy*, vol. 110, no. 1, pp. 21–26, 2009.
- [22] N. Nagy, T. Freudenberger, A. Melchior-Becker et al., "Inhibition of hyaluronan synthesis accelerates murine atherosclerosis: novel insights into the role of hyaluronan synthesis," *Circulation*, vol. 122, no. 22, pp. 2313–2322, 2010.
- [23] C. Desjardins and B. R. Duling, "Heparinase treatment suggests a role for the endothelial cell glycocalyx in regulation of capillary hematocrit," *The American Journal of Physiology—Heart and Circulatory Physiology*, vol. 258, no. 3, pp. H647–H654, 1990.
- [24] J. Han, F. Zhang, J. Xie, R. J. Linhardt, and L. M. Hiebert, "Changes in cultured endothelial cell glycosaminoglycans under hyperglycemic conditions and the effect of insulin and heparin," *Cardiovascular Diabetology*, vol. 8, article 46, 2009.
- [25] A. Rizzo, F. Mercuri, L. Quagliaro, G. Damante, and A. Ceriello, "Intermittent high glucose enhances apoptosis in human umbilical vein endothelial cells in culture," *The American Journal of Physiology—Endocrinology and Metabolism*, vol. 281, no. 5, pp. E924–E930, 2001.
- [26] C. J. Zuurbier, C. Demirci, A. Koeman, H. Vink, and C. Ince, "Short-term hyperglycemia increases endothelial glycocalyx permeability and acutely decreases lineal density of capillaries with flowing red blood cells," *Journal of Applied Physiology*, vol. 99, no. 4, pp. 1471–1476, 2005.
- [27] A. Zarbock, R. K. Polanowska-Grabowska, and K. Ley, "Platelet-neutrophil-interactions: linking hemostasis and inflammation," *Blood Reviews*, vol. 21, no. 2, pp. 99–111, 2007.
- [28] C. de la Motte, J. Nigro, A. Vasanji et al., "Platelet-derived hyaluronidase 2 cleaves hyaluronan into fragments that trigger monocyte-mediated production of proinflammatory cytokines," *The American Journal of Pathology*, vol. 174, no. 6, pp. 2254–2264, 2009.
- [29] S. Albeiroti, K. Ayasoufi, D. R. Hill, B. Shen, and C. A. de la Motte, "Platelet hyaluronidase-2: an enzyme that translocates to the surface upon activation to function in extracellular matrix degradation," *Blood*, vol. 125, no. 9, pp. 1460–1469, 2015.

- [30] C. M. McKee, M. B. Penno, M. Cowman et al., "Hyaluronan (HA) fragments induce chemokine gene expression in alveolar macrophages: the role of HA size and CD44," *The Journal of Clinical Investigation*, vol. 98, no. 10, pp. 2403–2413, 1996.
- [31] A. C. Petrey and C. A. de la Motte, "Hyaluronan, a crucial regulator of inflammation," *Frontiers in Immunology*, vol. 5, article 101, 2014.
- [32] K. A. Scheibner, M. A. Lutz, S. Boodoo, M. J. Fenton, J. D. Powell, and M. R. Horton, "Hyaluronan fragments act as an endogenous danger signal by engaging TLR2," *Journal of Immunology*, vol. 177, no. 2, pp. 1272–1281, 2006.
- [33] K. R. Taylor, K. Yamasaki, K. A. Radek et al., "Recognition of hyaluronan released in sterile injury involves a unique receptor complex dependent on toll-like receptor 4, CD44, and MD-2," *The Journal of Biological Chemistry*, vol. 282, no. 25, pp. 18265–18275, 2007.
- [34] G. M. Rubanyi, J. C. Romero, and P. M. Vanhoutte, "Flow-induced release of endothelium-derived relaxing factor," *American Journal of Physiology—Heart and Circulatory Physiology*, vol. 250, no. 6, part 2, pp. H1145–H1149, 1986.
- [35] K. L. Andrews, C. R. Triggle, and A. Ellis, "NO and the vasculature: where does it come from and what does it do?" *Heart Failure Reviews*, vol. 7, no. 4, pp. 423–445, 2002.
- [36] M. H. Ali and P. T. Schumacker, "Endothelial responses to mechanical stress: where is the mechanosensor?" *Critical Care Medicine*, vol. 30, no. 5, supplement, pp. S198–S206, 2002.
- [37] R. Kumagai, X. Lu, and G. S. Kassab, "Role of glycocalyx in flow-induced production of nitric oxide and reactive oxygen species," *Free Radical Biology and Medicine*, vol. 47, no. 5, pp. 600–607, 2009.
- [38] M. Y. Pahakis, J. R. Kosky, R. O. Dull, and J. M. Tarbell, "The role of endothelial glycocalyx components in mechanotransduction of fluid shear stress," *Biochemical and Biophysical Research Communications*, vol. 355, no. 1, pp. 228–233, 2007.
- [39] S. Mochizuki, H. Vink, O. Hiramatsu et al., "Role of hyaluronic acid glycosaminoglycans in shear-induced endothelium-derived nitric oxide release," *The American Journal of Physiology—Heart and Circulatory Physiology*, vol. 285, no. 2, pp. H722–H726, 2003.
- [40] J. A. Florian, J. R. Kosky, K. Ainslie, Z. Pang, R. O. Dull, and J. M. Tarbell, "Heparan sulfate proteoglycan is a mechanosensor on endothelial cells," *Circulation Research*, vol. 93, no. 10, pp. e136–e142, 2003.
- [41] S. F. Kemeny, D. S. Figueroa, and A. M. Clyne, "Hypo- and hyperglycemia impair endothelial cell actin alignment and nitric oxide synthase activation in response to shear stress," *PLoS ONE*, vol. 8, no. 6, Article ID e66176, 2013.
- [42] X. Chen, L. Feng, and H. Jin, "Constant or fluctuating hyperglycemias increases cytomembrane stiffness of human umbilical vein endothelial cells in culture: roles of cytoskeletal rearrangement and nitric oxide synthesis," *BMC Cell Biology*, vol. 14, no. 1, article 22, 2013.
- [43] C. B. S. Henry and B. R. Duling, "Permeation of the luminal capillary glycocalyx is determined by hyaluronan," *The American Journal of Physiology—Heart and Circulatory Physiology*, vol. 277, no. 2, pp. H508–H514, 1999.
- [44] P. A. Singleton, S. M. Dudek, S.-F. Ma, and J. G. N. Garcia, "Transactivation of sphingosine 1-phosphate receptors is essential for vascular barrier regulation: novel role for hyaluronan and CD44 receptor family," *The Journal of Biological Chemistry*, vol. 281, no. 45, pp. 34381–34393, 2006.
- [45] P. A. Singleton, T. Mirzapozova, Y. Guo et al., "High-molecular-weight hyaluronan is a novel inhibitor of pulmonary vascular leakiness," *The American Journal of Physiology—Lung Cellular and Molecular Physiology*, vol. 299, no. 5, pp. L639–L651, 2010.
- [46] W. Schubert, P. G. Frank, S. E. Woodman et al., "Microvascular hyperpermeability in caveolin-1 (–/–) knock-out mice. Treatment with a specific nitric-oxide synthase inhibitor, L-name, restores normal microvascular permeability in Cav-1 null mice," *Journal of Biological Chemistry*, vol. 277, no. 42, pp. 40091–40098, 2002.
- [47] M. Mohamadzadeh, H. DeGrendele, H. Arizpe, P. Estess, and M. Siegelman, "Proinflammatory stimuli regulate endothelial hyaluronan expression and CD44/HA-dependent primary adhesion," *Journal of Clinical Investigation*, vol. 101, no. 1, pp. 97–108, 1998.
- [48] A. Nandi, P. Estess, and M. H. Siegelman, "Hyaluronan anchoring and regulation on the surface of vascular endothelial cells is mediated through the functionally active form of CD44," *The Journal of Biological Chemistry*, vol. 275, no. 20, pp. 14939–14948, 2000.
- [49] A. A. Constantinescu, H. Vink, and J. A. E. Spaan, "Endothelial cell glycocalyx modulates immobilization of leukocytes at the endothelial surface," *Arteriosclerosis, Thrombosis, and Vascular Biology*, vol. 23, no. 9, pp. 1541–1547, 2003.
- [50] J. A. MacK, R. J. Feldman, N. Itano et al., "Enhanced inflammation and accelerated wound closure following tetraborborol ester application or full-thickness wounding in mice lacking hyaluronan synthases Has1 and Has3," *Journal of Investigative Dermatology*, vol. 132, no. 1, pp. 198–207, 2012.
- [51] Y. Wang, M. E. Lauer, S. An, J. A. Mack, and E. V. Maytin, "Hyaluronan synthase 2 protects skin fibroblasts against apoptosis induced by environmental stress," *The Journal of Biological Chemistry*, vol. 289, no. 46, pp. 32253–32265, 2014.
- [52] A. Wang, C. de la Motte, M. Lauer, and V. Hascall, "Hyaluronan matrices in pathobiological processes," *The FEBS Journal*, vol. 278, no. 9, pp. 1412–1418, 2011.
- [53] C. A. de la Motte, V. C. Hascall, J. Drazba, S. K. Bandyopadhyay, and S. A. Strong, "Mononuclear leukocytes bind to specific hyaluronan structures on colon mucosal smooth muscle cells treated with polyinosinic acid: polycytidylic acid. Inter-alpha-trypsin inhibitor is crucial to structure and function," *American Journal of Pathology*, vol. 163, no. 1, pp. 121–133, 2003.
- [54] A. K. Majors, R. C. Austin, C. A. de la Motte et al., "Endoplasmic reticulum stress induces hyaluronan deposition and leukocyte adhesion," *The Journal of Biological Chemistry*, vol. 278, no. 47, pp. 47223–47231, 2003.
- [55] M. E. Lauer, M. Aytakin, S. A. Comhair et al., "Modification of hyaluronan by heavy chains of inter- α -inhibitor in idiopathic pulmonary arterial hypertension," *Journal of Biological Chemistry*, vol. 289, no. 10, pp. 6791–6798, 2014.
- [56] M. E. Lauer, G. Cheng, S. Swaidanis, M. A. Aronica, P. H. Weigel, and V. C. Hascall, "Tumor necrosis factor-stimulated gene-6 (TSG-6) amplifies hyaluronan synthesis by airway smooth muscle cells," *The Journal of Biological Chemistry*, vol. 288, no. 1, pp. 423–431, 2013.
- [57] M. E. Lauer, T. T. Glant, K. Mikecz et al., "Irreversible heavy chain transfer to hyaluronan oligosaccharides by tumor necrosis factor-stimulated gene-6," *The Journal of Biological Chemistry*, vol. 288, no. 1, pp. 205–214, 2013.
- [58] M. E. Lauer, D. Mukhopadhyay, C. Fulop, C. A. de la Motte, A. K. Majors, and V. C. Hascall, "Primary murine airway smooth

- muscle cells exposed to poly(I,C) or tunicamycin synthesize a leukocyte-adhesive hyaluronan matrix," *The Journal of Biological Chemistry*, vol. 284, no. 8, pp. 5299–5312, 2009.
- [59] J. Ren, V. C. Hascall, and A. Wang, "Cyclin D3 mediates synthesis of a hyaluronan matrix that is adhesive for monocytes in mesangial cells stimulated to divide in hyperglycemic medium," *Journal of Biological Chemistry*, vol. 284, no. 24, pp. 16621–16632, 2009.
- [60] A. Wang and V. C. Hascall, "Hyaluronan structures synthesized by rat mesangial cells in response to hyperglycemia induce monocyte adhesion," *The Journal of Biological Chemistry*, vol. 279, no. 11, pp. 10279–10285, 2004.
- [61] A. Wang, R. J. Midura, A. Vasanthi, A. J. Wang, and V. C. Hascall, "Hyperglycemia diverts dividing osteoblastic precursor cells to an adipogenic pathway and induces synthesis of a hyaluronan matrix that is adhesive for monocytes," *Journal of Biological Chemistry*, vol. 289, no. 16, pp. 11410–11420, 2014.
- [62] P. Rossetti, J. Bondia, J. Vehí, and C. G. Fanelli, "Estimating plasma glucose from interstitial glucose: the issue of calibration algorithms in commercial continuous glucose monitoring devices," *Sensors*, vol. 10, no. 12, pp. 10936–10952, 2010.
- [63] U. Fischer, R. Ertle, P. Abel et al., "Assessment of subcutaneous glucose concentration: validation of the wick technique as a reference for implanted electrochemical sensors in normal and diabetic dogs," *Diabetologia*, vol. 30, no. 12, pp. 940–945, 1987.
- [64] J. P. Bantle and W. Thomas, "Glucose measurement in patients with diabetes mellitus with dermal interstitial fluid," *The Journal of Laboratory and Clinical Medicine*, vol. 130, no. 4, pp. 436–441, 1997.
- [65] D. B. Keenan, J. J. Mastrototaro, S. A. Weinzimer, and G. M. Steil, "Interstitial fluid glucose time-lag correction for real-time continuous glucose monitoring," *Biomedical Signal Processing and Control*, vol. 8, no. 1, pp. 81–89, 2013.
- [66] E. Kulcu, J. A. Tamada, G. Reach, R. O. Potts, and M. J. Lesho, "Physiological differences between interstitial glucose and blood glucose measured in human subjects," *Diabetes Care*, vol. 26, no. 8, pp. 2405–2409, 2003.
- [67] Y. H. Baek, H. Y. Jin, K. A. Lee et al., "The correlation and accuracy of glucose levels between interstitial fluid and venous plasma by continuous glucose monitoring system," *Korean Diabetes Journal*, vol. 34, no. 6, pp. 350–358, 2010.
- [68] I. M. Braverman, J. Sibley, and A. Keh, "Ultrastructural analysis of the endothelial-pericyte relationship in diabetic cutaneous vessels," *Journal of Investigative Dermatology*, vol. 95, no. 2, pp. 147–153, 1990.
- [69] H.-P. Hammes, J. Lin, O. Renner et al., "Pericytes and the pathogenesis of diabetic retinopathy," *Diabetes*, vol. 51, no. 10, pp. 3107–3112, 2002.
- [70] I. M. Braverman and A. Keh-Yen, "Ultrastructural abnormalities of the microvasculature and elastic fibers in the skin of juvenile diabetics," *Journal of Investigative Dermatology*, vol. 82, no. 3, pp. 270–274, 1984.
- [71] A. Sainio, T. Jokela, M. I. Tammi, and H. Järveläinen, "Hyperglycemic conditions modulate connective tissue reorganization by human vascular smooth muscle cells through stimulation of hyaluronan synthesis," *Glycobiology*, vol. 20, no. 9, pp. 1117–1126, 2010.
- [72] D. Vigetti, M. Rizzi, P. Moretto et al., "Glycosaminoglycans and glucose prevent apoptosis in 4-methylumbelliferone-treated human aortic smooth muscle cells," *The Journal of Biological Chemistry*, vol. 286, no. 40, pp. 34497–34503, 2011.
- [73] S. Meran, D. Thomas, P. Stephens et al., "Involvement of hyaluronan in regulation of fibroblast phenotype," *The Journal of Biological Chemistry*, vol. 282, no. 35, pp. 25687–25697, 2007.
- [74] J. Webber, R. H. Jenkins, S. Meran, A. Phillips, and R. Steadman, "Modulation of TGF β 1-dependent myofibroblast differentiation by hyaluronan," *The American Journal of Pathology*, vol. 175, no. 1, pp. 148–160, 2009.

Review Article

Hyaluronan Synthesis, Catabolism, and Signaling in Neurodegenerative Diseases

Larry S. Sherman,^{1,2} Steven Matsumoto,³ Weiping Su,¹
Taasin Srivastava,⁴ and Stephen A. Back⁴

¹*Division of Neuroscience, Oregon National Primate Research Center, Oregon Health & Science University, 505 NW 185th Avenue, Beaverton, OR 97006, USA*

²*Department of Cell, Developmental & Cancer Biology, Oregon Health & Science University, 3181 SW Sam Jackson Park Road, Portland, OR 97239, USA*

³*Department of Integrative Biosciences, School of Dentistry, Oregon Health & Science University, 3181 SW Sam Jackson Park Road, Portland, OR 97239, USA*

⁴*Department of Pediatrics, Oregon Health & Science University, 3181 SW Sam Jackson Park Road, Portland, OR 97239, USA*

Correspondence should be addressed to Larry S. Sherman; shermanl@ohsu.edu

Received 3 February 2015; Accepted 11 April 2015

Academic Editor: Wiljan J. A. J. Hendriks

Copyright © 2015 Larry S. Sherman et al. This is an open access article distributed under the Creative Commons Attribution License, which permits unrestricted use, distribution, and reproduction in any medium, provided the original work is properly cited.

The glycosaminoglycan hyaluronan (HA), a component of the extracellular matrix, has been implicated in regulating neural differentiation, survival, proliferation, migration, and cell signaling in the mammalian central nervous system (CNS). HA is found throughout the CNS as a constituent of proteoglycans, especially within perineuronal nets that have been implicated in regulating neuronal activity. HA is also found in the white matter where it is diffusely distributed around astrocytes and oligodendrocytes. Insults to the CNS lead to long-term elevation of HA within damaged tissues, which is linked at least in part to increased transcription of HA synthases. HA accumulation is often accompanied by elevated expression of at least some transmembrane HA receptors including CD44. Hyaluronidases that digest high molecular weight HA into smaller fragments are also elevated following CNS insults and can generate HA digestion products that have unique biological activities. A number of studies, for example, suggest that both the removal of high molecular weight HA and the accumulation of hyaluronidase-generated HA digestion products can impact CNS injuries through mechanisms that include the regulation of progenitor cell differentiation and proliferation. These studies, reviewed here, suggest that targeting HA synthesis, catabolism, and signaling are all potential strategies to promote CNS repair.

1. Introduction

Up to 20% of the volume of the mammalian central nervous system (CNS) is composed of an extracellular matrix (ECM) that includes proteins, proteoglycans, and glycosaminoglycans [1]. Evolving evidence indicates that the composition and organization of this matrix change throughout the course of normal aging, in neurodegenerative diseases and following CNS injury and that these alterations influence a wide range of cellular behaviors. The CNS ECM was originally believed to play mostly structural roles including supporting tissue architecture. Findings over the past few decades, however,

indicate that the CNS ECM is an information-rich environment that includes signals that influence cell proliferation, differentiation, migration, synapse formation and remodeling, and responses to injury [2–7].

The composition and function of the CNS ECM can differ within distinct areas of the CNS [8]. For example, white matter ECM is far more diffuse compared to gray matter ECM. Within gray matter, perineuronal nets that surround some neuron cell bodies and dendrites are composed of a dense matrix of glycosaminoglycans, proteoglycans, tenascin R, and link proteins. This specialized ECM can regulate synaptic

plasticity [9] while the negatively-charged glycosaminoglycans can influence the diffusion of cations that support rapid neuronal firing [10]. Another distinct ECM environment can be found in the basal lamina surrounding cerebral vessels, which is composed of collagen, fibronectin, perlecan, dystroglycan, and laminin-nidogen complexes. It surrounds the pial surface of the CNS and separates endothelial cells from the parenchyma, thus contributing to the blood-brain barrier [8].

Although numerous studies have implicated proteoglycans in the response to CNS damage and in mediating inflammatory responses and recovery (for excellent recent reviews see [11–13]) there is growing evidence that the glycosaminoglycan hyaluronan (HA) plays specific roles in regulating neural progenitor cell proliferation and differentiation. HA is a large unbranched, nonsulfated glycosaminoglycan composed of repeating disaccharide units of N-glucuronic acid and N-acetylglucosamine and is a major constituent of the ECM. HA can reach upwards of 25,000 disaccharide units, with molecular weights as high as 10^7 Da. HA can have distinct physiological functions depending on its size, concentration, and localization. These functions include altering tissue hydration and elasticity and creating cell-free spaces that are crucial for cell migration. In addition, HA can induce cell signaling through transmembrane HA receptors.

HA is synthesized at the inner face of the plasma membrane and secreted into the extracellular space as a linear undecorated molecule. In mammals, HA synthesis is achieved by a family of transmembrane proteins known as HA synthases (HASs). The mammalian genome codes for three such synthases, HAS1, HAS2, and HAS3. HA catabolism is carried out by hyaluronidases (HYALs) that differ in their cellular localization and pH optima. Mammals possess multiple hyaluronidase genes, including HYAL-1 through HYAL-5, PH20/SPAM1, and, in humans, a pseudogene designated PHYAL-1. The balance between HA synthesis and catabolism has long been recognized to play roles in CNS development (e.g., [14–17]). Here, we review data implicating alterations in HA synthesis, signaling, and catabolism in the responses of progenitor cell populations to neurodegenerative diseases and CNS injuries and provide a framework to assess the efficacy of targeting HA as a strategy to promote CNS repair.

2. HA Accumulates in the Damaged CNS

2.1. Ischemic Injury. In the uninjured CNS, HA is diffusely distributed throughout the white matter but is densely packed in gray matter, including perineuronal nets (Figure 1). Damage to the CNS leads to HA accumulation [4, 18] in both white and gray matter that can persist for long periods of time after the initial insult. In most cases, pathological elevation of HA is linked to increased HAS transcription and is often associated with reactive astrogliosis and glial scarring. This effect has been most thoroughly studied in the context of ischemic injuries. For example, HAS2 mRNA is normally expressed at very low levels in the CNS but increased significantly within 6 hours following middle cerebral artery occlusion in rats [19]. HA was also elevated up to six weeks following a photothrombotic stroke lesion in adult mouse cortex [20]. Consistent with these experimental findings, HAS1 and HAS2

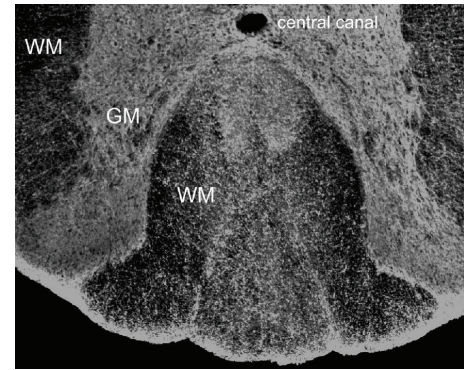


FIGURE 1: Distribution of HA (white) in lumbar spinal cord white matter (WM) and gray matter (GM). A section of a rat spinal cord was labeled with a biotinylated-HA-binding protein then visualized by fluorescence microscopy following staining with fluorescein-labeled streptavidin. Note that HA is diffusely distributed throughout white matter, but is much more dense in gray matter.

are elevated in infarcted and peri-infarcted tissues from patients following ischemic stroke [21]. Plasma levels of HA were also significantly elevated in acute stroke patients compared to controls and could predict 3-month functional outcomes, especially in patients with intracerebral hemorrhage [22].

In addition to the findings in adult patients and in adult models of stroke, HA is also markedly elevated in perinatal hypoxic-ischemic cerebral white matter injuries. Lesions resulting from these insults are the leading cause of cerebral palsy in survivors of premature birth and contribute to lifelong neurobehavioral disabilities. HA accumulates in the ECM in human preterm chronic cerebral white matter lesions coincident with extensive reactive astrogliosis [23]. Similarly, in a fetal sheep model of cerebral hypoxic-ischemic injury, HA rapidly increased by 24 hours after a single episode of fetal hypoxia-ischemia and remained persistently elevated for weeks [24].

2.2. Seizures. Seizures also alter HA synthesis in the CNS but whether seizure activity directly increases or decreases HA is not entirely clear. Epileptic seizures can influence both the behaviors of existing neurons and adult neurogenesis (the generation of new neurons). One consequence of these alterations is abnormal sprouting by granule cell axons (so-called mossy fiber sprouting) in the dentate gyrus of the hippocampus, an area of the brain involved in learning and memory. Degradation of HA in organotypic hippocampal slice cultures with a hyaluronidase significantly reduced kainic acid-induced mossy fiber sprouting, a synaptic rearrangement associated with temporal lobe epilepsy [25]. Interestingly, HA and HAS3 both decrease in perineuronal nets in the hippocampus following seizures in a rodent model of temporal lobe epilepsy [26] while *Has3*-null mice have reduced hippocampal volumes and develop epileptic seizures [17]. These data suggest that reduced HA could contribute to seizure onset and recurrence but HA digestion by a hyaluronidase may generate HA products that reduce mossy fiber sprouting

and, possibly, positive feedback circuits for seizure generation. In contrast to studies in rodents, HA was observed to increase in the hippocampus and temporal neocortex of patients with intractable mesial temporal lobe epilepsy [27]. It is possible that this discrepancy with the rodent studies is due to the fact that the human tissue samples had more chronic lesions with extensive astrogliosis compared to the rodent tissues and that HA was rebounding coincident with glial scarring.

2.3. Traumatic Brain and Spinal Cord Injuries. For up to 5 months after dorsal rhizotomy proximal to dorsal root ganglia, Mansour and coworkers [28] found increased glial hyaluronan-binding protein immunoreactivity (which typically reflects increased HA). In another study, spinal cord contusion injury in rats resulted in HA degradation at the site of injury with subsequent elevated accumulation within one month after injury [29]. HA was highest in areas where there was extensive astrogliosis. A study of controlled cortical impact injury in rats (as a model of traumatic brain injury) indicated that HAS1 and HAS2 mRNA increase anywhere from 4 hours to 3 days after injury compared to craniotomy alone [30]. This study did not, however, validate their findings by examining the distribution or levels of HA. Nonetheless, these data indicate that traumatic CNS injuries lead to long-term increases in HA in affected tissues.

2.4. Demyelinating Diseases. A number of studies have demonstrated increased HA in CNS lesions associated with neurodegenerative diseases that influence white matter. For example, HA is elevated in demyelinating white matter lesions from mice with experimental autoimmune encephalomyelitis and patients with multiple sclerosis, both of which are autoimmune diseases where myelin-reactive immune cells induce demyelination [31–33]. HA is also elevated in the brains of patients with Vanishing White Matter Disease, a genetic leukoencephalopathy caused by mutations in eukaryotic translation initiation factor 2B [34]. These patients experience a slowly progressive neurological deterioration with episodes of rapid clinical worsening triggered by stress. HA accumulation was especially pronounced in affected frontal white matter but not in the unaffected cerebellar white matter in these patients.

2.5. Normative Aging and Dementias. HA accumulation in the CNS also occurs during the course of normal aging. Moderate increases in HA were observed in 30-month-old rat brain tissue compared to tissues from younger animals [35]. HA levels also significantly increase with age in the gray matter of rhesus and Japanese macaques in areas with astrogliosis and coincident with increased transcription of *HAS1* expressed by reactive astrocytes [36]. HA is similarly elevated in gray matter from patients with Alzheimer's disease (AD) [37, 38] and the white matter of patients with vascular dementia who have a low burden of AD pathology accompanied by vascular injury consistent with vascular dementia [39]. In agreement with these findings, Nägga and coworkers [40] observed significantly increased levels of HA in

the cerebrospinal fluid (CSF) from patients with vascular dementia but not AD alone compared with controls. This is consistent with the findings of Laurent and coworkers [18], who observed elevated HA in the cerebrospinal fluid (CSF) of patients with a number of different neurological diseases. Increased levels of HA were also observed in the CSF of individuals with vascular abnormalities determined as significant white matter changes or in patients with previous infarction compared with individuals without these findings [40]. There was a positive correlation between the levels of HA and the CSF/serum albumin ratio, an indicator of blood-brain barrier integrity, in patients with both vascular dementia and AD. These findings support the notion that HA accumulates in gray matter during the course of normal aging, and further increases in white matter in cases of age-related vascular injury.

All together, the findings described above demonstrate that HA accumulates, likely due to increased HAS transcription, in a wide variety of insults to the CNS. HA accumulation is usually associated with astrogliosis, and indeed reactive astrocytes demonstrate elevated HAS. This likely accounts for the chronically high levels of HA within glial scars. As indicated by studies in models of spinal cord injury and seizures, HA may initially become degraded due to the possible induction of specific hyaluronidases or other factors in the early injury environment but, at least in chronic lesions, quickly accumulates to higher than normal levels that are sustained for long periods after the initial insult. At least in some insults, this elevated HA can be detected in CSF. Future studies focused on examining when HA concentrations become detectably elevated in the CSF following different insults to the CNS will demonstrate the potential of HA as a diagnostic biomarker for CNS injury.

3. HA Accumulation Alters Neural Progenitor Cell Proliferation and Differentiation

3.1. Effects of HA on Neural Progenitor Cells and Glia. What are the consequences of prolonged HA accumulation in CNS lesions? In addition to its roles in nervous system development and homeostasis, HA can have an impact on nervous system repair by altering the proliferation, migration, and differentiation of progenitor cell populations in the CNS. In demyelinating lesions, including those of multiple sclerosis patients, some recovery of function is associated with the recruitment of oligodendrocyte progenitor cells (OPCs) that differentiate into oligodendrocytes (OLs) that remyelinate spared axons [41]. However, in chronic white matter lesions, OPCs accumulate and fail to give rise to myelinating OLs [42–47]. The presence of HA within demyelinating lesions correlates with areas where remyelination fails, and the addition of high molecular weight preparations of HA (>10⁶ Da) to rodent OPCs *in vitro*, to white matter slice cultures, or to lysolecithin-induced demyelinating corpus callosum lesions blocks OPC differentiation and remyelination [31, 32, 48]. Interestingly, high molecular weight HA also blocks astrocyte proliferation [29] and inhibits glial scarring [49]. Thus, although the accumulation of HA in demyelinating lesions is

linked to the inhibition of OPC maturation and remyelination failure, it may also mediate glial scar formation.

HA may also play a role in OPC recruitment to demyelinating lesions. Following demyelinating insults, OPCs migrate towards damaged axons before differentiating into myelinating OLs. Using an OPC line, Piao and coworkers [50] found that reducing the expression of the HA receptor CD44 or treating cells with a CD44 blocking antibody inhibited OPC migration both *in vitro* and following transplantation into inflammatory demyelinating lesions. Although the authors reported elevated HA in these lesions, it remains to be determined if HA is directly required for the migratory behavior of these cells. Nonetheless, these data suggest that while HA can block OPC maturation when found in excess in demyelinating lesions, HA might also be required to facilitate OPC recruitment to lesions in a CD44-dependent manner.

3.2. Roles of HA in Neural Stem/Progenitor Cell Niches. While HA is mostly observed at low levels in the uninjured adult brain, it remains at high levels in the adult subventricular zone, the subgranular zone of the dentate gyrus of the hippocampus, and the rostral migratory stream, areas where neural stem/progenitor cells (NSPCs) reside throughout life [20, 51]. HA may, therefore, play a role in regulating NSPCs in their niches [52]. Although it is unclear what direct role HA plays in NSPC niches, a number of studies have examined the effects of HA gels on NSPCs and the use of these gels as vehicles in NSPC transplantation studies [52]. For example, HA hydrogels significantly improved the survival of a human NSPC line and glial-restricted precursor cells following transplantation into the brains of mice [53]. In another study, a biopolymer hydrogel composed of cross-linked HA and heparin sulfate significantly promoted the survival of NSPC lines *in vitro* in conditions of stress and *in vivo* following transplantation into the infarct cavity in a stroke model [54]. Degradation of the HA gels encapsulating neural progenitor cells caused differentiation and maturation of the progenitor cells.

Collectively, these studies suggest that HA within NSPC niches plays a critical role in regulating NSPC proliferation and differentiation. This function of HA is recapitulated in demyelinating and possibly other lesions, where OPCs encounter a niche-like environment rich in HA that can influence OPC migration, astrocyte proliferation, and glial cell differentiation. Presumably, the levels and distribution of HA within NSPC niches must be tightly controlled to regulate NSPC differentiation. The challenge will be to identify a means of controlling HA synthesis or catabolism within NSPC niches or areas of damaged CNS tissues in a way that promotes nervous system repair. The use of HA biomaterials, as described above, has the potential to regulate HA functions in both stem cell niches and CNS lesions, offering a potential approach to stem/progenitor cell-based therapies (reviewed in [52]).

4. Endogenous Hyaluronidases Influence CNS Repair

As discussed above, there are several mammalian hyaluronidases that catabolize HA in tissues. While digestion of high

molecular weight HA can have its own biological consequences, the accumulation of HA digestion products generated by hyaluronidases can also have distinct, size-dependent activities.

4.1. Roles of Hyaluronidases in CNS Injury and Disease. The first indication that hyaluronidases play a role in the CNS came from the observation that there is a high level of hyaluronidase activity in the developing brain and spinal cord that declines during the early perinatal period [14]. Hyaluronidase activity and expression are generally low in the adult CNS. However, following a number of insults to the nervous system, hyaluronidase expression and activity increase. For example, in both stroke and peri-infarct regions of ischemic stroke patients, HYAL1 and HYAL2 were elevated in inflammatory cells, microvessels, and neurons [21]. Elevated hyaluronidase expression was accompanied by the accumulation of low molecular mass (3–10 disaccharides) HA, suggesting that increased hyaluronidase expression within ischemic CNS lesions is accompanied by the accumulation of HA digestion products.

Hyall mRNA was also elevated in rats following a craniotomy or a controlled cortical impact injury [30]. Other hyaluronidases, including PH20/SPAM1, were also detected and showed trends of increased expression but the changes were not significant. Similarly, hyaluronidases were elevated in demyelinating lesions where HA accumulates. Sloane and coworkers [32] found that OPCs express multiple hyaluronidases including PH20/SPAM1 (referred to henceforth as PH20) by immunocytochemistry. This result was surprising, since previous studies had not detected PH20 in the brain. A subsequent study demonstrated that PH20 is expressed by mouse astrocytes and OPCs both *in vitro* and in demyelinating mouse and human lesions by immunohistochemistry and, in mice, by RT-PCR [55]. This amplified RT-PCR product was the same size as PH20 amplified from mouse testes, did not originate from genomic DNA, and was confirmed to be PH20 by sequencing. Furthermore, infecting OPCs with a lentivirus carrying the cDNA for PH20, but not for other hyaluronidases normally expressed by OPCs, blocked OPC differentiation [55]. Treatment of OPCs *in vitro* with a broad-spectrum hyaluronidase inhibitor (ascorbate 6-hexadecanoate) promoted OPC maturation [32, 55] while treatment of demyelinating lesions with the inhibitor overcame the inhibitory effects of high molecular weight HA on remyelination, leading to functional recovery [55].

Further evidence that PH20 is elevated in the CNS following injury comes from a sheep model of prenatal white matter injury described above, where elevated ovine PH20 expression was confirmed through multiple approaches [24]. A single PH20 transcript was detected using a nested RT-PCR assay of mRNAs isolated from control and injured white matter in two separate labs. This transcript was the same size as in fetal ovine testes, was obtained with multiple primer sets, did not originate from genomic DNA, and was confirmed by sequencing to be PH20. PH20 was also detected in fetal ovine white matter by RNA-Seq in data from 10 animals, with the fetal ovine PH20 sequence confirmed to be highly homologous to rodent and human PH20. Finally, PH20 was detected

by immunohistochemistry in fetal sheep brain tissues using two separate polyclonal antisera from rabbit and chicken. Lower levels of PH20 staining in controls relative to the white matter injury groups support the notion that PH20 expression is elevated following prenatal hypoxic-ischemic injury. All together, these data support the hypothesis that PH20 and possibly other hyaluronidases block OPC maturation and remyelination.

4.2. Hyaluronidases Can Influence Neuronal Activity. It is unclear if endogenous hyaluronidases influence neuronal function. However, a number of studies have suggested that HA within perineuronal nets can influence neuron activity that can be altered by hyaluronidase treatment. For example, the removal of perineuronal nets using hyaluronidase in hippocampal slices from young rats reduced the width of the synaptic cleft and increased the amplitude of excitatory post-synaptic potentials in CA1 axodendritic connections [56]. From this and other studies, it is reasonable to conclude that HA-rich perineuronal nets could influence both the efficacy and architecture of synapses. Furthermore, the controlled degradation of HA in perineuronal nets may be a mechanism used to alter synaptic plasticity underlying learning and memory. Hyaluronidase has also been reported to regulate α -amino-3-hydroxy-5-methyl-4-isoxazolepropionic acid (AMPA) receptor trafficking into and out of the synapse [57] suggesting that HA may control the plasticity of individual synapses by creating distinct membrane compartments and controlling the passive diffusion of molecules at the cell surface. Interestingly, perisynaptic HA may influence lateral mobility at the plasma membrane differently on spiny versus aspiny neurons [58]. How this perineuronal HA is regulated is unclear. It is intriguing to speculate, however, that hyaluronidases expressed by neurons or local glial cells may regulate neuronal activity through the regulated catabolism of HA.

4.3. HA Digestion Products Generated by Hyaluronidases Can Influence Neural Progenitor Cell Behaviors. While the digestion of HA by hyaluronidases may relieve signaling induced by high molecular weight HA, HA digestion products generated by hyaluronidases may also have their own distinct biological activities in the CNS. For example, digestion products of HA generated by bovine testicular hyaluronidase (whose activity is mostly PH20), but not those of another hyaluronidase directly blocked OPC differentiation and remyelination [55]. This finding is interesting in light of the observation that HA digestion products of sizes that are consistent with those predicted to be generated by hyaluronidase activity accumulate in demyelinated multiple sclerosis lesions [32]. It remains to be determined whether PH20 digestion products directly impact OPC maturation in ischemic CNS injuries the way they do in adult demyelinating lesions.

Additional evidence supporting the possibility that hyaluronidase-generated HA products could influence nervous system repair comes from studies utilizing HA oligosaccharides. For example, an HA tetrasaccharide was reported to improve functional recovery following spinal cord injury,

possibly by inducing the expression of brain-derived neurotrophic factor (BDNF) and vascular endothelial growth factor (VEGF) in astrocytes within the injury environment [59]. HA tetrasaccharides can also promote axonal outgrowth and promote peripheral nerve regeneration [60]. It is unclear if these tetrasaccharides are blocking interactions between other sizes of HA and their receptors, or if they are mimicking the effects of HA digestion products.

These studies indicate that high molecular weight and digested forms of HA each have distinct functions following nervous system injury and during recovery. Certain sizes of HA products that accumulate in the damaged CNS may induce cellular signals that prevent differentiation and inhibit repair, while others may induce distinct signals that support these activities. Identifying how these products are generated, the precise sizes of HA fragments that influence cell signaling in neural progenitor populations, and the receptors and downstream effectors that regulate these signals will likely lead to novel strategies to promote nervous system repair.

5. HA Receptors Are Elevated in the Damaged CNS

There are a number of receptors that signal in response to HA [61]. Among these receptors, CD44, the receptor for HA-mediated motility (RHAMM), Stabilin-2 (the HA receptor for endocytosis), lymphatic vessel endothelial hyaluronan receptor-1 (LYVE-1), and HA-binding Toll-Like Receptors (TLR-2 and TLR-4) are expressed in either the normal or diseased CNS. The roles for most of these receptors in the brain and spinal cord are not clear. However, several studies have implicated CD44 in nervous system development, homeostasis, repair, and injury responses.

5.1. CD44 Is Elevated following CNS Insults and Is Required for CNS Development. HA binds to CD44 via an extracellular domain that shares homology with cartilage link protein. Multiple forms of CD44 are generated as a result of extensive RNA splicing and posttranslational modifications [62], both of which can alter the binding affinity of HA to CD44. In general, CD44 preferentially binds high molecular weight forms of HA, although lower MW forms of HA may also signal via CD44. CD44 has been shown to influence multiple cellular behaviors including survival, proliferation, migration, and differentiation via interactions with a variety of downstream intracellular signaling molecules. These functions are linked to CD44-mediated signaling through the CD44 cytoplasmic tail, which interacts with a number of intracellular proteins including Src family kinases and members of the ezrin, radixin, moesin family of actin-associated proteins, including the merlin tumor suppressor protein [62].

CD44 is expressed throughout both the central and peripheral nervous systems predominantly by glial cells, although some neuronal populations are at least transiently CD44-positive [5]. In parallel with HA, CD44 expression increases in the injured CNS coincident with gliosis [63]. In traumatic CNS injuries, for example, CD44 is chronically elevated within areas of reactive gliosis [64, 65]. CD44 is also

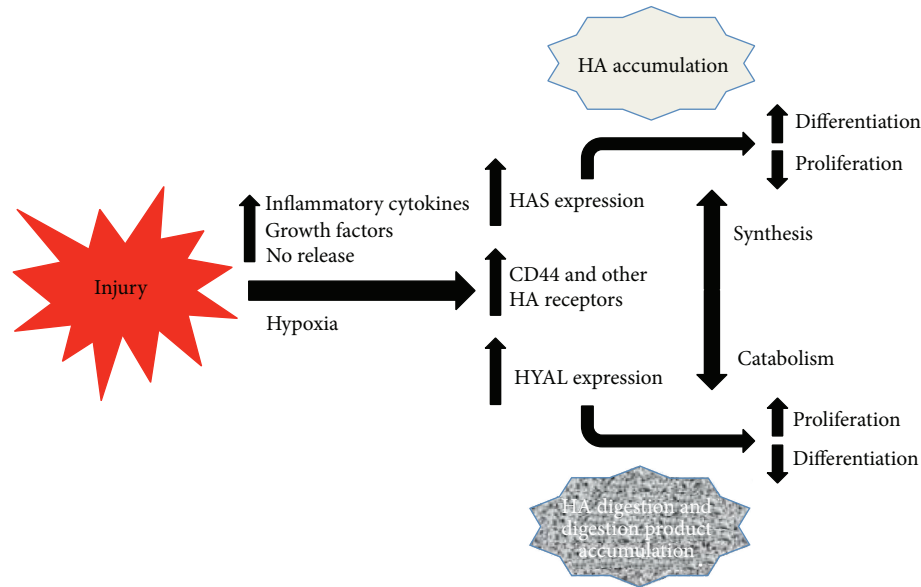


FIGURE 2: HA synthases, HA receptors, and hyaluronidases are transcriptionally upregulated in response to injury by inflammatory mediators and other injury-induced mediators. As a result, HA increases in injured tissues but also is digested. The balance between HA synthesis and catabolism influences cellular behaviors, such as proliferation and differentiation, either by influencing signals induced by high molecular weight HA or due to the accumulation of HA digestion products that have their own biological activities.

elevated following ischemia in the brains of adult animals and humans [19, 21, 66, 67] and may influence inflammatory responses following ischemic brain injury [68]. CD44 is similarly elevated in lesions from patients [23] and sheep [24] with perinatal hypoxic-ischemic cerebral white matter injuries, in the gray matter of aged macaques [36], and in patients with evidence of vascular brain injury associated with age-related cognitive decline [39]. Finally, CD44 expression is increased in a mouse model of amyotrophic lateral sclerosis (ALS; [69]). In each of these conditions, CD44 localized to reactive astrocytes or microglia.

Demyelinating lesions demonstrate highly elevated CD44 expression on reactive astrocytes and OPCs in conjunction with elevated HA [31, 63, 70]. Transgenic elevation of CD44 in OPCs leads to HA accumulation and the persistence of OPCs that fail to differentiate into OLs [71]. These mice are phenotypically similar to *shiverer* mice that lack CNS myelin. Furthermore, chronic elevation of CD44 on OPCs leads to pericellular HA accumulation [31]. Thus, chronically elevated CD44 can contribute to HA accumulation that contributes to the failure of OPC maturation. It remains unclear if CD44 is required for the effects of HA digestion products on OPC maturation and remyelination. In contrast, loss of CD44 leads to impaired OPC migration into demyelinating lesions [50] suggesting that CD44 may be required for OPC recruitment following CNS insults. Together, these findings suggest that CD44 expression must be tightly regulated in OPCs to ensure that they effectively migrate to CNS lesions and differentiate into myelinating oligodendrocytes.

CD44 is also elevated in the hippocampus following seizures [25, 72]. Although the significance of this expression is unclear, mossy fiber sprouting can be inhibited using CD44 function-blocking antibodies [25]. Furthermore, CD44 null

mice demonstrate hippocampal learning and memory deficits, consistent with abnormalities in adult hippocampal function [73]. These data suggest that, similar to OPCs, CD44 expression by cells in the hippocampus must be tightly regulated to maintain hippocampal function.

5.2. RHAMM May Influence Axon Outgrowth and Glial Cell Motility. Like CD44, RHAMM also exists in multiple isoforms and is expressed by at least subsets of neurons and glial cells, especially oligodendrocytes [74]. Unlike CD44, RHAMM can function both in the cytoplasm and at the cell surface as a glycoposphatidylinositol-anchored protein. Intracellular RHAMM binds to a number of structures including microtubules, actin, the centrosome and the mitotic spindle, and podosomes. HA binding to RHAMM can promote cell migration and growth through interactions with a variety of intracellular signaling molecules such as focal adhesion kinase (FAK), by inducing changes in actin and microtubule dynamics [75]. Interestingly, RHAMM can also interact with CD44 to influence extracellular signal-regulated kinase (ERK) activity that is required to promote cell migration [76].

Like CD44, RHAMM is observed in astrocytes in perinfarct areas following ischemia [20] and has been implicated in promoting axonal growth and astrocyte and microglial motility [77]. It is unclear, however, how RHAMM-HA interactions influence CNS injury outcomes. Interestingly, RHAMM can bind to the signaling mediator calmodulin in a calcium-dependent manner [78], suggesting a role for RHAMM in calmodulin-mediated cell signaling in the CNS.

5.3. Toll-Like Receptors May Regulate Responses to HA Digestion Products in the Injured CNS. A number of studies have

suggested that HA is a ligand for Toll-Like Receptors (TLRs). Both TLR2 and TLR4 have been reported to bind HA [79] and their expression has been detected in NSPCs [80] where they may play a role in regulating neurogenesis. TLRs are also expressed by microglia and astrocytes [81]. Sloane and coworkers [32] have reported that TLR2 is expressed by OPCs and that hyaluronidase-generated HA digestion products signal through TLR2 to inhibit OPC maturation, although roles for additional receptors in OPC responses to HA products have not been ruled out.

Altogether, studies to date support the notion that multiple HA receptors are involved in nervous system responses to injury, regulating cell migration, axon outgrowth, and differentiation. What remains to be determined is how these receptors interact to influence each of these cellular behaviors, how receptor activation influences specific intracellular signaling cascades, and which receptors respond to high molecular weight HA versus HA digestion products generated by hyaluronidases.

6. Conclusions

HA synthesis and catabolism are both induced following insults to various tissues, including the CNS. Following most if not all forms of CNS injury, the HA-based ECM is initially disrupted, leading to the loss of HA within new lesions. However, soon after the initial CNS insult, HA accumulates predominantly through transcriptional upregulation of *HAS* genes by astrocytes and other reactive glia. HA accumulation is accompanied by transcriptional upregulation of CD44 and possibly other transmembrane HA receptors leading to both enhanced HA signaling and anchoring of cell surface HA, contributing to further HA accumulation in the injury microenvironment. Such anchoring of HA to the cell surface by CD44 has been described in activated brain endothelial cells [82]. In conjunction with the transcriptional activation of *HAS* genes and HA receptors, the expression of one or more hyaluronidases is also induced, leading to the digestion and clearance of the accumulated HA in the lesions. The balance between HA accumulation and HA degradation by hyaluronidases can influence a number of cell behaviors, such as proliferation and differentiation in NSPC niches (Figure 2). Interestingly, *HAS*, HA receptor, and hyaluronidase expression may each be influenced by the same milieu of pro-inflammatory mediators that are induced following tissue damage. Disruption in the balance between HA synthesis and catabolism can lead to either excess high molecular weight HA accumulation or the accumulation of HA digestion products that can negatively impact CNS repair. The best example of this latter outcome has been demonstrated in the case of remyelination failure, where the accumulation of HA digestion products inhibits OPC maturation in demyelinating lesions (Figure 3).

In CNS diseases and injuries, it will be important to determine to what degree the disruption of high molecular weight HA versus the accumulation of HA digestion products is important for recovery. For example, following seizures, it is conceivable that maintaining the HA matrix is important

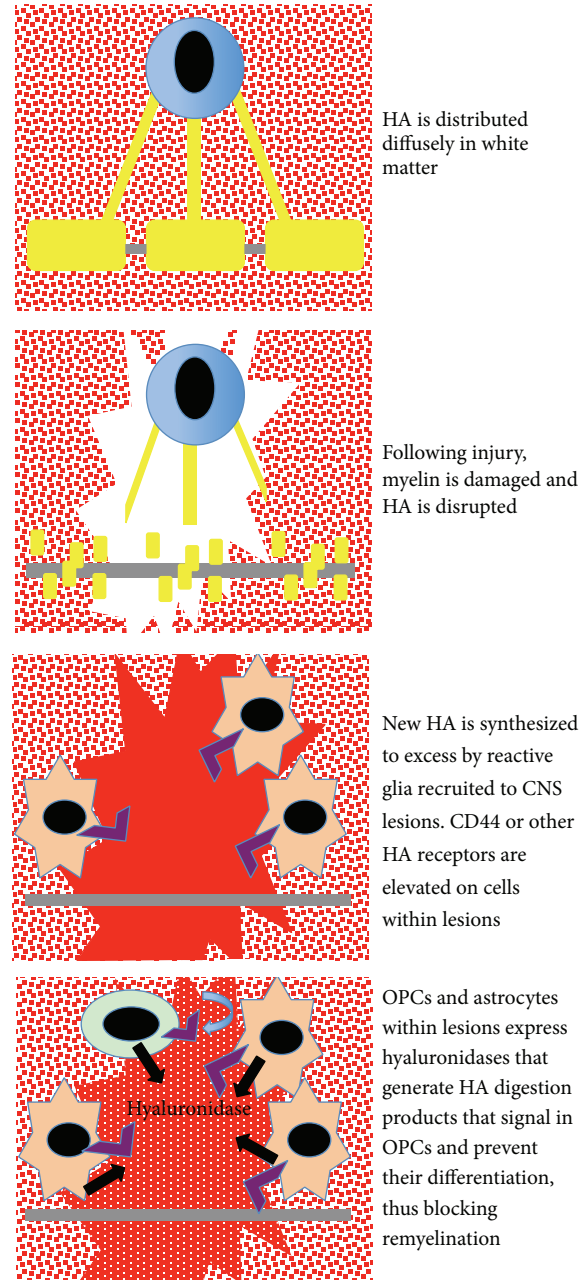


FIGURE 3: A single OL (blue cell) can form myelin (yellow) for multiple internodes of the same axon (gray) or for many axons. In uninjured white matter, HA (red) is diffuse while in perineuronal nets HA is at much higher density (not shown). Following injury, myelin and oligodendrocytes are destroyed and HA is initially disrupted. HA later accumulates at higher than normal levels coincident with the appearance of reactive astrocytes (orange cells). CD44 and possibly other HA receptors (purple) are elevated on astrocytes and OPCs recruited to lesions. Both astrocytes and recruited OPCs (green cell) then express hyaluronidases (including PH20; black arrows in lower panel) that digest the excess HA within lesions. The resulting HA digestion products that accumulate in the injury microenvironment feed back on OPCs (blue arrow in lower panel) and prevent their differentiation and subsequent remyelination.

to protect perineuronal nets and possibly NSPC survival and differentiation in NSPC niches. This could be achieved

by blocking hyaluronidase activity or expression if hyaluronidases are involved in HA degradation within NSPC niches or by elevating HAS activity. Inhibiting hyaluronidase activity has been effective in other biological systems, including blocking tumor growth in at least some cancer cells (e.g., [83]) and to promote OPC maturation [55]. Blocking the activation of receptors that respond to HA digestion products may also be an efficacious strategy to promote OPC maturation and myelination following perinatal hypoxia-ischemia and in demyelinating diseases. As the contributions of HA synthesis, catabolism and signaling become more clear in different types of CNS insults, we will gain new clues about how targeting HA synthases, hyaluronidases, and HA receptors could lead to novel therapies to promote CNS repair.

Conflict of Interests

The authors declare that there is no conflict of interests regarding the publication of this paper.

Acknowledgments

This work was supported by the National Institutes of Health (NIH): NINDS Awards: 1R01AG031892, OD011092, 1RO1NS054044, and R37NS045737-06S1/06S2 and Grant RG4843A5/1 from the National Multiple Sclerosis Society.

References

- [1] A. Bignami, M. Hosley, and D. Dahl, "Hyaluronic acid and hyaluronan-binding proteins in brain extracellular matrix," *Anatomy and Embryology*, vol. 188, no. 5, pp. 419–433, 1993.
- [2] C. E. Bandtlow and D. R. Zimmermann, "Proteoglycans in the developing brain: new conceptual insights for old proteins," *Physiological Reviews*, vol. 80, no. 4, pp. 1267–1290, 2000.
- [3] A. Dityatev and M. Schachner, "Extracellular matrix molecules and synaptic plasticity," *Nature Reviews Neuroscience*, vol. 4, no. 6, pp. 456–468, 2003.
- [4] L. S. Sherman and S. A. Back, "A 'GAG' reflex prevents repair of the damaged CNS," *Trends in Neurosciences*, vol. 31, no. 1, pp. 44–52, 2008.
- [5] M. Preston and L. S. Sherman, "Neural stem cell niches: roles for the hyaluronan-based extracellular matrix," *Frontiers in Bioscience*, vol. 3, no. 3, pp. 1165–1179, 2011.
- [6] L. B. Jakeman, K. E. Williams, and B. Brautigam, "In the presence of danger: the extracellular matrix defensive response to central nervous system injury," *Neural Regeneration Research*, vol. 9, no. 4, pp. 377–384, 2014.
- [7] A. D. Levy, M. H. Omar, and A. J. Koleske, "Extracellular matrix control of dendritic spine and synapse structure and plasticity in adulthood," *Frontiers in Neuroanatomy*, vol. 8, article 116, 2014.
- [8] L. W. Lau, R. Cua, M. B. Keough, S. Haylock-Jacobs, and V. W. Yong, "Pathophysiology of the brain extracellular matrix: a new target for remyelination," *Nature Reviews Neuroscience*, vol. 14, no. 10, pp. 722–729, 2013.
- [9] J. C. F. Kwok, G. Dick, D. Wang, and J. W. Fawcett, "Extracellular matrix and perineuronal nets in CNS repair," *Developmental Neurobiology*, vol. 71, no. 11, pp. 1073–1089, 2011.
- [10] W. Härtig, A. Derouiche, K. Welt et al., "Cortical neurons immunoreactive for the potassium channel Kv3.1b subunit are predominantly surrounded by perineuronal nets presumed as a buffering system for cations," *Brain Research*, vol. 842, no. 1, pp. 15–29, 1999.
- [11] J. M. Cregg, M. A. DePaul, A. R. Filous, B. T. Lang, A. Tran, and J. Silver, "Functional regeneration beyond the glial scar," *Experimental Neurology*, vol. 253, pp. 197–207, 2014.
- [12] A. D. Gaudet and P. G. Popovich, "Extracellular matrix regulation of inflammation in the healthy and injured spinal cord," *Experimental Neurology*, vol. 258, pp. 24–34, 2014.
- [13] E. R. Burnside and E. J. Bradbury, "Review: manipulating the extracellular matrix and its role in brain and spinal cord plasticity and repair," *Neuropathology and Applied Neurobiology*, vol. 40, no. 1, pp. 26–59, 2014.
- [14] J. R. Polansky, B. P. Toole, and J. Gross, "Brain hyaluronidase: changes in activity during chick development," *Science*, vol. 183, no. 4127, pp. 862–864, 1974.
- [15] L. O. Sampaio and C. P. Dietrich, "Changes of sulfated mucopolysaccharides and mucopolysaccharidases during fetal development," *The Journal of Biological Chemistry*, vol. 256, no. 17, pp. 9205–9210, 1981.
- [16] S. Shibata, K. H. Cho, J. H. Kim, H. Abe, G. Murakami, and B. H. Cho, "Expression of hyaluronan (hyaluronic acid) in the developing laminar architecture of the human fetal brain," *Annals of Anatomy*, vol. 195, no. 5, pp. 424–430, 2013.
- [17] A. M. Arranz, K. L. Perkins, F. Irie et al., "Hyaluronan deficiency due to Has3 knock-out causes altered neuronal activity and seizures via reduction in brain extracellular space," *Journal of Neuroscience*, vol. 34, no. 18, pp. 6164–6176, 2014.
- [18] U. B. G. Laurent, T. C. Laurent, L. K. Hellsing, L. Persson, M. Hartman, and K. Lilja, "Hyaluronan in human cerebrospinal fluid," *Acta Neurologica Scandinavica*, vol. 94, no. 3, pp. 194–206, 1996.
- [19] H. Wang, Y. Zhan, L. Xu, G. Z. Feuerstein, and X. Wang, "Use of suppression subtractive hybridization for differential gene expression in stroke: discovery of CD44 gene expression and localization in permanent focal stroke in rats," *Stroke*, vol. 32, no. 4, pp. 1020–1027, 2001.
- [20] C. Lindwall, M. Olsson, A. M. Osman, H. G. Kuhn, and M. A. Curtis, "Selective expression of hyaluronan and receptor for hyaluronan mediated motility (Rhamm) in the adult mouse subventricular zone and rostral migratory stream and in ischemic cortex," *Brain Research*, vol. 1503, pp. 62–77, 2013.
- [21] A. Al'Qteishat, J. Gaffney, J. Krupinski et al., "Changes in hyaluronan production and metabolism following ischaemic stroke in man," *Brain*, vol. 129, no. 8, pp. 2158–2176, 2006.
- [22] S. Tang, S. Yeh, L. Tsai et al., "Association between plasma levels of hyaluronic acid and functional outcome in acute stroke patients," *Journal of Neuroinflammation*, vol. 11, no. 1, article 101, 2014.
- [23] J. R. Buser, J. Maire, A. Riddle et al., "Arrested preoligodendrocyte maturation contributes to myelination failure in premature infants," *Annals of Neurology*, vol. 71, no. 1, pp. 93–109, 2012.
- [24] M. W. Hagen, A. Riddle, E. McClendon et al., "Role of recurrent hypoxia-ischemia in preterm white matter injury severity," *PLoS ONE*, vol. 9, no. 11, Article ID e112800, 2014.
- [25] S. B. Bausch, "Potential roles for hyaluronan and CD44 in kainic acid-induced mossy fiber sprouting in organotypic hippocampal slice cultures," *Neuroscience*, vol. 143, no. 1, pp. 339–350, 2006.

- [26] P. A. Mcrae, E. Baranov, S. L. Rogers, and B. E. Porter, "Persistent decrease in multiple components of the perineuronal net following status epilepticus," *European Journal of Neuroscience*, vol. 36, no. 11, pp. 3471–3482, 2012.
- [27] S. R. Perosa, M. A. Porcionatto, A. Cukiert et al., "Glycosaminoglycan levels and proteoglycan expression are altered in the hippocampus of patients with mesial temporal lobe epilepsy," *Brain Research Bulletin*, vol. 58, no. 5, pp. 509–516, 2002.
- [28] H. Mansour, R. Asher, D. Dahl, B. Labkovsky, G. Perides, and A. Bignami, "Permissive and non-permissive reactive astrocytes: Immunofluorescence study with antibodies to the glial hyaluronate-binding protein," *Journal of Neuroscience Research*, vol. 25, no. 3, pp. 300–311, 1990.
- [29] J. Struve, P. C. Maher, Y.-Q. Li et al., "Disruption of the hyaluronan-based extracellular matrix in spinal cord promotes astrocyte proliferation," *Glia*, vol. 52, no. 1, pp. 16–24, 2005.
- [30] G. Xing, M. Ren, and A. Verma, "Divergent temporal expression of hyaluronan metabolizing enzymes and receptors with craniotomy vs. controlled-cortical impact injury in rat brain: a pilot study," *Frontiers in Neurology*, vol. 5, article 173, 2014.
- [31] S. A. Back, T. M. F. Tuohy, H. Chen et al., "Hyaluronan accumulates in demyelinated lesions and inhibits oligodendrocyte progenitor maturation," *Nature Medicine*, vol. 11, no. 9, pp. 966–972, 2005.
- [32] J. A. Sloane, C. Batt, Y. Ma, Z. M. Harris, B. Trapp, and T. Vartanian, "Hyaluronan blocks oligodendrocyte progenitor maturation and remyelination through TLR2," *Proceedings of the National Academy of Sciences of the United States of America*, vol. 107, no. 25, pp. 11555–11560, 2010.
- [33] A. Chang, S. M. Staugaitis, R. Dutta et al., "Cortical remyelination: a new target for repair therapies in multiple sclerosis," *Annals of Neurology*, vol. 72, no. 6, pp. 918–926, 2012.
- [34] M. Bugiani, N. Postma, E. Polder et al., "Hyaluronan accumulation and arrested oligodendrocyte progenitor maturation in vanishing white matter disease," *Brain*, vol. 136, no. 1, pp. 209–222, 2013.
- [35] H. G. Jenkins and H. S. Bachelard, "Developmental and age-related changes in rat brain glycosaminoglycans," *Journal of Neurochemistry*, vol. 51, no. 5, pp. 1634–1640, 1988.
- [36] R. Cargill, S. G. Kohama, J. Struve et al., "Astrocytes in aged nonhuman primate brain gray matter synthesize excess hyaluronan," *Neurobiology of Aging*, vol. 33, no. 4, pp. 830.e13–830.e24, 2012.
- [37] H. G. Jenkins and H. S. Bachelard, "Glycosaminoglycans in cortical autopsy samples from Alzheimer brain," *Journal of Neurochemistry*, vol. 51, no. 5, pp. 1641–1645, 1988.
- [38] K. Suzuki, R. Katzman, and S. R. Korey, "Chemical studies on Alzheimer's disease," *Journal of Neuropathology and Experimental Neurology*, vol. 24, pp. 211–224, 1965.
- [39] S. A. Back, C. D. Kroenke, L. S. Sherman et al., "White matter lesions defined by diffusion tensor imaging in older adults," *Annals of Neurology*, vol. 70, no. 3, pp. 465–476, 2011.
- [40] K. Nägga, O. Hansson, D. van Westen, L. Minthon, and M. Wennström, "Increased levels of hyaluronic acid in cerebrospinal fluid in patients with vascular dementia," *Journal of Alzheimer's Disease*, vol. 42, no. 4, pp. 1435–1441, 2014.
- [41] R. J. Franklin and C. Ffrench-Constant, "Remyelination in the CNS: from biology to therapy," *Nature Reviews Neuroscience*, vol. 9, no. 11, pp. 839–855, 2008.
- [42] G. Wolswijk, "Chronic stage multiple sclerosis lesions contain a relatively quiescent population of oligodendrocyte precursor cells," *Journal of Neuroscience*, vol. 18, no. 2, pp. 601–609, 1998.
- [43] N. Scolding, R. Franklin, S. Stevens, C.-H. Heldin, A. Compston, and J. Newcombe, "Oligodendrocyte progenitors are present in the normal adult human CNS and in the lesions of multiple sclerosis," *Brain*, vol. 121, no. 12, pp. 2221–2228, 1998.
- [44] A. Chang, A. Nishiyama, J. Peterson, J. Prineas, and B. D. Trapp, "NG2-positive oligodendrocyte progenitor cells in adult human brain and multiple sclerosis lesions," *Journal of Neuroscience*, vol. 20, no. 17, pp. 6404–6412, 2000.
- [45] Y. Maeda, M. Solanky, J. Menonna, J. Chapin, W. Li, and P. Dowling, "Platelet-derived growth factor- α receptor-positive oligodendroglia are frequent in multiple sclerosis lesions," *Annals of Neurology*, vol. 49, no. 6, pp. 776–785, 2001.
- [46] A. Chang, W. W. Tourtellotte, R. Rudick, and B. D. Trapp, "Premyelinating oligodendrocytes in chronic lesions of multiple sclerosis," *The New England Journal of Medicine*, vol. 346, no. 3, pp. 165–173, 2002.
- [47] G. Wolswijk, "Oligodendrocyte precursor cells in the demyelinated multiple sclerosis spinal cord," *Brain*, vol. 125, no. 2, pp. 338–349, 2002.
- [48] J. M. Dean, A. Riddle, J. Maire et al., "An organotypic slice culture model of chronic white matter injury with maturation arrest of oligodendrocyte progenitors," *Molecular Neurodegeneration*, vol. 6, no. 1, article 46, 2011.
- [49] C.-M. Lin, J.-W. Lin, Y.-C. Chen et al., "Hyaluronic acid inhibits the glial scar formation after brain damage with tissue loss in rats," *Surgical Neurology*, vol. 72, no. 2, pp. S50–S54, 2009.
- [50] J.-H. Piao, Y. Wang, and I. D. Duncan, "CD44 is required for the migration of transplanted oligodendrocyte progenitor cells to focal inflammatory demyelinating lesions in the spinal cord," *Glia*, vol. 61, no. 3, pp. 361–367, 2013.
- [51] K. Fuxe, B. Tinner, G. Chadi, A. Härfstrand, and L. F. Agnati, "Evidence for a regional distribution of hyaluronic acid in the rat brain using a highly specific hyaluronic acid recognizing protein," *Neuroscience Letters*, vol. 169, no. 1-2, pp. 25–30, 1994.
- [52] M. A. Solis, Y.-H. Chen, T. Y. Wong, V. Z. Bittencourt, Y.-C. Lin, and L. L. H. Huang, "Hyaluronan regulates cell behavior: a potential niche matrix for stem cells," *Biochemistry Research International*, vol. 2012, Article ID 346972, 11 pages, 2012.
- [53] Y. Liang, P. Walczak, and J. W. M. Bulte, "The survival of engrafted neural stem cells within hyaluronic acid hydrogels," *Biomaterials*, vol. 34, no. 22, pp. 5521–5529, 2013.
- [54] J. Zhong, A. Chan, L. Morad, H. I. Kornblum, and S. T. Carmichael, "Hydrogel matrix to support stem cell survival after brain transplantation in stroke," *Neurorehabilitation and Neural Repair*, vol. 24, no. 7, pp. 636–644, 2010.
- [55] M. Preston, X. Gong, W. Su et al., "Digestion products of the PH20 hyaluronidase inhibit remyelination," *Annals of Neurology*, vol. 73, no. 2, pp. 266–280, 2013.
- [56] S. V. Kul'chitskii, N. V. Yakubovich, A. A. Emel'yanova, Y. S. Garkun, S. G. Pashkevich, and V. A. Kul'chitskii, "Changes in neuropil ultrastructure in hippocampal field CA1 in rat pups after application of hyaluronidase," *Neuroscience and Behavioral Physiology*, vol. 39, no. 6, pp. 517–521, 2009.
- [57] R. Frischknecht, M. Heine, D. Perrais, C. I. Seidenbecher, D. Choquet, and E. D. Gundelfinger, "Brain extracellular matrix affects AMPA receptor lateral mobility and short-term synaptic plasticity," *Nature Neuroscience*, vol. 12, no. 7, pp. 897–904, 2009.
- [58] J. Klueva, E. D. Gundelfinger, R. R. Frischknecht, and M. Heine, "Intracellular Ca^{2+} and not the extracellular matrix determines surface dynamics of AMPA-type glutamate receptors on aspiny neurons," *Philosophical Transactions of the Royal Society of*

- London B: Biological Science*, vol. 369, no. 1654, Article ID 20130605, 2014.
- [59] J. Wang, X. Wang, J. Wei, and M. Wang, "Hyaluronan tetrasaccharide exerts neuroprotective effect and promotes functional recovery after acute spinal cord injury in rats," *Neurochemical Research*, vol. 40, no. 1, pp. 98–108, 2015.
- [60] K. Torigoe, H. F. Tanaka, H. Ohkochi et al., "Hyaluronan tetrasaccharide promotes regeneration of peripheral nerve: in vivo analysis by film model method," *Brain Research*, vol. 1385, pp. 87–92, 2011.
- [61] D. Vigetti, E. Karousou, M. Viola, S. Deleonibus, G. De Luca, and A. Passi, "Hyaluronan: biosynthesis and signaling," *Biochimica et Biophysica Acta—General Subjects*, vol. 1840, no. 8, pp. 2452–2459, 2014.
- [62] H. Ponta, L. Sherman, and P. A. Herrlich, "CD44: from adhesion molecules to signalling regulators," *Nature Reviews Molecular Cell Biology*, vol. 4, no. 1, pp. 33–45, 2003.
- [63] H. Vogel, E. C. Butcher, and L. J. Picker, "H-CAM expression in the human nervous system: evidence for a role in diverse glial interactions," *Journal of Neurocytology*, vol. 21, no. 5, pp. 363–373, 1992.
- [64] S. S. Stylli, A. H. Kaye, and U. Novak, "Induction of CD44 expression in stab wounds of the brain: long term persistence of CD44 expression," *Journal of Clinical Neuroscience*, vol. 7, no. 2, pp. 137–140, 2000.
- [65] L. L. Jones, Z. Liu, J. Shen, A. Werner, G. W. Kreutzberg, and G. Raivich, "Regulation of the cell adhesion molecule CD44 after nerve transection and direct trauma to the mouse brain," *Journal of Comparative Neurology*, vol. 426, no. 3, pp. 468–492, 2000.
- [66] A. Al Qteishat, J. J. Gaffney, J. Krupinski, and M. Slevin, "Hyaluronan expression following middle cerebral artery occlusion in the rat," *NeuroReport*, vol. 17, no. 11, pp. 1111–1114, 2006.
- [67] W.-S. Kang, J.-S. Choi, Y.-J. Shin et al., "Differential regulation of osteopontin receptors, CD44 and the α_v and β_3 integrin subunits, in the rat hippocampus following transient forebrain ischemia," *Brain Research*, vol. 1228, pp. 208–216, 2008.
- [68] X. Wang, L. Xu, H. Wang, Y. Zhan, E. Puré, and G. Z. Feuerstein, "CD44 deficiency in mice protects brain from cerebral ischemia injury," *Journal of Neurochemistry*, vol. 83, no. 5, pp. 1172–1179, 2002.
- [69] T. Matsumoto, S. Imagama, K. Hirano et al., "CD44 expression in astrocytes and microglia is associated with ALS progression in a mouse model," *Neuroscience Letters*, vol. 520, no. 1, pp. 115–120, 2012.
- [70] S. Alldinger, S. Fonfara, E. Kremmer, and W. Baumgärtner, "Up-regulation of the hyaluronate receptor CD44 in canine distemper demyelinated plaques," *Acta Neuropathologica*, vol. 99, no. 2, pp. 138–146, 2000.
- [71] T. M. F. Tuohy, N. Wallingford, Y. Liu et al., "CD44 overexpression by oligodendrocytes: a novel mouse model of inflammation-independent demyelination and dysmyelination," *Glia*, vol. 47, no. 4, pp. 335–345, 2004.
- [72] K. Borges, D. L. McDermott, and R. Dingledine, "Reciprocal changes of CD44 and GAP-43 expression in the dentate gyrus inner molecular layer after status epilepticus in mice," *Experimental Neurology*, vol. 188, no. 1, pp. 1–10, 2004.
- [73] J. Raber, R. H. J. Olsen, W. Su et al., "CD44 is required for spatial memory retention and sensorimotor functions," *Behavioral Brain Research*, vol. 275, pp. 146–149, 2014.
- [74] B. D. Lynn, X. Li, P. A. Cattini, E. A. Turley, and J. I. Nagy, "Identification of sequence, protein isoforms, and distribution of the hyaluronan-binding protein RHAMM in adult and developing rat brain," *Journal of Comparative Neurology*, vol. 439, no. 3, pp. 315–330, 2001.
- [75] C. L. Hall, C. Wang, L. A. Lange, and E. A. Turley, "Hyaluronan and the hyaluronan receptor RHAMM promote focal adhesion turnover and transient tyrosine kinase activity," *The Journal of Cell Biology*, vol. 126, no. 2, pp. 575–588, 1994.
- [76] S. R. Hamilton, S. F. Fard, F. F. Paiwand et al., "The hyaluronan receptors CD44 and Rhamm (CD168) form complexes with ERK1,2 that sustain high basal motility in breast cancer cells," *The Journal of Biological Chemistry*, vol. 282, no. 22, pp. 16667–16680, 2007.
- [77] E. A. Turley, M. Z. Hossain, T. Sorokan, L. M. Jordan, and J. I. Nagy, "Astrocyte and microglial motility in vitro is functionally dependent on the hyaluronan receptor RHAMM," *Glia*, vol. 12, no. 1, pp. 68–80, 1994.
- [78] B. D. Lynn, E. A. Turley, and J. I. Nagy, "Subcellular distribution, calmodulin interaction, and mitochondrial association of the hyaluronan-binding protein RHAMM in rat brain," *Journal of Neuroscience Research*, vol. 65, no. 1, pp. 6–16, 2001.
- [79] J. A. Sloane, D. Blitz, Z. Margolin, and T. Vartanian, "A clear and present danger: endogenous ligands of Toll-like receptors," *NeuroMolecular Medicine*, vol. 12, no. 2, pp. 149–163, 2010.
- [80] A. Rolls, R. Shechter, A. London et al., "Toll-like receptors modulate adult hippocampal neurogenesis," *Nature Cell Biology*, vol. 9, no. 9, pp. 1081–1088, 2007.
- [81] C. Gurley, J. Nichols, S. Liu, N. K. Phulwani, N. Esen, and T. Kielian, "Microglia and astrocyte activation by toll-like receptor ligands: modulation by PPAR-gamma agonists," *PPAR Research*, vol. 2008, Article ID 453120, 15 pages, 2008.
- [82] C. W. Winkler, S. C. Foster, S. G. Matsumoto et al., "Hyaluronan anchored to activated CD44 on central nervous system vascular endothelial cells promotes lymphocyte extravasation in experimental autoimmune encephalomyelitis," *Journal of Biological Chemistry*, vol. 287, no. 40, pp. 33237–33251, 2012.
- [83] A. Benitez, T. J. Yates, L. E. Lopez, W. H. Cerwinka, A. Bakkar, and V. B. Lokeshwar, "Targeting hyaluronidase for cancer therapy: antitumor activity of sulfated hyaluronic acid in prostate cancer cells," *Cancer Research*, vol. 71, no. 12, pp. 4085–4095, 2011.